

Development of Innovative Methodologies for Transition Metal Catalyzed Syntheses of Fine Chemicals

Dissertation
zur Erlangung des akademischen Grades
doctor rerum naturalium (Dr. rer. nat.)
der Mathematisch-Naturwissenschaftlichen Fakultät
der Universität Rostock

Gutachter:

1. Prof. Dr. Matthias Beller (Leibniz-Institut für Katalyse e.V.)
2. Prof. Dr. Wolfram Seidel (Institut für Chemie, Universität Rostock)

vorgelegt von

Sören Hancker, geboren am 18.05.1990 in Eutin

Tag der Einreichung: 30.01.2019

Tag des Kolloquiums: 14.05.2019

https://doi.org/10.18453/rosdok_id00002481

Abstract

Development of Innovative Methodologies for Transition Metal Catalyzed Syntheses of Fine Chemicals

Sören Hancker

This thesis describes the development of novel methodologies for transition metal catalyzed syntheses of industrially relevant substances. Herein, the efficiency of innovative catalysts for environmentally-friendly hydrogen autotransfer conversions which enable molecular transformations displaying significant advantages over classical synthetic routes is investigated. Moreover, the thesis presents new heterogeneous materials for the atom efficient amidocarbonylation which allows access to the important substance class of N-acyl amino acids and thereby amino acid building blocks. The reported protocol significantly improves the well-known methodology by decreasing a critical co-catalyst loading. Finally, a new procedure for the selective synthesis of Z-alkenes *via* twofold utilization of palladium atoms – initially as homogeneous and subsequently as heterogeneous catalyst – is presented.

Die vorliegende Arbeit beschreibt die Entwicklung neuartiger Methoden für die Übergangsmetall-katalysierte Synthese industriell relevanter Substanzen. Hierbei wird die Effektivität innovativer Katalysatoren für umweltfreundliche Hydrogen Autotransfer Reaktionen untersucht, die molekulare Umsetzungen ermöglichen, welche signifikante Vorteile gegenüber klassisch-synthetischen Routen besitzen. Weiterhin evaluiert die Arbeit neue heterogene Materialien für die atom-effiziente Amidocarbonylierung, welche Zugang zu der wichtigen Stoffklasse der N-Acyl-Aminosäuren und damit Aminosäure-Bausteinen bietet. Das veröffentlichte Protokoll erlaubt eine deutliche Reduzierung der Konzentration eines entscheidenden Co-Katalysators. Schlussendlich präsentiert die Arbeit ein neues Prozedere für die selektive Synthese von Z-Alkenen über die zweifache Verwendung von Palladiumatomen – zunächst als homogener und anschließend als heterogener Katalysator.

Table of Contents

Selbstständigkeitserklärung	I
Acknowledgement.....	II
Abstract	VII
Table of Contents	VIII
List of Schemes	IX
List of Tables.....	XI
List of Abbreviations.....	XII
1. Preface.....	1
2. Hydrogen Autotransfer	5
2.1. Theory.....	5
2.2. Objectives	10
2.3. Results	12
2.4. Outlook.....	22
3. Amidocarbonylation	24
3.1. Theory.....	24
3.2. Objectives	29
3.3. Results	30
3.4. Outlook.....	44
4. Sonogashira-Semihydrogenation	46
4.1. Theory.....	46
4.2. Objectives	52
4.3. Results	53
4.4. Outlook.....	77
5. Summary.....	79
6. References.....	81
7. Appendix.....	91

List of Schemes

<i>Scheme 1. Share of each branch in the overall turnover in 2016.</i>	1
<i>Scheme 2. Development of the Production Index.</i>	2
<i>Scheme 3. General mechanistic concept of hydrogen autotransfer reactions.</i>	5
<i>Scheme 4. Selected examples of catalysts for hydrogen autotransfer reactions.</i>	6
<i>Scheme 5. Selected examples for substrates and reactions in hydrogen autotransfer chemistry.</i>	7
<i>Scheme 6. Selected examples for C-alkylation of C-H acidic compounds with alcohols.</i>	8
<i>Scheme 7. Alternative synthetic route towards valproic acid.</i>	10
<i>Scheme 8. Selected examples for non-noble metal Pincer complex catalyzed reactions from the Beller group.</i>	11
<i>Scheme 9. Synthesis of iridium complex 1.</i>	12
<i>Scheme 10. Optimization reaction for the α-alkylation of esters.</i>	12
<i>Scheme 11. Results for the attempted methyl valerate propylation.</i>	13
<i>Scheme 12. Successful α-alkylation of ^tbutyl acetate with n-propanol.</i>	13
<i>Scheme 13. Successful α-alkylation of ethyl acetate with n-propanol.</i>	13
<i>Scheme 14. Unsuccessful α-alkylation of ^tbutyl valerate with n-propanol.</i>	14
<i>Scheme 15. Structure of Fe- and Ru-MACHO-BH complexes.</i>	14
<i>Scheme 16. Suitable C-H acidic substrates for hydrogen autotransfer reactions.</i>	16
<i>Scheme 17. Results for the iron-catalyzed hydrogen autotransfer reaction.</i>	17
<i>Scheme 18. C-Alkylation of benzyl cyanide.</i>	18
<i>Scheme 19. Dehydrogenative coupling of primary alcohols to methyl esters.</i>	19
<i>Scheme 20. Dehydrogenative coupling towards symmetric esters.</i>	19
<i>Scheme 21. Alkylation of ketones with alcohols catalyzed by pyrolyzed heterogeneous catalysts.</i>	20
<i>Scheme 22. N-Alkylation of amines by pyrolyzed, heterogeneous catalysts.</i>	21
<i>Scheme 23. Law of mass action for the condensation reaction of hydrogen autotransfer conversions.</i>	22
<i>Scheme 24. Industrially important substances incorporating N-acyl amino acids.</i>	24
<i>Scheme 25. Selected examples for the synthesis of amino acids.</i>	25
<i>Scheme 26. Generally accepted mechanism for the Pd-catalyzed amidocarbonylation.</i>	26
<i>Scheme 27. Comparing classical and amidocarbonylation route for the synthesis of Piracetam and N-lauroyl sarcosine.</i>	27
<i>Scheme 28. Protocols for the amidocarbonylation of N-methyl dodecanamide.</i>	29
<i>Scheme 29. Results for the tested ligands in the palladium-catalyzed amidocarbonylation.</i>	30
<i>Scheme 30. Influence of the lithium bromide concentration on the reaction yield.</i>	35

<i>Scheme 31. Results for the recycling experiments.</i>	<i>36</i>
<i>Scheme 32. Substrate scope for the novel amidocarbonylation protocol.</i>	<i>37</i>
<i>Scheme 33. Reactivity of aldehydes towards nucleophiles and amides towards electrophiles.</i>	<i>38</i>
<i>Scheme 34. Comparison of the activity of pre-alkylated and non-alkylated amides.</i>	<i>39</i>
<i>Scheme 35. Application of the novel protocol for the 10 g synthesis of N-lauroyl sarcosine.</i>	<i>39</i>
<i>Scheme 36. Results for the recycling experiments.</i>	<i>40</i>
<i>Scheme 37. Synthetical approach to N-sulfonyl amino acids via amidocarbonylation.</i>	<i>41</i>
<i>Scheme 38. Substrate scope for the sulfonamidocarbonylation.</i>	<i>42</i>
<i>Scheme 39. Synthesis of acetamido malonic acid via amidocarbonylation.</i>	<i>43</i>
<i>Scheme 40. Conditions for the Sonogashira coupling.</i>	<i>46</i>
<i>Scheme 41. Pharmaceuticals produced via Sonogashira coupling.</i>	<i>46</i>
<i>Scheme 42. Generally accepted mechanism for the Sonogashira coupling.</i>	<i>47</i>
<i>Scheme 43. Industrial production of Prosulferon.</i>	<i>50</i>
<i>Scheme 44. Selected routes for the synthesis of Z-alkenes.</i>	<i>51</i>
<i>Scheme 45. Novel methodology for the synthesis of Z-alkenes.</i>	<i>52</i>
<i>Scheme 46. Product yield over time of the sequential one-pot synthesis.</i>	<i>59</i>
<i>Scheme 47. Ball-and-stick models of tolan (left) and 35 (right).</i>	<i>64</i>
<i>Scheme 48. Influence of DTOD in the semihydrogenation step of internal acetylene 71.</i>	<i>68</i>
<i>Scheme 49. Ball-and-stick models of compounds 73 (left) and 74 (right).</i>	<i>69</i>
<i>Scheme 50. XRD-analysis of the heterogeneous material obtained after the hydrogenation process.</i>	<i>70</i>
<i>Scheme 51. XPS-spectra of the heterogeneous material obtained after the hydrogenation process.</i>	<i>71</i>
<i>Scheme 52. Postulated mechanism for the sequential Sonogashira-semihydrogenation.</i>	<i>71</i>
<i>Scheme 53. Mechanism for the heterogeneous syn-addition.</i>	<i>73</i>
<i>Scheme 54. Arylacetylene side-reaction.</i>	<i>73</i>
<i>Scheme 55. Synthesis of E-Z-dienes via the novel methodology.</i>	<i>74</i>
<i>Scheme 56. Products from the initial attempt to generate E-Z-dienes.</i>	<i>74</i>
<i>Scheme 57. Synthesis of E-Z-dienes via the novel methodology.</i>	<i>74</i>
<i>Scheme 58. Synthetic pathways available by the novel Sonogashira-Semihydrogenation protocol.</i>	<i>75</i>

List of Tables

<i>Table 1. Optimization of the iron catalyzed α-alkylation of esters.</i>	<i>15</i>
<i>Table 2. Catalyst screening for the C-alkylation of ketones by pyrolyzed heterogeneous catalysts.</i>	<i>21</i>
<i>Table 3. Optimization of the PdBr₂-catalyzed conversion towards N-lauroyl sarcosine.</i>	<i>31</i>
<i>Table 4. Screening for efficient heterogeneous palladium catalysts in the amidocarbonylation.</i>	<i>32</i>
<i>Table 5. Screening of heterogeneous palladium catalyst incorporating acidic supports for the H₂SO₄-free amidocarbonylation.</i>	<i>33</i>
<i>Table 6. Optimization of the Pd black catalyzed amidocarbonylation.</i>	<i>34</i>
<i>Table 7. Optimization of the synthesis of N-sulfonyl amino acids via amidocarbonylation.</i>	<i>41</i>
<i>Table 8. Selected examples from literature reports on amidocarbonylations.</i>	<i>44</i>
<i>Table 9. Optimization of the copper- and amine-free Sonogashira reaction.</i>	<i>53</i>
<i>Table 10. Optimization of the semihydrogenation applying (CH₂O)_n/H₂O.</i>	<i>55</i>
<i>Table 11. Optimization of the selective semihydrogenation applying hydrogen gas.</i>	<i>57</i>
<i>Table 12. Substrate scope of the Sonogashira-semihydrogenation.</i>	<i>59</i>

List of Abbreviations

A

Ad Adamantyl-Moiety

B

Bu Butyl-Moiety

C

CHEM21 CHEM21-Project, see references

cod Cyclooctadiene

D

DME Dimethoxyethane

DMF Dimethylformamide

DMSO Dimethylsulfoxide

DTOD 3,6-Dithia-1,8-octanediol

E

e.g. *exempli gratia (lat.); for example*

Et Ethyl-Moiety

EU European Union

G

GC Gas Chromatography

H

Hex Hexyl-Moiety

I

ICDD *The International Centre of Diffraction Data*

ICP-OES Inductively Coupled Plasma – Optical Emission Spectrometry

in situ *(lat.); in place, on location*

M

MACHO *Bis[2-(di(organophosphino)ethyl)amine*

MS *Mass Spectrometry*

N

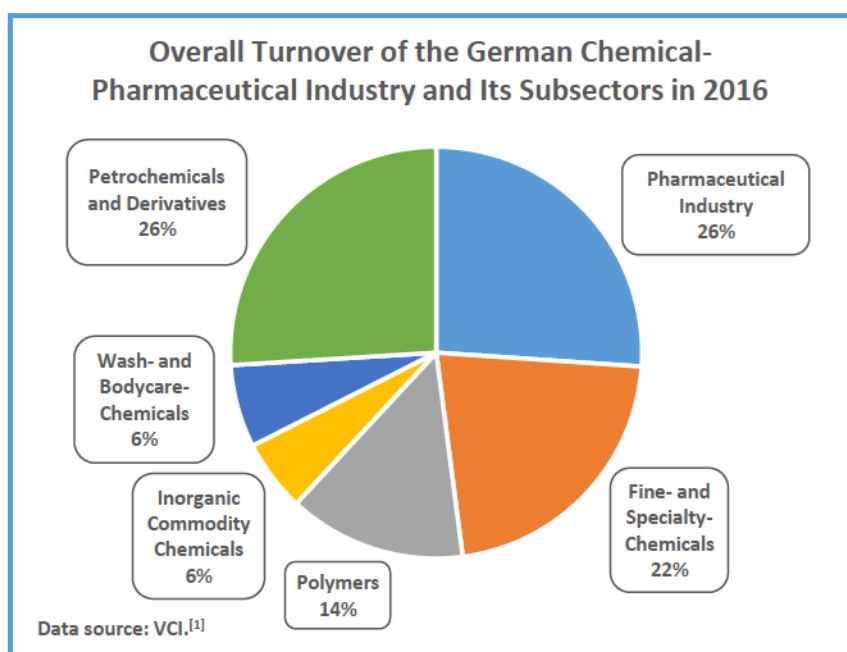
n *normal; linear*

ND Not Detected

NMDA	<i>N-Methyldodecanamide</i>
NMR	<i>Nuclear Magnetic Resonance (Spectroscopy)</i>
P	
PFA	<i>Paraformaldehyde</i>
PFPE	<i>Perfluoro-Polyether</i>
Ph	<i>Phenyl-Moiety</i>
PTFE	<i>Polytetrafluoroethylene</i>
S	
sp	<i>s- and p-Orbital Hybridization</i>
T	
^t , <i>tert</i>	<i>tertiary</i>
TOF	<i>Turnover Frequency</i>
TON	<i>Turnover Number</i>
V	
VCI	<i>Verband der Chemischen Industrie e.V.</i>
<i>via</i>	<i>by way of; through</i>
W	
WHO	<i>World Health Organization</i>
X	
XPS	<i>X-Ray Photoelectron Spectroscopy</i>
XRD	<i>X-Ray Diffraction</i>
Z	
ZSM-5	<i>Zeolite Socony Mobil-5, an aluminosilicate zeolite</i>
Δ	
Δ	<i>Elevated Temperature</i>

1. Preface

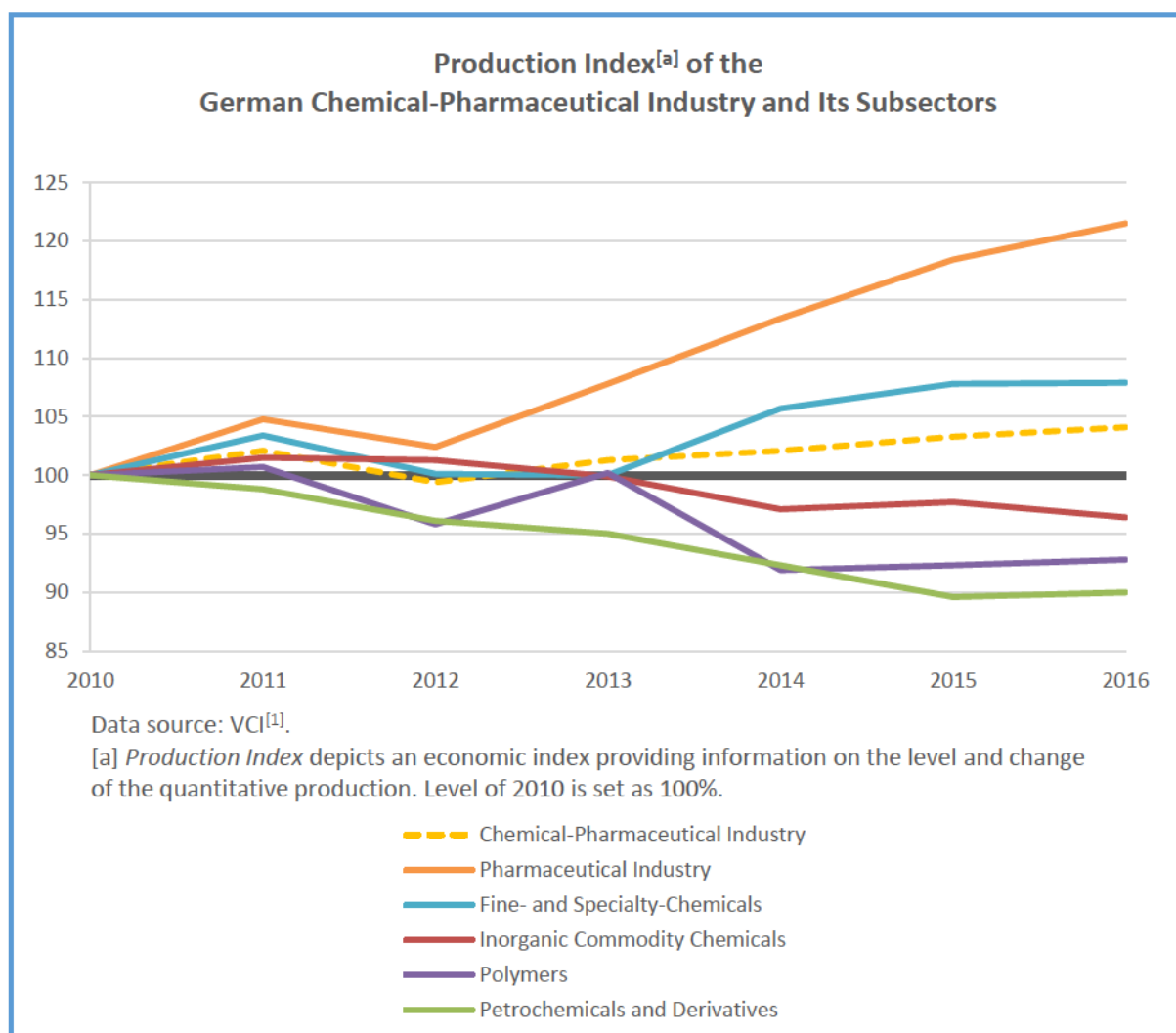
In 2016, the German chemical-pharmaceutical industries and its 447,000 employees generated an overall turnover of 184.7 billion euro and therefore constitute one of the most productive industrial sections. Moreover, the pharmaceutical industry and the fine- and specialty-chemicals branch combined for almost 50% of the overall turnover, thus emphasizing the economic relevance of both sections (Scheme 1).^[1]



Scheme 1. Share of each branch in the overall turnover in 2016.

In recent years, the significance of these two industrial branches has been emphasized as the production index of both industries has been increasing (Scheme 2). In contrast, other branches affiliated with the chemical-pharmaceutical industry recorded declining production indexes.^[1]

In general, the production of both pharmaceuticals and fine chemicals requires complex and multi-step syntheses since the target molecules include multiple and often challenging functionalities.^[2,3] Thus, processes have to be designed to selectively and efficiently afford the product while minimizing the formation of waste. In addition, the desire to decrease the energy consumption and the emission of greenhouse gases requires chemists to develop novel and sustainable methodologies and processes for the synthesis of industrially relevant products.^[4-8]



Scheme 2. Development of the Production Index.

Herein, catalysis constitutes a key factor to accomplish these tasks. The science of accelerating chemical reactions provides a tool box of possibilities not only to increase the reaction rates but also to provide alternative reaction pathways.^[9] Thereby, new chemical transformations are enabled while others can be performed with improved functional group tolerance. Thus, the necessity of waste-intense stoichiometric conversions and (de)protection transformations can be avoided while more direct synthetic routes are facilitated. As a result, catalytic conversions are currently involved in over 80% of all manufacturing processes in the chemical industry.^[10] Consequently, pharmaceutical and chemical companies demonstrate an incessant interest in the development of new catalysts and new catalytic methodologies.^[2,3]

Due to the superior selectivity and activity under milder conditions, homogeneous catalysis is widely applied in academic research as well as the industrial production of pharmaceuticals and fine chemicals.^[9,11,12] While the implementation on industrial scale

implies specific challenges, homogeneous catalysis has exceeded established stoichiometric methodologies in numerous examples.^[2,3,13] Herein, the most well-studied catalytic conversions include hydroformylation, hydrogenation, oxidation, metathesis, carbonylation and cross coupling reactions.^[14] Furthermore, the significance of homogeneous catalysis has been emphasized by the bestowal of several Nobel Prizes in Chemistry to contributors accomplished in this specific field including Knowles, Noyori (2001, chiral hydrogenation), Sharpless (2001, chiral epoxidation), Chauvin, Grubbs, Schrock (2005, metathesis) and most recently Heck, Negishi, and Suzuki (2010, cross-coupling reactions).^[15-17]

While the majority of these examples effect transformations of functional groups, cross coupling reactions enable alterations in the basic carbon structure.^[18-20] In the early 1970s, the initial work was conducted by Heck and Mizoroki by converting aryl halides with olefins to the corresponding substituted alkenes catalyzed by palladium salts.^[21,22] Ever since, numerous C-C coupling protocols utilizing various nucleophiles have emerged. Sonogashira and Hagihara introduced the coupling with acetylenes as nucleophiles^[23] while Suzuki and Miyaura employed organoboronic acids as coupling partner.^[24] In addition, various organometallic reagents such as organo-zinc,^[25] -tin,^[26,27] -magnesium^[28,29] and -silicon^[30] were found to be reactive organometallic reactants. Furthermore, C-H acidic compounds^[31-39] as well as amines,^[40,41] alcohols^[42,43] and thiols^[44-46] were identified as suitable coupling partners. Based on the wide application range and superior profitability, cross coupling methodologies are extensively applied in both industry and academic research.^[9,19,47-51]

Despite the success of homogeneous catalysts in industrial processes, heterogeneous catalysis is viewed as advantageous and more eligible on large scale due to the superior recyclability and reusability.^[52,53] However, insufficient catalytic performances often prevent the implementation of heterogeneous catalysts in the fine chemical and pharmaceutical industry.^[9] As an emerging strategy, the design and synthesis of well-defined heterogeneous materials has proven to afford novel materials with increased selectivity and efficiency combined with recyclability and durability.^[54-59] Surprisingly, the alternate approach to convert a homogeneous complex into a heterogeneous catalyst subsequently to an initial reaction in order to enable a second conversion by the newly formed material had been reported as early as 1994.^[60] However, despite this elegant solution to an otherwise challenging problem, this methodology has rarely been applied ever since.^[61,62] Still, this procedure turned the synthesis of the industrially relevant agrochemical Prosulfuron into an

economically feasible process as it combines the advantages of homogeneous and heterogeneous catalysis.^[63]

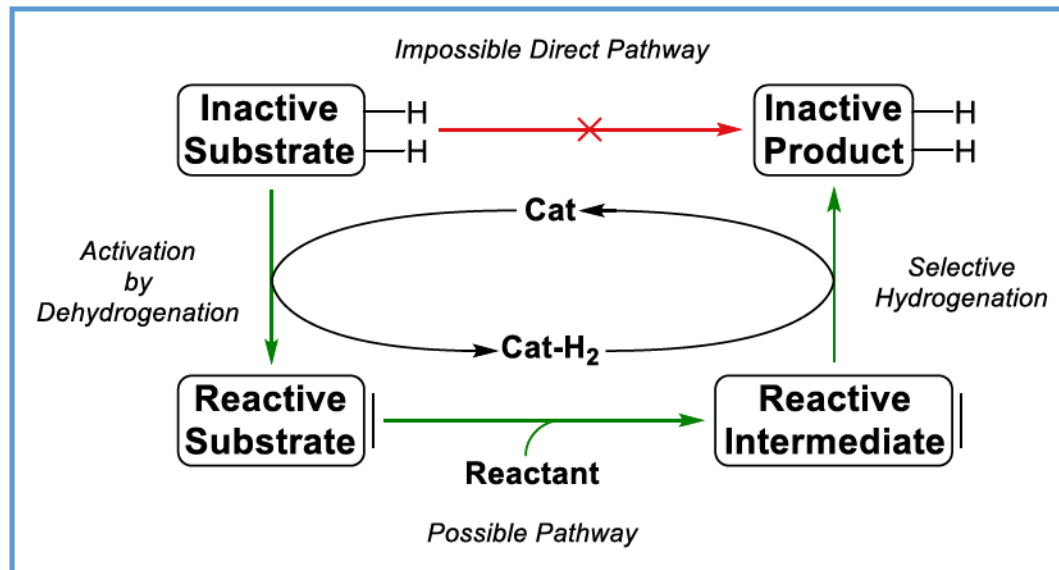
Complementary to traditional cross coupling reactions, hydrogen autotransfer reactions support the formation of sp^3 -carbon-nucleophile bonds.^[64,65] In recent years, the field of *hydrogen autotransfer* reactions, also known as *borrowing hydrogen*, and the related topic of *transfer hydrogenation* conversions have been gaining increased interest.^[66-68] Herein, an unreactive substrate is activated by dehydrogenation. Subsequently, the resulting intermediate performs a specific reaction. Finally, the initially abstracted hydrogen is added to the structural motif formed in the reaction of the intermediate. Advantageously, these reactions usually form only small amounts of non-toxic by-products which benefits the atom efficiency and reduces costs for waste-management. Moreover, inexpensive but unreactive compounds such as alcohols can be activated without additional stoichiometric and waste-intensive methodologies.^[69-71]

Aside from manipulations in the carbon structure, the insertion of functional groups constitutes a crucial aspect of syntheses in the pharmaceutical and fine chemical industry.^[2,3] Herein, amino acids and peptides have been of fundamental interest to chemists since the beginning of chemical research.^[72-74] Thus, the investigation of novel methodologies for the synthesis of amino acids and their derivatives depicts an omnipresent necessity.^[75] For this purpose, the amidocarbonylation displays an advantageous process as the reaction proceeds with 100% theoretical atom efficiency.^[76,77] In addition, the carbonylation employs readily accessible starting materials such as amides and aldehydes to give N-acyl amino acids.^[78]

2. Hydrogen Autotransfer

2.1. Theory

By describing the dimerization of linear alcohols to α -substituted alcohols catalyzed by sodium alkoxide at elevated temperatures, the first report of the Guerbet reaction dates back as far as 1899.^[79] However, the initial protocol proceeded *via* a different route than modern hydrogen autotransfer protocols.^[80] Whereas the original methodology involves a reaction step closely related to the Cannizzaro reaction,^[81,82] advanced (de-)hydrogenation catalysts avoid the generation of carboxylic acids as stoichiometric by-products.^[71,83] Instead, hydrogenation of the intermediate affords the final product.^[70,84,85] Prior to the era of modern homogeneous catalysts,^[68,86,87] heterogeneous copper,^[88,89] nickel^[90] and palladium^[80] materials were found to support the reaction at lower temperatures and improved selectivity. Consequently, novel catalysts perform the Guerbet reaction according to the general hydrogen autotransfer mechanism.^[70,71,85] In principle, this mechanism completes identical steps independent from the involved substance classes (Scheme 3).

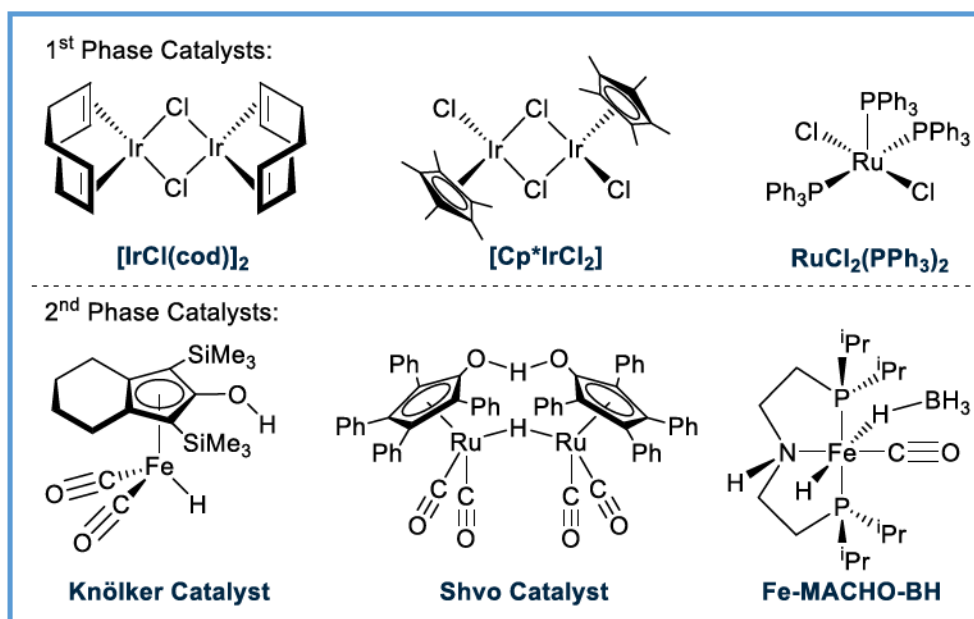


Scheme 3. General mechanistic concept of hydrogen autotransfer reactions.

Herein, an inactive substrate – commonly an alcohol – is activated through dehydrogenation by the hydrogen autotransfer catalyst. Thereby, hydrogen is attached to the catalyst which serves as an oxidizing agent. Subsequently, the reactive substrate forms the corresponding intermediate by interacting with additional reactants. Henceforward, the resulting compound is further reduced to the final product by the hydrogenated catalyst. The “inactive” product can formally be dehydrogenated again which constitutes the reversibility

of the entire process. However, the product is generated since the reduced form is thermodynamically favored under reaction conditions.^[65,84,85,91]

Due to necessary hydrogenation and dehydrogenation activity, the hydrogen autotransfer catalyst is required to support both reaction steps. Traditionally, specifically ruthenium(II)^[64,65] as well as iridium(I)^[92] and iridium (III)^[69,70] salts have proven to facilitate various hydrogen autotransfer reactions (Scheme 4).

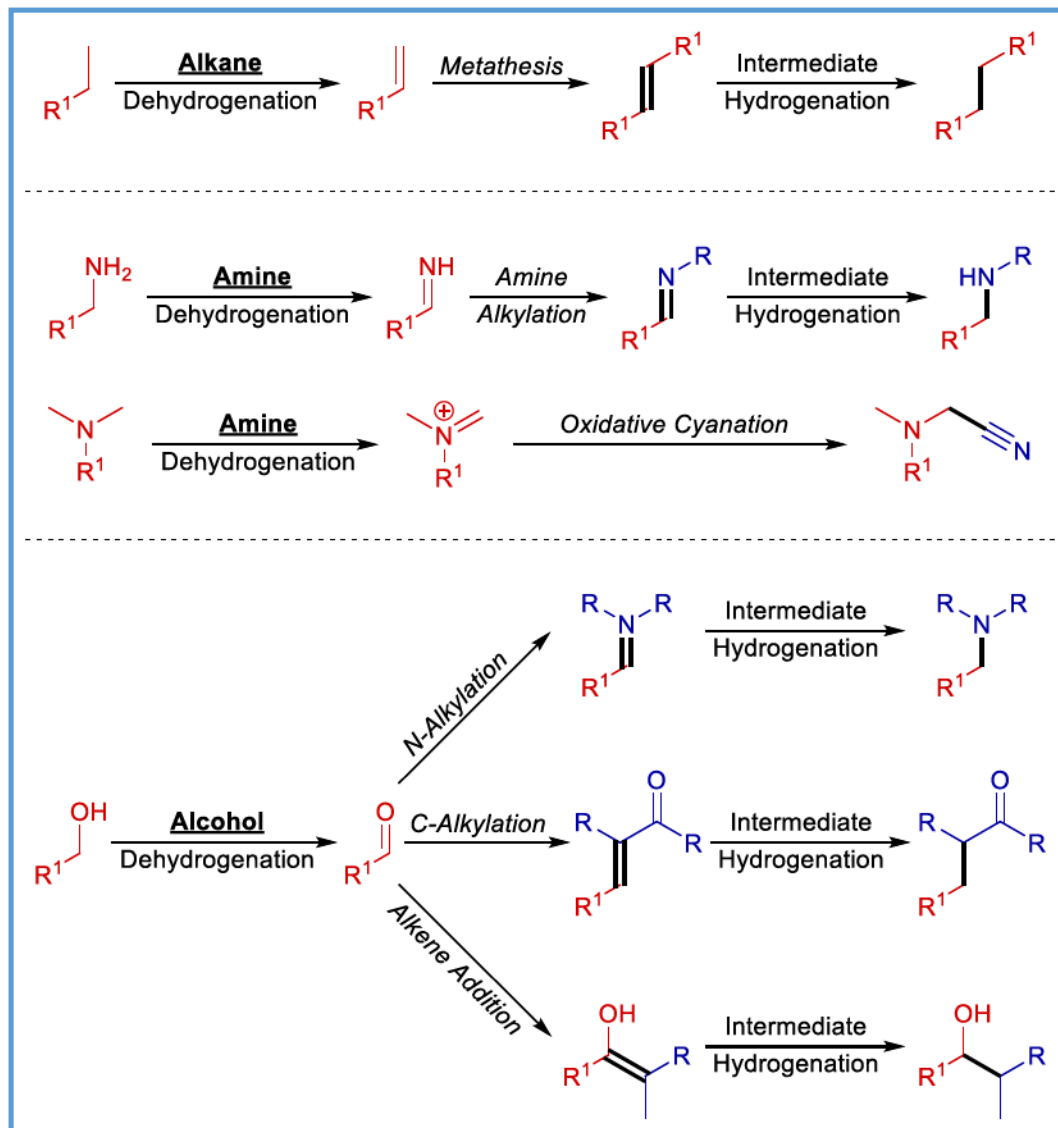


Scheme 4. Selected examples of catalysts for hydrogen autotransfer reactions.

These catalysts oxidize the starting material to the corresponding reactive intermediate (e.g. oxidation of a primary alcohol to the aldehyde) by formally abstracting H_2 as dihydrogen, dihydride or hydride complex.^[93,94] Therefore, stabilizing ligands such as phosphines or carbenes are commonly added to the noble metal salts. In contrast to these first phase catalysts, the development of *non-innocent* ligands such as pincer^[95-98] or Knölker-type^[99,100] ligands introduced an additional possibility for the storage of H_2 in hydrogen autotransfer reactions. These more recent catalysts abstract H_2 by binding one hydrogen atom as hydride to the transition metal while adding the second as a proton to the ligand. Whereas the Knölker and Shvo complexes transfer the proton from the hydroxy function present in the ligand,^[100] pincer complexes often contain a secondary amine capable of releasing a proton and simultaneously establishing formal nitrogen-metal double bonds.^[66,101] In the case of pyridine and acridine pincer ligands, the hydrogen is provided by a C-H proton.^[102,103] Due to their direct influence on the catalytic process, these ligands are referred to as *non-innocent*.^[104] Based on the increase in activity caused by this type of ligands, less active non-noble metals such as manganese,^[105] iron^[106,107] and cobalt^[108] demonstrated drastically

improved performances in hydrogen autotransfer reactions. Furthermore, such complexes provide excellent activity in transfer hydrogenations.^[67,109]

While alcohols remain the primary target for activation in hydrogen autotransfer research, alkanes and amines represent suitable substrates as well (Scheme 5).



Scheme 5. Selected examples for substrates and reactions in hydrogen autotransfer chemistry.

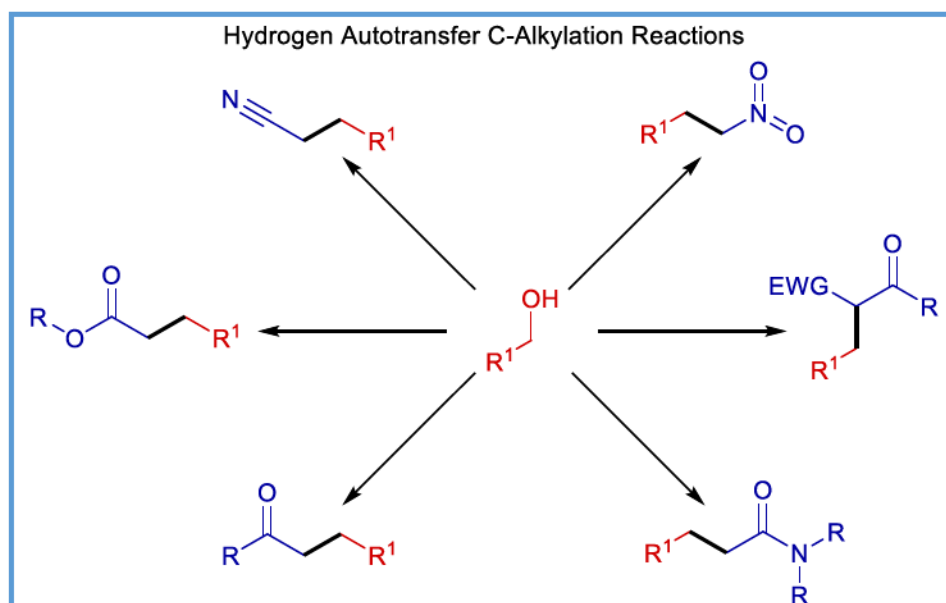
In principle, alkanes act as suitable substrates for the dehydrogenation through transition metal complexes.^[110-112] Combined with powerful metathesis catalysts, the resulting alkenes are converted into higher alkanes.^[113-115] However, the insufficient selectivity limits extended applications in the field of fine chemical synthesis.

Likewise, amines can be activated by the abstraction of hydrogen and the formation of the corresponding imines.^[116] Hereupon, the conversion with inert amines such as aniline provides access to secondary amines.^[117,118] In addition, the application of tertiary amines with hydrogen cyanide under oxidizing conditions offers amines containing nitriles as

functional group in the α -position.^[119] Nevertheless, the nucleophilic character of the amine limits the application since the substrate competes with potential nucleophiles.

Noteworthy, the most extensive application range is found for alcohols as reducible starting materials. More precisely, the alkylation of carbon- and nitrogen-nucleophiles with alcohols has been extensively studied by several groups.^[65,69-71,92,120] For this purpose, the alcohol is initially reduced to the corresponding aldehyde or ketone prior to a sequential condensation reaction. In the second step, imines are generated *in situ* in the case of nitrogen-nucleophiles while carbon-nucleophiles lead to alkenes. In general, the resulting C-X double bond is hydrogenated to give the final product. Thus, this methodology employs otherwise unreactive alcohols as efficient alkylation agent. Furthermore, water results as the exclusive by-product while more traditional alkylation agents produce stoichiometric amounts of metal salts.^[121,122] In addition to C- and N-alkylation, the hydrogen autotransfer methodology enables the alkylation of dienes^[123-127] and phosphonium ylides.^[128,129] Moreover, the *in situ* generated aldehydes can perform the Tishchenko condensation.^[121,122,130-133] Finally, the multitude of suitable nucleophiles and substrates enables the synthesis of numerous heterocycles.^[120,134-140]

Among the most powerful tools, the modification of the basic carbon network by alkylation of C-H acidic compounds represents a widely investigated strategy.^[69,70,92] Due to the number of applicable substrates containing acidic α -protons, this methodology allows for the condensation towards various substance classes. Thus, a variety of compounds containing numerous structural motives becomes accessible *via* hydrogen autotransfer (Scheme 6).



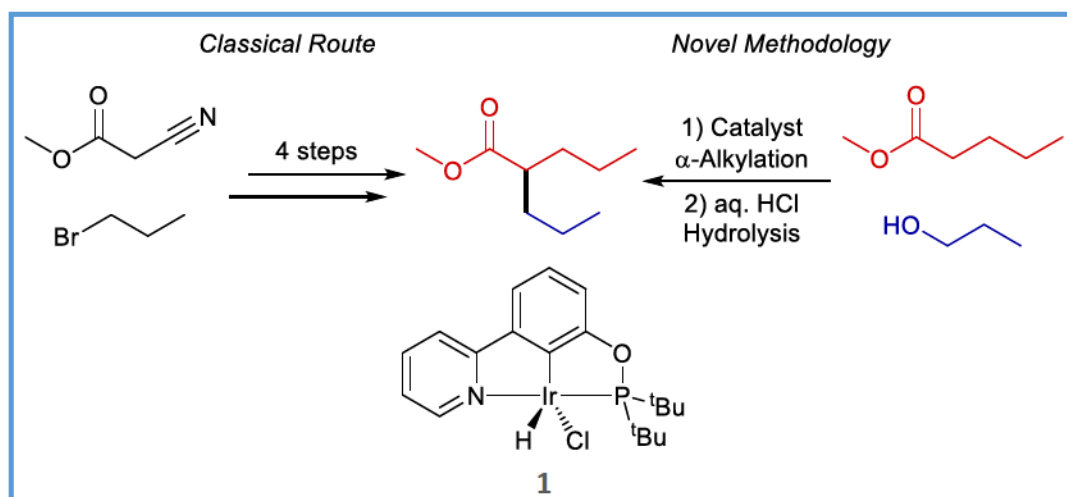
Scheme 6. Selected examples for C-alkylation of C-H acidic compounds with alcohols.

Herein, ketones have been intensively investigated for their reactivity in hydrogen autotransfer protocols. Among others, simple ruthenium^[141,142] and iridium catalysts^[143,144] such as $\text{RuCl}_2(\text{dmsO})_4$ and $[\text{IrCl}(\text{cod})]_2$ facilitate the formation of substituted ketones. In contrast to these and other early protocols,^[70,145] modern hydrogen autotransfer catalysts require only catalytic amounts of base. Furthermore, the utilization of advanced *non-innocent* ligands in catalysts such as pincer- and Knölker-type complexes allows the activation of otherwise unreactive metals such as cobalt, iron, manganese or rhenium.^[146-149] While the activation of higher alcohols is achieved with various catalysts, the dehydrogenation of methanol to formaldehyde requires powerful hydrogen autotransfer catalysts. Nevertheless, the alkylation of ketones employing methanol was achieved by different groups with rhodium, iridium and ruthenium complexes.^[150-152] In addition to substituted ketones, the hydrogen autotransfer methodology enables access to α -substituted alcohols when over-stoichiometric amounts of specific hydrogen donors are applied.^[65,71,141] Moreover, it was shown that the application of chiral catalysts gives enantiomerically pure alcohols.^[153]

Aside from ketones, various C-H acidic compounds such as nitroalkanes,^[92] malonic acid derivatives,^[92,154,155] esters,^[64,156] amides^[157,158] and nitriles^[159-165] have been converted successfully to the corresponding alkylated substances through hydrogen autotransfer protocols. While strongly C-H acidic substances such as nitroalkanes, malonic acid derivatives and ketones can be sufficiently activated by catalytic amounts of base, less C-H acidic compounds such as esters, amides and nitriles typically require over-stoichiometric amounts of strong bases to deprotonate the α -carbon atom. Moreover, the conversion of these challenging substrates generally demands powerful and highly active iridium and ruthenium hydrogen autotransfer catalysts.

2.2. Objectives

The main objective of the investigations in hydrogen autotransfer reactions was the reproduction and improvement of the ester alkylation reported by Huang and co-workers.^[70] The motivation for this study was reasoned by the described two-stepped synthesis of valproic acid by alkylation of methyl valerate with *n*-propanol catalyzed by iridium complex **1** and ensuing hydrolysis (Scheme 7).



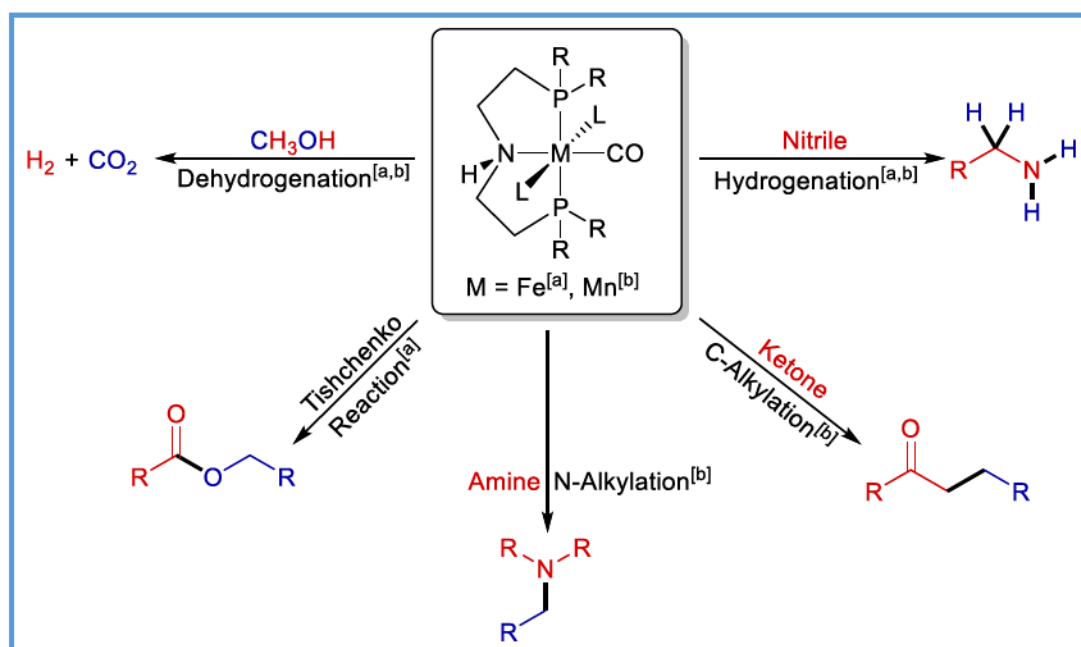
Scheme 7. Alternative synthetic route towards valproic acid.

The product represents one of the WHO's essential medicines^[166] as the pharmaceutical is applied to treat epilepsy, bipolar disorder and to prevent migraine.^[167] As a part of the EUs CHEM21 project,^[168] the Beller group collaborated with researchers at Sanofi due to the shared interest to find a more environmentally-friendly and economically-efficient synthesis of this important pharmaceutical. Currently, the production of valproic acid is accomplished *via* di-alkylation of ethyl cyanoacetate with two equivalents of bromopropane catalyzed by sodium ethoxide and subsequent decarboxylation prior to the hydrolysis of the nitrile as final step (Scheme 7).^[169]

In order to succeed, the published results had to be reproduced and ensuing experiments had to be conducted to identify new catalysts preferably composed of non-noble metals which improve the productivity. Thereby, it was desired to avoid the generation of several equivalents of salt by-products in the classical route and instead establish an alternative synthetic route. In fact, this approach had provided the target molecule while producing water and the residual catalysts as exclusive by-product. Moreover, non-noble metals such as iron are considered nonhazardous compared to noble metals which represents a critical aspect in the synthesis of pharmaceuticals.^[170,171] Another critical aspect remains in the

availability and sustainability of second and third row transition metals. According to Hunt, the known reserves for rhodium, iridium, platinum and ruthenium will be depleted within the next 50 years. Likewise, the existing palladium resources will be consumed within the next 100 years. While the time span allows the society enough time to find alternatives for these rare metals, this survey emphasizes the limited availability of these resources.^[172]

Aside from the main objective, the extension of the understanding of the application range of the MACHO-type ligands and the hydrogen autotransfer methodology in general was desired. In recent years, the Beller group successfully applied non-noble metal pincer complexes for the hydrogenation of nitriles and esters, C-alkylation of ketones, N-alkylation of amines, the Tishchenko reaction and the hydrogen production from methanol (Scheme 8).^[149,173-181]

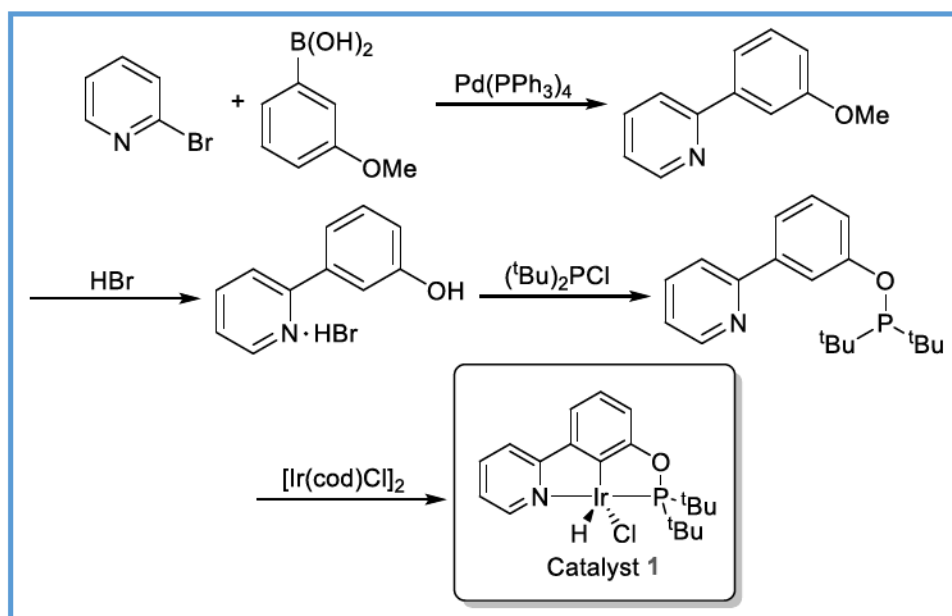


Scheme 8. Selected examples for non-noble metal pincer complex catalyzed reactions from the Beller group.

Hereupon, the development of novel hydrogen autotransfer protocols employing non-noble metals for the catalytic synthesis of fine chemicals represents a fundamental interest. Hence, iron-based catalysts such as the Fe-MACHO-BH complex were extensively tested for their activity in well-known hydrogen autotransfer reactions successfully catalyzed by noble metal catalysts.

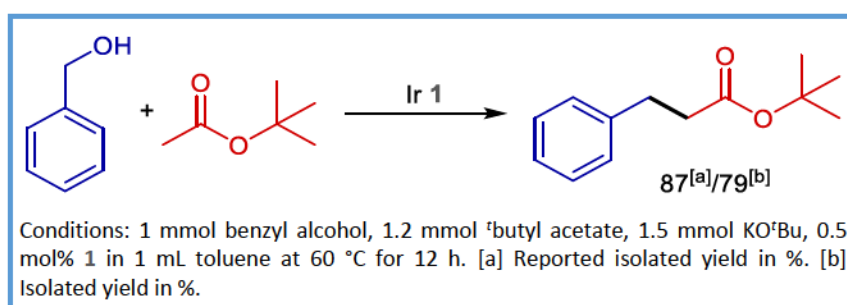
2.3. Results

In order to reproduce the reported results, the iridium complex **1** was synthesized according to the published procedure illustrated in Scheme 9.^[70]



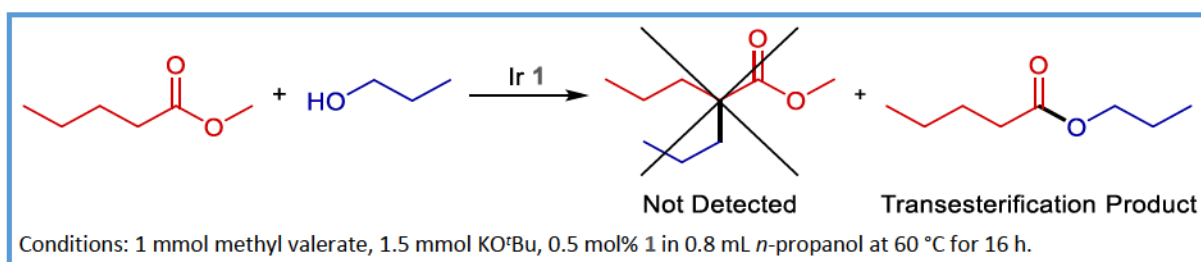
Scheme 9. Synthesis of iridium complex **1**.

The complex was obtained as described in the literature. Consequently, the generated substance was tested for its activity in the described optimization reaction of benzyl alcohol with *t*butyl acetate according to Scheme 10.



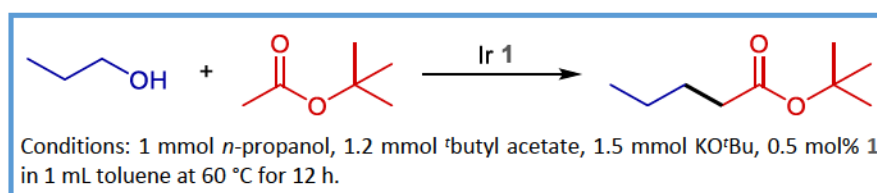
Scheme 10. Optimization reaction for the α -alkylation of esters.

Accordingly, *t*butyl 3-phenylpropanoate was successfully synthesized in 79% isolated yield compared to a reported isolated yield of 87%. Despite the slight deviation, the activity of the described complex in the α -alkylation of esters was proven. Consequently, the generated catalyst was applied in the desired alkylation of methyl valerate with *n*-propanol according to the described conditions. However, the conversion failed to give the target molecule or an intermediate despite multiple attempts to repeat the published results. Instead, the transesterification product *n*-propyl valerate was repeatedly identified by GC-MS analysis as the exclusive reaction product (Scheme 11).



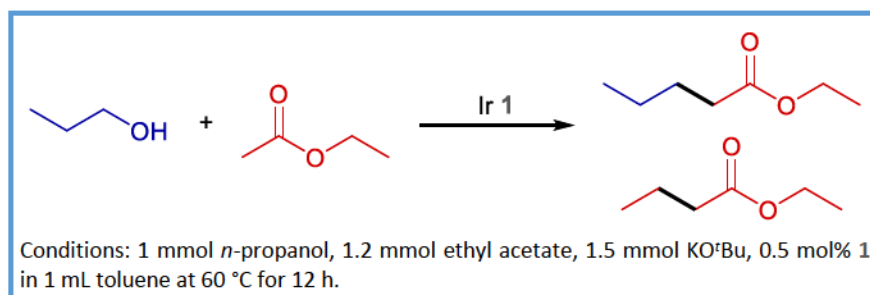
Scheme 11. Results for the attempted methyl valerate propylation.

Based on these results, extended manipulations were conducted to determine the crucial aspect of the methyl valerate alkylation causing the deviation from the reported results and the disagreement between the successful reproduction of the optimization study and the failed reproduction of the methyl valproate synthesis. Therefore, a series of experiments was executed in which the starting materials were subsequently altered to identify critical changes. Herein, the conditions from the optimization study constituted the foundation since this conversion proceeded effectively. Initially, the reactivity of *n*-propanol towards dehydrogenation was investigated by reacting the alcohol with ^tbutyl acetate under the optimized conditions (Scheme 12).



Scheme 12. Successful α -alkylation of ^tbutyl acetate with *n*-propanol.

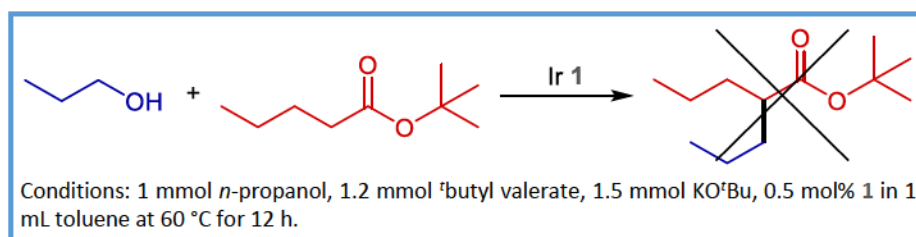
The corresponding product ^tbutyl valerate was successfully detected by GC-MS in repeated experiments. Consequently, *n*-propanol generally constitutes a suitable starting material for the α -alkylation of esters with iridium catalyst **1** under the implemented conditions. Next, the influence of the alcohol moiety within the ester was studied by exchanging ^tbutyl acetate for ethyl acetate in the conversion with *n*-propanol (Scheme 13).



Scheme 13. Successful α -alkylation of ethyl acetate with *n*-propanol.

The expected ethyl valerate was detected by GC-MS as well as the product of the α -alkylation of ethyl acetate with ethanol. Hence, the transesterification of ethyl acetate with *n*-propanol provided *n*-propyl acetate and ethanol which subsequently participated in the

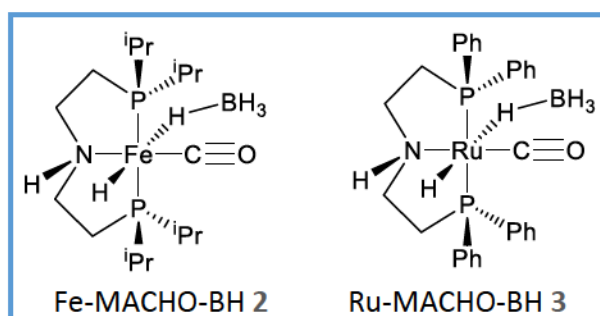
reaction as a suitable alkylation agent. Therefore, the corresponding esters *n*-propyl valerate and butyrate were identified by GC-MS as well. Thus, the ester-alkylation proceeds according to the hydrogen autotransfer protocol independently from the alcohol incorporated in the ester. Eventually, the standard conditions were applied to the transformation of *t*-butyl valerate with *n*-propanol in order to assess the influence of a pre-existing alkylation in the α -position of the ester (Scheme 14).



Scheme 14. Unsuccessful α -alkylation of *t*-butyl valerate with *n*-propanol.

Interestingly, the corresponding *t*-butyl valproate was not found by GC-MS. Consequently, the desired conversion was not observed. Instead, significant quantities of the starting material were identified as well as the transesterification product *n*-propyl valerate. Thereby, the pre-existing alkylation in the α -position of the ester was determined to be the critical aspect which presumably prevents the conversion of methyl valerate towards methyl valproate. The results were confirmed in several iterations. Further manipulations with esters incorporating pre-existing α -alkylations such as *t*-butyl 3-phenyl-propanoate supported this finding as the corresponding product was not detected.

Nevertheless, the development of alternative catalytic systems for the ester alkylation by hydrogen autotransfer protocols was approached. Herein, the Fe- and Ru-MACHO-BH complexes 2 and 3 were evaluated as catalysts (Scheme 15).



Scheme 15. Structure of Fe- and Ru-MACHO-BH complexes.

These catalysts were chosen based on the superior reactivity displayed in different applications involving the dehydrogenation of primary alcohols or the hydrogenation of C-X double bonds as key step.^[136,173,174,178,179,182-184]

After initial tests suggested a superior activity for the Fe-MACHO-BH complex **2**, the ongoing investigation was continued utilizing this catalyst (Table 1, entry 1).

Table 1. Optimization of the iron catalyzed α -alkylation of esters.

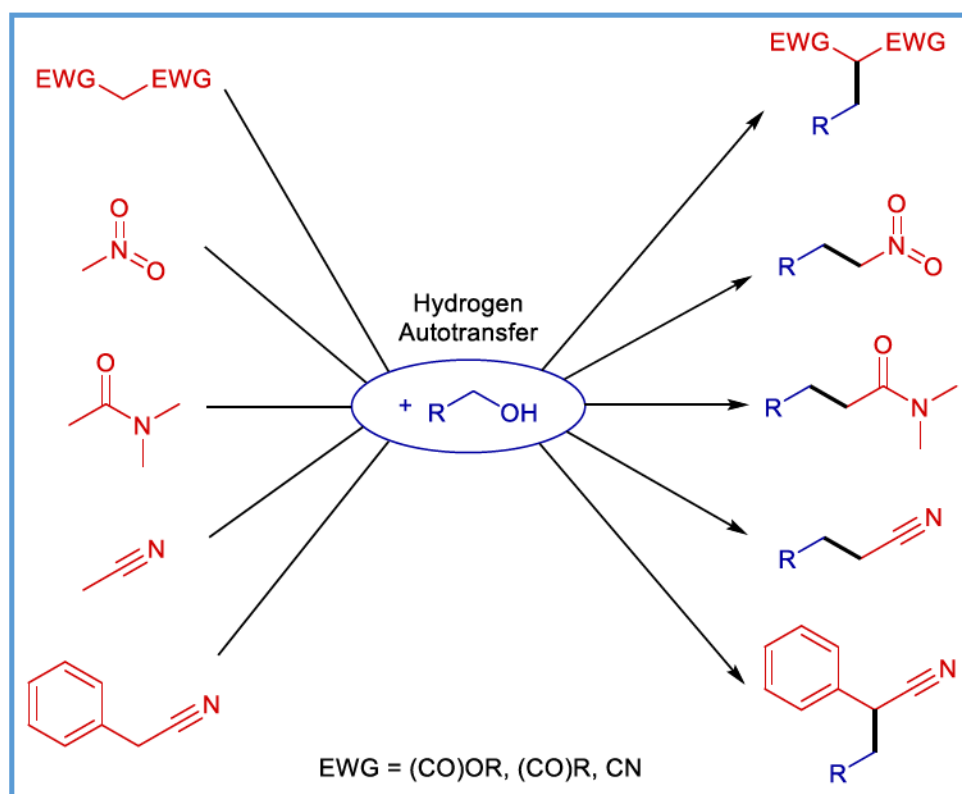
Entry	Alcohol [mmol]	Ester [mmol]	KO ^t Bu [mmol]	T [°C]	t [h]	Yield ^[a] [%]
1 ^[b]	1	1.2	1.5	60	16	5
2	1	1.2	1.5	60	16	8
3	1	1.2	0.75	60	16	5
4	1	1.2	1.5	60	5	15
5	5	1	1.5	60	5	<1
6	1	5	1.5	60	5	10
7	1	1.2	1.5	40	16	20
8	1	1.2	1.5	25	16	22
9	1	1.2	1.5	0	16	12
10 ^[c]	1	1.2	1.5	25	16	25 ^[d]

Standard conditions (entry 2): 1 mmol benzyl alcohol, 1.2 mmol ester, 1.5 mmol KO^tBu, 0.5 mol % Fe-MACHO-BH **2**, in 1 mL toluene at 60 °C for 16 h. [a] Yield determined by GC with hexadecane as internal standard. [b] 0.5 mol% Ru-MACHO-BH **3** [c] 1 mol% Fe-MACHO-BH **2** [d] NMR yield 24%, isolated yield 20 %.

Herein, the reduction of the base quantity led to an insignificantly lower yield of 5% (entry 3). Surprisingly, the outcome improved to 15% when the reaction time was reduced to 5 hours at 60 °C (entry 4). While further decreasing the duration led to similar results without significant improvement, the extension of the reaction time presumable caused decomposition of the final product by the strong basic conditions. As the next step, the influence of the alcohol and ester equivalents was tested by conducting the conversion with an excess of each starting material in two separated experiments. Under the effect of 5 equivalents of alcohol, the product was not detected (entry 5). In contrast, employing 5 equivalents of ester gave 10 % of the desired product (entry 6). Therefore, these experiments suggest that the ester does not limit the product formation while an excess of alcohol suppresses the generation of the alkylated ester. Noteworthy, the yield was further increased to 20% when the reaction temperature was reduced to 40 °C (entry 7). In fact, the product formation improved slightly to 22% when the reaction was conducted at room temperature (entry 8). However, this tendency was not extended at 0 °C as only 12% of the target molecule was synthesized (entry 9). In addition, the application of 1 mol% Fe-MACHO-BH **2** only slightly enhanced the reaction outcome to 25%. Upon isolation, 20% overall yield of the desired product was obtained and characterized.

Unfortunately, this result was not further improved despite various attempts to increase the outcome of the reaction. Herein, the application of different bases (including NaO^tBu , LiHMDS , NaBH_4 and NaH), solvents (benzene, heptane, diethyl ether, anisole and $^t\text{butanol}$), catalysts (Shvo catalyst, Knölker catalyst, Mn-MACHO-BH) and additives (AlCl_3 , $\text{BF}_3 \cdot \text{OEt}_2$) failed to raise the yield to a more satisfying level. Due to these results, the methodology has not been extended to other starting materials to date.

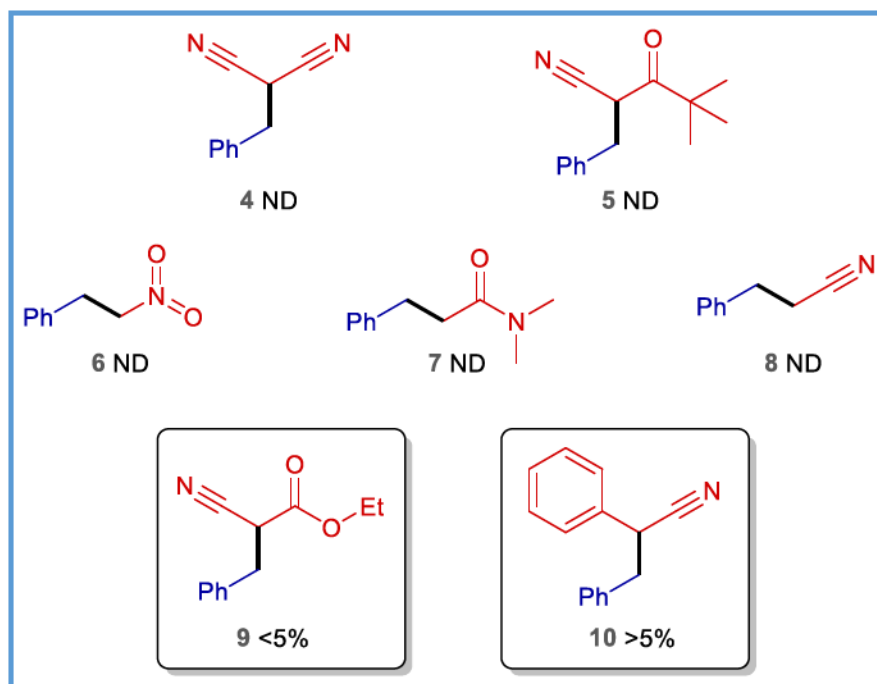
Entries 3 and 4 (Table 1) indicate that the reaction medium promotes the decomposition of the target molecule under specific conditions since the product yield declined over prolonged reaction times. In addition, the tendency of the observed higher yields at lower temperature further indicates a decomposition of the product at higher temperatures and increased reaction time (entries 4, 7 and 8).



Scheme 16. Suitable C-H acidic substrates for hydrogen autotransfer reactions.

Aside from the investigations on the α -alkylation of esters, the alkylation of various C-H acidic compounds utilizing the hydrogen autotransfer methodology and the homogeneous, iron-based catalysts was tested. Herein, malonic acid derivatives such as ethyl cyanoacetate, pivaloylacetonitrile and malononitrile as well as nitromethane, acetonitrile, acetamide and benzylnitrile (Scheme 16) were identified as suitable substrates due to their increased C-H acidity and reported tendency to readily condensate with aldehydes to the corresponding C-C double bond incorporating compound.

Generally, literature studies have proven that the conversion of the displayed substances with primary alcohols under hydrogen autotransfer conditions yields the corresponding C-alkylated α -acidic compounds.^[92,154,155,157-165] However, the corresponding products were mainly absent in the resulting reaction mixtures when the transformations were conducted with the iron-based catalysts (Scheme 17).



Scheme 17. Results for the iron-catalyzed hydrogen autotransfer reaction.

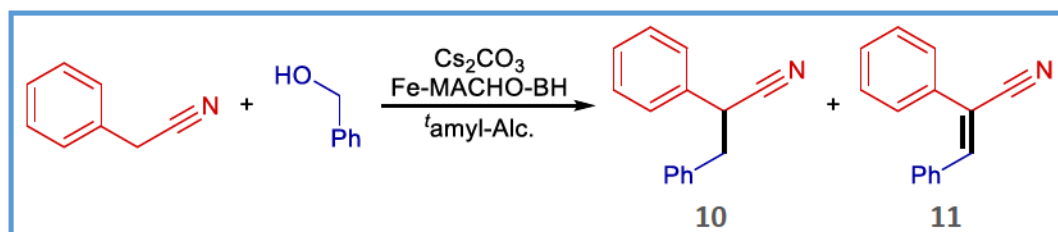
Herein, the C-benzylated malonic acid derivatives 4 and 5 as well as the compounds 6, 7 and 8 were not detected by GC-MS although various conditions including various catalysts, bases and solvents as well as altered concentrations were tested.

In order to better understand the failure of the desired conversions, mechanistic experiments were conducted. For all desired transformations, the presence of the required benzaldehyde in the corresponding reaction mixtures was confirmed by GC-MS. Thus, the formation of the condensation partner was achieved by the employed hydrogen autotransfer catalyst since no quantities of benzaldehyde were detected when the applied benzylic alcohol or an unreacted experiment solution were analyzed by GC-MS. Thus, the alcohol dehydrogenation required for the hydrogen autotransfer methodology successfully proceeded. Moreover, the reaction of benzaldehyde instead of benzylic alcohol with the corresponding C-H acidic substances yielded the desired condensation products in significant quantities under hydrogen autotransfer conditions. Therefore, since the condensation product was not observed in the regular experiments utilizing benzylic alcohol, the

experiment results indicate that either the concentration of the generated benzaldehyde was too low to support the condensation with the present reactant or the catalyst impeded the condensation reaction.

Nevertheless, the conversion of ethyl cyanoacetate afforded the corresponding α -alkylated derivative **9** (Scheme 17) in amounts sufficient for the identification of the molecule by GC-MS. Although the generation of the desired substance was confirmed, the overall yield remained unsatisfying as only minimal quantities were generated. Despite significant efforts, the reaction outcome was not improved and only traces of the product were detected by GC-MS.

In contrast, the transformation of benzyl cyanide with benzylic alcohol proceeded smoothly. However, aside from the desired hydrogenated condensation product **10**, the associated intermediate **11** was detected in significant quantities as well (Scheme 18).



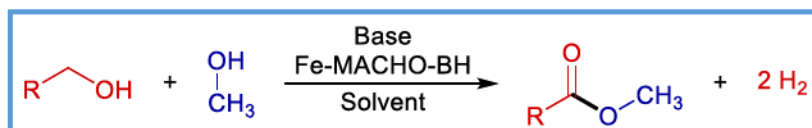
Scheme 18. C-Alkylation of benzyl cyanide.

Unfortunately, the intermediate to product ratio was not further elevated than 1:1 despite extended efforts to improve the overall yield of the desired nitrile **10**. Essentially, various bases (including K_2CO_3 , $KOtBu$, $NaBH_4$, $NaHMDS$ and KOH), solvents (including toluene, THF, dioxane and anisole), catalysts (Fe-MACHO-BH, Knölker-catalyst, ferrocenecarboxaldehyde) as well as temperatures and reaction periods were evaluated. Nevertheless, the corresponding intermediate was not completely converted to the desired product while the conversion of benzyl cyanide approximated full consumption.

Eventually, the experiment results indicate that while the dehydrogenation of the benzylic alcohol proceeds efficiently enough to allow the condensation of the resulting benzaldehyde with benzyl cyanide to the double bond incorporating product, the reaction rate of the ensuing hydrogenation of the afforded intermediate was not increased enough to achieve the complete conversion to the desired product. Herein, the cause remains unidentified as a decomposition of the catalyst as well as insufficient hydrogenation activity of the catalyst result in an unsatisfying hydrogenation outcome. However, the detection of significant intermediate amounts supports the generally accepted reaction pathway since the double

bond is generated from the condensation of aldehyde and C-H acidic compound and simultaneous elimination of water. In contrast, a direct substitution of the alcohol moiety by the α -carbon nucleophile has never been reported and does not afford the double bond intermediate **11**.

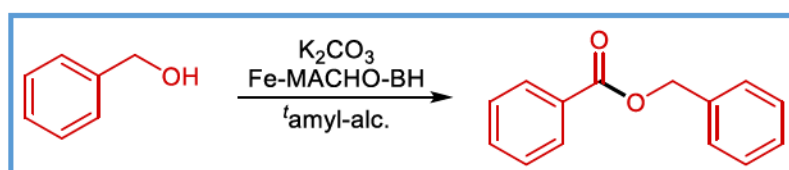
Continuing the studies on the dehydrogenative abilities of iron-based catalysts, the dehydrogenative couplingreaction of primary alcohols with methanol to generate the associated methyl esters was investigated (Scheme 19).



Scheme 19. Dehydrogenative coupling of primary alcohols to methyl esters.

Although this reaction has mainly been reported to be catalyzed by heterogeneous materials under aerobic and therefore oxidative conditions,^[185-189] recent results for the homogeneous synthesis of lactones from dioles by the Fe-MACHO-BH complex indicate the ability of the iron-based catalyst to facilitate this oxidative conversion.^[178] Moreover, this transformation was successfully achieved by ruthenium-based complexes and the application of sacrificial hydrogen acceptors.^[132,133]

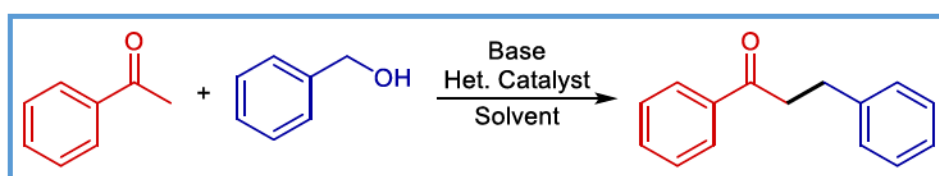
In the initial experiments, the desired methyl benzoate was generated in trace amounts and identified by GC-MS. In addition, the analysis revealed the presence of benzaldehyde. Herein, Fe-MACHO-BH was applied as catalyst whereas K_2CO_3 in *t*-amyl alcohol was employed as base-solvent system at 130 °C for 16 h. Unfortunately, further optimization of the transformation did not provide more satisfying results despite extended approaches to optimize the reaction conditions. Herein, the catalyst, base and solvent as well as their concentrations were altered to identify positive effects and tendencies. Moreover, additives (including H_2O , O_2 , crotononitrile, tolan) as well as conducting the reaction under atmospheric pressure and argon flow in order to remove evolved hydrogen gas did not improve the reaction outcome. In contrast, the application of toluene as solvent without additional base led to the formation of significant amounts of benzyl benzoate instead of the desired methyl ester (Scheme 20).



Scheme 20. Dehydrogenative coupling towards symmetric esters.

Consequently, the experiments suggest that while trace quantities of methyl benzoate were formed in initial experiments, the presence of methanol impedes the catalyst since the symmetric ester was generated in relevant amounts in the absence of the alcohol.

Aside from the studies utilizing the homogeneous iron complex **2**, the performance of various heterogeneous catalysts originating from the pyrolysis of distinct transition metal complexes in standard hydrogen autotransfer reactions such as ketone and amine alkylation was investigated. For this purpose, five different pyrolyzed heterogeneous catalysts were chosen and initially applied in the alkylation of benzophenone with benzylic alcohol (Scheme 21).



Scheme 21. Alkylation of ketones with alcohols catalyzed by pyrolyzed heterogeneous catalysts.

As catalysts, iron and ruthenium on charcoal as well as iron, cobalt and nickel on Al_2O_3 and cobalt on Co_3O_4 were tested. Herein, the catalysts were prepared by pyrolysis of molecularly-defined complexes which were previously adsorbed to the surface of the support. As a result, the transition metals form nitrogen-doped clusters serving as catalytically active centers. The catalyst screening results are displayed in Table 2.

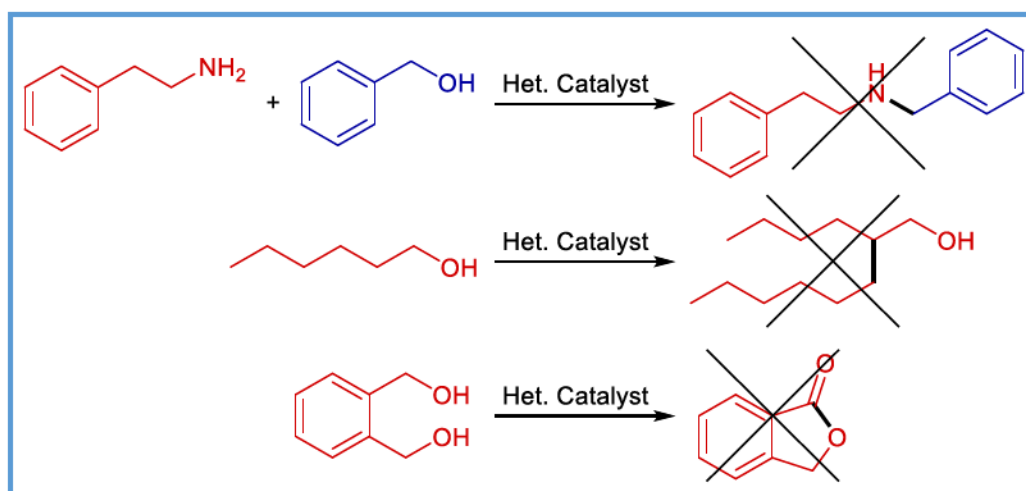
Controversially, the initially obtained promising yields in the first iteration especially for the carbon supported catalysts (Table 2, entries 2 and 3) were not confirmed. Despite significant efforts, the continuative experiments offered no significant reaction outcomes. In order to reproduce the initial results, various solvent- and Cs_2CO_3 -batches were tested but the moderate yet encouraging yields have not been reproduced despite various iterations and modifications. While the desired product was still present in the reaction mixture, the experiments constantly yielded less than 5% of the targeted substance. Since the cause for the severe loss of productivity was not identified, the further investigation of this specific reaction was concluded.

Table 2. Catalyst screening for the C-alkylation of ketones by pyrolyzed heterogeneous catalysts.

Entry	Catalyst	Yield Run 1 ^[a] [%]	Yield Run 2 ^[a] [%]
1	Co@Co ₃ O ₄	27	<5
2	Fe@C	39	<5
3	Ru@C	45	<5
4	Fe@Al ₂ O ₃	22	<5
5	Co@Al ₂ O ₃	35	<5
6	Ni@Al ₂ O ₃	15	<5
7	-	ND ^[b]	ND ^[b]

Standard conditions: 1 mmol acetophenone, 1.2 mmol benzylic alcohol, 10 mol% Cs₂CO₃, 3 mol% catalyst (referring to the amount of metal in relation to acetophenone) in 1 mL toluene at 150 °C for 16 h. [a] Yield determined by GC with hexadecane as internal standard. [b] Not Detected.

In addition to the C-alkylation with alcohols, the activity of the employed heterogeneous catalysts was briefly evaluated in several reactions requiring the dehydrogenation of primary alcohols. These conversions included the N-alkylation of amines, the synthesis of lactones from diols and the Guerbet reaction of *n*-hexanol (Scheme 22).

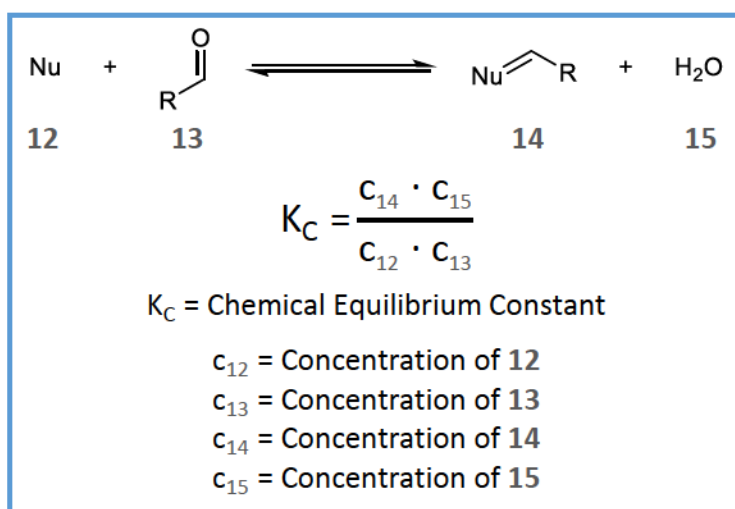


Scheme 22. N-Alkylation of amines by pyrolyzed, heterogeneous catalysts.

Unfortunately, the conducted manipulations did not generate the corresponding products. In accordance with previous results for the homogeneously catalyzed alkylation of C-H-acidic compounds, trace amounts of the required aldehyde were detected by GC-MS.

2.4. Outlook

Regarding the ester alkylation with alcohols, the application of novel and advanced iron-based complexes offers the possibility of superior catalysts which are more active in the desired transformation. However, the question remains how significant the influence of the catalyst on the substrate condensation is. While the catalyst is proposed to be active in the hydrogenation and dehydrogenation, the condensation is generally considered to be not directly affected by the catalyst (Scheme 23).



Scheme 23. Law of mass action for the condensation reaction of hydrogen autotransfer conversions.

Nevertheless, the concentrations of the reagents and products reason the chemical equilibrium. Due to the chemical equilibrium constant, an increased aldehyde concentration and a decreased product concentration lead to a more rapid generation of the overall product (Scheme 23). Consequently, the catalyst indirectly affects the condensation reaction since the aldehyde concentration is reasoned by the ability of the catalyst to dehydrogenate the corresponding alcohol. Moreover, the ability to hydrogenate the reactive intermediate to the desired reduced product influences the intermediate concentration. *Via* this pathway, the catalyst indirectly affects the condensation reaction.

To improve the alkylation of acetates with alcohols catalyzed by the Fe-MACHO-BH catalyst, the knowledge about the exact decomposition pathway leads to alternate reaction conditions preventing the degradation of the product. Moreover, the decomposition pathway might additionally effect and degrade the reactant. Thus, identifying and circumventing the degradation mechanism enables a more selective synthesis of the target molecule.

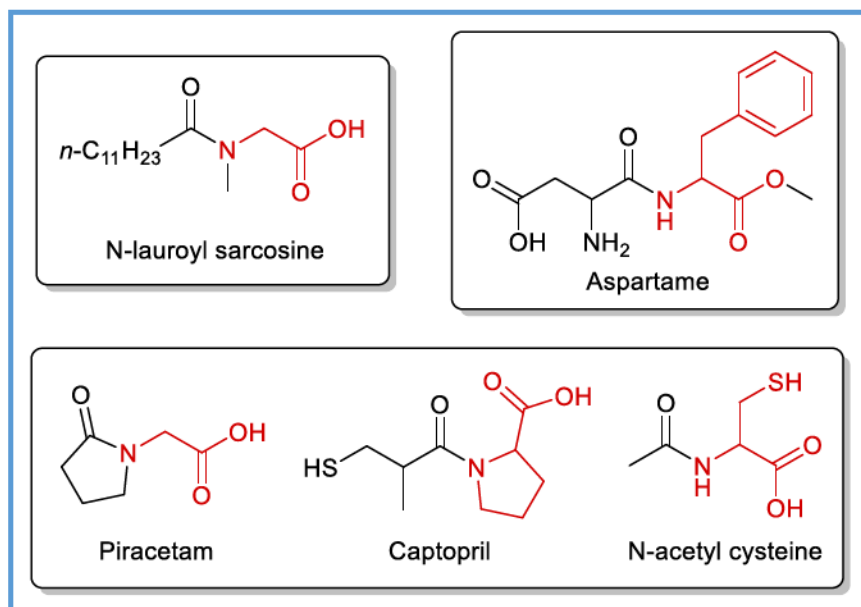
In general, the development of more effective and advanced non-noble metal-based complexes represents the central challenge as more efficient (de-)hydrogenation catalysts increase the concentration of the required aldehydes and improve the conversion of the reactive intermediate. In several targeted conversions, the reactions proceeded to the corresponding intermediate when the associated aldehyde was employed under hydrogen autotransfer conditions. However, the transformations did not give the desired product when the corresponding alcohol was employed despite the formation of detectable aldehyde quantities in the reaction solution. Thus, novel catalysts generating higher concentrations of the necessary aldehyde improve the condensation of the substrates to the desired compounds.

Regarding the heterogeneously catalyzed conversions, the synthesized catalysts displayed activity in the C-alkylation of ketones which emphasizes their general potential as (de-)hydrogenation catalysts. Therefore, a wider screening of novel materials as well as reaction conditions offers the possibility of more satisfying results. In addition, the reproducibility has to be assured and the cause for the deviation between the obtained results for the C-alkylation has to be determined.

3. Amidocarbonylation

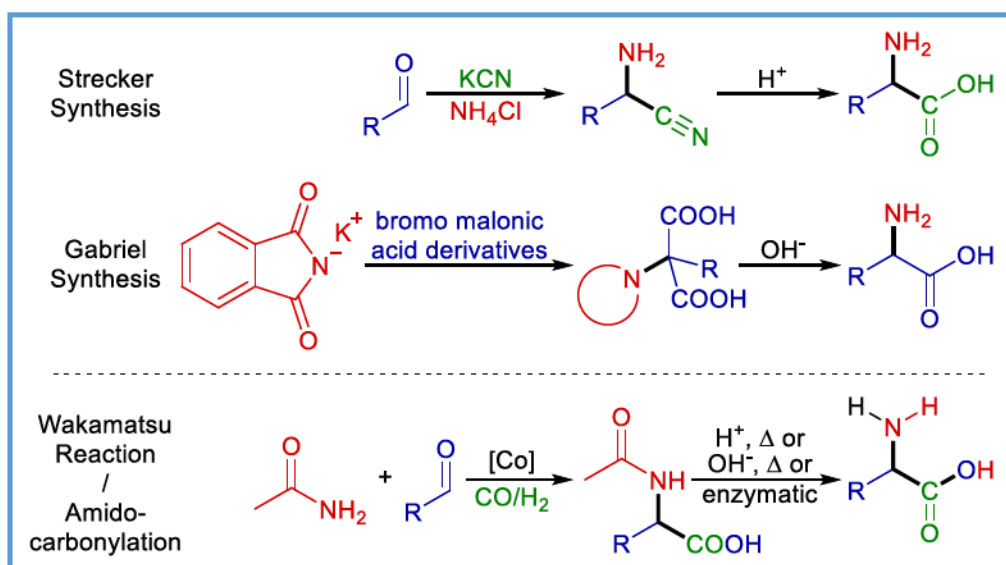
3.1. Theory

Due to the elementary importance for biological life, amino acids are of fundamental interest for chemists and biologists.^[72-75,121] In addition, N-acyl amino acids are applied in various fields and therefore represent a substance class which draws extended industrial interest. For example, the structural motif of N-acyl amino acids is present in numerous substances such as surfactants like N-lauroyl sarcosine, pharmaceuticals Piracetam, Captopril and N-acetyl cysteine as well as food additives such as Aspartame (Scheme 24).^[75] Moreover, N-acetyl amino acids constitute the reactant for the enantiomerically pure production of amino acids through enzymatic resolution.^[78,190]



Scheme 24. Industrially important substances incorporating N-acyl amino acids.

Furthermore, since amino acids depict the fundamental component of proteins as well as peptides and constitute significant building blocks for organic syntheses, chemists have paid plenty of attention to develop novel methodologies for their production.^[122,191]



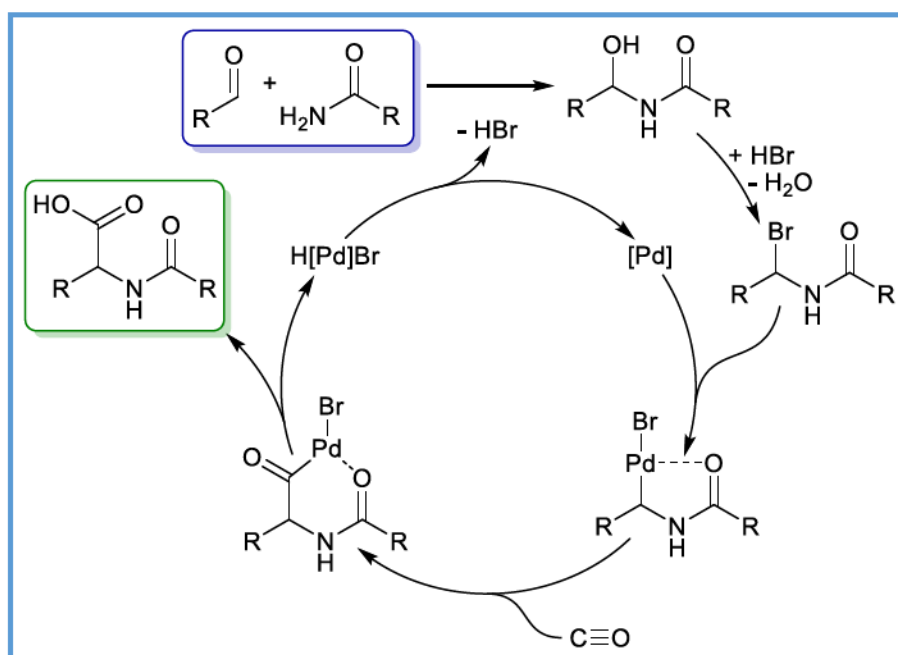
Scheme 25. Selected examples for the synthesis of amino acids.

Aside from numerous industrially applied methods, the Strecker synthesis employing aldehydes, potassium cyanide and ammonium chloride as reactants serves as one of the most well-known and established procedures for the synthesis of racemic amino acids (Scheme 25).^[192,193] Likewise, the Gabriel synthesis for primary amines constitutes a well-investigated synthetic approach which can be modified for the production of amino acids by utilizing bromo malonic acid derivatives.^[121] However, these and other classical methods produce stoichiometric quantities of organic by-products and inorganic salt waste.

In contrast, the amidocarbonylation,^[77] also referred to as Wakamatsu reaction,^[76] describes an alternate approach offering theoretically perfect atom economy. Herein, the single remaining by-product is the applied catalyst. Moreover, this procedure employs readily accessible starting materials such as (*in situ* formed) aldehydes, acetals or epoxides in combination with amides or nitriles.^[78]

While the initial report by Wakamatsu in 1971 described the conversion towards various N-acyl amino acids catalyzed by $\text{Co}_2(\text{CO})_8$,^[76] Beller and co-workers reported the successful amidocarbonylation utilizing $\text{PdBr}_2(\text{PPh}_3)_2$ and lithium bromide. This novel catalytic system expanded the substrate scope of the methodology.^[77,190,194,195] Ever since, protocols utilizing platinum and gold catalysts have emerged.^[196,197] Nevertheless, the focus of research continued with either palladium or cobalt catalyzed amidocarbonylation as these approaches offer superior selectivity and effectivity.^[198-201]

The mechanism of the conversion was the subject of several publications and case studies.^[78,201,202] The generally accepted mechanism is illustrated in Scheme 26.

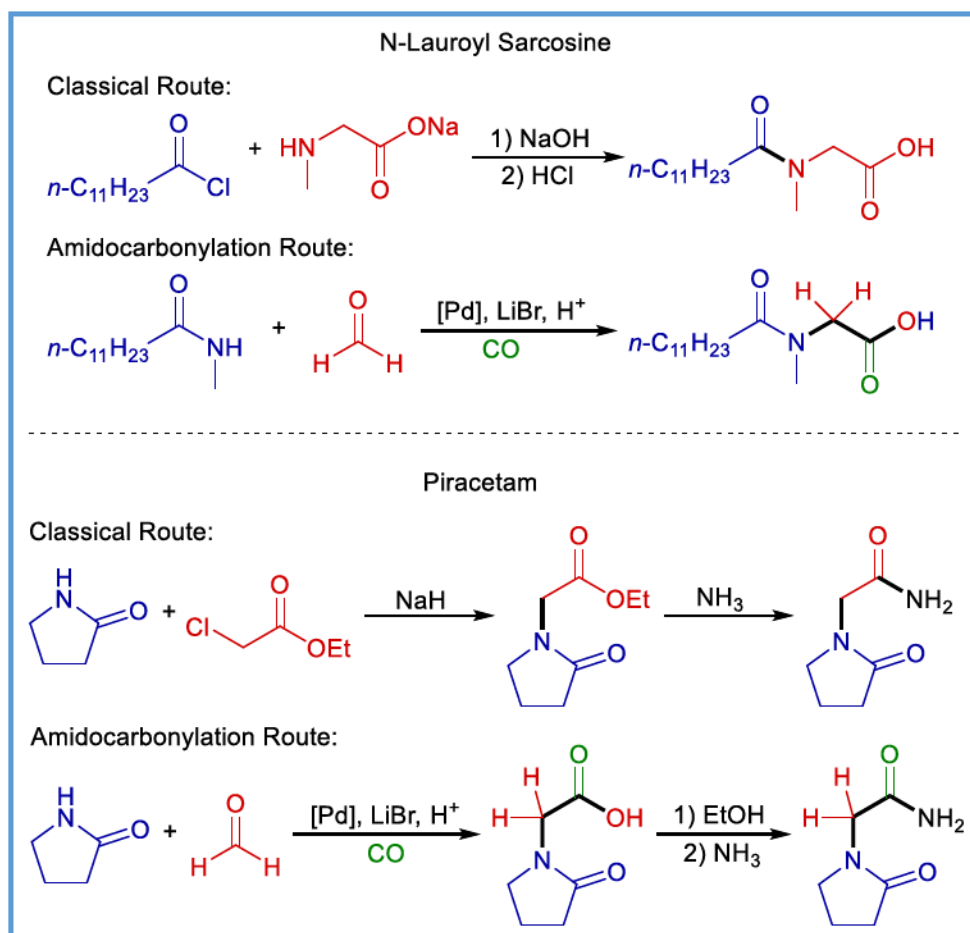


Scheme 26. Generally accepted mechanism for the Pd-catalyzed amidocarbonylation.

Herein, the active palladium catalyst adds oxidatively into the C-Br bond. This bond is generated *in situ* from the condensation product of the aldehyde and the amide. In particular, the bromine replaces the oxygen in the hemiamidal either directly through nucleophilic substitution or by addition of hydrogen bromide to an *in situ* formed C-N double bond resulting from the elimination of water. In an elegant mechanistic study, Freed and Kozlowski showed that imines as well as enamides represent suitable substrates for the amidocarbonylation.^[203] However, it is hereby noted that this does not prove that the conversion generally necessitates the formation of the double bond as this functional group can reverse to the hemiamidal upon the addition of water. Furthermore, the authors suggest the direct addition of an undefined palladium hydride bromide complex to the C-N double bond as an alternative pathway which does not require oxidative addition by the palladium.^[203] Nevertheless, the generated palladium complex is stabilized by coordination of the carbonyl oxygen to the metal center. Following the insertion of carbon monoxide into the Pd-C bond, the novel palladium complex is hydrolyzed. Thereby, the final product is released and further incorporates all atoms being present in the aldehyde and amide in the beginning of the reaction. Moreover, the water molecule stemming from the condensation is added to the final product in the palladium acyl hydrolysis. Furthermore, even the previously added hydrogen bromide is regenerated. Thus, the reaction proceeds with 100% theoretical atom efficiency. Interestingly, the study by Freed and Kozlowski further indicates that the *in situ* generated equivalent of water appears insufficient to facilitate the reaction

completely as only 10% of the desired product was formed under what is referred to as *rigorously anhydrous conditions*.^[203]

Among other economically attractive products, the surfactant N-lauroyl sarcosine and the pharmaceutical Piracetam are accessible *via* amidocarbonylation. Complementary to the classical synthetic routes, both substances can be prepared without the generation of significant amounts of waste (Scheme 27).



Scheme 27. Comparing classical and amidocarbonylation route for the synthesis of Piracetam and N-lauroyl sarcosine.

Both substances are synthesized through nucleophilic substitution reactions with alkyl or acyl halides, respectively. Aside from an energy-intensive synthesis of those reactants, the transformations generate stoichiometric salt by-products. However, long chain sarcosinates are perceived as green detergents due to their good dermatological compatibility and foam-forming qualities.^[75] Thus, this substance class is produced in quantities of approximately 10.000 tonnes per year.^[78]

Although the amidocarbonylation displays a diminished reactivity with N-alkylated amides, Lin and Knifton obtained 95% of N-lauroyl sarcosine when paraformaldehyde was reacted with N-methyl dodecanamide catalyzed by $\text{Co}_2(\text{CO})_8$ under 200 bar of syngas at 120 °C.

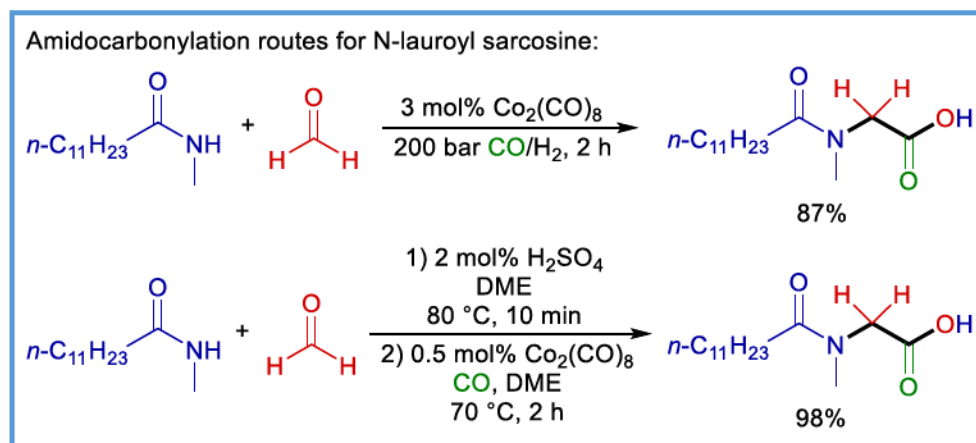
Further investigations led to a two staged pilot plant by Hoechst AG to provide the surfactant on industrial scales.^[78,204,205] According to the literature, the synthesis of Piracetam *via* amidocarbonylation has not been commercialized so far.

Unlike the cobalt catalyzed Wakamatsu reaction, the palladium-mediated amidocarbonylation requires significant amounts of lithium bromide (generally 35 mol%) and additional trace amounts of sulfuric acid (1 mol%).^[201,202] Indeed, these co-catalysts proved to be essential in the first heterogeneously promoted amidocarbonylation utilizing Pd/C.^[195]

3.2. Objectives

In the beginning of the study, two main objectives for the investigation in the amidocarbonylation were established. Since the development of the palladium catalyzed amidocarbonylation, experiments were mainly conducted utilizing either classic triphenylphosphine or no additional ligand. Since the spectrum of efficient phosphine-based ligands has been drastically extended in the last 20 years, the screening of various well-known ligands was executed in order to identify more powerful catalytic system for a TON- and TOF-efficient amidocarbonylation. In recent years, specifically pyridine containing phosphine ligands revealed outstanding qualities in acid-catalyzed carbonylation reactions such as the methoxycarbonylation.^[206-209] Therefore, various ligands developed in recent years were tested in the palladium catalyzed amidocarbonylation.

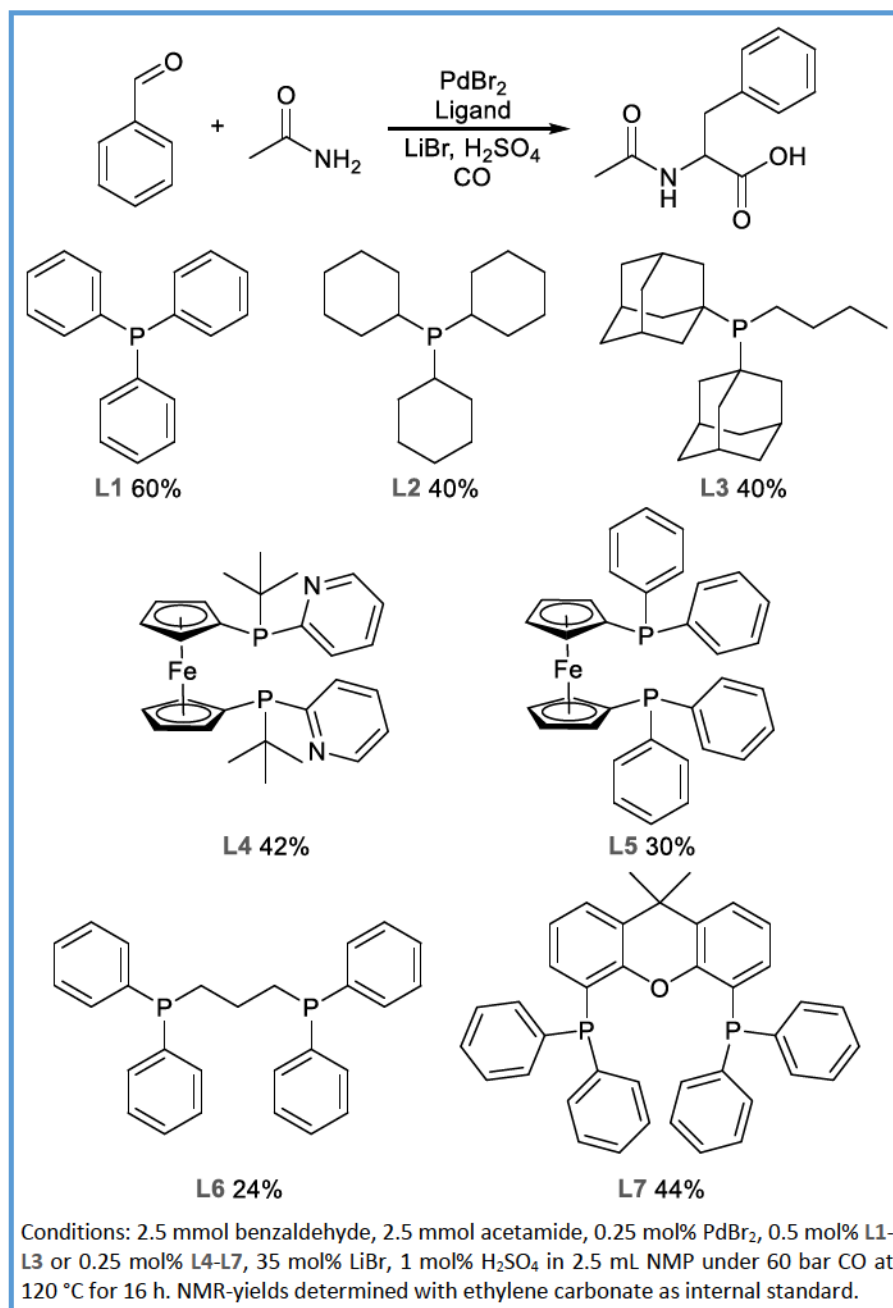
On the other hand, the possibility to develop a process for the synthesis of N-lauroyl sarcosine was examined reasoned by the collaboration of the Beller group with Eastman Chemical and the desire to find an efficient alternative route to produce the surfactant. Herein, especially the demand for high amounts of additives and the question of reusability of the catalyst displayed problematic aspects of the hitherto developed protocols (Scheme 28).



Scheme 28. Protocols for the amidocarbonylation of N-methyl dodecanamide.

3.3. Results

Initially, various ligands were tested as additives for the palladium catalyzed amidocarbonylation in order to determine their effect on the efficiency and reactivity. A selection of the tested ligands is shown in Scheme 29.



Scheme 29. Results for the tested ligands in the palladium-catalyzed amidocarbonylation.

The conversion of benzaldehyde and acetamide to N-acyl α-phenylglycine was chosen as a model system based on the challenging nature of the aromatic aldehyde substrate. Moreover, the catalyst concentration was selected with 0.25 mol% to enable the

differentiation of the performances of the ligands. Otherwise, the results were leveled if the catalyst concentration caused full conversion with all ligands. Unexpectedly, none of the widely-applied ligands **L2-L7** gave higher yields than triphenyl phosphine. Strongly electron-donating ligands such as tricyclohexylphosphine (**L2**) or BuPAD₂ (**L3**) as well as bidentate ligands **L4-L7** gave somewhat decreased yields. Most importantly, pyridine-containing ligand **L4** did not improve the reaction outcome compared to the standard phosphine **L1** despite the excellent performance of this ligand in carbonylations catalyzed under acidic conditions such as alkoxycarbonylations.^[206-209] Moreover, a control experiment revealed that the reaction proceeds comparably when no phosphine ligand is present in the reaction mixture. Under the described conditions (Scheme 29), 56% of the product was obtained without an additional organic phosphine compound.

These results were accounted when the reaction towards N-lauroyl sarcosine was investigated more closely. Initially, the reaction was conducted with PdBr₂ and **L1** under 60 bar CO at 130 °C for 16 h (Table 3, entry 1).

Table 3. Optimization of the PdBr₂-catalyzed conversion towards N-lauroyl sarcosine.

$n\text{-C}_{11}\text{H}_{23}\text{CONHCH}_3 + \text{HCHO} \xrightarrow[\text{NMP, CO}]{\text{PdBr}_2, \text{PPh}_3, \text{LiBr}, \text{H}_2\text{SO}_4} n\text{-C}_{11}\text{H}_{23}\text{CON(CH}_3\text{)CH}_2\text{COOH}$				
Entry	PFA [mmol]	PPh ₃ [mol%]	T [°C]	Yield ^[a] [%]
1	1	1	130	58 ^[b]
2	1	1	140	54 ^[b]
3	1	1	100	68 ^[b]
4	1	-	100	81 ^[b]
5	1	-	80	82 ^[b]
6	2	-	80	82
7	2	-	60	97
8	2	-	40	≈ 40% ^[b,c]

Standard conditions (entry 1): 2.5 mmol N-methyl dodecanamide, 2.5 mmol paraformaldehyde (PFA), 35 mol% LiBr, 1 mol% H₂SO₄, 0.5 mol% PdBr₂, 0.5 mol% PPh₃, in 2.5 mL NMP under 60 bar CO at 130 °C for 16 h. [a] Yield determined by NMR with ethylene carbonate as internal standard. Integration results based on R-CH₂-COOH. [b] Significant amounts of the starting material remained unconverted [c] Overlapping signals from the product, starting material and presumably intermediates.

Herein, the conversion afforded 58% of the desired product. Still, significant amounts of the starting material remained unconverted in the crude reaction mixture. However, raising the temperature to 140 °C did not improve the reaction outcome (entry 2). Surprisingly, the yield was increased by 10% when the temperature was lowered to 100 °C (entry 3). Nevertheless, significant quantities of the starting amide were still present in the solution. Based on the observation that ligands do not necessarily benefit the activity, an experiment

without triphenylphosphine was executed which yielded 81% of the surfactant (entry 4). Similar yields were observed when the reaction was exercised at 80 °C (entry 5). Upon employing two equivalents of PFA, the yield did not improve but the starting material was completely converted (entry 6). Advantageously, the surfactant was obtained almost quantitatively when the reaction temperature was decreased to 60 °C (entry 7). However, an additional decrease of 20 °C led to a diminished reaction outcome of 40% (entry 8). Herein, significant quantities of the substrate were found in the crude product mixture.

Nevertheless, the industrial application requires more efficient systems regarding the reusability and efficiency of the catalyst as well as the quantity of additives necessary for a complete conversion and high yield. Herein, the possibility of employing heterogeneous palladium catalysts for the requested transformation was further examined (Table 4).

Table 4. Screening for efficient heterogeneous palladium catalysts in the amidocarbonylation.

$n\text{-C}_{11}\text{H}_{23}\text{C}(=\text{O})\text{NHCH}_3 + \text{HCHO} \xrightarrow[\text{NMP, CO}]{\text{Pd-Cat.}, \text{LiBr}, \text{H}_2\text{SO}_4} n\text{-C}_{11}\text{H}_{23}\text{C}(=\text{O})\text{N}(\text{CH}_3)\text{CH}_2\text{COOH}$		
Entry	Pd-Catalyst	Yield ^[a] [%]
1 ^[b]	PdBr ₂	77
2	Pd black	52
3	Pd/C (ox.)	42
4	Pd/SiO ₂	48
5	Pd/Al ₂ O ₃	22
6	Pd/N@Gr	48
7	Pd/Faujasite A	30
8	Pd/ZSM-5 A	12
9	Pd/Faujasite B	<5
10	Pd/ZSM-5 B	50

Standard conditions (entry 2): 1 mmol N-methyl dodecanamide (NMDA), 2 mmol paraformaldehyde (PFA), 35 mol% LiBr, 1 mol% H₂SO₄, Pd-catalyst (1 mol% metal) in 1 mL NMP under 60 bar CO at 100 °C for 16 h. [a] Yield determined by NMR with ethylene carbonate as internal standard. Integration results based on R-CH₂-COOH. [b] 0.5 mol% PdBr₂.

For comparison, the amidocarbonylation catalyzed by PdBr₂ was repeated on the applied decreased scale (entry 1). Herein, the experiment afforded 77% of the N-acyl amino acid. Initially, the catalyst testing was performed employing 1 mol% sulfuric acid and 35 mol% lithium bromide under 60 bar CO at 100 °C for 16 hours while converting 1 mmol NMDA with two equivalents of PFA. The catalysts quantity was elected to represent exactly 1 mol% of palladium, independently from the metal loading of the material. These initial parameters were chosen based on the prior results and the report on the Pd/C-catalyzed

amidocarbonylation from 1999.^[195] Simple palladium black led to a modest yield of 52% (entry 2). When the reaction was carried out utilizing 1 mol% of charcoal supported palladium, a slightly decreased yield of 42% was recorded (entry 3). Further studies examined the effect of the acidic or basic nature of the support. Therefore, Pd/SiO₂ gave the surfactant in a similar yield of 48% (entry 4) while aluminum oxide afforded only 22% of N-lauroyl sarcosine (entry 5). Surprisingly, the more basic nitrogen-doped graphene supported palladium catalyst provided 48% of the glycine derivative (entry 6). Unexpectedly, the catalyst supports the conversion to the product despite the nitrogen doping of the graphene which constitutes basic centers expected to impede the acid-catalyzed transformation.

In addition, palladium catalysts based on acidic materials were synthesized to investigate these acidic supports for beneficial effects. Thus, the metal nanoparticles were prepared by applying both wet impregnation (A) and incipient wetness impregnation (B) on each material to give four diverse catalysts. Except for Pd/Faujasite B (entry 9), all generated catalyst demonstrated activity in the model reaction. Nevertheless, only 12% of the theoretical quantity was formed when Pd/ZSM-5 A was applied in the transformation towards N-lauroyl sarcosine (entry 8). The employment of Pd/Faujasite A generated 30% yield (entry 7) while utilizing Pd/ZSM-5 B led to a moderate reaction outcome of 50% (entry 10). Thus, a yield similar to the initially tested palladium black was observed.

In addition, the possibility to replace sulfuric acid as by the acidic supports was investigated by conducting experiments without the co-catalyst. The results are depicted in Table 5.

Table 5. Screening of heterogeneous palladium catalyst incorporating acidic supports for the H₂SO₄-free amidocarbonylation.

$n\text{-C}_{11}\text{H}_{23}\text{CONHCH}_3 + \text{HCHO} \xrightarrow[\text{NMP, CO}]{\text{Pd-Cat., LiBr}} n\text{-C}_{11}\text{H}_{23}\text{CON(CH}_3\text{)CH}_2\text{COOH}$		
Entry	Pd-Catalyst	Yield ^[a] [%]
1	Pd black	<5
2	Pd/Faujasite A	<5
3	Pd/ZSM-5 A	23
4	Pd/Faujasite B	<5
5	Pd/ZSM-5 B	28

Standard conditions (entry 1): 1 mmol N-methyl dodecanamide (NMDA), 1.5 mmol paraformaldehyde (PFA), 35 mol% LiBr, Pd-catalyst (1 mol% metal) in 1 mL NMP under 60 bar CO at 100 °C for 16 h. [a] Yield determined by NMR with ethylene carbonate as internal standard. Integration results based on R-CH₂-COOH.

As expected, the manipulation employing palladium black failed to give the desired product as no quantities of the surfactant were detected by NMR (entry 1). Thereby, the essential

role of sulfuric acid under classical conditions was emphasized. Similarly, the synthesis of the surfactant by the Faujasite-based palladium catalysts A and B remained unsuccessful (entries 2 and 4). In contrast to these results, the materials consisting of ZSM-5 both afforded the desired compound. Herein, Pd/ZSM-5 A offered 23% yield of the substance (entry 3) while Pd/ZSM-5 B yielded 28% of the surfactant (entry 5). Thus, the experiments suggest that heterogeneous supports incorporating acidic centers offer access to N-acyl amino acids *via* amidocarbonylation procedures conducted without the addition of acidic additives.

In general, the manipulations suggest that a catalyst support does not increase the reaction output. Moreover, no distinct tendency regarding the effect of the acidic or basic nature of the supporting material was observed. The study was continued with palladium black since the commercially available catalyst offered sufficient performance. Henceforward, the reaction parameters were screened for optimal reaction conditions (Table 6).

Table 6. Optimization of the Pd black catalyzed amidocarbonylation.

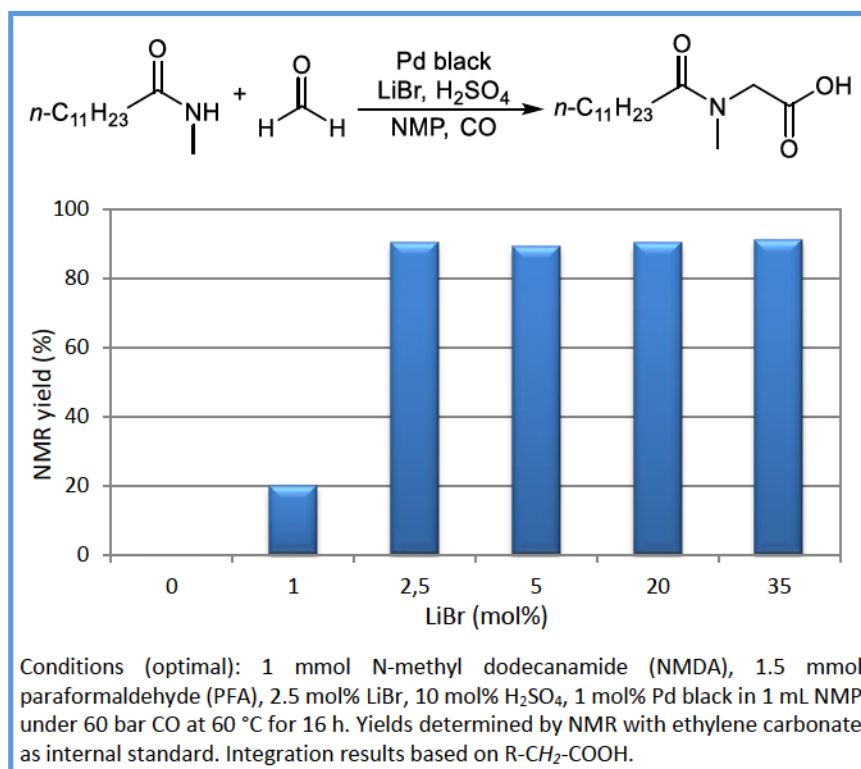
$n\text{-C}_{11}\text{H}_{23}\text{CONHCH}_3 + \text{HCHO} \xrightarrow[\text{NMP, CO}]{\text{Pd black, LiBr, H}_2\text{SO}_4} n\text{-C}_{11}\text{H}_{23}\text{CON(CH}_3\text{)CH}_2\text{COOH}$					
Entry	H ₂ SO ₄ [mol%]	Pd black [mol%]	PFA [mmol]	T [°C]	Yield ^[a] [%]
1	1	1	2	100	52
2	5	1	2	100	80
3	10	1	2	100	84
4	10	1	2	80	87
5	10	1	2	60	87
6	10	1	2	40	8
7	10	0.5	2	60	52
8	10	0.25	2	60	26
9	10	0.1	2	60	20
10	10	1	1	60	87
11	10	1	1.5	60	91
12	10	1	2.5	60	87

Standard conditions (entry 11): 1 mmol N-methyl dodecanamide (NMDA), 1.5 mmol paraformaldehyde (PFA), 35 mol% LiBr, 10 mol% H₂SO₄, 1 mol% Pd black in 1 mL NMP under 60 bar CO at 60 °C for 16 h. [a] Yield determined by NMR with ethylene carbonate as internal standard. Integration results based on R-CH₂-COOH.

Initially, the sulfuric acid concentration was varied in order to increase the reaction output. Herein, 10 mol% of the strong acid gave 84% of the target substance (entry 3) while half the amount accounted for an insignificantly decreased yield of 80% (entry 2). The experiment conducted under the starting parameters is displayed in entry 1 for comparison. The variation of the reaction temperature revealed that the product formation does not significantly depend on the temperature in a range from 60 to 100 °C since the results did

not differ strongly as 84% were obtained at 100 °C (entry 3) and 87% at both 80 and 60 °C, respectively (entries 4 and 5). In contrast, lowering the temperature to only 40 °C had a drastic influence as only 8% of the desired product was detected after 16 hours (entry 6). Naturally, manipulations to examine the effect of a decreased palladium loading were carried out. Herein, reducing the loading to 0.5 mol% resulted in a declined yield of 52% (entry 7). Accordingly, experiments with 0.25 mol% and 0.1 mol% afforded the surfactant in only 26% and 20%, respectively (entries 8 and 9). Therefore, the catalyst concentration strongly affects the reaction outcome and a catalyst loading of 1 mol% appears sufficient but also necessary to facilitate the transformation in a satisfying manner. Oppositely, the PFA quantity does not significantly influence the yield since N-lauroyl sarcosine was obtained in yields ranging from 87% to 91% when the PFA concentration was varied between 1 and 2.5 mmol (entries 5 and 10 to 12). Herein, a slight excess of 1.5 equivalents provided the best result.

Furthermore, the effect of the lithium bromide loading on the overall performance was examined (Scheme 30).

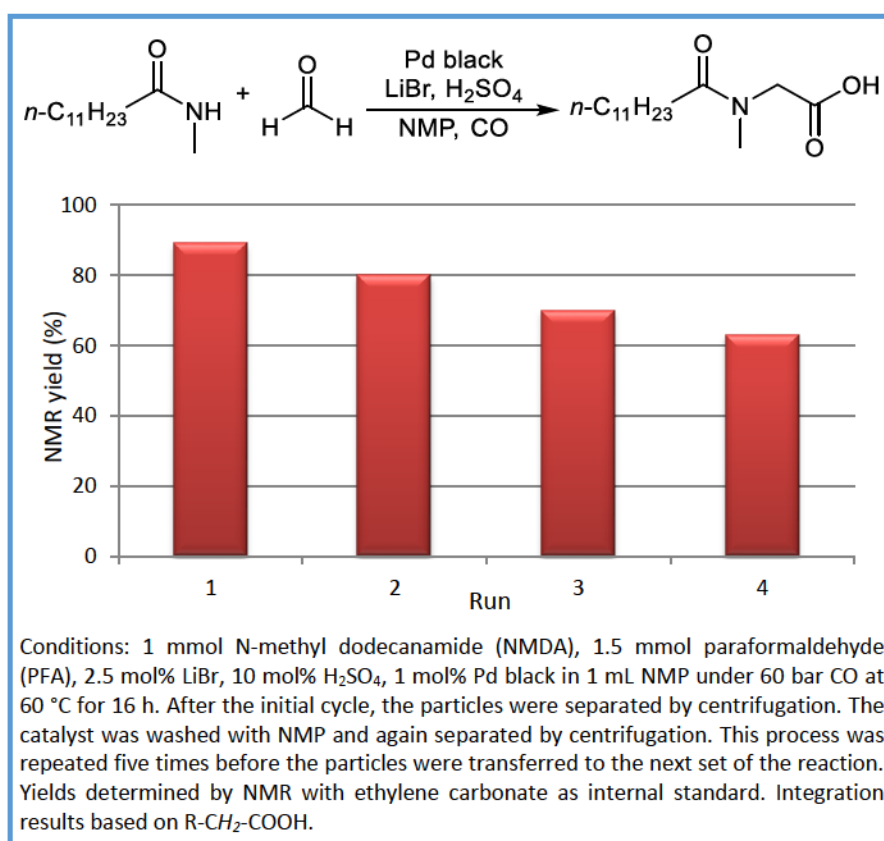


Scheme 30. Influence of the lithium bromide concentration on the reaction yield.

Advantageously, the lithium bromide content can be significantly decreased since a loading of 2.5 mol% offers sufficient activity and satisfying yields as 90% of the surfactant was detected (Scheme 30). However, the output excessively declines when only 1 mol% of

lithium bromide was employed. Moreover, the formation of the surfactant was not observed when the lithium salt was absent. In contrast, an increased concentration up to 35 mol% did not improve the reaction outcome. Obviously, the additive is necessary to facilitate the reaction. However, decreasing the co-catalysts loading to 2.5 mol% represents an enormous cost reduction for a potential industrial scale application whereas the increase of the employed sulfuric acid appears negligible since the base chemical can be obtained inexpensively in bulk quantities.

Addressing the reusability of the applied catalyst, recycling experiments were conducted (Scheme 31).

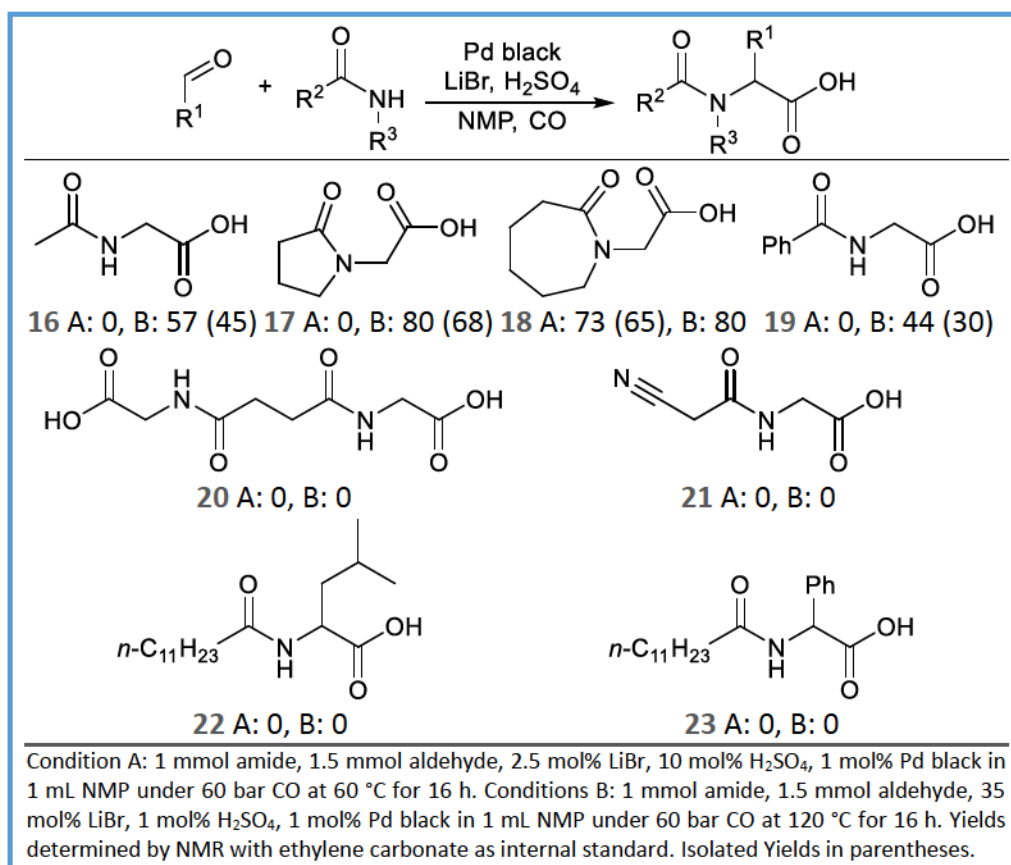


Scheme 31. Results for the recycling experiments.

For the evaluation of the reusability of the catalyst, the material was employed under optimized reaction conditions with subsequent separation of the heterogeneous material from the reaction solution by centrifugation. Afterwards, the particles were washed with NMP several times before these were applied again. Simultaneously, the organic layers were combined after which the solvent was removed in high vacuum in order to analyze the crude product for its N-lauroyl sarcosine content by NMR. Meanwhile, the heterogeneous material was transferred under argon *via* syringe with NMP into an autoclave vial already equipped with the next set of reagents and co-catalysts. As shown in Scheme 31, a productivity loss of

roughly 10% yield per cycle was documented after every run. However, the exact cause for the decreasing reaction output remains unidentified. The result of the centrifugation indicates that the palladium black particles differ tremendously in their size and weight. While the majority of the material was precipitated even at low centrifugation speed, visible quantities of the catalyst remained in the solution as particles were observed in the solution after separation even at the highest centrifugation speed. Therefore, a certain loss of palladium during the recycling must be accounted when interpreting the loss of activity. Moreover, the transfer of the isolated material *via* syringe and solvent does not represent an ideal method as loss of substance was observed as well. *Therefore, the author assumes the loss of catalytically active material during the recycling process to be the main reason for the declining productivity in the recycling experiments. Unfortunately, loss of catalytically active material affects small scale recycling experiment more significantly than manipulations on increased scales.* In addition, the loss of catalyst was increased if the heterogeneous catalyst had been transformed into a homogeneous palladium complex during the conversion through reaction with *in situ* generated hydrogen bromide and CO. A homogeneous complex is inseparable by centrifugation and therefore remains in the liquid phase.

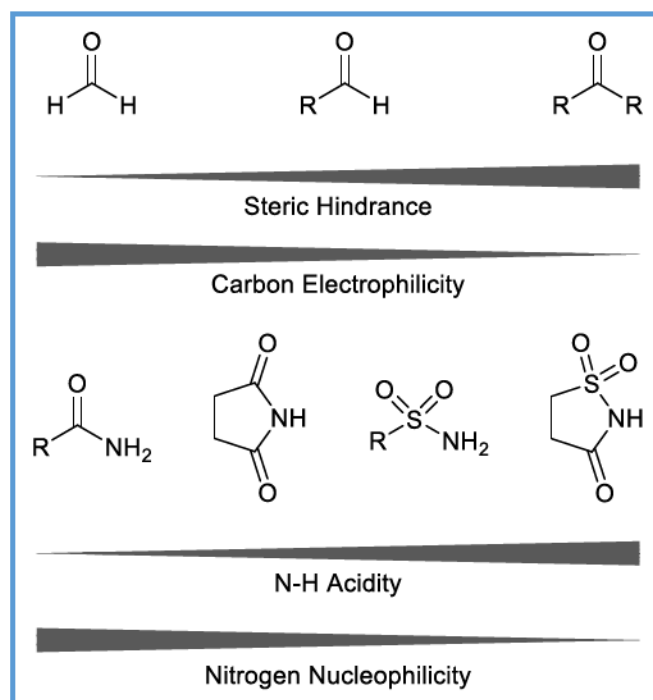
Continuative, the substrate scope of the reaction was further examined (Scheme 32).



Scheme 32. Substrate scope for the novel amidocarbonylation protocol.

Applying the optimized conditions for the synthesis of N-lauroyl sarcosine, acetamide was tested as substrate in the amidocarbonylation. Unexpectedly, no product formation was observed under the optimized conditions (conditions A, Scheme 32). Furthermore, none of the tested substrates provided the desired product except for amide **18** which was generated in 73% NMR yield while 65% were isolated. Nevertheless, the synthesis of the corresponding products was attempted by employing the initial conditions obtained from the literature report on the heterogeneously catalyzed amidocarbonylation (conditions B, Scheme 32).^[195] Herein, N-acetyl glycine (**16**) was afforded in 45% isolated yield catalyzed by 35 mol% lithium bromide and 1 mol% sulfuric acid at 120 °C for 16 hours. Furthermore, employing 2-pyrrolidinone gave 68% isolated yield of Piracetam (**17**) under conditions B while N-benzoyl glycine (**19**) was formed in 30% isolated yield. Unfortunately, when amides **20-23** were reacted with the corresponding aldehydes, the products were not detected in the reaction mixture under milder nor under more severe conditions. Thus, the reaction of NMDA proceeds with formaldehyde but not with higher aldehydes such as benzaldehyde or isovaleraldehyde.

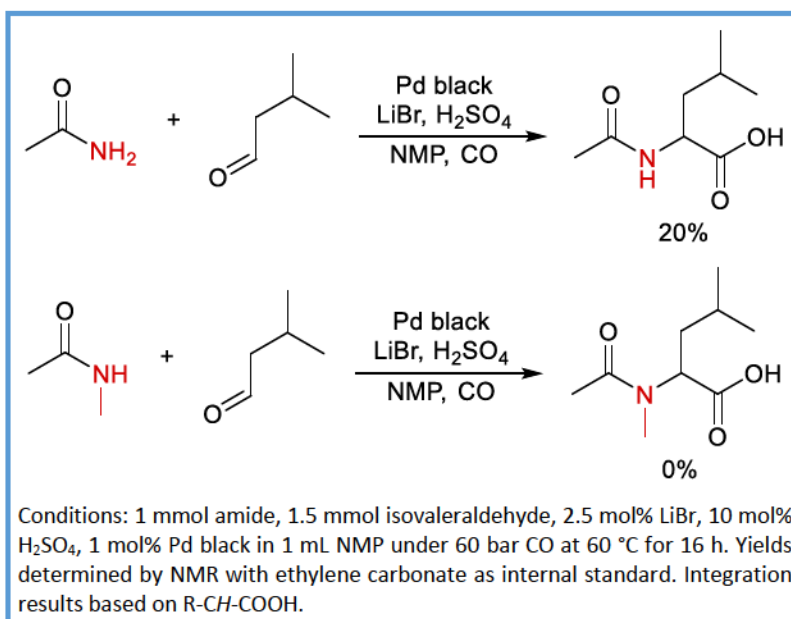
These results confirm the general reactivity of aldehydes in which formaldehyde represents the most active aldehyde due to the electron-poor character and the insignificant steric hindrance by the hydrogen atoms (Scheme 33).



Scheme 33. Reactivity of aldehydes towards nucleophiles and amides towards electrophiles.

Substituted aldehydes are generally less reactive due to the steric hindrance of the organic substituent and its electron-donating character. Overall, the amidocarbonylation does proceed with substituted aldehydes as well. However, the conversion with higher aldehydes fails under the milder conditions specifically optimized for the amidocarbonylation of the N-alkylated amide NMDA and formaldehyde. Nevertheless, the absence of reactivity for formaldehyde with other amides except for NMDA and substance **18** under milder conditions remains unexplained.

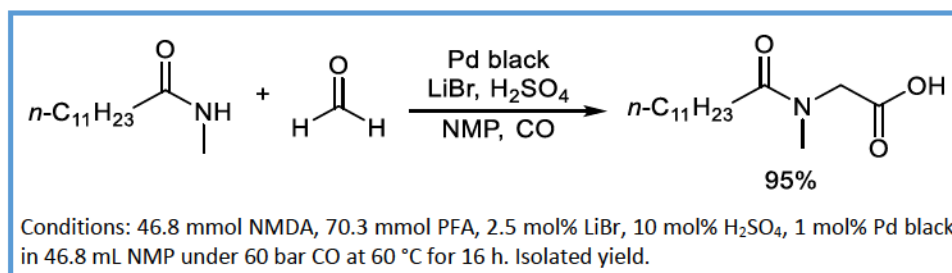
Next, the influence of a pre-existing N-alkylation of the amide was investigated (Scheme 34).



Scheme 34. Comparison of the activity of pre-alkylated and non-alkylated amides.

In earlier reports, a present N-alkylation impeded the palladium-catalyzed amidocarbonylation.^[77] The executed manipulations suggest that this tendency applies in the developed protocol as well since N-methyl acetamide was not converted to the desired N-acyl-N-methyl leucine whereas the non-methylated acetamide provided 20% of the leucine derivative under identical conditions.

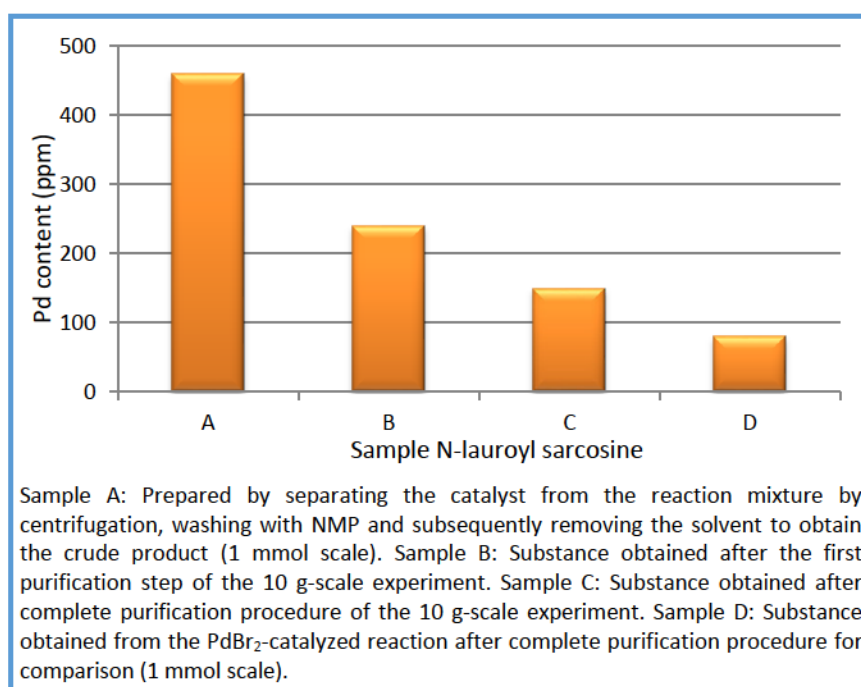
In order to address the scalability, a 10 g-scale experiment was performed (Scheme 35).



Scheme 35. Application of the novel protocol for the 10 g synthesis of N-lauroyl sarcosine.

Advantageously, the desired surfactant was afforded in >98% yield utilizing a slightly modified work-up procedure. The major impurity in the obtained product is the starting material NMDA with slightly less than 2%. Upon an additional acid-base extraction, the pure product was acquired in 95% overall yield. The results indicate that the production can be transferred to industrial scales without significant loss of activity. Moreover, the yield proved to be slightly higher than the NMR analyses suggested which is attributed to the inaccuracy of the NMR yield method.

With the intention of further characterizing the products, samples from the target compound were prepared in order to analyze the materials for their residual palladium content (Scheme 36).

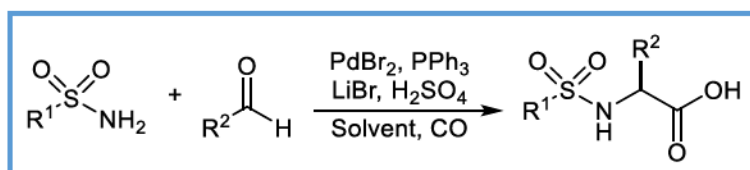


Scheme 36. Results for the recycling experiments.

Herein, the prepared materials were analyzed by ICP-OES analysis in order to determine the degree of leaching occurring through the reaction and the work-up procedure. In addition, a sample from the PdBr_2 -catalyzed amidocarbonylation towards N-lauroyl sarcosine was examined for comparison. As shown in Scheme 36, residual palladium was detected in all processed materials. Herein, especially the crude product constituting sample A contained high amounts of palladium with 460 ppm. Moreover, the observed contamination accounts for 17% of the originally employed palladium which explains the declining productivity in the recycling experiments. In addition, the results suggest that the loss stems from either insufficient separation by centrifugation or from leaching as homogeneous palladium complex. Furthermore, the purification steps successfully lowered the palladium

contamination. In fact, 250 ppm palladium were detected in sample B while the content was reduced to 150 ppm in sample C following the acid-base extraction. Unexpectedly, the sample obtained after applying the complete purification procedure to the PdBr_2 -catalyzed reaction offered the lowest quantity of palladium with 80 ppm.

In addition to the studies focused on industrially applicable N-acyl amino acids, the possibilities to extend the substrate spectrum of the amidocarbonylation were evaluated. Herein, the alteration of the amide appeared logical and the implementation of sulfonamides into the carbonylation process was examined (Scheme 37).



Scheme 37. Synthetic approach to N-sulfonyl amino acids *via* amidocarbonylation.

As starting conditions, the applied reaction parameters from the general amidocarbonylation were chosen for the desired conversion. Based on the experience with the optimization of N-lauroyl sarcosine, the critical parameters such as temperature, ligand and PFA concentration were varied. The results are depicted in Table 7.

Table 7. Optimization of the synthesis of N-sulfonyl amino acids *via* amidocarbonylation.

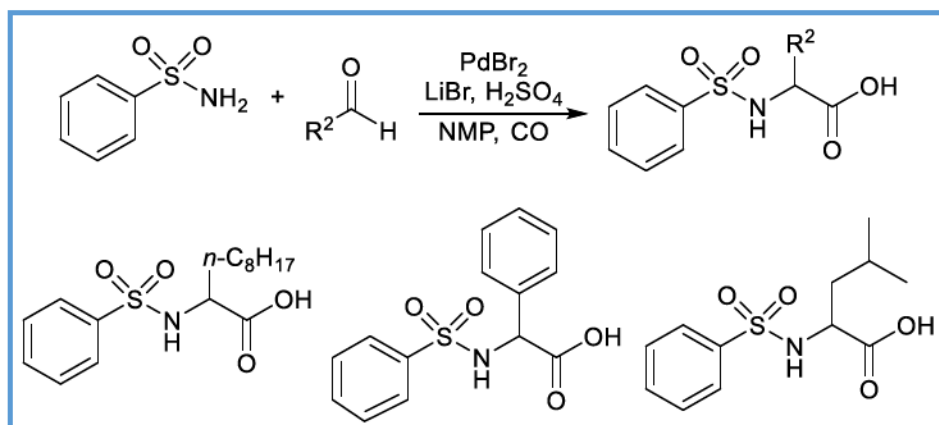
Entry	PFA [mmol]	PPh_3 [mol%]	T [°C]	Yield ^[a] [%]
1	2.5	1	130	60
2	2.5	1	140	52
3	2.5	1	100	65
4	2.5	-	100	70
5	2.5	-	80	41
6	5	-	100	39
7	3	-	100	74

Standard conditions (entry 7): 2.5 mmol N-methyl dodecanamide (NMDA), 3 mmol paraformaldehyde (PFA), 35 mol% LiBr, 1 mol% H_2SO_4 , 0.5 mol% PdBr_2 in 2.5 mL NMP under 60 bar CO at 100 °C for 16 h. [a] Yield determined by NMR with ethylene carbonate as internal standard. Integration results based on $\text{R-CH}_2\text{-COOH}$.

In general, the amidocarbonylation proceeds successfully when sulfonamides are applied as substrates. Under 60 bar carbon monoxide and 130 °C, the product is generated at 60% yield catalyzed by $\text{PdBr}_2/(\text{PPh}_3)_2$ and 35 mol% LiBr as well as 1 mol% sulfuric acid (entry 1). However, an increase of the temperature by 10 °C led to a decreased yield of 52% (entry 2).

Based on this effect, the temperature was further lowered to 100 °C. Henceforward, the glycine derivative was found in 65% and therefore a slightly improved yield was observed (entry 3). Due to the experience with the amidocarbonylation of NMDA, the influence of the ligand was examined by conducting an experiment according to entry 4 without the additive. Thus, the yield was further raised slightly to 70%. Nevertheless, the temperature of 100 °C appeared necessary since the product was formed in only 41% yield when the reaction was conducted at 80 °C (entry 5). Furthermore, the PFA concentration was varied in order to learn about the effect of the reagent's concentration. Thereby, the manipulations with 2 and 1.2 equivalents gave the compound in 39% and 74%, respectively (entries 6 and 7). Thus, the experiments indicate that a slight excess of the aldehyde has beneficial effects (entry 7) while a significant excess inhibits the conversion (entry 6).

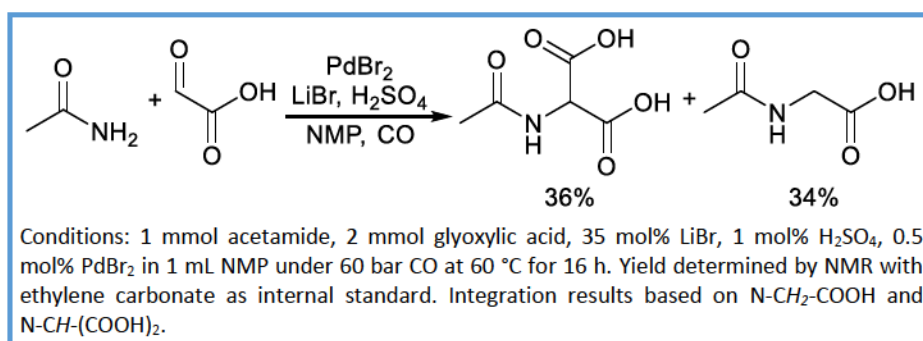
Following the initial optimization results, preliminary tests of the substrate scope were started in order to identify suitable aldehydes for the sulfonamidocarbonylation.



Scheme 38. Substrate scope for the sulfonamidocarbonylation.

Unfortunately, none of the applied aldehydes gave rise to the corresponding N-sulfonyl amino acids. Despite various attempts under more severe and forcing conditions, the desired compounds were not generated. *Thereinafter, the author became aware of the PhD thesis of Wahed Ahmed Moradi^[210] and the included results for the sulfonamidocarbonylation. Herein, comparable experiments provided similar results leading to the identical conclusion that the amidocarbonylation of sulfonamides is feasible with formaldehyde. However, the implementation of higher aldehydes fails to give the corresponding products. A comparison of the results can be found in the appendix.*

Next, the amidocarbonylation methodology was extended to the synthesis of malonic acid derivatives. Therefore, the application of glyoxylic acid with acetamide for the synthesis of acetamido malonic acid was investigated (Scheme 39).



Scheme 39. Synthesis of acetamido malonic acid *via* amidocarbonylation.

Advantageously, preliminary experiments indicated that the utilization of glyoxylic acid leads to the formation of the desired acylamido malonic acid. Thus, 70% of the substrate was successfully converted under 60 °C and 60 bar carbon monoxide catalyzed by 0.5 mol% PdBr₂, 35 mol% lithium bromide and 1 mol% sulfuric acid in 16 hours. However, approximately half of the targeted compound already underwent reductive decarboxylation at the point of analysis. Nevertheless, the desired acetamido malonic acid was formed in 36% overall yield.

3.4. Outlook

In conclusion, an improved catalytic system for the production of N-lauroyl sarcosine was developed and applied on a 10 g-scale. Moreover, the employed heterogeneous catalyst offers reusability and a drastic decrease of the lithium bromide loading while operating at significantly lower temperatures. Thus, an efficient and scalable methodology was successfully developed.

However, the results of the optimization study for the homogeneously catalyzed amidocarbonylation raised the main question whether the addition of phosphine ligands benefits the activity and productivity. The manipulations suggest that the reactivity of PdBr_2 exceeds the reaction rate of conversions with additional ligand. Moreover, a detailed literature study revealed examples in which the data suggest that the reaction proceeds more efficiently without an added phosphine ligand as well (Table 8).

Table 8. Selected examples from literature reports on amidocarbonylations.

Entry	Literature	Ligand	Conditions	Yield [%]
1	Beller et. al. 1998 ^[202]	PPh_3	A	37
2		-		80
5	Beller et. al. 2003 ^[201]	PPh_3	B	<70% ^[a]
6		-		>80% ^[a]

Conditions: A = 25 mmol acetamide, 25 mmol isovaleraldehyde, 35 mol% LiBr, 1 mol% H_2SO_4 , 0.25 mol% PdBr_2 , 0.5 mol% PPh_3 in 25 mL NMP under 60 bar CO at 80 °C for 1 h. B = 50 mmol acetamide, 100 mmol propionaldehyde, 35 mol% LiBr, 1.5 mol% H_2SO_4 , 0.25 mol% PdBr_2 , 0.5 mol% PPh_3 in 50 mL NMP under 60 bar CO at 100 °C for 12 h. [a] Obtained from Figure 3 and 6.

These findings support the results from the described study. However, the addition of triphenylphosphine proved to be beneficial in several cases as well. Nevertheless, since the heterogeneous catalyst performed excellent in the synthesis of N-lauroyl sarcosine and further displayed reusability, the question is raised whether the reaction is homogeneously or heterogeneously catalyzed. As often observed in homogeneous palladium catalysis, the solution contained (palladium) black particles after the reaction when homogeneously PdBr_2 was applied. On the other hand, the activity of palladium black declined after each reaction cycle. Although this decrease in the productivity might be assigned to loss of catalyst during the work-up, the necessity to better understand the nature of the active palladium species was emphasized when the applied ligands did not improve the amidocarbonylation of acetamide with benzaldehyde. Therefore, the identification of the catalytically active species will be a priority for future investigations of the amidocarbonylation. Furthermore, a

detailed understanding of the active catalyst allows for a more precise screening for more active catalyst.

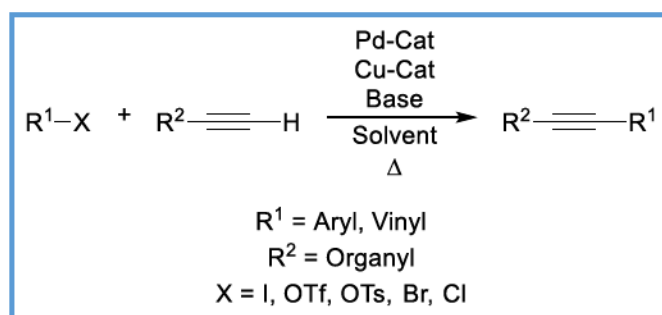
Moreover, a protocol for the amidocarbonylation of benzenesulfonamide towards N-phenylsulfonyl glycine was developed. Unfortunately, this protocol was not successfully applied to higher aldehydes. For further studies, the importance of identifying the critical aspect of the mechanistic cycle for the sulfonamidocarbonylation with higher aldehydes represents a significant priority in order to develop protocols enabling the conversion of these more challenging substrates.

In addition, the results prove that the formation of amido malonic acids from the conversion of an amide with glyoxylic acid was achieved. However, the reductive decarboxylation of the target molecule represents a critical aspect. Herein, an extensive optimization study offers the possibility to provide conditions under which the decomposition is suppressed. Herein, especially a temperature decrease and minimal amounts of sulfuric acid benefit the stability of malonic acid derivatives.

4. Sonogashira-Semihydrogenation

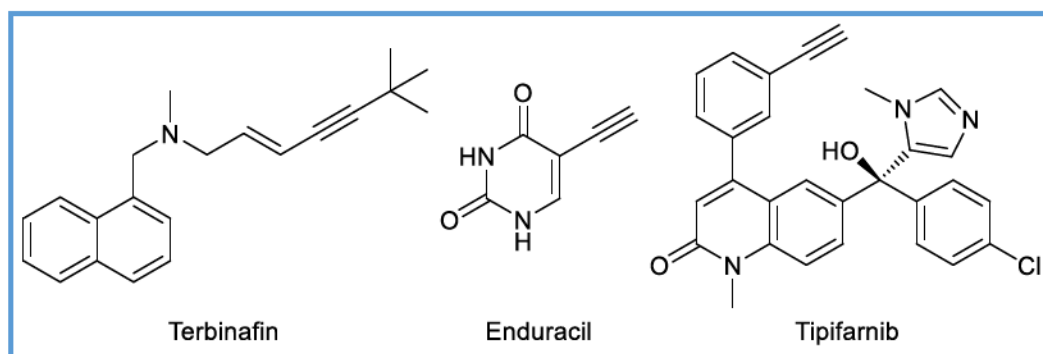
4.1. Theory

In 1975, Heck^[211] and Cassar^[212] individually reported the successful palladium-catalyzed coupling of iodobenzene and phenylacetylene. However, these conversions required rather forcing conditions. In contrast, Sonogashira and Hagihara described the successful palladium-catalyzed coupling of aryl iodides with terminal acetylenes employing copper iodide as co-catalyst at room temperature in the same year.^[23] Hence, the palladium-catalyzed formation of internal acetylenes assisted by copper salts is nowadays referred so as *Sonogashira* or *Sonogashira-Hagihara* coupling (Scheme 40).



Scheme 40. Conditions for the Sonogashira coupling.

Oppositely, the copper-free methodology is sometimes described as *Heck-Cassar* coupling. Thereby, the tool box for late-stage introductions of internal acetylenes was intensively extended as evidenced by various industrial and scientific applications (Scheme 41).^[11,19,213-216]

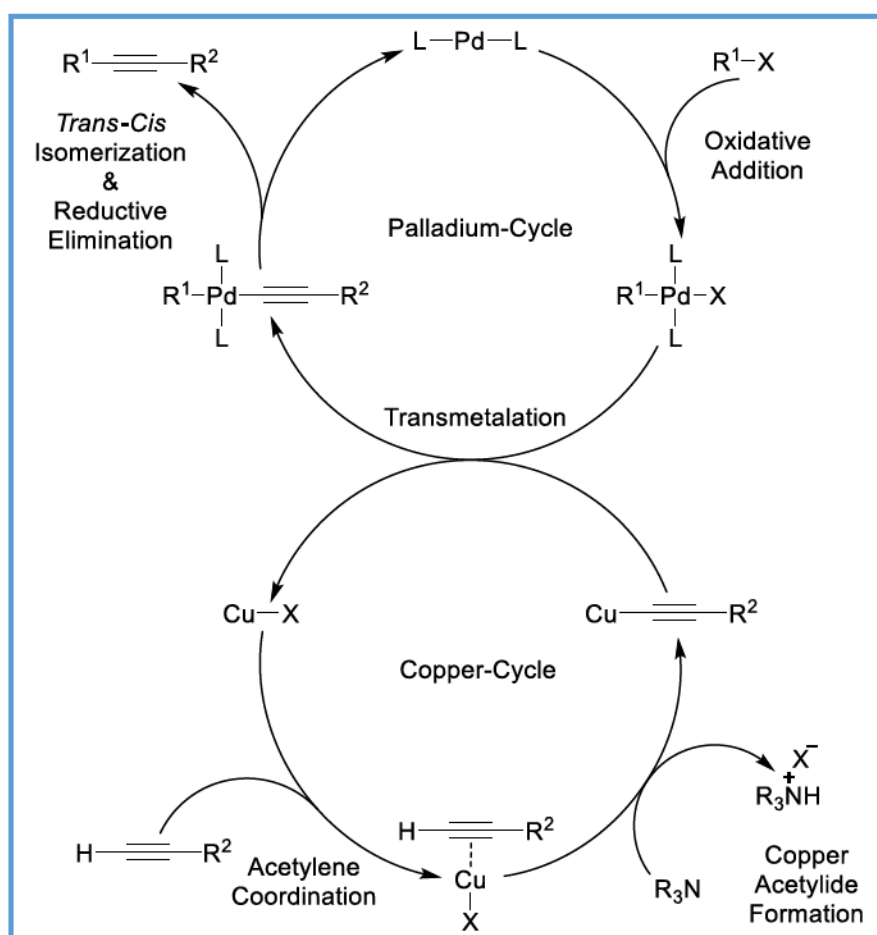


Scheme 41. Pharmaceuticals produced *via* Sonogashira coupling.

Herein, the aryl halide or pseudohalide is coupled with an organic acetylene *via* activation of the terminal C-H proton and the associated formation of a copper acetylide. As halides, iodides, triflates,^[217-219] and bromides^[220-222] as well as chlorides^[223,224] represent suitable coupling partners. The activity of these compounds decreases in the depicted sequence from

the most active iodides to the least reactive chlorides. Furthermore, tosylates^[225-227] as well as mesylates^[228] have been effectively employed as substrates. It is important to note that even the most unreactive vinyl halides (in general vinyl chlorides) perform at higher reaction rates than aryl iodides.^[213] Thus, even deactivated aryl bromides constitute challenging starting materials for Sonogashira coupling protocols. Herein, the starting material is referred to as deactivated when electron-rich substituents increase the electron density in the C-X bond whereas electron-poor aryl and vinyl halides constitute activated substrates. In addition, the reactivity of the acetylene is influenced as well since electron-withdrawing substituents activate the C-H bond and increase the acidity of the alkyne. In contrast, electron-donating moieties decrease the C-H acidity and the deprotonation of the substrate is inhibited.^[229]

Although the exact mechanism of the palladium/copper-catalyzed Sonogashira reaction is not entirely understood and proven, it is generally suggested to proceed *via* two independent cycles displayed in Scheme 42. For mechanistic studies, especially the investigation of the two catalytic cycles combined in the presence of both metals raises significant challenges to researchers in terms of experiment design.



Scheme 42. Generally accepted mechanism for the Sonogashira coupling.

Herein, the active palladium complex PdL_2 adds the aryl halide by oxidative addition into the carbon halide bond. Thereby, the oxidation state of the palladium complex is increased from zero to two and the *Umpolung* of the carbon atom is achieved. Consecutively, the palladium complex exchanges the halide for the acetylide with the *in situ* formed copper acetylide. This process is referred to as transmetalation. The copper complex is previously generated by abstraction of the halide acid from the π -alkyne copper complex. Typically, an amine base supports the abstraction of the proton by generating an organic ammonium salt. In addition, the transmetalation regenerates the copper halide salt which coordinates an additional alkyne to provide the π -alkyne copper complex. Thereinafter, the palladium complex undergoes *trans-cis*-isomerization and subsequent reductive elimination to give the desired internal alkyne. Moreover, the active palladium species PdL_2 is regenerated to initiate the next catalytic cycle.

As catalyst, various palladium salts and palladium-ligand combination have been reported to efficiently facilitate the transformation of terminal to internal acetylenes.^[213,214] Aside from the well-established palladium phosphine ligand combinations, N-heterocyclic carbenes^[230] as well as palladacycles^[231] have proven their respective activity in the C-C bond forming process. Moreover, the application of various heterogeneous materials and nanoparticles enabled the formation of internal alkynes by Sonogashira coupling protocols.^[232] However, the topic of heterogeneous catalysts for coupling reactions is controversially discussed as it is suggested that the heterogeneous palladium only serves as a reservoir and that leached homogeneous palladium constitutes the catalytically active species.^[233,234]

Internal acetylenes depict an interesting structural motif which can be found in natural products,^[215] pharmaceuticals^[216] and molecular organic materials^[235,236] such as organic LEDs.^[213,237] Moreover, the generated internal acetylenes are of specific interest due to the diverse functionalization possibilities of the C-C triple bond including hydrogenations,^[238-240] halogenation,^[241,242] cycloadditions^[243-245] as well as ozonolysis.^[246]

As indicated in the literature,^[213,214,237] one drawback in classical Sonogashira coupling protocols arises from the utilization of copper salts as co-catalysts. Thereby, the methodology has to be conducted under inert conditions since oxygen promotes copper-mediated Hay and Glaser couplings.^[247] Furthermore, the addition of another environmentally problematic and difficult to recover catalyst creates additional requirements for chemical processes. Herein, copper-free protocols offer an efficient

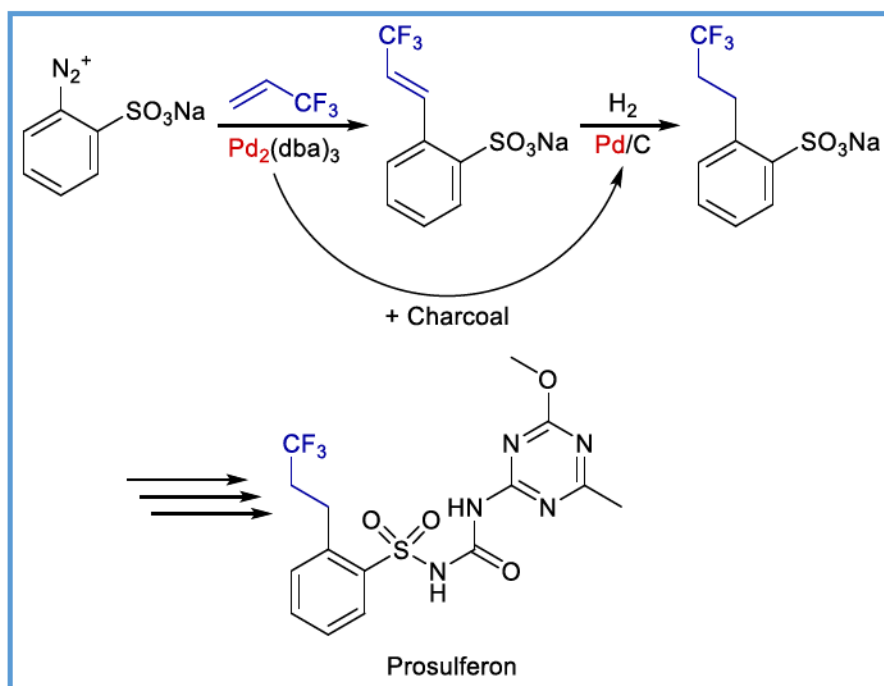
alternative. Unfortunately, the absence of copper decreases the reactivity of the catalytic system and constitutes the necessity of such synthetic protocols to employ amine bases or specific bases such as Cs_2CO_3 .^[213,214,248-257] In these cases, the amine bases are applied in excess or often even as solvents which creates environmental concerns as well.

However, scientists have been reporting several studies addressing the investigation of copper- and amine-free Sonogashira coupling methodologies.^[258-264] In these enhancements, the acetylene deprotonation is assumed to be achieved by an undefined palladium π -alkyne complex.^[213,214] Interestingly, numerous examples utilizing the combination of K_2CO_3 as inorganic and inexpensive base and DMF as solvent have been documented in the literature.^[265-274] Apparently, this solvent-base system increases the deprotonation of the acetylene without the assistance of copper enough to empower the reported catalytic systems to facilitate the Sonogashira coupling reactions. Thereby, drawbacks from utilizing copper co-catalysts and amines can be avoided.

Aside from cross-coupling reactions, hydrogenations are amongst the most-applied chemical transformations in the pharmaceutical and fine chemicals industry.^[2,14,18] While both homogeneous and heterogeneous transition metal catalysts offer activity in such reductions, heterogeneous materials are generally preferred in industrial-scale processes due to their advantageous separability and reusability.^[9] At the same time, homogeneous complexes usually display superior selectivity, activity and functional group tolerance under milder conditions.^[12] In recent years, several groups developed novel and well-designed heterogeneous materials displaying increased selectivity and activity while maintaining the beneficial separability and reusability.^[54-59] Among other techniques, the Beller group and others established the pyrolysis of molecularly distinct nitrogen-containing transition metal complexes as an advanced route for the synthesis of superior catalytically active materials.^[275-282] *Via* this methodology, heterogeneous catalysts possessing nitrogen-doped metal centers embedded into the material surface as catalytically active sites are accessible. The resulting highly active catalysts demonstrate tremendous reactivity in several conversions such as nitro- and aldehyde-hydrogenation, alkyne- and quinoline-semihydrogenation as well as aldehyde-amination and Guerbet-conversions.

Aside from the approach to develop novel heterogeneous materials, the strategy of converting an applied homogeneous catalyst into a solid which is further employed as heterogeneous catalyst in a subsequent reaction was already successfully realized on an

industrial scale in 1994.^[60] Notably, this approach allowed the production of the agrochemical Prosulferon on an economically feasible standard (Scheme 43).^[63]

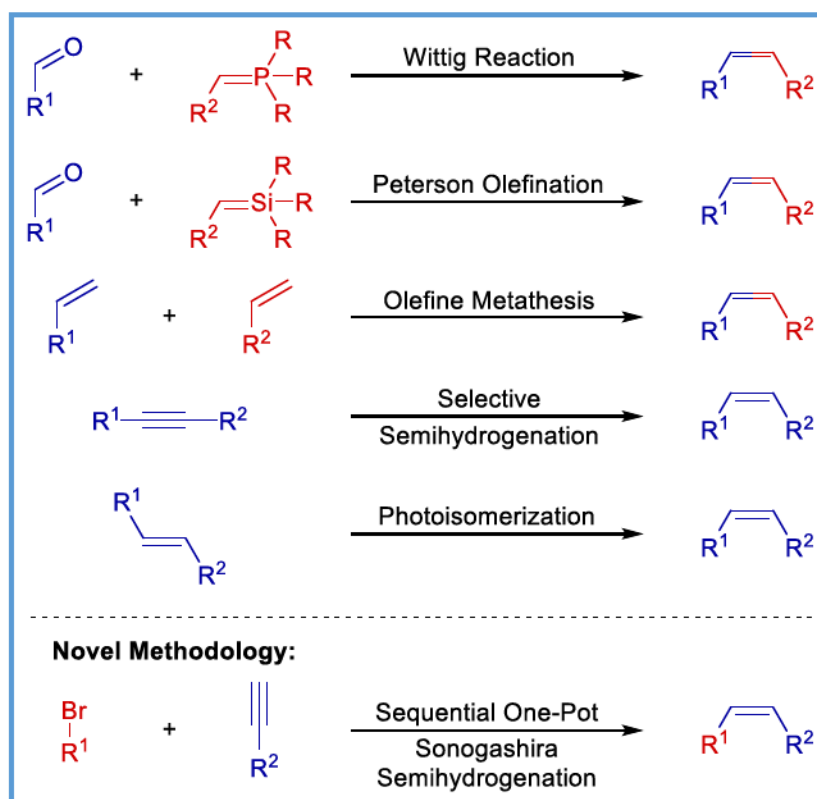


Scheme 43. Industrial production of Prosulferon.

However, despite the increased efficiency and the combination of the advantages from both homogeneous and heterogeneous catalysis, this strategy has not extensively found its way into industrially scale productions and scientific research regardless of its obvious advantages. Accordingly, this methodology has only been reported to be further applied for the synthesis of Naproxen.^[61]

In general, Z-alkenes represent an interesting and promising substance class as this functional group is found in numerous biologically active compounds and constitutes a valuable building block for organic syntheses of various substance classes due to its broad functionalization spectrum.

Classically, this structural motif can be generated *via* various well-known routes. However, the established routes are affiliated with several drawbacks including the formation of stoichiometric amounts of waste, the requirement for commercially non-available starting materials, implementation problems on industrial scales or deficient selectivity. A selection of methodologies is displayed in Scheme 44.

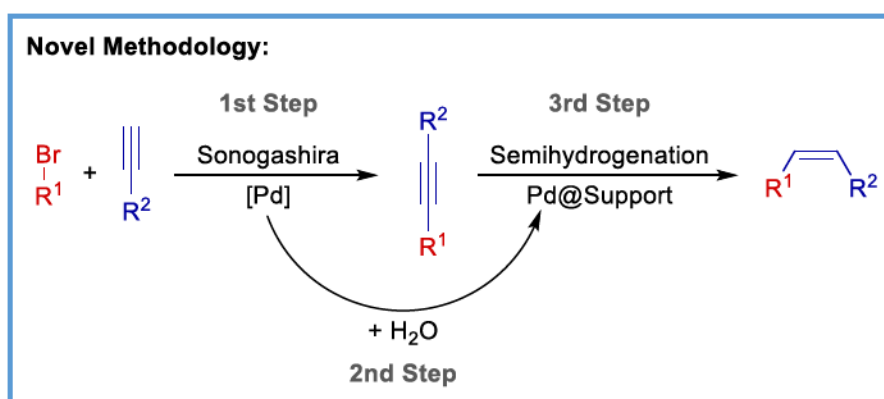


Scheme 44. Selected routes for the synthesis of Z-alkenes.

Herein, the selective semihydrogenation of internal acetylenes resembles the most direct pathway. However, this synthetic procedure requires specific hydrogenation catalysts capable of performing the selective semihydrogenation towards the desired product without over-hydrogenation and significant formation of the *E*-isomer. In this regard, the Lindlar catalysts represents the most well-known and investigated compound.^[283,284] While this Pd@CaCO₃ catalyst is typically poisoned with quinoline and lead acetate, more advanced heterogeneous materials based on noble metals^[285-290] and other transition metals^[291-294] have been developed in recent years and show high activity and selectivity without these additives. In contrast, the Wittig reaction offers selective access to Z-alkenes *via* stoichiometric reaction of aldehydes with phosphor ylides under specific reaction conditions.^[295] Similarly, the related Peterson olefination condenses aldehydes with α -silyl carbanions and the subsequent acidic or basic hydrolysis determines the diastereoselectivity.^[296] Nevertheless, both reaction protocols lead to the formation of stoichiometric waste. Furthermore, the isomer can be synthesized by photoisomerization of the corresponding *E*-alkene.^[297,298] Unfortunately, photoisomerizations are difficult to be realized on industrial scales. Finally, terminal olefins can be converted into internal Z-alkenes by suitable alkene metathesis catalysts.^[299] However, specifically intermolecular reactions represent challenging conversions for this methodology.

4.2. Objectives

Inspired by these reports, a sequential one-pot protocol for the selective synthesis of Z-alkenes was developed including a homogeneously catalyzed Sonogashira reaction and a heterogeneously performed selective semihydrogenation (Scheme 45). Both transformations are conducted by the same metal atoms as the homogeneous catalyst is heterogenized subsequently to its application as Sonogashira catalyst. The *in situ* heterogenized catalyst then performs the selective semihydrogenation using hydrogen gas as reducing agent.



Scheme 45. Novel methodology for the synthesis of Z-alkenes.

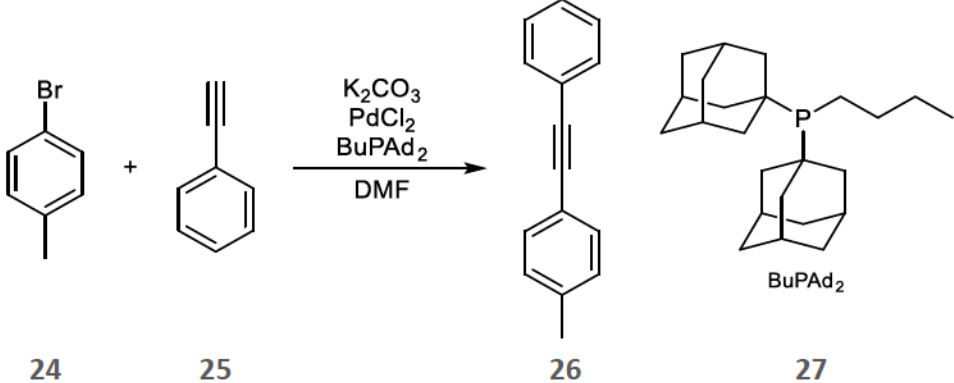
Aside from the optimization of the protocol, the investigation of the substrate scope of the innovative protocol was further planned. For the optimization study, the development of the heterogenization and the selectivity of the semihydrogenation as well as the overall one-pot sequence were specifically focused on in order to achieve a working methodology. While the enhancement of the Sonogashira reaction *via* alteration of the solvent and especially the catalyst-ligand-system offers tremendous possibilities in terms of improving the reactivity and selectivity of this reaction step, it was decided to maintain the catalyst, ligand and solvent known to work according to the literature for the carbonylative Sonogashira reaction in order to focus on the non-investigated and experimental sequence steps 2 and 3.

Noteworthy, the initial results from the study were reported in the master thesis of the author. The regarding experiments (entries 1-5) are marked in the optimization of the Sonogashira reaction (Table 9) presented in the following chapter.

4.3. Results

For this study, 4-bromotoluene (**24**) and phenylacetylene (**25**) were selected as starting materials to afford the corresponding product phenyl-p-tolyl-acetylene (**26**). This model system was chosen based on reports in the literature indicating that the conversion proceeds smoothly catalyzed by $\text{PdCl}_2/\text{BuPAD}_2$ (**27**) in a solution of $\text{K}_2\text{CO}_3/\text{DMF}$ without further additives (Cu salts, amines).^[266,271,272,300]

Table 9. Optimization of the copper- and amine-free Sonogashira reaction.

						
24	25			26	27	
Entry ^[a]	25 [mmol]	Pd:L [mol%]	T [°C]	t [h]	Conversion ^[b,c] [%]	Yield ^[c] [%]
1*	1	4:6	25	96	68	65
2*	1	4:6	40	24	>99	82
3*	1	4:6	60	4	>99	78
4*	1.5	4:6	60	4	>99	67
5* ^[d]	0.6	4:6	60	6	88 ^[e]	70
6	1	2:2	60	16	>99	84
7	1	1:1	60	16	>99	88
8 ^[d]	0.6	1:1	60	16	67 ^[e]	61
9	1	1:1	60	8	90	80
10	1	0.5:0.5	60	16	90	81
11	1	0.1:0.1	60	16	66	60
12	1	0:1	60	16	<1	<1
13	1	1:0	60	16	<1	<1

* These results were obtained in experiments conducted for the master thesis of the author.
 [a] Standard conditions (entry 7): 0.5 mmol 4-bromo-toluene (**24**), 1 mmol phenylacetylene (**25**), 1 mmol K_2CO_3 , 1 mol% PdCl_2 , 1 mol% BuPAD_2 , 2 mL DMF at 60 °C for 16 h. [b] Regarding **24**. [c] Determined by GC with hexadecane as internal standard. [d] **25** was dissolved in 1 mL DMF and added continuously over the first 2 hours of the experiment. [e] Conversion of **25**: >99%.

Prior to continuing the experiments from the master thesis regarding the Sonogashira coupling step, it was already established that the reaction affords the targeted compound in 65% yield when the protocol is executed at room temperature (Table 9, entry 1). While the selectivity at room temperature is exceptional, the conversion reached only 68% after 96

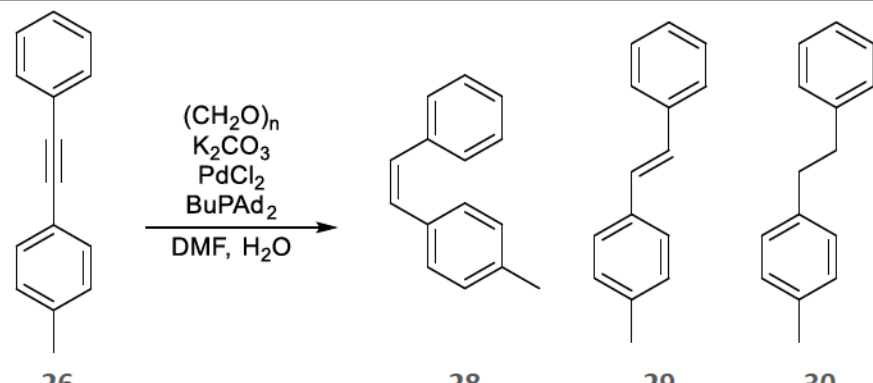
hours of reaction time. When the temperature was increased to 40 °C, the yield reached 82% at full conversion of the aryl bromide after 24 hours (entry 2). Therefore, the selectivity significantly drops when the reaction is performed at higher temperatures. However, the drastic improvement of the reaction rate benefits the applicability of the methodology greatly. In agreement, simply raising the temperature to 60 °C afforded 78% of **26** after only 4 hours (entry 3). In conclusion, the optimization was further executed at 60 °C despite the decreased selectivity due to the high reaction rate and the desire to minimize the necessary catalyst loading. Continuing the studies, the effect of the acetylene concentration was investigated as the complete consumption of this reagent was documented in several experiments. Noteworthy, the reaction outcome was further lowered to 67% when 3 equivalents of the terminal acetylene were applied (entry 4). In agreement with prior findings, the yield further declined to 70% when 1.2 equivalents were added continuously over the first 2 hours of the experiment (entry 5). While the selectivity stayed at 80% in comparison with experiments in which two equivalents of phenylacetylene were utilized (entries 2 and 3), the aryl bromide conversion was only completed to 88% while the acetylene was consumed entirely. These manipulations indicate the necessity for an excess of acetylene when the reaction is catalyzed by the PdCl₂/BuPAd₂-system.

Next, the minimization of the applied amount of catalyst was approached by reducing the loading of the palladium precursor and the ligand to 2 mol% (entry 6). Herein, the yield was increased to 84%. Noteworthy, the selectivity was generally enhanced when lower catalyst loadings were applied (entries 6 to 11). In agreement, 88% selectivity was observed at full conversion when 1 mol% palladium salt and ligand were applied (entry 7). The repeated attempt to lower the necessary concentration of **25** resulted in a declining yield of 61% at only 67% conversion with complete consumption of the acetylene (entry 8). Thus, the ensuing manipulations were conducted utilizing the original amount of 2 equivalents. Due to the decreased catalyst loading and the associated declining reaction rate, the product was afforded in only 80% overall yield and 90% selectivity when the experiment was executed for 8 hours at the reaction temperature (entry 9). Thus, the elaborated reaction time of 16 hours was chosen for the ongoing investigation. In accordance with previous results, the reaction rate further diminished at lower catalyst loadings while simultaneously displaying enhanced selectivity towards the product (**26**) (entries 10 and 11). Herein, the selectivity remained at 90% while the activity in the formation of **26** was lowered to 81% and 60%,

respectively. Importantly, the control experiments emphasized the necessity of both catalytically applied substances since the generation of the target molecule failed in the absence of either BuPAd₂ or palladium chloride (entries 12 and 13).

Next, the semihydrogenation of the intermediate **26** was studied. Initially, the protocol applying paraformaldehyde (PFA) and water as hydrogen source was tested and optimized (Table 10).

Table 10. Optimization of the semihydrogenation applying (CH₂O)_n/H₂O.

						
Entry ^[a]	(CH ₂ O) _n [mmol]	DMF:H ₂ O [mL]	Conversion ^[b,c] [%]	Yield 28 ^[c] [%]	Z:E-Ratio ^[c] [%:%]	Selectivity 28 ^[d] [%]
1	5	2:0	4	<1	-	-
2	5	2:0.1	26	22	22:4	85
3	2.5	2:0.1	20	17	17:2	85
4	10	2:0.1	31	26	26:4	84
5	5	2:0.2	54	48	48:3	89
6	5	2:0.4	61	50	50:5	82
7 ^[e]	5	2:0.2	32	26	26:3	81
8 ^[f]	5	2:0.2	68	61	61:4	90
9 ^[g]	5	2:0.2	51	42	42:5	82
10 ^[h]	5	2:0.2	66	60	60:3	91

[a] Standard conditions (entry 5): 0.5 mmol **26**, 5 mmol (CH₂O)_n, 1 mmol K₂CO₃, 1 mol% PdCl₂, 1 mol% BuPAd₂, 2 mL DMF, 0.2 mL H₂O at 120 °C for 24 h. [b] Regarding **26**. [c] Determined by GC with hexadecane as internal standard. [d] Referring to the ratio of yield to conversion. [e] 2 mmol K₂CO₃. [f] 140 °C. [g] 160 °C. [h] 140 °C, 12 h.

This methodology originated from the attempt to conduct a carbonylative Sonogashira coupling reaction with paraformaldehyde as carbon monoxide source. In the associated experiments, the non-carbonylated acetylenes and the corresponding hydrogenated alkenes were observed instead of the desired alkynones. Further manipulations suggested that the combination of residual water and PFA led to the hydrogenation of the *in situ* formed alkynes. Thus, the established conditions were applied in order to identify suitable reaction parameters for a satisfying hydrogenation of the internal acetylene. To begin with, the hydrogenation step was optimized separately to guarantee that changes in the reaction

outcome were caused by effects of the reaction parameters on the semihydrogenation and not on the prior Sonogashira coupling.

Accordingly, the presence of water was tested for its effect on the semihydrogenation of **26** using PFA as hydrogen source. Herein, entries 1 and 2 emphasize the significance of water as its absence prevented the formation of the desired *Z*-alkene entirely (Table 10). In addition, the internal alkyne remained unconverted in the reaction solution. In contrast, employing 0.1 mL H₂O led to the formation of 22% of the semihydrogenation product with 85% overall selectivity (entry 2). Thus, the presence of water displays a critical factor for the desired conversion. Continuing the optimization, the PFA concentration was varied in order to enhance the conversion and the product formation. Herein, reducing the PFA excess to 2.5 mmol lowered the reaction outcome to 17% and the conversion to 20% (entry 3). Unfortunately, increasing the PFA excess to 20 equivalents only slightly affected the overall yield as 26% of the *Z*-alkene **28** was formed (entry 4). Moreover, the PFA concentration insignificantly influenced the overall *Z*-selectivity (entries 2 to 4).

On the other hand, the water concentration in the solution directly impacted the overall yield and selectivity since increasing the content to 10% and 20% of water gave rise to 48% and 50% yield, respectively (entries 5 and 6). However, the selectivity decreased to 82% when 0.4 mL of water were present (entry 6). Therefore, further studies were continued employing 10% water in respect to DMF (entry 5). Furthermore, the addition of 4 equivalents of K₂CO₃ drastically reduced the productivity as only 26% of **28** was detected (entry 7). At the same time, the selectivity declined to 81%. Noteworthy, the reaction yield and conversion reached its maximum during the optimization when the experiment was modified to run at 140 °C (entry 8). Thereby, **28** was provided in 61% yield under 68% conversion of **26** and an overall *Z*-selectivity of 90%. Unfortunately, an additional increase in the reaction temperature by 20 °C failed to offer further enhancement of the productivity but instead decreased the reaction outcome to 42% and the selectivity to 82% (entry 9). Although various approaches to further improve the reactivity of the transformation were conducted, the utilization of paraformaldehyde as hydrogen source proved to be insufficient to reach a satisfying level in terms of selectivity and activity for the synthesis of *Z*-alkenes. In fact, entry 10 implies that the semihydrogenation stagnates after 12 hours of reaction time. Consequentially, the results suggest that either the evolution of hydrogen is stopped at a certain point during the reaction or that the catalyst is deactivated during the

semihydrogenation process since the reaction outcome after 12 and 24 hours of reaction time only showed insignificant variation (entries 8 and 10). Thus, numerous alternative hydrogen sources were tested for their activity in the selective semihydrogenation of **26** by the PdCl₂/BuPAd₂-system in K₂CO₃/DMF/H₂O mixture. The solvents as well as the base and the catalytic system were not altered for the optimization of the semihydrogenation step in order to guarantee the compatibility with the Sonogashira coupling step.

Attempting to find other suitable hydrogen sources, different compounds were tested for their specific efficiency in the selective semihydrogenation with the catalytic system. While different hydrides as well as formic acid resulted in insufficient selectivity, the application of different alcohols offered no activity in the hydrogenation. Advantageously, hydrogen gas afforded the desired substance in satisfying yield and selectivity. Moreover, molecular hydrogen represents an efficient hydrogen source as no by-products are formed. For the implementation of the gas, the reaction solution was heated for 8 hours to 120 °C. Subsequently, the mixture was cooled down to room temperature and hydrogen gas was bubbled through the solution (Table 11).

Table 11. Optimization of the selective semihydrogenation applying hydrogen gas.

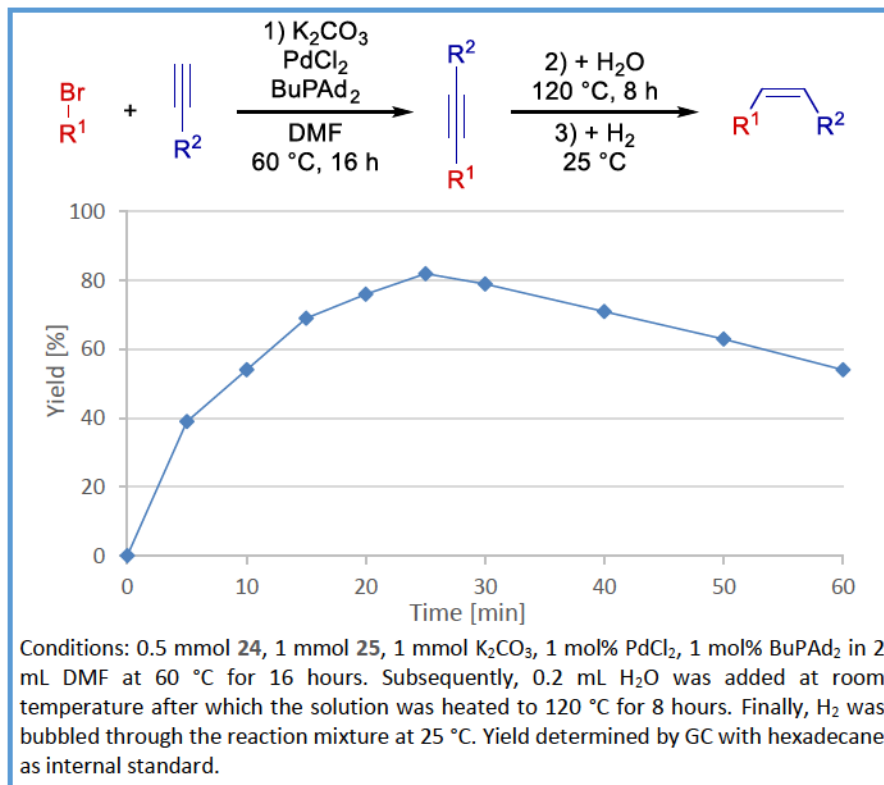
				28	29	30
Entry ^[a]	t ₁ [h]	t ₂ [min]	Conversion ^[b,c] [%]	Yield 28 ^[c] [%]	Z:E-Ratio ^[c] [%: %]	Selectivity 28 ^[d] [%]
1	8	150	>99	<1	-	-
2	8	80	>99	33	33:9	33
3	8	40	>99	80	80:8	80
4	8	20	>99	91	91:6	91
5	8	10	60	51	51:5	85
6	4	20	46	38	38:4	83
7	2	20	21	14	14:3	67
8	0	20	<1	<1	-	-

[a] Standard conditions (entry 4): 0.5 mmol **26**, 1 mmol K₂CO₃, 1 mol% PdCl₂, 1 mol% BuPAd₂, 2 mL DMF, 0.2 mL H₂O at 120 °C for 8 h. Subsequently, hydrogen gas was bubbled through the solution at 25 °C for 20 min at 0.5 mL/s gas flow.
 [b] Regarding **26**. [c] Determined by GC with hexadecane as internal standard. [d] Referring to the ratio of yield to conversion.

Herein, full conversion of the internal acetylene was achieved when the hydrogenation was conducted for 150 min. However, no detectable amounts of the target molecule were present in the reaction mixture (entry 1). Instead, the *Z*-alkene was completely hydrogenated to the corresponding alkane. Consequently, the product yield increased when the hydrogenation period was reduced. After 80 minutes of hydrogenation, the targeted product was synthesized in 33% yield at full conversion of the starting material (entry 2). Nevertheless, the *Z*:*E*-ratio as well as the *Z*-selectivity remained unsatisfying as the majority of the product was converted to the undesired alkane. These criteria were significantly improved by further shortening the hydrogenation period to 40 min. Thereby, the *Z*:*E*-ratio was enhanced to 80:8 at full conversion of the internal acetylene paired with an overall yield of 80 % (entry 3). After a hydrogenation period of 20 minutes, *Z*-alkene **28** was provided in 91% yield with a *Z*:*E*-ratio of 91:6 and complete consumption of the starting material (entry 4). Thus, the implementation of hydrogen gas as direct reducing agent offered the optimal procedure for the selective hydrogenation of the internal acetylene. Further experiments revealed that a hydrogenation period of 10 minutes failed to assure complete conversion of the starting material as 40% of the internal acetylene was detected in the reaction mixture (entry 5). Furthermore, the heterogenization period at 120 °C had to be conducted for 8 hours as the incomplete consumption of the reactant was observed when the heterogenization was decreased to 4 or 2 hours, respectively (entries 6 and 7). In these cases, the modification led to a diminished yield of 38% and 14% after 20 minutes of hydrogenation. Noteworthy, the product was not detected when the heterogenization period was eliminated (entry 8). Thus, the homogeneous palladium complex showed no activity in the hydrogenation of acetylenes utilizing hydrogen gas emphasizing the necessity of the presented catalyst transformation sequence.

As the next step, the isolated reaction steps were combined to a sequential one-pot protocol. For this purpose, the Sonogashira coupling was conducted under the conditions developed in the optimization of step 1 (Table 9, entry 7). Hereinafter, the optimal amount of water was added after the reaction cooled down to room temperature (Table 10, entry 5). Subsequently, the solution was heated to 120 °C for 8 hours in order to heterogenize the palladium catalyst. Following this step, the mixture was hydrogenated by passing the gas through the solution. Determining the optimal duration for the hydrogenation period, the reaction was executed while samples from the reaction solution were prepared in specific

intervals and analyzed for their content. The resulting yield over time sequence is displayed in Scheme 46. The optimal hydrogenation duration was determined at 25 minutes of hydrogen flow. Therefore, the results slightly differed from the semihydrogenation optimization demonstrated in Table 11.



Scheme 46. Product yield over time of the sequential one-pot synthesis.

Next, the activity of various terminal acetylenes and aryl bromides to generate the corresponding Z-alkenes was investigated utilizing the developed protocol (Table 12).

Table 12. Substrate scope of the Sonogashira-semihydrogenation.

$\text{Br}-\text{R}^1 + \text{R}^2\text{-C}\equiv\text{CH} \xrightarrow[\text{DMF, 60 }^\circ\text{C, 16 h}]{1) \text{ K}_2\text{CO}_3, \text{ PdCl}_2, \text{ BuPAd}_2} \text{R}^1\text{-C}\equiv\text{C-R}^2 \xrightarrow[\text{25 }^\circ\text{C, 20 min}]{2) + \text{H}_2\text{O, 120 }^\circ\text{C, 8 h; 3) + \text{H}_2} \text{R}^1\text{-CH=CH-R}^2$				
Entry ^[a]	Intermediate	Yield ^[b] Alkyne [%]	Z-Alkene	Yield ^[b] Alkene [%]
1		85		75
	31		32	

Table 12. Substrate scope of the Sonogashira-semihydrogenation.

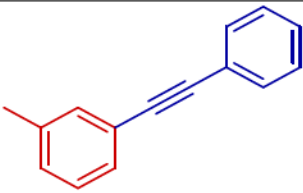
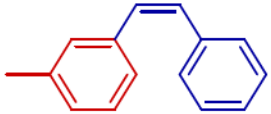
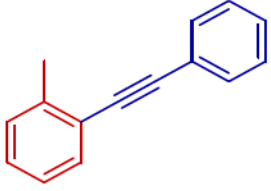
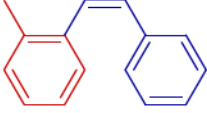
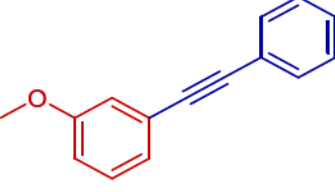

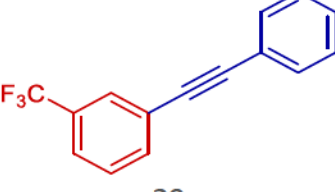
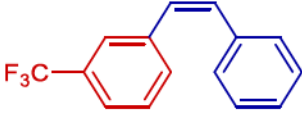
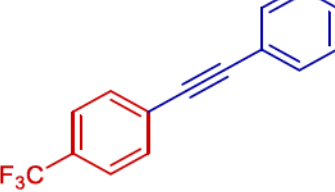

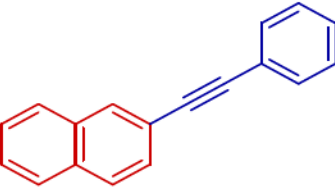

$ \begin{array}{c} \text{Br} \\ \\ \text{R}^1 \end{array} + \begin{array}{c} \text{R}^2 \\ \text{---} \\ \text{---} \\ \text{---} \end{array} \xrightarrow[\text{DMF, } 60^\circ\text{C, 16 h}]{\text{1) K}_2\text{CO}_3, \text{PdCl}_2, \text{BuPAd}_2} \begin{array}{c} \text{R}^2 \\ \text{---} \\ \text{---} \\ \\ \text{R}^1 \end{array} \xrightarrow[\text{25 }^\circ\text{C, 20 min}]{\text{2) + H}_2\text{O, 120 }^\circ\text{C, 8 h; 3) + H}_2} \begin{array}{c} \text{R}^1 \\ \text{---} \\ \text{---} \\ \text{---} \end{array} \text{R}^2 $				
Entry ^[a]	Intermediate	Yield ^[b] Alkyne [%]	Z-Alkene	Yield ^[b] Alkene [%]
2	 33	87	 34	75
3 ^[c]	 35	84	 36	72
4 ^[d]	 37	72	 38	68
5	 39	93	 40	83
6	 41	88	 42	79
7	 43	82	 44	72

Table 12. Substrate scope of the Sonogashira-semihydrogenation.

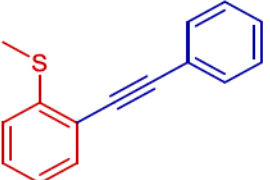

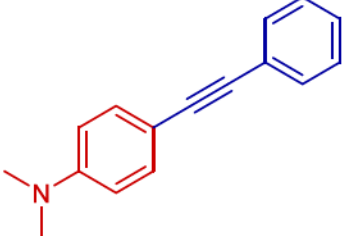
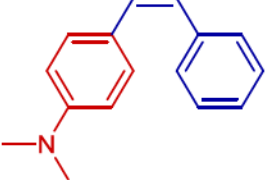
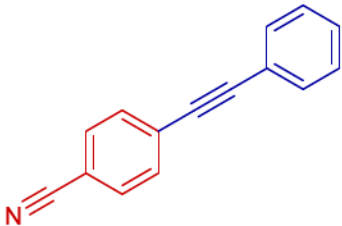
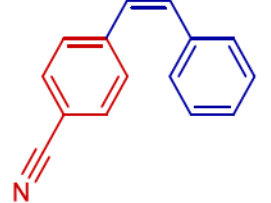
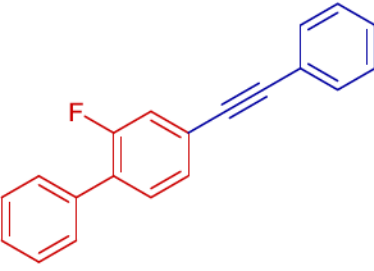
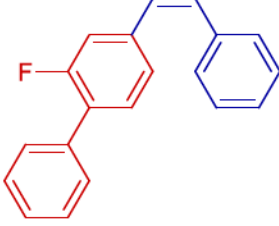
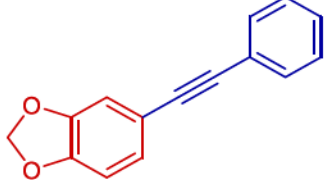
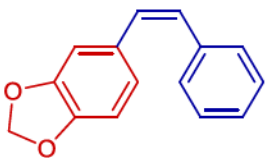
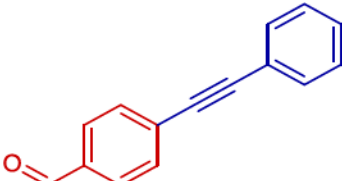
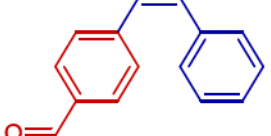
$ \begin{array}{c} \text{Br} \\ \\ \text{R}^1 \end{array} + \begin{array}{c} \text{R}^2 \\ \text{---} \\ \text{---} \\ \text{---} \end{array} \xrightarrow[\text{DMF, } 60^\circ\text{C, 16 h}]{\text{1) K}_2\text{CO}_3, \text{PdCl}_2, \text{BuPAd}_2} \begin{array}{c} \text{R}^2 \\ \text{---} \\ \text{---} \\ \\ \text{R}^1 \end{array} \xrightarrow[\text{25 }^\circ\text{C, 20 min}]{\text{2) + H}_2\text{O, 120 }^\circ\text{C, 8 h; 3) + H}_2} \begin{array}{c} \text{R}^1 \\ \text{---} \\ \text{---} \\ \text{---} \end{array} \text{R}^2 $				
Entry ^[a]	Intermediate	Yield ^[b] Alkyne [%]	Z-Alkene	Yield ^[b] Alkene [%]
8 ^[e]	 45	69	 46	35 ^[f]
9 ^[d]	 47	70	 48	41 ^[g]
10	 49	98	 50	84
11	 51	96	 52	86
12 ^[h]	 53	68	 54	64
13	 55	87	 56	0 ^[i]

Table 12. Substrate scope of the Sonogashira-semihydrogenation.

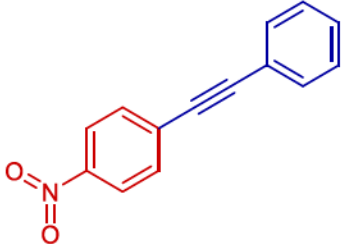
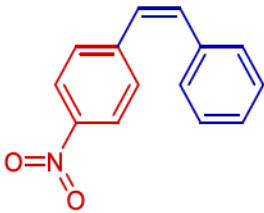
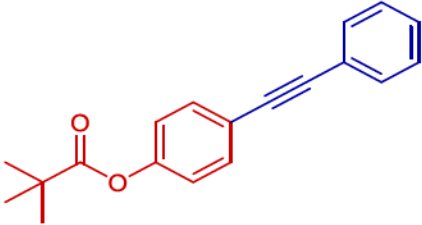
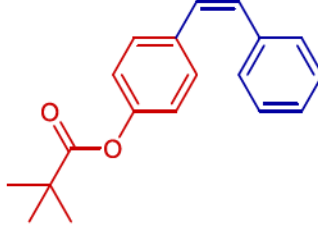
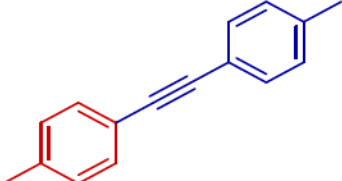
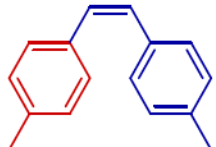
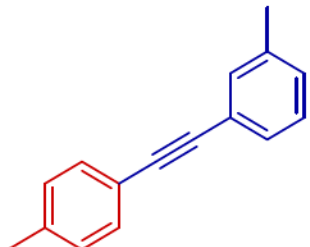
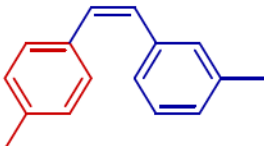
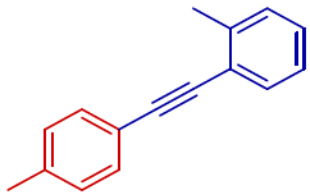
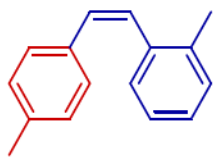
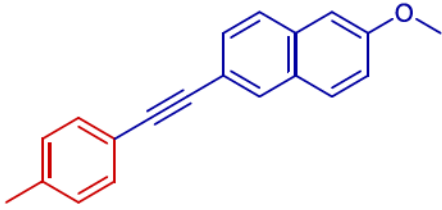
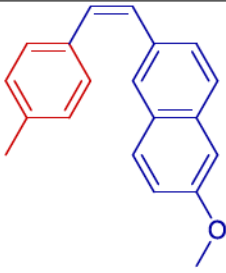
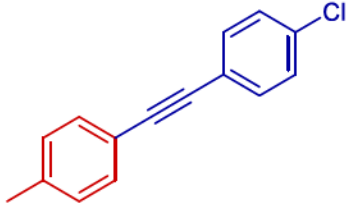
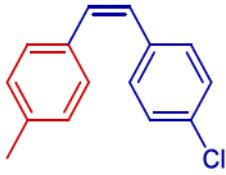
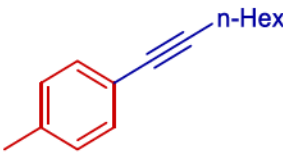
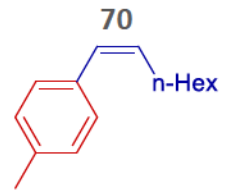
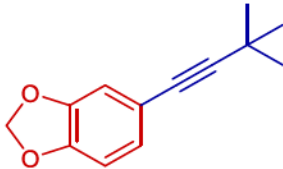
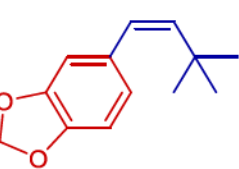
$ \begin{array}{c} \text{Br} \\ \\ \text{R}^1 \end{array} + \begin{array}{c} \text{R}^2 \\ \text{---} \\ \text{---} \\ \text{---} \end{array} \xrightarrow[\text{DMF, 60 } ^\circ\text{C, 16 h}]{\text{1) K}_2\text{CO}_3, \text{PdCl}_2, \text{BuPAd}_2} \begin{array}{c} \text{R}^2 \\ \\ \text{---} \\ \\ \text{R}^1 \end{array} \xrightarrow[\text{25 } ^\circ\text{C, 20 min}]{\text{2) + H}_2\text{O, 120 } ^\circ\text{C, 8 h; 3) + H}_2} \begin{array}{c} \text{R}^1 \text{---} \text{CH=CH} \text{---} \text{R}^2 \end{array} $				
Entry ^[a]	Intermediate	Yield ^[b] Alkyne [%]	Z-Alkene	Yield ^[b] Alkene [%]
14		83		0 ^[i]
15		86		0 ^[i]
16		82		76
17		84		76
18 ^[c]		80		71

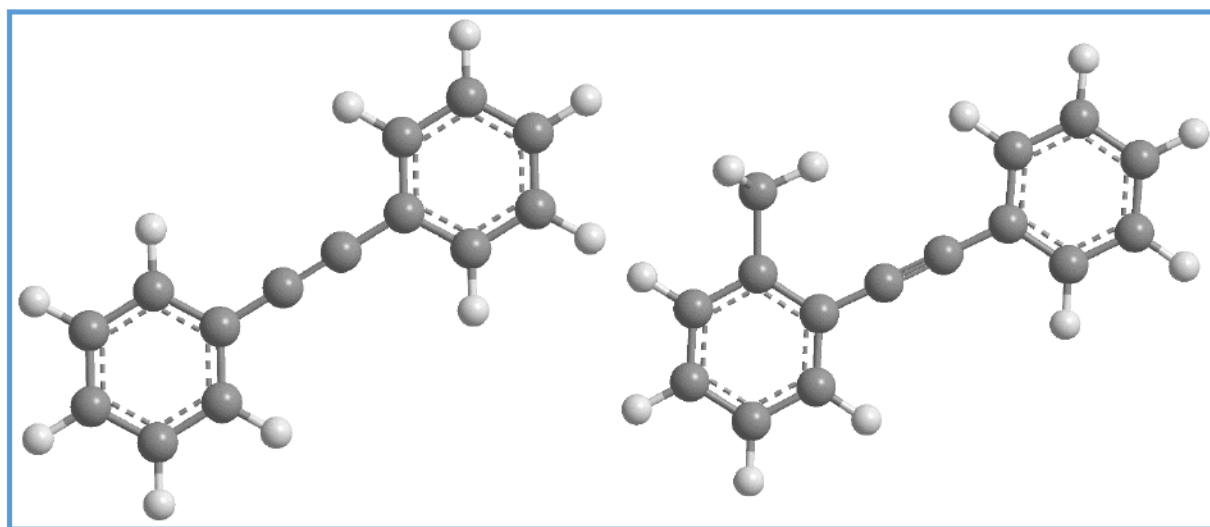
Table 12. Substrate scope of the Sonogashira-semihydrogenation.

$ \begin{array}{c} \text{Br} \\ \\ \text{R}^1 \end{array} + \begin{array}{c} \text{R}^2 \\ \text{---} \\ \text{---} \\ \text{---} \end{array} \xrightarrow[\text{DMF, 60 } ^\circ\text{C, 16 h}]{\text{1) K}_2\text{CO}_3, \text{PdCl}_2, \text{BuPAD}_2} \begin{array}{c} \text{R}^2 \\ \text{---} \\ \text{---} \\ \\ \text{R}^1 \end{array} \xrightarrow[\text{25 } ^\circ\text{C, 20 min}]{\text{2) + H}_2\text{O, 120 } ^\circ\text{C, 8 h; 3) + H}_2} \begin{array}{c} \text{R}^1 \text{---} \text{CH=CH} \text{---} \text{R}^2 \end{array} $				
Entry ^[a]	Intermediate	Yield ^[b] Alkyne [%]	Z-Alkene	Yield ^[b] Alkene [%]
19 ^[c]		90		85
20		80		0 ^[j]
21 ^[k]		75		52
22 ^[l]		69		34

[a] Standard conditions: 0.5 mmol aryl bromide, 1 mmol terminal acetylene, 1 mmol K₂CO₃, 1 mol% PdCl₂, 1 mol% BuPAD₂ in 2 mL DMF at 60 °C for 16 hours. Subsequently, 0.2 mL H₂O was added at room temperature followed by heating to 120 °C for 8 hours. Finally, H₂ was bubbled through the reaction mixture at 25 °C for 25 min. [b] Isolated yield. [c] 30 min hydrogenation. [d] 35 min hydrogenation. [e] 180 min hydrogenation. [f] Significant amounts of the intermediate remained unconverted [g] The isolated product contained significant amounts of the corresponding *E*-alkene which emerged to be inseparable from the desired product by preparative methods. [h] 40 min hydrogenation. [i] The resulting complex mixture was not further isolated [j] Despite prolonged hydrogenation, only insignificant amounts of the corresponding product were detected and not further isolated. [k] 80 min hydrogenation with 25 mol% 3,6-dithia-1,8-octanediole (DTOD) at 0 °C. [l] 20 min hydrogenation at 0 °C.

Herein, the elaborated reaction conditions were applied to the conversion of *ortho*-, *meta*- and *para*-methyl-substituted bromobenzenes with phenylacetylene to identify the influence of the substitution pattern. Entries 1 to 3 in Table 12 demonstrate that the corresponding intermediates **31**, **33** and **35** were synthesized in 85%, 87% and 84% overall yield, respectively. Consequently, no significant substituent effect on the Sonogashira coupling

was documented. Nonetheless, the final products were only offered in comparable yields when the hydrogenation period was adjusted. Thus, the compounds were afforded in similar yields of 75% (**32**), 75% (**34**) and 72% (**36**) when the duration of the hydrogenation of the ortho-substituted methyl bromobenzene was extended to 30 minutes. The prolonged hydrogenation period for the ortho-substituted bromotoluene was presumably reasoned by the steric hindrance of the methyl substituent (Scheme 47).



Scheme 47. Ball-and-stick models of tolan (left) and **35** (right).

Herein, the steric proximity to the reaction center limits the access of the catalyst surface to the C-C triple bond. As a result, the reaction rate is impeded. Thus, the semihydrogenation was significantly affected by the steric properties of the aryl bromide while the Sonogashira reaction demonstrated insignificant variation in relation to the substituents position. Furthermore, the electronic effect of the substituent was analyzed by conducting the reaction with an aryl bromide with electron-donating substituent and, for comparison, a starting material with electron-withdrawing group. Consequently, 3-trifluoromethyl-bromobenzene (entry 5) and 3-methoxy-bromobenzene (entry 4) were applied in the Sonogashira-semihydrogenation. In accordance with general findings,^[213,214] the electron-withdrawing trifluoromethyl group increases the activity of the aryl bromide in the Sonogashira coupling as 93% of the corresponding intermediate **39** were synthesized. In contrast, only 72% of the internal alkyne **37** containing the methoxy group was found which confirms the tendency of electron-donating groups to inhibit coupling reactions. Moreover, the hydrogenation of the intermediates **37** and **39** towards the *Z*-alkenes **38** and **40** was affected by the electronic properties as well. Herein, the internal alkyne containing the electron-withdrawing group was entirely hydrogenated to the product **40** after 25 minutes in

83% yield (entry 5) while the electron-donating methoxy substituent caused a decline in the reaction rate of the semihydrogenation. Thus, the hydrogenation period for compound **37** had to be extended to 35 minutes in order to achieve 68% yield (entry 4). During the investigation of the substrate scope, the tendency of coordinating functional groups to necessitate extended hydrogenation periods was observed in multiple cases (entries 4, 8, 9, 12 and 19). In general, the duration of the hydrogenation had to be prolonged for substrates incorporating coordinating groups such as methoxy, thiomethoxy and amine functionalities. In addition, the hydrogenation period had to be varied to identify the optimal duration in dependency on the electronic and steric properties of the alkyne. Extending the substrate scope, the reactivity of 4-trifluoromethyl-bromobenzene was examined for the two reaction steps (entry 6). Employing this specific aryl bromide, the conversions afforded 88% of the internal alkyne **41** and 79% of the *Z*-alkene **42**. 2-Bromonaphthalene was successfully tested when the internal alkyne **43** was provided in 82% overall yield while the hydrogenation product **44** was afforded in 72% yield (entry 7). Moreover, the thiomethoxy containing starting material was converted to the corresponding alkyne **45** with an overall yield of 69% (entry 8). Due to the sulfur containing functionality, the hydrogenation period had to be prolonged to 3 hours to give the final product **46** in 35%. Still, the resulting reaction mixture contained significant amounts of the intermediate **45**. Herein, the thiomethoxy group represents a severe example for the effect of coordinating functionalities on the hydrogenation. Moreover, the conversion of 4-dimethylamino-bromobenzene gave 70% of the internal alkyne **47** whereas the final product **48** was afforded in 41% overall yield upon hydrogenation (entry 9). Nevertheless, the obtained compound further incorporated 15% *E*-alkene which emerged to be inseparable from the desired *Z*-alkene by preparative methods. Thus, this starting material gave the most unsatisfying *Z*:*E*-ratio with 85:15. Furthermore, 4-bromo-benzonitrile was applied in the Sonogashira coupling to afford the internal alkyne **49** in 98% overall yield while the subsequent semihydrogenation gave the desired product **50** in 84% (entry 10). In addition, the result for the Sonogashira reaction further emphasizes the tendency of electron-withdrawing groups to improve the results for the aryl bromide coupling. Continuing the study, 4-phenyl-3-fluoro-bromobenzene was examined in the conversion to the internal acetylene **51** as well as the *Z*-alkene **52** and identified both desired substances to be synthesized in 96% (**51**) and 86% (**52**) (entry 11). Expanding the substrate scope, the intermediate **53** was generated in 68% yield whereas the corresponding final

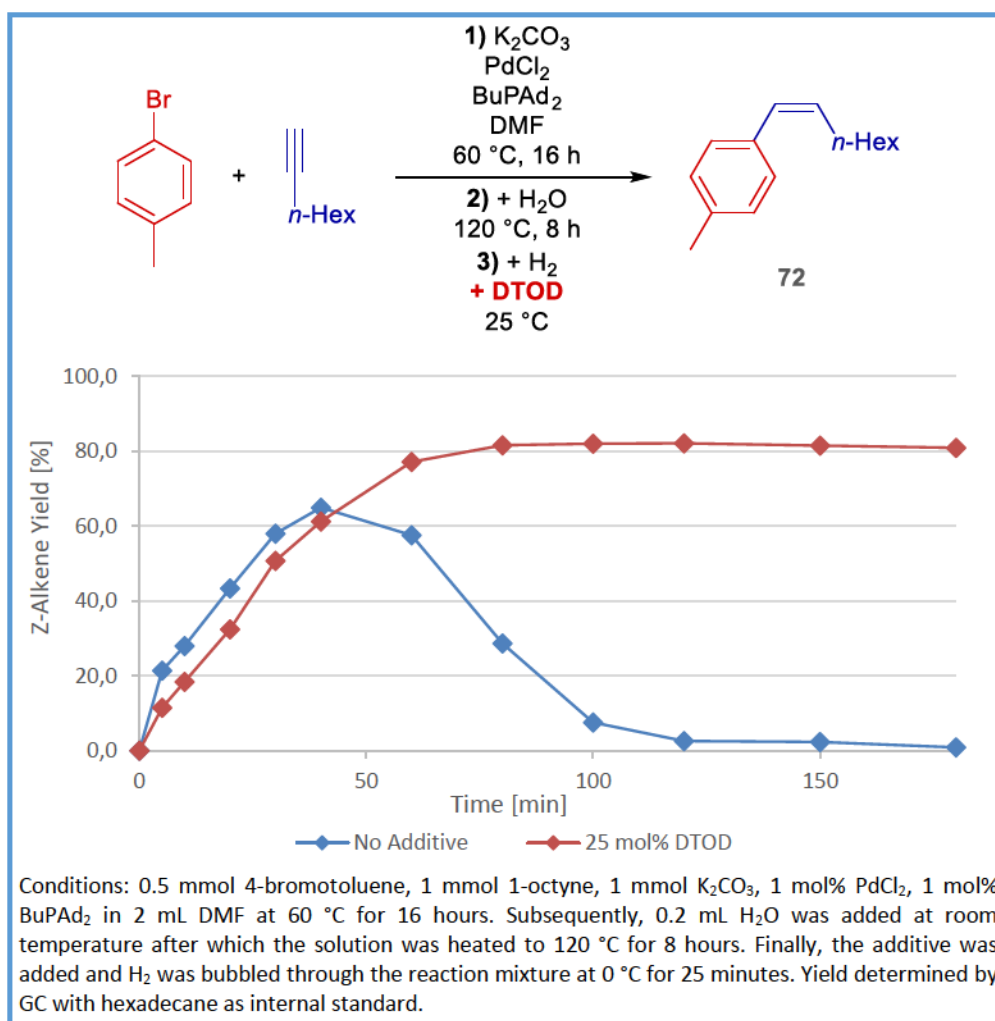
product **54** was afforded in 64% overall yield (entry 12). Noteworthy, a number of substrates with specific functionalities failed to give the targeted products. Herein, aldehyde- and nitro-containing aryl bromides successfully gave the associated internal alkynes **55** and **57** in 87% and 83% overall yield, respectively (entries 13 and 14). However, the subsequent hydrogenation offered a complex mixture of various products including alkanes, alkenes and alkynes containing either reduced or non-reduced aldehyde- or nitro-functionalities and its intermediates. Thus, substrates containing easily reducible functional groups represent challenging and problematic compounds as the heterogeneous palladium acts as potent hydrogenation catalyst. However, while readily reducible functionalities such as nitro or aldehyde groups were hydrogenated, functional groups such as nitriles possess higher activation barriers which results in inert behavior towards hydrogenation as evidenced by product **50**. Utilizing a pivaloyl-containing ester, the internal alkyne **59** was isolated in 86% yield (entry 15). However, the intermediate decomposed during the heterogenization by partial hydrolysis due to the basic aqueous medium at elevated temperature. Consequently, a complex mixture of hydrolyzed, non-hydrolyzed, reduced and non-reduced compounds was obtained and not further analyzed by work-up. Therefore, the starting materials and intermediates have to fulfill three main requirements to be convertible to Z-alkenes by the novel methodology.

1. The functional groups have to be tolerated by the Sonogashira coupling conditions.
2. The functionalities have to be inert to the basic aqueous conditions of the heterogenization at high temperatures.
3. The characteristics have to be inert to the hydrogenation conditions in the final reaction step.

As presented in the substrate scope, a broad variety of starting materials meet these criteria, thus emphasizing the various possible applications of the novel methodology.

In addition, the reactivity of various acetylenes with the innovative methodology was examined. Herein, the effect of substituents was investigated similar to the experiments in entries 1 to 3. Therefore, *ortho*-, *meta*- and *para*-methyl substituted phenyl acetylene were employed as starting materials for the conversion with 4-bromotoluene (entries 16 to 18). Regarding the Sonogashira coupling, a marginal position effect was observed as the corresponding intermediates **61**, **63** and **65** were obtained in 82%, 84% and 80% yield, respectively. Instead, the described *ortho*-effect of functional groups displaying steric

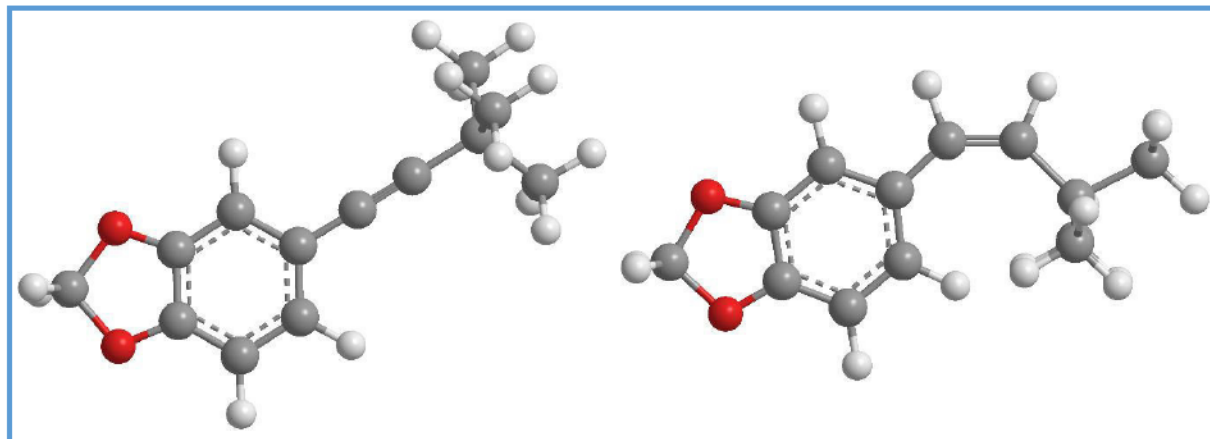
proximity to the C-C triple bond was observed for the terminal alkyne as well. Due to the impeded hydrogenation, the application of 2-methylphenylacetylene led to 71% of the desired Z-alkene **66** after the hydrogenation period was adjusted to 30 minutes. After 25 minutes of hydrogenation, both compounds **62** and **64** were received in 76% yield. Moreover, the transformation of 4-bromotoluene with 2-methoxy-6-ethynyl-naphthalene resulted in an isolated yield of 90% of the intermediate **67** while the final product **68** was obtained in 85% overall yield (entry 19). Unfortunately, 4-chloro-phenylacetylene denied the conversion to the final product **70** upon hydrogenation while the Sonogashira reaction proceeded smoothly under the formation of 80% of the intermediate **69** (entry 20). Despite numerous attempts under various conditions, the selective hydrogenation of the C-C triple bond was not achieved. Although minor amounts of the desired compound were detected by GC-MS, the manipulations failed to give full conversion of the intermediate **69**. Instead, the conversion maximum reached 10% after 60 minutes of hydrogen flow. Noteworthy, the reaction of 4-bromotoluene with 1-octyne offered the internal alkyne **71** in 75% yield (entry 21). However, the initial test for the hydrogenation step suggested that the selectivity of the reduction remained unsatisfying although promising. Most importantly, the targeted Z-alkene **72** was produced and identified by analytical methods. Nevertheless, the Z-selectivity reached only 58% under slightly modified conditions at 0 °C. While the majority of the remaining material was already converted to the corresponding alkane, traces of the intermediate **71** were still present in the reaction mixture. In order to improve the performance especially in regard to the chemoselectivity, the desired transformation was performed under the influence of 3,6-dithia-1,8-octanediole (DTOD), also referred to as *Lindlar Catalyst Poison*,^[301] as additive. Herein, a positive effect of this additive on the chemoselectivity was observed which allowed the synthesis of the final product **72** in 52% isolated yield. Moreover, the Z-alkene was generated with 80% Z-selectivity. Furthermore, the synthesis proceeded more practically as the additive suppressed the over-hydrogenation of the desired product towards the alkane. The results of both experiments are depicted in Scheme 48 for comparison.



Scheme 48. Influence of DTOD in the semihydrogenation step of internal acetylene 71.

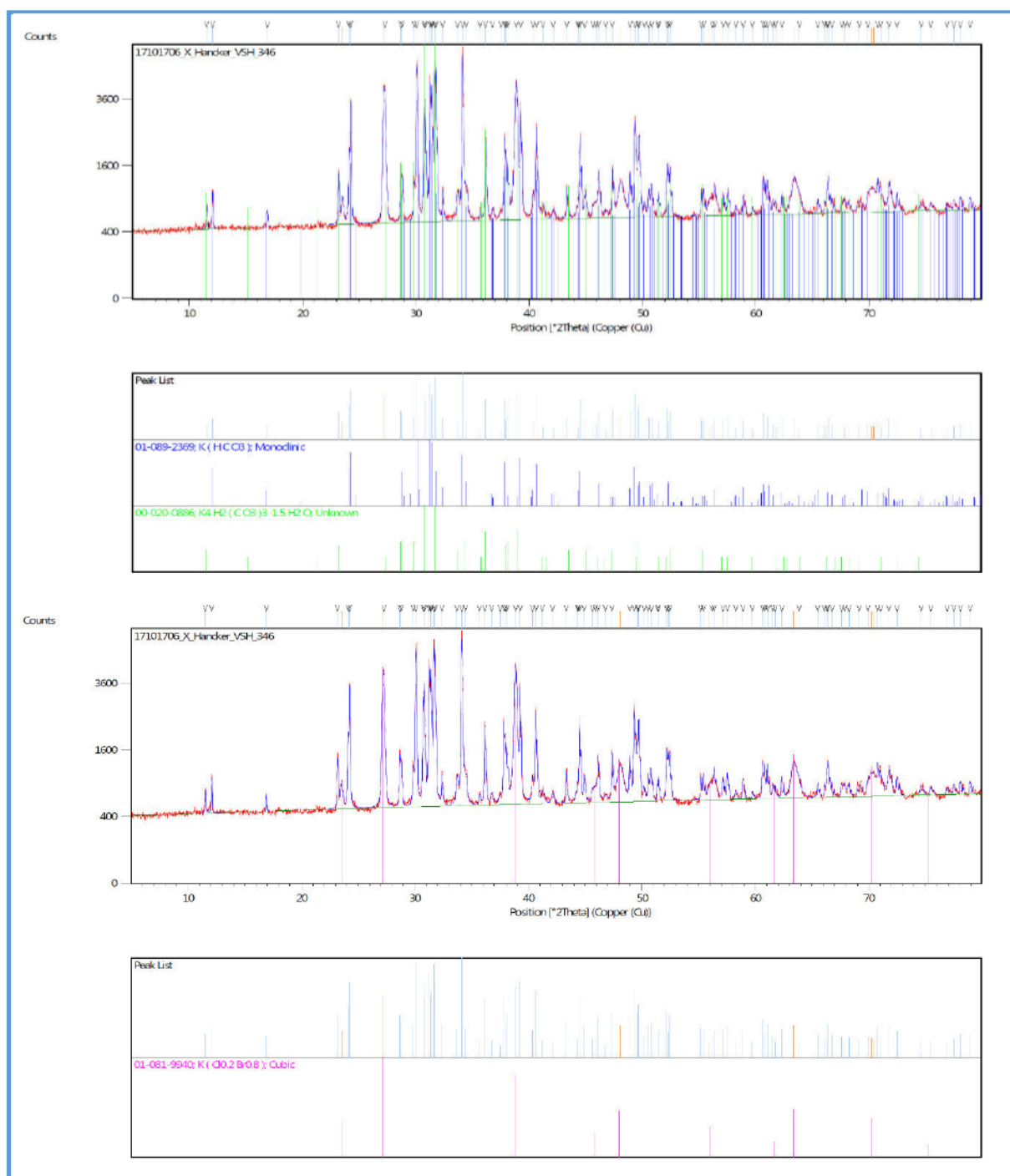
Thus, terminal alkyl-substituted alkynes are convertible to the corresponding Z-alkenes by the novel methodology under assistance of the additive DTOD as well. Nonetheless, the formation of the corresponding product from 1-bromo-3,4-(methylenedioxy)benzene and *t*-butyl acetylene was almost completely prevented when the additive was applied. Instead, the desired compound **74** was obtained in 34% overall yield when the experiment was conducted at $0\text{ }^\circ\text{C}$. In this case, two opposite tendencies reason the reactivity of this specific substrate. On the one hand, the alkyl substitution increases the electron density of the C-C triple bond which improves the reaction rate of the hydrogenation. Therefore, the reaction proceeds faster at lower temperatures as observed for the internal alkyne **71**. On the other hand, the steric hindrance caused by the *t*-butyl group reasons an increased activation barrier which reduces the reaction rate as observed for the intermediates **36**, **46** and **66** (Table 12). Consequently, the addition of DTOD to the reaction with *t*-butyl acetylene poisoned the catalyst and therefore further inhibited the conversion of the resulting alkyne **73** towards the Z-alkene **74**. However, when the internal alkyne was transformed to the corresponding

Z-alkene, the product was hydrogenated to the alkane faster since the activation barrier of the Z-alkene towards hydrogenation is lowered due to the steric constitution of the Z-alkene. For comparison, the compounds **73** and **74** are displayed in Scheme 49 to illustrate the steric access to the C-C triple and double bond, respectively.



Scheme 49. Ball-and-stick models of compounds **73** (left) and **74** (right).

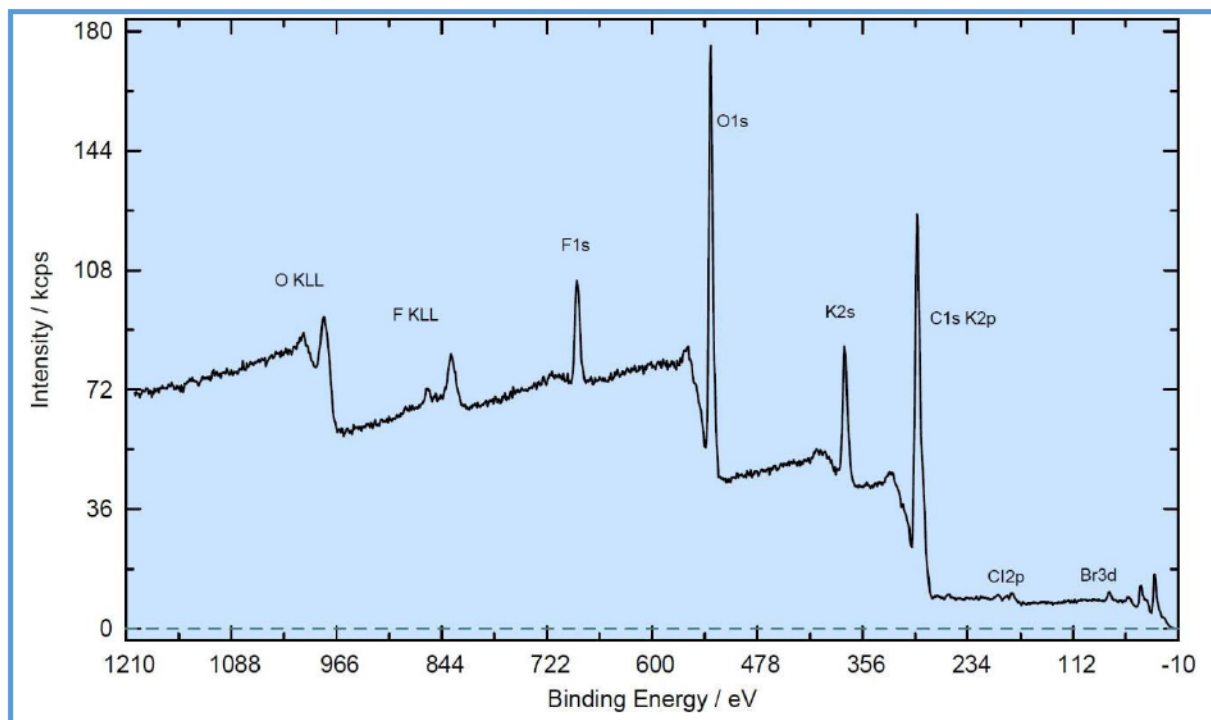
In order to further extend the understanding of the ongoing process, the heterogeneous compounds were isolated after each reaction step and analyzed by ICP-OES for its palladium content. In addition, the solvent was removed from the remaining homogeneous solution and ICP-OES analysis of the residue was conducted as well. The experiments suggested that the transition metal still exists as homogeneous complex after the Sonogashira coupling step as no palladium was observed in the heterogeneous residue while 94% of the originally employed amount was found in the sample prepared from the solution. In contrast, the samples prepared after the heterogenization step under aqueous conditions at elevated temperatures contained 26% of the applied palladium whereas the residue from the homogeneous solution incorporated 69% of the theoretical palladium amount. Apparently, the homogeneous complex is not completely converted to a heterogeneous species after the second reaction step. However, since significant amounts of the transition metal were found in the solid phase, a heterogeneous catalyst was formed during this step. Therefore, this step is described as *heterogenization*. Consequently, similar results were obtained from the samples prepared after the hydrogenation as 29% of the palladium was detected in the heterogeneous material while 68% remained in the solution residue. Moreover, the solid phase obtained after the hydrogenation was further analyzed by XRD and XPS methodologies to improve the understanding of the nature of the *in situ* formed catalyst. The results from the XRD-investigation are displayed in Scheme 50.



Scheme 50. XRD-analysis of the heterogeneous material obtained after the hydrogenation process.

Herein, the investigation supported the expectation that the majority of the heterogeneous material consisted of a K_2CO_3 - $KHCO_3$ mixture while the methodology detected potassium bromide impurities and residual potassium chloride as well. Precisely, a comparison of the generated diffractogram with the ICDD-database suggested correlation between the obtained data and the characteristics of monoclinic $KHCO_3$, $K_4H_2(CO_3)_3 \cdot 1.5H_2O$ and $KBr_{0.8}Cl_{0.2}$. Unfortunately, the analysis did not reveal further information on the nature of the palladium catalyst since the concentration of the transition metal in the solid was too low for

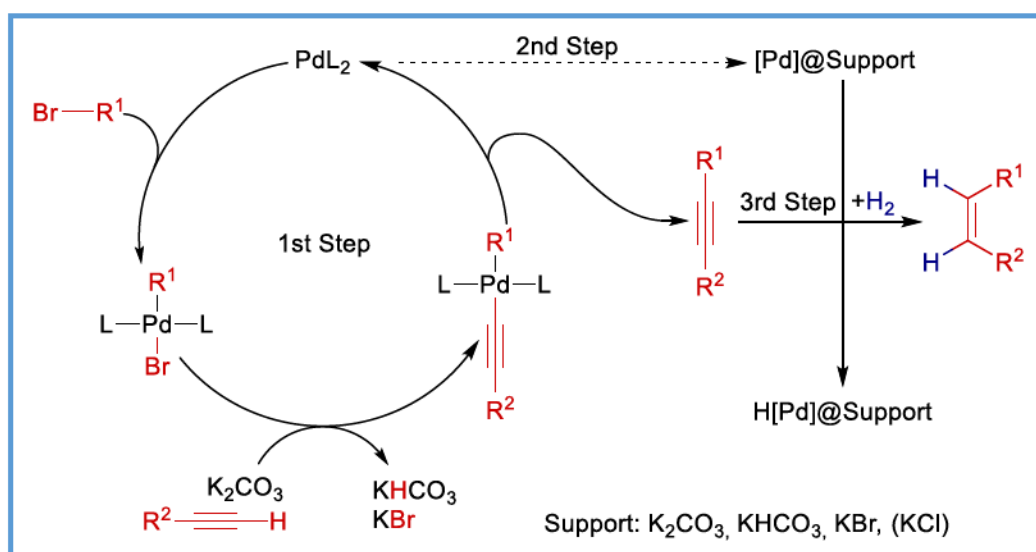
the employed analytical method. Furthermore, XPS-analysis of the synthesized material was conducted (Scheme 51).



Scheme 51. XPS-spectra of the heterogeneous material obtained after the hydrogenation process.

Unfortunately, the XPS-analysis only confirmed the composition of the substance to be mainly oxygen ($O_{1s} = 532$ eV), carbon ($C_{1s} = 289$ eV) and potassium ($K_{2p} = 293$ eV; $K_{2s} = 378$ eV) with trace quantities of bromine ($Br_{3d} = 69$ eV) and chlorine ($Cl_{2p} = 199$ eV). Organic fluorine is commonly observed as surface contamination from *e.g.* PFPE or PTFE.

Based on these results, the mechanism illustrated in Scheme 52 is postulated.



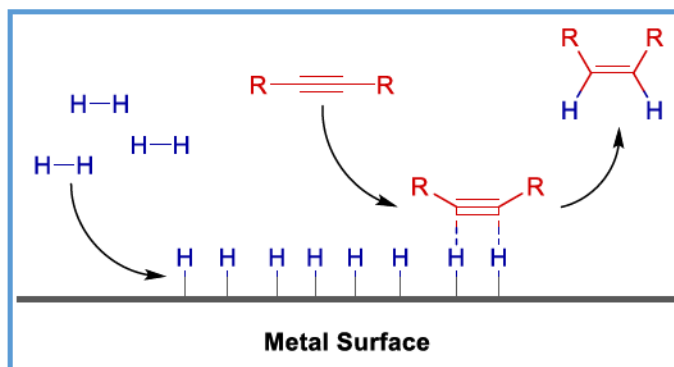
Scheme 52. Postulated mechanism for the sequential Sonogashira-semihydrogenation.

Initially, the generation of the catalytically active, homogeneous palladium complex is achieved by coordination of the BuPAD₂-ligand to the metal center. Noteworthy, the exact

characteristics of this complex remain undetermined. However, literature findings and discussions suggest the formation of di- and even more active mono-coordinated palladium complexes for bulky electron-rich phosphine ligands in cross coupling reactions.^[302,303] The active catalyst adds the aryl bromide by oxidative addition into the C-Br bond generating the organopalladium complex. Subsequently, the formed complex is converted into the organopalladium acetylide complex by initially coordinating the acetylene *via* the C-C triple bond following deprotonation assisted by the base K_2CO_3 to give the palladium acetylide. Overall, this process exchanges the bromide resulting from the oxidative addition with the acetylide. Moreover, the deprotonation of the acetylene converts the K_2CO_3 to $KHCO_3$ and potassium bromide, thus forming two of the materials found in the heterogeneous catalysts support. Hereupon, the internal acetylene is released from the organopalladium complex by reductive elimination of the aryl and acetylide moiety. Hereby, the catalytically active species is restored to initiate the next catalytic cycle. Essentially, these sequences constitute the first step of the one-pot procedure.

After step 1, the heterogenization of the homogeneous catalyst is accomplished by adding water to the reaction solution and heating the resulting mixture to 120 °C for 8 hours. However, the exact processes of the heterogenization remain speculative. In this regard, the presence of water appears essential as evidenced by Table 10. While an excess of water leads to the dissolution of the K_2CO_3 - $KHCO_3$ -KBr-KCl mixture and therefore to the dissolution of the required heterogeneous catalysts support since all described potassium salts are water soluble. During this process, the synthesized internal alkyne remains unconverted in the reaction solution and thus has to be inert to the basic aqueous conditions at elevated temperatures.

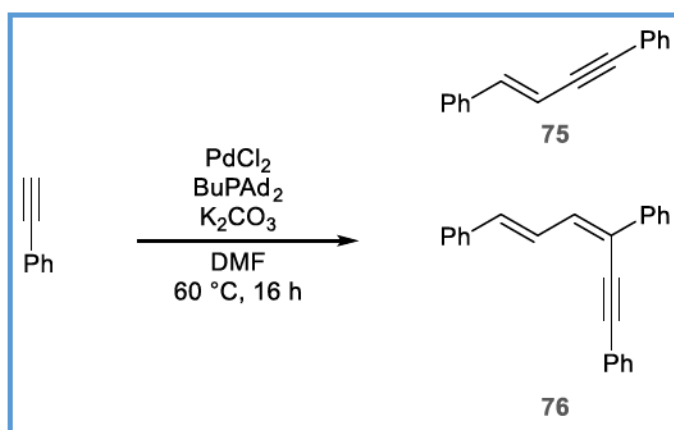
The generated heterogeneous catalyst is applied in the final step of the one-pot Sonogashira-semihydrogenation. Through hydrogen gas, the catalyst is activated by reduction and the internal alkyne is selectively hydrogenated to the corresponding Z-alkene *via* a standard heterogeneous hydrogenation mechanism. Herein, the surface structure of the catalyst allows for the reduction towards the desired Z-alkenes but prevents the over-hydrogenation to the corresponding alkanes. As expected, the heterogeneous hydrogenation suppresses the formation of the thermodynamically favored E-alkenes as the mechanism proceeds *via syn*-addition (Scheme 53).



Scheme 53. Mechanism for the heterogeneous *syn*-addition.

Herein, the hydrogen adds to the metal surface due to the strong tendency of palladium to form metal hydrides. In a sequential step, the alkyne is coordinating to the surface and reduced by transfer of two hydrogen atoms to the C-C triple bond. Since the atoms are added to the same side of the alkyne, the corresponding *Z*-alkene is generated with both hydrogen atoms placed on the same side of the C-C bond (*syn*-addition).

As earlier described, the reaction requires a significant excess of the employed terminal alkyne to proceed with satisfying conversion and yield of the desired internal alkyne. Despite various efforts, the necessary excess was not significantly reduced. In order to better understand the problematic side reactions, the conversion of phenylacetylene by the catalytic system was further analyzed by GC-MS to identify by-products. Thereby, two undesired major side products were found (Scheme 54).

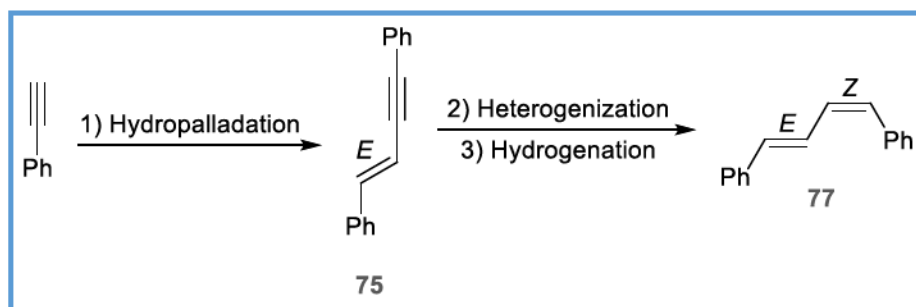


Scheme 54. Arylacetylene side-reaction.

Interestingly, the two observed side products stemmed from dimerization reactions since the molecules displayed the twice (75) and triple (76) mass of phenylacetylene as molecular peak in GC-MS analyses. While the dimerization of phenylacetylene towards the corresponding enyne by various transition metals including electron-rich palladium complexes has been documented in the literature,^[304-307] the trimerization towards the

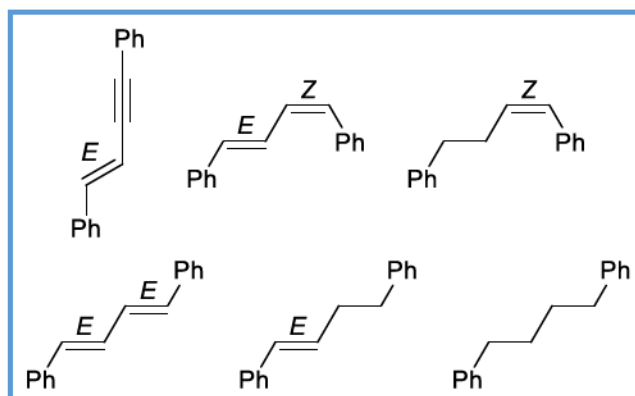
associated conjugated dienyne has only been reported to be facilitated by a specific cobalt catalyst once.

However, the hydropalladation of phenylacetylene towards the corresponding enyne **75** offers the possibility to synthesize the associated *E-Z*-dienes *via* the developed methodology according to Scheme 55.



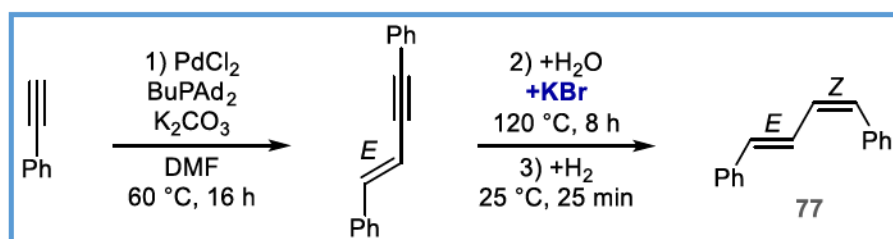
Scheme 55. Synthesis of *E-Z*-dienes *via* the novel methodology.

Noteworthy, the initial experiment employing the well-known reaction system including the catalysts and K_2CO_3 in DMF gave a complex mixture with undesired over-hydrogenated compounds as major products. Albeit, the desired compound **77** was formed as a minor by-product. However, the conversion yielded all displayed compounds (Scheme 56).



Scheme 56. Products from the initial attempt to generate *E-Z*-dienes.

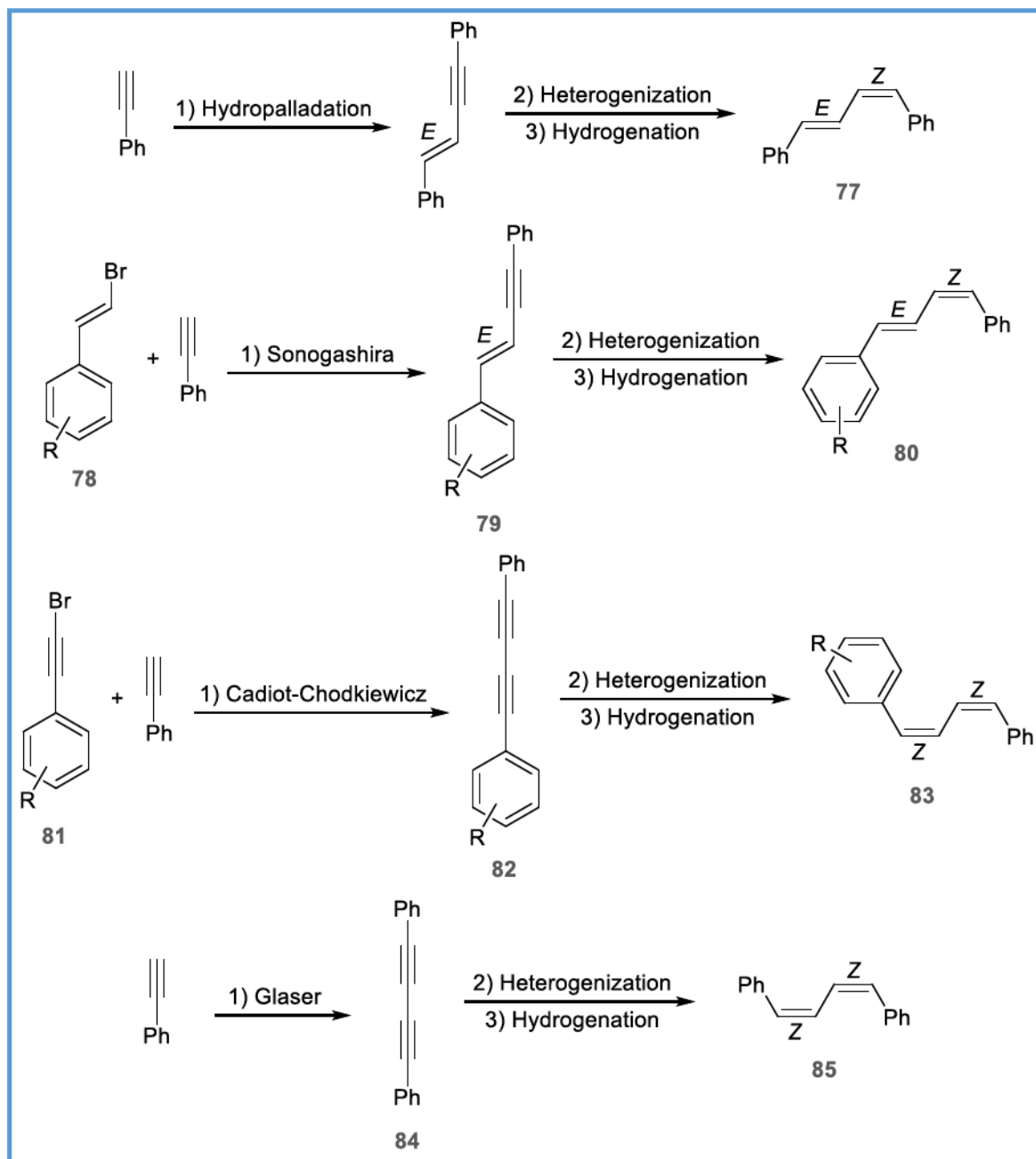
However, the desired *E-Z*-diene **77** was obtained as major product when potassium bromide was added prior to the second step.



Scheme 57. Synthesis of *E-Z*-dienes *via* the novel methodology.

This indicates the importance of the generated potassium halide for the selectivity of the *in situ* formed heterogenous catalyst in the original reaction of aryl bromides with terminal

acetylenes. With additional potassium bromide, the synthesis of the *E-Z*-diene **77** as major product was achieved while the displayed by-products (Scheme 56) were detected by GC-MS as well. The additional C-C double bond results in an increased number of possible hydrogenation products which further increases the demands for the catalysts selectivity. Nevertheless, the novel protocol offers access to the otherwise difficult to synthesize *E-Z*-dienes. In this regard, the new methodology further allows for additional transformations (Scheme 58).



Scheme 58. Synthetic pathways available by the novel Sonogashira-Semihydrogenation protocol.

As a part of an initial investigation of the possible synthetic pathways, the reaction of bromo-*E*-alkene **78** with phenylacetylene under Sonogashira coupling conditions provided

the corresponding asymmetric enyne **79**. Moreover, the subsequent heterogenization and hydrogenation generated the desired asymmetric *E-Z*-diene **80** as major product. However, as no extensive optimization was conducted, the selectivity remained at improvable levels. Furthermore, the catalytic system of PdCl₂ and BuPAd₂ enabled the transformation of phenylacetylene with bromoalkyne **81** according to Cadiot-Chodkiewicz to give the corresponding diyne **82**. Upon heterogenization and hydrogenation, the associated asymmetric *Z-Z*-diene **83** was identified by GC-MS analyses as one main product in a complex mixture of compounds. Unfortunately, the Glaser-type coupling of phenylacetylene failed to give the associated symmetric diyne **84** when the established catalytic system was employed under atmospheric conditions. However, literature findings indicate that Pd(II) salts in combination with polar aprotic solvents and inorganic carbonates as well as benzoquinone as oxidizing agent offer access to the corresponding symmetric diynes.^[308] Thus, a modification of the developed protocol offers to give the desired compounds and enable the subsequent heterogenization and hydrogenation towards the symmetric diene **85**. Overall, the elaborated methodology can be extended to the synthesis of complex conjugated structures which otherwise require demanding multi-step syntheses.

4.4. Outlook

Regarding the developed synthesis of Z-alkenes, the focus of continuative studies is set on the minimization of the necessary phenylacetylene concentration in order to increase the efficiency of the overall process. Therefore, especially the screening for more selective (phosphine) ligands displays a promising approach. Since the applied phosphine ligand is assumed to insignificantly influence the following steps two and three, these processes of the one-pot procedure will be insignificantly affected by the replacement of BuPAd₂. On the other hand, the literature on copper- and amine-free Sonogashira coupling reactions suggests that this type of conversions requires electron-rich palladium complexes which benefit the alkyne dimerization as well. Thus, any efficient ligand supporting the additive-free Sonogashira coupling presumably leads to the formation of the undesired dimerization product. Therefore, the implementation of a copper mediated Sonogashira coupling offers the possibility of an improved efficiency regarding the required phenylacetylene concentration while the hydrogenative abilities of the resulting heterogenous Cu-Pd catalyst have to be determined for its support of the selective semihydrogenation since copper-based Z-alkene-selective catalysts have been described as well.^[240]

Moreover, the improvement and reduction of the heterogenization period constitutes a central aspect of further investigations. Herein, the drastic reduction of the duration of the second step is desired in order to increase the efficiency of the overall process. More importantly, the effectivity of the heterogenization requires improvement since only 26% of the employed palladium is found in the heterogenous material after the second step. Thus, the majority of the transition metal is still present as homogeneous complex. Thereby, the recyclability and reusability of the expensive catalyst is impeded since the recovering of the dissolved palladium demands more sophisticated techniques while the solids can be filtered off the reaction mixture or separated by centrifugation without significant difficulties. To achieve a complete heterogenization, different approaches have to be tested for their effect on the process. Herein, various additives have to be tested to identify pathways to accelerate the heterogenization. Alternatively, the discharge of oxygen to the solution before the second reaction step leads to the oxidation of the BuPAd₂-ligand. While the bulky phosphine is inert to atmospheric oxygen as a solid, the ligand is rapidly oxidized in solution. Consequently, this suggests that the presence of the phosphine prevents the precipitation of

the transition metal under argon atmosphere by coordinating and thus shielding the metal center. Furthermore, the application of oxidizing additives offers the possibility to increase the precipitation rate of the heterogenization. However, the desired internal alkyne has to be inert to the employed oxidizing agent. Nevertheless, the resulting catalyst is required to be tested for its efficiency and selectivity in the subsequent hydrogenation since all alterations might affect the catalyst performance.

In addition, the improvement of the semihydrogenation selectivity is the subject of further investigations. For the described methodology, the Z-alkene is favored by the heterogeneous hydrogenation and the surface structure of the catalyst which inhibits the over-hydrogenation. However, especially the over-hydrogenation is not entirely prevented. Unfortunately, especially when the internal alkyne is completely converted, the hydrogenation rate for the desired product increases. Noteworthy, this circumstance is illustrated in Scheme 48. Without the additive DTOD, the Z-alkene is further hydrogenated to the corresponding alkane as soon as the concentration of the reactant accounts for less than 10% of the original amount. While the effect was observed for all employed starting materials, the aryl-alkyl-alkynes demonstrated a more drastic over-hydrogenation. Advantageously, the additive DTOD successfully suppressed the over-hydrogenation in the case of compound **71** almost entirely (Scheme 48). Nevertheless, the application of this substance prevented the semihydrogenation for the diaryl-acetylenes completely. Thus, the inhibiting characteristics of the sulfur-containing compound emerged to be too severe for the majority of the tested substances. Herein, the investigation of other additives for their selectivity improving characteristics offers the possibility to improve the overall yield and efficiency. Moreover, the selectivity of the catalyst is affected by the addition of additives to the heterogenization process.

5. Summary

In conclusion, novel reaction conditions for the synthesis of α -substituted esters from acetates and primary alcohols catalyzed by the Fe-MACHO-BH complex have been developed. Although the yield of the corresponding product remained at insufficient levels, the product was characterized by NMR and GC-MS.

In addition, the critical aspect of the alkylation of methyl valerate to methyl valproate by iridium complex **1** was identified to originate from the pre-existing α -alkylation of the substrate. Moreover, the reproduction of the optimization experiment from literature findings was achieved and the feasibility of the reaction with *n*-propanol was proven as well. While the desired transformation towards methyl valproate failed, it was shown that the alkylation of ethyl esters proceeded despite transesterification and the resulting product mixture.

Unfortunately, the well-established Fe-MACHO-BH catalyst could not successfully be applied to the conversion of several C-H-acidic compounds with primary alcohols. Nevertheless, the presence of the important corresponding aldehydes in the reaction solutions was proven for the targeted reactions. In contrast, the associated aldehydes performed the desired condensation under hydrogen autotransfer conditions. Thereby, the general dehydrogenation activity was observed while the condensation of the substrates was identified as crucial and failing intermediate step.

Aside from the investigation into the hydrogen autotransfer methodology, the development of a heterogeneously palladium-catalyzed amidocarbonylation of N-methyldodecanamide towards N-lauroyl sarcosine was achieved. Herein, the necessary additive loading was reduced to 2.5 mol% of lithium bromide which constitutes a significant decrease compared to the originally applied 35 mol%. Although the concentration of sulfuric acid had to be increased, the development represents a major improvement in regard to the economic efficiency of a theoretical industrial process since the additive's costs exceed the expenses for sulfuric acid drastically.

Despite a decreasing selectivity, the general recyclability and reusability of the catalyst was proven by recycling experiments indicating a reaction outcome decrease of 10% yield per run. As physical material loss influences small scale experiments more drastically than conversions on increased scales, this effect diminishes on multi g-scales. In this regard, the

conversion was conducted on a 10 g-scale resulting in an excellent yield of 95% upon isolation. Nevertheless, trace metal analyses indicate and emphasize the problematic removal of residual amounts of palladium from the product.

Moreover, the selective synthesis of Z-alkenes from aryl bromides and terminal acetylenes in a sequential one-pot procedure *via* homogeneously catalyzed Sonogashira coupling and subsequent selective semihydrogenation by the heterogenized catalyst was developed. Thereby, the expensive palladium catalyst is employed twice – once as homogeneous catalyst by coordination of the BuPAd₂-ligand and once as heterogeneous catalyst obtained from the previously homogeneous catalyst by heterogenization under basic conditions. Although the aqueous conditions of the heterogenization step limit the substrate scope of the described procedure, the conversion of various aryl bromides and terminal acetylenes was proven. Therefore, the novel methodology offers tremendous upside to well-known synthetic pathways since no prior formation of the corresponding internal alkyne or the utilization of stoichiometric reagents is required. Advantageously, the methodology can be applied to the synthesis of diaryl-Z-alkenes as well as aryl-alkyl-Z-alkenes. Herein, it was shown that additives can significantly improve the performance of the hydrogenation by increasing the selectivity and inhibiting the over-hydrogenation. In addition, minor modifications of the procedure offer the possibility to extend the product scope to various dienes including symmetric and asymmetric *E-Z*- as well as *Z-Z*-dienes. Based on the results of experiments and ICP-analyses, a general mechanism was developed and illustrated. Moreover, the competing side reaction in the Sonogashira coupling which causes the necessity for an excess of terminal alkyne was identified.

6. References

1. *Chemiewirtschaft in Zahlen 2016*, Verband der Chemischen Industrie e.V. (VCI), Frankfurt am Main, 2016.
2. J. S. Carey, D. Laffan, C. Thomson and M. T. Williams, *Org. Biomol. Chem.*, 2006, **4**, 2337-2347.
3. S. D. Roughley and A. M. Jordan, *J. Med. Chem.*, 2011, **54**, 3451-3479.
4. P. T. Anastas and J. C. Warner, *Green Chemistry: Theory and Practice*, Oxford University Press, New York, 1998.
5. P. Anastas and N. Eghbali, *Chem. Soc. Rev.*, 2010, **39**, 301-312.
6. C. Song, *Catal. Today*, 2006, **115**, 2-32.
7. R. A. Sheldon, *Catal. Today*, 2015, **247**, 4-13.
8. F. Roschangar, R. A. Sheldon and C. H. Senanayake, *Green Chem.*, 2015, **17**, 752-768.
9. M. Beller, *Catalysis: From Principle to Application*, Wiley-VCH, Weinheim, 2012.
10. D. Steinborn, *Fundamentals of Organometallic Catalysis*, Wiley-VCH, Weinheim, 2012.
11. M. Beller and C. Bolm, *Transition Metals for Organic Synthesis: Building Blocks and Fine Chemicals*, Wiley-VCH, Weinheim, 1998.
12. A. Behr, *Angewandte Homogene Katalyse*, Wiley-VCH, Weinheim, 2008.
13. V. F. Slagt, A. H. M. de Vries, J. G. de Vries and R. M. Kellogg, *Org. Process Res. Dev.*, 2010, **14**, 30-47.
14. B. Cornils, W. A. Herrmann, M. Beller and R. Paciello, *Applied Homogeneous Catalysis with Organometallic Compounds: A Comprehensive Handbook in Four Volumes*, Wiley-VCH, Weinheim, 2018.
15. The Royal Swedish Academy of Sciences, *The 2001 Nobel Prize in Chemistry*, http://www.nobelprize.org/nobel_prizes/chemistry/laureates/2001/press.html, Accessed 02.05., 2018.
16. The Royal Swedish Academy of Sciences, *The Nobel Prize in Chemistry 2005*, http://www.nobelprize.org/nobel_prizes/chemistry/laureates/2005/press.html, Accessed 02.05., 2018.
17. The Royal Swedish Academy of Sciences, *The Nobel Prize in Chemistry 2010*, http://www.nobelprize.org/nobel_prizes/chemistry/laureates/2010/press.html, Accessed 02.05., 2018.
18. A. d. Meijere, S. Bräse and M. Oestreich, *Metal-Catalyzed Cross-Coupling Reactions and More*, Wiley-VCH, Weinheim, 2014.
19. Y. Nishihara, *Applied Cross-Coupling Reactions*, Springer, Berlin, Heidelberg, 2013.
20. N. Miyaura, *Cross-Coupling Reactions: A Practical Guide*, Springer, Berlin, Heidelberg, 2002.
21. R. F. Heck and J. P. Nolley, *J. Org. Chem.*, 1972, **37**, 2320-2322.
22. T. Mizoroki, K. Mori and A. Ozaki, *Bull. Chem. Soc. Jpn.*, 1971, **44**, 581-581.
23. K. Sonogashira, Y. Tohda and N. Hagihara, *Tetrahedron Lett.*, 1975, **16**, 4467-4470.
24. N. Miyaura and A. Suzuki, *J. Chem. Soc., Chem. Commun.*, 1979, 866.
25. A. O. King, N. Okukado and E.-i. Negishi, *J. Chem. Soc., Chem. Commun.*, 1977, 683.
26. D. Milstein and J. K. Stille, *J. Am. Chem. Soc.*, 1978, **100**, 3636-3638.
27. M. Kosugi, K. Sasazawa, Y. Shimizu and T. Migita, *Chem. Lett.*, 1977, **6**, 301-302.
28. K. Tamao, K. Sumitani and M. Kumada, *J. Am. Chem. Soc.*, 1972, **94**, 4374-4376.
29. R. J. P. Corriu and J. P. Masse, *J. Chem. Soc., Chem. Commun.*, 1972, 144a.

30. Y. Hatanaka and T. Hiyama, *J. Org. Chem.*, 1988, **53**, 918-920.
31. T. Satoh, Y. Kawamura, M. Miura and M. Nomura, *Angew. Chem. Int. Ed.*, 1997, **36**, 1740-1742.
32. M. Palucki and S. L. Buchwald, *J. Am. Chem. Soc.*, 1997, **119**, 11108-11109.
33. B. C. Hamann and J. F. Hartwig, *J. Am. Chem. Soc.*, 1997, **119**, 12382-12383.
34. W. A. Moradi and S. L. Buchwald, *J. Am. Chem. Soc.*, 2001, **123**, 7996-8002.
35. H. Muratake and H. Nakai, *Tetrahedron Lett.*, 1999, **40**, 2355-2358.
36. G. D. Vo and J. F. Hartwig, *Angew. Chem. Int. Ed.*, 2008, **47**, 2127-2130.
37. T. Hama, D. A. Culkin and J. F. Hartwig, *J. Am. Chem. Soc.*, 2006, **128**, 4976-4985.
38. K. H. Shaughnessy, B. C. Hamann and J. F. Hartwig, *J. Org. Chem.*, 1998, **63**, 6546-6553.
39. D. A. Culkin and J. F. Hartwig, *J. Am. Chem. Soc.*, 2002, **124**, 9330-9331.
40. J. Louie and J. F. Hartwig, *Tetrahedron Lett.*, 1995, **36**, 3609-3612.
41. A. S. Guram, R. A. Rennels and S. L. Buchwald, *Angew. Chem. Int. Ed.*, 1995, **34**, 1348-1350.
42. G. Mann, C. Incarvito, A. L. Rheingold and J. F. Hartwig, *J. Am. Chem. Soc.*, 1999, **121**, 3224-3225.
43. K. E. Torraca, X. Huang, C. A. Parrish and S. L. Buchwald, *J. Am. Chem. Soc.*, 2001, **123**, 10770-10771.
44. U. Schopfer and A. Schlapbach, *Tetrahedron*, 2001, **57**, 3069-3073.
45. T. Migita, T. Shimizu, Y. Asami, J.-i. Shiobara, Y. Kato and M. Kosugi, *Bull. Chem. Soc. Jpn.*, 1980, **53**, 1385-1389.
46. M. A. Fernandez-Rodriguez, Q. Shen and J. F. Hartwig, *J. Am. Chem. Soc.*, 2006, **128**, 2180-2181.
47. J. Hassan, M. Sévignon, C. Gozzi, E. Schulz and M. Lemaire, *Chem. Rev.*, 2002, **102**, 1359-1470.
48. X. Chen, K. M. Engle, D. H. Wang and J. Q. Yu, *Angew. Chem. Int. Ed.*, 2009, **48**, 5094-5115.
49. S. L. Buchwald, C. Mauger, G. Mignani and U. Scholz, *Adv. Synth. Catal.*, 2006, **348**, 23-39.
50. A. Zapf and M. Beller, *Chem. Commun.*, 2005, 431-440.
51. A. Zapf and M. Beller, *Top. Catal.*, 2002, **19**, 101-109.
52. G. Ertl, *Handbook of Heterogeneous Catalysis*, Wiley-VCH, Weinheim, 1997.
53. G. V. Smith and F. Notheisz, *Heterogeneous Catalysis in Organic Chemistry*, Academic Press, San Diego, Calif., 1999.
54. M. J. Climent, A. Corma and S. Iborra, *Chem. Rev.*, 2011, **111**, 1072-1133.
55. P. Munnik, P. E. de Jongh and K. P. de Jong, *Chem. Rev.*, 2015, **115**, 6687-6718.
56. M. Sankar, N. Dimitratos, P. J. Miedziak, P. P. Wells, C. J. Kiely and G. J. Hutchings, *Chem. Soc. Rev.*, 2012, **41**, 8099-8139.
57. H.-U. Blaser, A. Indolese, A. Schnyder, H. Steiner and M. Studer, *J. Mol. Catal. A: Chem.*, 2001, **173**, 3-18.
58. J. B. Ernst, C. Schwermann, G. I. Yokota, M. Tada, S. Muratsugu, N. L. Doltsinis and F. Glorius, *J. Am. Chem. Soc.*, 2017, **139**, 9144-9147.
59. J. B. Ernst, S. Muratsugu, F. Wang, M. Tada and F. Glorius, *J. Am. Chem. Soc.*, 2016, **138**, 10718-10721.
60. P. Baumeister, G. Seifert and H. Steiner, EP0584043A1, 1994.
61. M. Picquet, *Platinum Met. Rev.*, 2013, **57**, 272-280.
62. K. Geoghegan, S. Kelleher and P. Evans, *J. Org. Chem.*, 2011, **76**, 2187-2194.

63. P. Baumeister, W. Meyer, K. Oertle, G. Seifert and H. Steiner, *Chimia*, 1997, **51**, 144.
64. G. E. Dobereiner and R. H. Crabtree, *Chem. Rev.*, 2010, **110**, 681-703.
65. M. H. S. A. Hamid, P. A. Slatford and J. M. J. Williams, *Adv. Synth. Catal.*, 2007, **349**, 1555-1575.
66. S. Chakraborty, P. O. Lagaditis, M. Förster, E. A. Bielinski, N. Hazari, M. C. Holthausen, W. D. Jones and S. Schneider, *ACS Catal.*, 2014, **4**, 3994-4003.
67. S. Werkmeister, J. Neumann, K. Junge and M. Beller, *Chemistry*, 2015, **21**, 12226-12250.
68. A. Quintard and J. Rodriguez, *ChemSusChem*, 2016, **9**, 28-30.
69. Y. Obora, *ACS Catal.*, 2014, **4**, 3972-3981.
70. F. Huang, Z. Liu and Z. Yu, *Angew. Chem. Int. Ed.*, 2016, **55**, 862-875.
71. T. D. Nixon, M. K. Whittlesey and J. M. Williams, *Dalton Trans.*, 2009, 753-762.
72. D. Whitford, *Proteins: Structure and Function*, Wiley, Chichester, 2005.
73. M. Connor, C. W. Vaughan and R. J. Vandenberg, *Br. J. Pharmacol.*, 2010, **160**, 1857-1871.
74. L. Hanus, E. Shohami, I. Bab and R. Mechoulam, *BioFactors*, 2014, **40**, 381-388.
75. A. P. Mikhalkin, *Russ. Chem. Rev.*, 1995, **64**, 259-275.
76. H. Wakamatsu, J. Uda and N. Yamakami, *Journal of the Chemical Society D: Chemical Communications*, 1971, 1540.
77. M. Beller, M. Eckert, F. Vollmüller, S. Bogdanovic and H. Geissler, *Angew. Chem. Int. Ed.*, 1997, **36**, 1494-1496.
78. M. Beller and M. Eckert, *Angew. Chem. Int. Ed.*, 2000, **39**, 1010-1027.
79. M. Guerbet, *Comptes rendus de l'Académie des sciences*, 1899, **128**, 511-513.
80. S. Veibel and J. I. Nielsen, *Tetrahedron*, 1967, **23**, 1723-1733.
81. S. Cannizzaro, *Annalen der Chemie und Pharmacie*, 1853, **88**, 129-130.
82. U. Lüning, *Organische Reaktionen: Eine Einführung in Reaktionswege und Mechanismen*, Elsevier, München, 2007.
83. D. Gabriëls, W. Y. Hernández, B. Sels, P. Van Der Voort and A. Verberckmoes, *Catal. Sci. Technol.*, 2015, **5**, 3876-3902.
84. D. Balcells, A. Nova, E. Clot, D. Gnanamgari, R. H. Crabtree and O. Eisenstein, *Organometallics*, 2008, **27**, 2529-2535.
85. G. Guillena, J. R. D and M. Yus, *Chem. Rev.*, 2010, **110**, 1611-1641.
86. C. Carlini, *J. Mol. Catal. A: Chem.*, 2003, **204-205**, 721-728.
87. K. N. Tseng, S. Lin, J. W. Kampf and N. K. Szymczak, *Chem. Commun.*, 2016, **52**, 2901-2904.
88. L. Haskelberg, E. Bergmann and C. Weizmann, *J. Soc. Chem. Ind.*, 2010, **56**, 587-591.
89. C. Weizmann, E. Bergmann and M. Sulzbacher, *J. Org. Chem.*, 1950, **15**, 54-57.
90. R. E. Miller and G. E. Bennett, *Ind. Eng. Chem.*, 1961, **53**, 33-36.
91. S. Ruiz-Botella and E. Peris, *Chemistry*, 2015, **21**, 15263-15271.
92. P. J. Black, G. Cami-Kobeci, M. G. Edwards, P. A. Slatford, M. K. Whittlesey and J. M. Williams, *Org. Biomol. Chem.*, 2006, **4**, 116-125.
93. X. Ma, C. Su and Q. Xu, *Top. Curr. Chem.*, 2016, **374**, 27.
94. R. H. Crabtree, *Acc. Chem. Res.*, 2002, **23**, 95-101.
95. C. J. Moulton and B. L. Shaw, *J. Chem. Soc., Dalton Trans.*, 1976, 1020-1024.
96. J. T. Singleton, *Tetrahedron*, 2003, **59**, 1837-1857.
97. M. E. van der Boom and D. Milstein, *Chem. Rev.*, 2003, **103**, 1759-1792.
98. C. Gunanathan and D. Milstein, *Chem. Rev.*, 2014, **114**, 12024-12087.

99. H.-J. Knölker, E. Baum, H. Goesmann and R. Klauss, *Angew. Chem. Int. Ed.*, 1999, **38**, 2064-2066.
100. R. M. Bullock, *Angew. Chem. Int. Ed.*, 2007, **46**, 7360-7363.
101. S. Chakraborty, W. W. Brennessel and W. D. Jones, *J. Am. Chem. Soc.*, 2014, **136**, 8564-8567.
102. C. Gunanathan and D. Milstein, *Acc. Chem. Res.*, 2011, **44**, 588-602.
103. R. Tanaka, M. Yamashita, L. W. Chung, K. Morokuma and K. Nozaki, *Organometallics*, 2011, **30**, 6742-6750.
104. C. K. Jørgensen, *Coord. Chem. Rev.*, 1966, **1**, 164-178.
105. M. Garbe, K. Junge and M. Beller, *Eur. J. Org. Chem.*, 2017, **2017**, 4344-4362.
106. S. Chakraborty, P. Bhattacharya, H. Dai and H. Guan, *Acc. Chem. Res.*, 2015, **48**, 1995-2003.
107. T. Zell and D. Milstein, *Acc. Chem. Res.*, 2015, **48**, 1979-1994.
108. S. Murugesan and K. Kirchner, *Dalton Trans.*, 2016, **45**, 416-439.
109. P. Dani, T. Karlen, R. A. Gossage, S. Gladiali and G. van Koten, *Angew. Chem. Int. Ed.*, 2000, **39**, 743-745.
110. T. Aokit and R. H. Crabtree, *Organometallics*, 1993, **12**, 294-298.
111. W.-W. Xu, G. P. Rosini, M. Gupta, C. M. Jensen, W. C. Kaska, K. Krogh-Jespersen and A. S. Goldman, *Chem. Commun.*, 1997, 2273-2274.
112. F. Liu and A. S. Goldman, *Chem. Commun.*, 1999, 655-656.
113. A. S. Goldman, A. H. Roy, Z. Huang, R. Ahuja, W. Schinski and M. Brookhart, *Science*, 2006, **312**, 257-261.
114. R. Ahuja, S. Kundu, A. S. Goldman, M. Brookhart, B. C. Vicente and S. L. Scott, *Chem. Commun.*, 2008, 253-255.
115. B. C. Bailey, R. R. Schrock, S. Kundu, A. S. Goldman, Z. Huang and M. Brookhart, *Organometallics*, 2009, **28**, 355-360.
116. C.-H. Jun, K.-Y. Chung and J.-B. Hong, *Org. Lett.*, 2001, **3**, 785-787.
117. D. Hollmann, S. Bahn, A. Tillack and M. Beller, *Angew. Chem. Int. Ed.*, 2007, **46**, 8291-8294.
118. A. Prades, R. Corberan, M. Poyatos and E. Peris, *Chemistry*, 2008, **14**, 11474-11479.
119. S. Murahashi, N. Komiya, H. Terai and T. Nakae, *J. Am. Chem. Soc.*, 2003, **125**, 15312-15313.
120. Q. Yang, Q. Wang and Z. Yu, *Chem. Soc. Rev.*, 2015, **44**, 2305-2329.
121. K. P. C. Vollhardt, N. E. Schore, H. Butenschön and K.-M. Roy, *Organic Chemistry, Structure and Function*, Wiley-VCH, Weinheim, 2011.
122. A. Streitwieser, C. H. Heathcock and E. M. Kosower, *Introduction to Organic Chemistry*, Wiley-VCH, Weinheim, 1994.
123. F. Shibahara, J. F. Bower and M. J. Krische, *J. Am. Chem. Soc.*, 2008, **130**, 6338-6339.
124. M. Y. Ngai, E. Skucas and M. J. Krische, *Org. Lett.*, 2008, **10**, 2705-2708.
125. J. F. Bower, R. L. Patman and M. J. Krische, *Org. Lett.*, 2008, **10**, 1033-1035.
126. R. L. Patman, V. M. Williams, J. F. Bower and M. J. Krische, *Angew. Chem. Int. Ed.*, 2008, **47**, 5220-5223.
127. F. Shibahara, J. F. Bower and M. J. Krische, *J. Am. Chem. Soc.*, 2008, **130**, 14120-14122.
128. P. J. Black, M. G. Edwards and J. M. J. Williams, *Eur. J. Org. Chem.*, 2006, **2006**, 4367-4378.
129. S. Burling, B. M. Paine, D. Nama, V. S. Brown, M. F. Mahon, T. J. Prior, P. S. Pregosin, M. K. Whittlesey and J. M. Williams, *J. Am. Chem. Soc.*, 2007, **129**, 1987-1995.

130. S.-I. Murahashi, T. Naota, K. Ito, Y. Maeda and H. Taki, *J. Org. Chem.*, 1987, **52**, 4319-4327.
131. J. Zhang, G. Leitus, Y. Ben-David and D. Milstein, *J. Am. Chem. Soc.*, 2005, **127**, 10840-10841.
132. N. A. Owston, A. J. Parker and J. M. Williams, *Chem. Commun.*, 2008, 624-625.
133. J. Williams, N. Owston, T. Nixon, A. Parker and M. Whittlesey, *Synthesis*, 2009, **2009**, 1578-1581.
134. S. Michlik and R. Kempe, *Nat Chem*, 2013, **5**, 140-144.
135. B. Gnanaprakasam, E. Balaraman, Y. Ben-David and D. Milstein, *Angew. Chem. Int. Ed.*, 2011, **50**, 12240-12244.
136. M. Pena-Lopez, H. Neumann and M. Beller, *Chem. Commun.*, 2015, **51**, 13082-13085.
137. D. Srimani, Y. Ben-David and D. Milstein, *Angew. Chem. Int. Ed.*, 2013, **52**, 4012-4015.
138. M. Zhang, X. Fang, H. Neumann and M. Beller, *J. Am. Chem. Soc.*, 2013, **135**, 11384-11388.
139. S. Michlik and R. Kempe, *Angew. Chem. Int. Ed.*, 2013, **52**, 6326-6329.
140. N. Deibl, K. Ament and R. Kempe, *J. Am. Chem. Soc.*, 2015, **137**, 12804-12807.
141. R. Martínez, G. J. Brand, D. J. Ramón and M. Yus, *Tetrahedron Lett.*, 2005, **46**, 3683-3686.
142. R. Martínez, D. J. Ramón and M. Yus, *Tetrahedron*, 2006, **62**, 8988-9001.
143. K. Taguchi, H. Nakagawa, T. Hirabayashi, S. Sakaguchi and Y. Ishii, *J. Am. Chem. Soc.*, 2004, **126**, 72-73.
144. C. Xu, X.-M. Dong, Z.-Q. Wang, X.-Q. Hao, Z. Li, L.-M. Duan, B.-M. Ji and M.-P. Song, *J. Organomet. Chem.*, 2012, **700**, 214-218.
145. C. S. Cho, B. T. Kim, T.-J. Kim and S. C. Shim, *J. Org. Chem.*, 2001, **66**, 9020-9022.
146. S. Elangovan, J. B. Sortais, M. Beller and C. Darcel, *Angew. Chem. Int. Ed.*, 2015, **54**, 14483-14486.
147. G. Zhang, J. Wu, H. Zeng, S. Zhang, Z. Yin and S. Zheng, *Org. Lett.*, 2017, **19**, 1080-1083.
148. P. Piehl, M. Pena-Lopez, A. Frey, H. Neumann and M. Beller, *Chem. Commun.*, 2017, **53**, 3265-3268.
149. M. Pena-Lopez, P. Piehl, S. Elangovan, H. Neumann and M. Beller, *Angew. Chem. Int. Ed.*, 2016, **55**, 14967-14971.
150. L. K. Chan, D. L. Poole, D. Shen, M. P. Healy and T. J. Donohoe, *Angew. Chem. Int. Ed.*, 2014, **53**, 761-765.
151. D. Shen, D. L. Poole, C. C. Shotton, A. F. Kornahrens, M. P. Healy and T. J. Donohoe, *Angew. Chem. Int. Ed.*, 2015, **54**, 1642-1645.
152. Y. Li, H. Li, H. Junge and M. Beller, *Chem. Commun.*, 2014, **50**, 14991-14994.
153. G. Onodera, Y. Nishibayashi and S. Uemura, *Angew. Chem. Int. Ed.*, 2006, **45**, 3819-3822.
154. P. A. Slatford, M. K. Whittlesey and J. M. J. Williams, *Tetrahedron Lett.*, 2006, **47**, 6787-6789.
155. R. Grigg, C. Lofberg, S. Whitney, V. Sridharan, A. Keep and A. Derrick, *Tetrahedron*, 2009, **65**, 849-854.
156. L. Guo, X. Ma, H. Fang, X. Jia and Z. Huang, *Angew. Chem. Int. Ed.*, 2015, **54**, 4023-4027.
157. T. Kuwahara, T. Fukuyama and I. Ryu, *RSC Adv.*, 2013, **3**, 13702.
158. L. Guo, Y. Liu, W. Yao, X. Leng and Z. Huang, *Org. Lett.*, 2013, **15**, 1144-1147.
159. T. Sawaguchi and Y. Obora, *Chem. Lett.*, 2011, **40**, 1055-1057.

160. B. Anxionnat, D. G. Pardo, G. Ricci and J. Cossy, *Org. Lett.*, 2011, **13**, 4084-4087.
161. T. Kuwahara, T. Fukuyama and I. Ryu, *Chem. Lett.*, 2013, **42**, 1163-1165.
162. K. Motokura, D. Nishimura, K. Mori, T. Mizugaki, K. Ebitani and K. Kaneda, *J. Am. Chem. Soc.*, 2004, **126**, 5662-5663.
163. K. Motokura, N. Fujita, K. Mori, T. Mizugaki, K. Ebitani, K. Jitsukawa and K. Kaneda, *Chem. Eur. J.*, 2006, **12**, 8228-8239.
164. C. Lofberg, R. Grigg, M. A. Whittaker, A. Keep and A. Derrick, *J. Org. Chem.*, 2006, **71**, 8023-8027.
165. F. Li, X. Zou and N. Wang, *Adv. Synth. Catal.*, 2015, **357**, 1405-1415.
166. *WHO Model List of Essential Medicines*, World Health Organization, Geneva, 2017.
167. American Society of Health-System Pharmacists, Inc., *Valproic Acid*, <https://www.drugs.com/monograph/valproic-acid.html>, Accessed 03.05., 2018.
168. CHEM21-Project Representatives, *The CHEM21-Project*, <https://www.chem21.eu>, Accessed 03.05., 2018.
169. M. Santaniello, C. A. Bagolini, A. Uttaro and S. Fontana, US5856569, 1997.
170. C. f. H. M. Products, *Guideline on the Specification Limits for Residues of Metal Catalysts*, European Medicines Agency, London, 2007.
171. F. a. D. Administration, *Q3D Elemental Impurities - Guidance for Industry*, Food and Drug Administration, 2015.
172. A. J. Hunt, T. J. Farmer and J. H. Clark, *Element Recovery and Sustainability*, Royal Society of Chemistry, Cambridge, 2013.
173. C. Bornschein, S. Werkmeister, B. Wendt, H. Jiao, E. Alberico, W. Baumann, H. Junge, K. Junge and M. Beller, *Nat. Commun.*, 2014, **5**, 4111.
174. E. Alberico, P. Sponholz, C. Cordes, M. Nielsen, H. J. Drexler, W. Baumann, H. Junge and M. Beller, *Angew. Chem. Int. Ed.*, 2013, **52**, 14162-14166.
175. S. Elangovan, C. Topf, S. Fischer, H. Jiao, A. Spannenberg, W. Baumann, R. Ludwig, K. Junge and M. Beller, *J. Am. Chem. Soc.*, 2016, **138**, 8809-8814.
176. S. Elangovan, M. Garbe, H. Jiao, A. Spannenberg, K. Junge and M. Beller, *Angew. Chem. Int. Ed.*, 2016, **55**, 15364-15368.
177. S. Elangovan, J. Neumann, J. B. Sortais, K. Junge, C. Darcel and M. Beller, *Nat. Commun.*, 2016, **7**, 12641.
178. M. Peña-López, H. Neumann and M. Beller, *ChemCatChem*, 2015, **7**, 865-871.
179. S. Elangovan, B. Wendt, C. Topf, S. Bachmann, M. Scalone, A. Spannenberg, H. Jiao, W. Baumann, K. Junge and M. Beller, *Adv. Synth. Catal.*, 2016, **358**, 820-825.
180. M. Anderez-Fernandez, L. K. Vogt, S. Fischer, W. Zhou, H. Jiao, M. Garbe, S. Elangovan, K. Junge, H. Junge, R. Ludwig and M. Beller, *Angew. Chem. Int. Ed.*, 2017, **56**, 559-562.
181. J. Neumann, S. Elangovan, A. Spannenberg, K. Junge and M. Beller, *Chem. Eur. J.*, 2017, **23**, 5410-5413.
182. A. Monney, M. Pena-Lopez and M. Beller, *Chimia (Aarau)*, 2014, **68**, 231-234.
183. J. Neumann, C. Bornschein, H. Jiao, K. Junge and M. Beller, *Eur. J. Org. Chem.*, 2015, **2015**, 5944-5948.
184. A. Monney, E. Barsch, P. Sponholz, H. Junge, R. Ludwig and M. Beller, *Chem. Commun.*, 2014, **50**, 707-709.
185. D. S. Mannel, M. S. Ahmed, T. W. Root and S. S. Stahl, *J. Am. Chem. Soc.*, 2017, **139**, 1690-1698.
186. F. Mao, Z. Qi, H. Fan, D. Sui, R. Chen and J. Huang, *RSC Adv.*, 2017, **7**, 1498-1503.

187. A. Gallas-Hulin, R. K. Kotni, M. Nielsen and S. Kegnæs, *Top. Catal.*, 2017, **60**, 1380-1386.
188. Y. X. Zhou, Y. Z. Chen, L. Cao, J. Lu and H. L. Jiang, *Chem. Commun.*, 2015, **51**, 8292-8295.
189. C.-H. Tsai, M. Xu, P. Kunal and B. G. Trewyn, *Catal. Today*, 2018, **306**, 81-88.
190. M. Beller, M. Eckert, H. Geissler, B. Napierski, H.-P. Rebenstock and E. W. Holla, *Chem. Eur. J.*, 1998, **4**, 935-941.
191. A. B. Hughes, *Amino Acids, Peptides and Proteins in Organic Chemistry*, Wiley-VCH, Weinheim, 2009.
192. A. Strecker, *Annalen der Chemie und Pharmacie*, 1850, **75**, 27-45.
193. A. Strecker, *Annalen der Chemie und Pharmacie*, 1854, **91**, 349-351.
194. M. Beller, M. Eckert, W. A. Moradi and H. Neumann, *Angew. Chem. Int. Ed.*, 1999, **38**, 1454-1457.
195. M. Beller, W. A. Moradi, M. Eckert and H. Neumann, *Tetrahedron Lett.*, 1999, **40**, 4523-4526.
196. A. Hamasaki, X. Liu and M. Tokunaga, *Chem. Lett.*, 2008, **37**, 1292-1293.
197. T. Sagae, M. Sugiura, H. Hagio and S. Kobayashi, *Chem. Lett.*, 2003, **32**, 160-161.
198. R. M. Gómez, A. Cabrera and C. G. Velázquez, *J. Mol. Catal. A: Chem.*, 2007, **274**, 65-67.
199. K. W. Yang and X. Z. Jiang, *Bull. Chem. Soc. Jpn.*, 2006, **79**, 806-809.
200. A. Cabrera, P. Sharma, J. L. Arias, J. L. Velasco, J. Pérez-Flores and R. M. Gómez, *J. Mol. Catal. A: Chem.*, 2004, **212**, 19-23.
201. D. Gördes, H. Neumann, A. J. von Wangelin, C. Fischer, K. Drauz, H.-P. Krimmer and M. Beller, *Adv. Synth. Catal.*, 2003, **345**, 510-516.
202. M. Beller, M. Eckert and F. Vollmüller, *J. Mol. Catal. A: Chem.*, 1998, **135**, 23-33.
203. D. A. Freed and M. C. Kozlowski, *Tetrahedron Lett.*, 2001, **42**, 3403-3406.
204. S. Bogdanovic, H. Geisler, K. Raab, M. Beller and H. Fischer, EP 0779102A1, 1997.
205. M. Beller, H. Fischer, T. Gerdau and P. Gross, EP 0680948A1, 1995.
206. R. Sang, P. Kucmierczyk, K. Dong, R. Franke, H. Neumann, R. Jackstell and M. Beller, *J. Am. Chem. Soc.*, 2018, **140**, 5217-5223.
207. K. Dong, X. Fang, S. Gulak, R. Franke, A. Spannenberg, H. Neumann, R. Jackstell and M. Beller, *Nat. Commun.*, 2017, **8**, 14117.
208. K. Dong, R. Sang, Z. Wei, J. Liu, R. Dühren, A. Spannenberg, H. Jiao, H. Neumann, R. Jackstell, R. Franke and M. Beller, *Chem. Sci.*, 2018, **9**, 2510-2516.
209. L. Wang, H. Neumann and M. Beller, *Angew. Chem. Int. Ed.*, 2018, **57**, 6910-6914.
210. W. A. Moradi, Technische Universität München, 1999.
211. H. A. Dieck and F. R. Heck, *J. Organomet. Chem.*, 1975, **93**, 259-263.
212. L. Cassar, *J. Organomet. Chem.*, 1975, **93**, 253-257.
213. R. Chinchilla and C. Najera, *Chem. Rev.*, 2007, **107**, 874-922.
214. R. Chinchilla and C. Najera, *Chem. Soc. Rev.*, 2011, **40**, 5084-5121.
215. K. C. Nicolaou, P. G. Bulger and D. Sarlah, *Angew. Chem. Int. Ed.*, 2005, **44**, 4442-4489.
216. C. Torborg and M. Beller, *Adv. Synth. Catal.*, 2009, **351**, 3027-3043.
217. M. Erdélyi and A. Gogoll, *J. Org. Chem.*, 2001, **66**, 4165-4169.
218. E. Shirakawa, T. Kitabata, H. Otsuka and T. Tsuchimoto, *Tetrahedron*, 2005, **61**, 9878-9885.
219. Q.-Y. Chen and Z.-Y. Yang, *Tetrahedron Lett.*, 1986, **27**, 1171-1174.

220. Volker P. W. Böhm and Wolfgang A. Herrmann, *Eur. J. Org. Chem.*, 2000, **2000**, 3679-3681.
221. S. Thorand and N. Krause, *J. Org. Chem.*, 1998, **63**, 8551-8553.
222. T. Hundertmark, A. F. Littke, S. L. Buchwald and G. C. Fu, *Org. Lett.*, 2000, **2**, 1729-1731.
223. D. Gelman and S. L. Buchwald, *Angew. Chem. Int. Ed.*, 2003, **42**, 5993-5996.
224. K. W. Anderson and S. L. Buchwald, *Angew. Chem. Int. Ed.*, 2005, **44**, 6173-6177.
225. H. Lu, L. Wang, F. Yang, R. Wu and W. Shen, *RSC Adv.*, 2014, **4**, 30447-30452.
226. O. R'Kyek, N. Halland, A. Lindenschmidt, J. Alonso, P. Lindemann, M. Urmann and M. Nazare, *Chemistry*, 2010, **16**, 9986-9989.
227. H. Nakatsuji, K. Ueno, T. Misaki and Y. Tanabe, *Org. Lett.*, 2008, **10**, 2131-2134.
228. P. Y. Choy, W. K. Chow, C. M. So, C. P. Lau and F. Y. Kwong, *Chemistry*, 2010, **16**, 9982-9985.
229. M. Schilz and H. Plenio, *J. Org. Chem.*, 2012, **77**, 2798-2807.
230. G. C. Fortman and S. P. Nolan, *Chem. Soc. Rev.*, 2011, **40**, 5151-5169.
231. W. A. Herrmann, K. Öfele, D. v. Preysing and S. K. Schneider, *J. Organomet. Chem.*, 2003, **687**, 229-248.
232. L. Yin and J. Liebscher, *Chem. Rev.*, 2007, **107**, 133-173.
233. N. T. S. Phan, M. Van Der Sluys and C. W. Jones, *Adv. Synth. Catal.*, 2006, **348**, 609-679.
234. J. G. de Vries, *Dalton Trans.*, 2006, 421-429.
235. M. Kivala and F. Diederich, *Acc. Chem. Res.*, 2009, **42**, 235-248.
236. T. Baumgartner and R. Reau, *Chem. Rev.*, 2006, **106**, 4681-4727.
237. K. Sonogashira, *J. Organomet. Chem.*, 2002, **653**, 46-49.
238. K. C. K. Swamy, A. S. Reddy, K. Sandeep and A. Kalyani, *Tetrahedron Lett.*, 2018, **59**, 419-429.
239. Á. Molnár, A. Sárkány and M. Varga, *J. Mol. Catal. A: Chem.*, 2001, **173**, 185-221.
240. M. Crespo-Quesada, F. Cárdenas-Lizana, A.-L. Dessimoz and L. Kiwi-Minsker, *ACS Catal.*, 2012, **2**, 1773-1786.
241. A. Podgorsek, M. Zupan and J. Iskra, *Angew. Chem. Int. Ed.*, 2009, **48**, 8424-8450.
242. S. R. Chemler and M. T. Bovino, *ACS Catal.*, 2013, **3**, 1076-1091.
243. W. Reppe, O. Schlichting and H. Meister, *Liebigs Ann. Chem.*, 1948, **560**, 93-104.
244. W. Reppe, O. Schlichting, K. Klager and T. Toepel, *Liebigs Ann. Chem.*, 1948, **560**, 1-92.
245. W. Reppe and W. J. Schweckendiek, *Liebigs Ann. Chem.*, 1948, **560**, 104-116.
246. P. S. Bailey, *Ozonation in Organic Chemistry*, Academic Press, Inc., London, 1978.
247. G. Evano, N. Blanchard and M. Toumi, *Chem. Rev.*, 2008, **108**, 3054-3131.
248. B. Liang, M. Huang, Z. You, Z. Xiong, K. Lu, R. Fathi, J. Chen and Z. Yang, *J. Org. Chem.*, 2005, **70**, 6097-6100.
249. A. Soheili, J. Albaneze-Walker, J. A. Murry, P. G. Dormer and D. L. Hughes, *Org. Lett.*, 2003, **5**, 4191-4194.
250. B. Liang, M. Dai, J. Chen and Z. Yang, *J. Org. Chem.*, 2005, **70**, 391-393.
251. D. Méry, K. Heuzé and D. Astruc, *Chem. Commun.*, 2003, 1934-1935.
252. N. E. Leadbeater and B. J. Tominack, *Tetrahedron Lett.*, 2003, **44**, 8653-8656.
253. X. Fu, S. Zhang, J. Yin and D. P. Schumacher, *Tetrahedron Lett.*, 2002, **43**, 6673-6676.
254. L. Yu, Z. Han and Y. Ding, *Org. Process Res. Dev.*, 2016, **20**, 2124-2129.
255. C. Dasaradhan, Y. S. Kumar, K. Prabakaran, F.-R. N. Khan, E. D. Jeong and E. H. Chung, *Tetrahedron Lett.*, 2015, **56**, 784-788.

256. C. Yi and R. Hua, *J. Org. Chem.*, 2006, **71**, 2535-2537.
257. S. J. Sabounchei and M. Ahmadi, *Catal. Commun.*, 2013, **37**, 114-121.
258. J. Cheng, Y. Sun, F. Wang, M. Guo, J. H. Xu, Y. Pan and Z. Zhang, *J. Org. Chem.*, 2004, **69**, 5428-5432.
259. M. Sarmah, A. Dewan, A. J. Thakur and U. Bora, *Tetrahedron Lett.*, 2016, **57**, 914-916.
260. N. Touj, S. Yaşar, N. Özdemir, N. Hamdi and İ. Özdemir, *J. Organomet. Chem.*, 2018, **860**, 59-71.
261. T. Yi, M. Mo, H.-Y. Fu, R.-X. Li, H. Chen and X.-J. Li, *Catal. Lett.*, 2012, **142**, 594-600.
262. S. K. Das, M. Sarmah and U. Bora, *Tetrahedron Lett.*, 2017, **58**, 2094-2097.
263. A. Gogoi, A. Dewan and U. Bora, *RSC Adv.*, 2015, **5**, 16-19.
264. R. Zhou, W. Wang, Z.-j. Jiang, H.-y. Fu, X.-l. Zheng, C.-c. Zhang, H. Chen and R.-x. Li, *Catal. Sci. Technol.*, 2014, **4**, 746.
265. T. He, L. L. Wu, X. L. Fu, H. Y. Fu, H. Chen and R. X. Li, *Chin. Chem. Lett.*, 2011.
266. B. Agrahari, S. Layek, Anuradha, R. Ganguly and D. D. Pathak, *Inorg. Chim. Acta*, 2018, **471**, 345-354.
267. R. Bhaskar, A. K. Sharma, M. K. Yadav and A. K. Singh, *Dalton Trans.*, 2017, **46**, 15235-15248.
268. S. Kumar, F. Saleem, M. K. Mishra and A. K. Singh, *New J. Chem.*, 2017, **41**, 2745-2755.
269. Z. Mandegani, M. Asadi and Z. Asadi, *Appl. Organomet. Chem.*, 2016, **30**, 657-663.
270. M. Esmaeilpour, J. Javidi, F. N. Dodeji and M. M. Abarghoui, *Transition Met. Chem.*, 2014, **39**, 797-809.
271. S. Jadhav, A. Jagdale, S. Kamble, A. Kumbhar and R. Salunkhe, *RSC Adv.*, 2016, **6**, 3406-3420.
272. S. J. Sabounchei, M. Ahmadi, Z. Nasri, E. Shams and M. Panahimehr, *Tetrahedron Lett.*, 2013, **54**, 4656-4660.
273. B. Tamami, M. M. Nezhad, S. Ghasemi and F. Farjadian, *J. Organomet. Chem.*, 2013, **743**, 10-16.
274. R. Najman, J. K. Cho, A. F. Coffey, J. W. Davies and M. Bradley, *Chem. Commun.*, 2007, 5031-5033.
275. R. V. Jagadeesh, K. Murugesan, A. S. Alshammari, H. Neumann, M. M. Pohl, J. Radnik and M. Beller, *Science*, 2017, **358**, 326-332.
276. F. A. Westerhaus, R. V. Jagadeesh, G. Wienhofer, M. M. Pohl, J. Radnik, A. E. Surkus, J. Rabeah, K. Junge, H. Junge, M. Nielsen, A. Bruckner and M. Beller, *Nat. Chem.*, 2013, **5**, 537-543.
277. R. V. Jagadeesh, A. E. Surkus, H. Junge, M. M. Pohl, J. Radnik, J. Rabeah, H. Huan, V. Schunemann, A. Bruckner and M. Beller, *Science*, 2013, **342**, 1073-1076.
278. L. L. Zhang, A. Q. Wang, W. T. Wang, Y. Q. Huang, X. Y. Liu, S. Miao, J. Y. Liu and T. Zhang, *ACS Catal.*, 2015, **5**, 6563-6572.
279. T. Cheng, H. Yu, F. Peng, H. Wang, B. Zhang and D. Su, *Catal. Sci. Technol.*, 2016, **6**, 1007-1015.
280. X. Ma, Y. X. Zhou, H. Liu, Y. Li and H. L. Jiang, *Chem. Commun.*, 2016, **52**, 7719-7722.
281. Y. Li, Y. X. Zhou, X. Ma and H. L. Jiang, *Chem. Commun.*, 2016, **52**, 4199-4202.
282. Z. Z. Wei, Y. Q. Chen, J. Wang, D. F. Su, M. H. Tang, S. J. Mao and Y. Wang, *ACS Catal.*, 2016, **6**, 5816-5822.
283. H. Lindlar and R. Dubuis, *Org. Synth.*, 1966, **46**, 89.
284. H. Lindlar, *Helv. Chim. Acta*, 1952, **35**, 446-450.
285. S. Liang, G. B. Hammond and B. Xu, *Chem. Commun.*, 2016, **52**, 6013-6016.

286. W. Niu, Y. Gao, W. Zhang, N. Yan and X. Lu, *Angew. Chem. Int. Ed.*, 2015, **54**, 8271-8274.
287. E. D. Slack, C. M. Gabriel and B. H. Lipshutz, *Angew. Chem. Int. Ed.*, 2014, **53**, 14051-14054.
288. R. Venkatesan, M. H. G. Precht, J. D. Scholten, R. P. Pezzi, G. Machado and J. Dupont, *J. Mater. Chem.*, 2011, **21**, 3030.
289. O. Verho, H. Zheng, K. P. J. Gustafson, A. Nagendiran, X. Zou and J.-E. Bäckvall, *ChemCatChem*, 2016, **8**, 773-778.
290. D. Köhler, M. Heise, A. I. Baranov, Y. Luo, D. Geiger, M. Ruck and M. Armbrüster, *Chem. Mater.*, 2012, **24**, 1639-1644.
291. F. Chen, C. Kreyenschulte, J. Radnik, H. Lund, A.-E. Surkus, K. Junge and M. Beller, *ACS Catal.*, 2017, **7**, 1526-1532.
292. T. N. Gieshoff, A. Welther, M. T. Kessler, M. H. Precht and A. Jacobi von Wangelin, *Chem. Commun.*, 2014, **50**, 2261-2264.
293. H. Konnerth and M. H. Precht, *Chem. Commun.*, 2016, **52**, 9129-9132.
294. K. K. Tanabe, M. S. Ferrandon, N. A. Siladke, S. J. Kraft, G. Zhang, J. Niklas, O. G. Poluektov, S. J. Lopykinski, E. E. Bunel, T. R. Krause, J. T. Miller, A. S. Hock and S. T. Nguyen, *Angew. Chem. Int. Ed.*, 2014, **53**, 12055-12058.
295. G. Wittig and U. Schöllkopf, *Chem. Ber.*, 1954, **87**, 1318-1330.
296. D. J. Peterson, *J. Org. Chem.*, 1968, **33**, 780-784.
297. H. Görner and H. J. Kuhn, in *Adv. Photochem.*, eds. D. C. Neckers, D. H. Volman and G. v. Büna, John Wiley, New York, 2007, pp. 1-117.
298. J. Kagan, in *Organic Photochemistry*, Academic Press, San Diego, 1993, pp. 34-54.
299. G. C. Vougioukalakis and R. H. Grubbs, *Chem. Rev.*, 2010, **110**, 1746-1787.
300. X. F. Wu, H. Neumann and M. Beller, *Chem. - Eur. J.*, 2010, **16**, 12104-12107.
301. Sigma Aldrich, *3,6-Dithia-1,8-octanediol - Lindlar Catalyst Poison*, Accessed 07.07., 2018.
302. C. A. Fleckenstein and H. Plenio, *Chem. Soc. Rev.*, 2010, **39**, 694-711.
303. U. Christmann and R. Vilar, *Angew. Chem. Int. Ed.*, 2005, **44**, 366-374.
304. M. Rubina and V. Gevorgyan, *J. Am. Chem. Soc.*, 2001, **123**, 11107-11108.
305. C. Yang and S. P. Nolan, *J. Org. Chem.*, 2002, **67**, 591-593.
306. C. Jahier, O. V. Zatolochyna, N. V. Zvyagintsev, V. P. Ananikov and V. Gevorgyan, *Org. Lett.*, 2012, **14**, 2846-2849.
307. O. S. Morozov, A. F. Asachenko, D. V. Antonov, V. S. Kochurov, D. Y. Paraschuk and M. S. Nechaev, *Adv. Synth. Catal.*, 2014, **356**, 2671-2678.
308. S. S. Ichake, A. Konala, V. Kavala, C. W. Kuo and C. F. Yao, *Org. Lett.*, 2017, **19**, 54-57.

7. Appendix

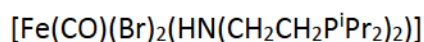
The appendix includes the general procedures for the conducted experiments as well as analytical results. In addition to the written data, the NMR spectra are displayed. Generally, the synthesized and isolated products have been characterized by ^1H - and ^{13}C -NMR, GC-MS and HR-MS as well as to some extent EA. Moreover, the technical characteristics of the employed analytical equipment are documented. Finally, the authors publications are presented.

7.1. Hydrogen Autotransfer

General Information

All manipulations were conducted under argon with exclusion of moisture and oxygen by using standard techniques for the manipulation of air sensitive compounds. Reaction temperatures refer to silicon oil in an additional pressure tube within the heated alumina block or to the silicon oil bath. NMR data were recorded on either Bruker ARX 300, Bruker ARX 400 or Bruker Fourier 300 spectrometers. ^{13}C - and ^1H -NMR spectra are given in ppm and referenced to signals of deuterated solvents and residual protonated solvents, respectively (CDCl_3 : ^1H : 7.260 ppm, ^{13}C : 77.160 ppm; C_6D_6 : ^1H : 7.260 ppm, ^{13}C : 128.060 ppm). Gas chromatography-mass analysis was carried out on an Agilent HP-5890 instrument with an Agilent HP-5973 Mass Selective Detector (EI) and HP-5 capillary column using helium carrier gas. TOF HR-MS measurements were performed on an Agilent 1200/6210 Time-of-Flight LC-MS. Flash chromatography was performed on a Teledyne Isco CombiFlash Rf 200 system. Chemicals were purchased from Sigma Aldrich, Alfar Aesar, TCI or Strem and were used as received. DMF was dried by a SPS from Innovative Technology while H_2O was flushed with argon for one hour. Solvents were stored in Aldrich Sure/store flasks under argon. The iridium complex **1** was synthesized according to the literature procedure.^[70]

General procedure for the synthesis of Fe-MACHO-BH 2

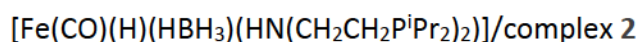


1.02 equivalents of FeBr_2 (718 mg; 3.33 mmol) were dissolved in 30 mL Ethanol (abs.) at room temperature. The ligand $((\text{HN}(\text{CH}_2\text{CH}_2\text{P}^i\text{Pr}_2)_2)$ (1 g; 3.27 mmol) was added dropwise over a period of 5-10 minutes. After the addition of 1-2 mL ligand-solution, a white precipitate was formed. It is not necessary to further purify this product as the excess of FeBr_2 will be easily removed in the next step.

After stirring at room temperature overnight, the solid was allowed to precipitate. The supernatant solution was removed via syringe and the solid was washed three times with 10 mL of Ethanol (abs.). The slightly yellow liquid contains residual FeBr_2 . After removing the solvent, a white-light greenish solid is obtained (1.4 g; no NMR-characterization due its paramagnetic characteristic).

30 mL THF (abs.) was added (the solid is poorly soluble in THF, complete dissolving is not required). Carbon monoxide was bubbled through the suspension for 1 h until the precipitate is dissolved completely and the solution has turned to dark blue. After removing the residual carbon monoxide by bubbling argon through the solution, 40 mL of n-heptane (abs.) were added. The solvents were removed under reduced pressure to obtain a dark blue, crystalline solid which was washed with Ethanol (abs.) to remove the residual excess of FeBr_2 .

The procedure gives 1.35 g (2.46 mmol, 75.2% yield) of the desired intermediate iron complex. NMR spectra can be obtained at this stage (C_6D_6 , THF- d_8 or CD_2H_2)



To 1.35 g (2.46 mmol) of $[\text{Fe}(\text{CO})(\text{H})(\text{HBH}_3)(\text{HN}(\text{CH}_2\text{CH}_2\text{P}^i\text{Pr}_2)_2)]$ in 50 mL THF (abs.), a solution of NaBH_4 (0.93 g; 24.6 mmol) in 30 mL Ethanol (abs.) was added. The blue solution turns to bright yellow. After stirring for 2 h at room temperature, the solvent was removed under reduced pressure. The product should not be heated as the complex decomposes towards the non-stable dihydride. The yellow residue was dissolved in toluene (abs.) and filtered to remove the salts.

After removing the solvent, an orange-yellow solid was isolated. Recrystallisation from THF/n-heptane (dissolving the solid in 3-5 mL THF and adding 20-30 mL n-heptane) affords fine yellow needles (537.2 mg, 1.33 mmol, 53.9% yield).

General Procedure for Hydrogen Autotransfer Reactions

The experiments were carried out in pressure tubes equipped with a magnetic stirring bar. Prior to the reaction, the solid reaction compounds were added to the pressure tube which was subsequently placed in an evacuation tube. The corresponding screw cap with septum was added into the evacuation tube as well. The closed tube was evacuated and flushed with argon three times. Afterwards, the tubes lid was slightly lifted and the liquid substances as well as the solvent (water-free stored under Argon) were added via syringe into the pressure tube. 4-Bromotoluene was slightly heated and added as a liquid as well since this compound sublimates significantly upon the exposition to vacuum. Finally, the lid of the evacuation tube was removed and the pressure tube was sealed with the screw cap under argon counter flow before the tube was placed in an aluminum heating block. The temperature was controlled by a thermocouple in an additional pressure tube with silicon oil placed in the aluminum block.

After the reaction was finished and cooled down to room temperature, the tube was opened and hexadecane was added as internal standard. A sample was prepared by filtering the crude solution through cotton. The sample was analyzed by GC-MS.

Example of Scheme 10 (page 12):

Benzyl alcohol: 1 mmol = 104 μ L

^tButyl acetate: 1.2 mmol = 162 μ L

KO^tBu: 1.5 mmol = 168.3 mg

Complex 1: 0.5 mol% = 2.7 mg

1 mL toluene, 60 °C, 12 h

Analytica Data

ITSD ^1H & ^{13}C NMR: CDCl_3 : ^1H : 7.260 ppm, ^{13}C : 77.160 ppm; C_6D_6 : ^1H : 7.260 ppm, ^{13}C : 128.060 ppm.

All $\delta^1\text{H}$ and $\delta^{13}\text{C}$ in ppm, all coupling constants J in Hz.

Iridium complex 1: ^1H NMR (300.1 MHz, C_6D_6): $\delta^1\text{H}$ = -38.53 (1H, s, IrH), 1.19-1.24 (9H, m, CH_3), 1.31-1.36 (9H, m, CH_3), 6.53-6.58 (1H, m, ArH), 6.84-6.93 (3H, m, ArH), 7.01-7.07 (2H, m, ArH), 9.73 (1H, m, ArH); ^{31}P NMR (121.5 MHz, C_6D_6): $\delta^{31}\text{P}$ = 160.4 ($P\text{-}^t\text{Bu}_2$); HRMS (CI, m/z): calcd. for $\text{Ir}_1\text{C}_{19}\text{H}_{26}\text{Cl}_1\text{N}_1\text{O}_1\text{P}_1$ (M): 543, found: 543; (M- ^{35}Cl): 508, found: 508; (M- ^{37}Cl): 506, found 506.

Fe-MACHO-BH 2: ^{13}C NMR (75.5 MHz, C_6D_6): $\delta^{13}\text{C}$ = 18.3 (2 CH_3), 19.0 (2 CH_3), 20.4 (2 CH_3), 20.8 (2 CH_3), 25.3 (2 CH), 29.0 (2 CH_2), 29.6 (2 CH), 54.1 (2 CH_2); ^{31}P NMR (121.5 MHz, C_6D_6): $\delta^{31}\text{P}$ = 99.3 ($P\text{-}^i\text{Pr}_2$), 99.4 ($P\text{-}^i\text{Pr}_2$)

Note: The NMR sample contained residual amounts of THF and heptane from the purification step.

3-Phenylpropanoic acid tert-butyl ester: ^1H NMR (300.1 MHz, CDCl_3): $\delta^1\text{H}$ = 1.44 (9H, s, CH_3), 2.53-2.58 (2H, m, CH_2), 2.90-2.95 (2H, m, CH_2), 7.17-7.22 (3H, m, ArH), 7.25-7.32 (2H, m, ArH); ^{13}C NMR (75.5 MHz, CDCl_3): $\delta^{13}\text{C}$ = 28.1 (CH_3), 31.2 (CH_2), 37.1 (CH_2), 80.3 (C^q), 126.2 (CH), 128.4 (2 CH), 128.4 (2 CH), 140.8 (C^q), 172.3 (C^q); GC/MS-EI (70 eV): m/z (%) = 150 ((MH - $\text{C}(\text{CH}_3)_3$) $^+$, 100), 57 (87), 91 (75), 104 (72), 105 (69), 133 (42), 77 (23), 78 (15), 103 (14), 79 (13), 51 (11), 151 (10).

Pentanoic acid tert-butyl ester: GC/MS-EI (70 eV): m/z (%) = 85 ((M - $\text{OC}(\text{CH}_3)_3$) $^+$, 100), 103 ((MH $_2$ - $\text{C}(\text{CH}_3)_3$) $^+$, 78), 57 (44), 60 (26), 61 (25), 73 (18), 102 (11).

Pentanoic acid ethyl ester: GC/MS-EI (70 eV): m/z (%) = 85 ((M - OC_2H_5) $^+$, 100), 103 ((MH $_2$ - C_2H_5) $^+$, 77), 57 (42), 61 (25), 73 (22), 60 (20), 75 (11).

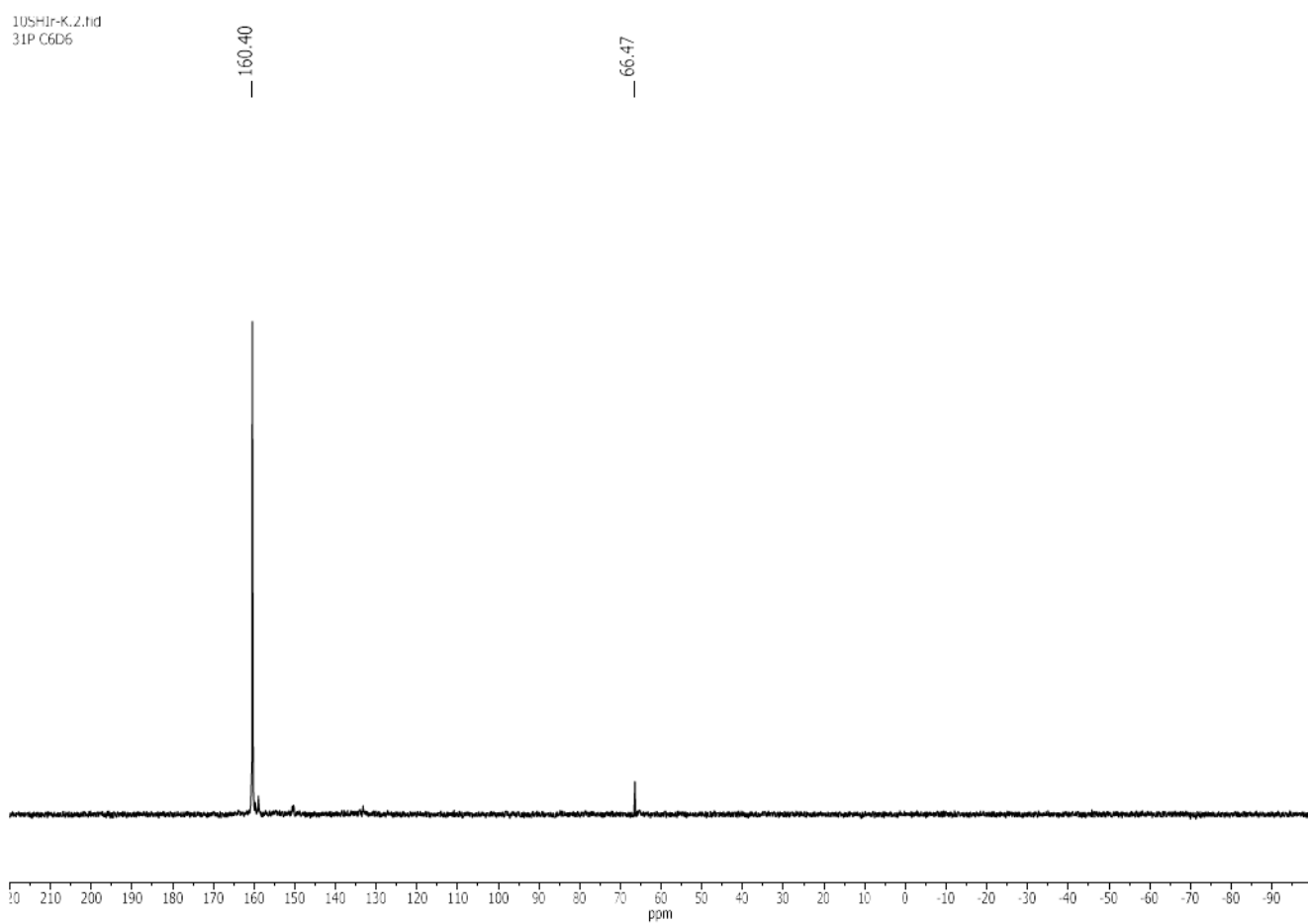
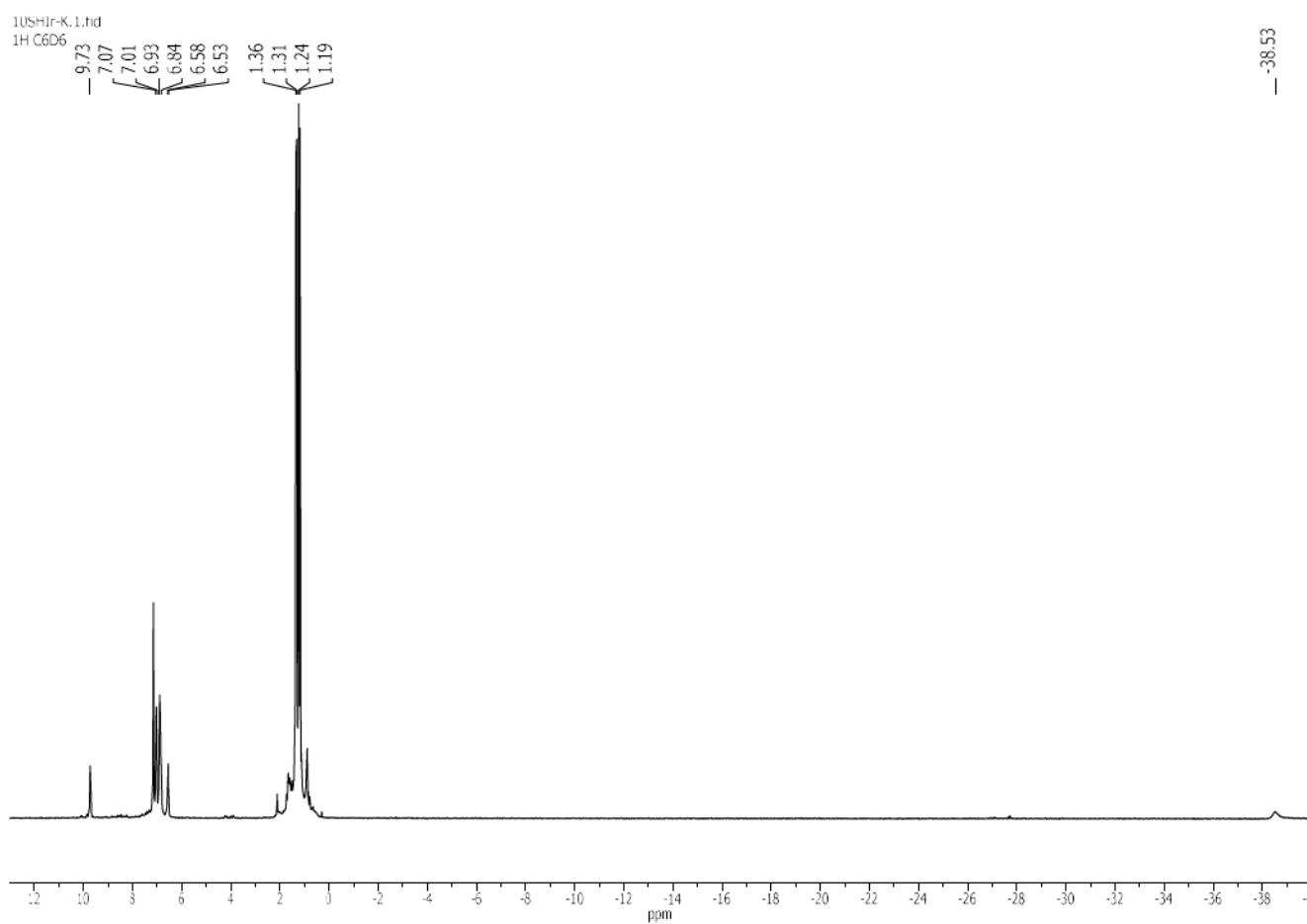
Butanoic acid ethyl ester: GC/MS-EI (70 eV): m/z (%) = 71 ((M - OC_2H_5) $^+$, 100), 89 ((MH $_2$ - C_2H_5) $^+$, 58).

2,3-Diphenyl-propionitrile: GC/MS-EI (70 eV): m/z (%) = 91 (100), 207 (M^+ , 19).

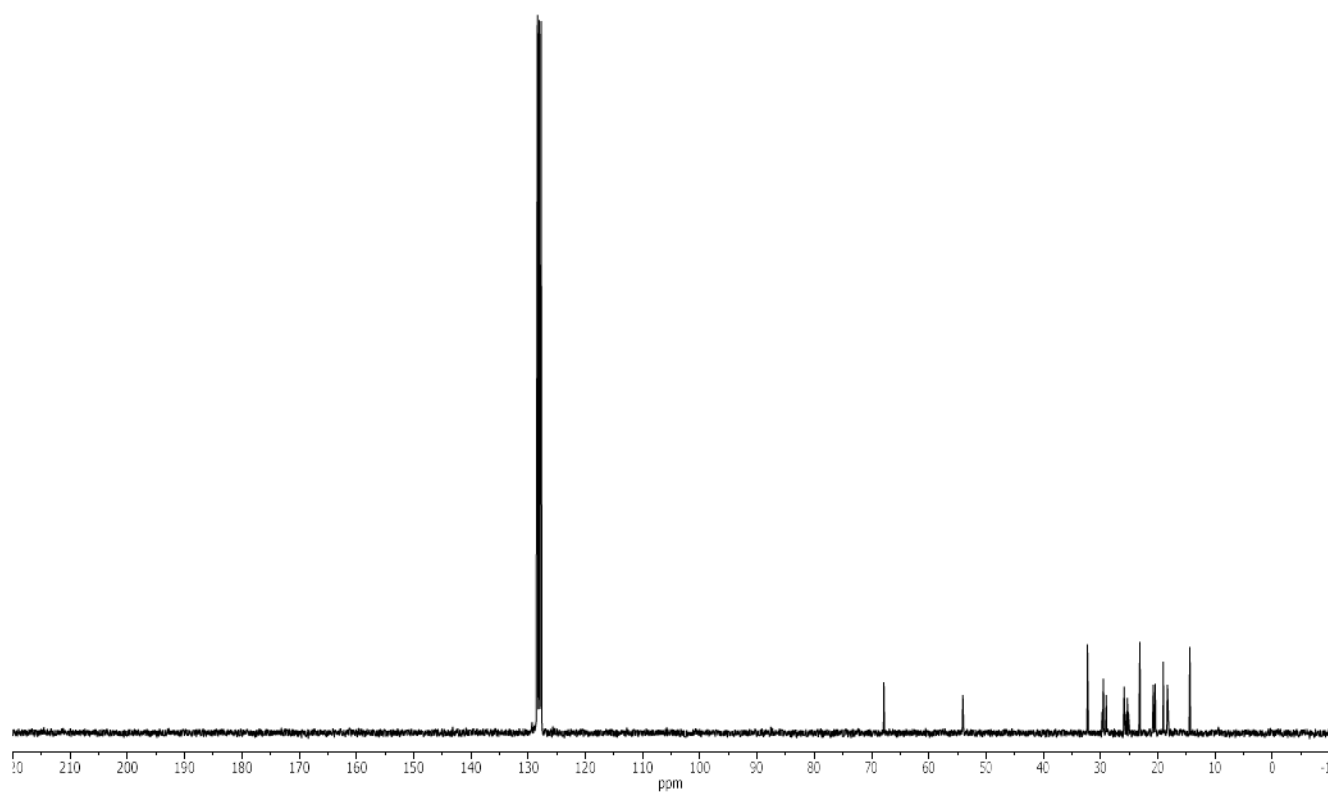
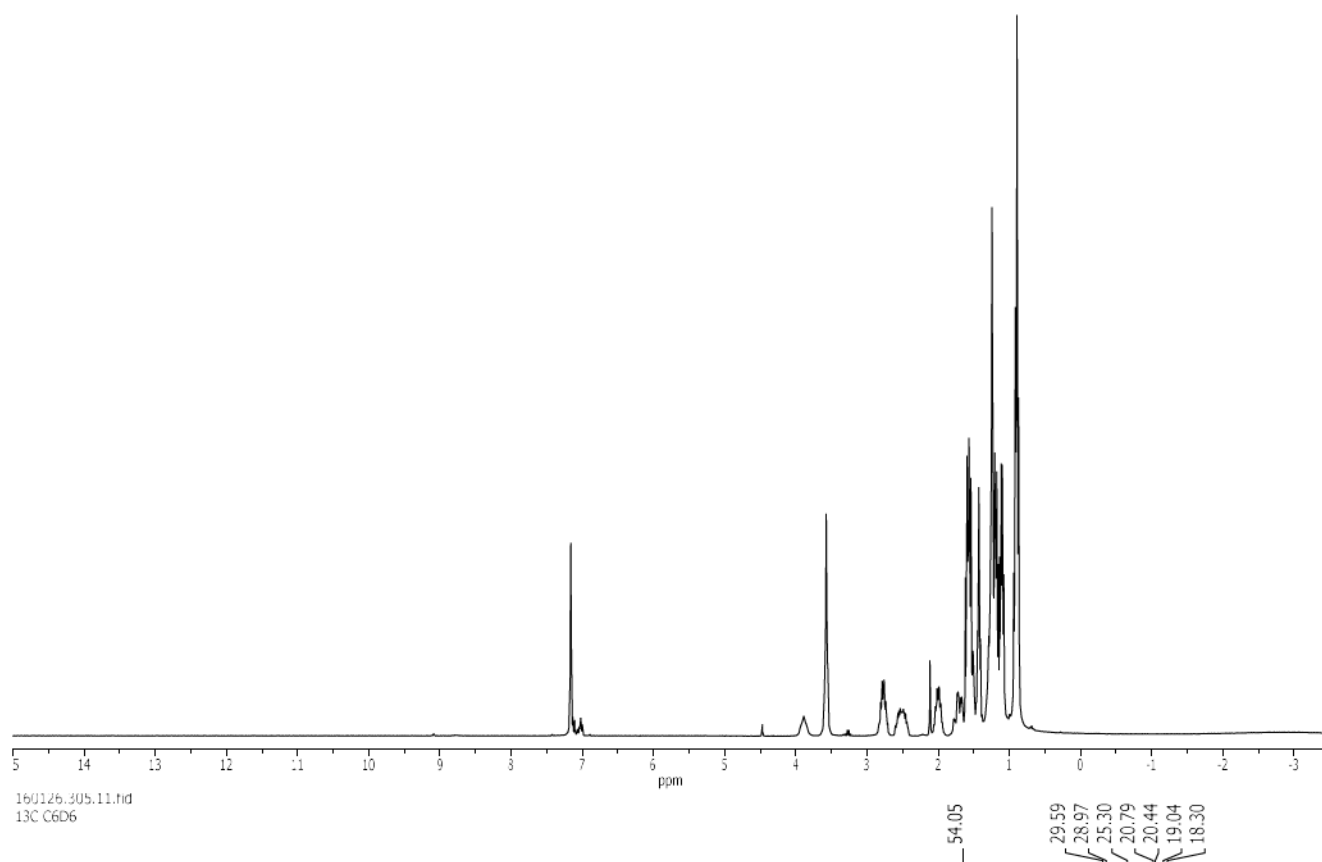
2,3-Diphenyl-acrylonitrile: GC/MS-EI (70 eV): m/z (%) = 205 (M^+ , 100), 204 (87), 190 (42), 203 (23), 177 (18), 176 (17), 206 (16), 178 (16).

Benzoic acid benzyl ester: GC/MS-EI (70 eV): m/z (%) = 105 (100), 91 (45), 212 (M^+ , 38), 77 (27), 194 (17), 51 (10), 167 (10).

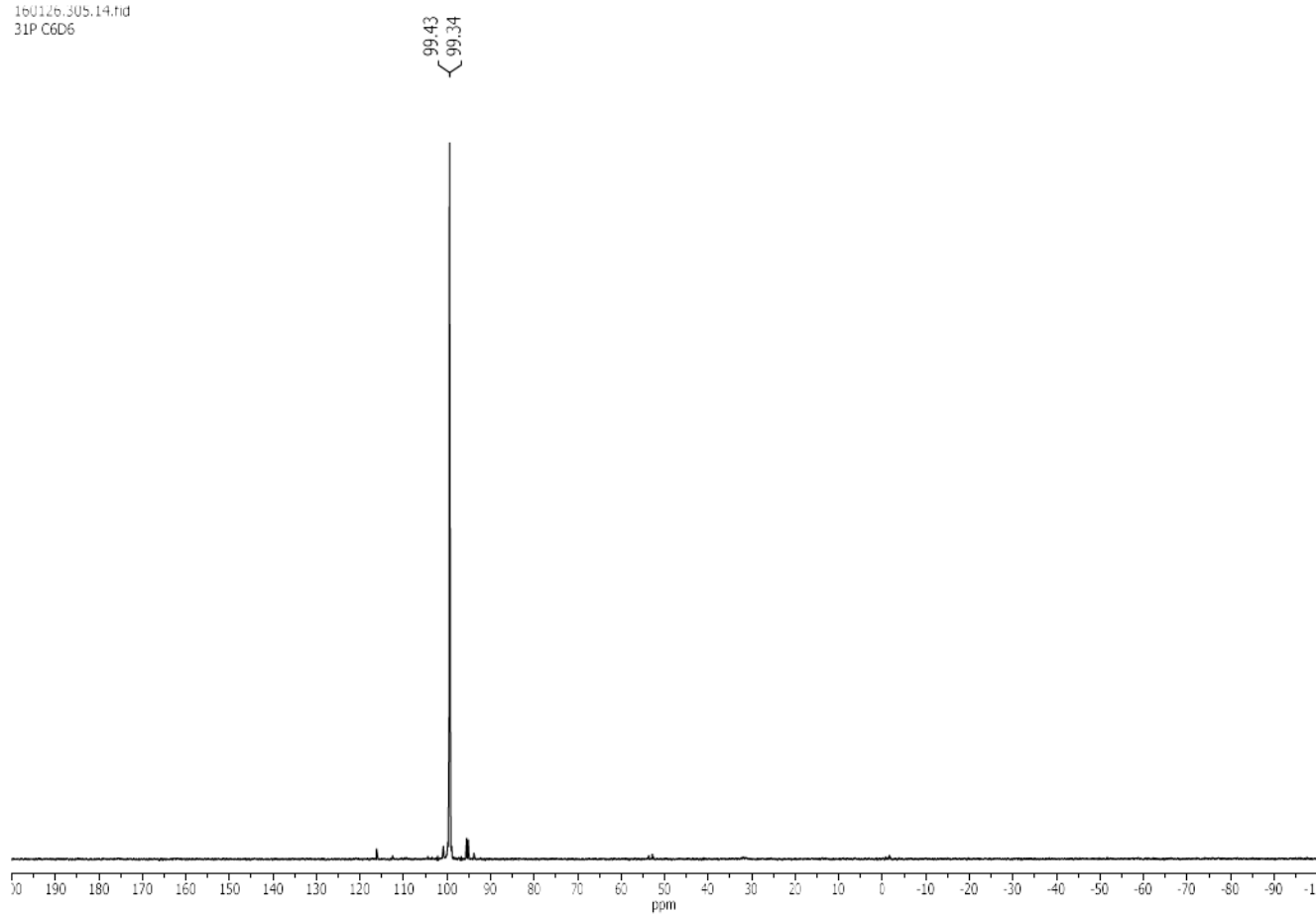
3-Phenyl-propiophenone: GC/MS-EI (70 eV): m/z (%) = 105 (100), 210 (M^+ , 52), 77 (31).



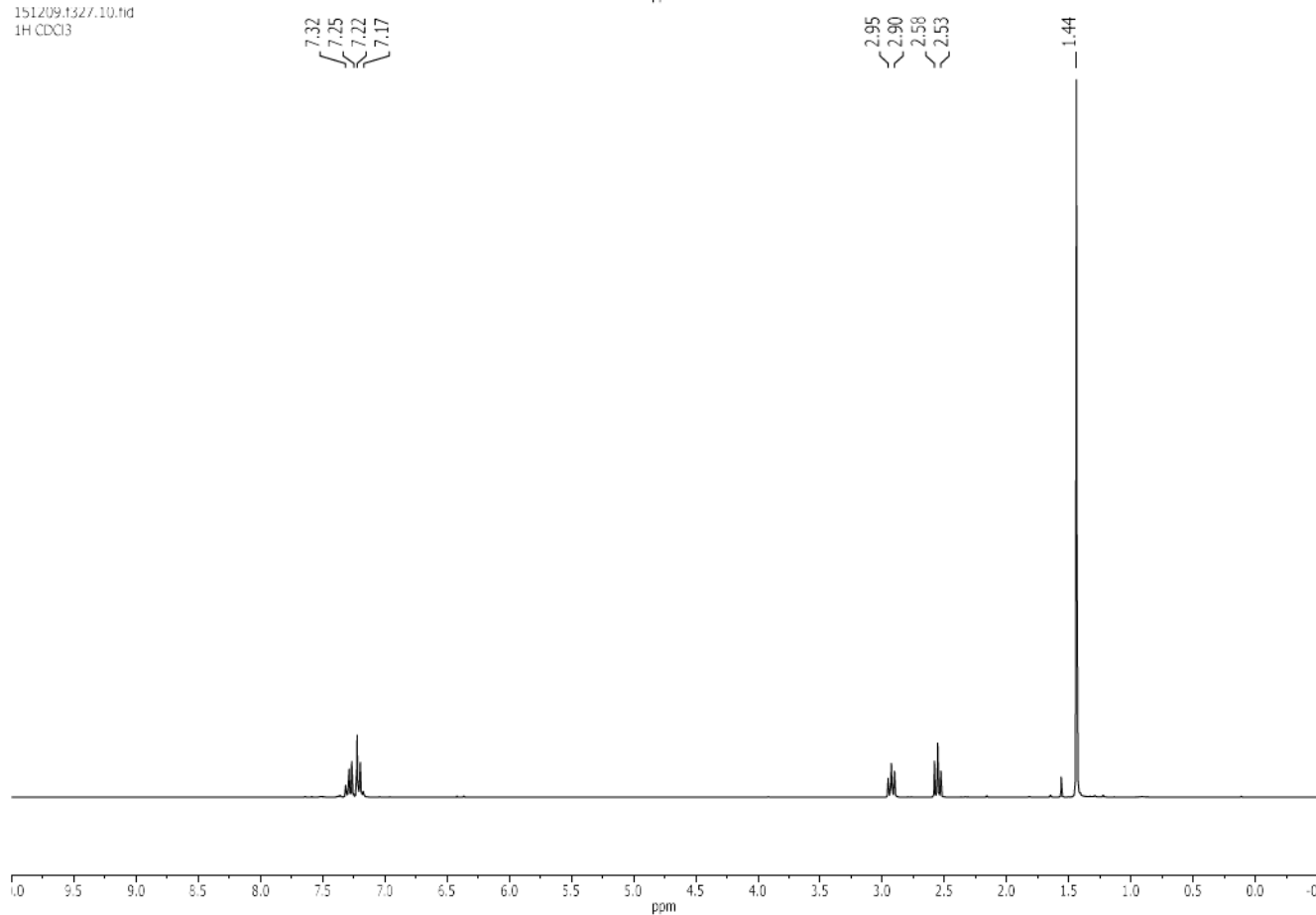
160126.305.10.fid
1H C6D6



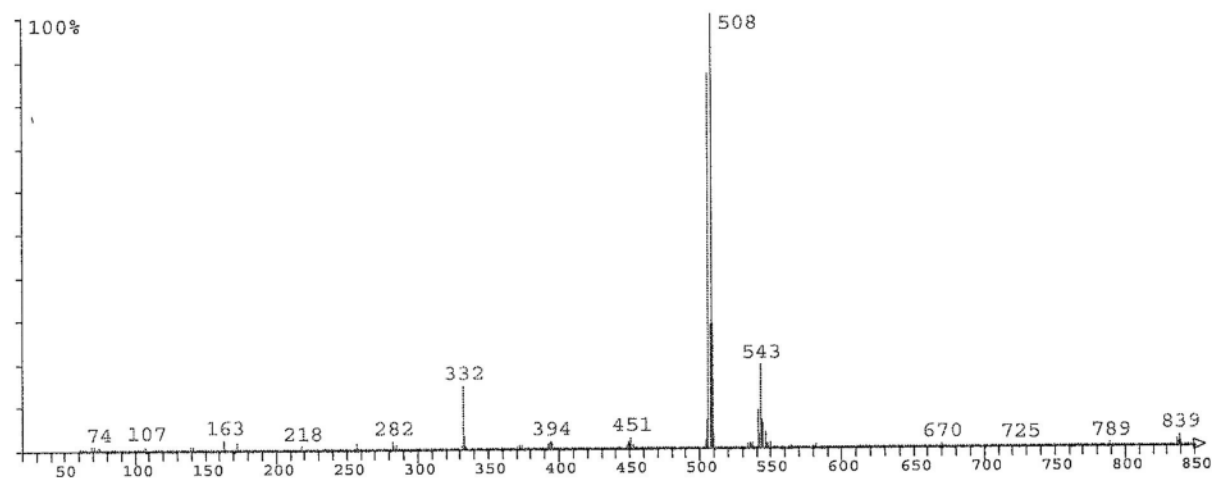
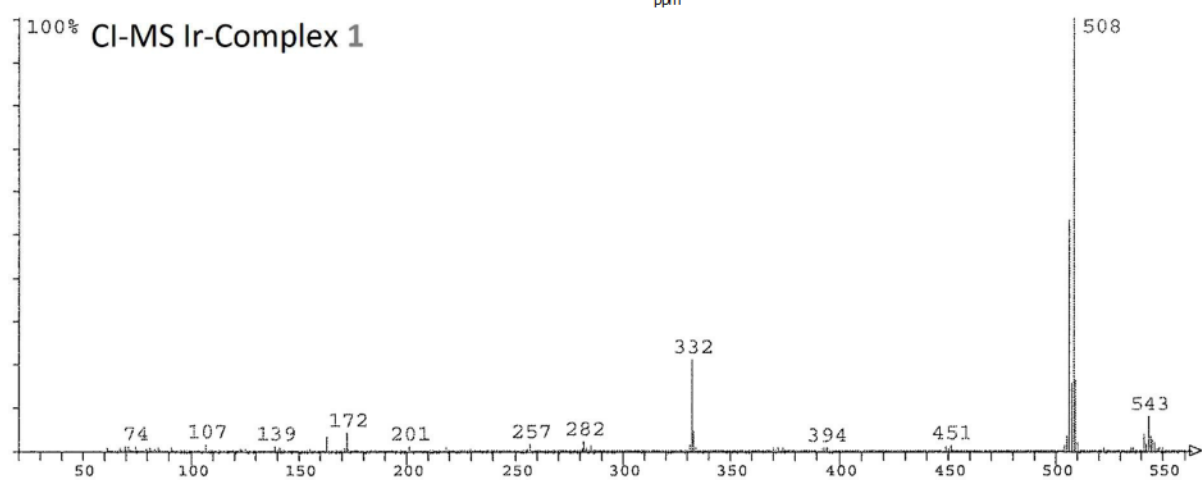
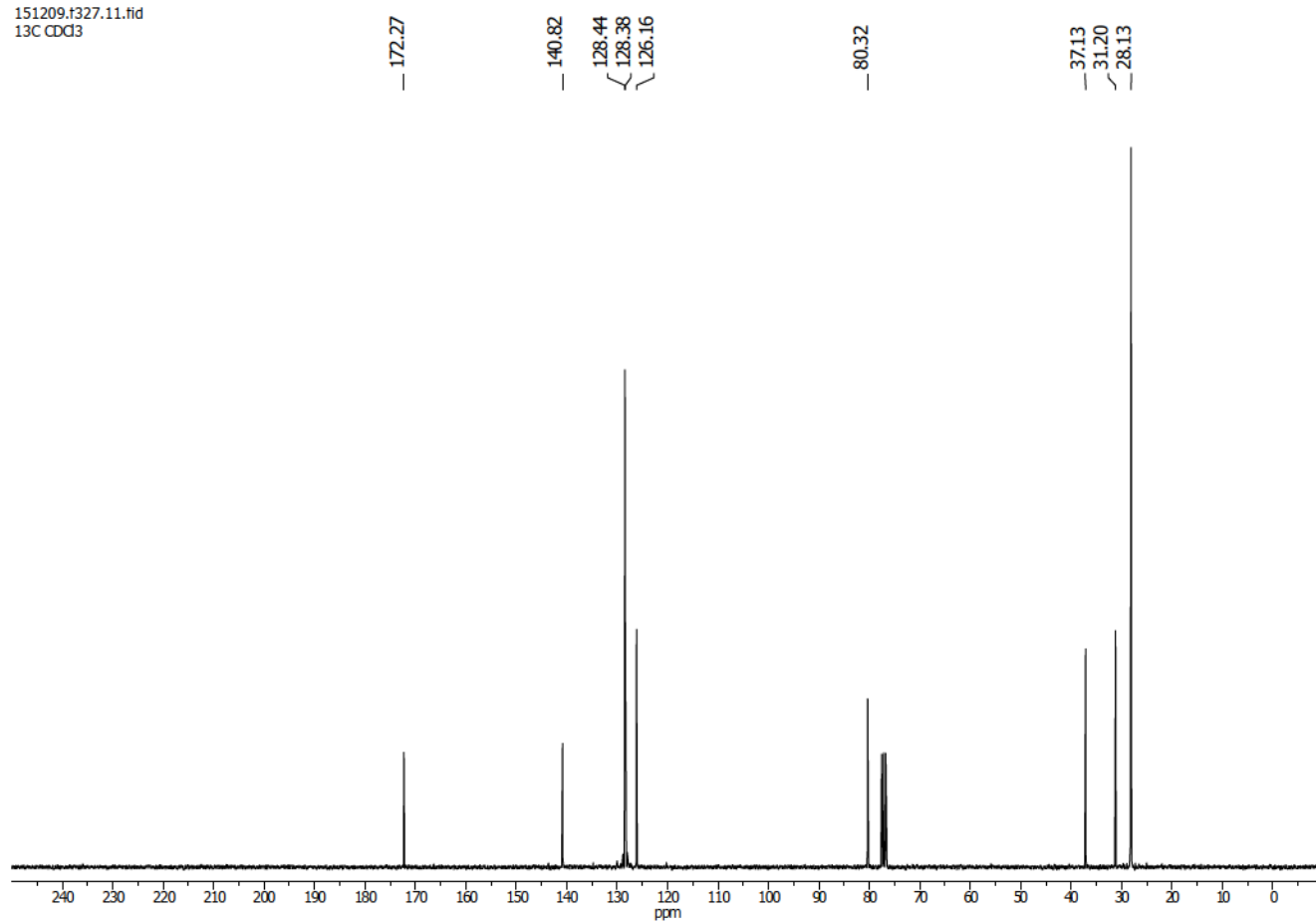
160126.305.14.fid
31P C6D6



151209.1327.10.fid
1H CDCl3



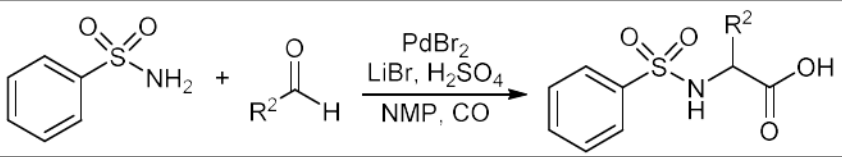
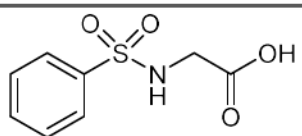
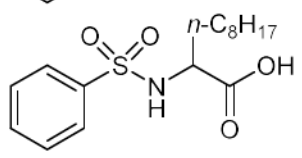
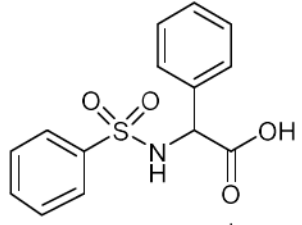
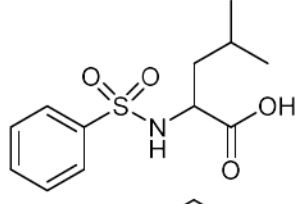
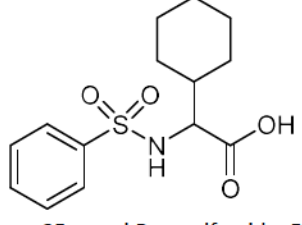
151209.1327.11.fid
13C CDCl₃



7.2. Amidocarbonylation

The following table includes a comparison of the obtained results for the sulfonamidocarbonylation by the author and the findings given in the dissertation of Wahed Ahmed Moradi.

Comparison of the results for the sulfonamidocarbonylation.

			
Entry	Compound	Yield previous work / % ^[a]	Yield this work / % ^[b]
1		65	74
2		n.e. ^[c]	<1
3		n.e. ^[c]	<1
4		<1	<1
5		<1	n.e. ^[c]

^[a] Conditions: 25 mmol Benzulfamide, 50 mmol paraformaldehyde (PFA), 35 mol% LiBr, 1 mol% H₂SO₄, 0.25 mol% PdBr₂, 0,5 mol% PPh₃ in 25 mL NMP under 60 bar CO at 120 °C for 12 h. ^[b] Conditions: 2.5 mmol Benzulfamide, 3.125 mmol paraformaldehyde (PFA), 35 mol% LiBr, 1 mol% H₂SO₄, 0.5 mol% PdBr₂ in 2.5 mL NMP under 60 bar CO at 100 °C for 16 h. ^[c] n.e. = not executed.

The following section includes the publication as well as the according supporting information. Herein, detailed experimental instructions on the conducted manipulations are given as well as analytical data.

Supporting Information

Synthesis of N-Lauroyl Sarcosine by Amidocarbonylation: Comparing Homogeneous and Heterogeneous Palladium Catalysts

Sören Hancker, Stefanie Kreft, Helfried Neumann and Matthias Beller*

*Leibniz-Institut für Katalyse e.V. an der Universität Rostock
Albert-Einstein-Straße 29a, 18059 Rostock (Germany)*

Table of Contents

- General amidocarbonylation procedure
- Catalyst preparation
- Optimisation reactions
- Recycling experiments
- Substrate scope
- 10 g-scale experiment
- ICP-OES analysis
- Analytical data of the synthesised products
- ^1H and ^{13}C NMR spectra
- Analytical instruments
- Substances
- References

General amidocarbonylation procedure

The manipulations were carried out in a 300 mL Parr high pressure autoclave. The small-scale experiments were conducted in 4 mL glass vials using magnetic stirring bars. Prior to the reaction, the vials were placed on an appropriate plate and equipped with the solid compounds which were subsequently sealed with a septum cap and evaporated and flushed with argon for three times. Afterwards, the solvent (water-free stored under Argon) was added prior to sulfuric acid (concentrated, neither purified nor oxygen- or water-free). The autoclave was closed before it was evaporated and flushed with Argon for three times as well. The autoclave was opened and the plate with the vials was placed inside quickly before the autoclave was closed again. Afterwards, the autoclave was flushed with argon for 15 minutes. The autoclave was sealed tightly before it was flushed with carbon monoxide up to 3 bars for three times. The reaction pressure (60 bars CO) was added by aid of the digital pressure indication. The autoclave was regulated by a control unit which monitored the reaction temperature *via* an integrated thermometer. The temperature was adjusted to the given value by the control unit automatically. The experiment was conducted at the corresponding reaction temperature for 16 hours.

Subsequently to the reaction, the autoclave was cooled in an ice bath. At room temperature, the pressure was released slowly. The heterogeneous catalyst was separated either by centrifugation (recycling experiments, preparation of sample A) or by filtration (optimisation reactions, substrate scope, 10 g-scale experiment, preparation of samples B-D) and washed at least three times within the process. Whenever NMP was removed (70 °C in high vacuum), an anti-splash guard with return-hole (Sigma Aldrich) was utilized since the solvent condensed before reaching the condensation trap. After the removal of NMP, the crude product was obtained.

Example on the basis of table 2, entry 11:

N-methyl dodecanamide:	1 mmol = 213.4 mg.
PFA (paraformaldehyde):	1.5 mmol = 45 mg.
Lithium bromide:	35 mol% = 30.4 mg.
Pd black:	1 mol% = 1.1 mg.
H ₂ SO ₄ :	10 mol% = 5 µL.

In 1 mL NMP at 60 bars CO and 60 °C for 16 hours.

Catalyst preparation

Pd/SiO₂, Pd/Faujasite A and Pd/ZSM-5 A (all 1 wt.% Pd)

Pd/SiO₂ was prepared by wet impregnation. Silica (990 mg, 0.035-0.070 mm, pore diameter 6 nm) was added to a solution of 30 mL water and Pd(NO₃)₂·XH₂O (25 mg, ca. 40% Pd content). After 30 minutes of stirring, the liquid was removed by rotary evaporation. Subsequently, the material was further dried at 80 °C overnight. Finally, the catalyst was calcined at 500 °C for 2 hours to give the final product. Pd/Faujasite A and Pd/ZSM-5 A were synthesised accordingly.

Pd/Faujasite B and Pd/ZSM-5 B (both 1 wt.% Pd)

Pd/Faujasite B and Pd/ZSM-5 B were prepared by incipient wet impregnation. Therefore, Pd(NO₃)₂·XH₂O (25 mg, ca. 40% Pd content) was dissolved in water (1.2 mL for Faujasite and 0.8 mL for ZSM-5). The solution was added to 990 mg of supporting material. Finally, the catalysts were dried at 80 °C overnight and finally calcined at 500 °C for 2 hours to give the final product.

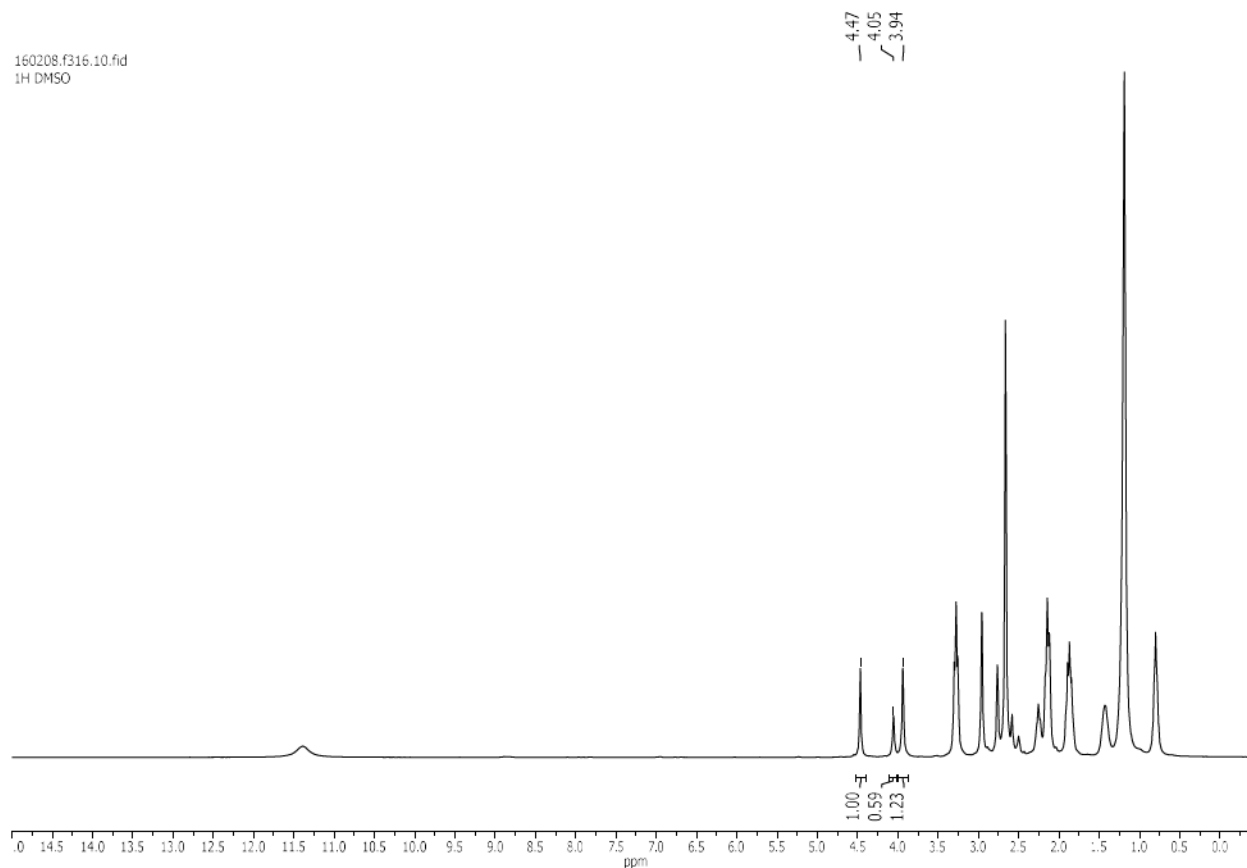
Pd/N@Gr (3 wt.% Pd)

Pd/N@Gr was synthesised by pyrolysis of a mixture of [Pd(phenanthroline)Cl₂] and carbon powder. For the synthesis of [Pd(phenanthroline)Cl₂], [Pd(CH₃CN)₂Cl₂] (2.233 mmol, 579 mg) was added dropwise to a stirred solution of phenanthroline·H₂O (4.925 mmol, 976 mg) and 60 mL DMF at 150 °C. After the formation of a precipitate within a few minutes, the mixture is heated under reflux conditions for another 3 hours. The product was obtained as orange needles after filtration. Subsequently, [Pd(phenanthroline)Cl₂] (0.314 mmol, 112.23 mg) was dissolved in 60 mL DMF at 120 °C. Henceforward, carbon powder (888.42 mg, VULCAN XC72R) was added and the mixture was kept at 120 °C for 2 hours. The solvent was removed by vacuum and the solid was further dried for 15 h at 120 °C in high vacuum. Finally, the catalyst was obtained by pyrolysis of the material at 800 °C for 2 h under argon atmosphere.

Optimisation reactions

The reaction solution was filtered through filter paper. The paper was washed with NMP several times. Ethylene carbonate (0.25 mol% to the amide) was added to the crude product (viscous liquid). Acetone was added to guarantee equal dispersion of the NMR standard within the sample. The acetone was removed by high vacuum. The integration results are based on the four protons from ethylene carbonate and the two protons from the glycine moiety ($\text{N-CH}_2\text{-COOH}$). Noteworthy, N-acyl sarcosines exist as *cis*- and *trans*-isomers.¹ Therefore, the $\text{N-CH}_2\text{-COOH}$ signal is split into one singlet at 3.96 ppm and one at 4.09 ppm. The intensity distribution for N-lauroyl sarcosine is 66:34. The signal splitting can also be observed for the methyl group N-CH_3 (2.79 ppm and 2.98 ppm, 34:66, singlet) and the first CH_2 -group of the alkyl chain $\text{CH}_2\text{-CH}_2\text{-CO-N}$ (2.16 ppm and 2.30 ppm, 34:66, triplet, $J = 7.4$ Hz).

Examples for NMR-analysis of the crude product:

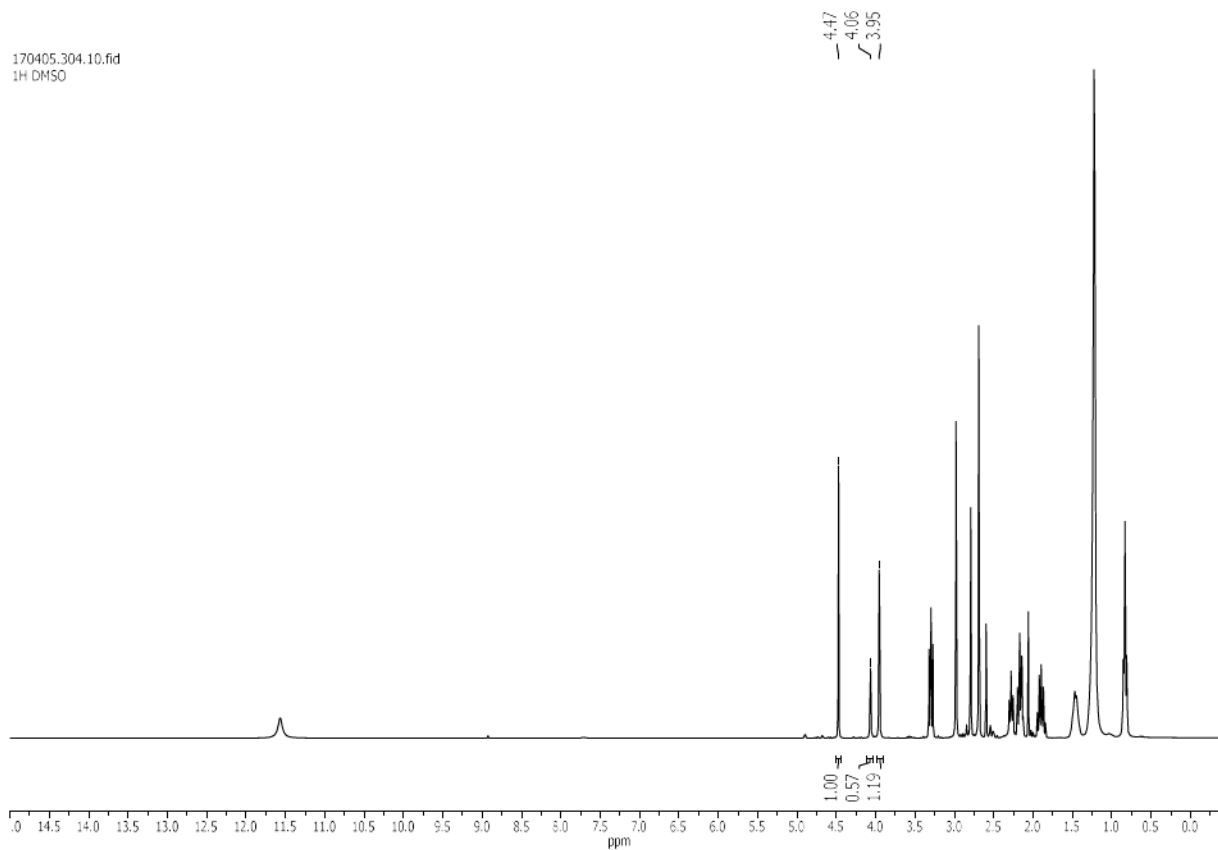


Recycling experiments

After the reaction, the mixture was transferred under argon into a septum sealed centrifuge tube. After centrifugation (5000 U/min for 20 min), the supernatant solution was removed *via* syringe and collected. The particles in the tube were washed with NMP five times. The combined NMP layers were prepared for NMR analysis (analogue to “Optimisation reactions”). The particles were transferred *via* syringe with NMP under argon into the next vial already containing the next set of reaction substrates as well as lithium bromide. In order to transfer the catalyst as entirely as possible, NMP was added in 0.1 mL portions and then transferred into the vial. This was repeated 10 times in order to add 1 mL NMP over the entire process as solvent for the next run. Finally, sulfuric acid was added and the manipulations were pursued as usual (see “General amidocarbonylation procedure”). After the reaction, the particles were treated with this procedure again until the forth cycle.

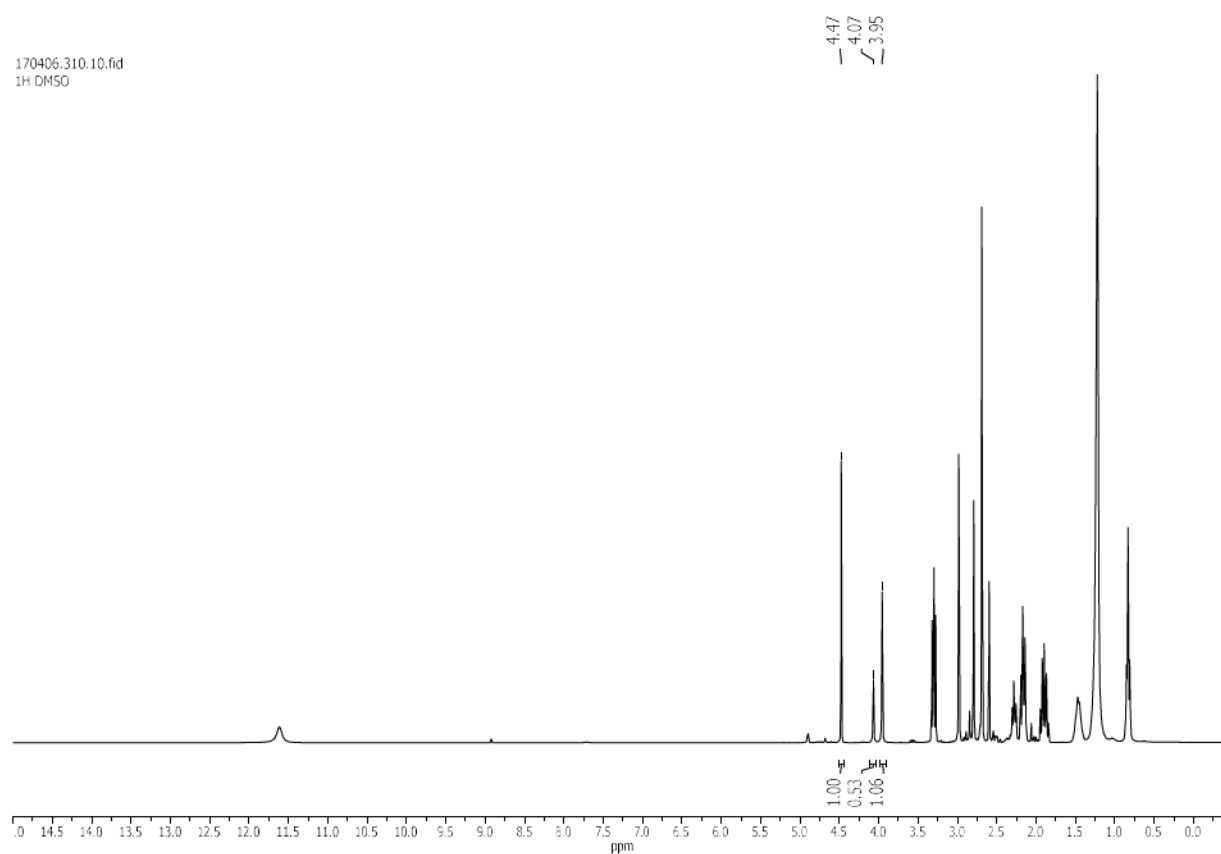
NMR-analysis of runs 1-4:

Run 1



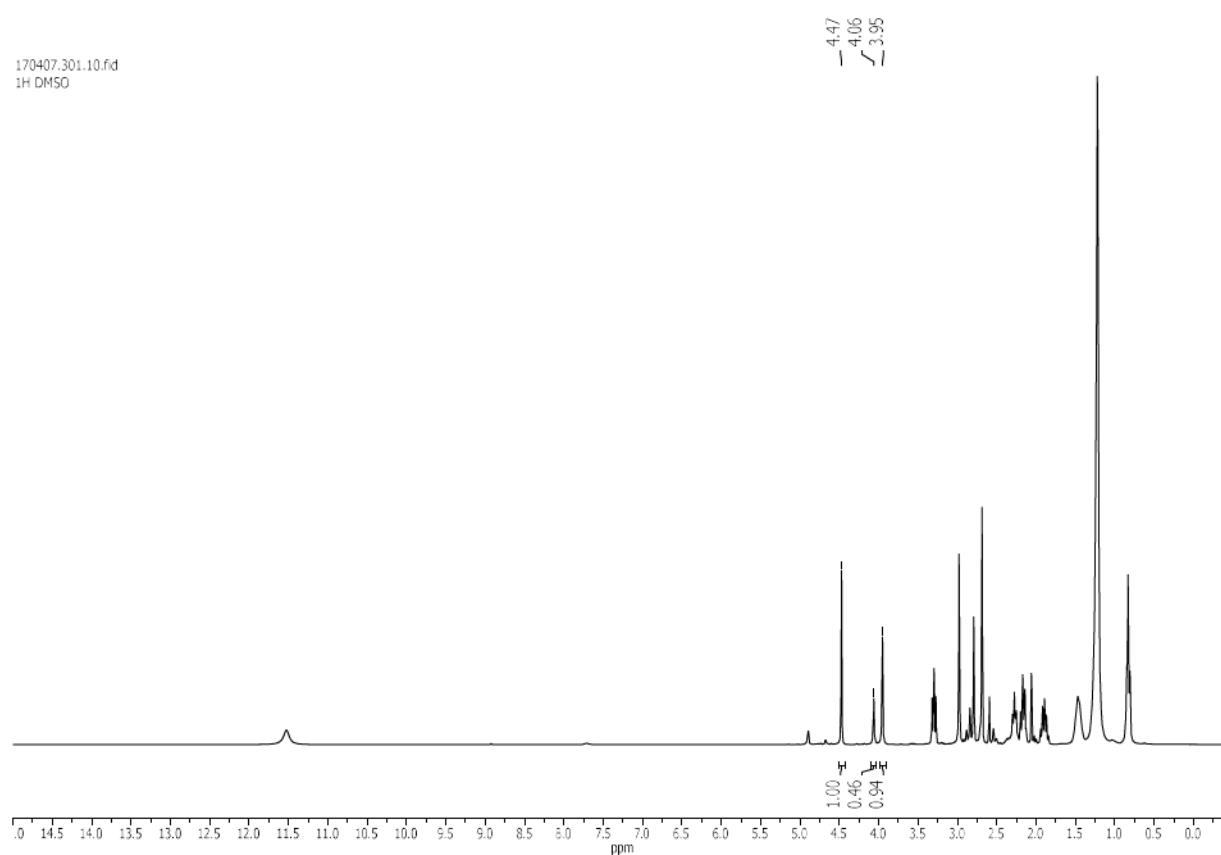
Run 2

170406.310.10.fid
1H DMSO



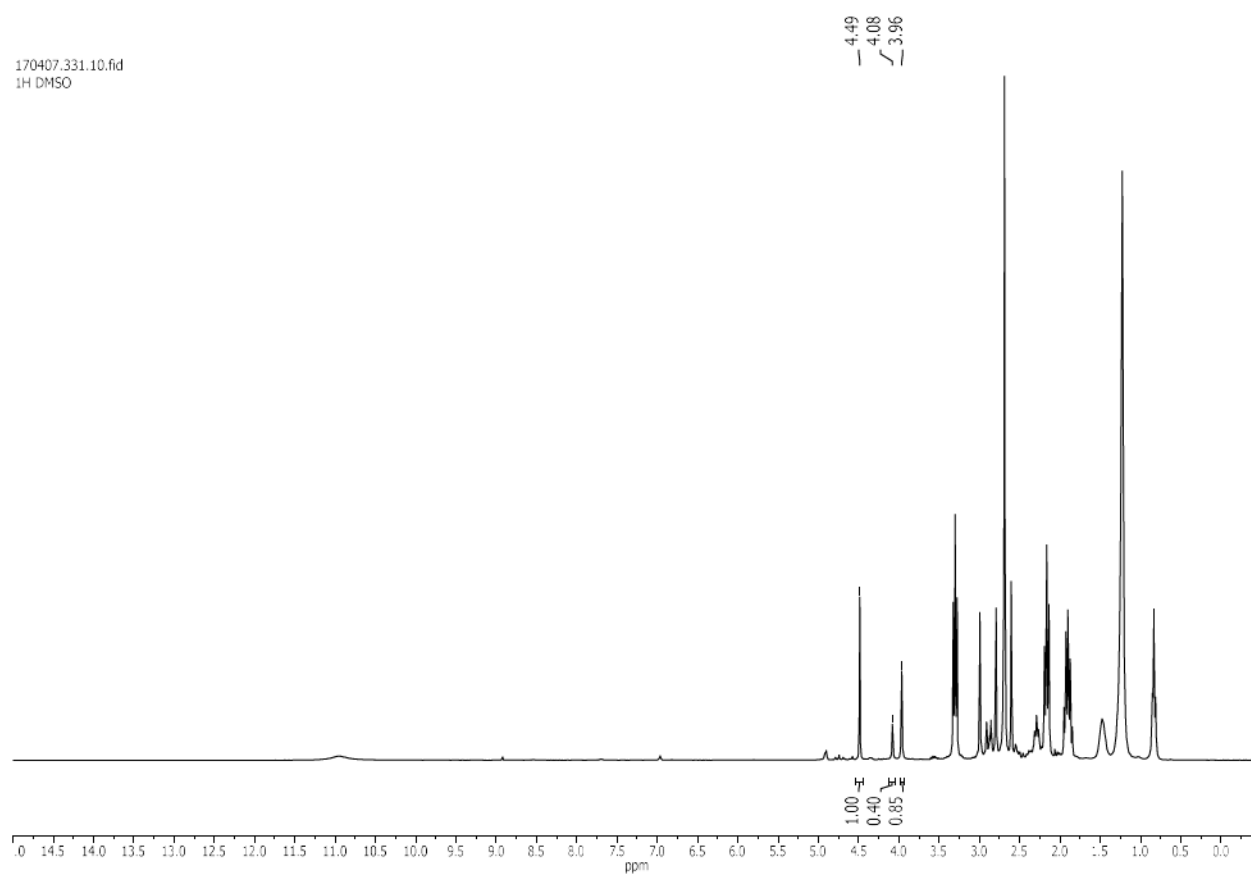
Run 3

170407.301.10.fid
1H DMSO



Run 4

170407.331.10.fid
1H DMSO



Substrate scope

The reactions were conducted and analysed by NMR and therefore treated according to the manipulations described in the sections “General amidocarbonylation procedure” and “Optimisation reactions”.

In order to determine the isolated yield, the reaction was repeated and an acid-base extraction was conducted in contrast to the optimisation reactions. Therefore, the crude product was dissolved in saturated aqueous NaHCO_3 solution (reaction is complete when evolution of gas stops and the liquid/particles are dissolved). The aqueous solution was extracted with ethyl acetate three times. Subsequently, the aqueous phase was acidified with concentrated phosphorus acid to pH 3. The aqueous phase was extracted with ethyl acetate again three times. The combined organic layers were dried over Na_2SO_4 which was later filtered off. Ethyl acetate was removed on the rotary evaporator. The products were dried in high vacuum.

10 g-scale experiment

The solid substrates and catalysts were added directly into the autoclave which was equipped with a mechanic stirrer. The autoclave was closed, evaporated and flushed with argon for three times. Meanwhile, a Schlenk flask was evaporated and flushed with argon as well. NMP and sulfuric acid were added and mixed by stirring with a magnetic stirring bar. The resulting solvent was added into a syringe and the autoclave was opened carefully. Under argon counter flow, the top of the autoclave was slightly lifted and the solvents were injected into the autoclave. Subsequently, the autoclave was closed and flushed with argon for 15 minutes. The carbon monoxide pressure was added after flushing with CO and heating as well as stirring was started. After the reaction, the pressure was released very slowly. The reaction mixture was filtered through filter paper before the solvent was removed in high vacuum at 70 °C (see "General amidocarbonylation procedure").

Water was added to the crude product at atmospheric pressure and 70 °C. After stirring for a few minutes, the two phased system was stored in a deep freezer at -28 °C for one hour. Afterwards, the solid was allowed to warm up to room temperature until the water melted. The solid raw product was crushed into small particles with a scoopula on a frit (POR 3) and subsequently washed with water five times. The product resulting from this purification step was analysed by ICP-OES and NMR as sample B. For additional purification, the acid-base extraction described within the section "Substrate scope" was conducted. For N-lauroyl sarcosine, the product starts to separate from the aqueous phase between pH of 4-6. The separation occurs immediately during the addition of concentrated phosphorus acid. After the two phased system was formed, a few more drops of concentrated phosphorus acid were added in order to ensure that the product can be obtained entirely. Additionally, the aqueous phase was extracted with ethyl acetate three times. The combined organic layers were dried over Na₂SO₄. After the solid was filtered off, ethyl acetate was removed using a rotary evaporator. The resulting viscous liquid was dried in high vacuum. The resulting N-lauroyl sarcosine was further analysed as sample C by ICP-OES and NMR.

NMR-analysis for samples B and C: see section "ICP-OES analysis".

ICP-OES analysis

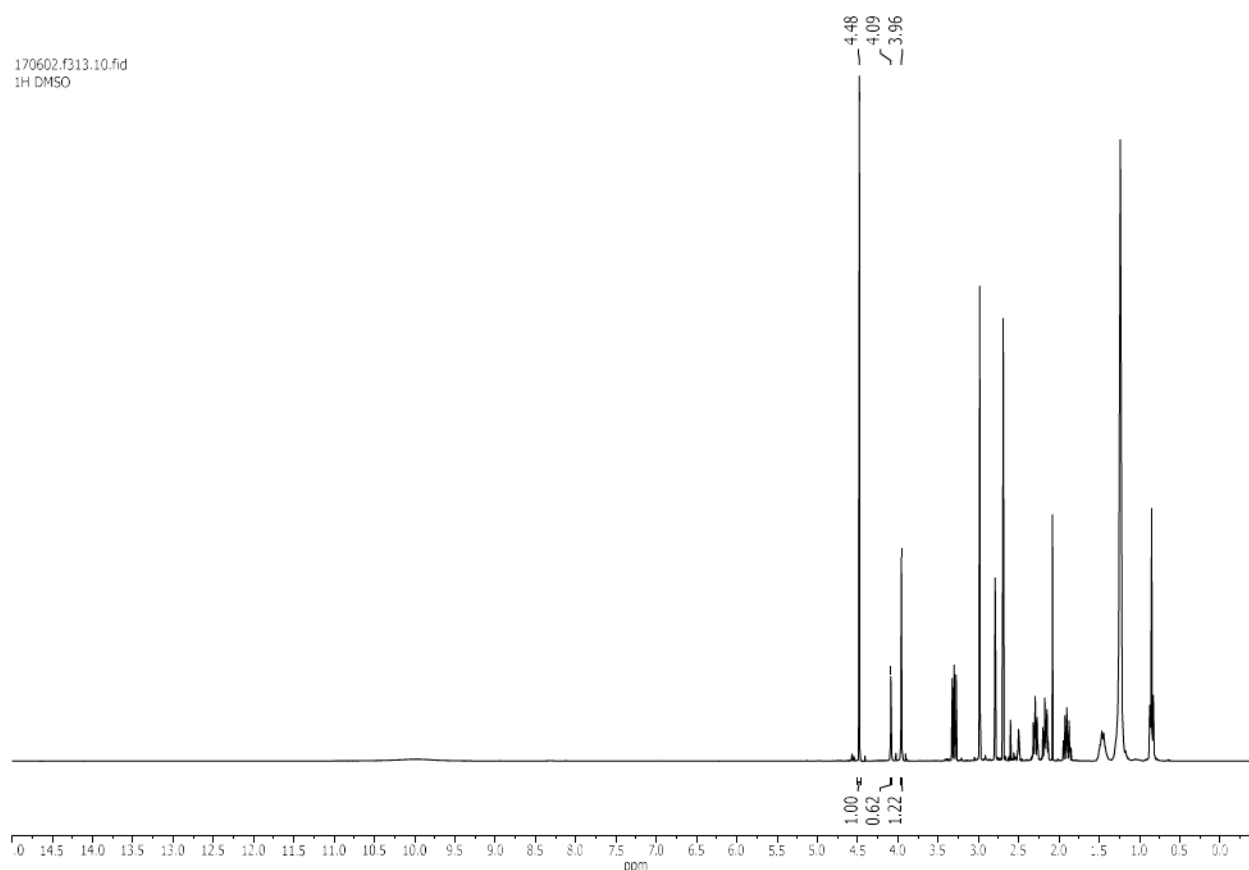
Samples B and C were prepared as described in the section “10 g-scale experiment”.

Sample A was prepared by conducting the experiment on the optimisation scale (conditions table 2, entry 11; see section “General amidocarbonylation procedure”). After the reaction, the particles were removed by centrifugation (5000 U/min for 20 min) and the remaining solid was washed with NMP five times. The crude product was analysed by ICP-OES and NMR as Sample A.

Sample D was prepared by conducting the reaction utilising PdBr_2 (0.5 mol%, 6.2 mg) as catalyst under otherwise optimised reaction conditions on a 1 g-scale (4.69 mmol N-methyl dodecanamide) in a 8 mL vial (see section “General amidocarbonylation procedure”). The product was isolated according to the conditions described in section “10 g-scale experiment”. Therefore, the sample was generated in the identical manner as sample C. The substance obtained from the PdBr_2 -catalysed reaction was analysed as sample D by ICP-OES and NMR.

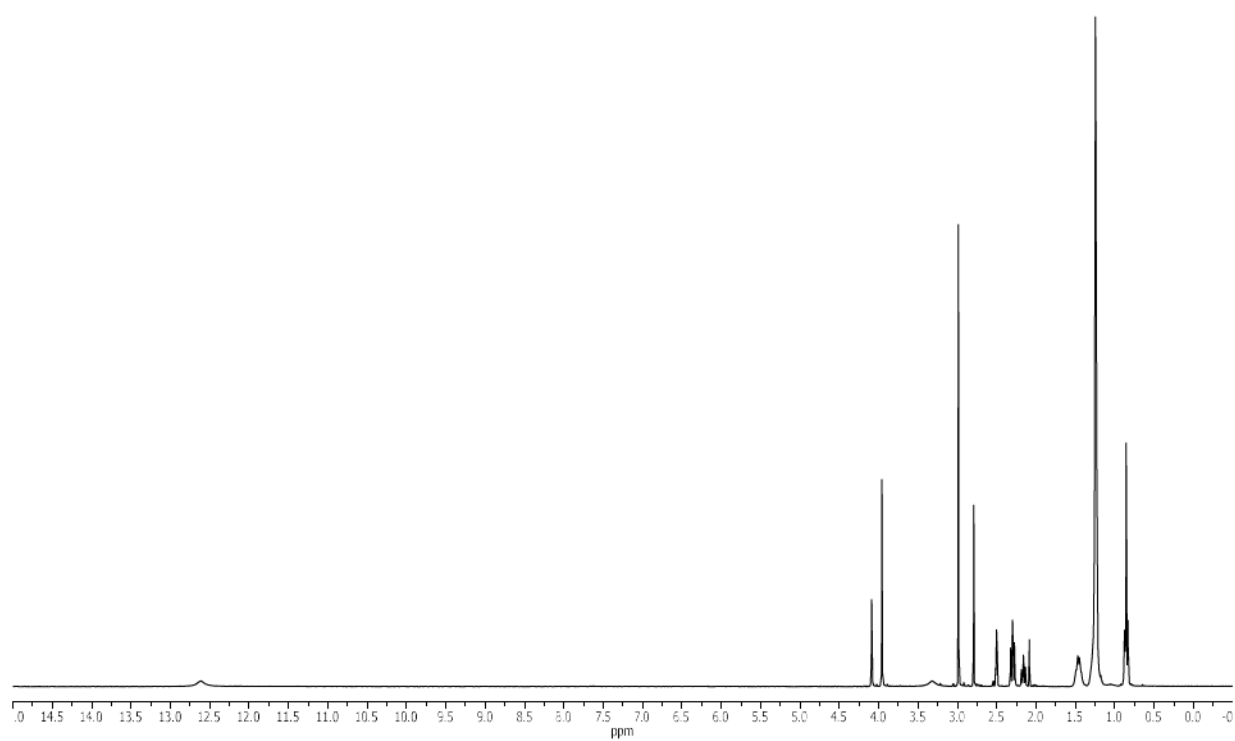
NMR-analysis for Samples A-D:

Sample A

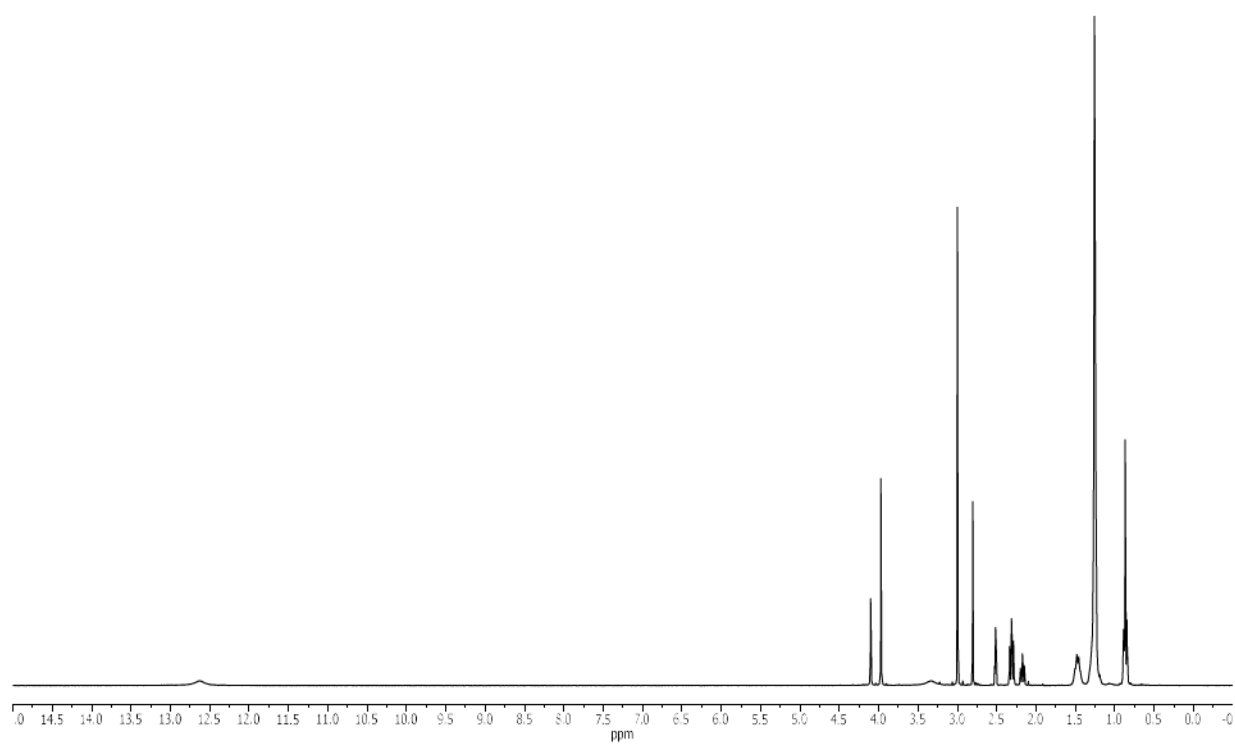


Sample B

170622.f301.10.fid
1H DMSO

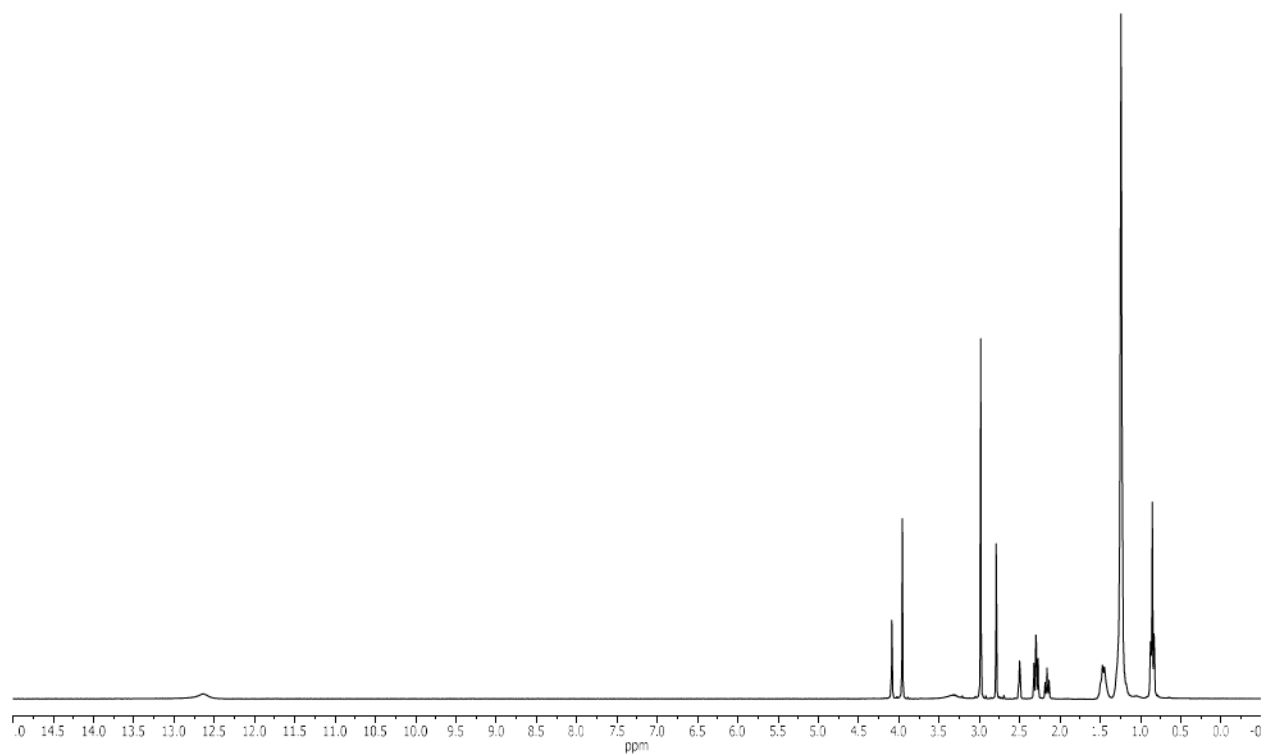
**Sample C**

170627.f307.10.fid
1H DMSO



Sample D

170728.f305.10.fid
1H DMSO

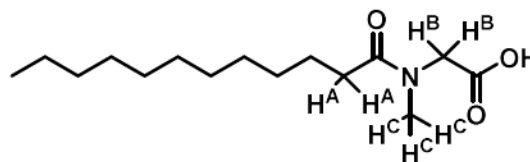


Analytical data of the synthesised products

^1H & ^{13}C NMR: DMSO- d_6 (ITSD: ^1H NMR: 2.500 ppm; ^{13}C : 39.520 ppm)

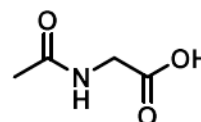
All $\delta^1\text{H}$ and $\delta^{13}\text{C}$ in ppm, all coupling constants J in Hz.

N-Lauroyl sarcosine (1): Off-white solid (12.04 g, 95%). ^1H NMR (300.1 MHz, DMSO- d_6): $\delta^1\text{H}$ = 0.83-0.88 (3H, m, CH_3), 1.19-1.30 (16H, m, 8 CH_2), 1.40-1.52 (2H, m, CH_2), 2.16 (0.68H, t, J = 7.4, H^{A}), 2.30 (1.32H, t, J = 7.4, H^{A}), 2.79 (1.02H, s, H^{C}), 2.98 (1.99H, s, H^{C}), 3.96

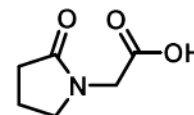


(1.32H, s, H^{B}), 4.09 (0.68H, s, H^{B}), 12.61 (1H, br s, COOH); ^{13}C NMR (75.5 MHz, DMSO- d_6): $\delta^{13}\text{C}$ = 13.9 (CH_3), 22.1 (CH_2), 24.5 & 24.6 (CH_2), 28.7 (2 C, CH_2), 28.9-29.0 (4 C, CH_2), 31.3 (CH_2), 31.8 & 32.1 ($\text{C}^{\text{A}}\text{H}_2$), 34.2 & 36.0 ($\text{C}^{\text{C}}\text{H}_3$), 48.9 & 50.9 ($\text{C}^{\text{B}}\text{H}_2$), 170.8 & 171.0 (CO-N), 172.6 & 172.6 (COOH); HRMS (ESI, m/z): calcd. for $\text{C}_{15}\text{H}_{28}\text{NO}_3^-$ (M-H^+): 270.20747, found: 270.20746; EA: calcd. for $\text{C}_{15}\text{H}_{29}\text{NO}_3$: C 66.38%, H 10.77%, N 5.16, found C 66.55%, H 10.55%, N 5.00%.

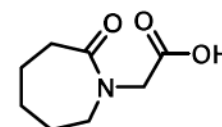
N-Acetylglycine (2): Off-white solid (52.7 mg, 45%). ^1H NMR (300.1 MHz, DMSO- d_6): $\delta^1\text{H}$ = 1.84 (3H, s, CH_3), 3.71 (2H, d, J = 5.7, CH_2), 8.15 (1H, t, J = 5.7, NH); ^{13}C NMR (75.5 MHz, DMSO- d_6): $\delta^{13}\text{C}$ = 22.3 (CH_3), 40.7 (CH_2), 169.7 (C^{q}), 171.5 (C^{q}); HRMS (ESI, m/z): calcd. for $\text{C}_4\text{H}_6\text{NO}_3^-$ (M-H^+): 116.03532, found: 116.03529; EA: calcd. for $\text{C}_4\text{H}_7\text{NO}_3$: C 41.03%, H 6.03%, N 11.96%, found C 41.19%, H 6.01%, N 11.63%.



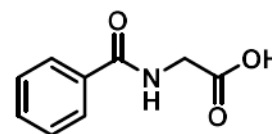
2-Oxo-1-pyrrolidineacetic acid (3): This product was further purified by sublimation in high vacuum (10^{-3} mbar) at 100 °C. Off-white solid (97.3 mg, 68%). ^1H NMR (300.1 MHz, DMSO- d_6): $\delta^1\text{H}$ = 1.94 (2H, p, J = 7.4, CH_2), 2.23 (2H, t, J = 8.1, CH_2), 3.38 (2H, t, J = 7.0, CH_2), 3.90 (2H, s, CH_2), 12.71 (1H, br s, COOH); ^{13}C NMR (75.5 MHz, DMSO- d_6): $\delta^{13}\text{C}$ = 17.5 (CH_2), 29.9 (CH_2), 43.6 (CH_2), 47.0 (CH_2), 170.2 (C^{q}), 174.4 (C^{q}); HRMS (ESI, m/z): calcd. for $\text{C}_6\text{H}_8\text{NO}_3^-$ (M-H^+): 142.05097, found: 142.05063; EA: calcd. for $\text{C}_6\text{H}_9\text{NO}_3$: C 50.35%, H 6.34%, N 9.79%, found C 50.61%, H 6.50%, N 9.77%.

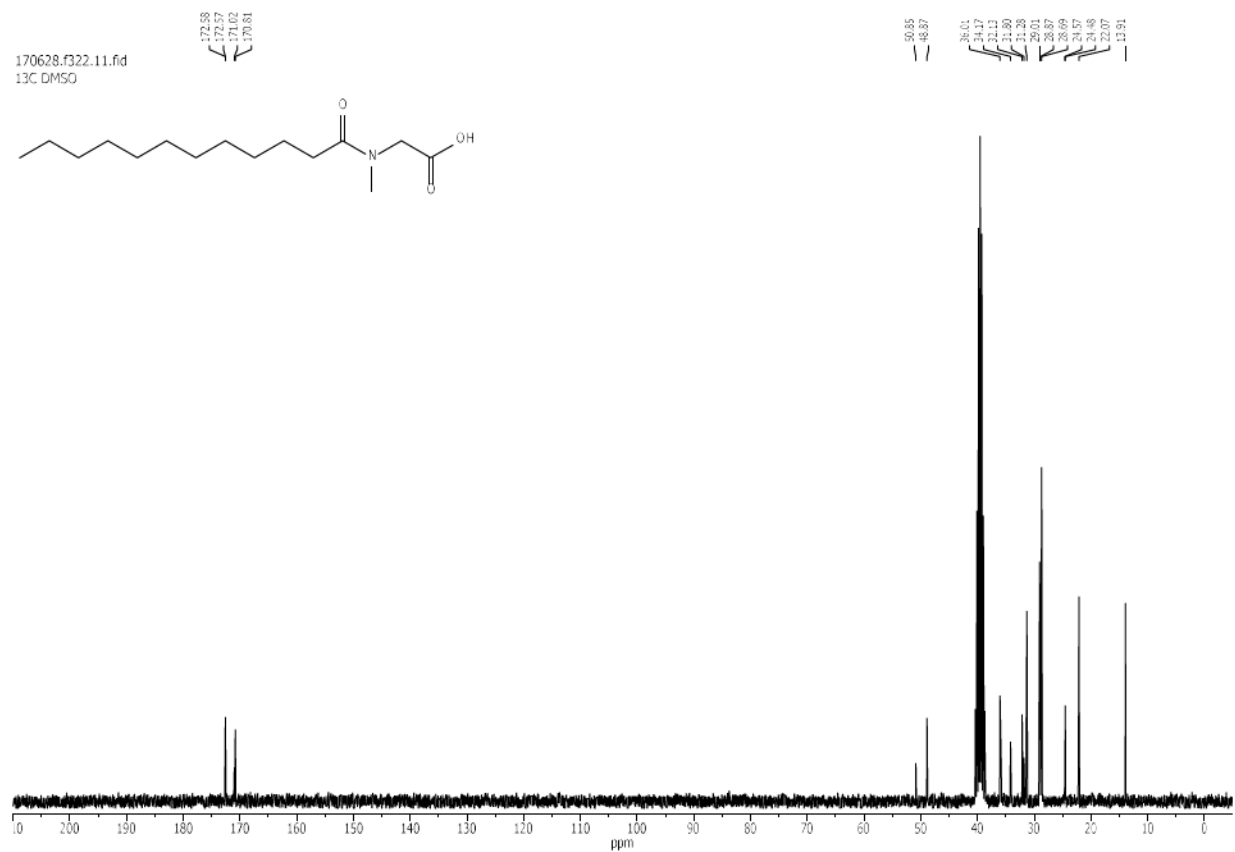
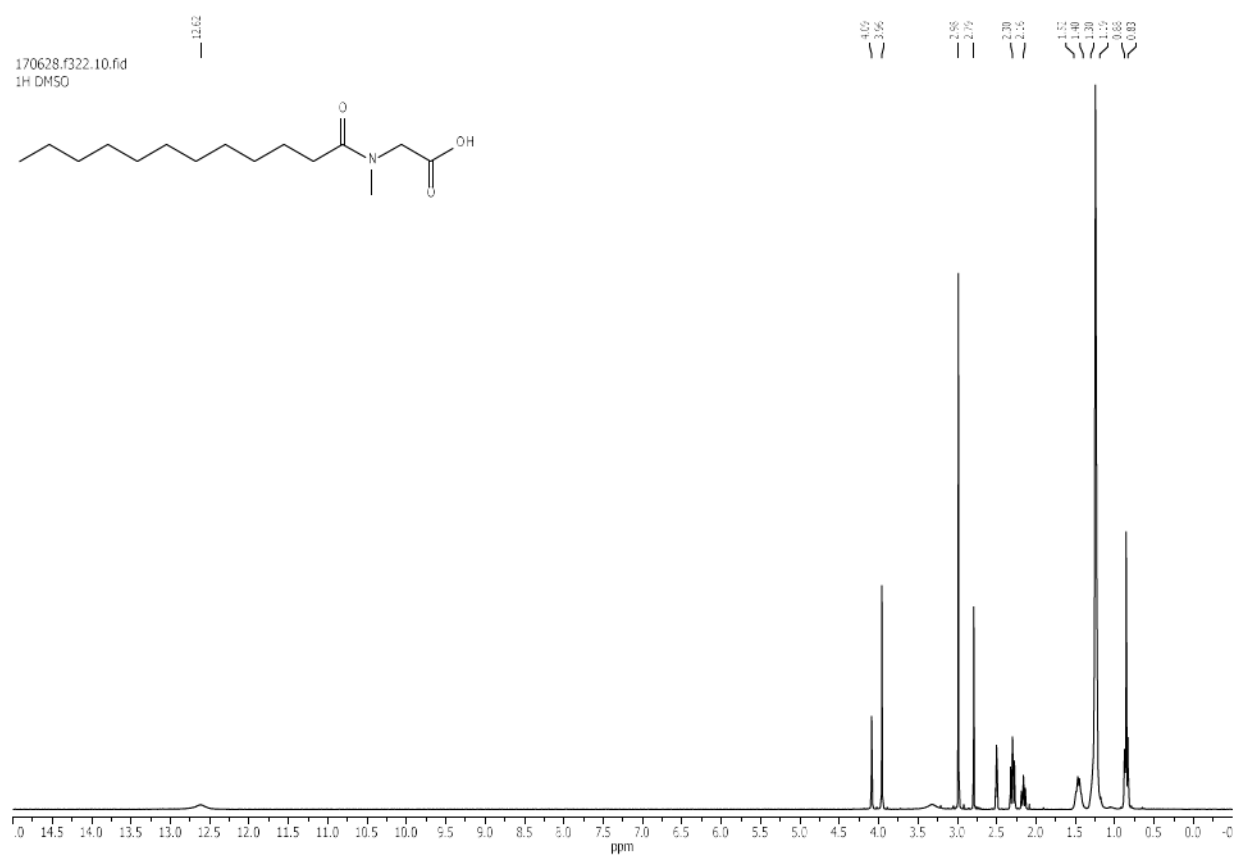


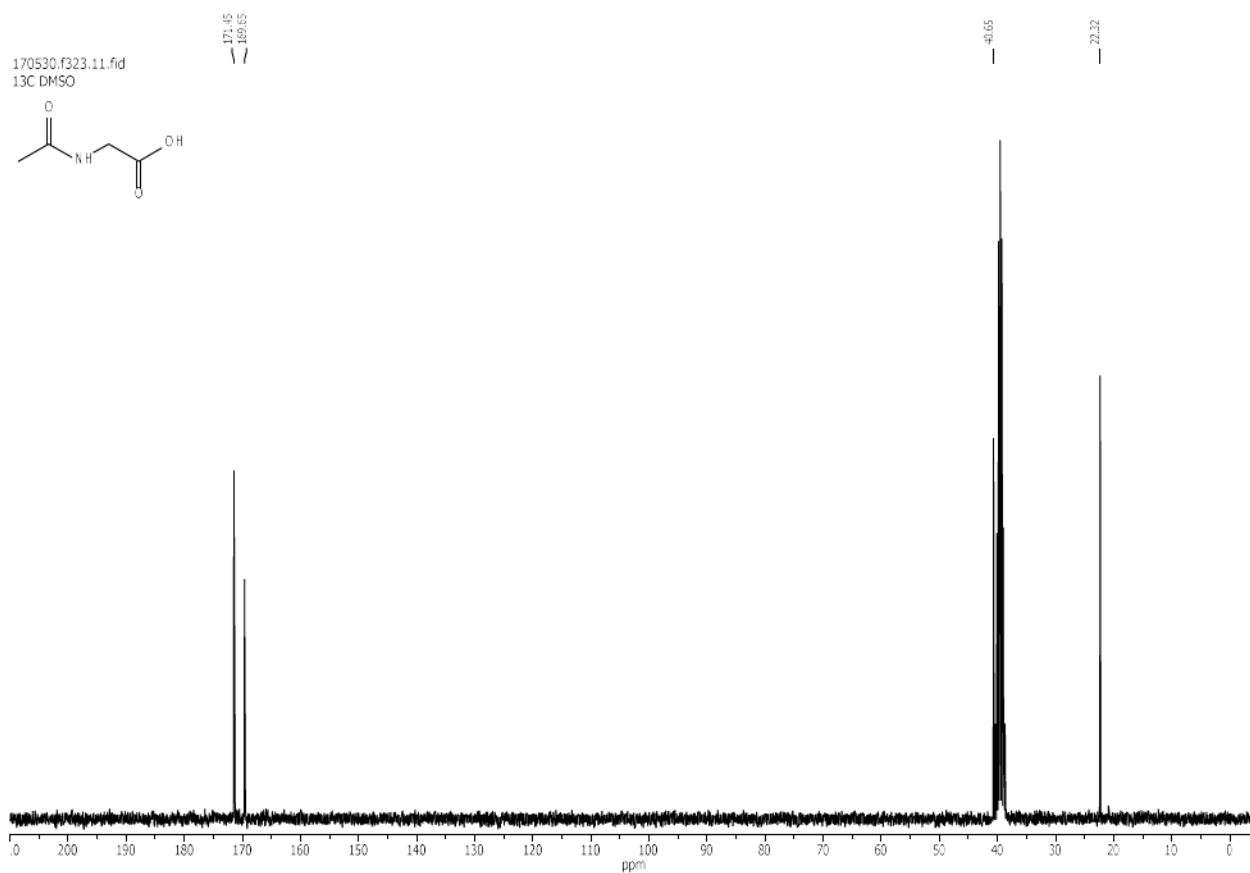
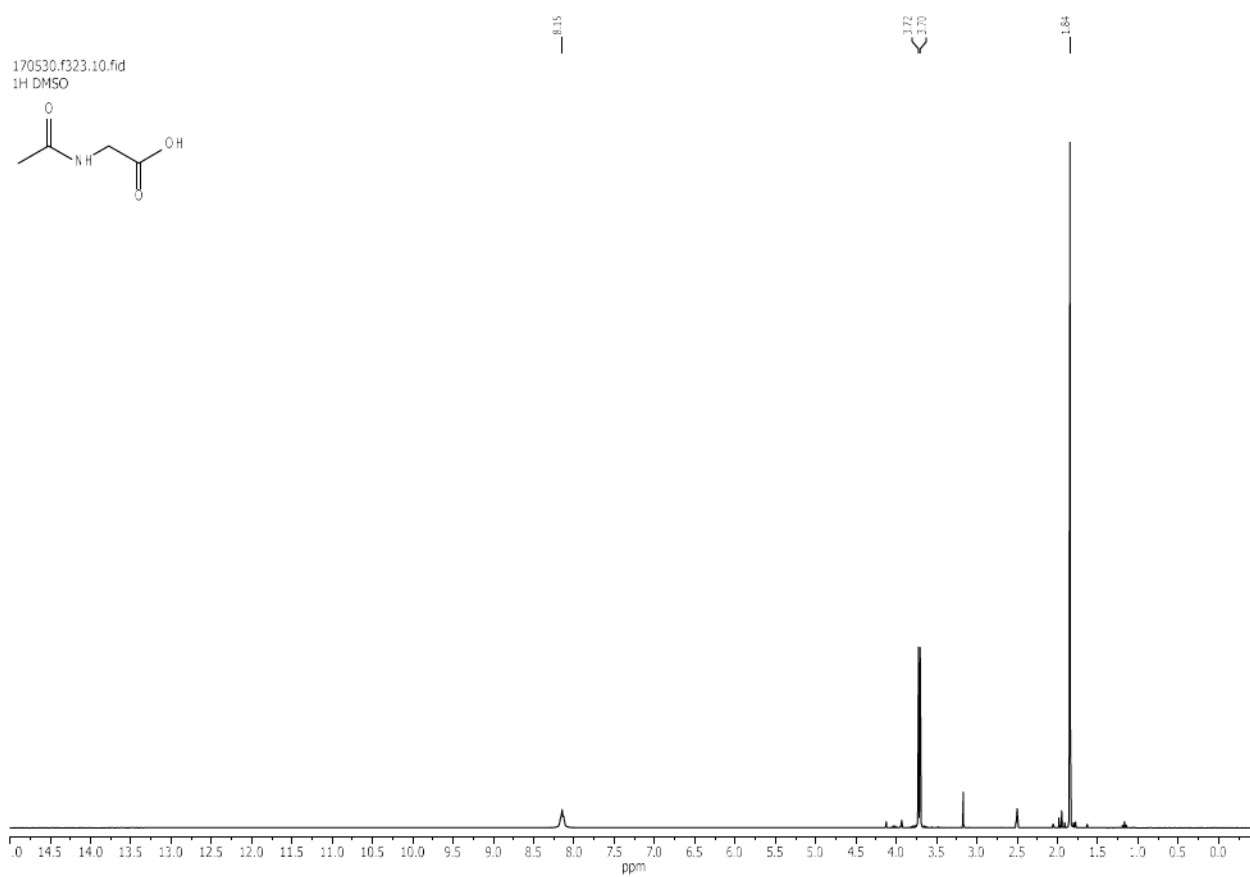
Hexahydro-2-oxo-1H-azepine-1-acetic acid (4): Off-white solid (111.3 mg, 65%). ^1H NMR (300.1 MHz, DMSO- d_6): $\delta^1\text{H}$ = 1.51-1.58 (2H, m, CH_2), 1.60-1.70 (4H, m, 2 CH_2), 2.41-2.45 (2H, m, CH_2), 3.37-3.40 (2H, m, CH_2), 3.98 (2H, s, CH_2); ^{13}C NMR (75.5 MHz, DMSO- d_6): $\delta^{13}\text{C}$ = 22.9 (CH_2), 27.7 (CH_2), 29.3 (CH_2), 36.3 (CH_2), 49.9 (CH_2), 50.2 (CH_2), 171.1 (C^{q}), 175.0 (C^{q}); HRMS (ESI, m/z): calcd. for $\text{C}_8\text{H}_{12}\text{NO}_3^-$ (M-H^+): 170.08227, found: 170.08218; EA: calcd. for $\text{C}_8\text{H}_{13}\text{NO}_3$: C 56.13%, H 7.65%, N 8.18%, found C 55.99%, H 7.52%, N 7.84%.

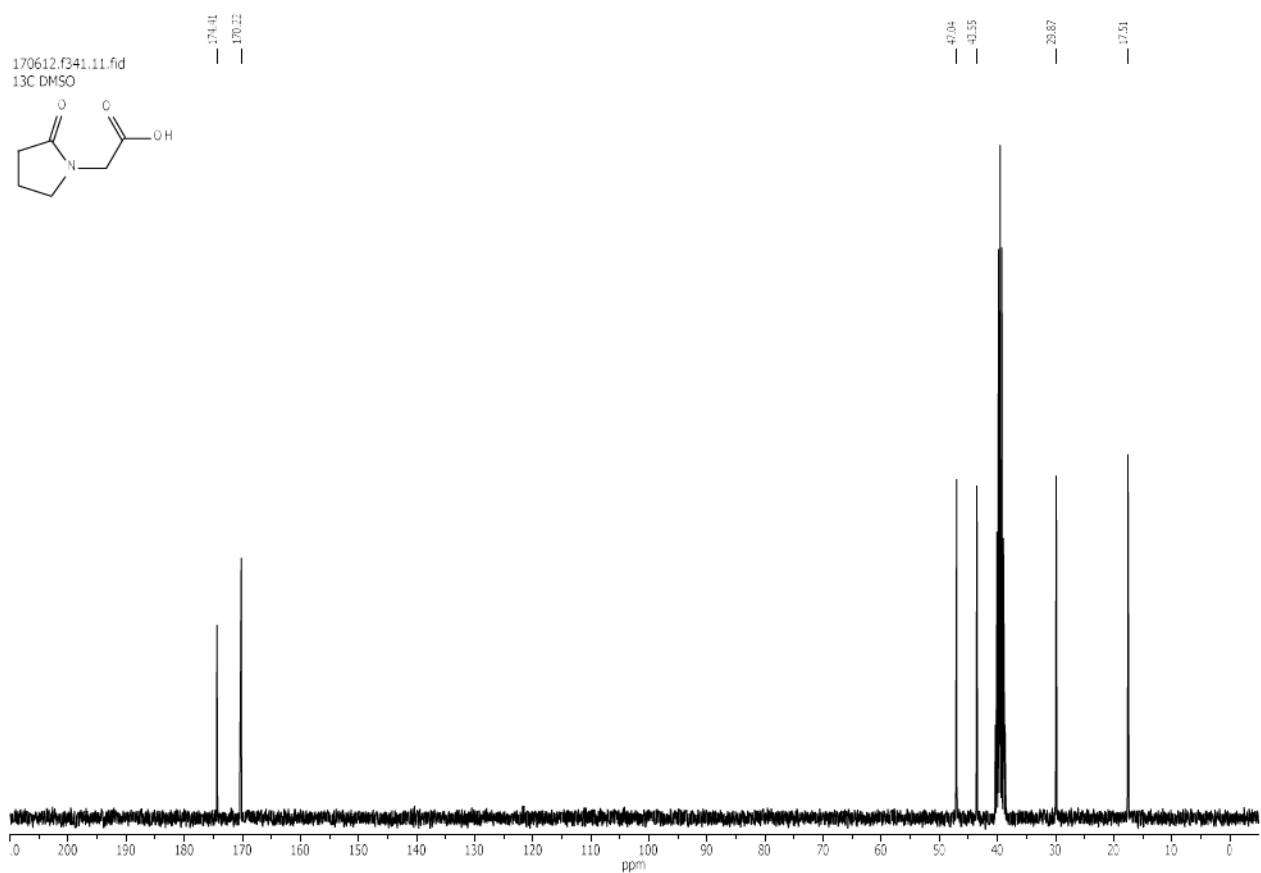
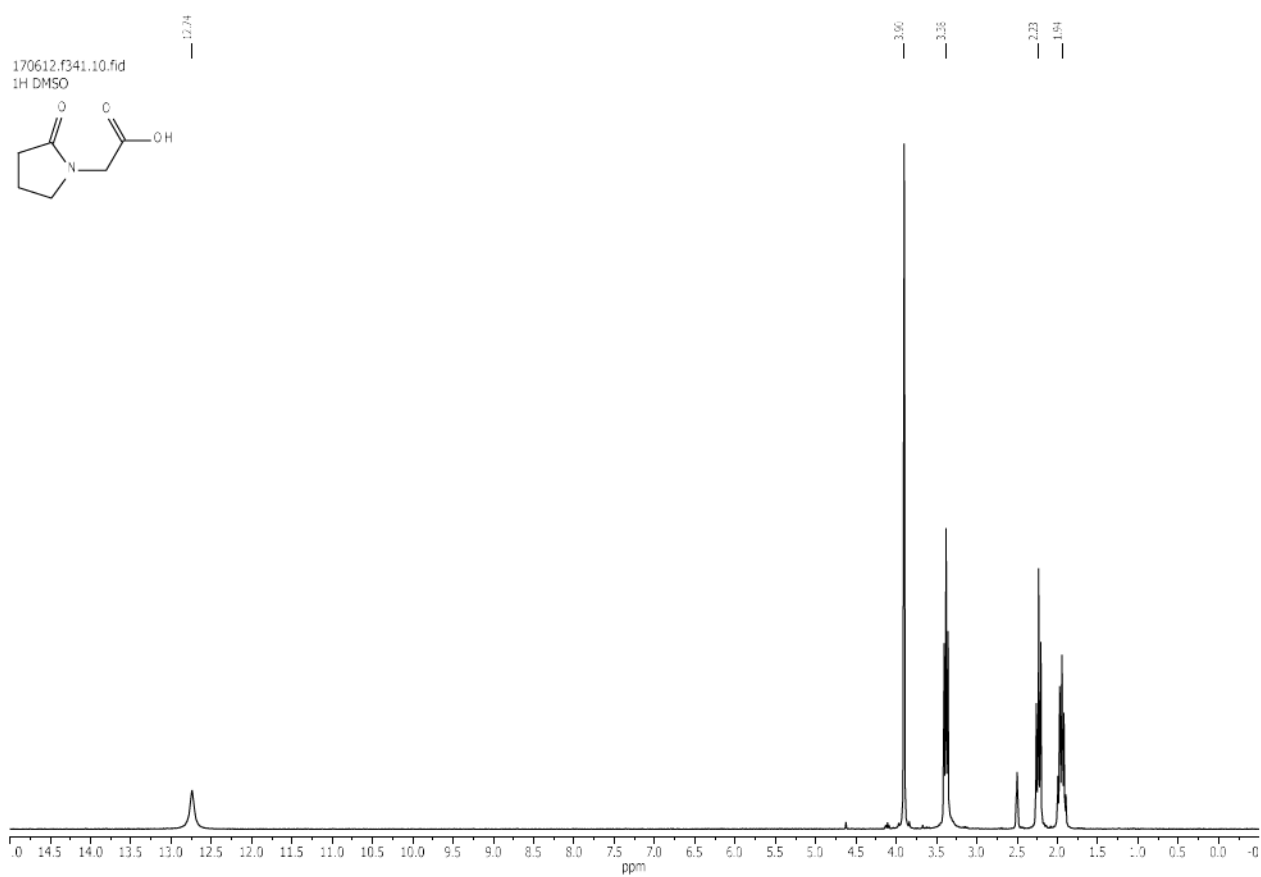


N-Benzoylglycine (5): Off-white solid (53.8 mg, 30%). ^1H NMR (300.1 MHz, DMSO- d_6): $\delta^1\text{H}$ = 3.94 (2H, d, J = 5.9, CH_2), 7.44-7.57 (3H, m, CH), 7.86-7.89 (2H, m, CH), 8.83 (1H, t, J = 5.9, NH); ^{13}C NMR (75.5 MHz, DMSO- d_6): $\delta^{13}\text{C}$ = 41.3 (CH_2), 127.3 (2C, CH), 128.5 (2C, CH), 131.5 (CH), 133.9 (C^{q}), 166.7 (C^{q}), 171.4 (C^{q}); HRMS (ESI, m/z): calcd. for $\text{C}_9\text{H}_8\text{NO}_3^-$ (M-H^+): 178.05097, found: 178.05084; EA: calcd. for $\text{C}_9\text{H}_9\text{NO}_3$: C 60.33%, H 5.06%, N 7.82%, found C 60.61%, H 5.04%, N 7.72%.

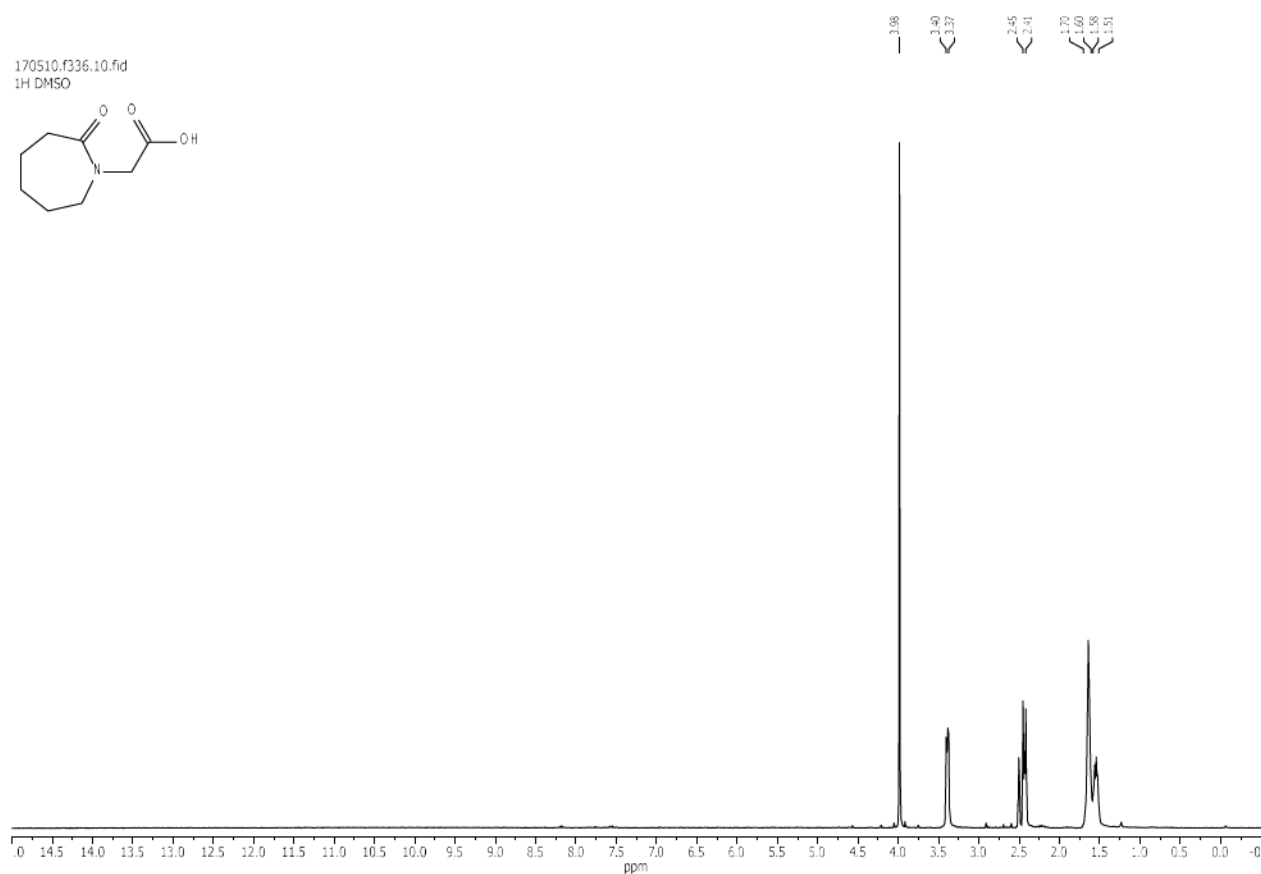
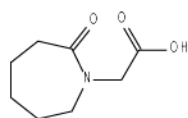


^1H and ^{13}C NMR Spectra

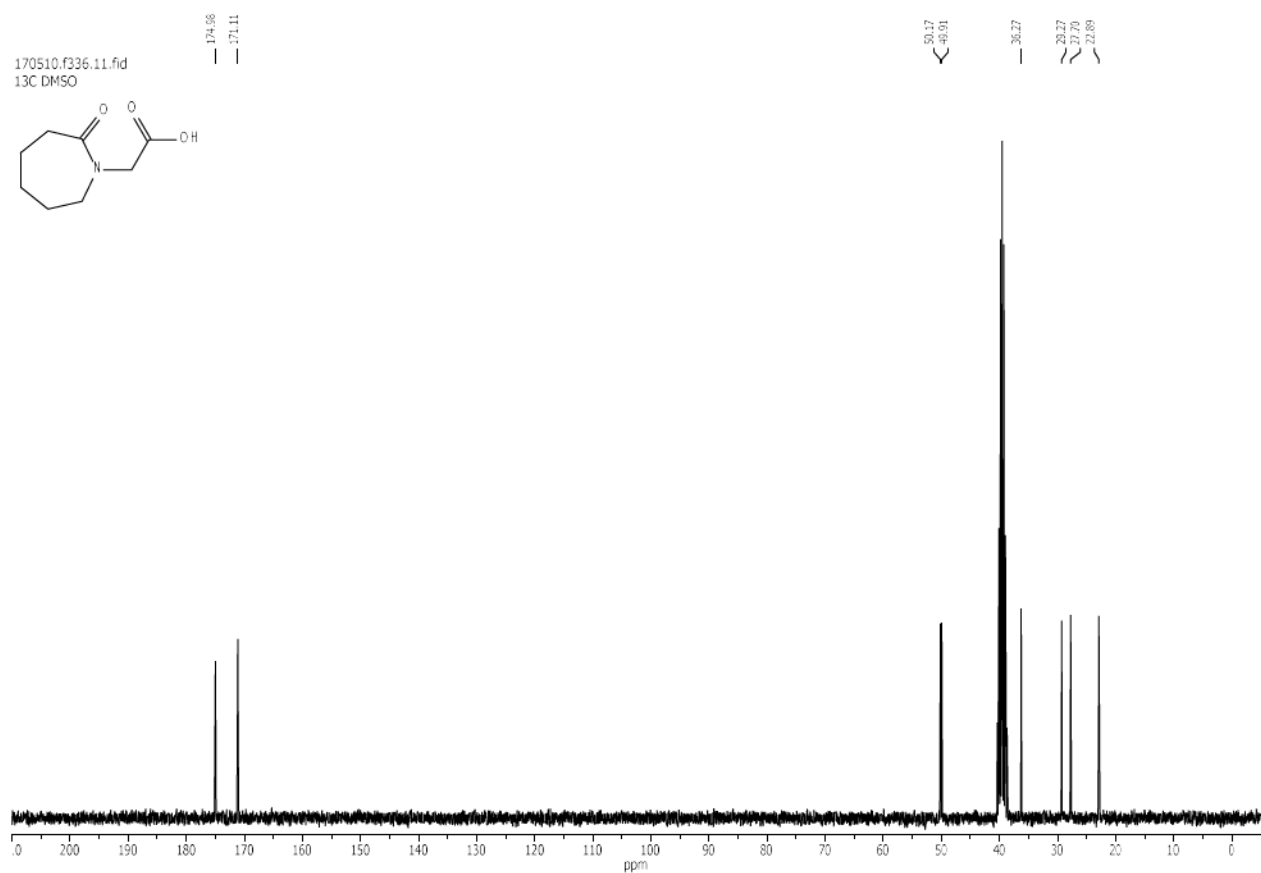
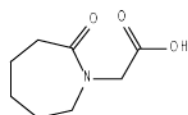


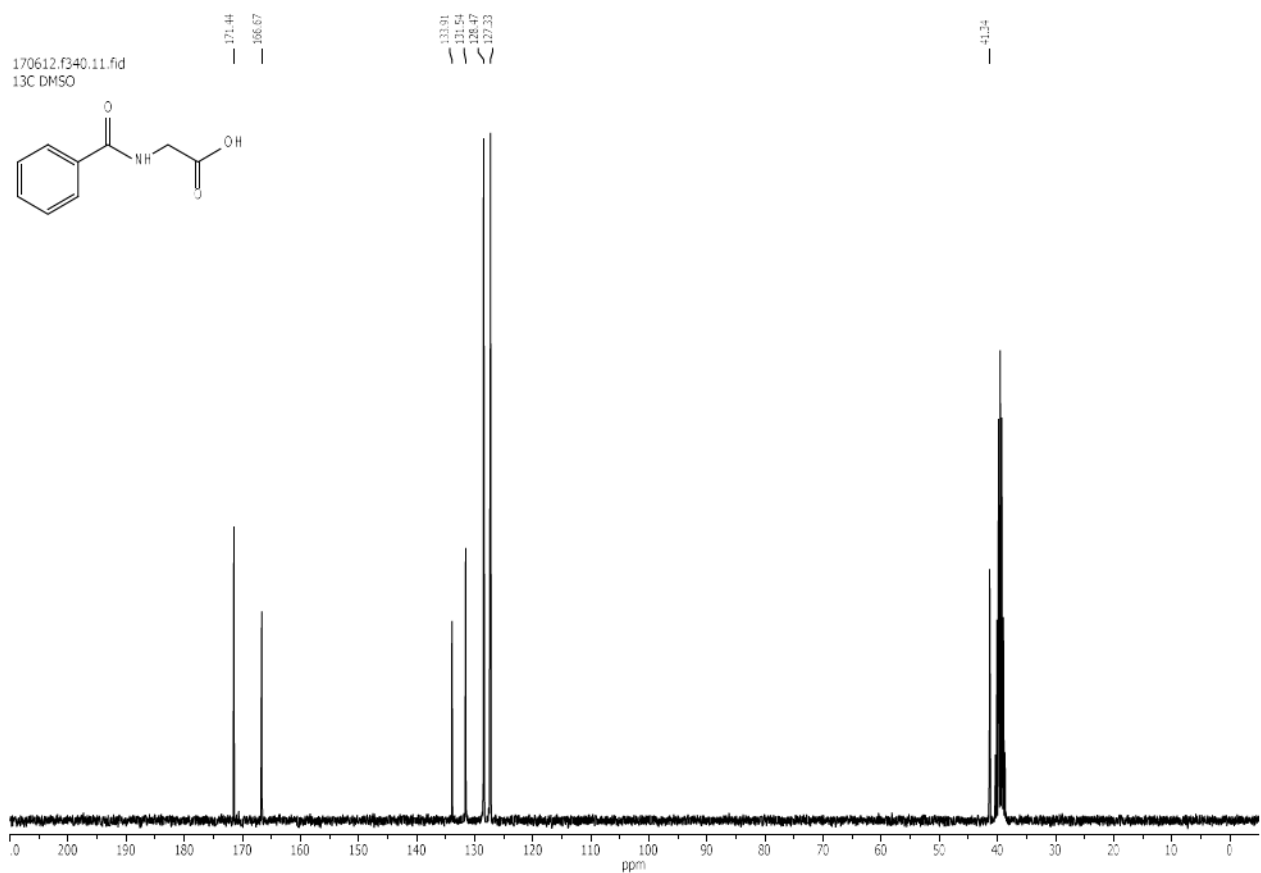
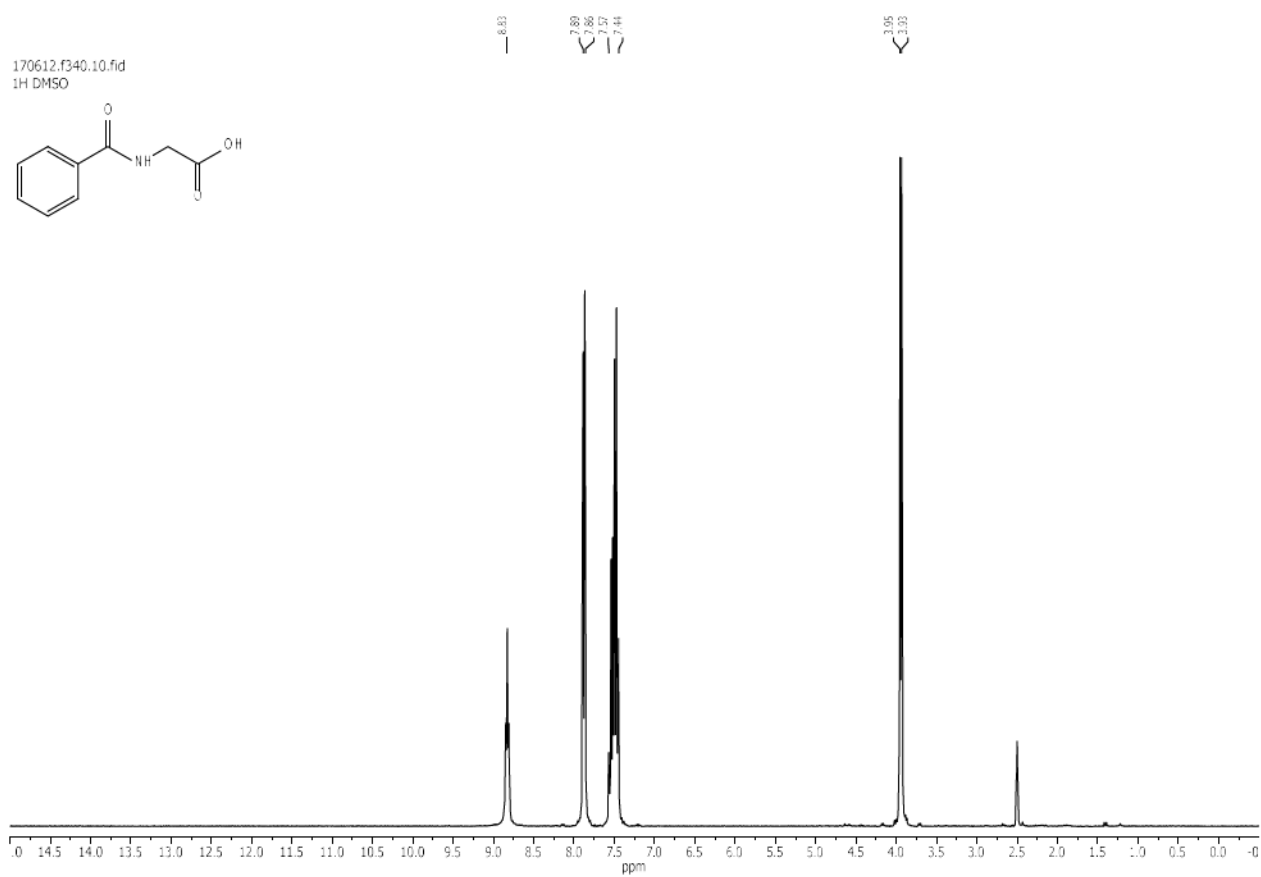


170510.f336.10.fid
1H DMSO



170510.f336.11.fid
13C DMSO





Analytical instruments

NMR

- AV 400 (Bruker)

Build 2005, Magnetic field 9.4 Tesla, Proton-Resonance-Frequency 400 MHz.

- AV 300 (Bruker)

Build 2005, Magnetic field 7.0 Tesla, Proton-Resonance-Frequency 300 MHz.

- Fourier 300 (Bruker)

Build 2012, Magnetic field 7.0 Tesla, Proton-Resonance-Frequency 300 MHz.

HRMS

- Agilent 1200/6210 Time-of-Flight LC-MS

EA

- Leco TruSpec Micro CHNS Element Analysator

ICP-OES

- Varian/Agilent 715-ES

Substances

Paraformaldehyde (PFA) – Sigma Aldrich

NMP – Acros Organics

N-Methyldodecanamide – TCI

Lithium bromide – Fluka

Sulfuric acid – Fisher Chemical

Acetamide – TCI

N-Methylacetamide – TCI

2-Pyrrolidinone – TCI

2-Cyanacetamide – Sigma Aldrich

ϵ -Caprolactame – Sigma Aldrich

Benzamide – Sigma Aldrich

Succindiamide – Sigma Aldrich

Benzaldehyde – Sigma Aldrich

Isovaleraldehyde – TCI

Pd black – Sigma Aldrich

Pd/C (ox.), 10 wt.% – Merck

Pd/Al₂O₃, 5 wt.% – Sigma Aldrich

PdBr₂ – Sigma Aldrich

Pd(NO₃)₂ hydrate (ca. 40% Pd) – Strem

[Pd(CH₃CN)₂Cl₂] – Sigma

Phenanthroline·H₂O – Sigma

References

- 1 A. P. Mikhalkin, *Russ. Chem. Rev.*, 1995, **64**, 259.

Synthesis of *N*-Lauroyl Sarcosine by Amidocarbonylation: Comparing Homogeneous and Heterogeneous Palladium Catalysts

SOREN HANCKER, STEFANIE KREFT, HEUFRIED NEUMANN, AND MATTHIAS BELLER[✉]

Leibniz-Institut für Katalyse e. V. an der Universität Rostock, Albert-Einstein-Straße 29a, 18059 Rostock, Germany

* Supporting Information

ABSTRACT: An improved system for the synthesis of *N*-acyl amino acids via Pd-catalyzed amidocarbonylation is reported. Utilizing inexpensive Pd black gives the industrially important surfactant *N*-lauroyl sarcosine in excellent yields (95%) on a multi-gram scale. Advantages of the new system include reusability, decreased process temperature, and, importantly, drastically decreased co-catalyst loading.

INTRODUCTION

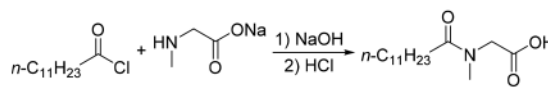
N-Acyl amino acids are of fundamental importance for chemistry and biology.^{1–5} In addition, they are of specific industrial interest as this class of compounds possesses a variety of different application fields. For example, pharmaceuticals such as Captopril or *N*-acetyl cysteine, food additives like Aspartame, and surfactants such as *N*-lauroyl sarcosine (**1**) depict *N*-acyl amino acid derivatives as structural motives.⁴ The broad application range of amino acids as an integral part of peptides as well as proteins and the importance of amino acid derivatives as building blocks for organic syntheses continue to attract interest for developing more effective synthetic methodologies for their production.^{6,7}

Within the numerous possible syntheses for amino acids and their derivatives, amidocarbonylation,⁸ also known as the Wakamatsu reaction,⁹ is an interesting approach due to its perfect atom efficiency. Complementary to the more common carbonylation reactions of olefins^{10–12} or aryl halides,^{13–15} this methodology employs readily accessible (*in situ* generated) aldehydes combined with either amides, nitriles, acetals, or epoxides.

While commercial routes for *N*-acyl amino acids, combining the Strecker reaction with subsequent acylation, produce overstoichiometric amounts of salt waste, amidocarbonylation only results in the (co)catalysts as “byproducts”. Originally developed using Co₂(CO)₈ as catalyst,^{16–18} nowadays the palladium-catalyzed methodology utilizing lithium bromide and sulfuric acid as co-catalysts prevails in this area.¹⁹ Notably, this latter protocol further enhanced the substrate scope of the reaction.^{19–21}

Due to their high foam-forming quality and good dermatological compatibility, long chain sarcosinates are of increasing interest as green detergents,⁴ which are produced in a quantity of 10 000 tonnes per year.⁸ As an example, the commercial synthesis of *N*-lauroyl sarcosine is realized by reacting sarcosine with *N*-lauroyl chloride under Schotten-Baumann reaction conditions (Figure 1).⁴ Despite a decreased reactivity toward secondary amides, Lin and Knifton successfully synthesized *N*-lauroyl sarcosine in 95% overall yield employing 1 mol % of Co₂(CO)₈ and 200 bar CO/H₂ at 120 °C via amidocarbonylation of *N*-methyl dodecanamide with

Classical route:



Amidocarbonylation:

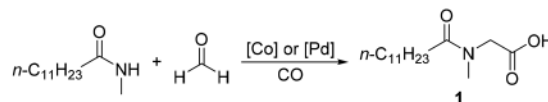


Figure 1. Comparison of the industrial synthesis of *N*-lauroyl sarcosine and the amidocarbonylation pathway.

paraformaldehyde (PFA).¹⁸ Further investigations by Hoechst AG gave the surfactant in a two staged pilot plant process.^{22,23}

While the amidocarbonylation theoretically incorporates every substrate atom in the product molecule, the Pd-catalyzed procedure requires significant amounts of lithium bromide (35 mol %) and sulfuric acid (1 mol %) as co-catalysts.^{24,25} Likewise, these additives were essential in the first reported heterogeneously catalyzed amidocarbonylation using Pd/C.²⁶

Herein, we describe an improved amidocarbonylation procedure using a novel heterogeneous Pd catalyst, which allowed a drastic reduction in lithium bromide loading to 2.5 mol %.

RESULTS AND DISCUSSION

The amidocarbonylation of *N*-methyl dodecanamide with PFA toward *N*-lauroyl sarcosine was chosen as the model reaction since the industrially relevant product represented the main interest of this study. An initial catalyst examination was conducted employing 35 mol % lithium bromide and 1 mol % sulfuric acid at 100 °C and 60 bar of CO as reaction parameters (Table 1). These conditions were selected based on prior findings from the first reported heterogeneously catalyzed amidocarbonylation applying Pd/C. For comparison, the reaction utilizing 0.5 mol % PdBr₂ resulted in an overall yield of 77%. When the reaction was carried out with 1 mol % of simple palladium black, 52% of the desired surfactant was

Received: October 12, 2017

Published: November 14, 2017

Table 1. Comparison of Various Heterogeneous Catalysts with PdBr₂ for the Model Reaction

$$n\text{-C}_{11}\text{H}_{23}\text{CONHCH}_3 + \text{HCHO} \xrightarrow[\text{1 mL NMP, 100 }^\circ\text{C, 60 bar CO, 16 h}]{\text{[Pd] 35 mol\% LiBr, 1 mol\% H}_2\text{SO}_4} n\text{-C}_{11}\text{H}_{23}\text{CON(CH}_3\text{)CH}_2\text{COOH}$$

1

entry ^a	catalyst	NMR yield ^b
1	PdBr ₂ ^c	77
2	Pd black	52
3	Pd/C (ox.)	42
4	Pd/SiO ₂	48
5	Pd/Al ₂ O ₃	22
6	Pd/N@Gr	48
7	Pd/Faujasite A	30
8	Pd/ZSM-5 A	12
9	Pd/Faujasite B	<5
10	Pd/ZSM-5 B	50

^aGeneral reaction conditions: 1 mmol of *N*-methyl dodecanamide, 2 mmol of PFA, 35 mol % LiBr, 1 mol % H₂SO₄, 1 mL of NMP, Pd catalyst (1 mol % metal) at 100 °C and 60 bar CO for 16 h. ^bEthylene carbonate was added as an internal standard. Integration results are based on R-CH₂-COOH. ^c0.5 mol % PdBr₂.

detected. Charcoal supported palladium in the oxidic form led to a slightly decreased yield of 42%. In order to survey common supports for heterogeneous catalysts, SiO₂- and Al₂O₃-based palladium catalysts were evaluated. While Pd/SiO₂ gave the desired product in an insignificantly lower yield of 48%, using aluminum oxide as support resulted in only 22% of *N*-lauroyl sarcosine. Surprisingly, a more basic nitrogen-doped graphene supported palladium catalyst resulted in the formation of 48% of the glycine derivative. Apparently, this catalyst performs in a similar manner as palladium black, which is contrary to expectations since nitrogen doping of the graphene results in basic centers assumed to impede the acid-catalyzed amidocarbonylation. Additionally, ZSM-5- and Faujasite-based palladium catalysts were synthesized in order to test those acidic materials for positive effects.²⁷ For each support, wet impregnation (A) and incipient wetness impregnation (B) were used to prepare the heterogeneous metal nanoparticles. In general, all resulting catalysts demonstrated a certain activity in the model amidocarbonylation reaction. However, only minor conversion was observed in the presence of Pd/Faujasite B (<5%) and Pd/ZSM-5 A (12%). A moderate yield of 30% was provided by Pd/Faujasite A, whereas using Pd/ZSM-5 B as catalyst resulted in the product being obtained in 50% yield, similar to the initially tested palladium black. Apparently, the catalyst support does not improve the reaction output. In addition, there is no obvious tendency regarding the basic or acidic character of the support. Due to its commercial availability and sufficient performance, we continued our investigations utilizing Pd black as catalyst.

To improve the product yield, temperature as well as acid and catalyst concentrations were varied (Table 2). For example, an increased loading of sulfuric acid up to 10 mol % enhanced the yield of **1** to 84%. Half of the amount of the acid gave 80% *N*-lauroyl sarcosine. To our delight, the overall yield was further enhanced when the reaction was carried out at lower temperatures. Both at 80 and 60 °C, product **1** was formed with 87% efficiency. However, at 40 °C the reaction yielded only 8% of the desired surfactant. Investigations aiming to decrease the necessary palladium loading proved that a catalyst

Table 2. Optimization of the Reaction Conditions in the Amidocarbonylation of *N*-Methyl Dodecanamide with PFA toward *N*-Lauroyl Sarcosine

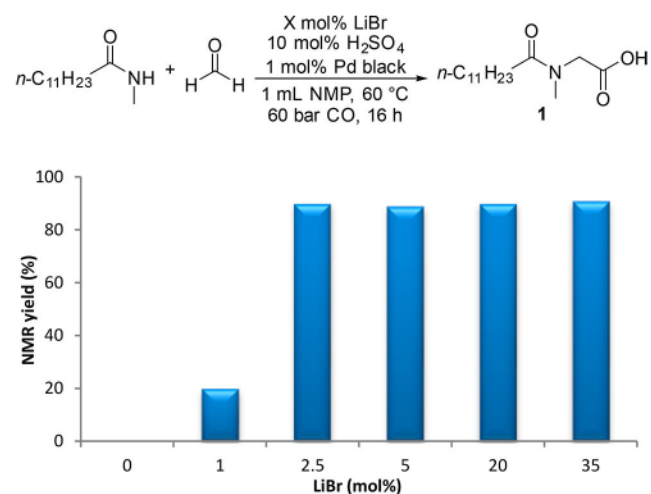
$$n\text{-C}_{11}\text{H}_{23}\text{CONHCH}_3 + \text{HCHO} \xrightarrow[\text{1 mL NMP, X }^\circ\text{C, 60 bar CO, 16 h}]{\text{35 mol\% LiBr, X mol\% H}_2\text{SO}_4, \text{X mol\% Pd black}} n\text{-C}_{11}\text{H}_{23}\text{CON(CH}_3\text{)CH}_2\text{COOH}$$

entry ^a	H ₂ SO ₄ (mol %)	Pd black (mol %)	PFA (mmol)	T (°C)	NMR yield ^b
1	1	1	2	100	52
2	5	1	2	100	80
3	10	1	2	100	84
4	10	1	2	80	87
5	10	1	2	60	87
6	10	1	2	40	8
7	10	0.5	2	60	52
8	10	0.25	2	60	26
9	10	0.1	2	60	20
10	10	1	1	60	87
11	10	1	1.5	60	91
12	10	1	2.5	60	87

^aGeneral reaction conditions: 1 mmol of *N*-methyl dodecanamide, X mmol of PFA, 35 mol % LiBr, X mol % H₂SO₄, X mol % Pd black, 1 mL of NMP at X °C and 60 bar CO for 16 h. ^bEthylene carbonate was added as an internal standard. Integration results are based on R-CH₂-COOH. and are given in %.

content of 1 mol % is required to achieve approximately full conversion. A reduction to 0.5 mol % palladium black led to a diminished output of 52% of **1**. While the influence of the catalyst content appears to be strong, neither a significant excess nor the application of exactly 1 equiv of PFA drastically affected the outcome of the amidocarbonylation as the deviation in the overall yield accounts for only 4% in both cases.

Next, the effect caused by the concentration of lithium bromide was briefly evaluated. As shown in Chart 1, the amount necessary to obtain good product yields can be

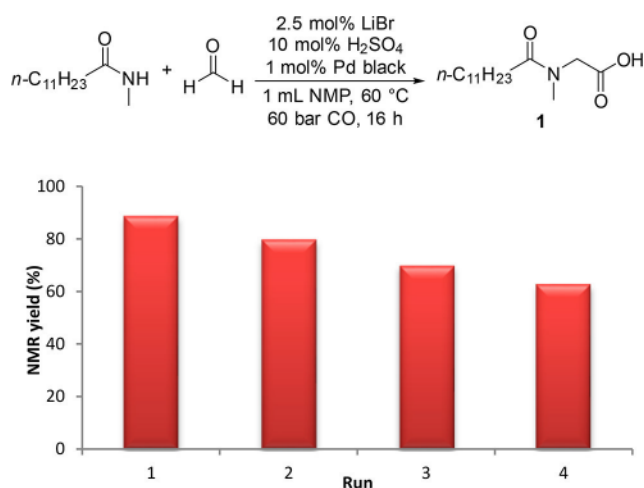
Chart 1. Influence of Lithium Bromide Content^a

^aGeneral reaction conditions: 1 mmol of *N*-methyl dodecanamide, 1.5 mmol of PFA, X mol % LiBr, 10 mol % H₂SO₄, 1 mol % Pd black, 1 mL of NMP at 60 °C and 60 bar CO for 16 h. Ethylene carbonate was added as an internal standard. Integration results are based on R-CH₂-COOH.

significantly decreased from 35 mol % down to 2.5 mol %. Clearly, reducing the loading of the co-catalyst by more than 90% lowers the expense for the process considerably. Likewise, the overall atom efficiency is improved as well. The results indicate that a lithium bromide addition of more than 2.5 mol % does not positively affect product formation since the experiments utilizing 2.5, 5, 20, and 35 mol % each lead to 90–1% overall yield. However, reducing the co-catalyst loading to 1 mol % gave only 20% of the target substance. In agreement with previous work, no surfactant was produced in the absence of lithium bromide.

In order to evaluate the reusability of palladium black, this material was tested in recycling experiments. Therefore, the reaction was conducted under optimized conditions with subsequent isolation of the catalyst particles by centrifugation. In order to both reuse the particles and determine the reaction yield by NMR, the isolated particles were washed with NMP several times. The solvent was removed from the combined organic layers, and the crude product was analyzed by NMR with an internal standard while the particles were transferred into the vial equipped with the next set of reaction compounds. As shown in Chart 2, a loss of activity of ca. 10% was detected

Chart 2. Recycling Experiments^a



^aGeneral reaction conditions: 1 mmol of *N*-methyl dodecanamide, 1.5 mmol of PFA, 2.5 mol % LiBr, 10 mol % H₂SO₄, 1 mol % Pd black, 1 mL of NMP at 60 °C and 60 bar CO for 16 h. After the initial cycle, the particles were separated by centrifugation. The catalyst was washed with NMP and again separated by centrifugation. This process was repeated three times before the particles were transferred to the next set of reaction compounds. Ethylene carbonate was added as an internal standard. Integration results are based on R-CH₂-COOH.

after every run. The decreasing yield is explained either by deactivation of the catalyst or by loss of catalytically active material in the recycling process.

Having an improved protocol for the preparation of *N*-lauroyl sarcosine in hand, we investigated the reaction of three aldehydes and seven amides using the optimal protocol and compared it to more severe conditions (Figure 2). Unfortunately, the reaction of PFA with acetamide, 2-pyrrolidinone, and benzamide using conditions A did not provide access to the corresponding glycine derivatives. On the other hand, the corresponding products were obtained when the reaction was carried out at 120 °C with 35 mol % lithium bromide and 1 mol % sulfuric acid (conditions B). More specifically, *N*-acetyl-

glycine (2) was formed in 57% NMR yield (45% isolated) and the conversion of 2-pyrrolidinone gave 80% NMR yield (68% isolated yield) of the corresponding 2-oxo-1-pyrrolidineacetic acid (3). Notably, the corresponding amide Piracetam is of interest as a pharmaceutical for the potential treatment of dementia. Furthermore, *N*-benzoyl glycine (5) was synthesized with 44% NMR yield (30% isolated yield). However, when caprolactam was reacted with PFA at 60 °C (conditions A), the corresponding caprolactam acetic acid (4) was obtained in 73% NMR yield (65% isolated yield). Under more severe conditions at 120 °C, the product was synthesized in 80% NMR yield. Despite reaction conditions B being more forcing, butanedi- amide and 2-cyano acetamide failed to convert to the corresponding glycine derivatives (6 and 7).

Next, we compared the amidocarbonylation of isovaleraldehyde with acetamide and *N*-methylacetamide in order to elucidate the influence of an additional *N*-alkyl substituent (Figure 3). Under identical reaction conditions, *N*-acetyl leucine can be synthesized in 20% NMR yield, whereas *N*-acetyl-*N*-methyl leucine is not formed at all.

As shown in Figure 4, our improved protocol can be easily performed on a 10 g scale. To our delight, when employing a slightly modified workup procedure, the compound is obtained in >98% overall yield with the starting material as the major impurity (<2%). An additional acid–base extraction further enhanced the purity of the product while the yield decreased to 95%. This experiment suggests that the synthesis of 1 can be transferred to larger scales without a significant loss of catalyst activity.

To get insight into the degree of palladium leaching from the heterogeneous catalyst, analysis of the metal contamination in product 1 was executed. Therefore, the palladium contents of the (crude) products from 1 and 47 mmol scale experiments were determined by ICP analysis. For comparison, a sample generated by carrying out the reaction with PdBr₂ was also investigated. As depicted in Chart 3, in all samples a significant amount of palladium was observed ranging from 80 to 460 ppm. The crude product of sample A contained the most palladium, which accounts for a loss of around 17% of the originally employed palladium black. The reasons for this loss of palladium remain currently unknown. Sample B, which was obtained after the first purification step, contained lower amounts of palladium (250 ppm). The palladium content could be further reduced to 150 ppm by subsequent acid–base extraction. Surprisingly, the product prepared by employing the homogeneous catalyst was the lowest in residual palladium (80 ppm).

CONCLUSIONS

An improved palladium catalyst for the synthesis of the industrially important surfactant *N*-lauroyl sarcosine is described. Investigating the amidocarbonylation reaction of *N*-methyl dodecanamide with paraformaldehyde (PFA) in the presence of inexpensive Pd black gives the desired product 1 in excellent yields (95%). Advantages of the new protocol include reusability, decreased process temperature, and significantly decreased co-catalyst loading.

EXPERIMENTAL SECTION

General Information. The solvent (NMP) was washed with argon and dried with molecular sieves overnight. Subsequently, the sieves were filtered off and the resulting

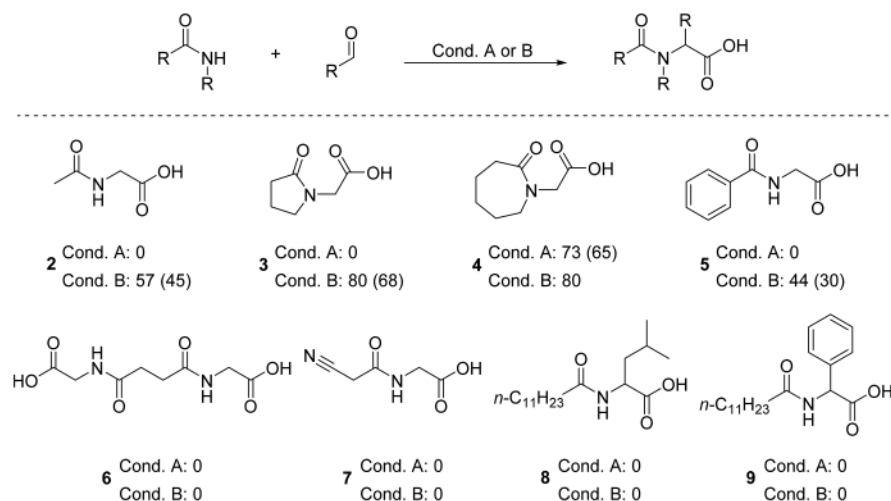


Figure 2. Substrate scope of the Pd black catalyzed amidocarbonylation. Conditions A: 1 mmol of amide, 1.5 mmol of aldehyde, 2.5 mol % LiBr, 10 mol % H₂SO₄, 1 mol % Pd black, 1 mL of NMP at 60 °C and 60 bar CO for 16 h. Conditions B: 1 mmol of amide, 1.5 mmol of aldehyde, 35 mol % LiBr, 1 mol % H₂SO₄, 1 mol % Pd black, 1 mL of NMP at 120 °C and 60 bar CO for 16 h. NMR yields were determined using ethylene carbonate as an internal standard. Integration results are based on R-CH₂-COOH. Yields are given in %; isolated yields are given in parentheses.

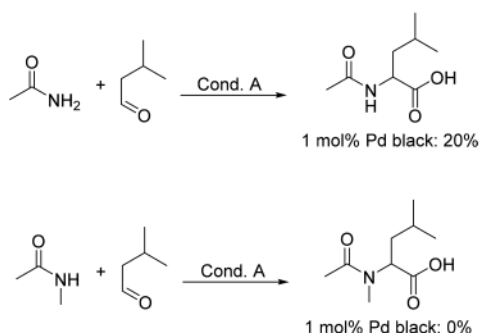


Figure 3. Comparison of the influence of an *N*-alkyl substituent on the activity of the substrate in the amidocarbonylation with substituted aldehydes. Conditions A: 1 mmol of amide, 1.5 mmol of aldehyde, 2.5 mol % LiBr, 10 mol % H₂SO₄, 1 mol % Pd black, 1 mL of NMP at 60 °C and 60 bar CO for 16 h. NMR yields were determined using ethylene carbonate as an internal standard. Integration results are based on R-CH₂-COOH.

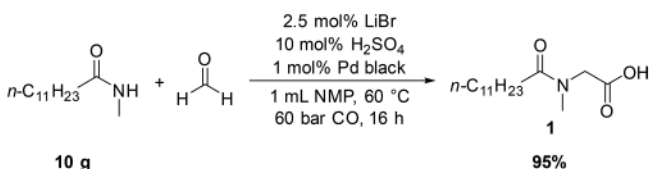
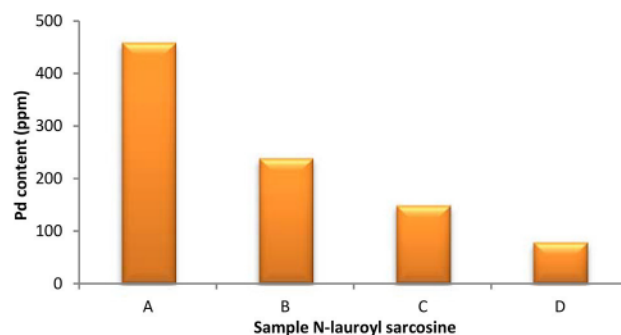


Figure 4. Amidocarbonylation of *N*-methyl dodecanamide with PFA toward *N*-lauroyl sarcosine on a 10 g scale. Conditions: 46.8 mmol of *N*-methyl dodecanamide, 70.3 mmol of PFA, 2.5 mol % LiBr, 10 mol % H₂SO₄, 1 mol % Pd black, 46.8 mL of NMP at 60 °C and 60 bar CO for 16 h.

NMP was distilled at 70 °C in high vacuum (10^{-3} mbar). Both steps were conducted under an argon atmosphere. ^1H and ^{13}C NMR spectra were recorded on Bruker AV 300, Bruker Fourier 300, and Bruker AV 400 NMR spectrometers. Chemical shifts are reported in ppm relative to the deuterated solvent (DMSO- d_6 ; ^1H : 2.500 ppm; ^{13}C : 39.520 ppm). High-resolution mass spectra were recorded on an Agilent 1200/6210 time-of-flight LC-MS by electrospray ionization. Elemental analyses were conducted utilizing a Leco TruSpec Micro CHNS element

Chart 3. ICP-OES Results for Pd Content of Different N-Lauroyl Sarcosine Samples^A



^aSample A: Prepared by separating the catalyst from the reaction mixture by centrifugation, washing with NMP, and subsequently removing the solvent to obtain the crude product. Sample B: Substance obtained after the 1st purification step. Sample C: Substance obtained after complete purification procedure. Sample D: Substance obtained after complete purification procedure of the PdBr₂-catalyzed reaction.

analyzer. ICP-OES measurements were conducted on a Varian/Agilent 715-ES instrument.

Catalyst Preparation. Pd/SiO₂, Pd/Faujasite A, and Pd/ZSM-5 A (All 1 wt % Pd). Pd/SiO₂ was prepared by wet impregnation. Silica (990 mg, 0.035 • 0.070 mm, pore diameter 6 nm) was added to a solution of 30 mL of water and Pd(NO₃)₂•XH₂O (25 mg, ca. 40% Pd content). After 30 min of stirring, the liquid was removed by rotary evaporation. Subsequently, the material was further dried at 80 • C overnight. Finally, the catalyst was calcined at 500 • C for 2 h to give the final product. Pd/Faujasite A and Pd/ZSM-5 A were synthesized accordingly.

Pd/Faujasite B and Pd/ZSM-5 B (Both 1 wt % Pd). Pd/Faujasite B and Pd/ZSM-5 B were prepared by incipient wet impregnation. Therefore, Pd(NO₃)₂·xH₂O (25 mg, ca. 40% Pd content) was dissolved in water (1.2 mL for Faujasite and 0.8 mL for ZSM-5). The solution was added to 990 mg of supporting material. The catalysts were dried at 80 °C

overnight and finally calcined at 500 °C for 2 h to give the final product.

Pd/N@Gr (3 wt % Pd). Pd/N@Gr (3 wt % Pd) was synthesized by pyrolysis of a mixture of [Pd(phenanthroline)₂Cl₂] and carbon powder. For the synthesis of [Pd(phenanthroline)Cl₂], [Pd(CH₃CN)₂Cl₂] (2.233 mmol, 579 mg) was added dropwise to a stirred solution of phenanthroline·H₂O (4.925 mmol, 976 mg) and 60 mL of DMF at 150 °C. After the formation of a precipitate within a few minutes, the mixture was heated under reflux conditions for another 3 h. The product was obtained as orange needles after filtration. Subsequently, [Pd(phenanthroline)Cl₂] (0.314 mmol, 112.23 mg) was dissolved in 60 mL of DMF at 120 °C. Then, carbon powder (888.42 mg, VULCAN XC72R) was added, and the mixture was kept at 120 °C for 2 h. The solvent was removed by vacuum, and the solid was further dried for 15 h at 120 °C in high vacuum. Finally, the catalyst was obtained by pyrolysis of the material at 800 °C for 2 h under an argon atmosphere.

General Amidocarbonylation Procedure. The manipulations were carried out in a 300 mL Parr high-pressure autoclave. The small scale experiments were conducted in 4 mL glass vials using magnetic stirring bars. Prior to the reaction (example Table 2, entry 11 in parentheses), the vials were placed on an appropriate plate and equipped with the solid compounds (213.4 mg *N*-methyl dodecanamide (1 mmol), 45 mg of PFA (1.5 mmol), 30.4 mg of lithium bromide (35 mol %), 1.1 mg of Pd black (1 mol %)), which were subsequently sealed with a septum cap and evaporated and flushed with argon three times. Afterward, NMP (1 mL; water-free stored under argon) was added prior to 5 mL of sulfuric acid (10 mol %; concentrated, neither purified nor oxygen- or water-free). The autoclave was closed before it was evaporated and flushed with argon three times as well. The autoclave was opened, and the plate with the vials was placed inside quickly before the autoclave was closed again. Afterward, the autoclave was flushed with argon for 15 min. The autoclave was sealed tightly before it was flushed with carbon monoxide up to 3 bar three times. The reaction pressure (60 bar CO) was added by aid of the digital pressure indication. The autoclave was regulated by a control unit that monitored the reaction temperature via an integrated thermometer. The temperature was adjusted to the given value by the control unit automatically. The experiment was conducted at the corresponding reaction temperature for 16 h. Subsequent to the reaction, the autoclave was cooled in an ice bath. At room temperature, the pressure was released slowly. The heterogeneous catalyst was separated either by centrifugation (recycling experiments, preparation of sample A) or by filtration (optimization reactions, substrate scope, 10 g scale experiment, preparation of samples B–D) and washed at least three times within the process. Whenever NMP was removed (70 °C in high vacuum), an antispash guard with a return hole (Sigma-Aldrich) was utilized since the solvent condensed before reaching the condensation trap. After the removal of NMP, the crude product was obtained.

Optimization Reactions. The reaction solution was filtered through filter paper. The paper was washed with NMP several times. Ethylene carbonate (0.25 mol % to the amide) was added to the crude product (viscous liquid). Acetone was added to guarantee equal dispersion of the NMR standard within the sample. The acetone was removed by high vacuum. The integration results are based on the four protons from ethylene carbonate and the two protons from the glycine moiety (N-CH₂-COOH). Noteworthy, *N*-acyl sarcosines exist

as *cis*- and *trans*-isomers.⁴ Therefore, the N-CH₂-COOH signal is split into one singlet at 3.96 ppm and one at 4.09 ppm. The intensity distribution for *N*-lauroyl sarcosine is 66:34. The signal splitting can also be observed for the methyl group N-CH₃ (2.79 and 2.98 ppm, 34:66, singlet) and the first CH₂ group of the alkyl chain CH₂-CH₂-CO-N (2.16 and 2.30 ppm, 34:66, triplet, *J* = 7.4 Hz).

Recycling Experiments. After the reaction, the mixture was transferred under argon into a septum sealed centrifuge tube. After centrifugation (5000 U/min for 20 min), the supernatant solution was removed via syringe and collected. The particles in the tube were washed with NMP five times. The combined NMP layers were prepared for NMR analysis (analogously to Optimization Reactions). The particles were transferred via syringe with NMP under argon into the next vial already containing the next set of reaction substrates as well as lithium bromide. In order to transfer the catalyst as entirely as possible, NMP was added in 0.1 mL portions and then transferred into the vial. This was repeated 10 times in order to add 1 mL of NMP over the entire process as solvent for the next run. Finally, sulfuric acid was added and the manipulations were pursued as usual (see General Amidocarbonylation Procedure). After the reaction, the particles were treated with this procedure again until the fourth cycle.

Substrate Scope. The reactions were conducted and analyzed by NMR and therefore treated according to the manipulations described in the sections General Amidocarbonylation Procedure and Optimization Reactions. In order to determine the isolated yield, the reaction was repeated and an acid–base extraction was conducted, in contrast to the optimization reactions. Therefore, the crude product was dissolved in saturated aqueous NaHCO₃ solution (the reaction is complete when the evolution of gas stops and the liquid/particles are dissolved). The aqueous solution was extracted with ethyl acetate three times. Subsequently, the aqueous phase was acidified with concentrated phosphorus acid to pH 3. The aqueous phase was extracted with ethyl acetate again three times. The combined organic layers were dried over Na₂SO₄, which was later filtered off. Ethyl acetate was removed on the rotary evaporator. The products were dried in high vacuum.

Ten Gram Scale Experiment. The solid substrates and catalysts were added directly into the autoclave, which was equipped with a mechanic stirrer. The autoclave was closed, evaporated, and flushed with argon three times. Meanwhile, a Schlenk flask was evaporated and flushed with argon as well. NMP and sulfuric acid were added and mixed by stirring with a magnetic stirring bar. The resulting solvent was added into a syringe, and the autoclave was opened carefully. Under argon counterflow, the top of the autoclave was lifted slightly and the solvents were injected into the autoclave. Subsequently, the autoclave was closed and flushed with argon for 15 min. The carbon monoxide pressure was added after flushing with CO and heating as well as stirring was started. After the reaction, the pressure was released very slowly. The reaction mixture was filtered through filter paper before the solvent was removed in high vacuum at 70 °C (see General Amidocarbonylation Procedure). Water was added to the crude product at atmospheric pressure and 70 °C. After stirring for a few minutes, the two phase system was stored in a deep freezer at -28 °C for 1 h. Afterward, the solid was allowed to warm to room temperature until the water melted. The solid raw product was crushed into small particles with a scoopula on a frit (POR 3) and subsequently washed with water five times.

The product resulting from this purification step was analyzed by ICP-OES and NMR as sample B. For additional purification, the acid–base extraction described within the section [Substrate Scope](#) was conducted. For *N*-lauroyl sarcosine, the product starts to separate from the aqueous phase as an additional liquid phase between pH 4 and 6. The separation occurs immediately during the addition of concentrated phosphorus acid. After the two phase system was formed, a few more drops of concentrated phosphorus acid were added in order to ensure that the product can be obtained entirely. Additionally, the aqueous phase was extracted with ethyl acetate three times. The combined organic layers were dried over Na_2SO_4 . After the solid was filtered off, ethyl acetate was removed using a rotary evaporator. The resulting viscous liquid was dried in high vacuum. The resulting *N*-lauroyl sarcosine was further analyzed as sample C by ICP-OES and NMR.

ICP-OES Analysis. Samples B and C were prepared as described in the section [Ten Gram Scale Experiment](#). Sample A was prepared by conducting the experiment on the optimization scale (conditions [Table 2](#), entry 11; see section [General Amidocarbonylation Procedure](#)). After the reaction, the particles were removed by centrifugation (5000 U/min for 20 min) and the remaining solid was washed with NMP five times. The crude product was analyzed by ICP-OES and NMR as Sample A. Sample D was prepared by conducting the reaction utilizing PdBr_2 (0.5 mol %, 6.2 mg) as catalyst under otherwise optimized reaction conditions on a 1 g scale (4.69 mmol *N*-methyl dodecanamide) in an 8 mL vial (see section [General Amidocarbonylation Procedure](#)). The product was isolated according to the conditions described in section [Ten Gram Scale Experiment](#). Therefore, the sample was generated in an identical manner as sample C. The substance obtained from the PdBr_2 -catalyzed reaction was analyzed as sample D by ICP-OES and NMR.

Analytical Data. All ^1H and ^{13}C are in ppm, and all coupling constants J are in Hz.

***N*-Lauroyl Sarcosine (1).** O•-white solid (12.04 g, 95%). ^1H NMR (300.1 MHz, $\text{DMSO}-d_6$): δ 0.83•0.88 (3H, m, CH_3), 1.19•1.30 (16H, m, 8 CH_2), 1.40•1.52 (2H, m, CH_2), 2.16 (0.68H, t, J = 7.4, H^A), 2.30 (1.32H, t, J = 7.4, H^A), 2.79 (1.02H, s, H^C), 2.98 (1.99H, s, H^C), 3.96 (1.32H, s, H^B), 4.09 (0.68H, s, H^B), 12.61 (1H, br s, COOH); ^{13}C NMR (75.5 MHz, $\text{DMSO}-d_6$): δ 13.9 (CH_3), 22.1 (CH_2), 24.5 and 24.6 (CH_2), 28.7 (2 C, CH_2), 28.9•29.0 (4 C, CH_2), 31.3 (CH_2), 31.8 and 32.1 (C^AH_2), 34.2 and 36.0 (C^CH_3), 48.9 and 50.9 (C^BH_2), 170.8 and 171.0 (CO-N), 172.6 and 172.6 (COOH); HRMS (ESI, m/z): calcd. for $\text{C}_{15}\text{H}_{28}\text{NO}_3$ • (M•H $^+$): 270.20747, found: 270.20746; EA: calcd. for $\text{C}_{15}\text{H}_{29}\text{NO}_3$: C 66.38%, H 10.77%, N 5.16%; found C 66.55%, H 10.55%, N 5.00%.

***N*-Acetylglutamine (2).** O•-white solid (52.7 mg, 45%). ^1H NMR (300.1 MHz, $\text{DMSO}-d_6$): δ 1.84 (3H, s, CH_3), 3.71 (2H, d, J = 5.7, CH_2), 8.15 (1H, t, J = 5.7, NH); ^{13}C NMR (75.5 MHz, $\text{DMSO}-d_6$): δ 22.3 (CH_3), 40.7 (CH_2), 169.7 (C^q), 171.5 (C^q); HRMS (ESI, m/z): calcd. for $\text{C}_4\text{H}_8\text{NO}_3$ • (M•H $^+$): 116.03532, found: 116.03529; EA: calcd. for $\text{C}_4\text{H}_7\text{NO}_3$: C 41.03%, H 6.03%, N 11.96%; found C 41.19%, H 6.01%, N 11.63%.

2-Oxo-1-pyrrolidineacetic Acid (3). This product was further purified by sublimation in high vacuum (10^{-3} mbar) at 100 •C. O•-white solid (97.3 mg, 68%). ^1H NMR (300.1 MHz, $\text{DMSO}-d_6$): δ 1.94 (2H, p, J = 7.4, CH_2), 2.23 (2H, t, J = 8.1, CH_2), 3.38 (2H, t, J = 7.0, CH_2), 3.90 (2H, s, CH_2),

12.71 (1H, br s, COOH); ^{13}C NMR (75.5 MHz, $\text{DMSO}-d_6$): δ 17.5 (CH_2), 29.9 (CH_2), 43.6 (CH_2), 47.0 (CH_2), 170.2 (C^q), 174.4 (C^q); HRMS (ESI, m/z): calcd. for $\text{C}_6\text{H}_9\text{NO}_3$ • (M•H $^+$): 142.05097, found: 142.05063; EA: calcd. for $\text{C}_6\text{H}_9\text{NO}_3$: C 50.35%, H 6.34%, N 9.79%; found C 50.61%, H 6.50%, N 9.77%.

Hexahydro-2-oxo-1H-azepine-1-acetic Acid (4). O•-white solid (111.3 mg, 65%). ^1H NMR (300.1 MHz, $\text{DMSO}-d_6$): δ 1.51•1.58 (2H, m, CH_2), 1.60•1.70 (4H, m, 2 CH_2), 2.41•2.45 (2H, m, CH_2), 3.37•3.40 (2H, m, CH_2), 3.98 (2H, s, CH_2); ^{13}C NMR (75.5 MHz, $\text{DMSO}-d_6$): δ 22.9 (CH_2), 27.7 (CH_2), 29.3 (CH_2), 36.3 (CH_2), 49.9 (CH_2), 50.2 (CH_2), 171.1 (C^q), 175.0 (C^q); HRMS (ESI, m/z): calcd. for $\text{C}_8\text{H}_{12}\text{NO}_3$ • (M•H $^+$): 170.08227, found: 170.08218; EA: calcd. for $\text{C}_8\text{H}_{13}\text{NO}_3$: C 56.13%, H 7.65%, N 8.18%; found C 55.99%, H 7.52%, N 7.84%.

***N*-Benzoylglutamine (5).** O•-white solid (53.8 mg, 30%). ^1H NMR (300.1 MHz, $\text{DMSO}-d_6$): δ 3.94 (2H, d, J = 5.9, CH_2), 7.44•7.57 (3H, m, CH), 7.86•7.89 (2H, m, CH), 8.83 (1H, t, J = 5.9, NH); ^{13}C NMR (75.5 MHz, $\text{DMSO}-d_6$): δ 41.3 (CH_2), 127.3 (2C, CH), 128.5 (2C, CH), 131.5 (CH), 133.9 (C^q), 166.7 (C^q), 171.4 (C^q); HRMS (ESI, m/z): calcd. for $\text{C}_9\text{H}_8\text{NO}_3$ • (M•H $^+$): 178.05097, found: 178.05084; EA: calcd. for $\text{C}_9\text{H}_9\text{NO}_3$: C 60.33%, H 5.06%, N 7.82%; found C 60.61%, H 5.04%, N 7.72%.

● ASSOCIATED CONTENT

* Supporting Information

The Supporting Information is available free of charge on the ACS Publications website at DOI: [10.1021/acs.oprd.7b00326](https://doi.org/10.1021/acs.oprd.7b00326).

^1H and ^{13}C NMR spectra and a list of the commercial sources for all chemicals (PDF)

● AUTHOR INFORMATION

Corresponding Author

•E-mail: matthias.beller@catalysis.de.

ORCID

MATTHIAS BELLER: 0000-0001-5709-0965

Author Contributions

The manuscript was written through contributions of all authors. All authors have given approval to the final version of the manuscript.

Notes

The authors declare no competing financial interest.

● ACKNOWLEDGMENTS

We thank Maximilian Hertrich, Patrick Piehl, Sandra Leiminger, Karin Struve, and the analytical department for fruitful discussions and technical support. This work was supported by the state of Mecklenburg-Vorpommern and the BMBF.

● REFERENCES

- (1) Whitford, D. *Proteins*; Wiley-VCH: Chichester, 2005.
- (2) Connor, M.; Vaughan, C. W.; Vandenberg, R. J. *Br. J. Pharmacol.* 2010, 160, 1857.
- (3) Hanus, L.; Shohami, E.; Bab, I.; Mechoulam, R. *BioFactors* 2014, 40, 381.
- (4) Mikhalkin, A. P. *Russ. Chem. Rev.* 1995, 64, 259.
- (5) Vollhardt, K. P. C.; Schore, N. E. *Organische Chemie*; Wiley-VCH: Weinheim, 2011.

- (6) Streitwieser, A.; Heathcock, C. H. *Organische Chemie*; Verlag Chemie: Weinheim, 1994.
- (7) Hughes, A. B. *Amino Acids, Peptides and Proteins in Organic Chemistry*; Wiley-VCH: Weinheim, 2009.
- (8) Beller, M.; Eckert, M. *Angew. Chem., Int. Ed.* **2000**, *39*, 1010.
- (9) Wakamatsu, H.; Uda, J.; Yamakami, N. *J. Chem. Soc. D* **1971**, 1540.
- (10) Beller, M.; Bolm, C. *Transition Metals for Organic Synthesis*; Wiley-VCH: Weinheim, 2004.
- (11) Wu, X. F.; Fang, X.; Wu, L.; Jackstell, R.; Neumann, H.; Beller, M. *Acc. Chem. Res.* **2014**, *47*, 1041.
- (12) van Leeuwen, P. W. N. M.; Chadwick, J. C. *Homogeneous Catalysis*; Wiley VCH: Weinheim, 2001.
- (13) Barnard, C. F. J. *Organometallics* **2008**, *27*, 5402.
- (14) Gadge, S. T.; Bhanage, B. M. *RSC Adv.* **2014**, *4*, 10367.
- (15) Kollár, L. *Modern Carbonylation Methods*; Wiley: Weinheim, 2008.
- (16) Cabrera, A.; Sharma, P.; Arias, J. L.; Velasco, J. L.; Pérez-Flores, J.; Gomez, R. M. *J. Mol. Catal. A: Chem.* **2004**, *212*, 19.
- (17) Gomez, R. M.; Cabrera, A.; Velazquez, C. G. *J. Mol. Catal. A: Chem.* **2007**, *274*, 65.
- (18) Knifton, J. F.; Lin, J. J.; Storm, D. A.; Wong, S. F. *Catal. Today* **1993**, *18*, 355.
- (19) Beller, M.; Eckert, M.; Vollmueller, F.; Bogdanovic, S.; Geissler, H. *Angew. Chem., Int. Ed. Engl.* **1997**, *36*, 1494.
- (20) Beller, M.; Eckert, M.; Geissler, H.; Napierski, B.; Rebenstock, H.-P.; Holla, E. W. *Chem. - Eur. J.* **1998**, *4*, 935.
- (21) Beller, M.; Eckert, M.; Moradi, W. A.; Neumann, H. *Angew. Chem., Int. Ed.* **1999**, *38*, 1454.
- (22) Bogdanovic, S.; Geisler, H.; Raab, K.; Beller, M.; Fischer, H. Process for recovering cobalt carbonyl catalysts used in the preparation of N-acyl- α -amino acid derivatives by amidocarbonylation. EP 0779102A1, 1997.
- (23) Beller, M.; Fischer, H.; Gerdau, T.; Gross, P. Process for preparing N-acylglycin derivatives. EP 0680948A1, 1995.
- (24) Gordes, D.; Neumann, H.; von Wangelin, A. J.; Fischer, C.; Drauz, K.; Krimmer, H.-P.; Beller, M. *Adv. Synth. Catal.* **2003**, *345*, 510.
- (25) Beller, M.; Eckert, M.; Vollmueller, F. *J. Mol. Catal. A: Chem.* **1998**, *135*, 23.
- (26) Beller, M.; Moradi, W. A.; Eckert, M.; Neumann, H. *Tetrahedron Lett.* **1999**, *40*, 4523.
- (27) Yang, K. W.; Jiang, X. Z. *Bull. Chem. Soc. Jpn.* **2006**, *79*, 806.

7.3. Sonogashira-Semihydrogenation

The following section includes the publication as well as the according supporting information. Herein, detailed experimental instructions on the conducted manipulations are given as well as analytical data.

Supporting Information

Development of a Novel Palladium-Catalyzed Process for the Synthesis of Z-Alkenes by Sequential Sonogashira-Hydrogenation-Reaction

Sören Hancker, Helfried Neumann and Matthias Beller*

*Leibniz-Institut für Katalyse e.V. an der Universität Rostock
Albert-Einstein-Straße 29a, 18059 Rostock (Germany)*

Table of Contents

- General information
- General Procedure for Sonogashira Optimization
- General Procedure for Hydrogenation Optimization
- General Procedure for Substrate Scope
- ICP-OES Analysis
- XRD-Analysis
- XPS-Analysis
- Analytical data
- ^1H and ^{13}C NMR spectra
- Analytical instruments
- Substances
- References

General Information

General Information: All manipulations were conducted under argon with exclusion of moisture and oxygen by using standard techniques for the manipulation of air sensitive compounds. Reaction temperatures refer to silicon oil in an additional pressure tube within the heated alumina block. NMR data were recorded on either Bruker ARX 300, Bruker ARX 400 or Bruker Fourier 300 spectrometers. ^{13}C and ^1H NMR spectra are given in ppm and referenced to signals of deuterated solvents and residual protonated solvents, respectively (Acetone- d_6 : ^1H : 2.050 ppm, ^{13}C : 29.840 ppm; CD_2Cl_2 : ^1H : 5.320 ppm, ^{13}C : 54.000 ppm). Gas chromatography analysis was performed on an Agilent HP-5890 instrument with a FID detector and HP-5 capillary column using H_2 as carrier gas. Gas chromatography-mass analysis was carried out on an Agilent HP-5890 instrument with an Agilent HP-5973 Mass Selective Detector (EI) and HP-5 capillary column using helium carrier gas. TOF HR-MS measurements were performed on an Agilent 1200/6210 Time-of-Flight LC-MS. Flash chromatography was performed on a Teledyne Isco CombiFlash R_f 200 system. Chemicals were purchased from Sigma Aldrich, Alfa Aesar, TCI or Strem and were used as received. DMF was dried by a SPS from Innovative Technology while H_2O was flushed with argon for one hour. Solvents were stored in Aldrich Sure/store flasks under argon.

General Procedure for Sonogashira Optimization

The experiments were carried out in pressure tubes equipped with a magnetic stirring bar. Prior to the reaction, the solid reaction compounds were added to the pressure tube which was subsequently placed in an evacuation tube. The corresponding screw cap with septum was added into the evacuation tube as well. The closed tube was evacuated and flushed with argon three times. Afterwards, the tubes lid was slightly lifted and the liquid substances as well as the solvent (water-free stored under Argon) were added *via* syringe into the pressure tube. 4-Bromotoluene was slightly heated and added as a liquid as well since this compound sublimates significantly upon the exposition to vacuum. Finally, the lid of the evacuation tube was removed and the pressure tube was sealed with the screw cap under argon counter flow before the tube was placed in an aluminum heating block. The temperature was controlled by a thermocouple in an additional pressure tube with silicon oil placed in the aluminum block.

After the reaction was finished and cooled down to room temperature, the tube was opened and hexadecane was added as internal standard. A sample was prepared by filtering the crude solution through cotton. The sample was analyzed by GC.

Example on the basis of table 1, entry 7:

4-Bromotoluene:	0.5 mmol	=	63.5 μ L
Phenylacetylene:	1 mmol	=	110 μ L
K ₂ CO ₃ :	1 mmol	=	138 mg
PdCl ₂ :	1 mol%	=	0.9 mg
BuPAd ₂ (CataCXium A):	1 mol%	=	1.8 mg

2 mL DMF, 60 °C, 16 h

General Procedure for Hydrogenation Optimization

The experiments were carried out in pressure tubes equipped with a magnetic stirring bar. Prior to the reaction, the solid reaction compounds were added to the pressure tube which was subsequently placed in an evacuation tube. The corresponding screw cap with septum was added into the evacuation tube as well. The closed tube was evacuated and flushed with argon three times. Afterwards, the tubes lid was slightly lifted and the liquid substances as well as the solvent (water-free stored under Argon) were added *via* syringe into the pressure tube. Finally, the lid of the evacuation tube was removed and the pressure tube was sealed with the screw cap under argon counter flow before the tube was placed in an aluminum heating block. The temperature was controlled by a thermocouple in an additional pressure tube with silicon oil placed in the aluminum block.

After the reaction was finished and cooled down to room temperature, the tube was opened and hydrogen gas was bubbled through the reaction solution. After the hydrogenation is finished, argon was bubbled through the solution to end the reaction prior to the addition of hexadecane as internal standard. A sample was prepared by filtering the crude solution through cotton. The sample was analyzed by GC.

Example on the basis of table 2, entry 4:

(4-methyl-phenyl)phenylacetylene:	0.5 mmol	=	96 mg
K ₂ CO ₃ :	1 mmol	=	138 mg
PdCl ₂ :	1 mol%	=	0.9 mg
BuPAd ₂ (CataCXium A):	1 mol%	=	1.8 mg

2 mL DMF, 0.2 mL H₂O, 120 °C, 8 h

After step 1:

+ H₂-bubble, 0.5 mL/s gas flow, 25 °C, 20 min

After step 2:

+ Argon-bubble, 10 min

General Procedure for Substrate Scope

The experiments were carried out in pressure tubes equipped with a magnetic stirring bar. Prior to the reaction, the solid compounds were added to the pressure tube which was subsequently placed in an evacuation tube. The corresponding screw cap with septum was added into the evacuation tube as well. The closed tube was evacuated and flushed with argon three times. Afterwards, the tubes lid was slightly lifted and the liquid substances as well as the solvent (water-free stored under Argon) were added *via* syringe into the pressure tube. Finally, the lid of the evacuation tube was removed and the pressure tube was sealed with the screw cap under argon counter flow before the tube was placed in an aluminum heating block. The temperature was controlled by a thermocouple in an additional pressure tube with silicon oil placed in the aluminum block.

When the intermediate alkyne was the desired product, the work-up (see below) was started after this reaction step.

Otherwise, after finishing the reaction and cooling down to room temperature, the pressure tube was placed in the evacuation tube which was evacuated and flushed with argon prior to this. Under argon counter flow, the screw cap was removed and the second solvent was added into the reaction mixture. The pressure tube was sealed again and placed in the aluminum block again to start the second reaction step.

After this second step was finished and the solution was cooled down to room temperature, the tube was opened and hydrogen gas was bubbled through the reaction solution. When the hydrogenation was finished, argon was bubbled through the solution to end the reaction.

For work-up, the solvents were removed by high vacuum. Especially DMF should be removed to improve the performance of the flash chromatography. Afterwards, the resulting crude product was dissolved by EtOAc/H₂O and extracted with EtOAc three times. The combined organic layers were extracted with H₂O again for three times. The combined organic layers were dried over Na₂SO₄ which was subsequently filtered off. Silica gel was added and the solvent was removed by rotary evaporator. A flash chromatography was conducted using heptane. In some cases (substances **h**, **i**, **l**, **n**, **u**), 5% EtOAc was added. Especially when Z-Alkenes are the desired products, the flash chromatography had to be repeated in some cases until a satisfying separation from the intermediate alkyne and the over-hydrogenated alkane was achieved.

Example on the basis of table 3, entry 1 (substance 4a):

4-Bromotoluene:	0.5 mmol	=	63.5 µL
Phenylacetylene:	1 mmol	=	110 µL
K ₂ CO ₃ :	1 mmol	=	138 mg
PdCl ₂ :	1 mol%	=	0.9 mg
BuPAD ₂ (CataCXium A):	1 mol%	=	1.8 mg

2 mL DMF, 60 °C, 16 h

After step 1:

+ 0.2 mL H₂O, 120 °C, 8 h

After step 2:

+ H₂, 0.5 mL/s gas flow, 25 °C, 25 min

After step 3:

+ Ar, 10 min

ICP-OES Analysis

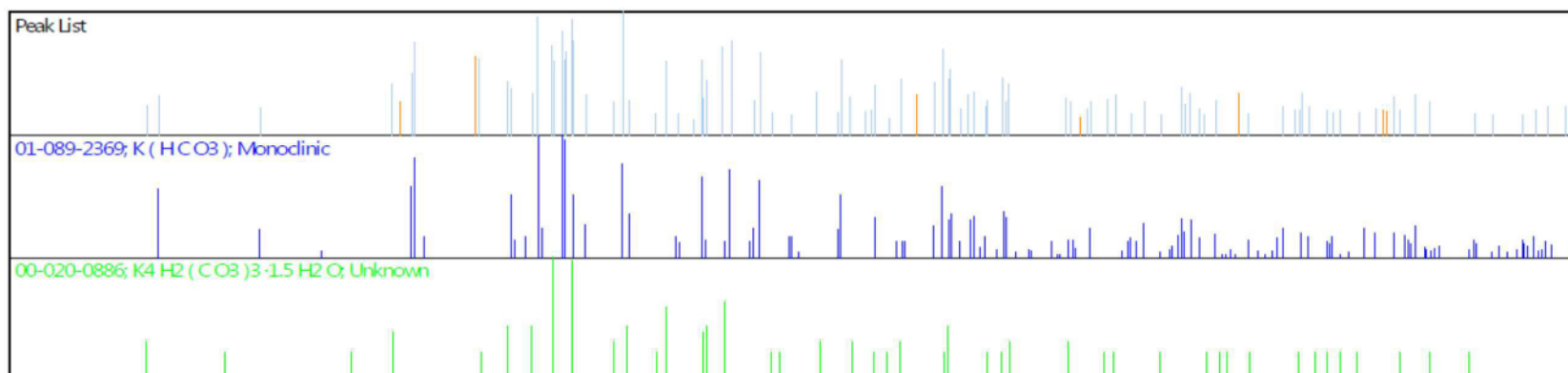
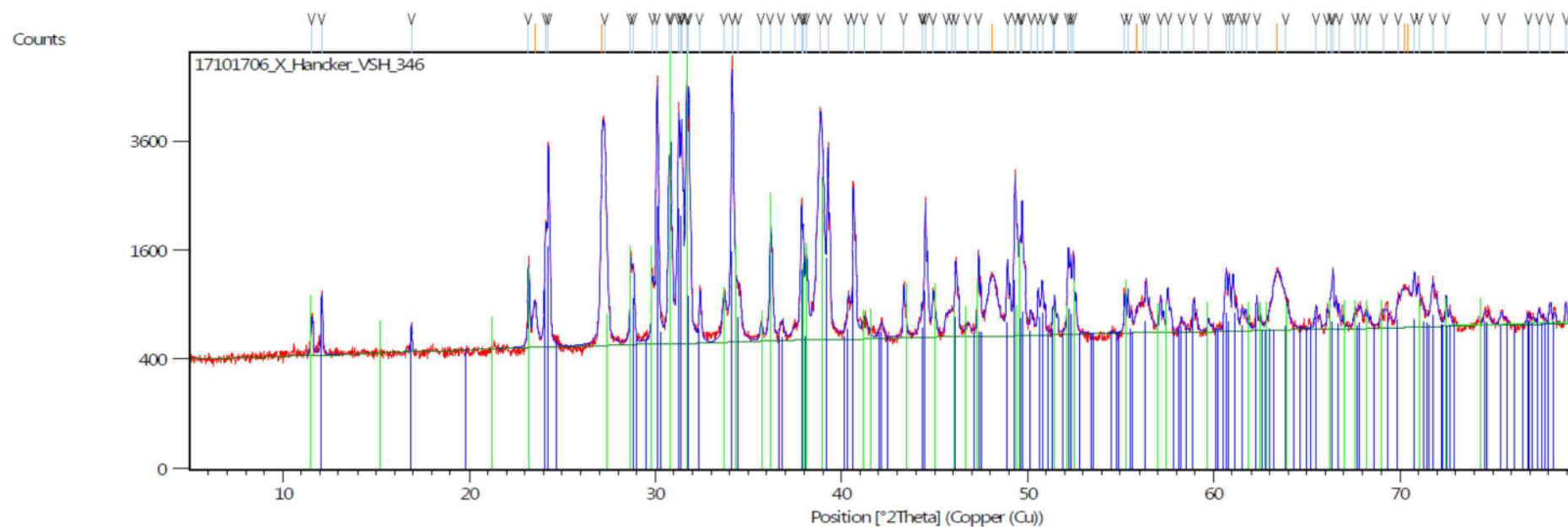
The reactions were carried out as described in section 2. and stopped at each reaction step for the preparation of both ICP-Samples. Herein, the homogeneous and heterogeneous phases were separated by centrifugation. The heterogeneous material was additionally washed with acetone five times. Afterwards, the solvents were removed by rotary evaporator. The heterogeneous material was used as obtained. The homogeneous samples were prepared by adding silica gel to the mixture and removing the solvent subsequently.

XRD-Analysis

Date: 20.10.2017 Time: 11:53:06

File: 17101706_X_Hancker_VSH_346

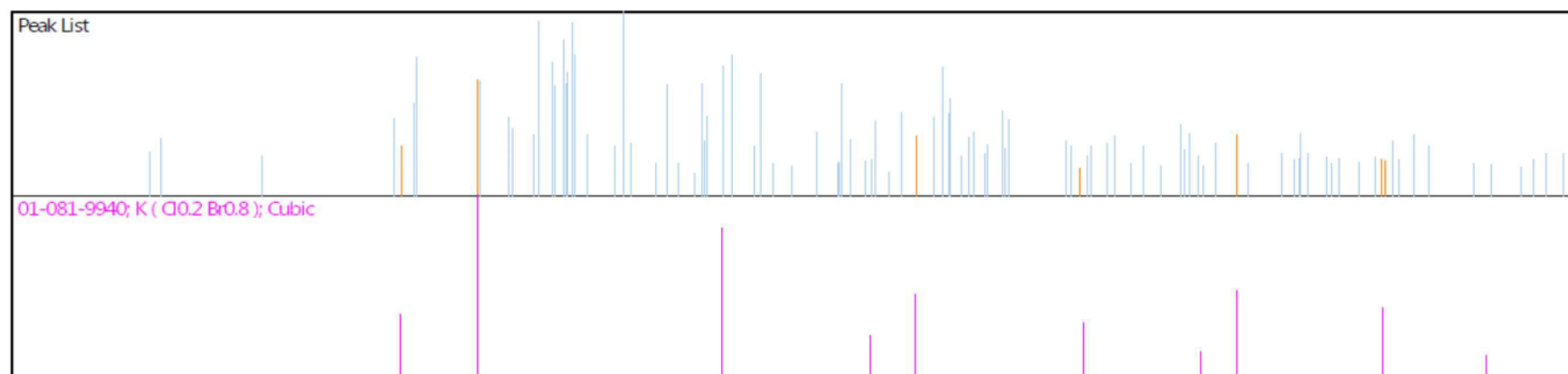
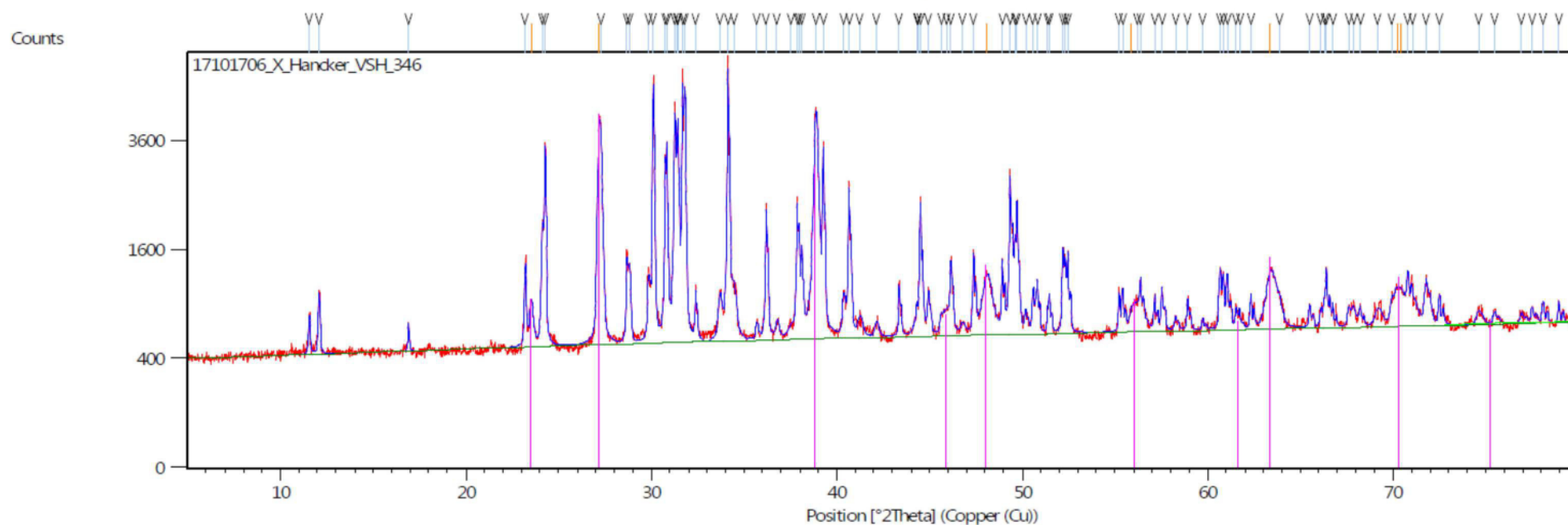
User: xrd



Date: 20.10.2017 Time: 11:53:25

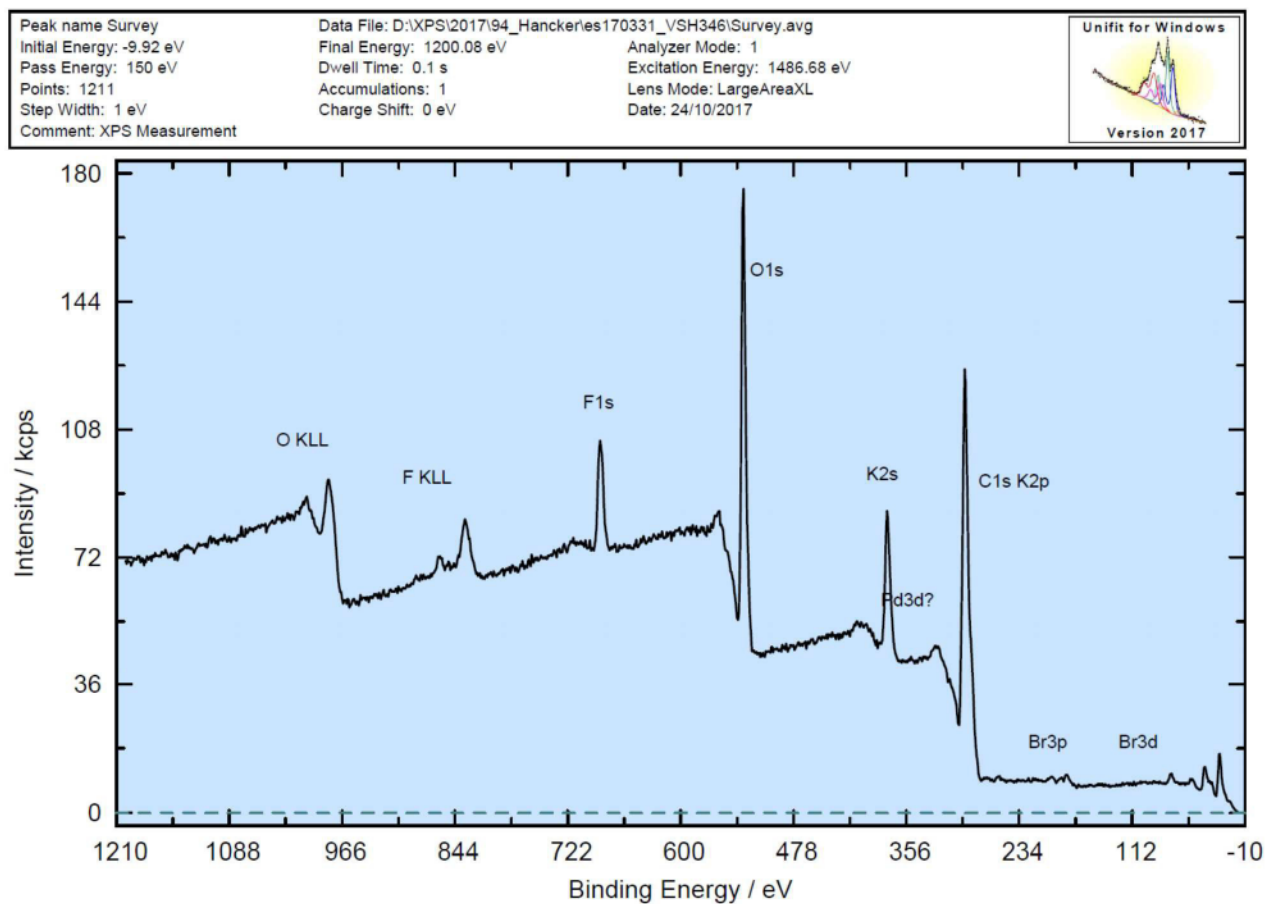
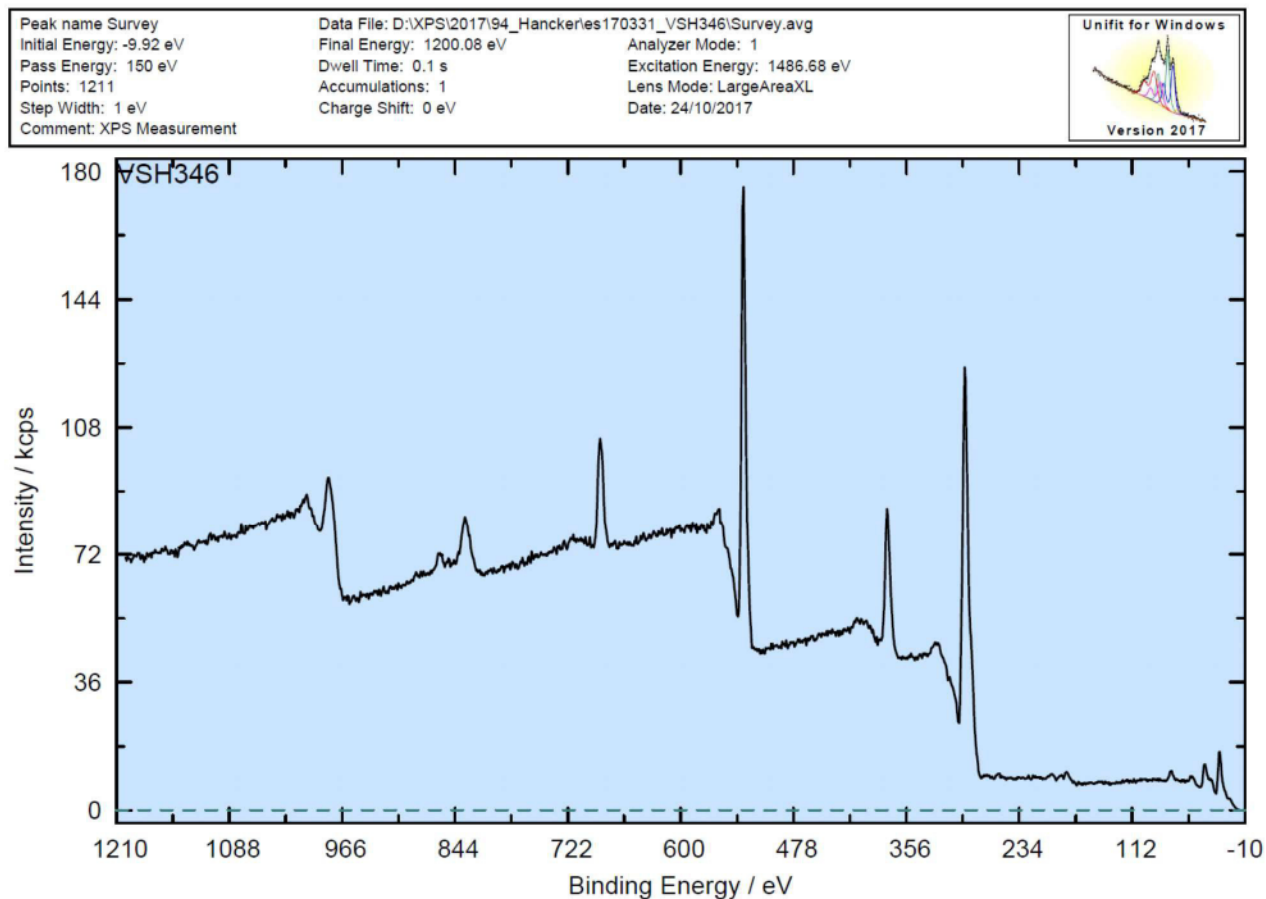
File: 17101706_X_Hancker_VSH_346

User: xrd



The heterogeneous material obtained after the hydrogenation step was analyzed by powder diffraction (powder-XRD). The generated diffractogram was interpreted by aid of a database (ICDD) which compares the generated diffractogram to data of listed compounds and identifies substances matching the recorded data. In the case of the generated catalyst, significant correlations between the generated data and the diffractograms of monoclinic KHCO_3 , $\text{K}_4\text{H}_2(\text{CO}_3)_3 \cdot 1.5\text{H}_2\text{O}$ and $\text{KBr}_{0.8}\text{Cl}_{0.2}$ were documented. Based on these observations and the fact that these compounds are theoretically expected to be formed from the Sonogashira coupling, the composition of the catalysts support is postulated as a K_2CO_3 - KHCO_3 mixture with additional KBr and trace amounts of KCl.

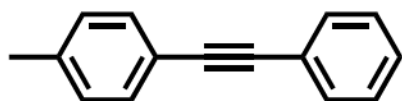
XPS-Analysis



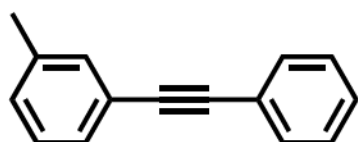
The XPS analysis displays a photoemission-spectroscopic methodology which mainly serves as a non-invasive analytical method for the determination of the elemental composition on the surface of materials. Herein, the binding energies (X-axis) of the generated photoelectrons are characteristic for the specific atom orbitals. Thus, the intensity peaks can be assigned to the characteristic atom orbitals and enable information about the elemental composition of the analyzed substance. As shown, the surface of the heterogeneous material obtained after the hydrogenation step consists mainly of oxygen, potassium and carbon. However, while evidence of bromine and chlorine is found in the data, the concentration of the palladium, whose presence was confirmed by ICP-OES, on the investigated surface is too low to generate the corresponding peaks.

The employed amount of palladium accounts for only 0.54 mg (0.9 mg PdCl₂ per reaction). Since the obtained heterogeneous residue amounted for 132 mg, the maximum palladium content would be 0.41% (assuming the complete heterogenization of the applied palladium). As only 26% of the employed palladium was heterogenized according to ICP-OES results for the generated heterogeneous material, the actual palladium loading in the measured sample was 0.11%. In addition, the distribution of the palladium and therefore its content on the surface remain unknown as well.

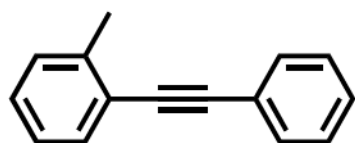
Analytical Data



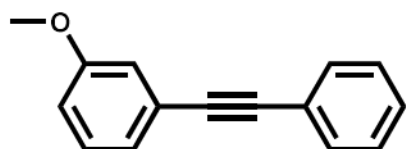
3a (4-methyl-phenyl)phenylacetylene: Off-white solid, isolated yield: 81.9 mg, 85%. $^1\text{H NMR}$ (300.1 MHz, Acetone- d_6): δ = 2.35 (s, 3 H), 7.19-7.24 (m, 2 H), 7.37-7.47 (m, 5 H), 7.52-7.57 (m, 2 H); $^{13}\text{C NMR}$ (75.5 MHz, Acetone- d_6): δ = 21.5 (CH_3), 89.4 (C^q), 90.2 (C^q), 121.0 (C^q), 124.2 (C^q), 129.1 (CH), 129.4 (2 CH), 130.1 (2 CH), 132.2 (4 CH), 139.4 (C^q); **HRMS** (EI, m/z): calcd. for $\text{C}_{15}\text{H}_{12}$ (M^+): 192.09335, found: 192.09364; **GC/MS-EI** (70 eV): m/z (%) = 192 (M^+ , 100), 191 (47), 189 (23), 193 (16), 165 (12), 190 (11).



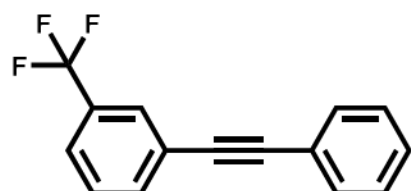
3b (3-methyl-phenyl)phenylacetylene: Off-white solid, isolated yield: 83.4 mg, 87%. $^1\text{H NMR}$ (300.1 MHz, Acetone- d_6): δ = 2.34 (s, 3 H), 7.19-7.23 (m, 1 H), 7.26-7.31 (m, 1 H), 7.34-7.45 (m, 5 H), 7.52-7.59 (m, 2 H); $^{13}\text{C NMR}$ (75.5 MHz, Acetone- d_6): δ = 21.2 (CH_3), 89.7 (C^q), 90.2 (C^q), 123.8 (C^q), 124.1 (C^q), 129.2 (CH), 129.3 (CH), 129.4 (CH), 129.4 (2 CH), 130.1 (CH), 132.3 (2 CH), 132.8 (CH), 139.1 (C^q); **HRMS** (EI, m/z): calcd. for $\text{C}_{15}\text{H}_{12}$ (M^+): 192.09335, found: 192.09311; **GC/MS-EI** (70 eV): m/z (%) = 192 (M^+ , 100), 191 (30), 189 (21), 193 (16), 165 (12), 190 (11),.



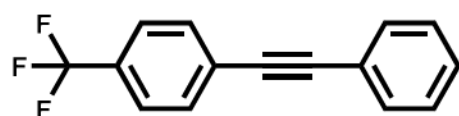
3c (2-methyl-phenyl)phenylacetylene: Off-white solid, isolated yield: 80.5 mg, 84%. $^1\text{H NMR}$ (300.1 MHz, Acetone- d_6): δ = 2.51 (s, 3 H), 7.18-7.24 (m, 1 H), 7.25-7.31 (m, 2 H), 7.38-7.45 (m, 3 H), 7.49-7.53 (m, 1 H), 7.54-7.61 (m, 2 H); $^{13}\text{C NMR}$ (75.5 MHz, Acetone- d_6): δ = 20.8 (CH_3), 88.9 (C^q), 94.1 (C^q), 123.7 (C^q), 124.2 (C^q), 126.6 (CH), 129.3 (CH), 129.4 (CH), 129.4 (2 CH), 130.4 (CH), 132.2 (2 CH), 132.5 (CH), 140.7 (C^q); **HRMS** (EI, m/z): calcd. for $\text{C}_{15}\text{H}_{12}$ (M^+): 192.09335, found: 192.09281; **GC/MS-EI** (70 eV): m/z (%) = 192 (M^+ , 100), 191 (95), 189 (35), 165 (22), 190 (17), 193 (15), 115 (11).



3d (3-methoxy-phenyl)phenylacetylene: Off-white solid, isolated yield: 75 mg, 72%. $^1\text{H NMR}$ (300.1 MHz, Acetone- d_6): δ = 3.83 (s, 3 H), 6.97 (ddd, J = 8.3, 2.6, 1.0 Hz, 1 H) 7.09-7.14 (m, 2 H), 7.29-7.35 (m, 1 H), 7.49-7.44 (m, 3 H), 7.53-7.57 (m, 2 H); $^{13}\text{C NMR}$ (75.5 MHz, Acetone- d_6): δ = 55.7 (CH_3), 89.7 (C^q), 90.0 (C^q), 115.8 (CH), 117.2 (CH), 124.0 (C^q), 124.7 (CH), 125.0 (C^q), 129.4 (CH), 129.5 (2 CH), 130.5 (CH), 132.3 (2 CH), 160.6 (C^q); **HRMS** (EI, m/z): calcd. for $\text{C}_{15}\text{H}_{12}\text{O}_1$ (M^+): 208.08827, found: 208.08883; **GC/MS-EI** (70 eV): m/z (%) = 208 (M^+ , 100), 178 (24), 165 (23), 209 (16).

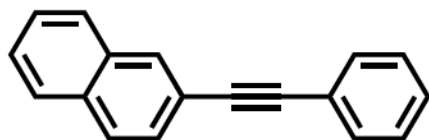


3e (3-trifluoromethyl-phenyl)phenylacetylene: Off-white solid, isolated yield: 114.5 mg, 93%. $^1\text{H NMR}$ (300.1 MHz, Acetone- d_6): δ = 7.41-7.48 (m, 3 H), 7.57-7.66 (m, 3 H), 7.71-7.74 (m, 1 H), 7.80-7.86 (m, 2 H); $^{13}\text{C NMR}$ (75.5 MHz, Acetone- d_6): δ = 88.3 (C^q), 91.7 (C^q), 123.3 (C^q), 124.8 (q, 1J = 271.7 Hz, CF_3), 125.1 (C^q), 125.8 (q, 3J = 3.9 Hz, $\text{CH}-\text{C}-\text{CF}_3$), 128.7 (q, 3J = 3.9 Hz, $\text{CH}-\text{C}-\text{CF}_3$), 129.5 (2 CH), 129.8 (CH), 130.5 (CH), 131.4 (q, 2J = 32.2 Hz, $\text{C}-\text{CF}_3$), 132.5 (2 CH), 135.8 (CH); $^{19}\text{F NMR}$ (282.4 MHz, Acetone- d_6): δ = -63.0 (CF_3); **HRMS** (EI, m/z): calcd. for $\text{C}_{15}\text{H}_9\text{F}_3$ (M^+): 246.06509, found: 246.06550; **GC/MS-EI** (70 eV): m/z (%) = 246 (M^+ , 100), 247 (16).

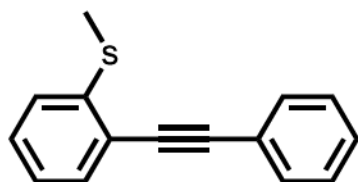


3f (4-trifluoromethyl-phenyl)phenylacetylene: Off-white solid, isolated yield: 108.1 mg, 88%. $^1\text{H NMR}$ (300.1 MHz, Acetone- d_6): δ = 7.42-7.47 (m, 3 H), 7.57-7.62 (m, 2 H), 7.77 (s, 4 H); $^{13}\text{C NMR}$ (75.5 MHz, Acetone- d_6): δ = 88.5 (C^q), 92.6 (C^q), 123.3 (C^q), 125.1 (q, 1J = 271.5 Hz, CF_3), 126.4 (q, 3J = 3.9 Hz, $\text{CH}-\text{C}-\text{CF}_3$), 128.2 (C^q), 129.6 (2 C, CH), 130.0 (CH), 130.4 (q, 2J = 32.4 Hz, $\text{C}-\text{CF}_3$), 132.5 (2 CH), 132.9 (2 CH); $^{19}\text{F NMR}$ (282.4 MHz, Acetone- d_6): δ = -62.9 (CF_3);

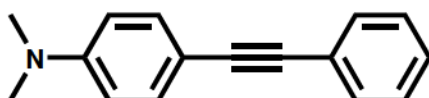
HRMS (EI, m/z): calcd. for $C_{15}H_9F_3$ (M)⁺: 246.06509, found: 246.06532 **GC/MS-EI** (70 eV): m/z (%) = 246 (M⁺, 100), 247 (16).



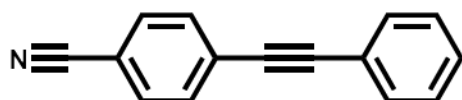
3g (2-naphthyl)phenylacetylene: Off-white solid, isolated yield: 93.7 mg, 82%. **¹H NMR** (300.1 MHz, Acetone- d_6): δ = 7.40-7.46 (m, 3 H), 7.54-7.63 (m, 5 H), 7.89-7.96 (m, 3 H), 8.13-8.14 (m, 1 H); **¹³C NMR** (75.5 MHz, Acetone- d_6): δ = 90.4 (2 C^q), 121.3 (C^q), 124.0 (C^q), 127.7 (CH), 127.8 (CH), 128.6 (2 CH), 129.0 (CH), 129.1 (CH), 129.4 (CH), 129.5 (2 CH), 132.1 (CH), 132.4 (2 CH), 133.8 (C^q), 134.0 (C^q); **HRMS** (EI, m/z): calcd. for $C_{18}H_{12}$ (M)⁺: 228.09335, found: 228.09330; **GC/MS-EI** (70 eV): m/z (%) = 228 (M⁺, 100), 226 (32), 229 (19), 227 (10).



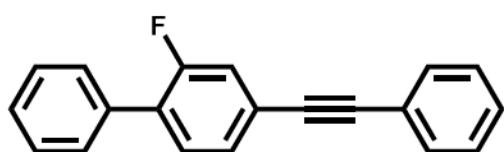
3h (2-methylthio-phenyl)phenylacetylene: Off-white solid, isolated yield: 77.4 mg, 69%. **¹H NMR** (300.1 MHz, Acetone- d_6): δ = 2.52 (s, 3 H), 7.14-7.19 (m, 1 H), 7.27-7.30 (m, 1 H), 7.35-7.38 (m, 1 H), 7.40-7.45 (m, 3 H), 7.48-7.51 (m, 1 H), 7.56-7.60 (m, 2 H); **¹³C NMR** (75.5 MHz, Acetone- d_6): δ = 14.7 (CH₃), 87.7 (C^q), 96.2 (C^q), 121.5 (C^q), 124.0 (C^q), 124.8 (CH), 125.0 (CH), 129.4 (2 CH), 129.5 (CH), 130.0 (CH), 132.1 (2 CH), 132.8 (CH), 143.0 (C^q); **HRMS** (EI, m/z): calcd. for $C_{15}H_{12}S$ (M)⁺: 224.06542, found: 224.06487; **GC/MS-EI** (70 eV): m/z (%) = 224 (M⁺, 100), 223 (92), 229 (19), 221 (23), 208 (22), 225 (20), 165 (15), 222 (13), 178 (10), 163 (10).



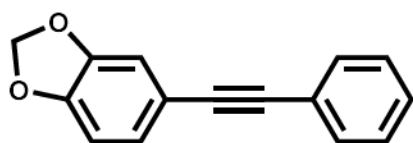
3i (4-N,N-dimethylamino-phenyl)phenylacetylene: Off-white solid, isolated yield: 77.1 mg, 70%. **¹H NMR** (300.1 MHz, Acetone- d_6): δ = 2.96 (s, 6 H), 6.69-6.73 (m, 2 H), 7.32-7.41 (m, 5 H), 7.47-7.51 (m, 2 H); **¹³C NMR** (75.5 MHz, Acetone- d_6): δ = 40.2 (2 CH₃), 87.9 (C^q), 91.6 (C^q), 110.4 (C^q), 112.7 (2 CH), 125.1 (C^q), 128.4 (CH), 129.3 (2 CH), 131.8 (2 CH), 133.3 (2 CH), 151.2 (C^q); **HRMS** (EI, m/z): calcd. for $C_{16}H_{15}N$ (M)⁺: 221.11990, found: 221.11961; **GC/MS-EI** (70 eV): m/z (%) = 221 (M⁺, 100), 220 (52), 222 (17), 205 (15), 176 (14).



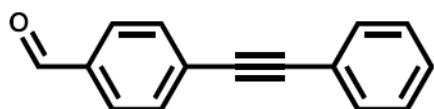
3j (4-cyano-phenyl)phenylacetylene: Off-white solid, isolated yield: 99.4 mg, 98%. $^1\text{H NMR}$ (300.1 MHz, Acetone- d_6): δ = 7.42-7.47 (m, 3 H), 7.56-7.62 (m, 2 H), 7.70-7.74 (m, 2 H), 7.79-7.83 (m, 2 H); $^{13}\text{C NMR}$ (75.5 MHz, Acetone- d_6): δ = 88.5 (C^q), 94.0 (C^q), 112.5 (C^q), 118.9 (C^q), 123.0 (C^q), 128.7 (C^q), 129.5 (2 CH), 130.1 (CH), 132.5 (2 CH), 133.0 (2 CH), 133.2 (2 CH); **HRMS** (EI, m/z): calcd. for $\text{C}_{15}\text{H}_9\text{N}$ (M^+): 203.07295, found: 203.07284; **GC/MS-EI** (70 eV): m/z (%) = 203 (M^+ , 100), 204 (17).



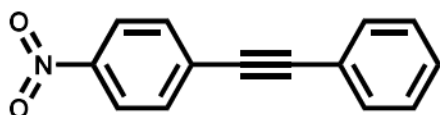
3k (4-phenyl-3-fluoro-phenyl)phenylacetylene: Off-white solid, isolated yield: 130.3 mg, 96%. $^1\text{H NMR}$ (300.1 MHz, Acetone- d_6): δ = 7.39-7.53 (m, 8 H), 7.54-7.63 (m, 5 H); $^{13}\text{C NMR}$ (75.5 MHz, Acetone- d_6): δ = 88.6 (d, J = 3.1 Hz, C^q), 91.4 (C^q), 119.6 (d, J = 24.8 Hz, CH), 123.5 (C^q), 124.9 (d, J = 9.8 Hz, C^q), 128.8 (d, J = 3.4 Hz, CH), 129.0 (CH), 129.5 (2 CH), 129.5 (2 CH), 129.7 (CH), 129.7 (2 CH), 130.2 (d, J = 13.6 Hz, C^q), 131.9 (d, J = 4.2 Hz, CH), 132.4 (2 CH), 135.8 (d, J = 1.0 Hz, C^q), 160.1 (d, J = 247.4 Hz, C^q); $^{19}\text{F NMR}$ (282.4 MHz, Acetone- d_6): δ = -118.9 (CF); **HRMS** (EI, m/z): calcd. for $\text{C}_{20}\text{H}_{13}\text{F}$ (M^+): 272.09958, found: 272.09978; **GC/MS-EI** (70 eV): m/z (%) = 272 (M^+ , 100), 273 (21), 270 (18).



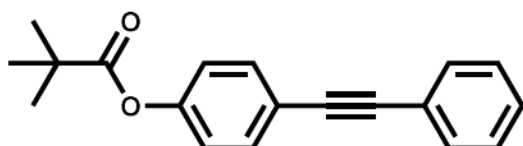
3l (3,4-methylenedioxy-phenyl)phenylacetylene: Off-white solid, isolated yield: 75.8 mg, 68%. $^1\text{H NMR}$ (300.1 MHz, Acetone- d_6): δ = 6.06 (s, 2 H), 6.87-6.90 (m, 1 H), 7.01-7.01 (m, 1 H), 7.07-7.10 (m, 1 H), 7.37-7.42 (m, 3 H), 7.49-7.54 (m, 2 H); $^{13}\text{C NMR}$ (75.5 MHz, Acetone- d_6): δ = 87.5 (C^q), 89.2 (C^q), 101.7 (CH_2), 108.5 (CH), 111.1 (CH), 116.3 (C^q), 123.3 (C^q), 126.2 (CH), 128.2 (CH), 128.5 (2 CH), 131.3 (2 CH), 147.8 (C^q), 148.3 (C^q); **HRMS** (EI, m/z): calcd. for $\text{C}_{15}\text{H}_{10}\text{O}_2$ (M^+): 222.06753, found: 222.06695; **GC/MS-EI** (70 eV): m/z (%) = 222 (M^+ , 100), 163 (32), 221 (25), 223 (16), 165 (11).



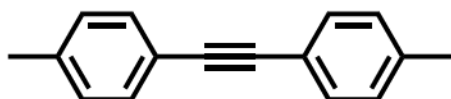
3m (4-carbaldehyde-phenyl)phenylacetylene: Off-white solid, isolated yield: 89.5 mg, 87%. $^1\text{H NMR}$ (300.1 MHz, Aceton- d_6): δ = 7.42-7.46 (m, 3 H), 7.57-7.62 (m, 2 H), 7.71-7.75 (m, 2 H), 7.93-7.96 (m, 2 H), 10.63 (s, 1 H); $^{13}\text{C NMR}$ (75.5 MHz, Aceton- d_6): δ = 89.2 (C^{q}), 93.6 (C^{q}), 123.2 (C^{q}), 129.5 (2 CH), 129.7 (C^{q}), 130.0 (CH), 130.3 (2 CH), 132.5 (2 CH), 132.8 (2 CH), 136.8 (C^{q}), 192.1 (CH); **HRMS** (EI, m/z): calcd. for $\text{C}_{15}\text{H}_{10}\text{O}$ (M^+): 206.07262, found: 206.07281; **GC/MS-EI** (70 eV): m/z (%) = 206 (M^+ , 100), 205 (70), 176 (46), 177 (18), 207 (16), 151 (16), 178 (12), 150 (12).



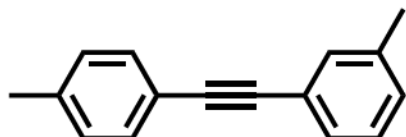
3n (4-nitro-phenyl)phenylacetylene: Off-white solid, isolated yield: 93.0 mg, 83%. $^1\text{H NMR}$ (300.1 MHz, Aceton- d_6): δ = 7.43-7.48 (m, 3 H), 7.57-7.63 (m, 2 H), 7.76-7.81 (m, 2 H), 8.24-8.28 (m, 2 H); $^{13}\text{C NMR}$ (75.5 MHz, Aceton- d_6): δ = 88.3 (C^{q}), 94.9 (C^{q}), 122.9 (C^{q}), 124.5 (2 CH), 129.6 (2 CH), 130.3 (CH), 130.7 (C^{q}), 132.6 (2 CH), 133.3 (2 CH), 148.1 (C^{q}); **HRMS** (EI, m/z): calcd. for $\text{C}_{14}\text{H}_9\text{NO}_2$ (M^+): 223.06278, found: 233.06281; **GC/MS-EI** (70 eV): m/z (%) = 223 (M^+ , 100), 176 (62), 193 (47), 165 (25), 151 (22), 177 (19), 224 (16).



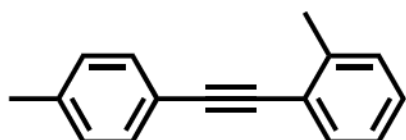
3o (4-phenyl-pivalate)phenylacetylene: Off-white solid, isolated yield: 120.1 mg, 86%. $^1\text{H NMR}$ (300.1 MHz, Aceton- d_6): δ = 1.35 (s, 9 H), 7.14-7.19 (m, 2 H), 7.39-7.44 (m, 3 H), 7.54-7.61 (m, 4 H); $^{13}\text{C NMR}$ (75.5 MHz, Aceton- d_6): δ = 27.3 (3 CH_3), 39.6 (C^{q}), 89.3 (C^{q}), 90.0 (C^{q}), 121.3 (C^{q}), 123.0 (2 CH), 123.9 (C^{q}), 129.4 (CH), 129.4 (2 CH), 132.3 (2 CH), 133.4 (2 CH), 152.3 (C^{q}), 176.9 (C^{q}); **HRMS** (EI, m/z): calcd. for $\text{C}_{19}\text{H}_{18}\text{O}_2$ (M^+): 278.13013, found: 278.12987; **GC/MS-EI** (70 eV): m/z (%) = 194 (100), 278 (M^+ , 22), 165 (15), 195 (15).



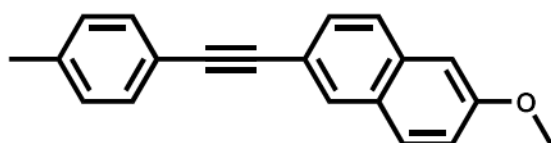
3p Di-(4-methyl-phenyl)acetylene: Off-white solid, isolated yield: 84.4 mg, 82%. $^1\text{H NMR}$ (300.1 MHz, Acetone- d_6): δ = 2.35 (s, 6 H), 7.20-7.24 (m, 4 H), 7.40-7.44 (m, 4 H); $^{13}\text{C NMR}$ (75.5 MHz, Acetone- d_6): δ = 21.4 (2 CH_3), 89.5 (2 C^q), 121.2 (2 C^q), 130.1 (4 CH), 132.3 (4 CH), 139.3 (2 C^q); **HRMS** (EI, m/z): calcd. for $\text{C}_{16}\text{H}_{14}$ (M^+): 206.10900, found: 206.10924; **GC/MS-EI** (70 eV): m/z (%) = 206 (M^+ , 100), 205 (25), 189 (18), 207 (17), 191 (15).



3q (4-methyl-phenyl)(3-methyl-phenyl)acetylene: Off-white solid, isolated yield: 87.0 mg, 84%. $^1\text{H NMR}$ (300.1 MHz, Acetone- d_6): δ = 2.34-2.34 (m, 3 H), 2.35-2.36 (m, 3 H), 7.18-7.24 (m, 3 H), 7.25-7.31 (m, 1 H), 7.31-7.36 (m, 2 H), 7.41-7.45 (m, 2 H); $^{13}\text{C NMR}$ (75.5 MHz, Acetone- d_6): δ = 21.2 (CH_3), 21.4 (CH_3), 89.6 (C^q), 89.8 (C^q), 121.1 (C^q), 124.1 (C^q), 129.3 (2 CH), 130.0 (CH), 130.1 (2 CH), 132.2 (2 CH), 132.7 (CH), 139.1 (C^q), 139.4 (C^q); **HRMS** (EI, m/z): calcd. for $\text{C}_{16}\text{H}_{14}$ (M^+): 206.10900, found: 206.10932; **GC/MS-EI** (70 eV): m/z (%) = 206 (M^+ , 100), 205 (21), 189 (19), 207 (17), 191 (13).

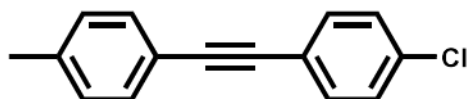


3r (4-methyl-phenyl)(2-methyl-phenyl)acetylene: Off-white solid, isolated yield: 82.2 mg, 80%. $^1\text{H NMR}$ (300.1 MHz, Acetone- d_6): δ = 2.35-2.36 (m, 3 H), 2.49-2.50 (m, 3 H), 7.19-7.25 (m, 3 H), 7.26-7.30 (m, 2 H), 7.43-7.50 (m, 3 H); $^{13}\text{C NMR}$ (75.5 MHz, Acetone- d_6): δ = 20.0 (CH_3), 20.6 (CH_3), 87.4 (C^q), 93.5 (C^q), 120.4 (C^q), 123.1 (C^q), 125.8 (CH), 128.4 (CH), 129.3 (2 CH), 129.5 (CH), 131.3 (2 CH), 131.6 (CH), 138.5 (C^q), 139.8 (C^q); **HRMS** (EI, m/z): calcd. for $\text{C}_{16}\text{H}_{14}$ (M^+): 206.10900, found: 206.10921; **GC/MS-EI** (70 eV): m/z (%) = 206 (M^+ , 100), 191 (67), 205 (44), 189 (28), 207 (17), 202 (17), 190 (16), 203 (13), 165 (13), 192 (11),.

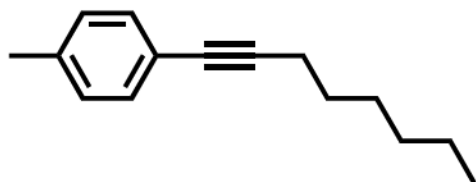


3s (4-methyl-phenyl)(6-(2-methoxy-naphthalene))acetylene: Off-white solid, isolated yield: 121.9 mg, 90%. $^1\text{H NMR}$ (300.1 MHz, Acetone- d_6): δ = 2.37 (s, 3 H), 3.94 (s, 3 H), 7.18-7.22

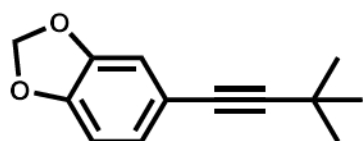
(m, 1 H), 7.23-7.26 (m, 2 H), 7.32-7.33 (m, 1 H), 7.45-7.48 (m, 2 H), 7.52-7.56 (m, 1 H), 7.81-7.85 (m, 2 H), 8.02-8.02 (m, 1 H); ^{13}C NMR (75.5 MHz, Aceton- d_6): δ = 21.4 (CH_3), 55.8 (CH_3), 89.8 (C^q), 90.0 (C^q), 106.8 (CH), 119.1 (C^q), 120.4 (CH), 121.3 (C^q), 128.0 (CH), 129.5 (C^q), 129.6 (CH), 130.1 (2 CH), 130.2 (CH), 131.8 (CH), 132.2 (2 CH), 135.3 (C^q), 139.4 (C^q), 159.5 (C^q); HRMS (EI, m/z): calcd. for $\text{C}_{20}\text{H}_{16}\text{O}$ (M^+): 272.11957, found: 272.11977; GC/MS-EI (70 eV): m/z (%) = 272 (M^+ , 100), 229 (43), 273 (21), 257 (15), 226 (14), 228 (13),.



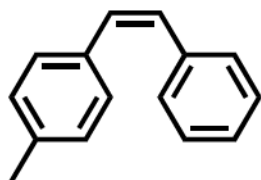
3t (4-methyl-phenyl)(4-chloro-phenyl)acetylene: Off-white solid, isolated yield: 90.7 mg, 80%. ^1H NMR (300.1 MHz, CD_2Cl_2): δ = 2.37 (s, 3 H), 7.17-7.20 (m, 2 H), 7.33-7.36 (m, 2 H), 7.41-7.44 (m, 2 H), 7.45-7.48 (m, 2 H); ^{13}C NMR (75.5 MHz, CD_2Cl_2): δ = 21.8 (CH_3), 88.0 (C^q), 91.0 (C^q), 120.3 (C^q), 122.6 (C^q), 129.2 (2 CH), 129.8 (2 CH), 132.0 (2 CH), 133.3 (2 CH), 134.5 (C^q), 139.5 (C^q); HRMS (EI, m/z): calcd. for $\text{C}_{15}\text{H}_{11}^{35}\text{Cl}$ (M^+): 226.05438, found: 226.05405, calcd. for $\text{C}_{15}\text{H}_{11}^{37}\text{Cl}$ (M^+): 228.05143, found: 228.05166; GC/MS-EI (70 eV): m/z (%) = 226 ($\text{M}_{35\text{Cl}}^+$, 100), 189 (35), 228 ($\text{M}_{37\text{Cl}}^+$, 33), 227 (22), 225 (19), 190 (16), 191 (12).



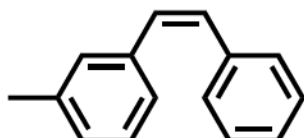
3u (4-methyl-phenyl)(n-hexyl)acetylene: Off-white solid, isolated yield: 74.8 mg, 75%. ^1H NMR (300.1 MHz, Acetone- d_6): δ = 0.87-0.93 (m, 3 H), 1.28-1.51 (m, 6 H), 1.53-1.63 (m, 2 H), 2.30-2.31 (m, 3 H), 2.37-2.41 (t, J = 6.9 Hz, 2 H), 7.11-7.15 (m, 2 H), 7.24-7.28 (m, 2 H); ^{13}C NMR (75.5 MHz, Aceton- d_6): δ = 14.3 (CH_3), 19.7 (CH_2), 21.3 (CH_3), 23.3 (CH_2), 29.3 (CH_2), 29.6 (CH_2), 32.1 (CH_2), 81.3 (C^q), 90.1 (C^q), 122.1 (C^q), 129.9 (2 CH), 132.1 (2 CH), 138.3 (C^q); HRMS (EI, m/z): calcd. for $\text{C}_{15}\text{H}_{20}$ (M^+): 200.15595, found: 200.15571; GC/MS-EI (70 eV): m/z (%) = 129 (100), 131 (79), 128 (55), 157 (43), 143 (40), 142 (40), 200 (M^+ , 35), 115 (32), 105 (24), 127 (21), 141 (19), 158 (17), 144 (14), 130 (14), 116 (14), 171 (12), 91 (12), 132 (11).



3v (3,4-methylenedioxy-phenyl)(tert-butyl)acetylene: Off-white solid, isolated yield: 70.0 mg, 69%. **¹H NMR** (300.1 MHz, Aceton-d₆): δ = 1.28 (s, 9 H), 6.00 (s, 2 H), 6.77-6.81 (m, 2 H), 6.88 (dd, *J* = 8.0, 1.6 Hz, 1 H); **¹³C NMR** (75.5 MHz, Aceton-d₆): δ = 28.5 (C^q), 31.3 (3 CH₃), 79.7 (C^q), 97.0 (C^q), 102.3 (CH₂), 109.1 (CH), 112.0 (CH), 118.2 (C^q), 126.5 (CH), 148.3 (C^q), 148.4 (C^q); **HRMS** (EI, *m/z*): calcd. for C₁₃H₁₄O₂ (M)⁺: 202.09883, found: 202.09882; **GC/MS-EI** (70 eV): *m/z* (%) = 187 (100), 202 (M⁺, 55), 128 (20), 129 (17), 188 (13).



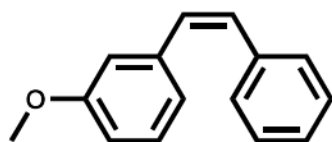
4a 1-(4-methyl-phenyl)-2-phenyl-Z-ethene: Colorless oil, isolated yield: 73.0 mg, 75%. ^1H NMR (300.1 MHz, Acetone- d_6): δ = 2.28 (s, 3 H), 6.58 (s, 2 H), 7.03-7.06 (m, 2 H), 7.12-7.15 (m, 2 H), 7.19-7.27 (m, 5 H); ^{13}C NMR (75.5 MHz, Acetone- d_6): δ = 21.2 (CH_3), 127.9 (CH), 129.1 (2 CH), 129.6 (4 CH), 129.7 (2 CH), 130.3 (CH), 131.0 (CH), 135.2 (C^q), 137.7 (C^q), 138.4 (C^q); HRMS (EI, m/z): calcd. for $\text{C}_{15}\text{H}_{14}$ (M^+): 194.10900, found: 194.10891; GC/MS-EI (70 eV): m/z (%) = 179 (100), 194 (M^+ , 86), 178 (82), 193 (21), 165 (15), 180 (14), 195 (14), 115 (13), 152 (11).



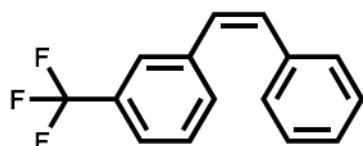
4b 1-(3-methyl-phenyl)-2-phenyl-Z-ethene: Colorless oil, isolated yield: 72.7 mg, 75%. ^1H NMR (300.1 MHz, Acetone- d_6): δ = 2.23 (d, J = 0.6 Hz, 3 H), 6.61 (s, 2 H), 7.01-7.04 (m, 2 H), 7.07-7.13 (m, 2 H), 7.20-7.25 (m, 5 H); ^{13}C NMR (75.5 MHz, Acetone- d_6): δ = 21.3 (CH_3), 126.6 (CH), 128.0 (CH), 128.7 (CH), 129.0 (CH), 129.0 (2 CH), 129.6 (2 CH), 130.3 (CH), 130.8 (CH), 131.1 (CH), 138.1 (C^q), 138.2 (C^q), 138.5 (C^q); HRMS (EI, m/z): calcd. for $\text{C}_{15}\text{H}_{14}$ (M^+): 194.10900, found: 194.10882; GC/MS-EI (70 eV): m/z (%) = 179 (100), 194 (M^+ , 86), 178 (84), 193 (23), 195 (14), 180 (14), 165 (13), 115 (11), 152 (10).



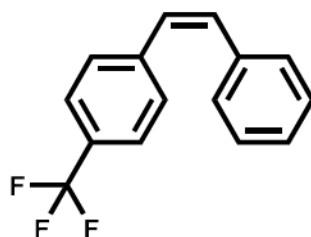
4c 1-(2-methyl-phenyl)-2-phenyl-Z-ethene: Colorless oil, isolated yield: 69.6 mg, 72%. ^1H NMR (300.1 MHz, Acetone- d_6): δ = 2.24 (s, 3 H), 6.68 (s, 2 H), 7.02-7.09 (m, 2 H), 7.09-7.11 (m, 1 H), 7.12-7.13 (m, 1 H), 7.14-7.20 (m, 4 H), 7.21-7.25 (m, 1 H); ^{13}C NMR (75.5 MHz, Acetone- d_6): δ = 19.9 (CH_3), 126.5 (CH), 128.0 (CH), 128.2 (CH), 128.9 (2 CH), 129.6 (CH), 129.6 (2 CH), 130.3 (CH), 130.9 (CH), 131.4 (CH), 136.7 (C^q), 138.0 (C^q), 138.0 (C^q); HRMS (EI, m/z): calcd. for $\text{C}_{15}\text{H}_{14}$ (M^+): 194.10900, found: 194.10883; GC/MS-EI (70 eV): m/z (%) = 179 (100), 194 (M^+ , 80), 178 (67), 115 (23), 116 (15), 193 (14), 180 (14), 195 (13), 165 (12).



4d 1-(3-methoxyphenyl)-2-phenyl-Z-ethene: Colorless oil, isolated yield: 71.8 mg, 68%. ^1H NMR (300.1 MHz, Acetone- d_6): δ = 3.64 (s, 3 H), 6.60 (d, J = 12.3 Hz, 1 H), 6.65 (d, J = 12.3 Hz, 1 H), 6.75-6.84 (m, 3 H), 7.13-7.16 (m, 1 H), 7.18-7.27 (m, 5 H); ^{13}C NMR (75.5 MHz, Acetone- d_6): δ = 55.2 (CH_3), 114.0 (CH), 114.7 (CH), 122.1 (CH), 128.0 (CH), 129.1 (2 CH), 129.6 (2 CH), 130.1 (CH), 131.0 (CH), 131.2 (CH), 138.3 (C^q), 139.4 (C^q), 160.5 (C^q); **HRMS** (EI, m/z): calcd. for $\text{C}_{15}\text{H}_{14}\text{O}$ (M^+): 210.10392, found: 210.10441; **GC/MS-EI** (70 eV): m/z (%) = 210 (M^+ , 100), 165 (59), 179 (41), 178 (40), 209 (34), 152 (27), 194 (26), 167 (25), 166 (19), 177 (19), 195 (18), 211 (16), 176 (10).

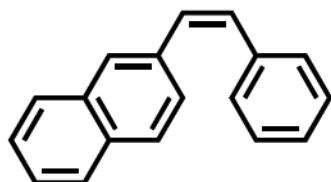


4e 1-(3-trifluoromethylphenyl)-2-phenyl-Z-ethene: Colorless oil, isolated yield: 102.8 mg, 83%. ^1H NMR (300.1 MHz, Acetone- d_6): δ = 6.68-6.72 (d, J = 12.2 Hz, 1 H), 6.77-6.82 (d, J = 12.2 Hz, 1 H), 7.21-7.31 (m, 5 H), 7.43-7.55 (m, 4 H); ^{13}C NMR (75.5 MHz, Acetone- d_6): δ = 124.5 (q, 3J = 3.9 Hz, CH-C- CF_3), 125.1 (q, 1J = 271.7 Hz, CF_3), 126.2 (q, 3J = 3.9 Hz, CH-C- CF_3), 128.4 (CH), 129.3 (2 CH), 129.4 (CH), 129.5 (2 CH), 130.0 (CH), 130.9 (q, 2J = 31.9 Hz, C- CF_3), 132.9 (CH), 133.4 (CH), 137.5 (C^q), 139.1 (C^q); ^{19}F NMR (282.4 MHz, Acetone- d_6): δ = -63.4 (CF_3); **HRMS** (EI, m/z): calcd. for $\text{C}_{15}\text{H}_{11}\text{F}_3$ (M^+): 248.08074, found: 248.08030; **GC/MS-EI** (70 eV): m/z (%) = 248 (M^+ , 100), 178 (71), 179 (70), 233 (21), 247 (20), 227 (19), 249 (16).

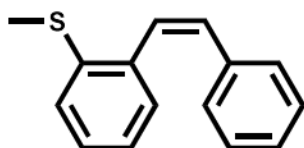


4f 1-(4-trifluoromethylphenyl)-2-phenyl-Z-ethene: Colorless oil, isolated yield: 98.5 mg, 79%. ^1H NMR (300.1 MHz, Acetone- d_6): δ = 6.70 (d, J = 12.3 Hz, 1 H), 6.80 (d, J = 12.3 Hz, 1 H), 7.21-7.31 (m, 5 H), 7.42-7.46 (m, 2 H), 7.56-7.61 (m, 2 H); ^{13}C NMR (75.5 MHz, Acetone- d_6): δ = 125.3 (q, 1J = 271 Hz, CF_3), 126.0 (q, 3J = 3.9 Hz, 2 CH-C- CF_3), 128.5 (CH), 129.3 (2 CH),

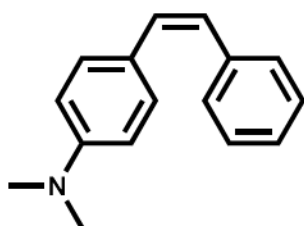
129.3 (q, $^2J = 32$ Hz, C-CF₃), 129.5 (CH), 129.6 (2 CH), 130.3 (2 CH), 133.3 (CH), 137.5 (C^q), 142.4 (C^q); **¹⁹F NMR** (282.4 MHz, Aceton-d₆): $\delta = -63.0$ (CF₃); **HRMS** (EI, m/z): calcd. for C₁₅H₁₁F₃ (M)⁺: 248.08074, found: 248.08027; **GC/MS-EI** (70 eV): m/z (%) = 248 (M⁺, 100), 179 (89), 178 (84), 227 (20), 247 (20), 233 (17), 249 (16), 180 (13), 229 (12), 176 (10).



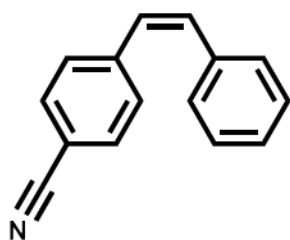
4g 1-(2-naphthyl)-2-phenyl-Z-ethene: Colorless oil, isolated yield: 82.7 mg, 72%. **¹H NMR** (300.1 MHz, Acetone-d₆): $\delta = 6.73$ (d, $J = 12.3$ Hz, 1 H), 6.82 (d, $J = 12.3$ Hz, 1 H), 7.21-7.32 (m, 5 H), 7.33-7.37 (m, 1 H), 7.43-7.49 (m, 2 H), 7.70-7.78 (m, 3 H), 7.80-7.86 (m, 1 H); **¹³C NMR** (75.5 MHz, Aceton-d₆): $\delta = 126.9$ (CH), 127.0 (CH), 127.6 (CH), 128.2 (CH), 128.3 (CH), 128.5 (CH), 128.7 (CH), 128.8 (CH), 129.1 (2 CH), 129.7 (2 CH), 131.0 (CH), 131.5 (CH), 133.6 (C^q), 134.5 (C^q), 135.8 (C^q), 138.2 (C^q); **HRMS** (EI, m/z): calcd. for C₁₈H₁₄ (M)⁺: 230.10900, found: 230.10867; **GC/MS-EI** (70 eV): m/z (%) = 230 (M⁺, 100), 229 (100), 228 (52), 215 (26), 226 (20), 231 (18), 227 (14), 202 (13).



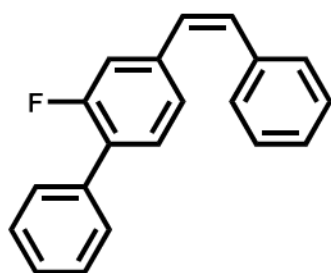
4h 1-(2-methylthio-phenyl)-2-phenyl-Z-ethene: Slightly yellow oil, isolated yield: 39.3 mg, 35%. **¹H NMR** (300.1 MHz, Acetone-d₆): $\delta = 2.49$ (s, 3 H), 6.62-6.66 (d, $J = 12.2$ Hz, 1 H), 6.68-6.72 (d, $J = 12.2$ Hz, 1 H), 6.96-7.01 (m, 1 H), 7.05-7.09 (m, 1 H), 7.13-7.21 (m, 5 H), 7.24-7.29 (m, 1 H), 7.32-7.35 (m, 1 H); **¹³C NMR** (75.5 MHz, Aceton-d₆): $\delta = 15.3$ (CH₃), 125.3 (CH), 126.0 (CH), 128.1 (CH), 128.9 (CH), 128.9 (CH), 128.9 (2 CH), 129.7 (2 CH), 130.0 (CH), 132.1 (CH), 136.8 (C^q), 137.6 (C^q), 138.9 (C^q); **HRMS** (EI, m/z): calcd. for C₁₅H₁₄S (M)⁺: 226.08107, found: 226.08112; **GC/MS-EI** (70 eV): m/z (%) = 211 (100), 226 (M⁺, 46), 178 (44), 212 (17), 210 (14), 165 (11).



4i 1-(4-N,N-dimethylamino-phenyl)-2-phenyl-Z-ethene: yellow oil, isolated yield of the E-Z-mixture: 54.0 mg, 48%. ~ 15% E-Isomer according to ^1H NMR. ^1H NMR (300.1 MHz, Acetone- d_6): δ = 2.91 (s, 6 H), 6.37-6.41 (d, 3J = 12.1 Hz, 1 H), 6.46-6.50 (d, 3J = 12.1 Hz, 1 H), 6.55-6.60 (m, 2 H), 7.09-7.33 (m, 7 H); ^{13}C NMR (75.5 MHz, Acetone- d_6): δ = 40.3 (2 CH_3), 112.6 (2 CH), 125.6 (C^q), 127.2 (CH), 127.5 (CH), 129.0 (2 CH), 129.4 (2 CH), 130.6 (2 CH), 131.2 (CH), 139.2 (C^q), 150.7 (C^q); HRMS both Isomers (EI, m/z): calcd. for $\text{C}_{16}\text{H}_{17}\text{N}$ (M^+): 223.13555, found: 223.13505; GC/MS-EI (70 eV): Z-Isomer: m/z (%) = 223 (M^+ , 100), 222 (42), 178 (22), 224 (17), 179 (12), 207 (11); E-Isomer: m/z (%) = 223 (M^+ , 100), 222 (41), 178 (19), 224 (18), 207 (12), 179 (11).

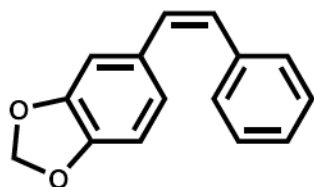


4j 1-(4-cyano-phenyl)-2-phenyl-Z-ethene: Colorless oil, isolated yield: 86.1 mg, 84%. ^1H NMR (300.1 MHz, Acetone- d_6): δ = 6.66-6.70 (d, 3J = 12.2 Hz, 1 H), 6.80-6.84 (d, 3J = 12.2 Hz, 1 H), 7.21-7.29 (m, 5 H), 7.39-7.42 (m, 2 H), 7.61-7.65 (m, 2 H); ^{13}C NMR (75.5 MHz, Acetone- d_6): δ = 111.3 (C^q), 119.3 (C^q), 128.6 (CH), 129.3 (3 CH), 129.5 (2 CH), 130.5 (2 CH), 132.9 (2 CH), 133.9 (CH), 137.3 (C^q), 143.0 (C^q); HRMS (EI, m/z): calcd. for $\text{C}_{15}\text{H}_{11}\text{N}$ (M^+): 205.08860, found: 205.08895; GC/MS-EI (70 eV): m/z (%) = 204 (100), 205 (M^+ , 98), 190 (40), 203 (33), 206 (15), 176 (14), 177 (13), 165 (12).

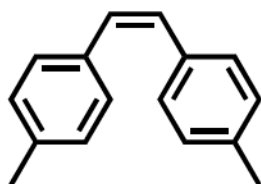


4k 1-(4-phenyl-3-fluoro-phenyl)-2-phenyl-Z-ethene: Colorless oil, isolated yield: 118.1 mg, 86%. ^1H NMR (300.1 MHz, Acetone- d_6): δ = 6.62-6.66 (d, 3J = 12.3 Hz, 1 H), 6.73-6.77 (d, 3J = 12.3 Hz, 1 H), 7.05-7.10 (m, 1 H), 7.14-7.17 (m, 1 H), 7.22-7.48 (m, 9 H), 7.53-7.58 (m, 2 H); ^{13}C NMR (75.5 MHz, Acetone- d_6): δ = 116.9 (d, J = 23.8 Hz, CH), 126.2 (d, J = 3.2 Hz, CH), 128.4 (CH), 128.4 (d, J = 13.5 Hz, C^q), 128.6 (CH), 129.3 (2 CH), 129.4 (2 CH), 129.4 (d, J = 2.3 Hz,

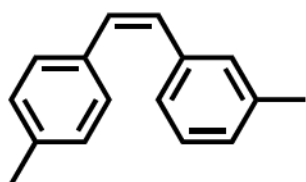
CH), 129.5 (2 CH), 129.6 (CH), 129.6 (CH), 131.3 (d, $J = 4.1$ Hz, CH), 132.4 (CH), 136.2 (d, $J = 1.4$ Hz, C^q), 137.8 (C^q), 139.5 (d, $J = 8.3$ Hz, C^q), 160.2 (d, $J = 246.2$ Hz, C^q); **¹⁹F NMR** (282.4 MHz, Aceton-d₆): $\delta = -119.6$ (CF); **HRMS** (EI, m/z): calcd. for C₂₀H₁₅F (M)⁺: 274.11523, found: 274.11528; **GC/MS-EI** (70 eV): m/z (%) = 274 (100), 275 (21), 252 (21), 273 (17), 253 (16), 196 (15), 259 (11), 197 (11).



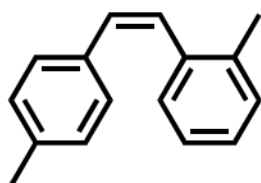
4l 1-(3,4-methylenedioxy-phenyl)-2-phenyl-Z-ethene: Colorless oil, isolated yield: 72.2 mg, 64%. **¹H NMR** (300.1 MHz, Acetone-d₆): $\delta = 5.95$ (s, 2 H), 6.54 (s, 2 H), 6.68-6.78 (m, 3 H), 7.19-7.28 (m, 5 H); **¹³C NMR** (75.5 MHz, Aceton-d₆): $\delta = 102.0$ (CH), 108.9 (CH), 109.3 (CH), 123.8 (CH), 127.9 (CH), 129.2 (2 CH), 129.5 (2 CH), 129.9 (CH), 130.7 (CH), 132.0 (C^q), 138.3 (C^q), 147.8 (C^q), 148.4 (C^q); **HRMS** (EI, m/z): calcd. for C₁₅H₁₂O₂ (M)⁺: 224.08318, found: 224.08301; **GC/MS-EI** (70 eV): m/z (%) = 224 (100), 165 (67), 166 (25), 223 (21), 225 (16), 193 (13), 164 (12).



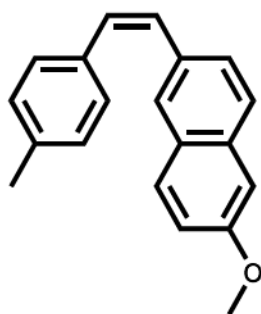
4p 1,2-di-(4-methyl-phenyl)-Z-ethene: Colorless oil, isolated yield: 79.3 mg, 76%. **¹H NMR** (300.1 MHz, Acetone-d₆): $\delta = 2.28$ (s, 6 H), 6.53 (s, 2 H), 7.03-7.07 (m, 4 H), 7.13-7.16 (m, 4 H); **¹³C NMR** (75.5 MHz, Aceton-d₆): $\delta = 21.2$ (CH₃), 129.5 (4 CH), 129.7 (4 CH), 130.3 (2 CH), 135.4 (2 C^q), 137.5 (2 C^q); **HRMS** (EI, m/z): calcd. for C₁₆H₁₆ (M)⁺: 208.12465, found: 208.12442; **GC/MS-EI** (70 eV): m/z (%) = 208 (100), 178 (67), 193 (59), 192 (31), 191 (22), 209 (17), 179 (14), 115 (14), 207 (12), 189 (12), 165 (12).



4q 1-(4-methyl-phenyl)-2-(3-methyl-phenyl)-Z-ethene: Colorless oil, isolated yield: 79.5 mg, 76%. $^1\text{H NMR}$ (300.1 MHz, Acetone- d_6): δ = 2.23-2.24 (m, 3 H), 2.27-2.28 (m, 3 H), 6.55 (s, 2 H), 7.00-7.04 (m, 2 H), 7.05-7.06 (m, 2 H), 7.09-7.11 (m, 2 H), 7.13-7.17 (m, 2 H); $^{13}\text{C NMR}$ (75.5 MHz, Acetone- d_6): δ = 21.2 (CH_3), 21.4 (CH_3), 126.5 (CH), 128.6 (CH), 128.9 (CH), 129.6 (2 CH), 129.6 (2 CH), 130.2 (CH), 130.4 (CH), 130.8 (CH), 135.2 (C^q), 137.6 (C^q), 138.3 (C^q), 138.5 (C^q); **HRMS** (EI, m/z): calcd. for $\text{C}_{16}\text{H}_{16}$ (M^+): 208.12465, found: 208.12444; **GC/MS-EI** (70 eV): m/z (%) = 208 (100), 178 (79), 193 (70), 192 (34), 191 (24), 209 (17), 179 (16), 115 (16), 189 (14), 165 (14), 207 (12), 194 (11).

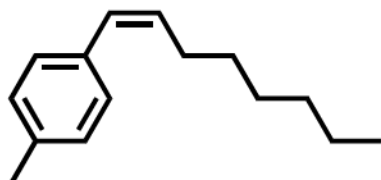


4r 1-(4-methyl-phenyl)-2-(2-methyl-phenyl)-Z-ethene: Colorless oil, isolated yield: 73.1 mg, 71%. $^1\text{H NMR}$ (300.1 MHz, Acetone- d_6): δ = 2.23-2.24 (m, 6 H), 6.62 (s, 2 H), 6.95-7.03 (m, 4 H), 7.04-7.08 (m, 1 H), 7.09-7.12 (m, 1 H), 7.13-7.19 (m, 1 H), 7.20-7.24 (m, 1 H); $^{13}\text{C NMR}$ (75.5 MHz, Acetone- d_6): δ = 19.9 (CH_3), 21.1 (CH_3), 126.5 (CH), 128.0 (CH), 129.4 (CH), 129.6 (5 CH), 130.9 (CH), 131.3 (CH), 135.1 (C^q), 136.7 (C^q), 137.6 (C^q), 138.2 (C^q); **HRMS** (EI, m/z): calcd. for $\text{C}_{16}\text{H}_{16}$ (M^+): 208.12465, found: 208.12452; **GC/MS-EI** (70 eV): m/z (%) = 208 (100), 178 (82), 193 (72), 115 (29), 192 (23), 116 (22), 191 (19), 209 (18), 179 (17), 165 (15), 189 (13), 194 (12).

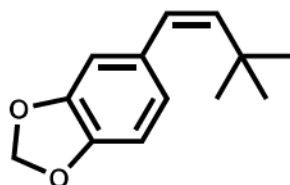


4s 1-(4-methyl-phenyl)-2-(6-(2-methoxy-naphthalene))-Z-ethene: Colorless oil, isolated yield: 116.1 mg, 85%. $^1\text{H NMR}$ (300.1 MHz, Acetone- d_6): δ = 2.28 (m, 3 H), 3.90 (m, 3 H), 6.62 (d, J = 12.2 Hz, 1 H), 6.71 (d, J = 12.2 Hz, 1 H), 7.03-7.07 (m, 2 H), 7.09-7.13 (m, 1 H), 7.16-7.20 (m, 2 H), 7.23-7.24 (m, 1 H), 7.31-7.35 (m, 1 H), 7.60-7.63 (m, 1 H), 7.65-7.68 (m, 1 H), 7.69-7.71 (m, 1 H); $^{13}\text{C NMR}$ (75.5 MHz, Acetone- d_6): δ = 21.2 (CH_3), 55.6 (CH_3), 106.7 (CH), 119.7 (CH),

127.3 (CH), 128.0 (CH), 128.6 (CH), 129.6 (2 CH), 129.7 (2 CH), 129.9 (C^q), 130.2 (CH), 130.4 (CH), 130.6 (CH), 133.7 (C^q), 134.9 (C^q), 135.4 (C^q), 137.7 (C^q), 158.9 (C^q); **HRMS** (EI, m/z): calcd. for C₂₀H₁₈O (M)⁺: 274.13522, found: 274.13544; **GC/MS-EI** (70 eV): m/z (%) = 274 (M⁺, 100), 215 (42), 216 (26), 259 (24), 275 (22).



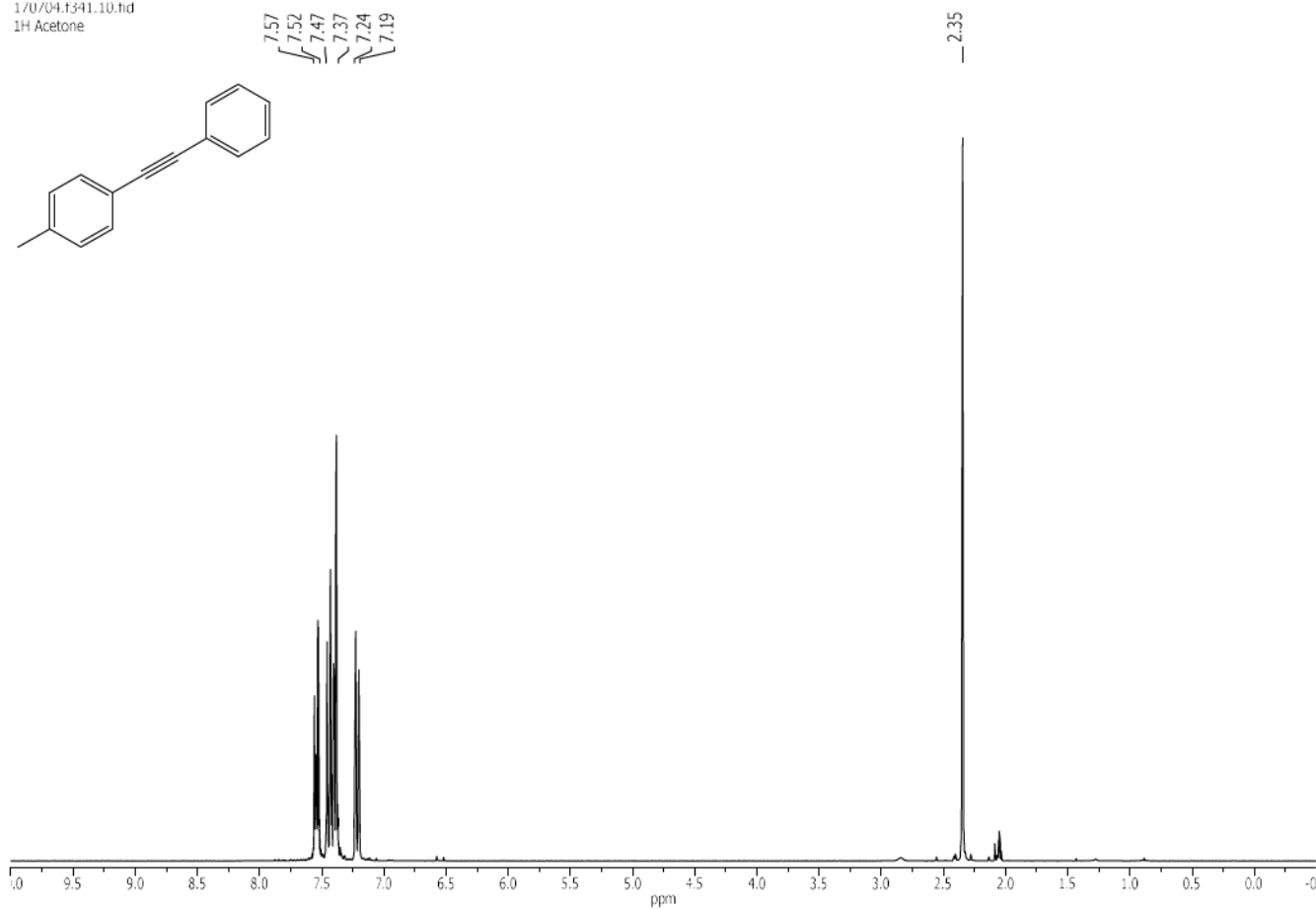
4u 1-(4-methylphenyl)-2-*n*-hexyl-*Z*-ethene: Colorless oil, isolated yield: 52.8 mg, 52%. **¹H NMR** (300.1 MHz, Acetone-d₆): δ = 0.87 (m, 3 H), 1.22-1.38 (m, 8 H), 1.40-1.50 (m, 2 H), 2.31 (s, 3 H), 5.62 (dt, *J* = 11.7, 7.3, 1 H), 6.37 (dt, *J* = 11.7, 1.8, 1 H), 7.13-7.20 (m, 4 H); **¹³C NMR** (75.5 MHz, Acetone-d₆): δ = 14.3 (CH₃), 21.1 (CH₃), 23.3 (CH₂), 29.3 (CH₂), 29.8 (CH₂), 30.7 (CH₂), 32.5 (CH₂), 129.5 (2 CH), 129.6 (CH), 129.6 (2 CH), 132.9 (CH), 135.8 (C^q), 136.9 (C^q); **HRMS** (EI, m/z): calcd. for C₁₅H₂₂ (M)⁺: 202.17160, found: 202.17166; **GC/MS-EI** (70 eV): m/z (%) = 131 (100), 118 (49), 202 (29), 115 (21), 91 (18), 116 (16), 129 (15), 117 (15), 105 (15), 132 (13), 128 (11).



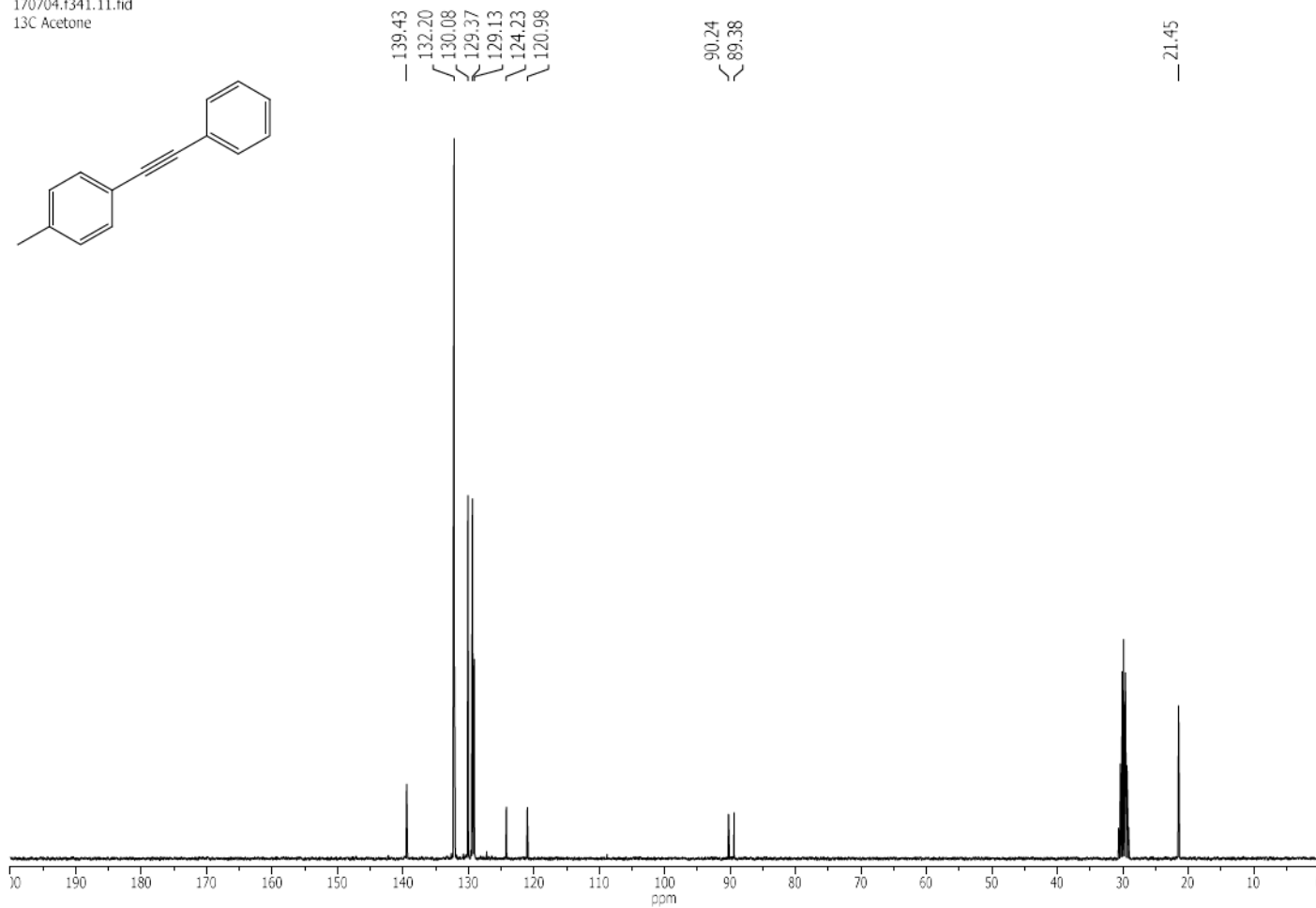
4v 1-(3,4-methylenedioxyphenyl)-2-*tert*-butyl-*Z*-ethene: Colorless oil, isolated yield: 35.1 mg, 34%. **¹H NMR** (300.1 MHz, Acetone-d₆): δ = 0.99 (s, 9 H), 5.55 (d, *J* = 12.5 Hz, 1 H), 5.97 (s, 2 H), 6.28-6.33 (m, 1 H), 6.63-6.67 (m, 2 H), 6.77-6.79 (m, 1 H); **¹³C NMR** (75.5 MHz, Acetone-d₆): δ = 31.5 (3 CH₃), 34.6 (C^q), 101.8 (CH₂), 108.3 (CH), 110.0 (CH), 122.9 (CH), 127.7 (CH), 133.7 (C^q), 143.2 (CH), 147.1 (C^q), 148.1 (C^q); **HRMS** (EI, m/z): calcd. for C₁₃H₁₆O₂ (M)⁺: 204.11448, found: 204.11436; **GC/MS-EI** (70 eV): m/z (%) = 159 (100), 189 (70), 204 (M⁺, 68), 131 (34), 115 (22), 91 (16), 160 (13), 144 (13), 116 (13), 77 (10).

^1H and ^{13}C NMR spectra

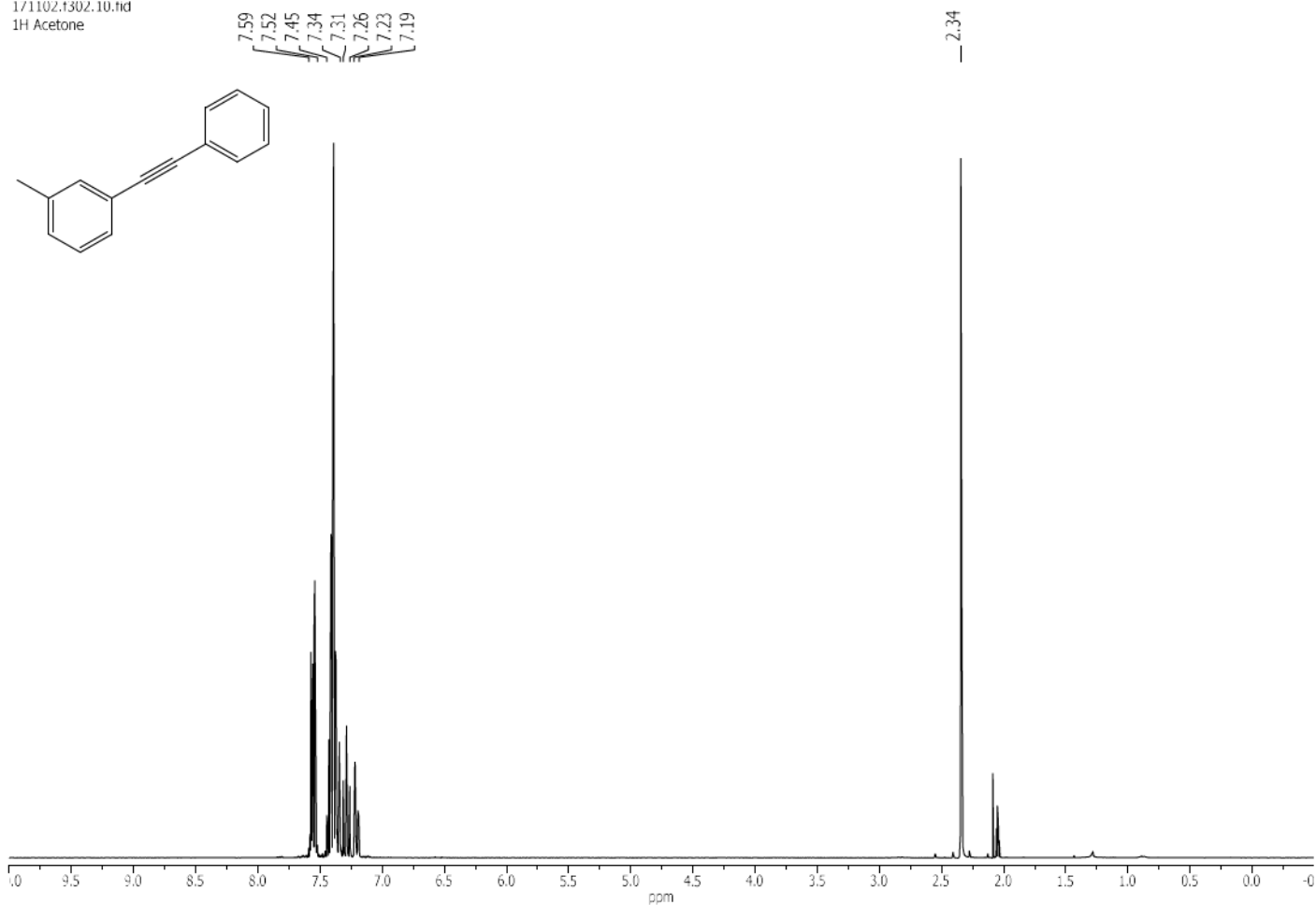
17/07/04.1341.10.fid
 ^1H Acetone



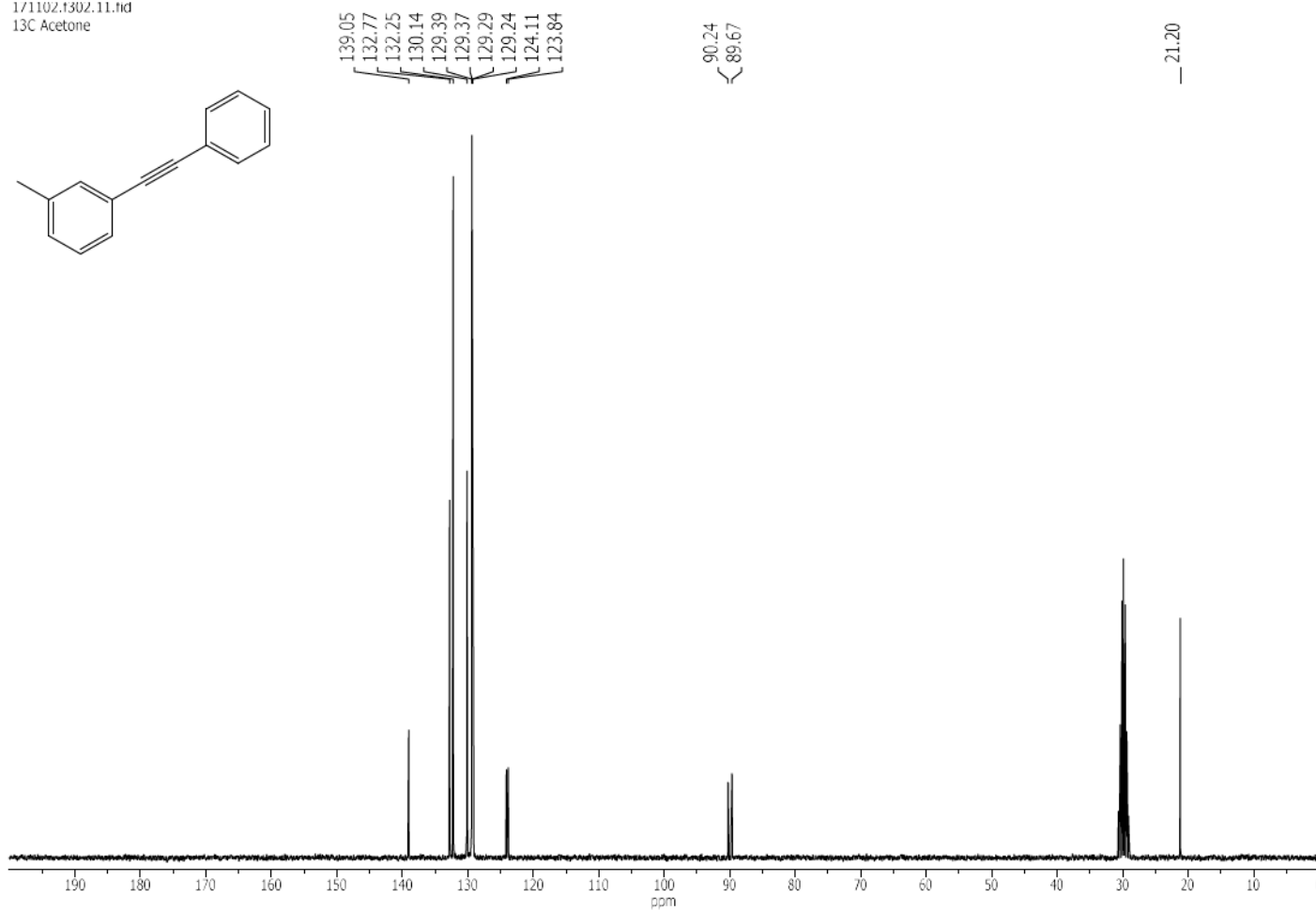
17/07/04.1341.11.fid
 ^{13}C Acetone



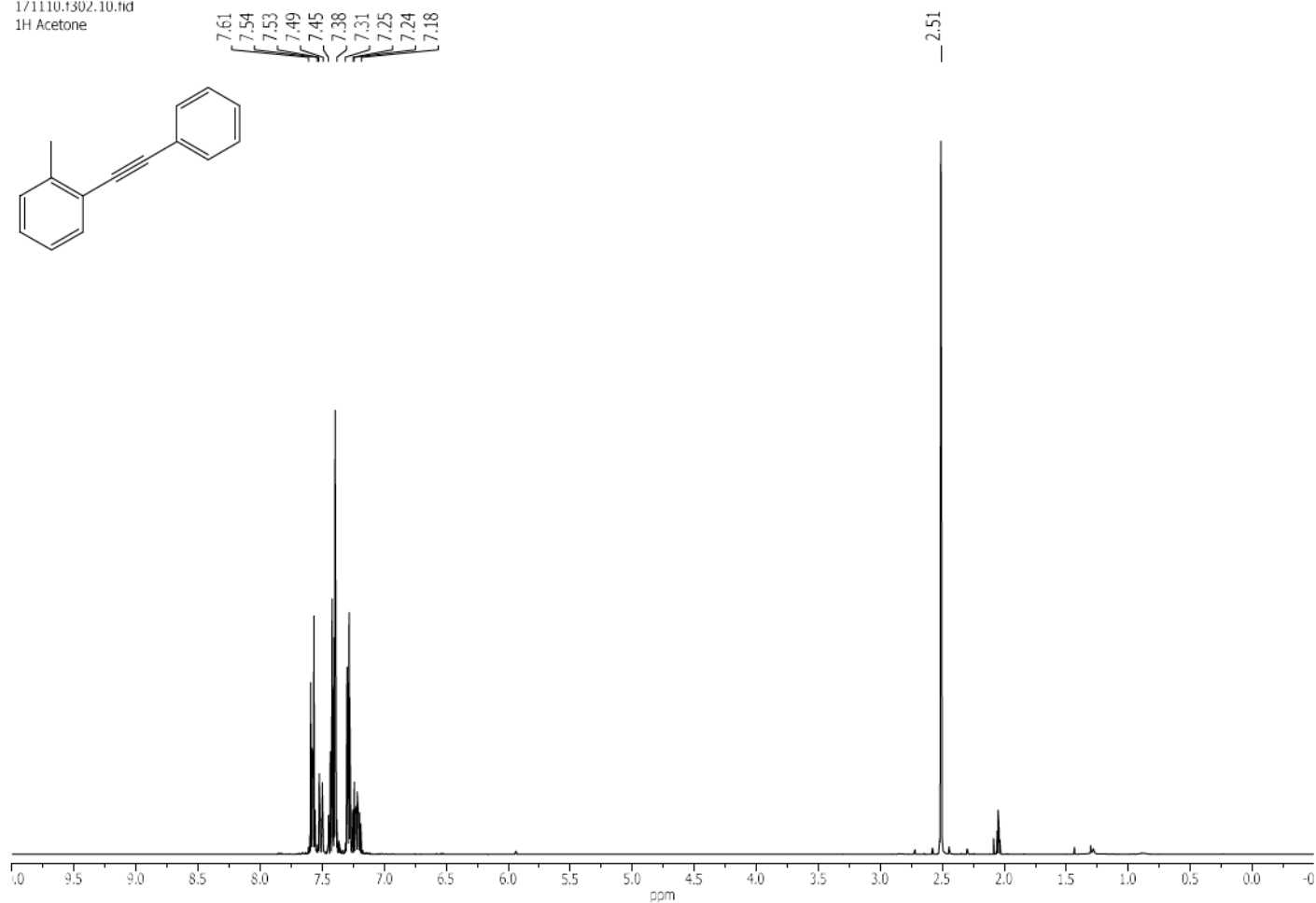
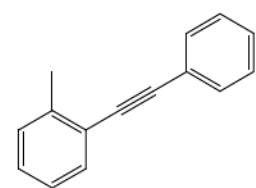
1/1102.1302.10.fid
1H Acetone



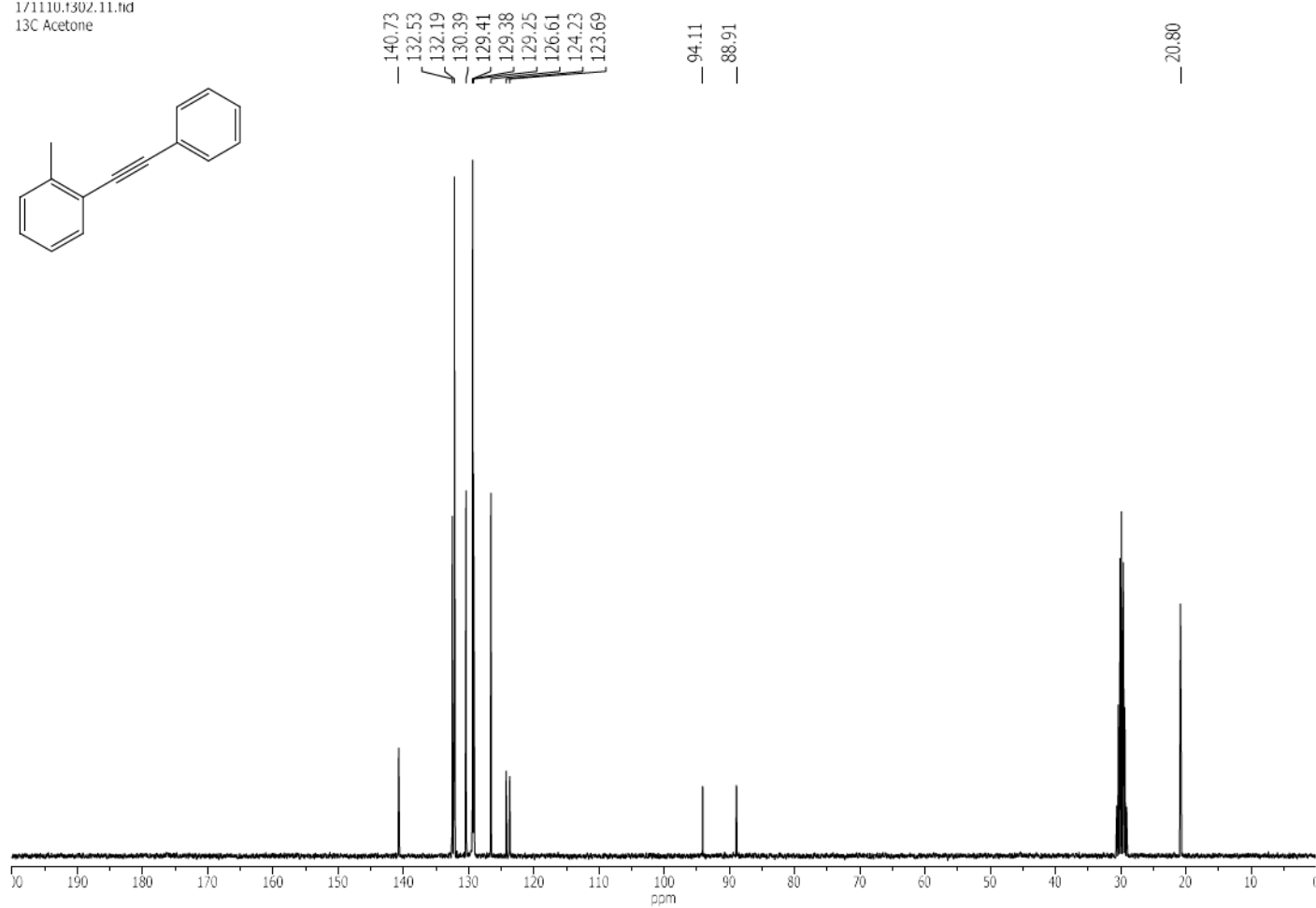
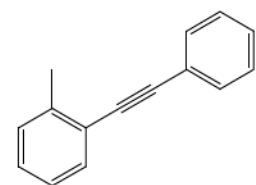
1/1102.1302.11.fid
13C Acetone



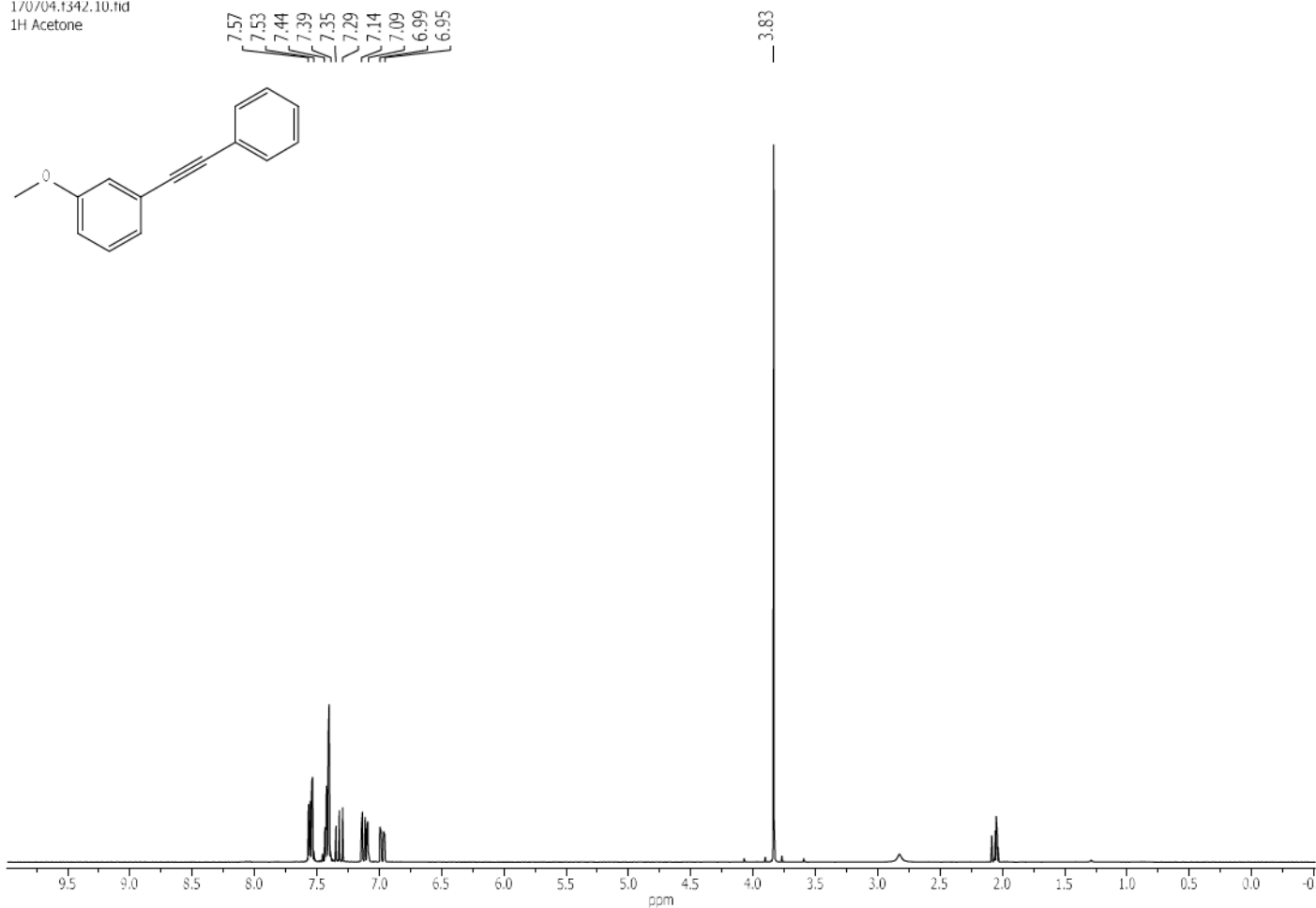
1/11110.1302.10.fid
1H Acetone



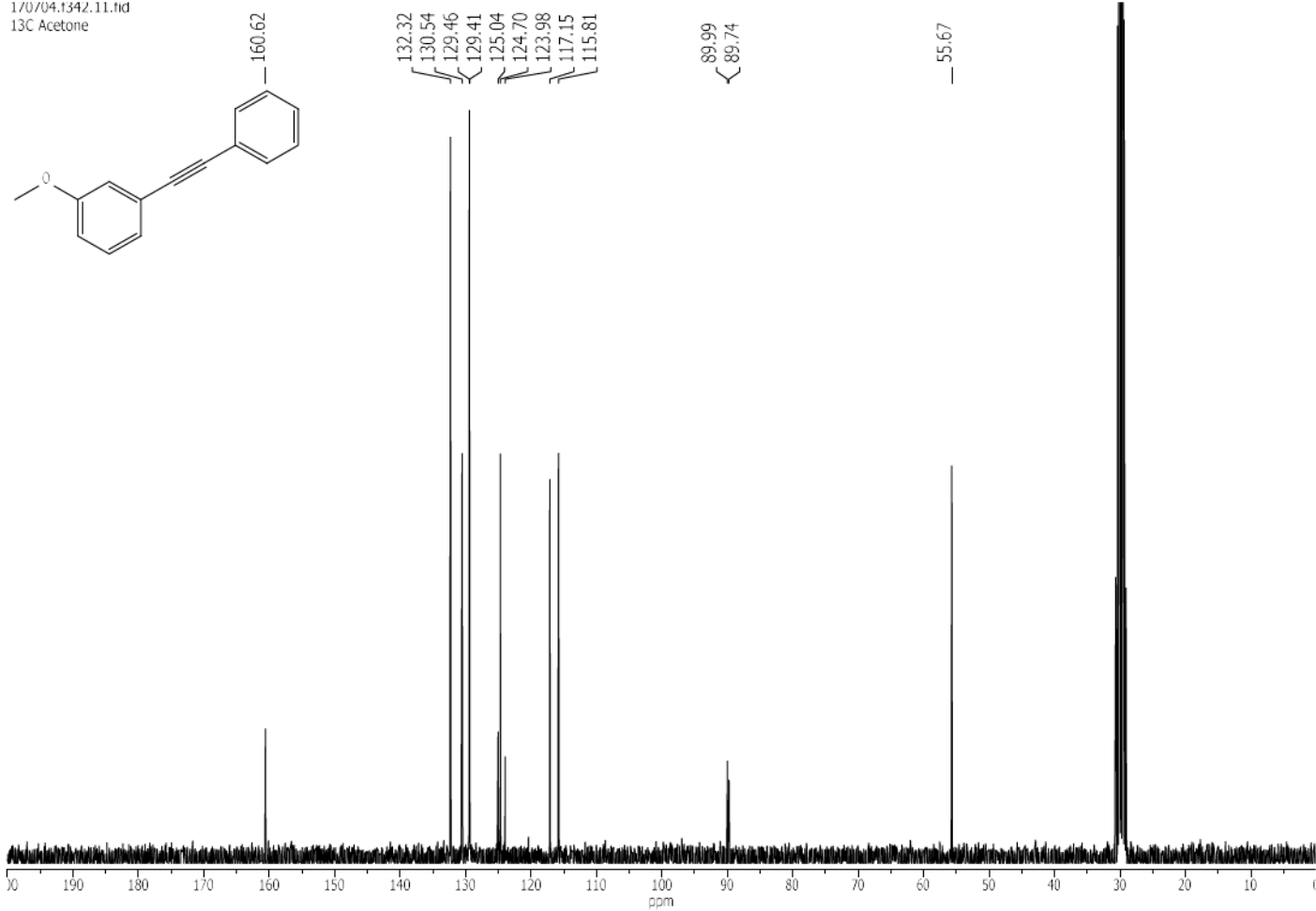
1/11110.1302.11.fid
13C Acetone



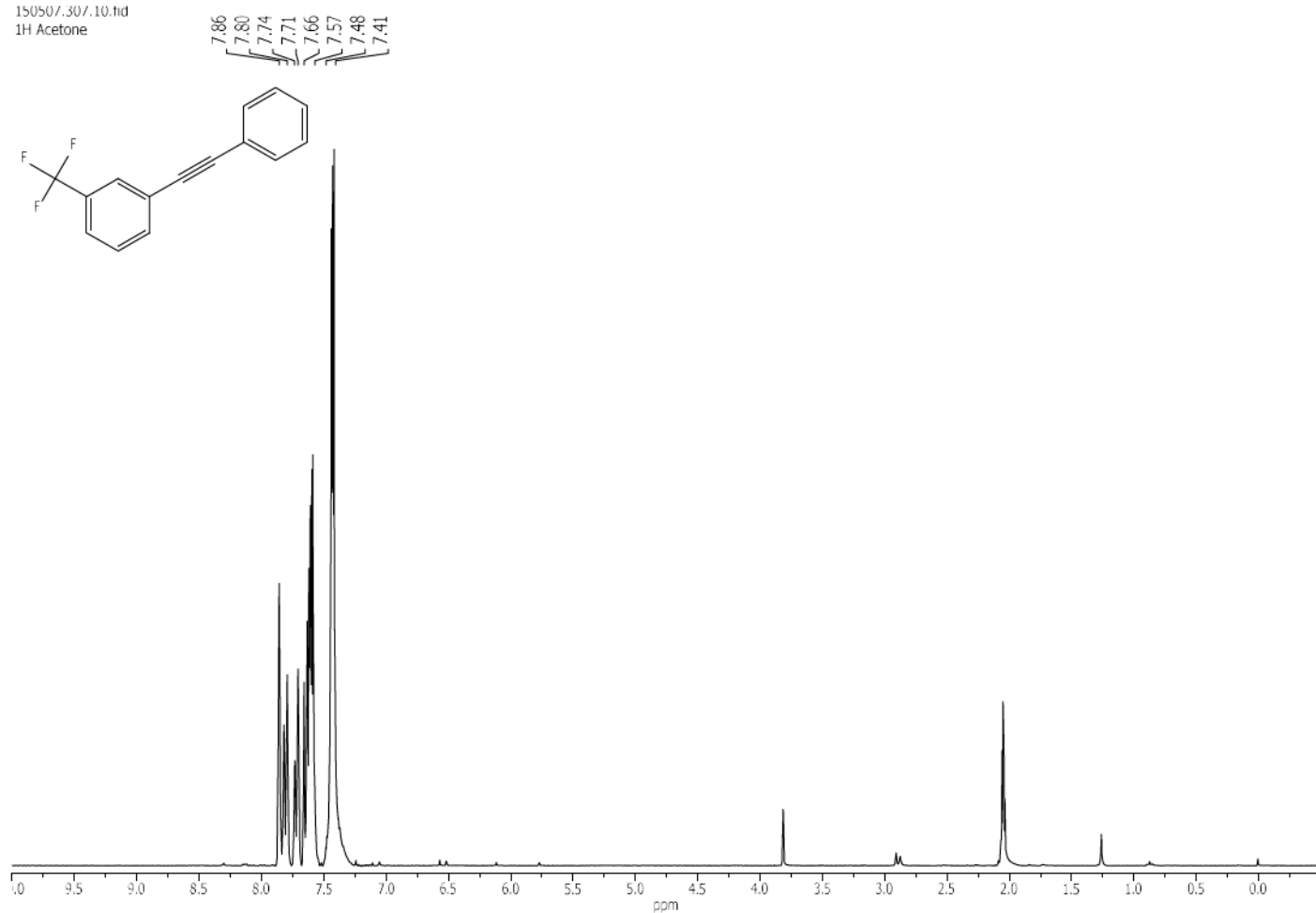
17/07/04.1342.10.fid
1H Acetone



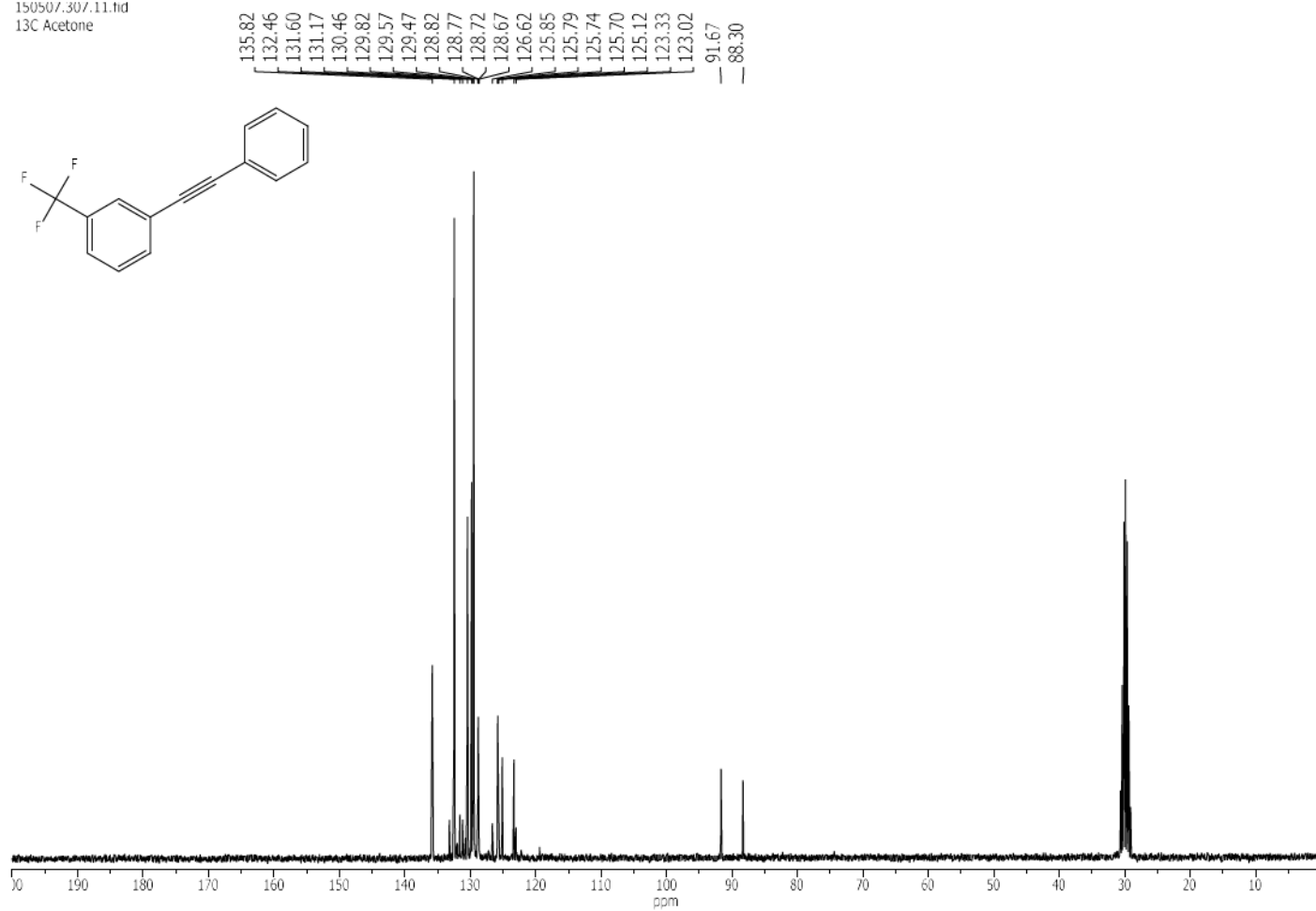
17/07/04.1342.11.fid
13C Acetone



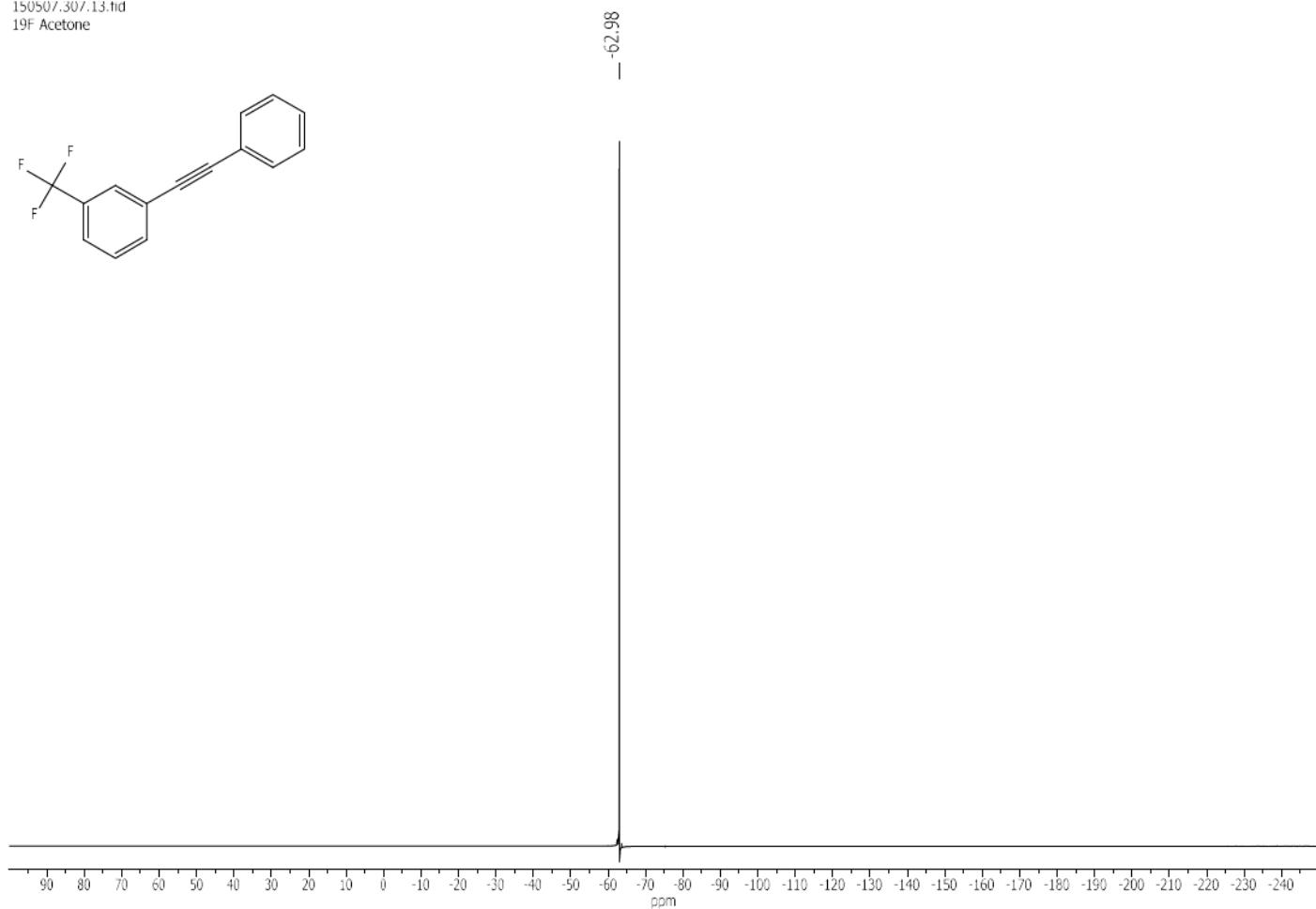
150507.307.10.tid
1H Acetone



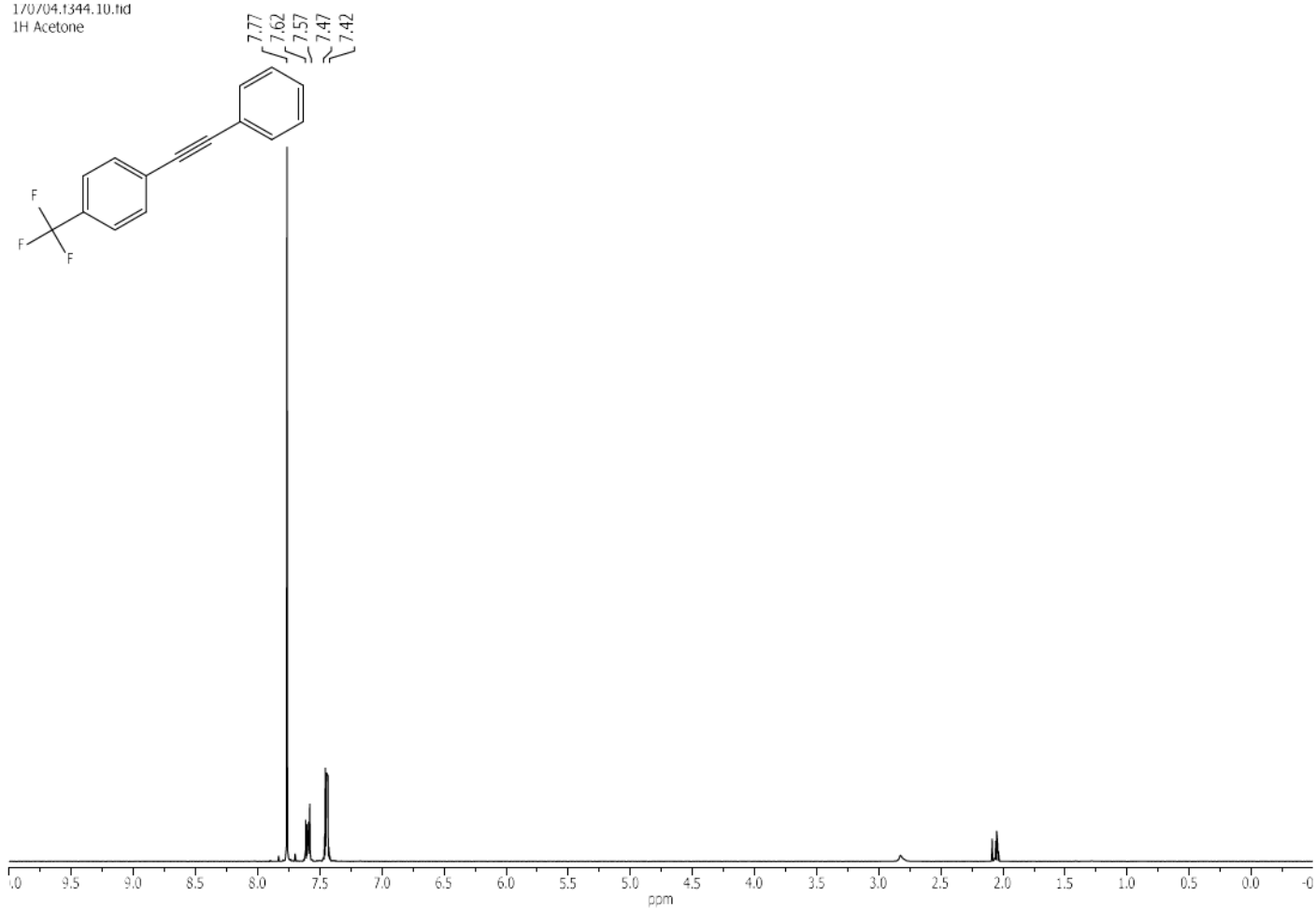
150507.307.11.tid
13C Acetone



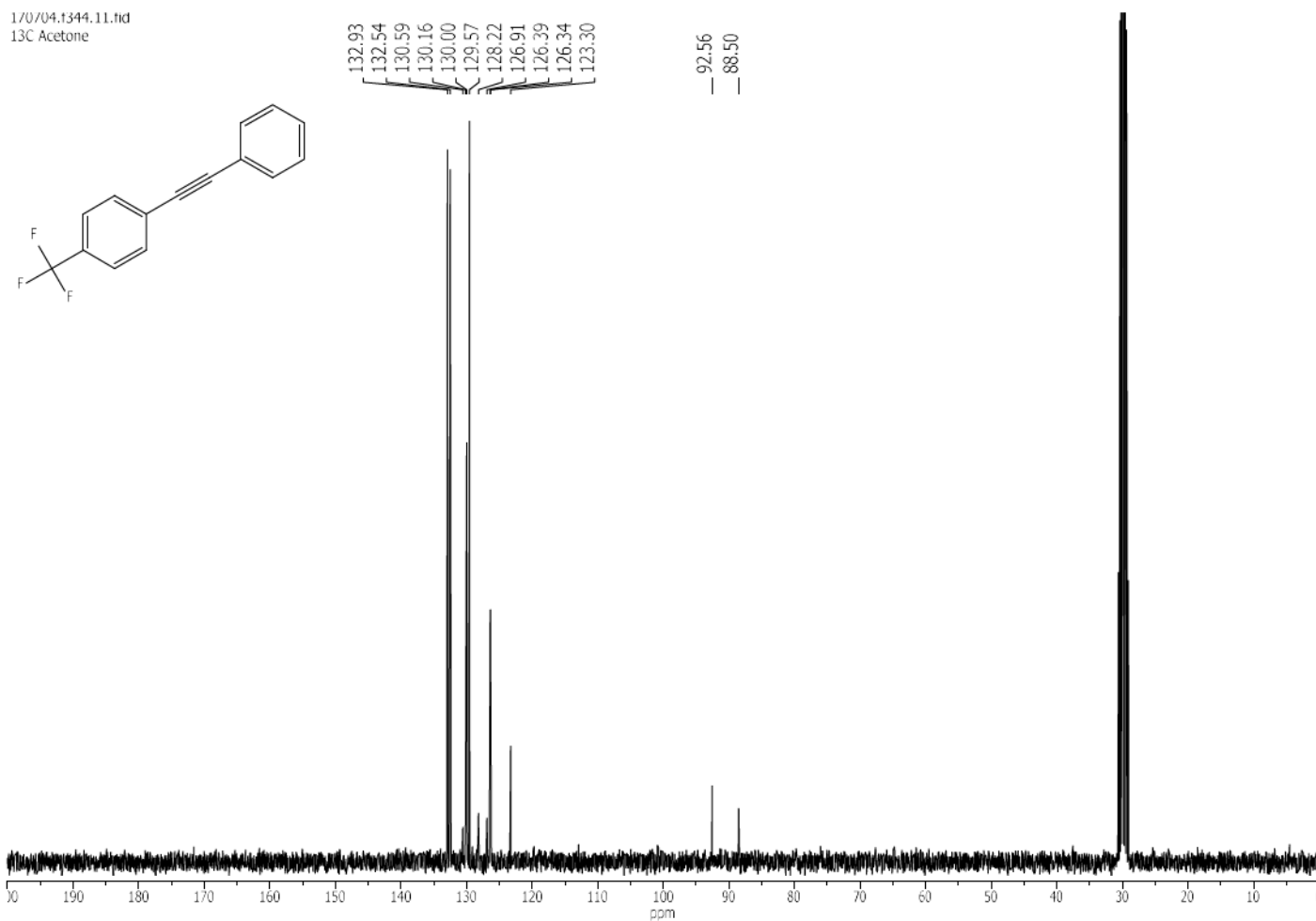
150507.307.13.fid
19F Acetone



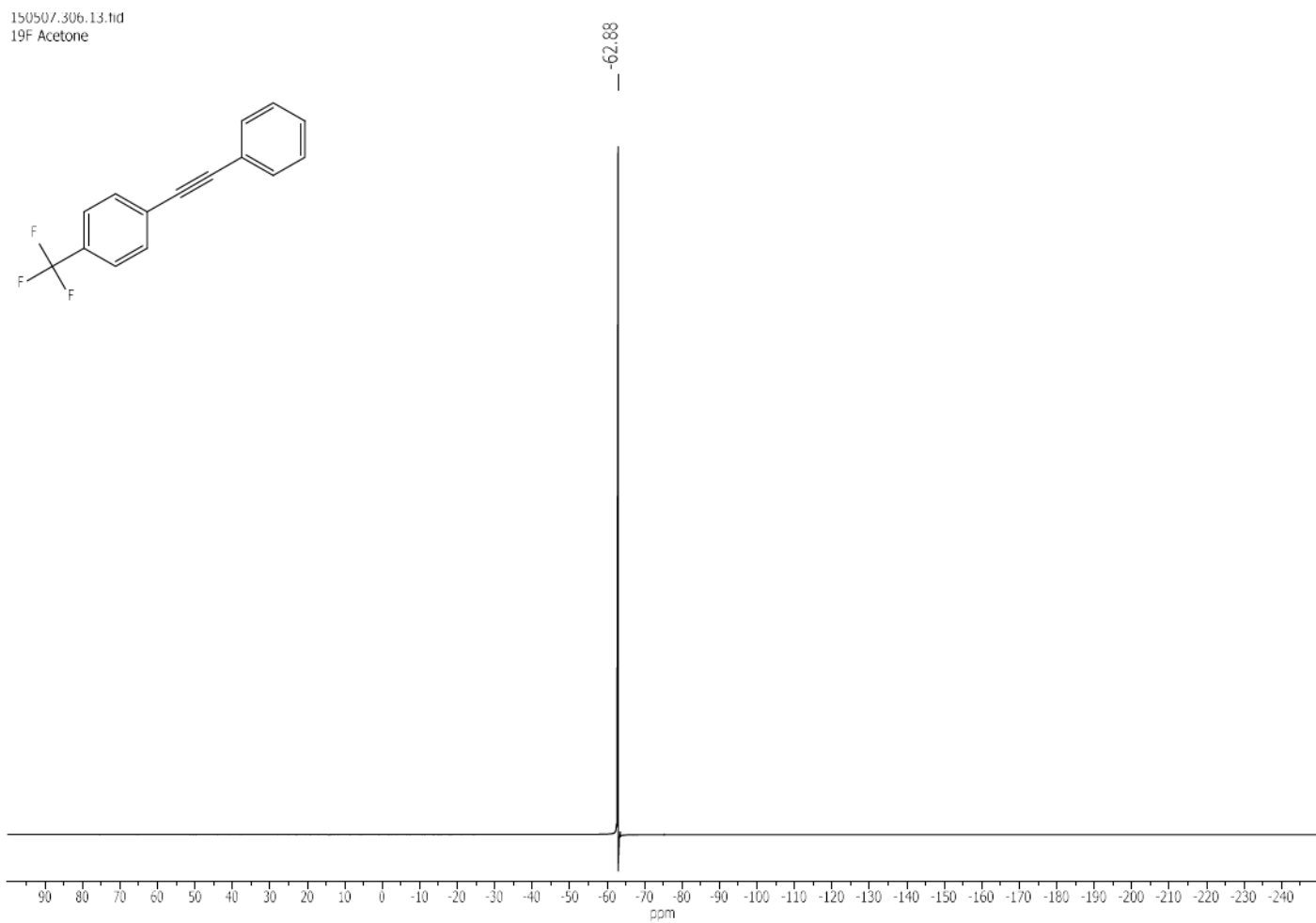
170704.1344.10.fid
1H Acetone



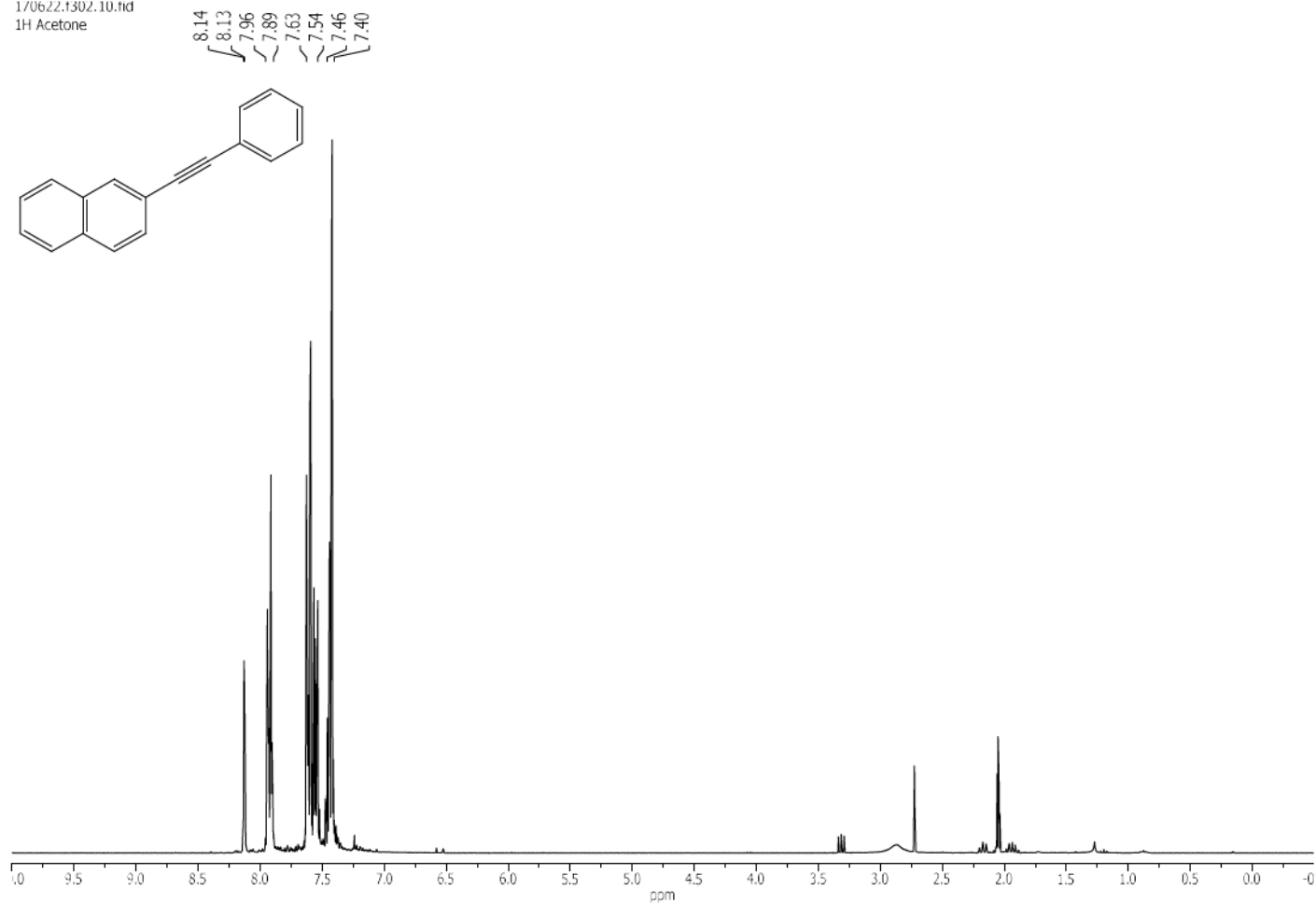
170704.1344.11.tid
13C Acetone



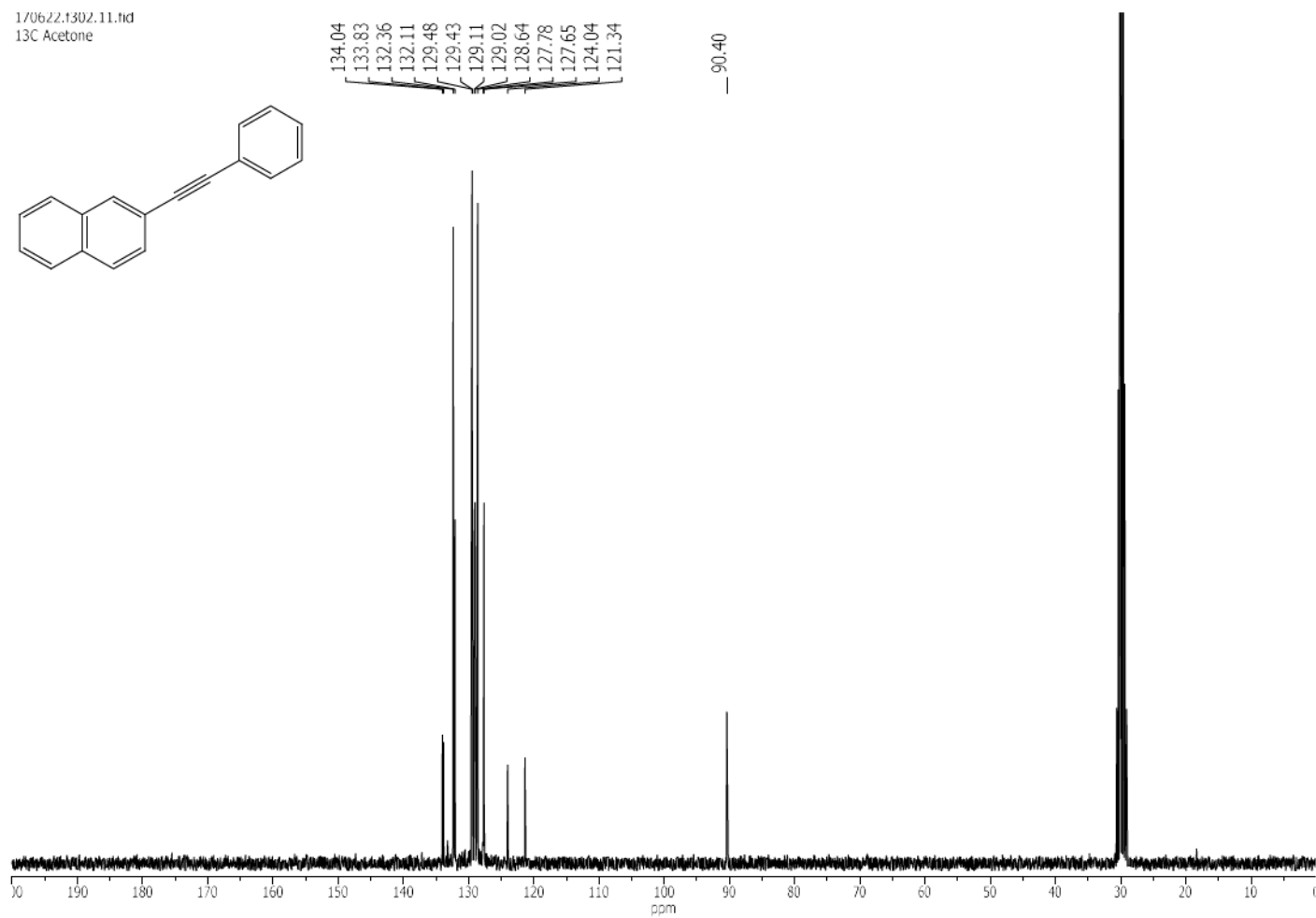
150507.306.13.tid
19F Acetone



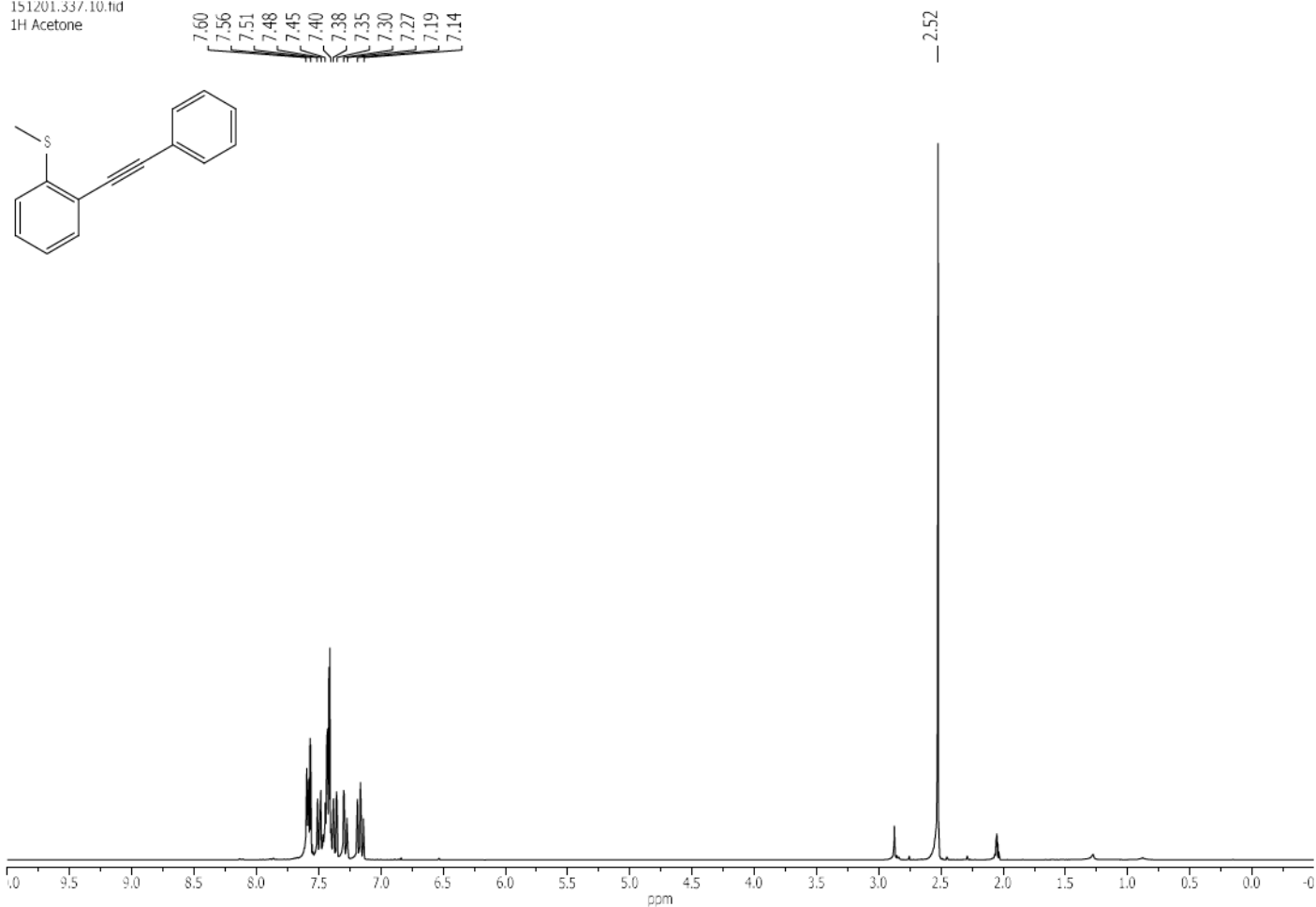
170622.1302.10.fid
1H Acetone



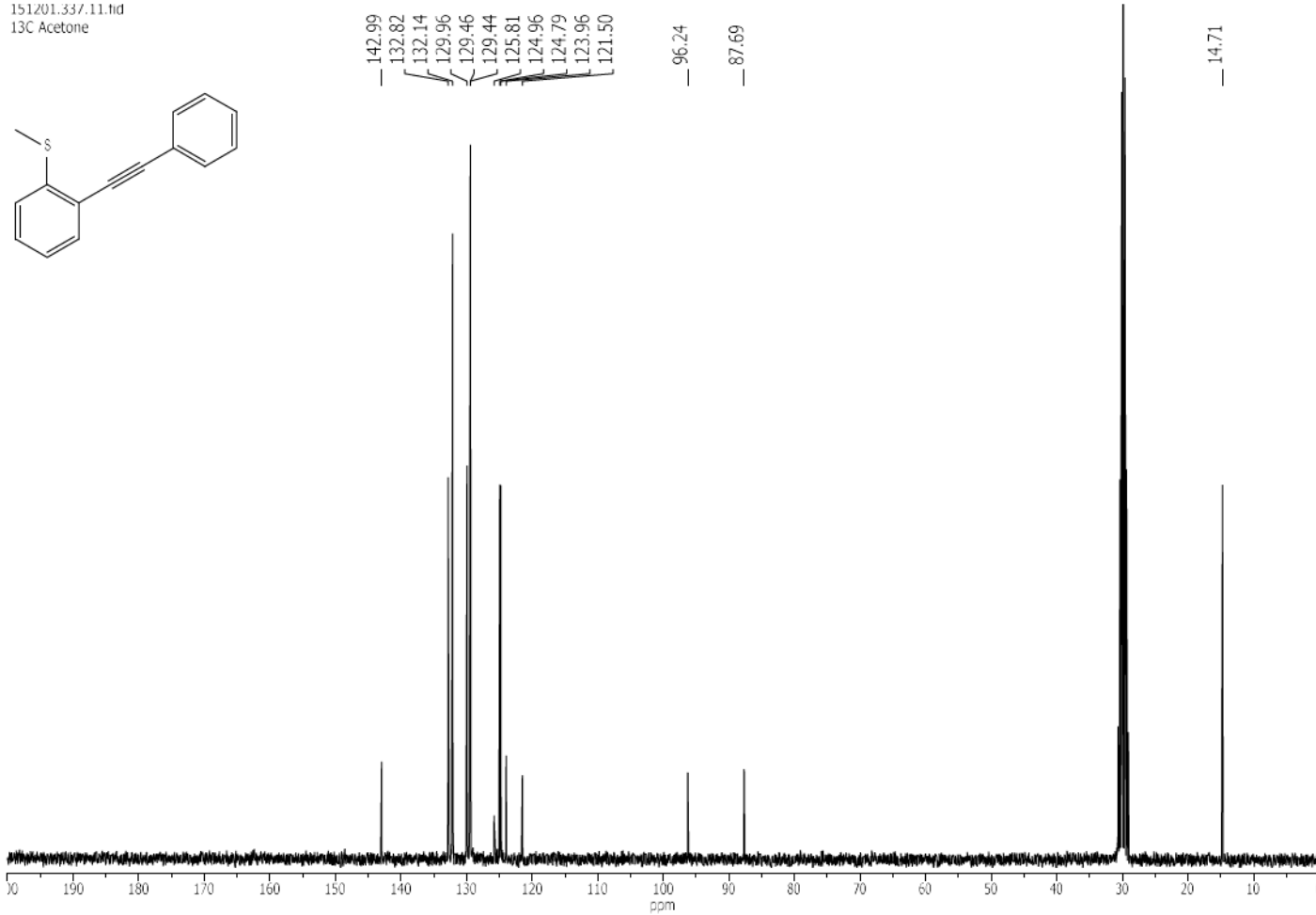
170622.1302.11.fid
13C Acetone



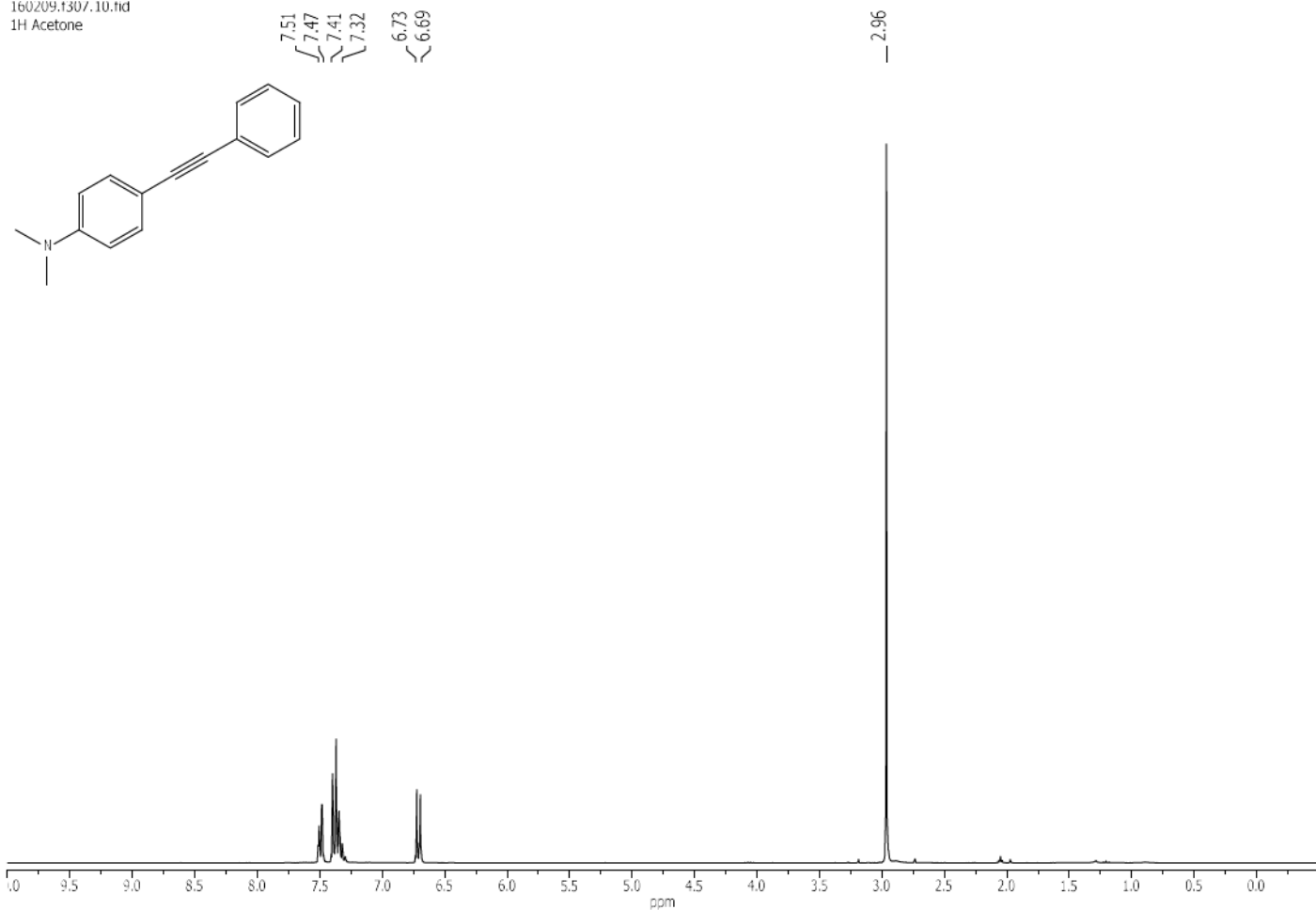
151201.337.10.tid
1H Acetone



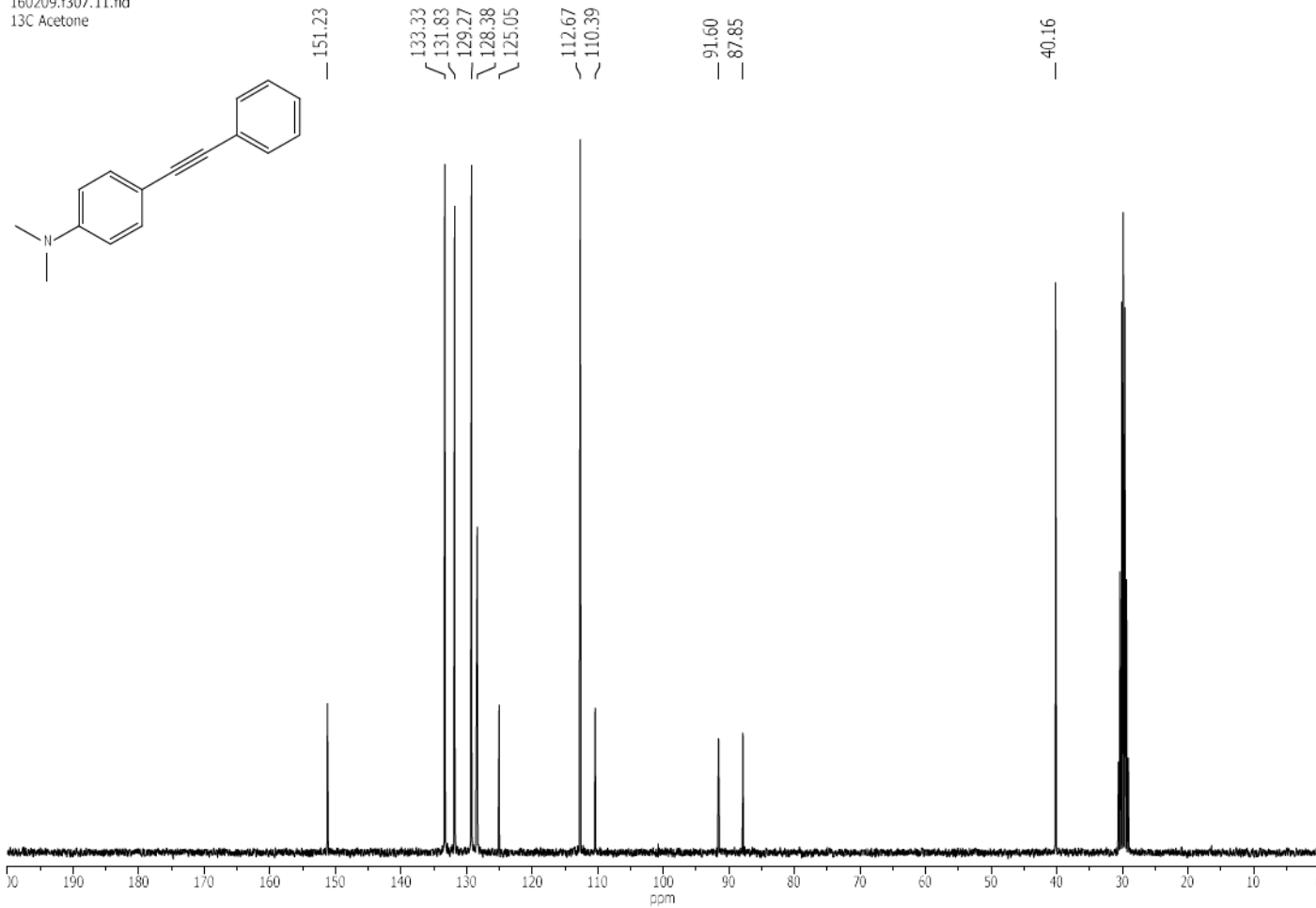
151201.337.11.tid
13C Acetone



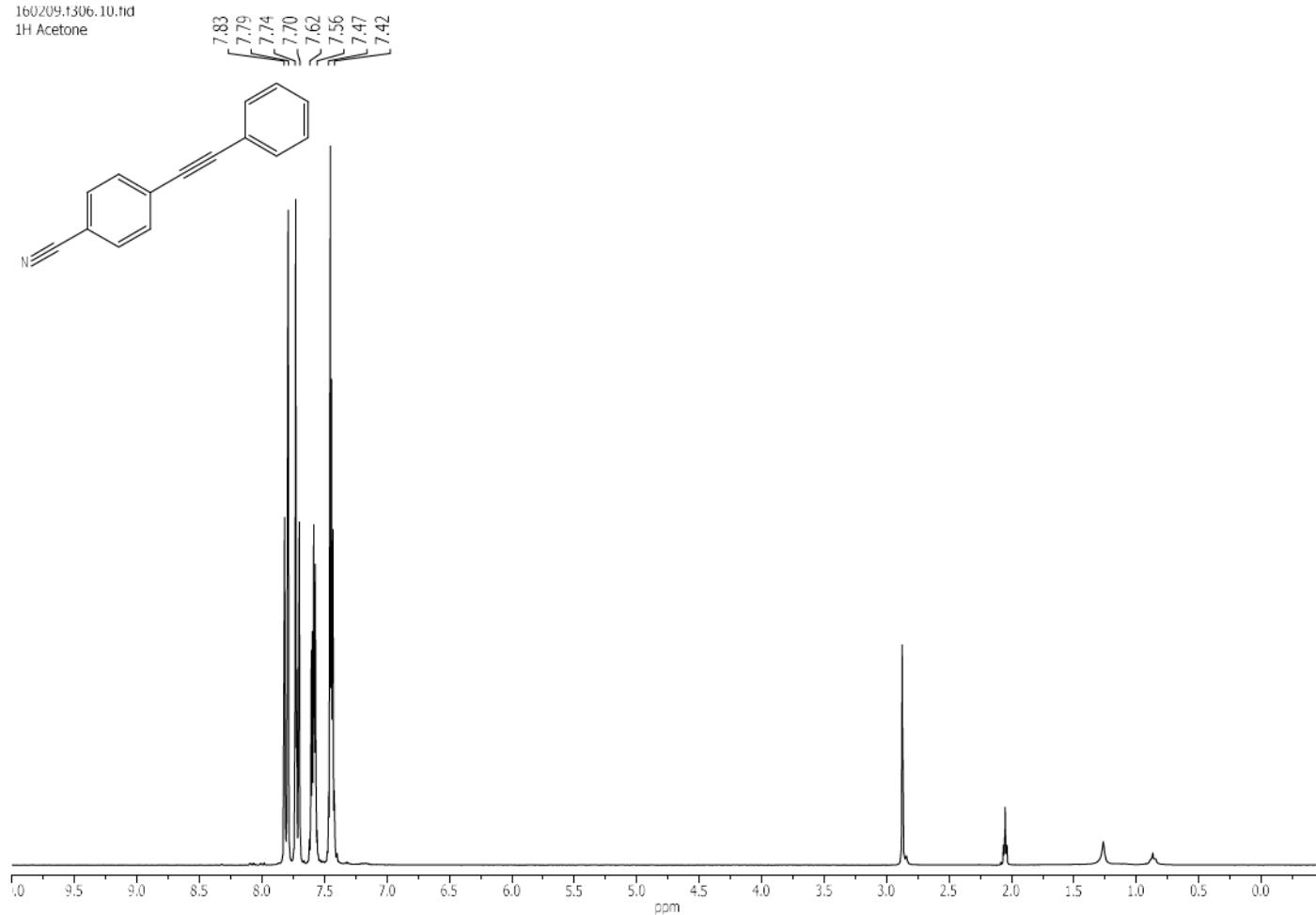
160209.1307.10.fid
1H Acetone



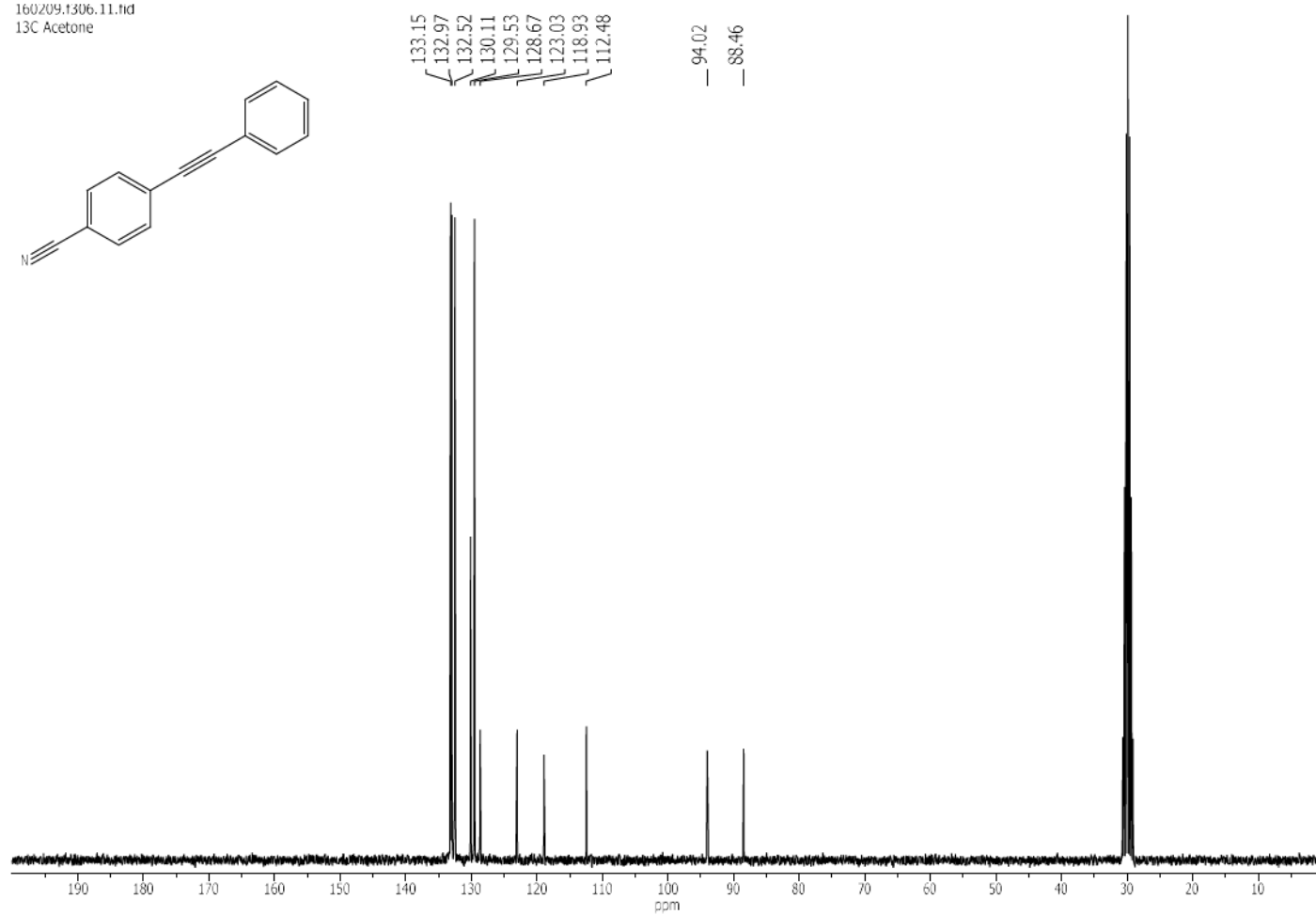
160209.1307.11.fid
13C Acetone



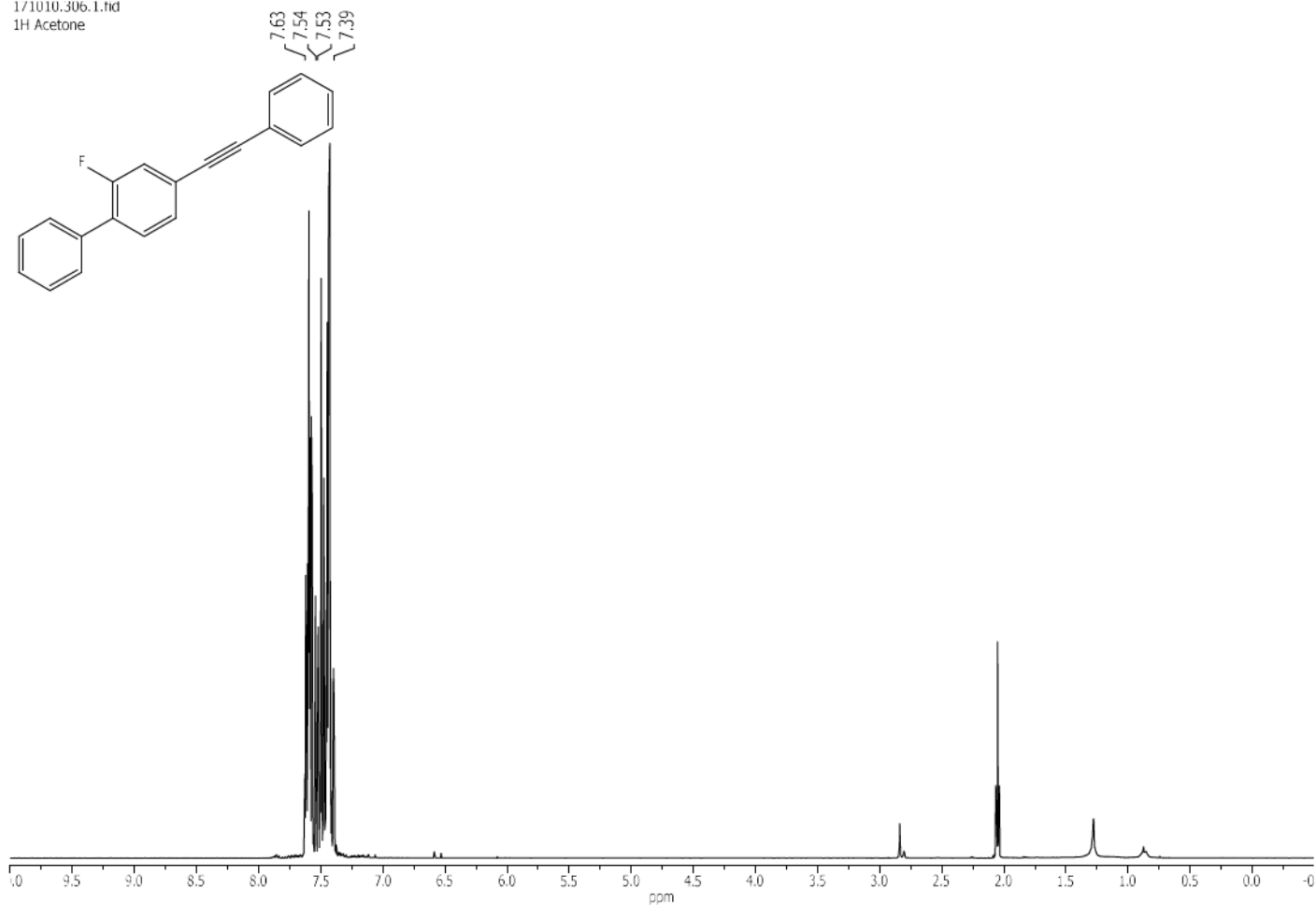
160209.1306.10.fid
1H Acetone



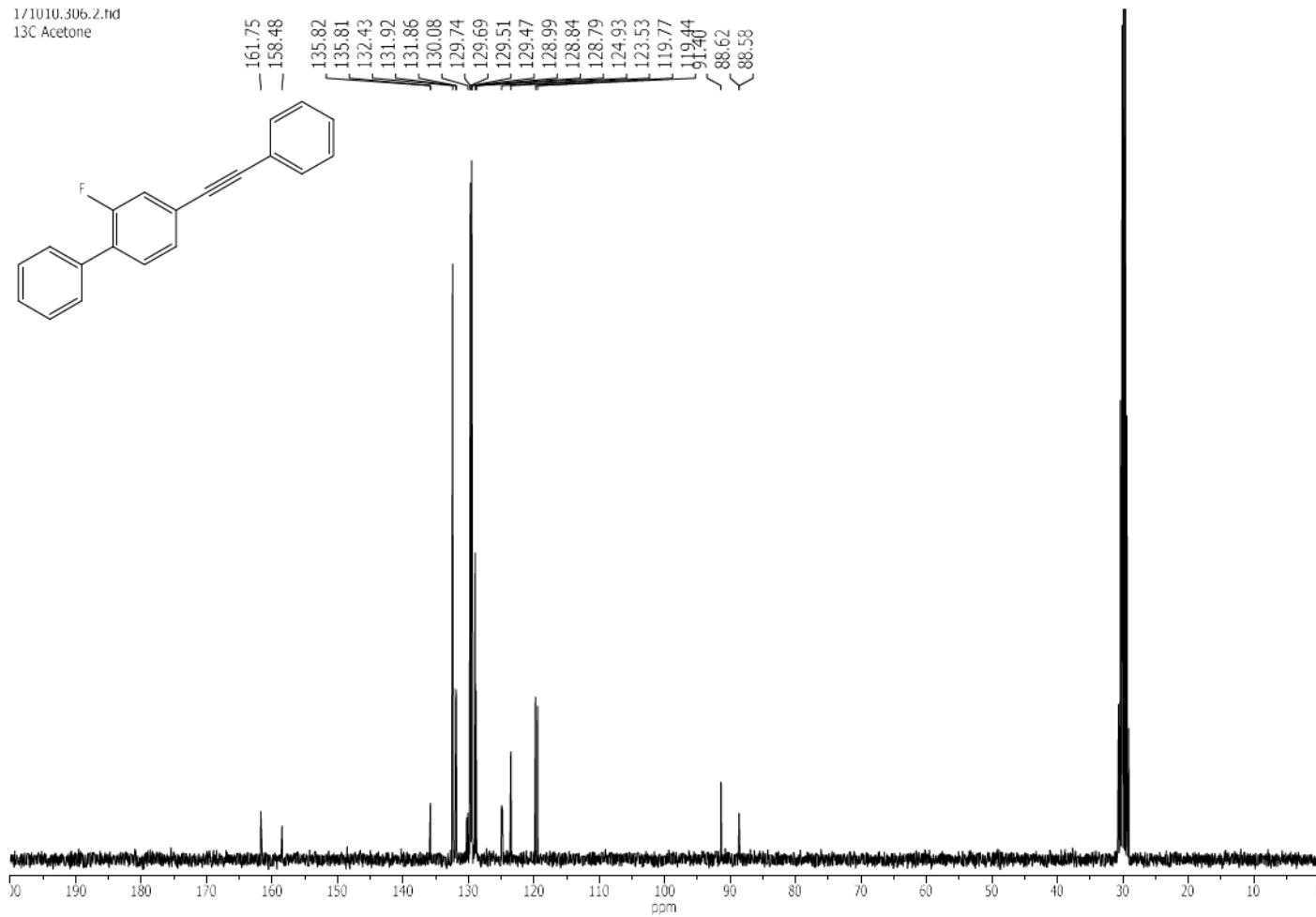
160209.1306.11.fid
13C Acetone



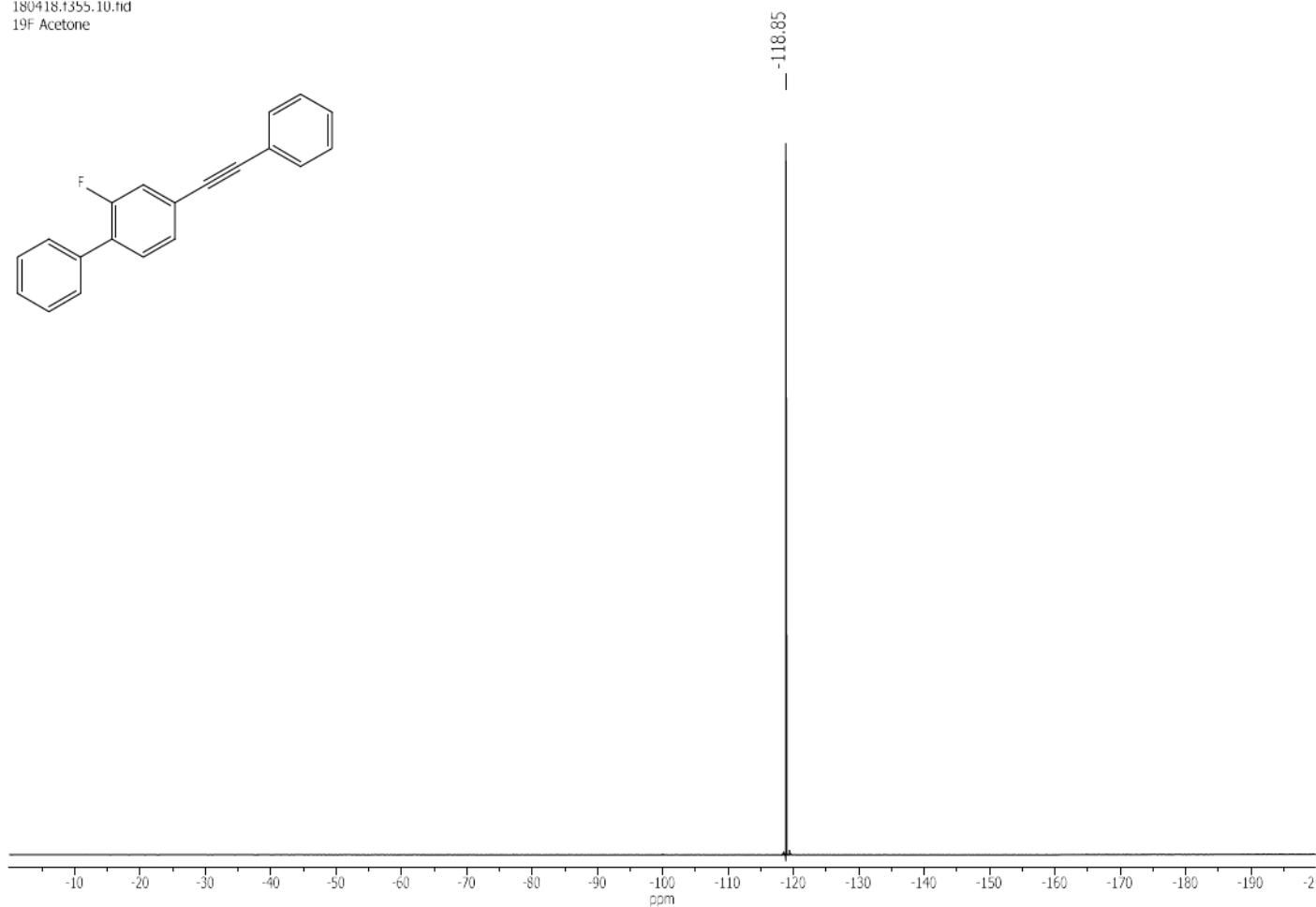
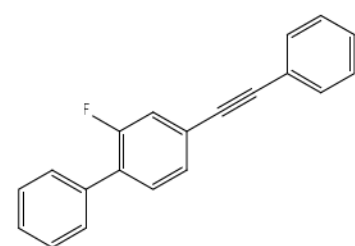
1/1010.306.1.fid
1H Acetone



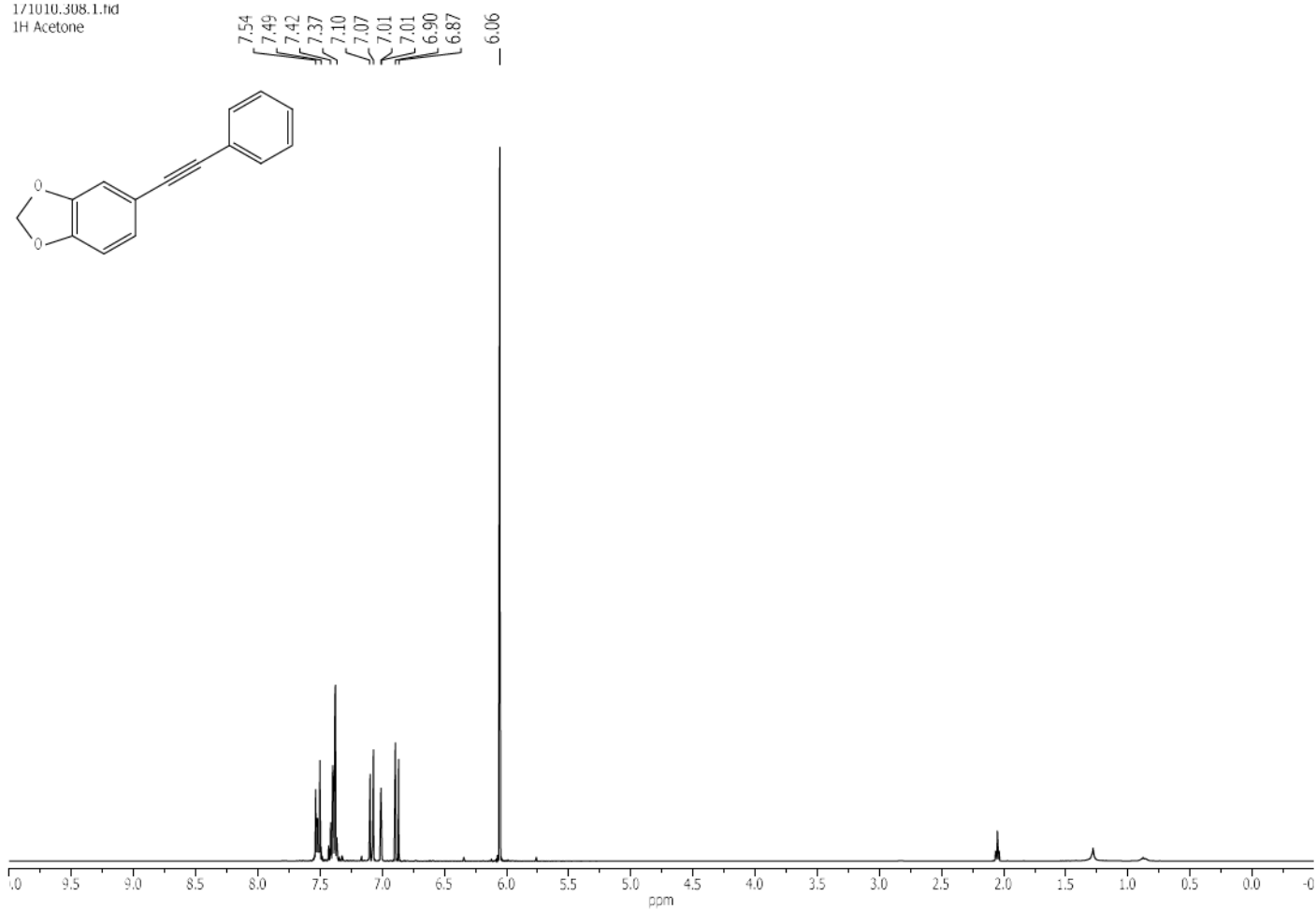
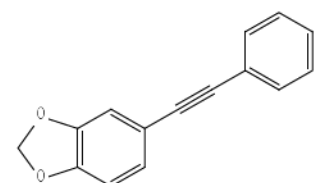
1/1010.306.2.fid
13C Acetone



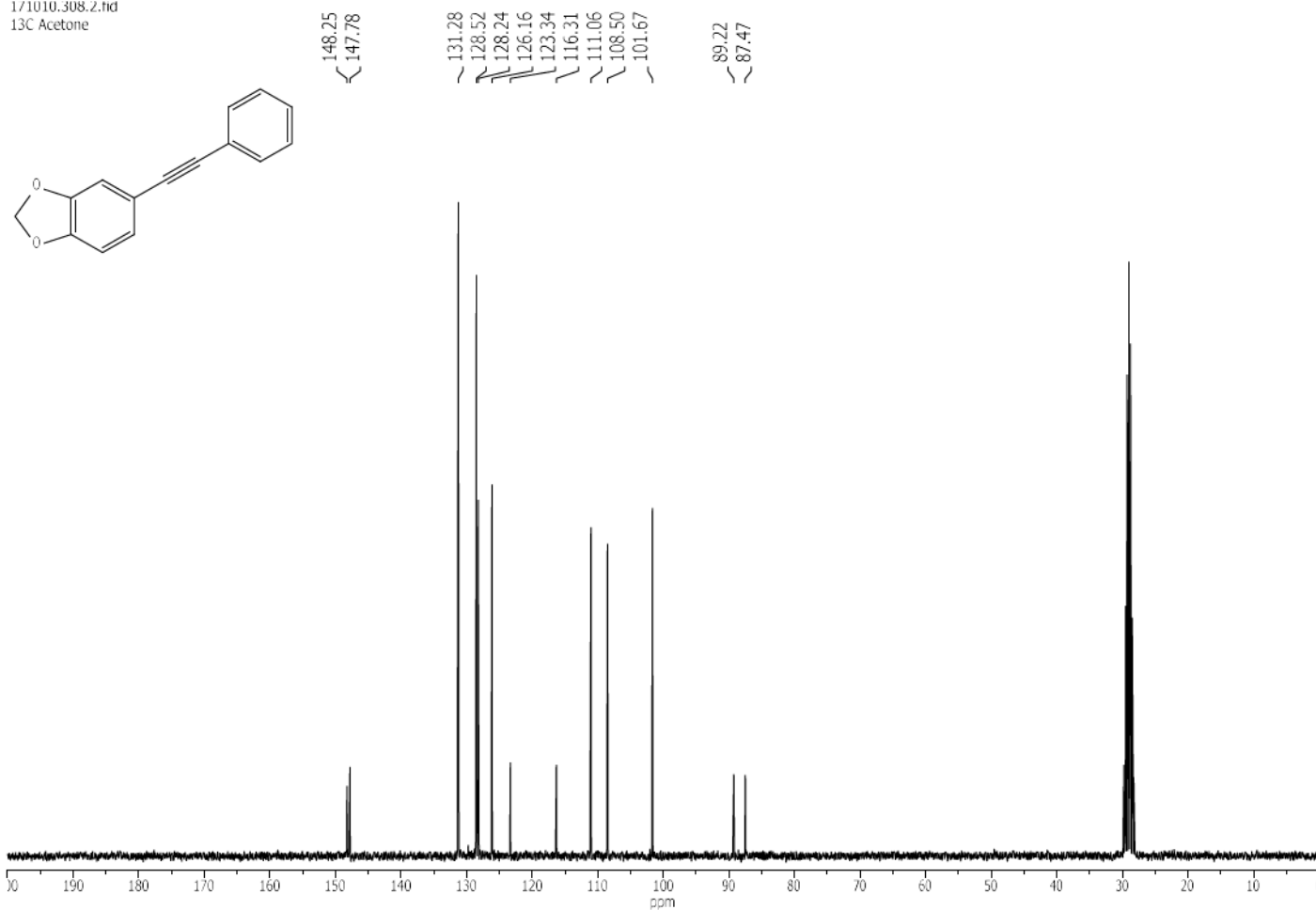
180418.1355.10.fid
19F Acetone



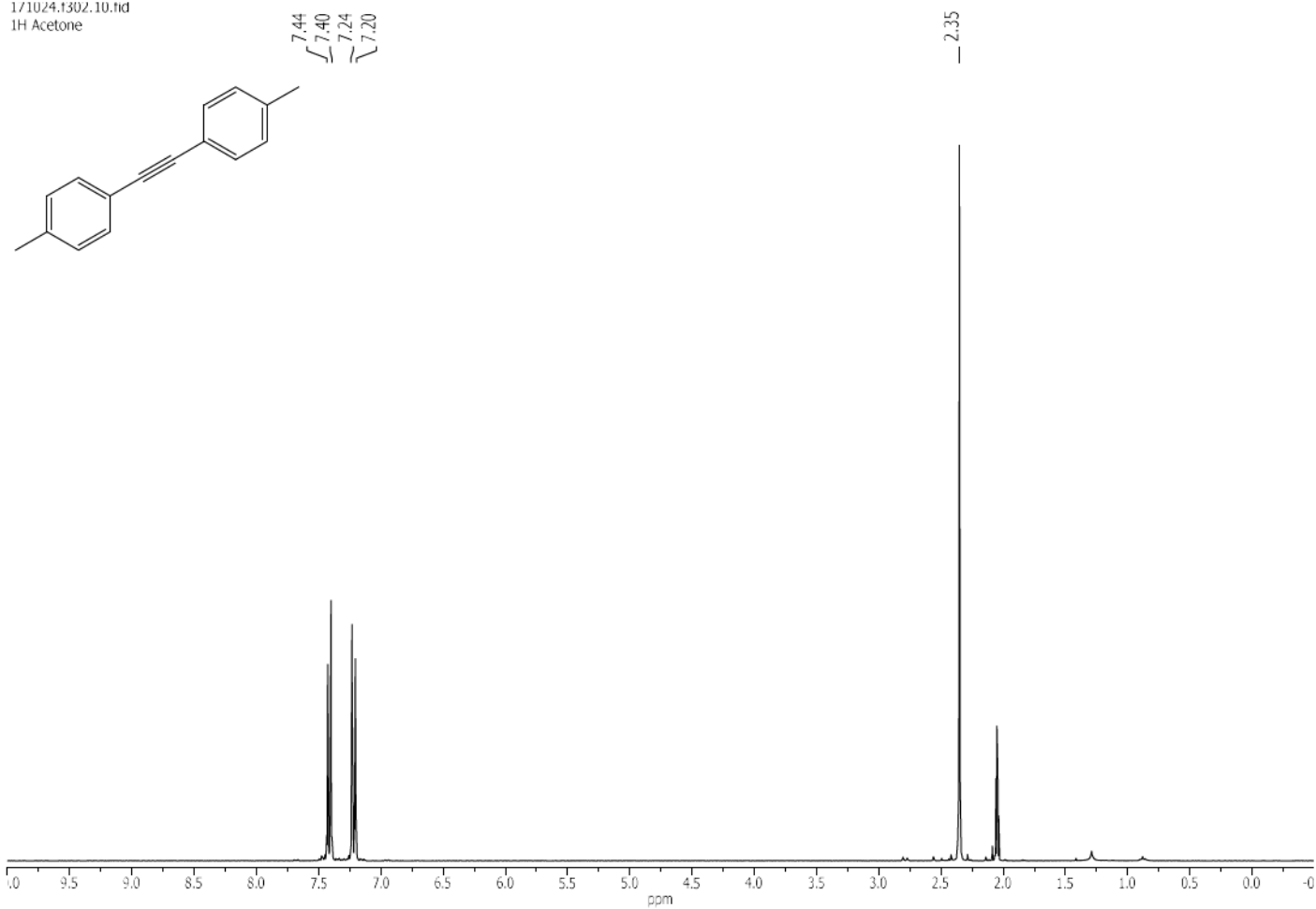
171010.308.1.fid
1H Acetone



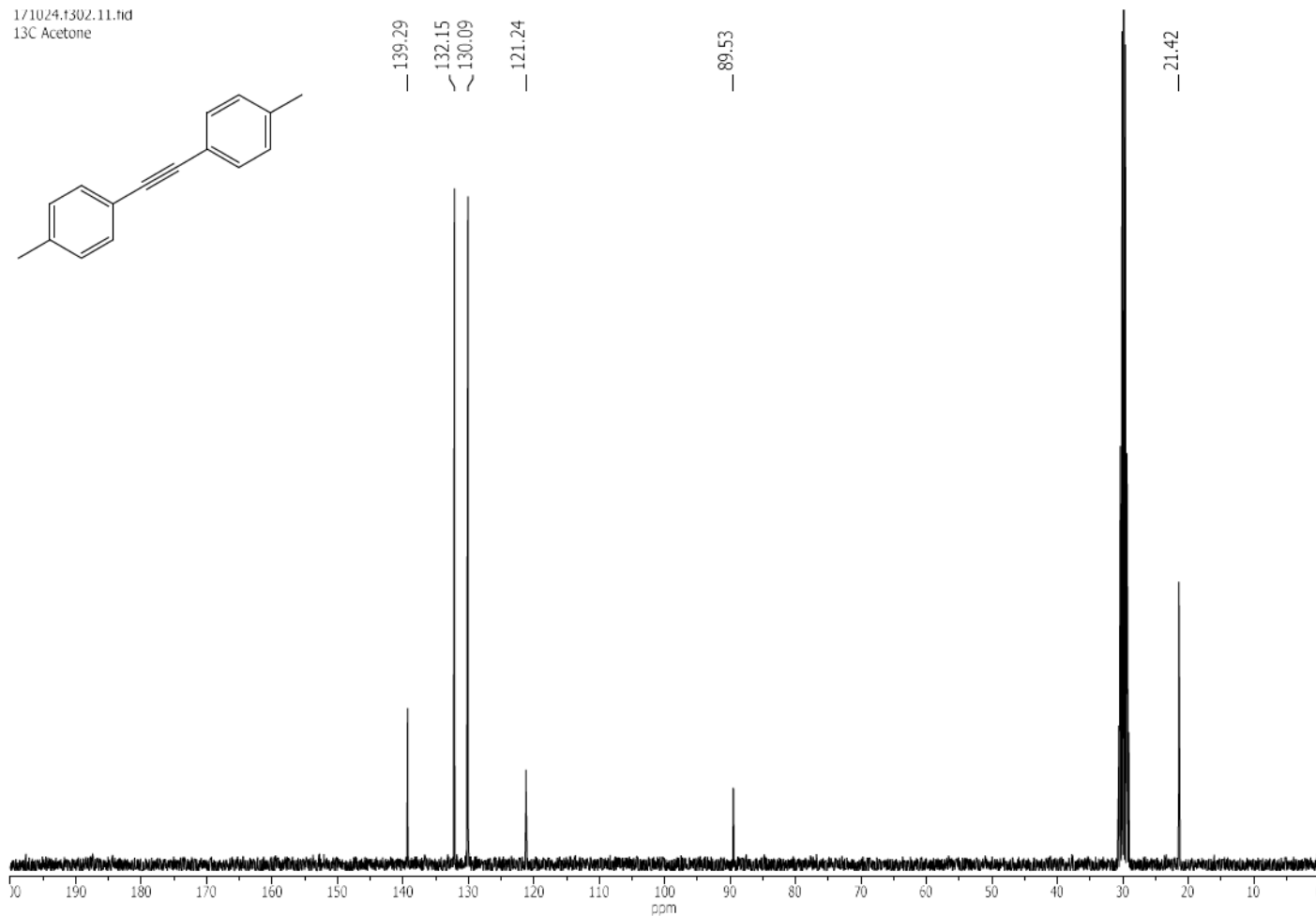
171010.308.2.fid
13C Acetone



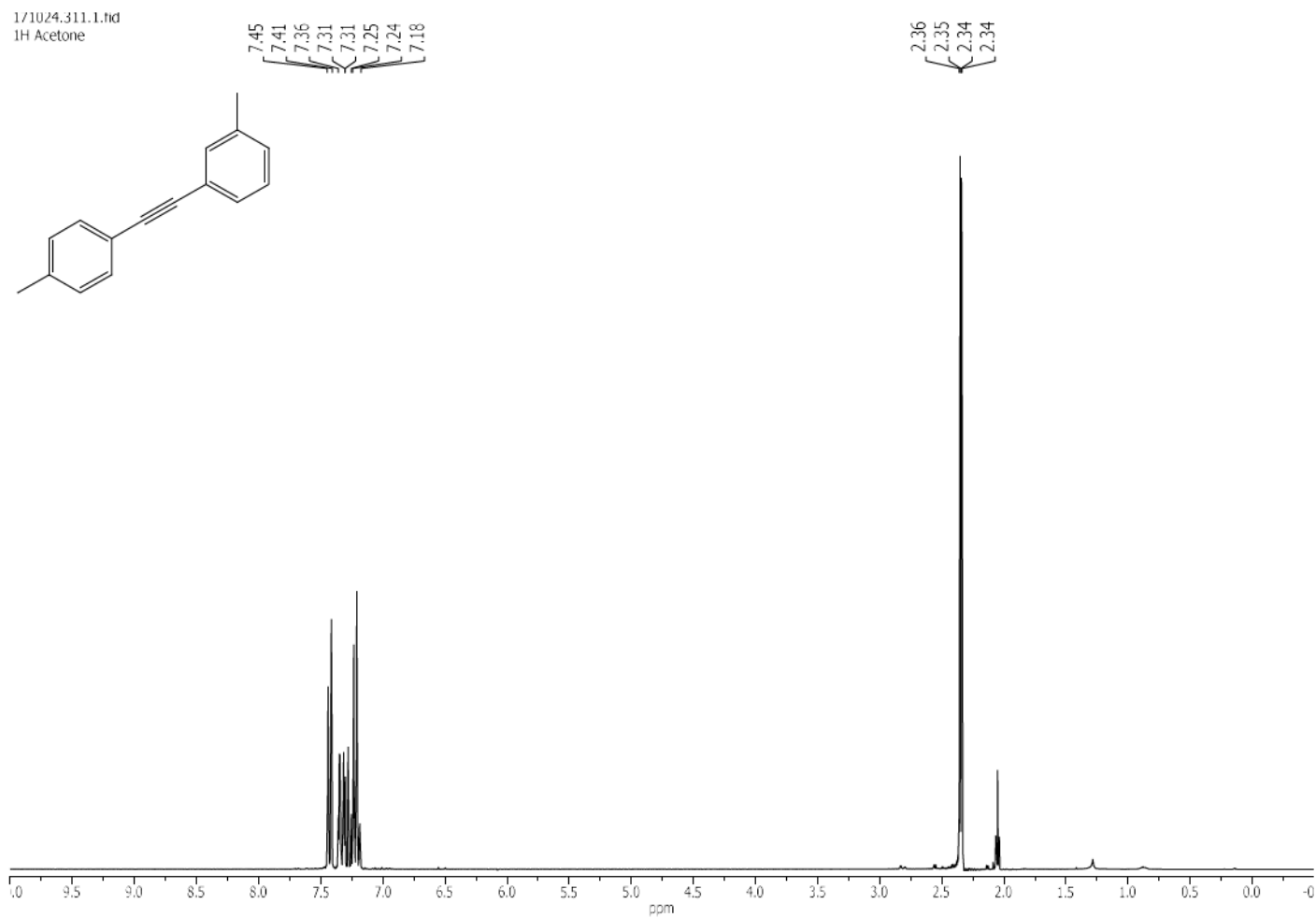
171024.1302.10.fid
1H Acetone



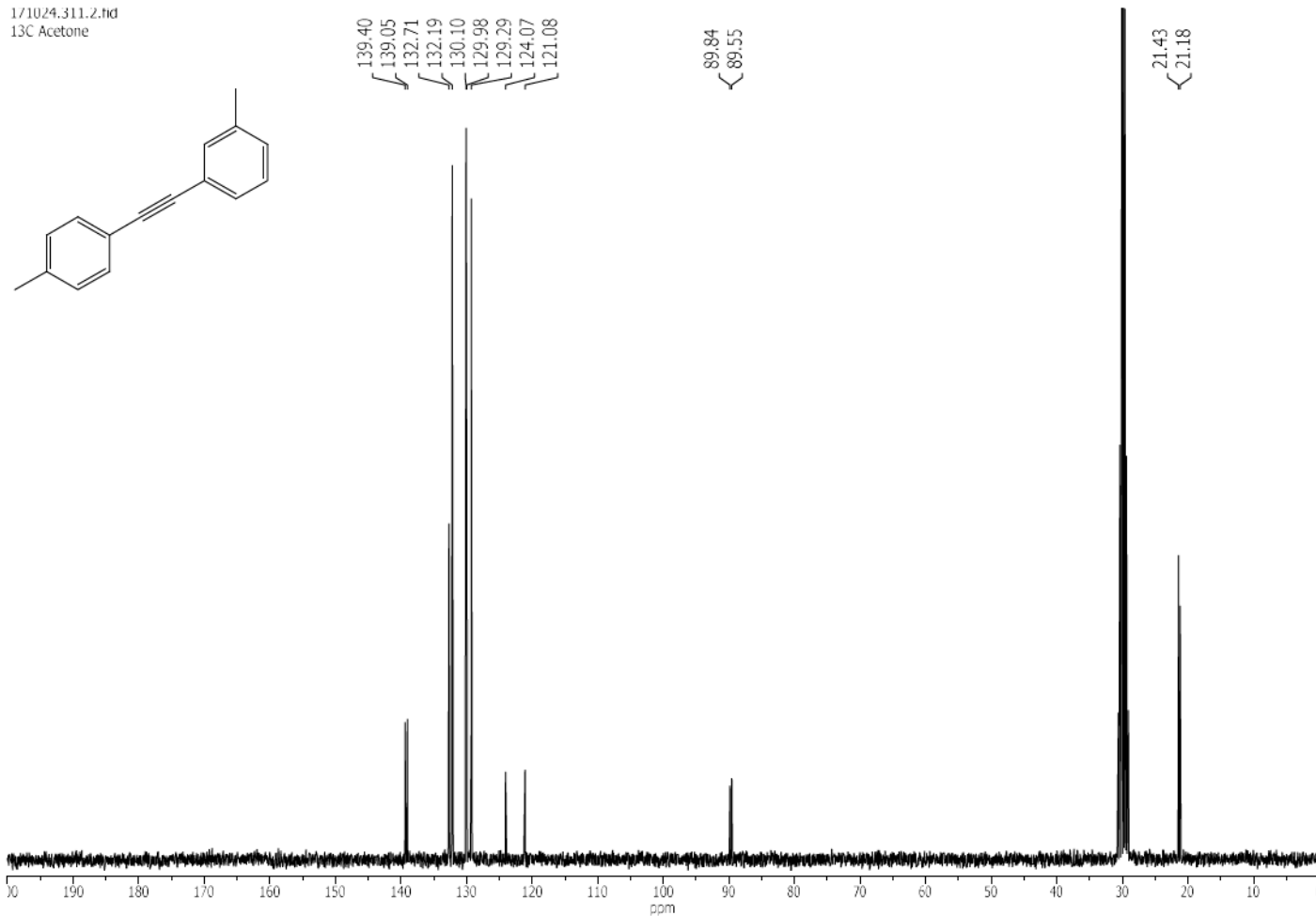
1/10/24.1302.11.fid
13C Acetone



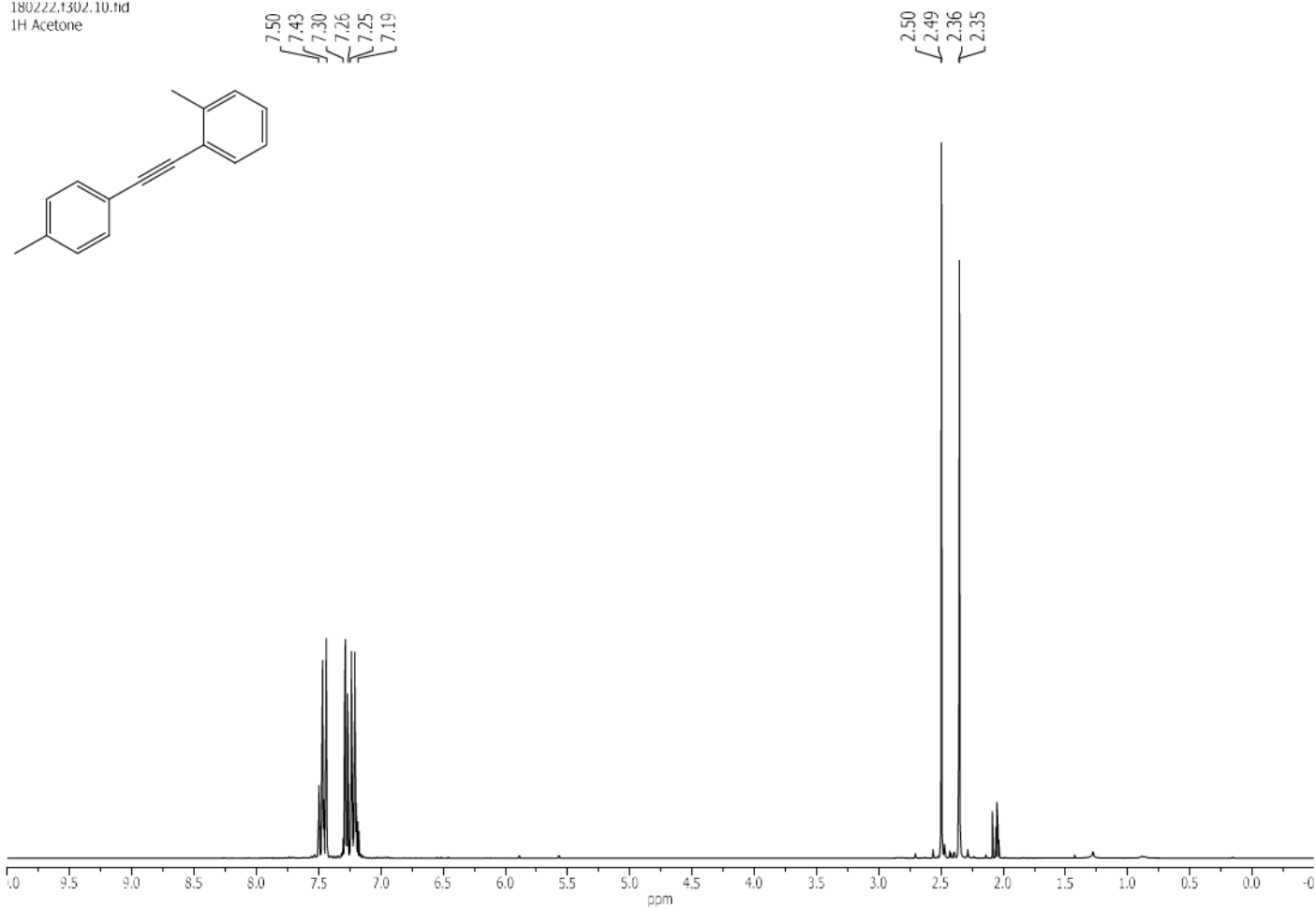
1/10/24.311.1.fid
1H Acetone



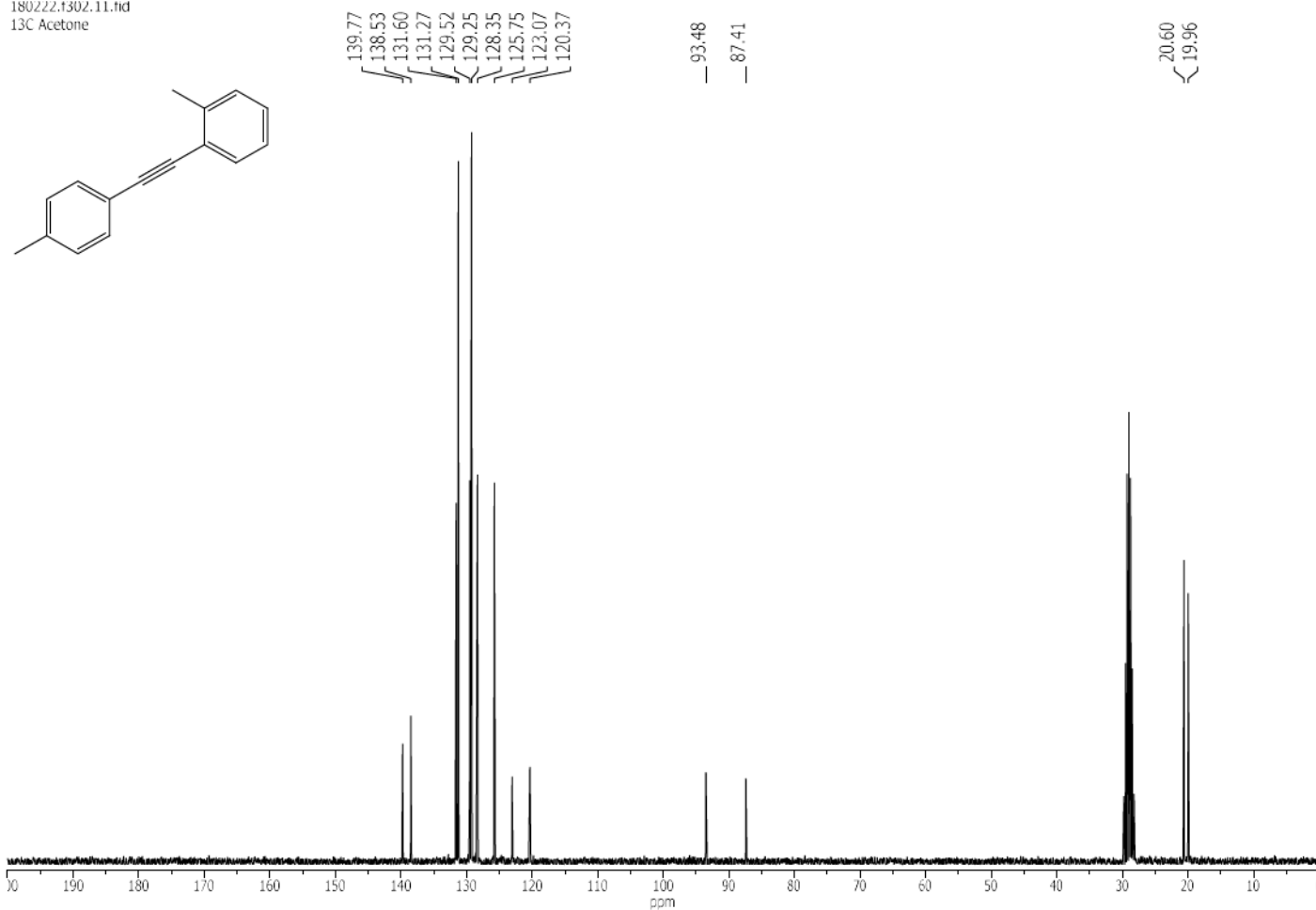
171024.311.2.fid
13C Acetone



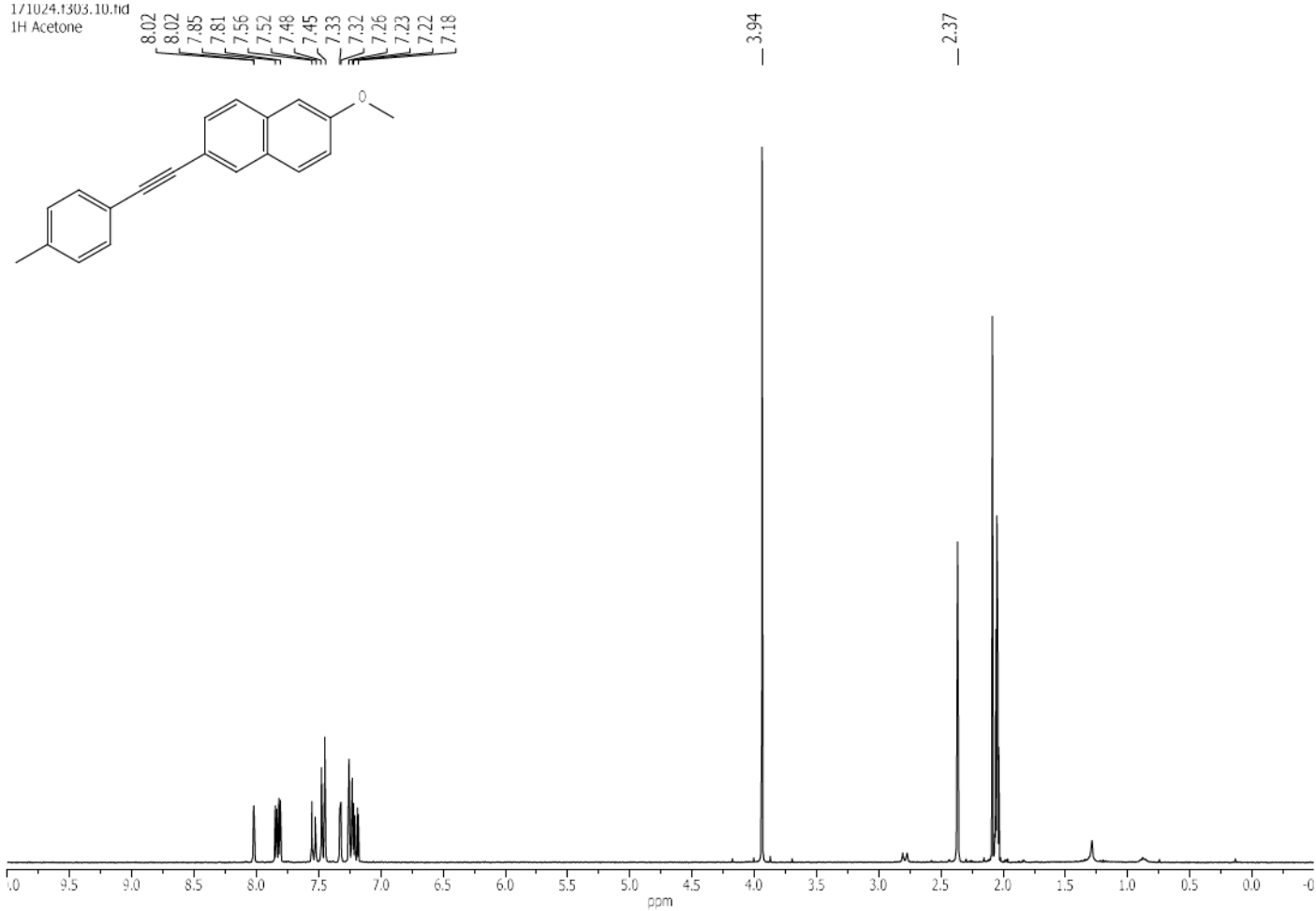
180222.1302.10.fid
1H Acetone



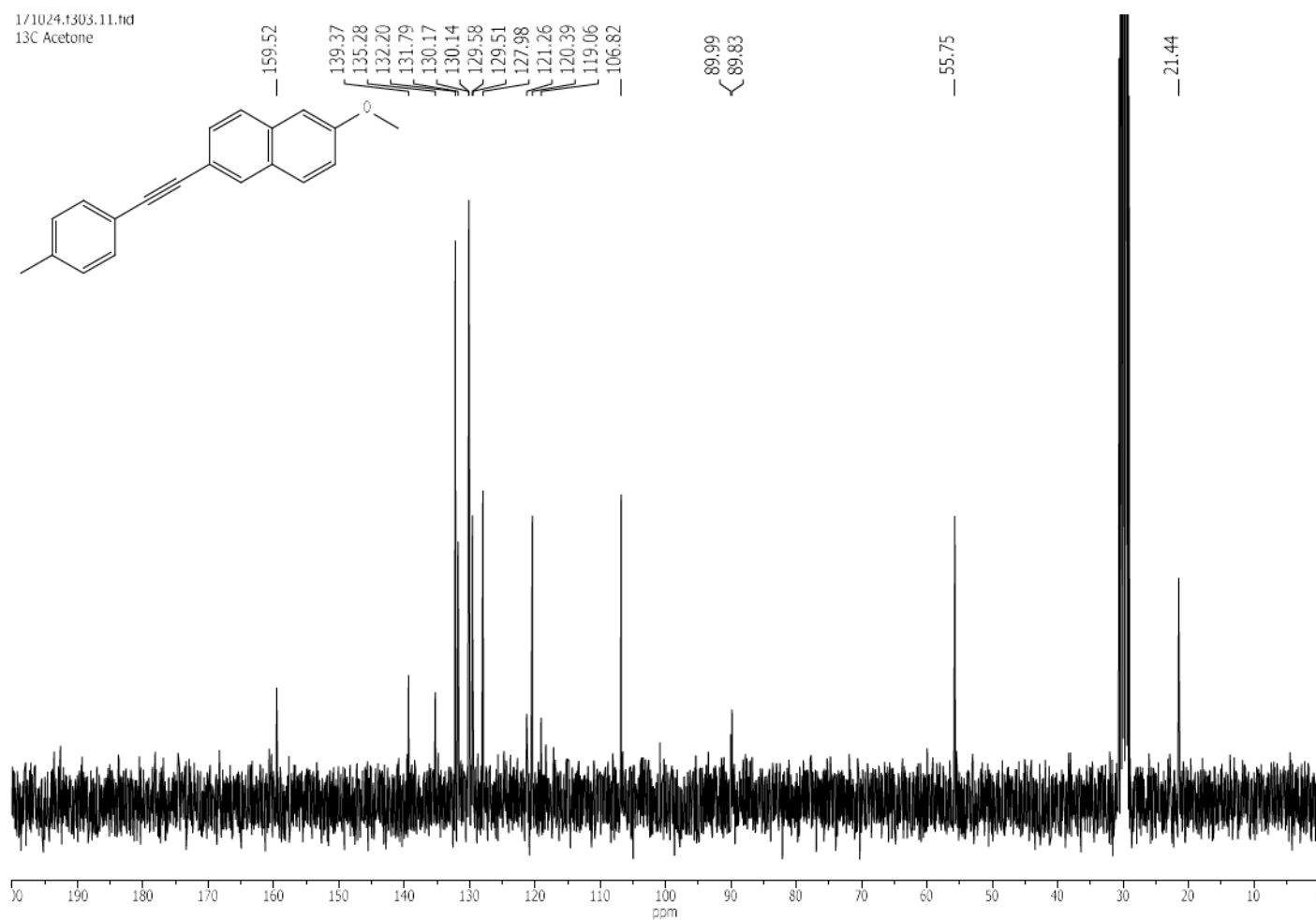
180222.1302.11.fid
13C Acetone



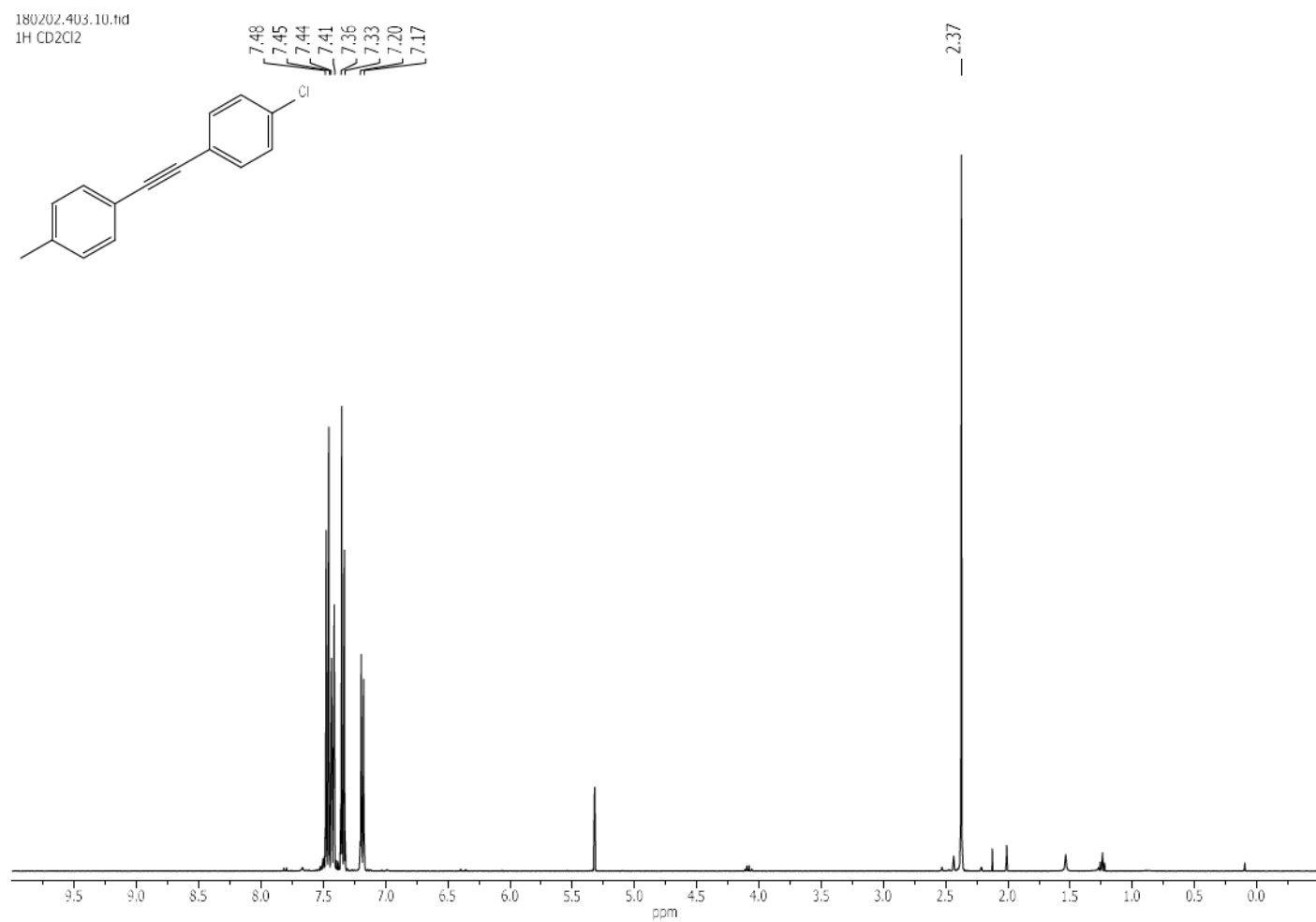
171024.1303.10.fid
1H Acetone



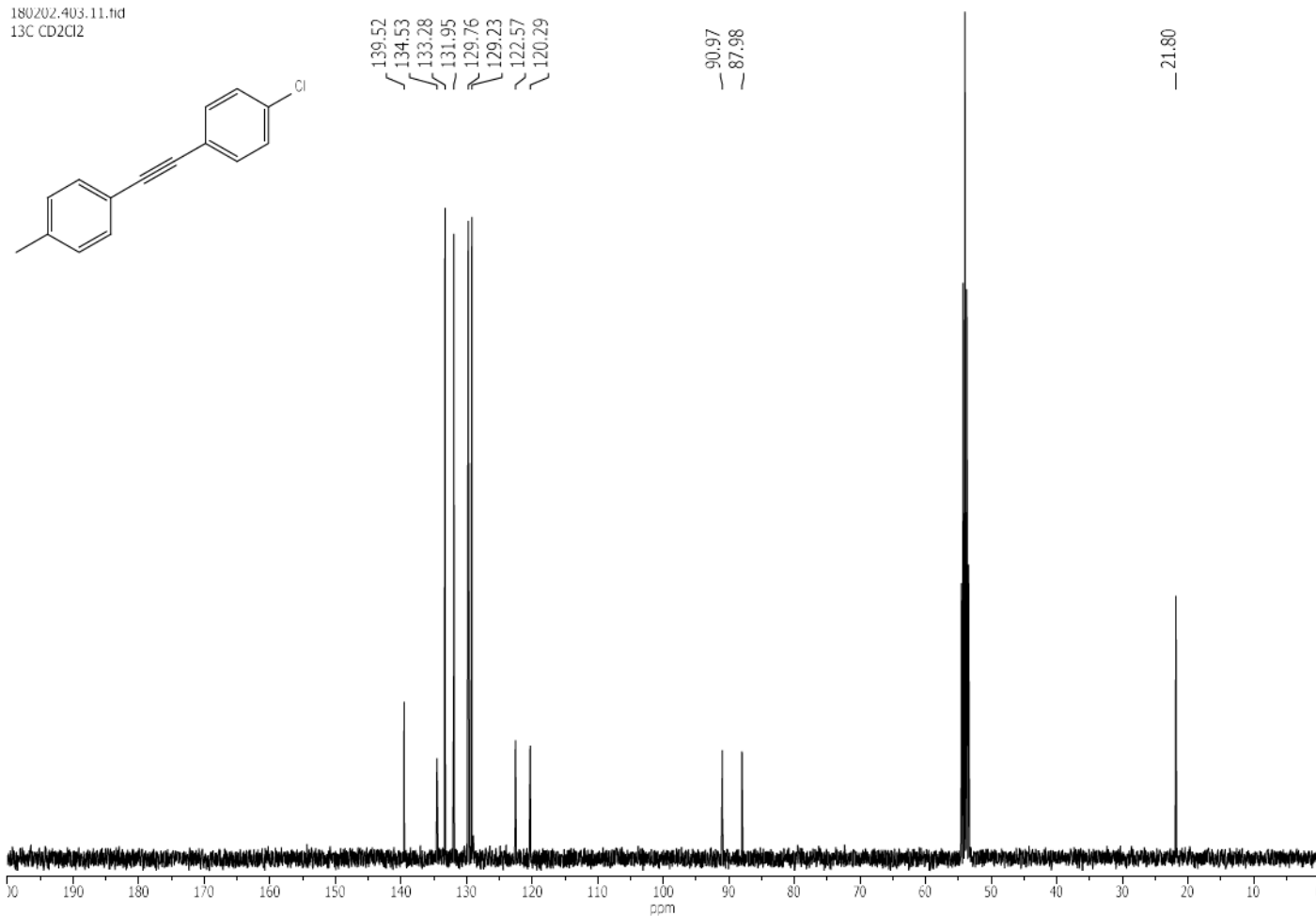
171024.1303.11.tid
13C Acetone



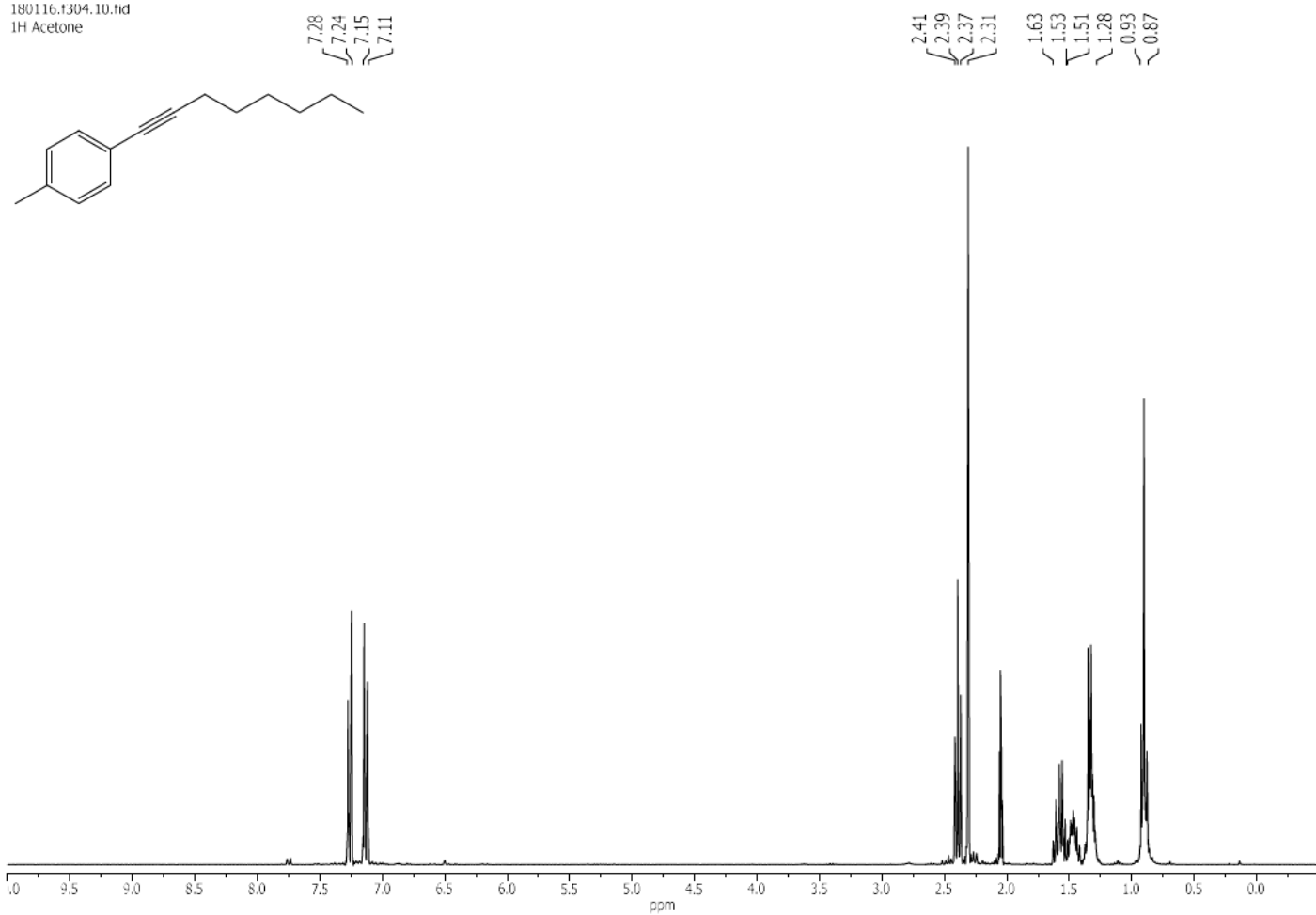
180202.403.10.tid
1H CD2Cl2



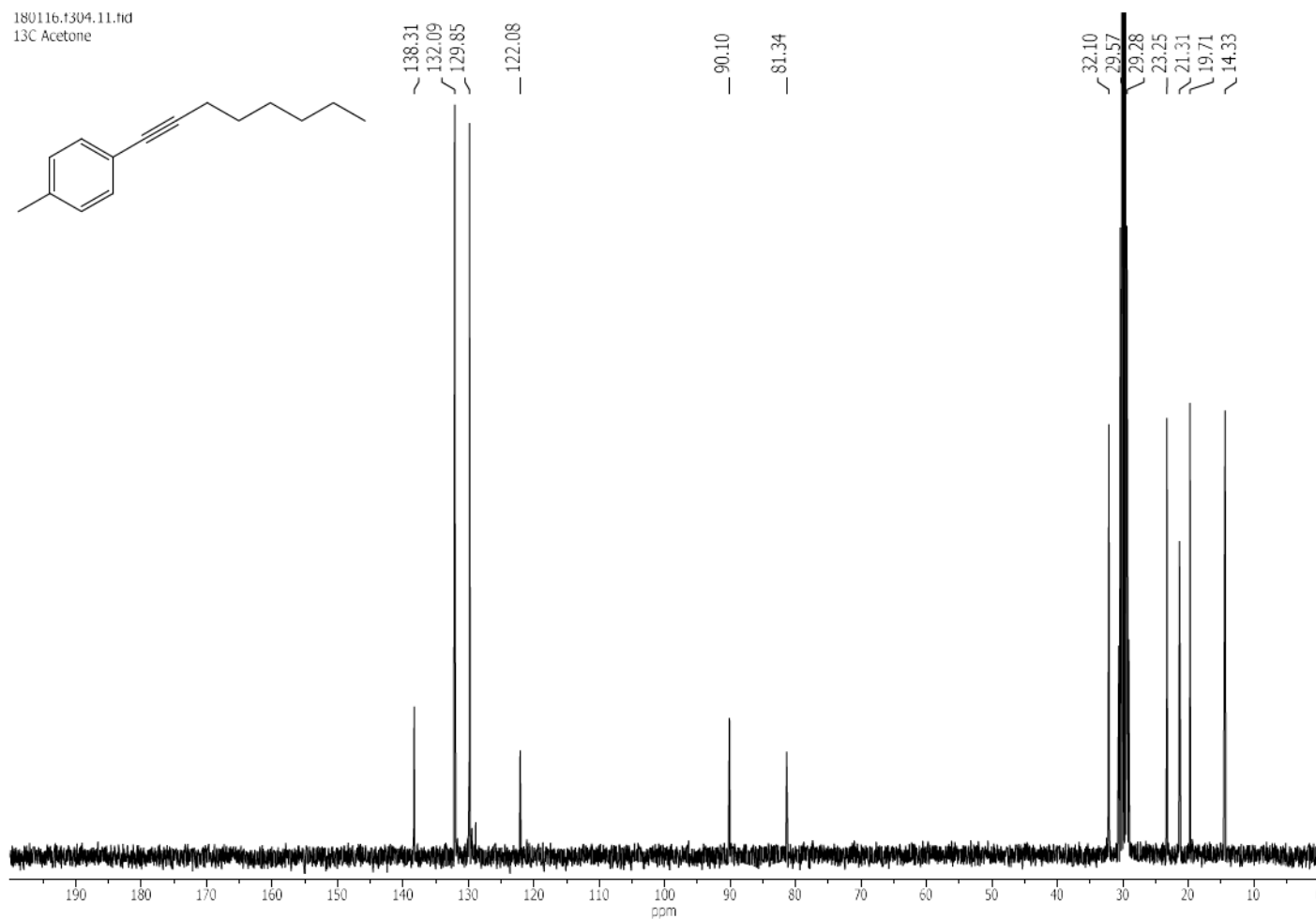
180202.403.11.fid
13C CD2Cl2



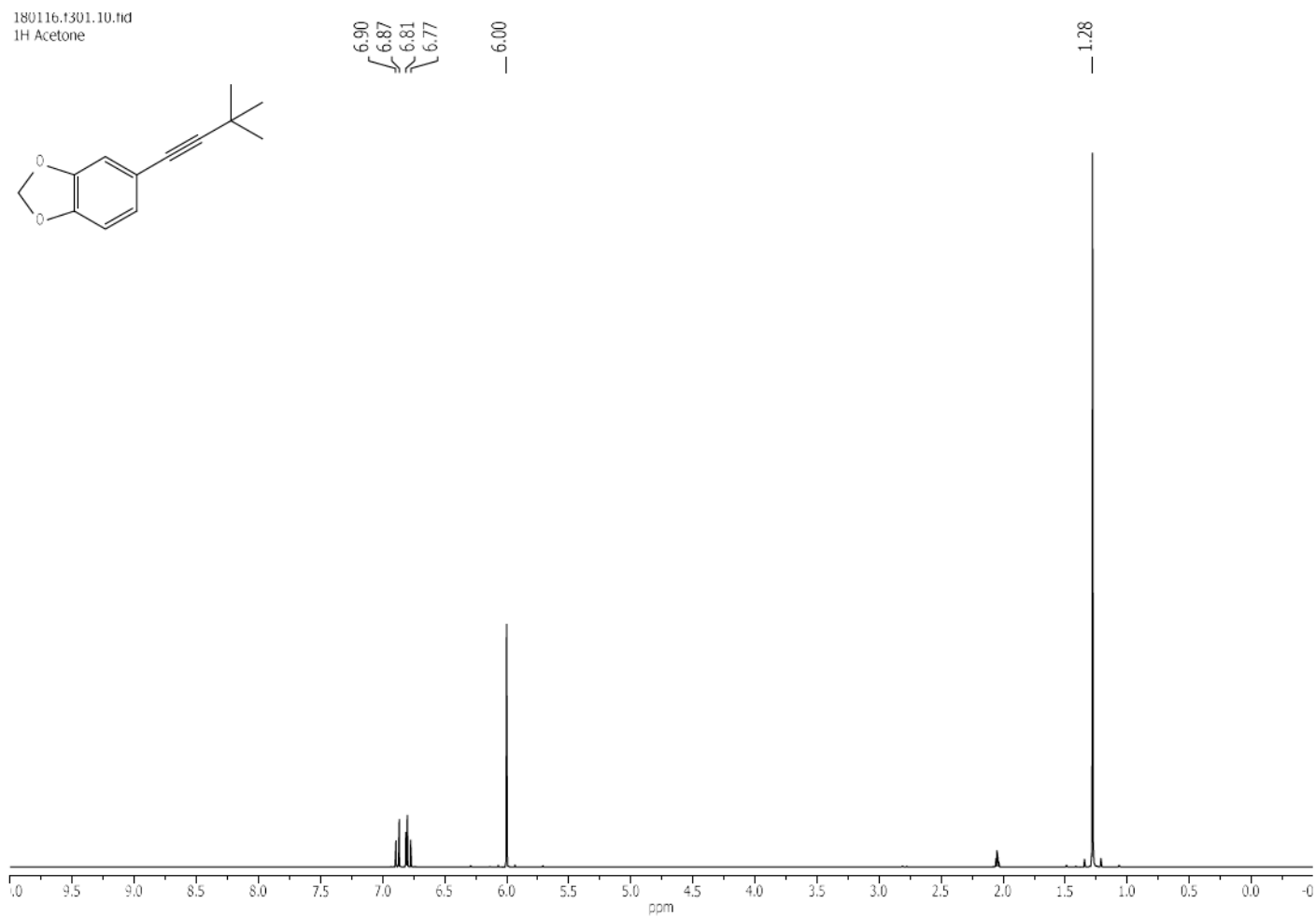
180116.1304.10.fid
1H Acetone



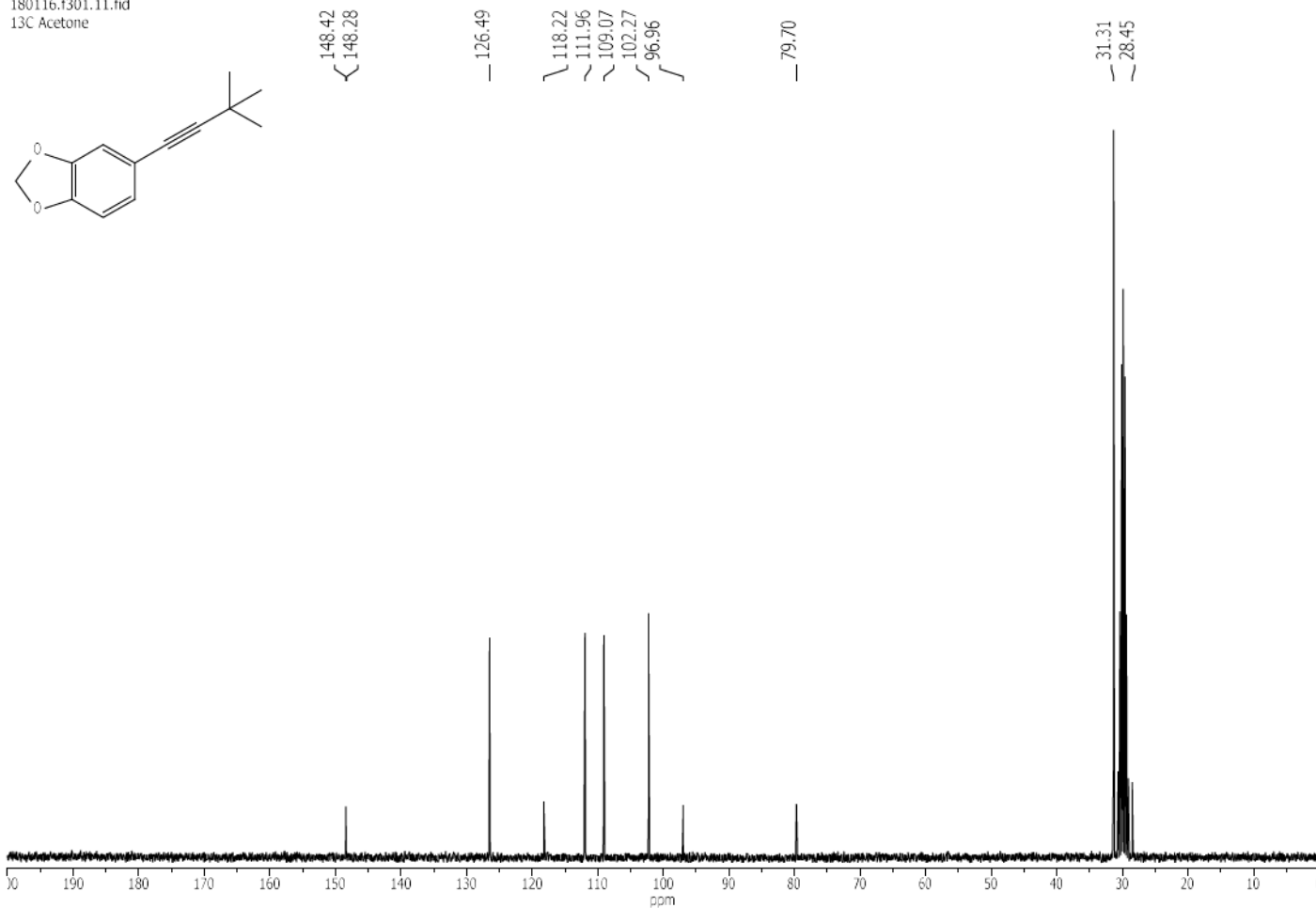
180116.1304.11.fid
13C Acetone



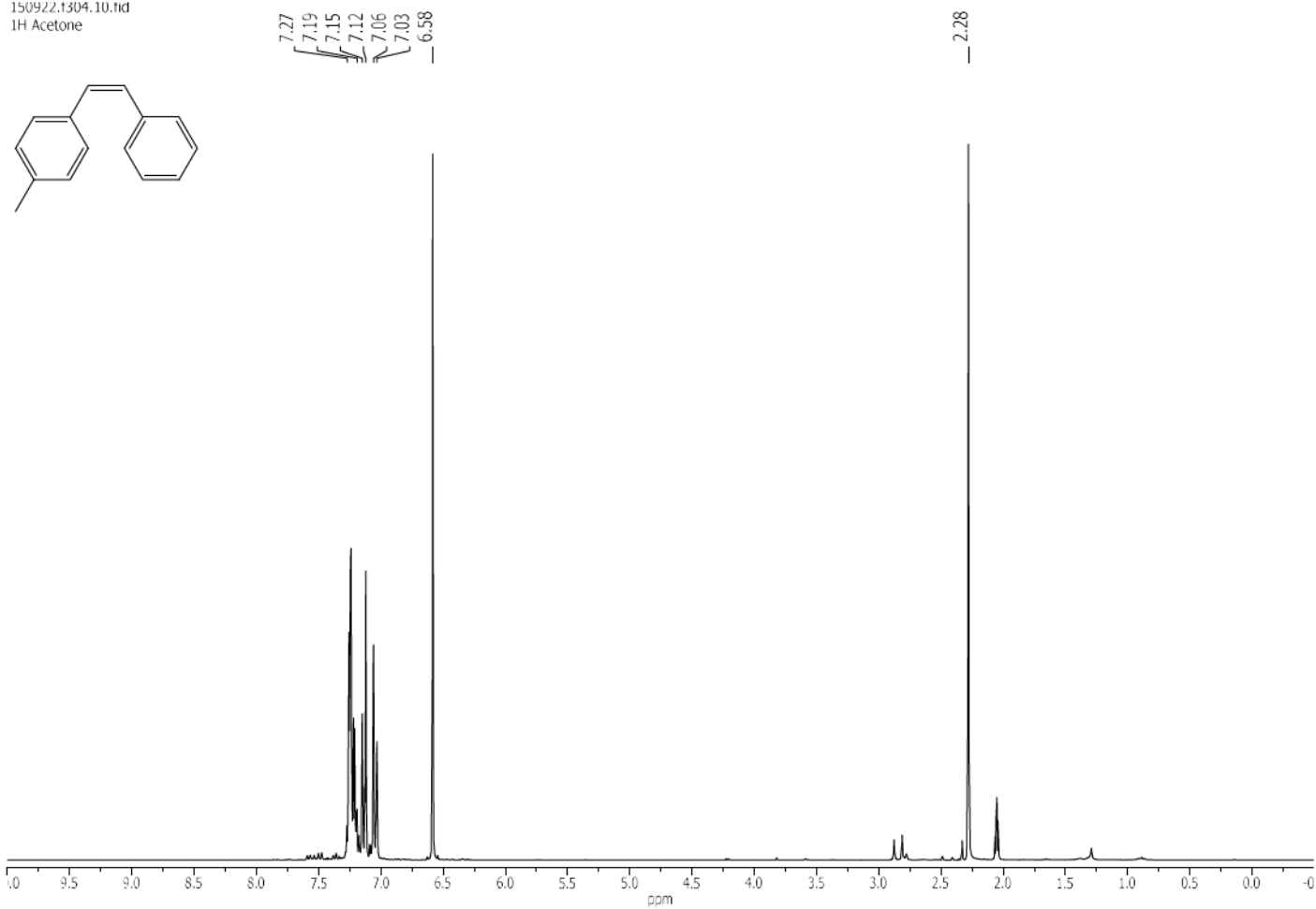
180116.1301.10.fid
1H Acetone



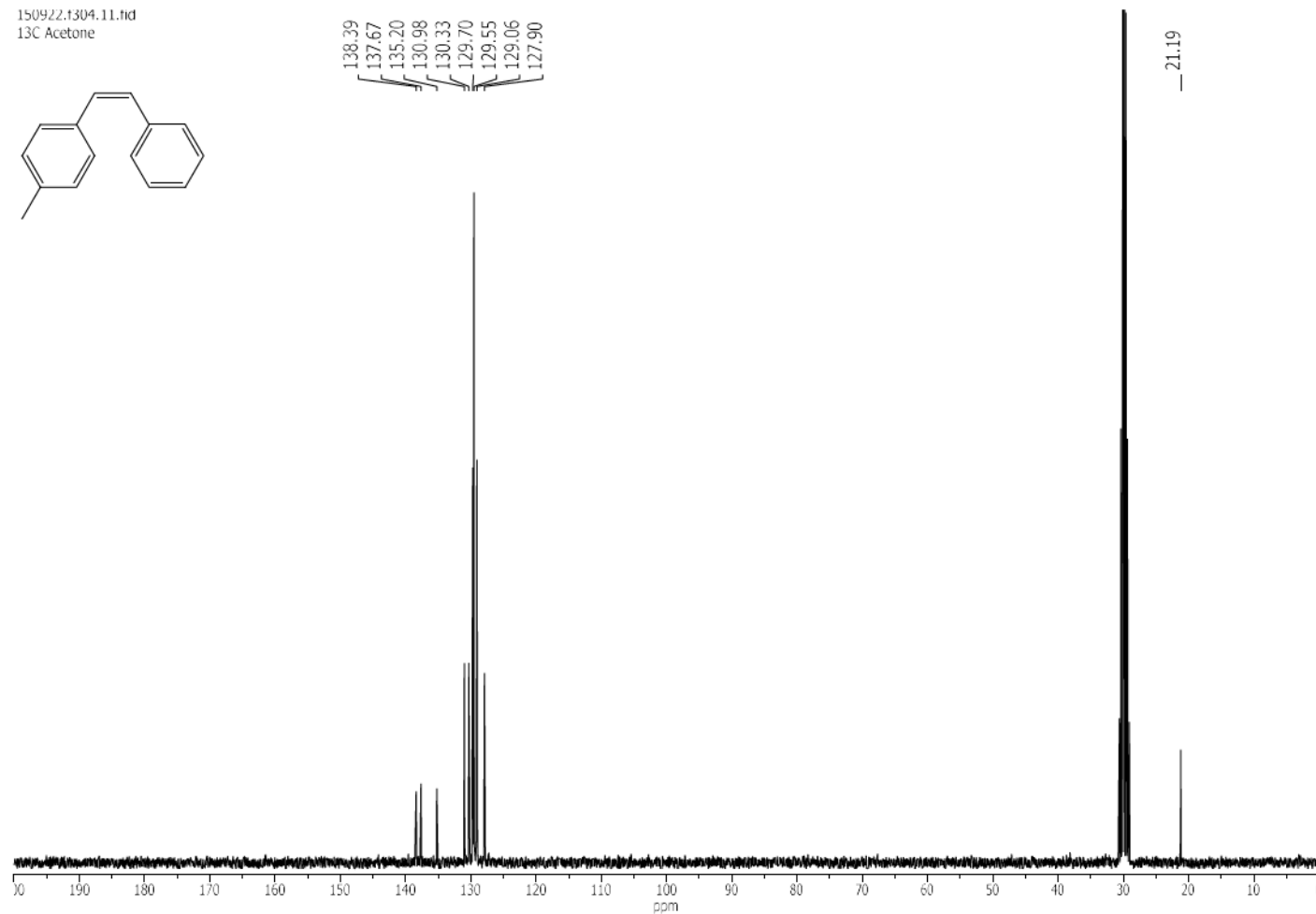
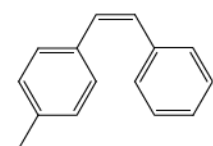
180116.1301.11.fid
13C Acetone



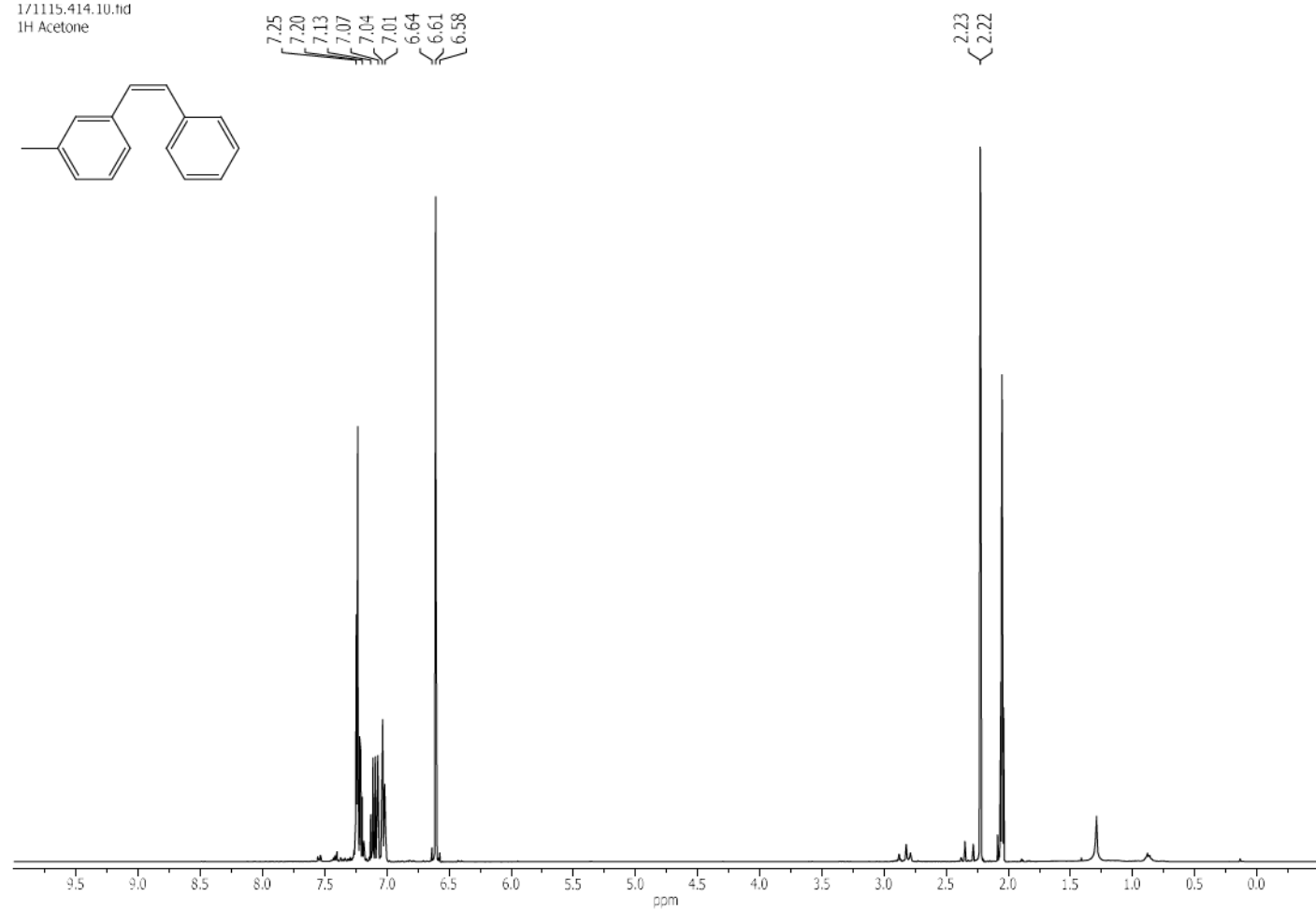
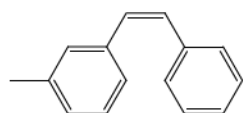
150922.1304.10.fid
1H Acetone



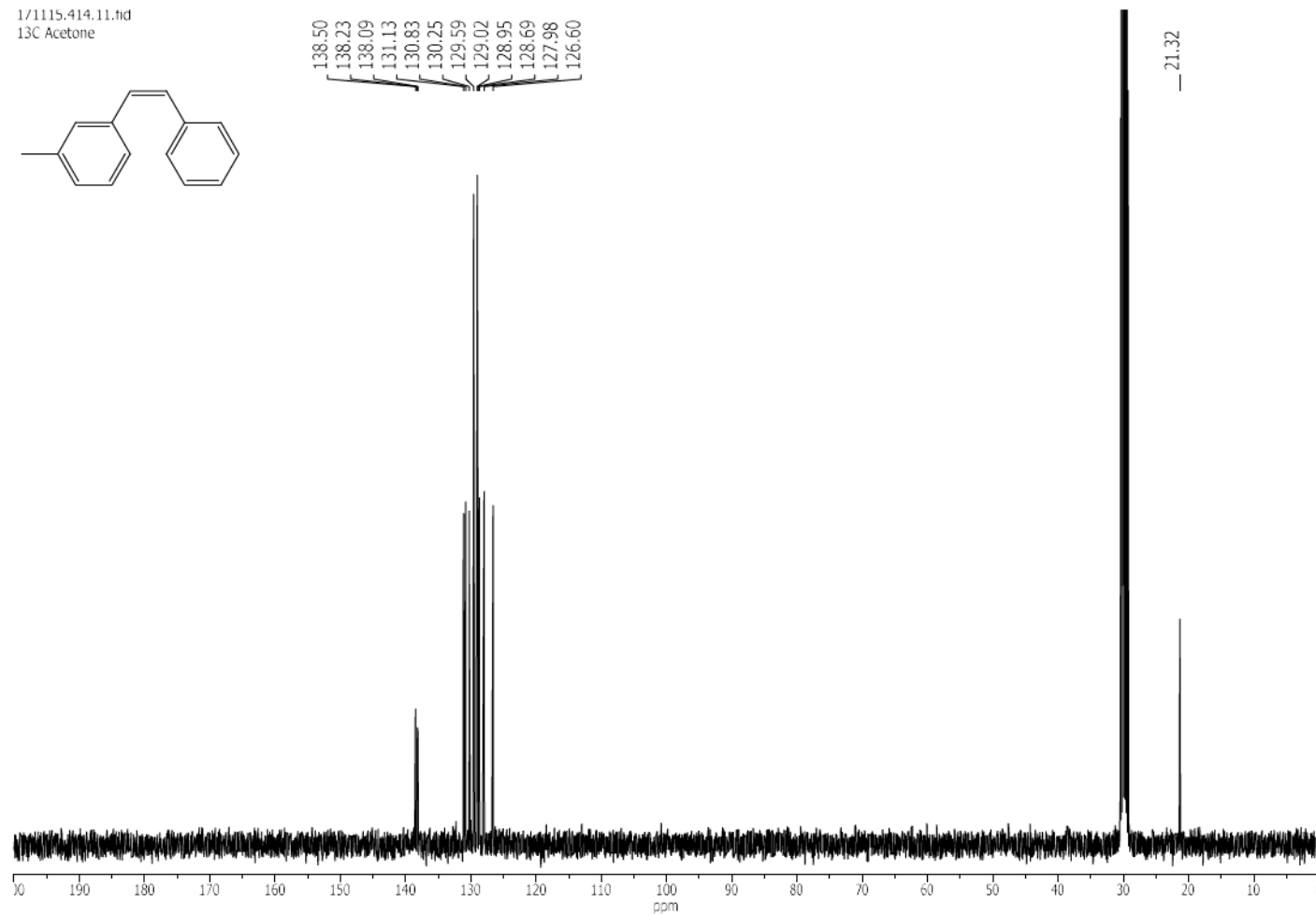
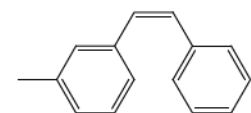
150922.1304.11.fid
13C Acetone



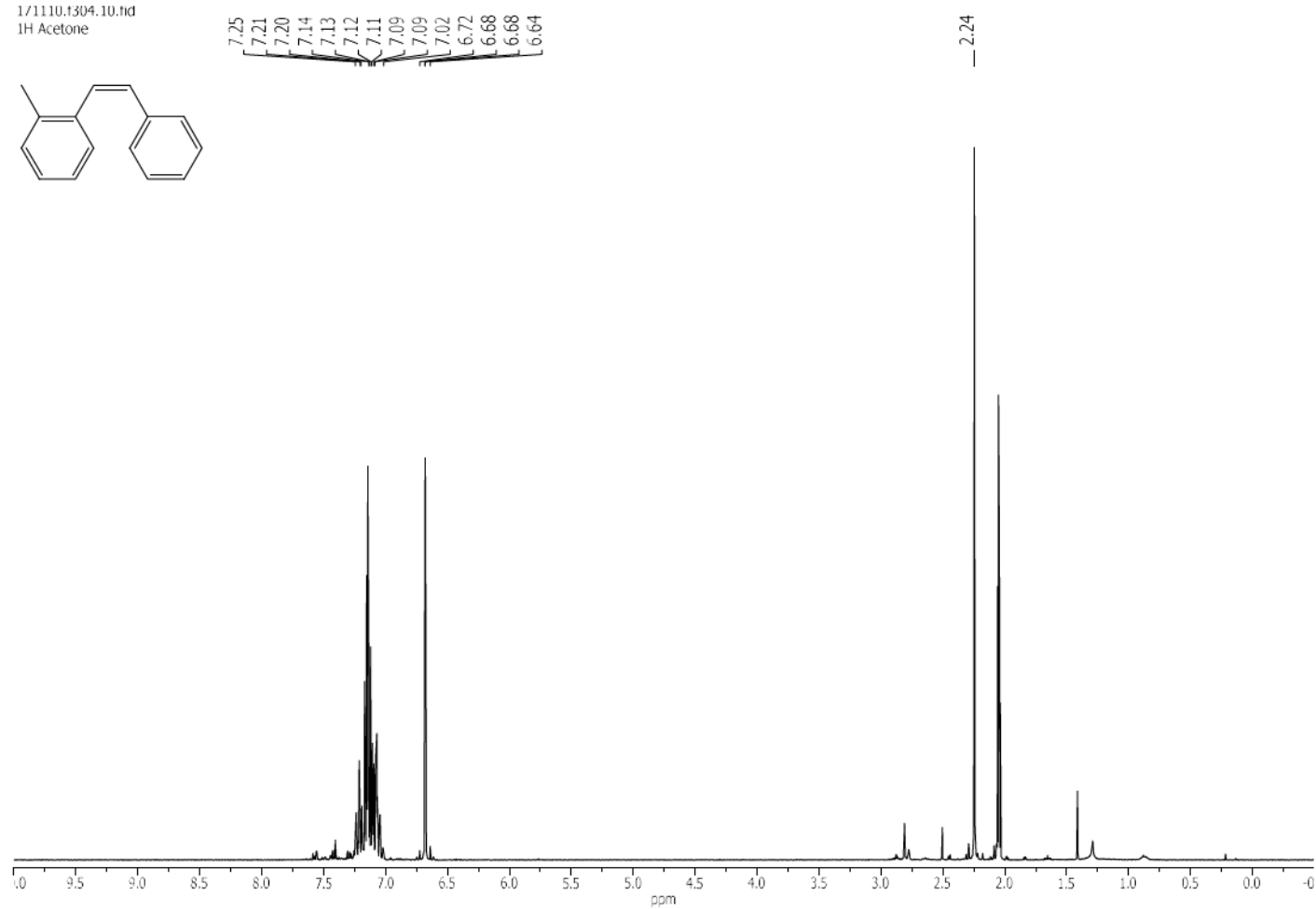
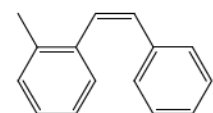
171115.414.10.fid
1H Acetone



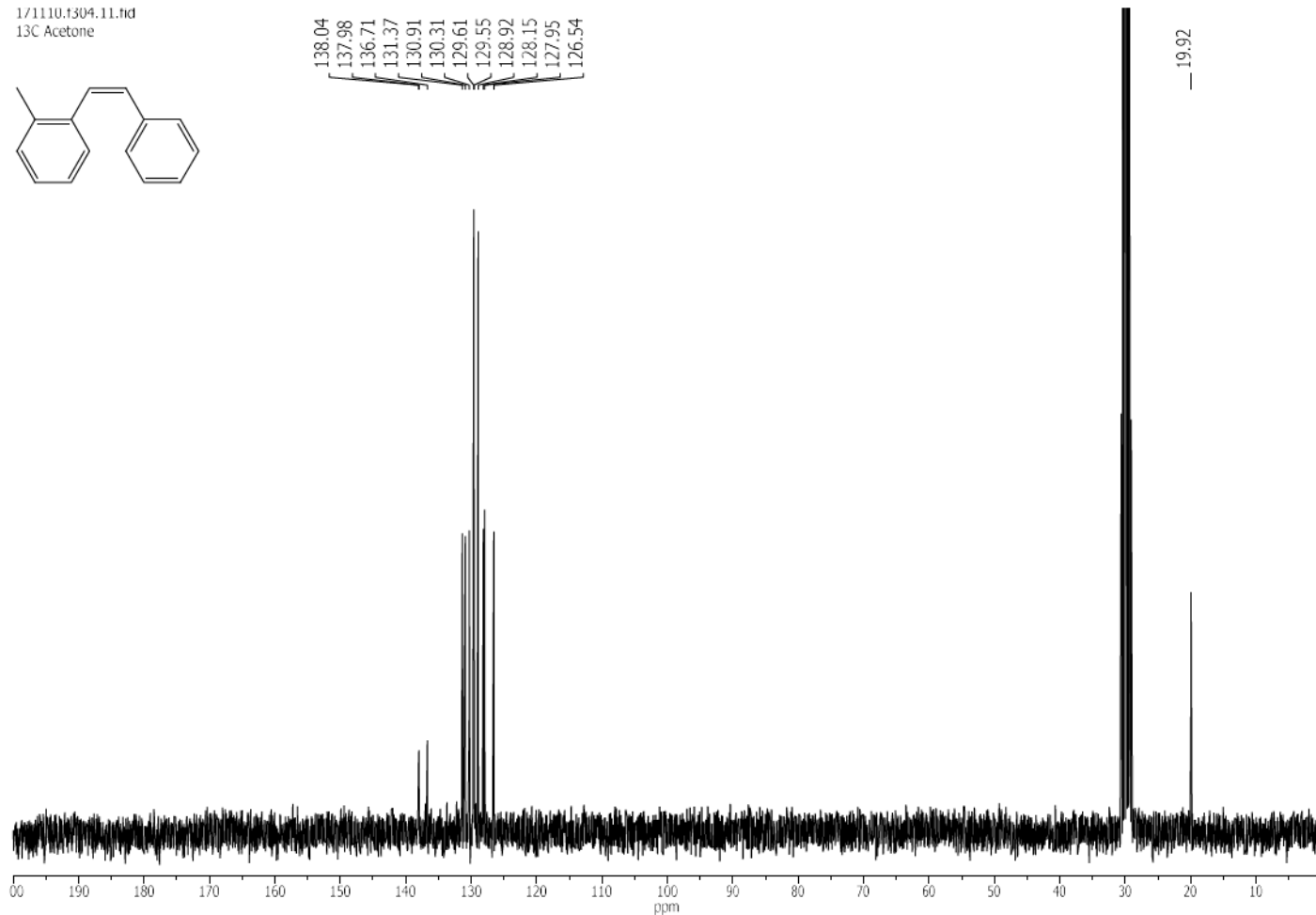
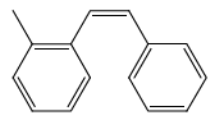
1/1115.414.11.fid
13C Acetone



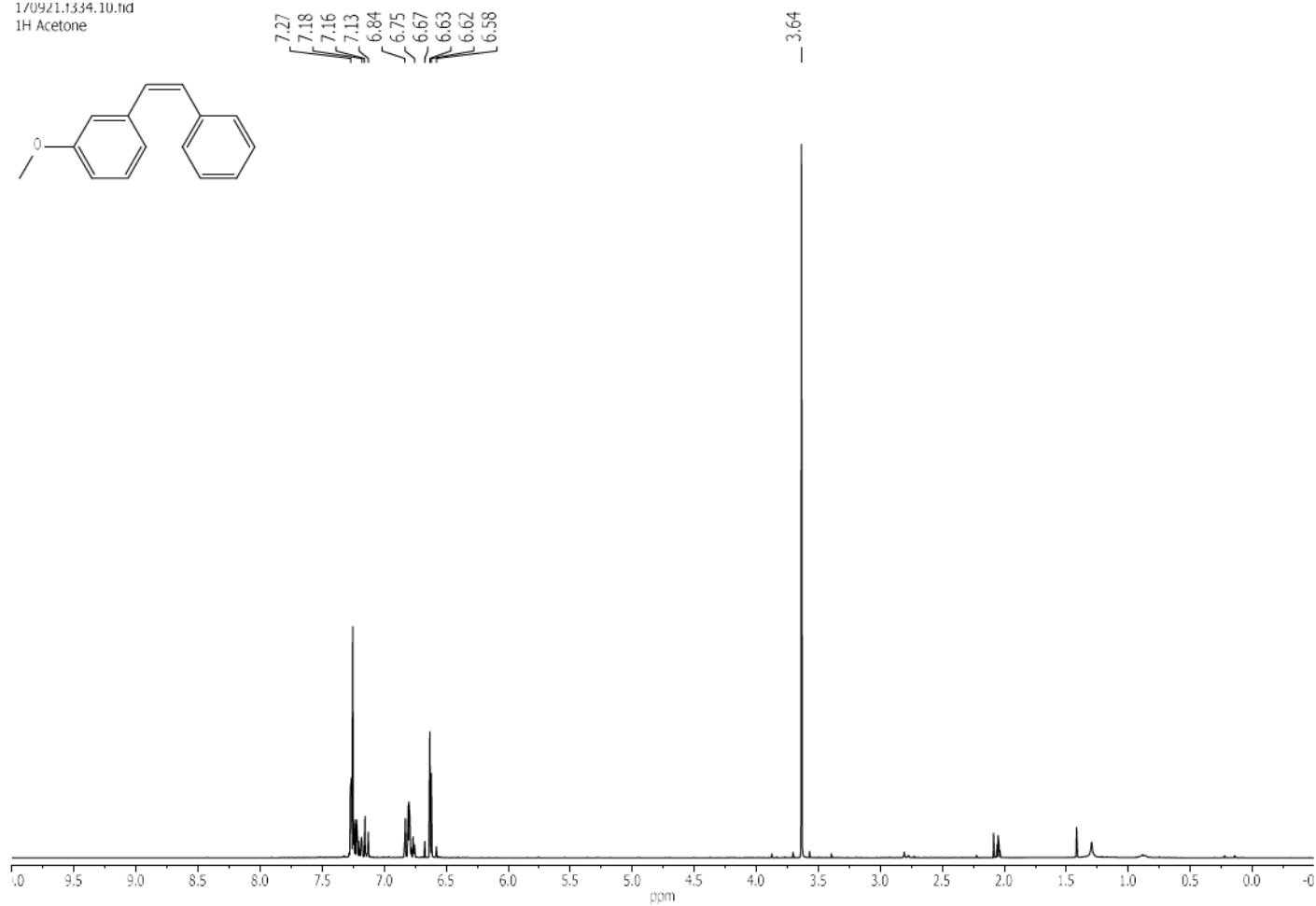
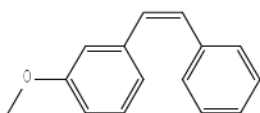
1/1110.1304.10.fid
1H Acetone



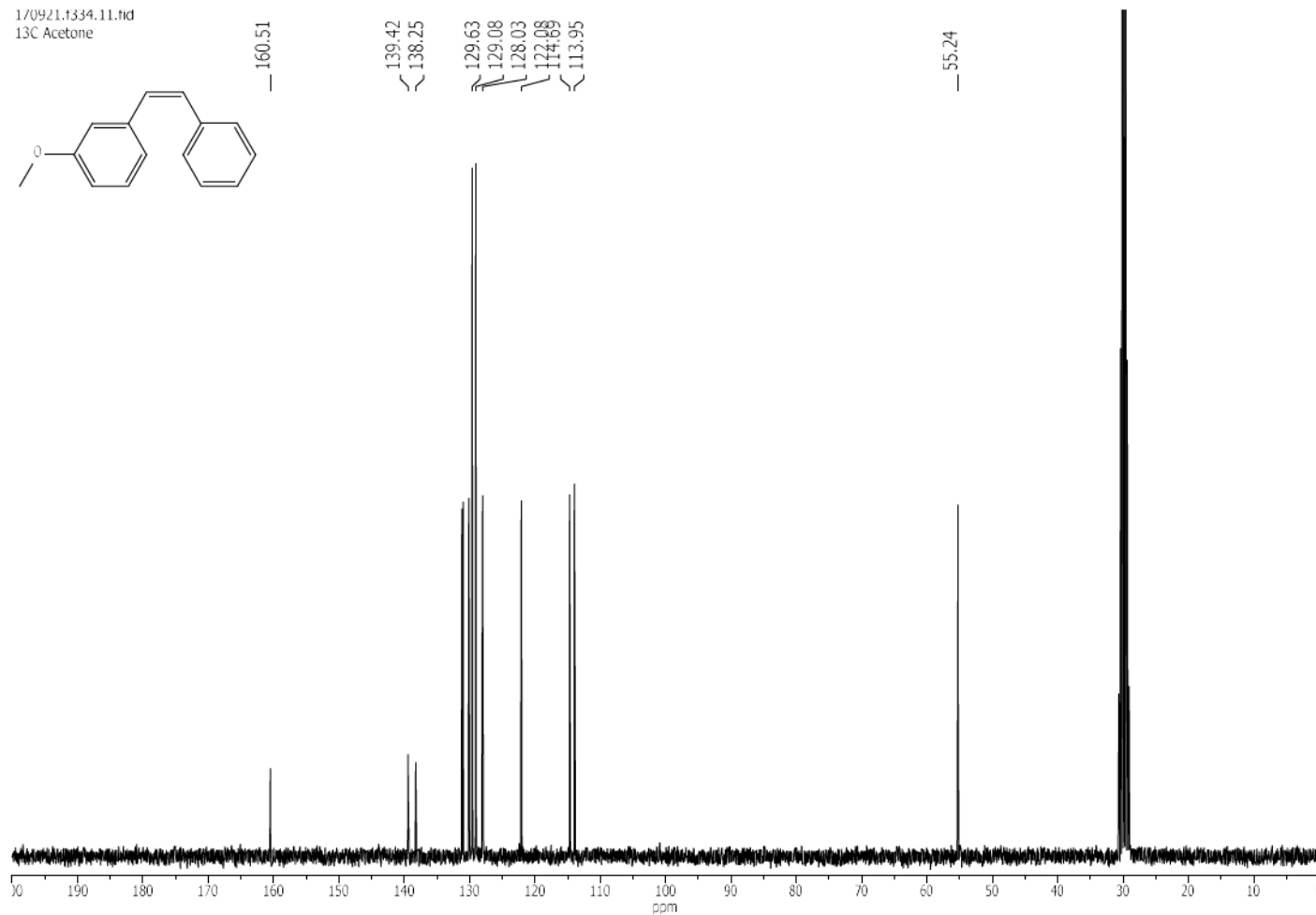
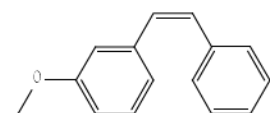
1/1110.1304.11.fid
13C Acetone



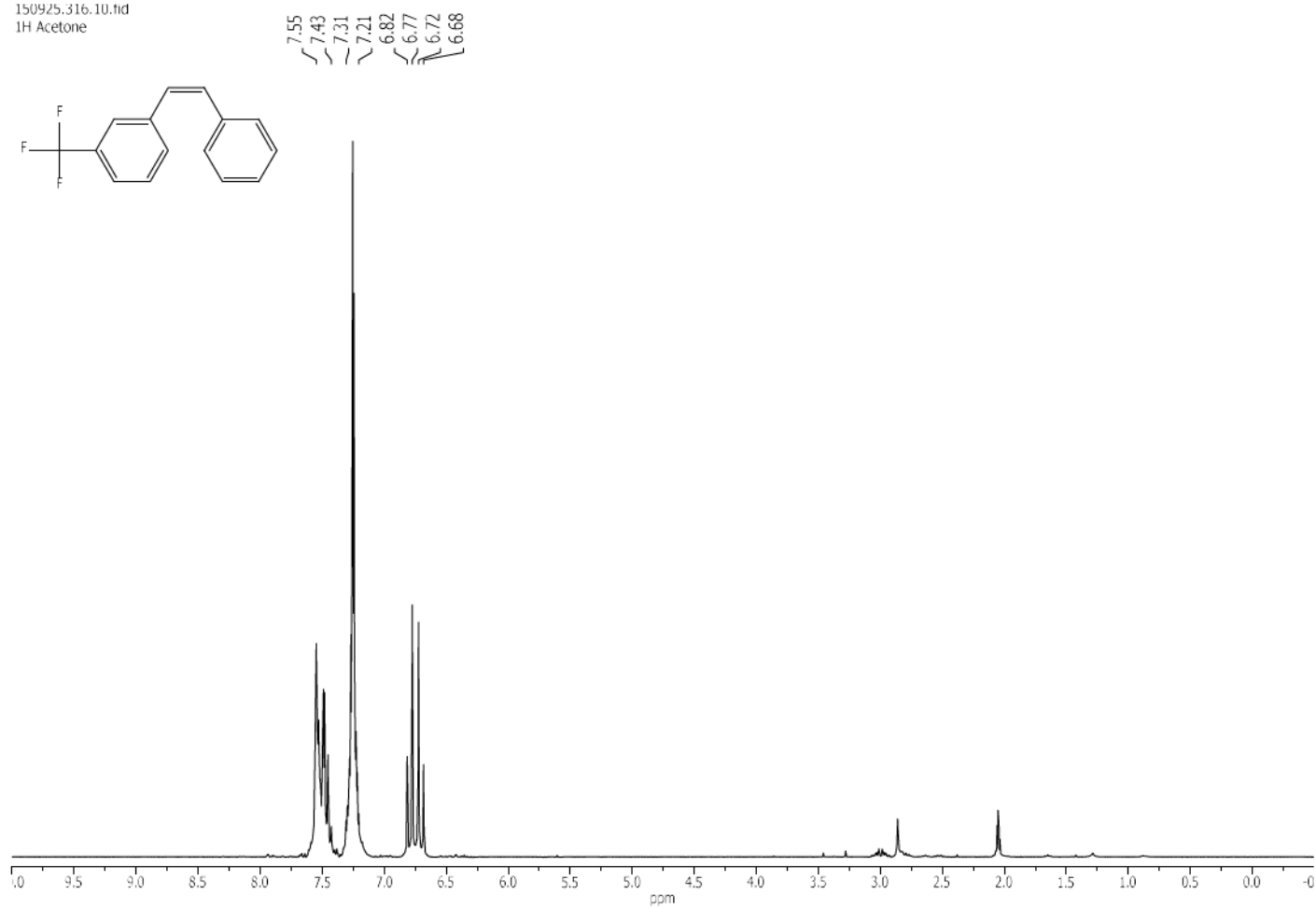
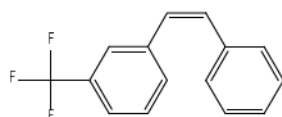
1/0921.1334.10.fid
1H Acetone



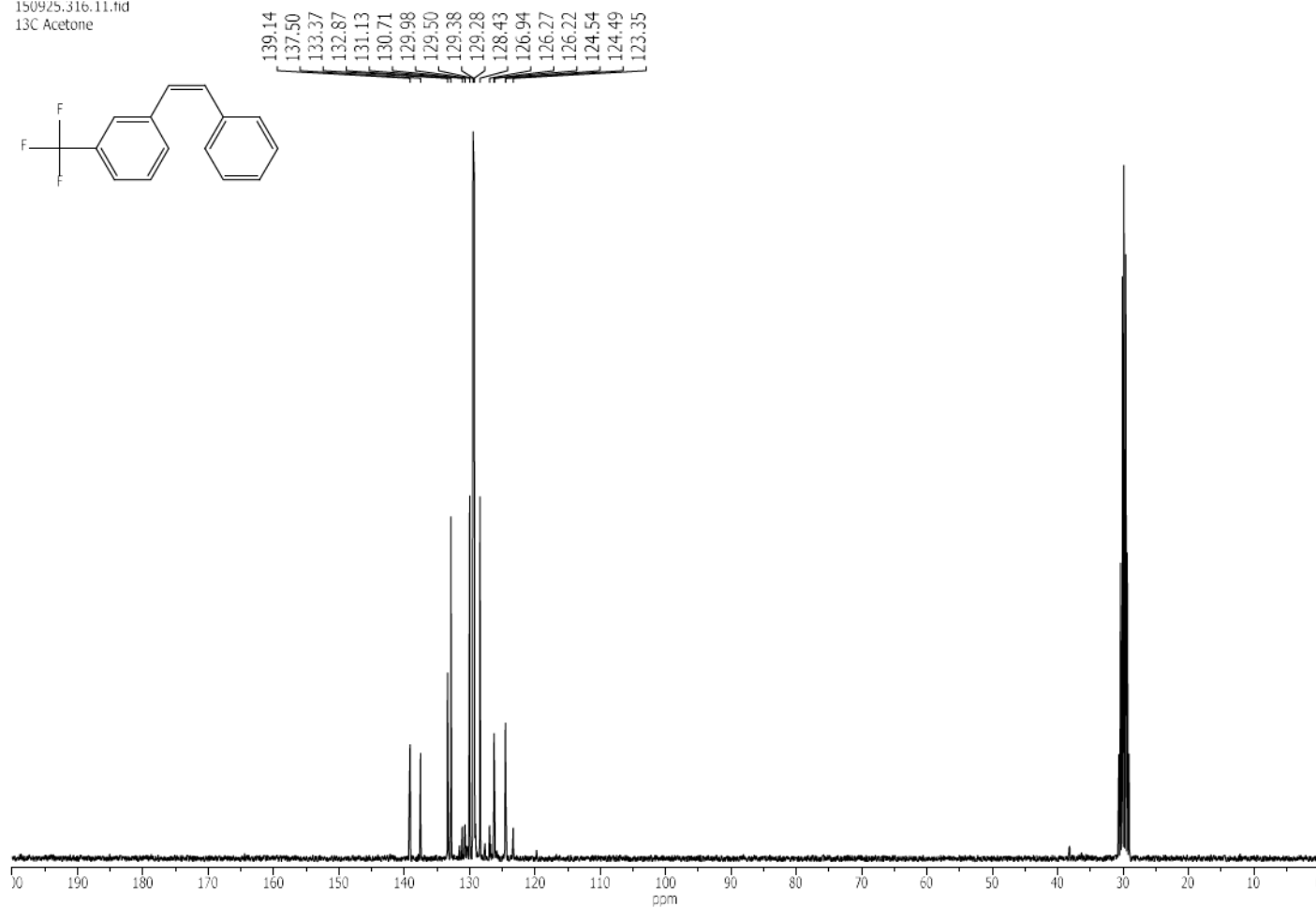
170921.1334.11.tid
13C Acetone



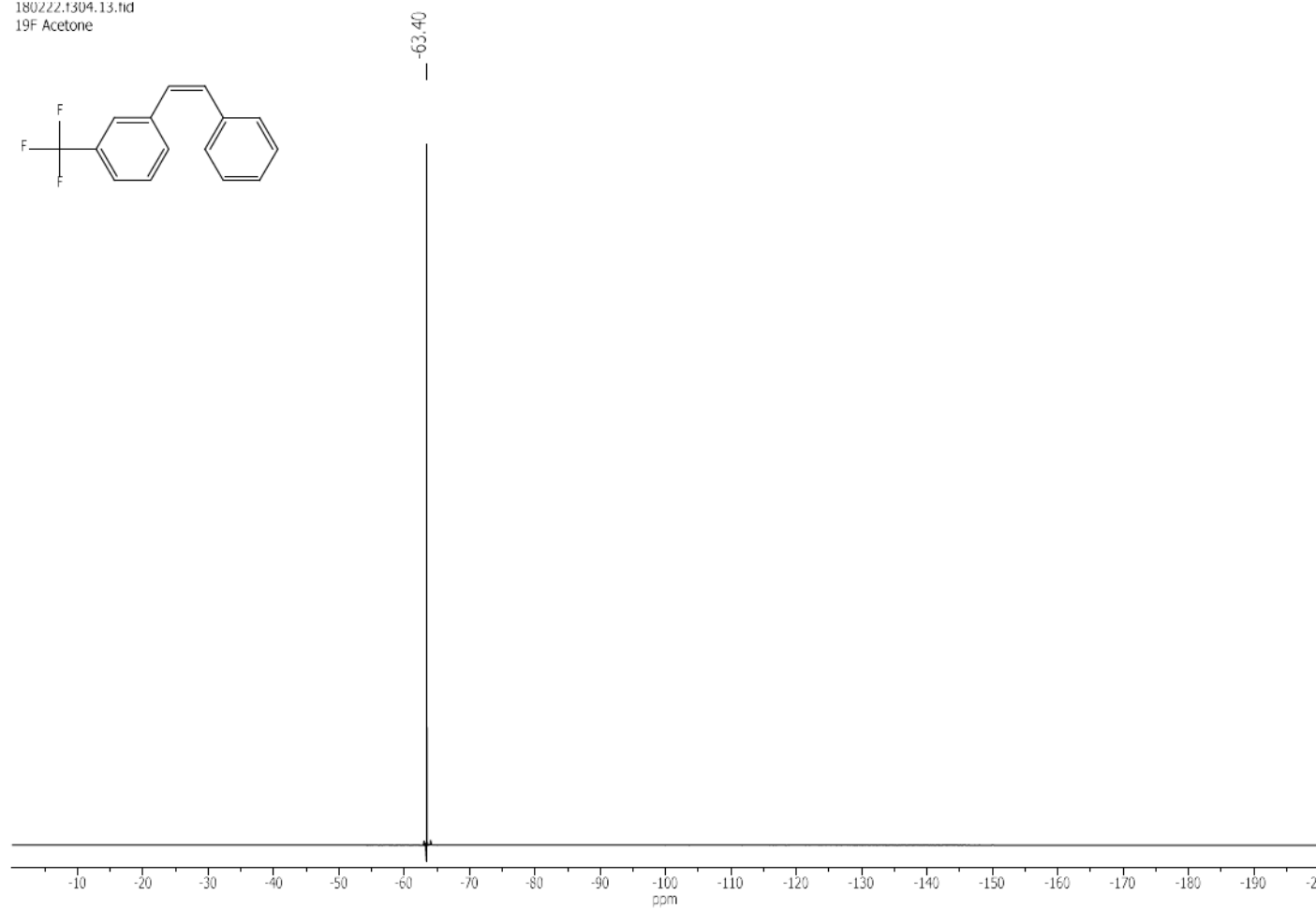
150925.316.10.tid
1H Acetone



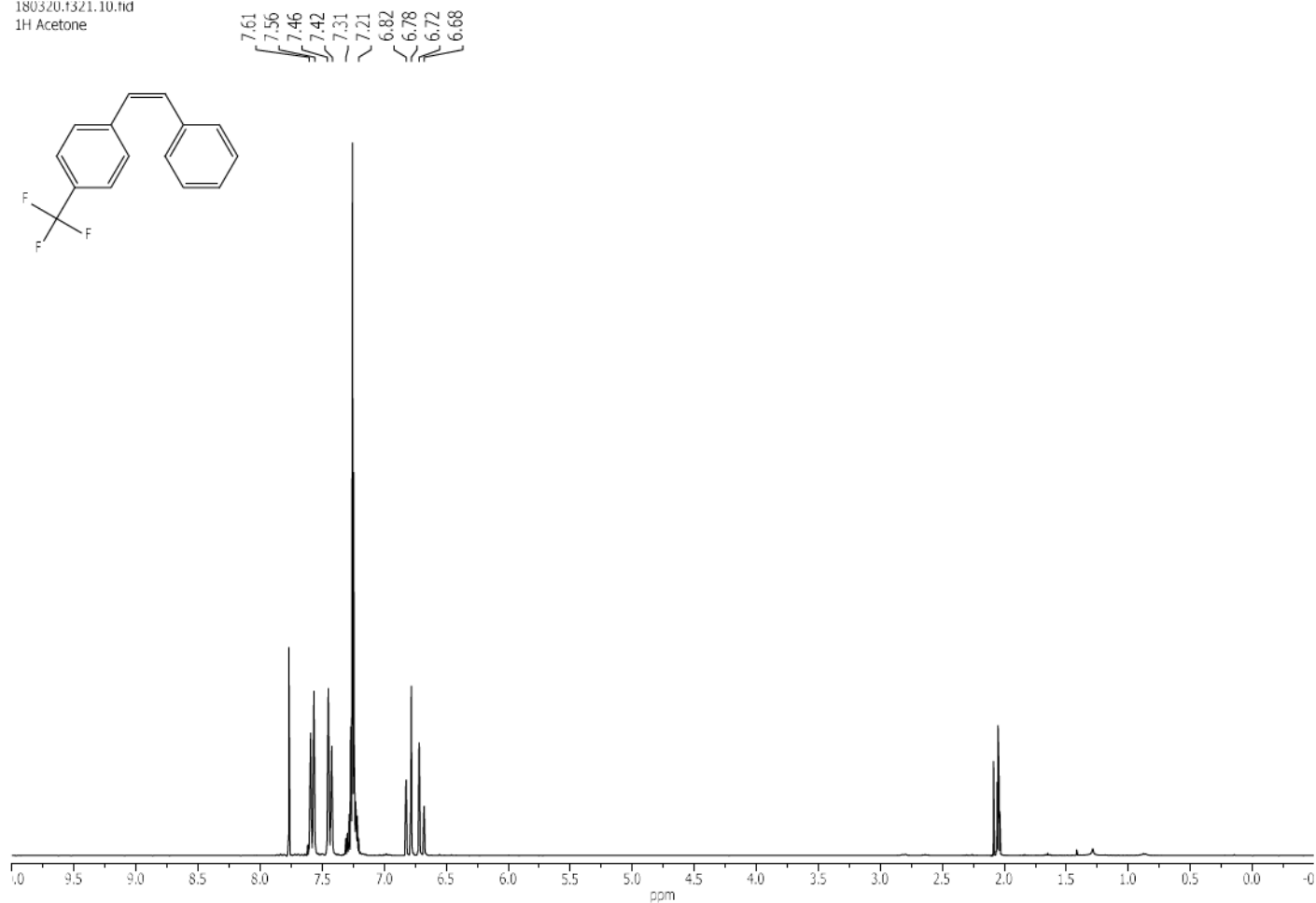
150925.316.11.fid
13C Acetone



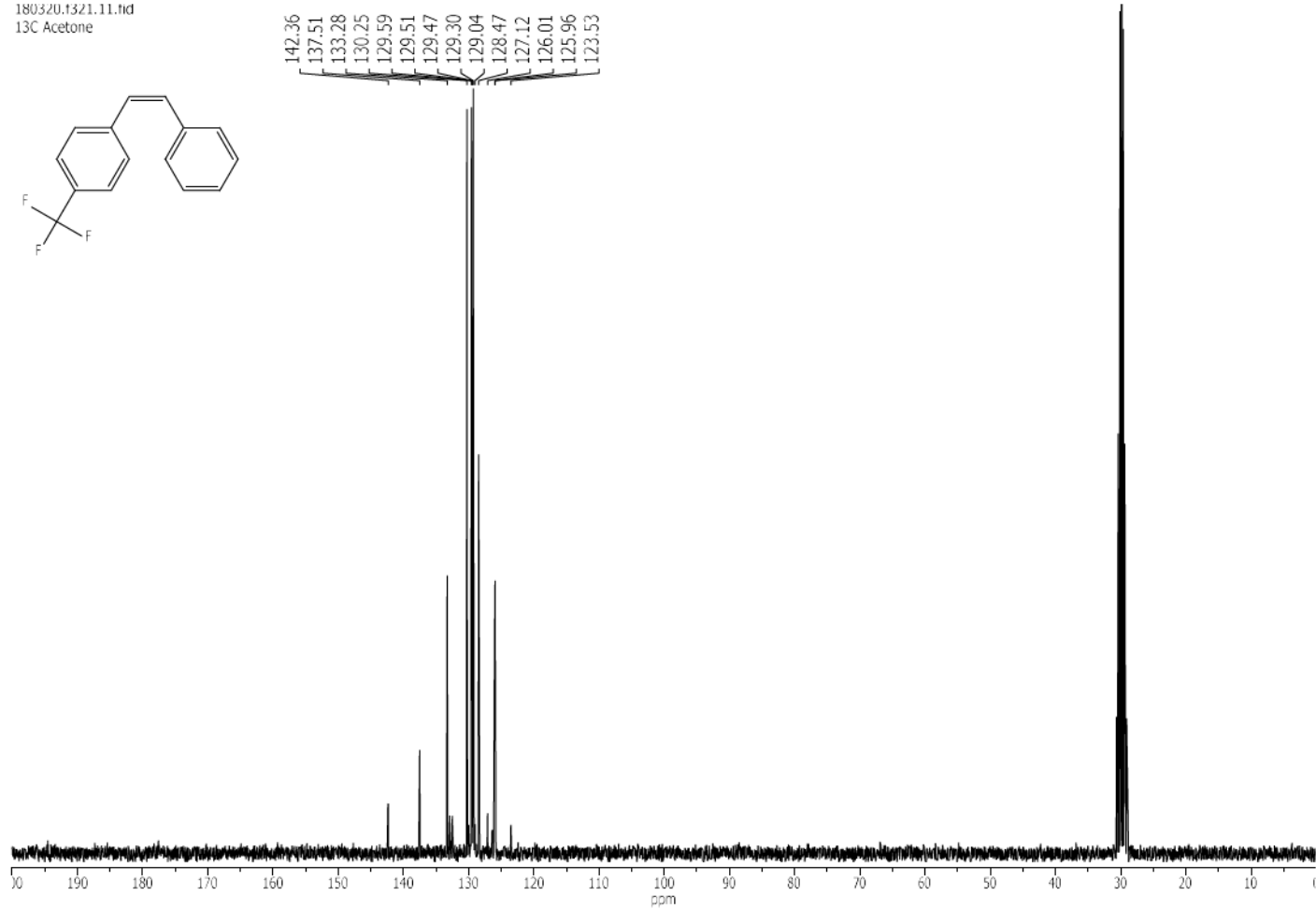
180222.1304.13.fid
19F Acetone



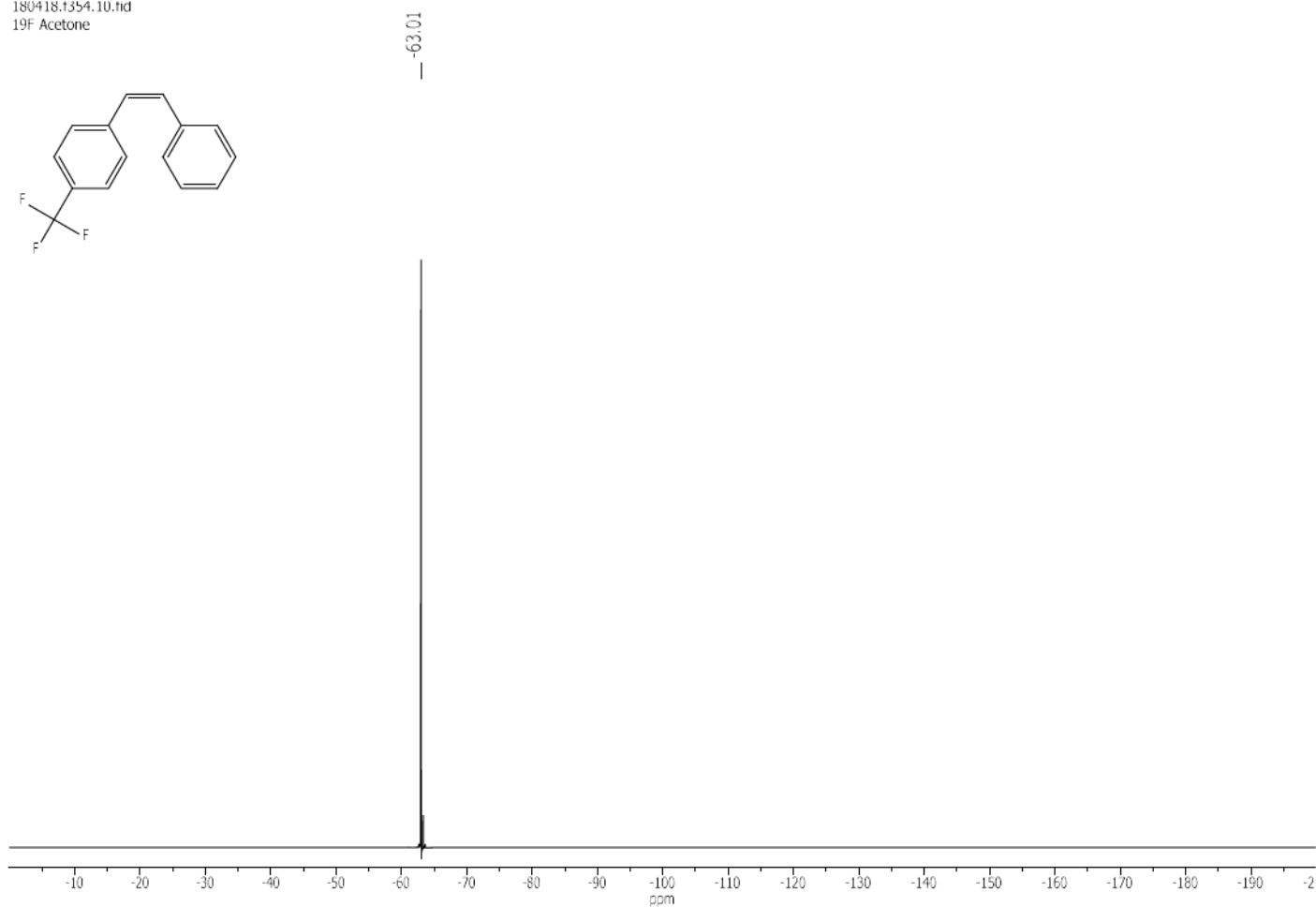
180320.1321.10.fid
1H Acetone



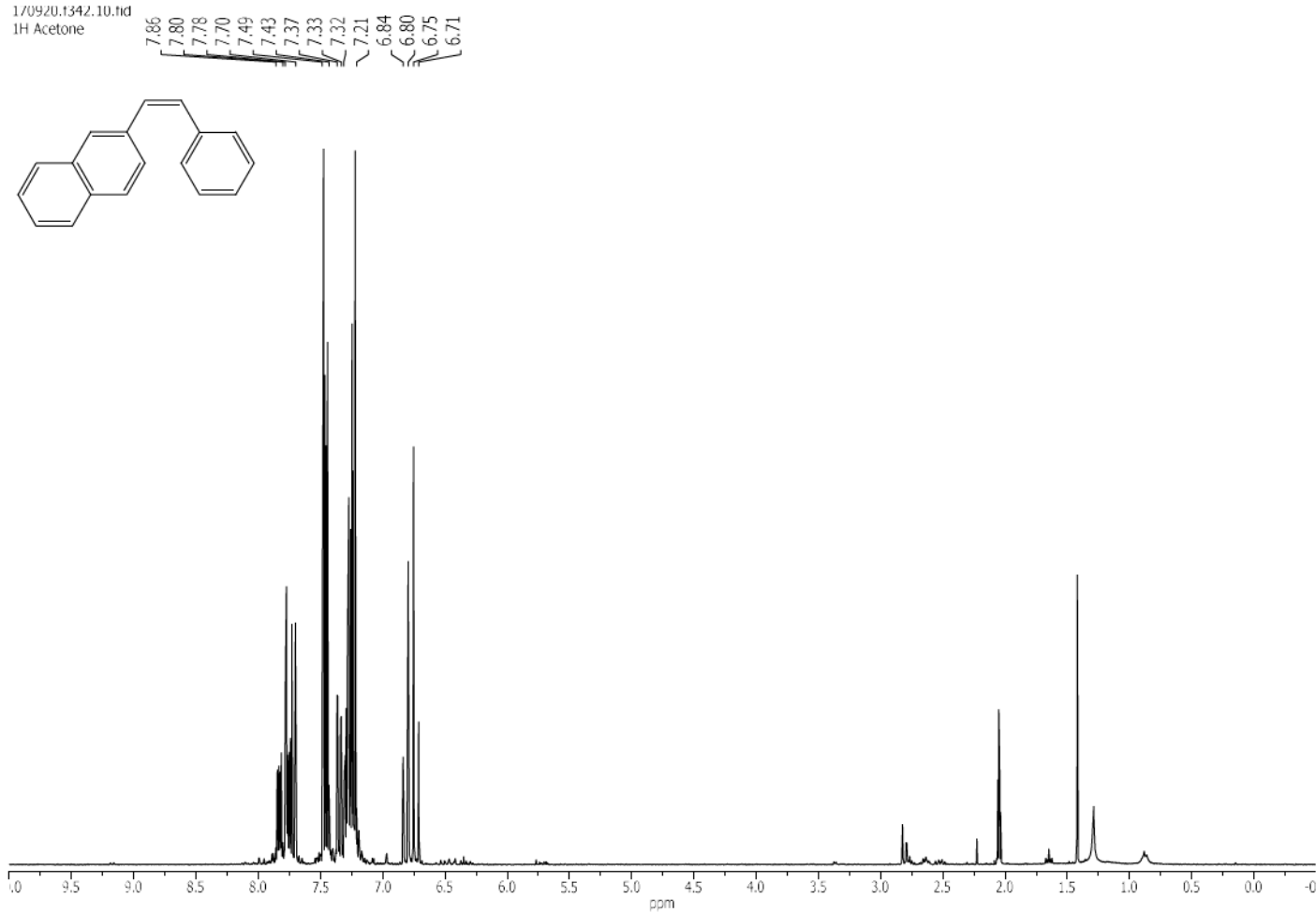
180320.1321.11.fid
13C Acetone



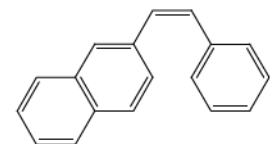
180418.1354.10.fid
19F Acetone



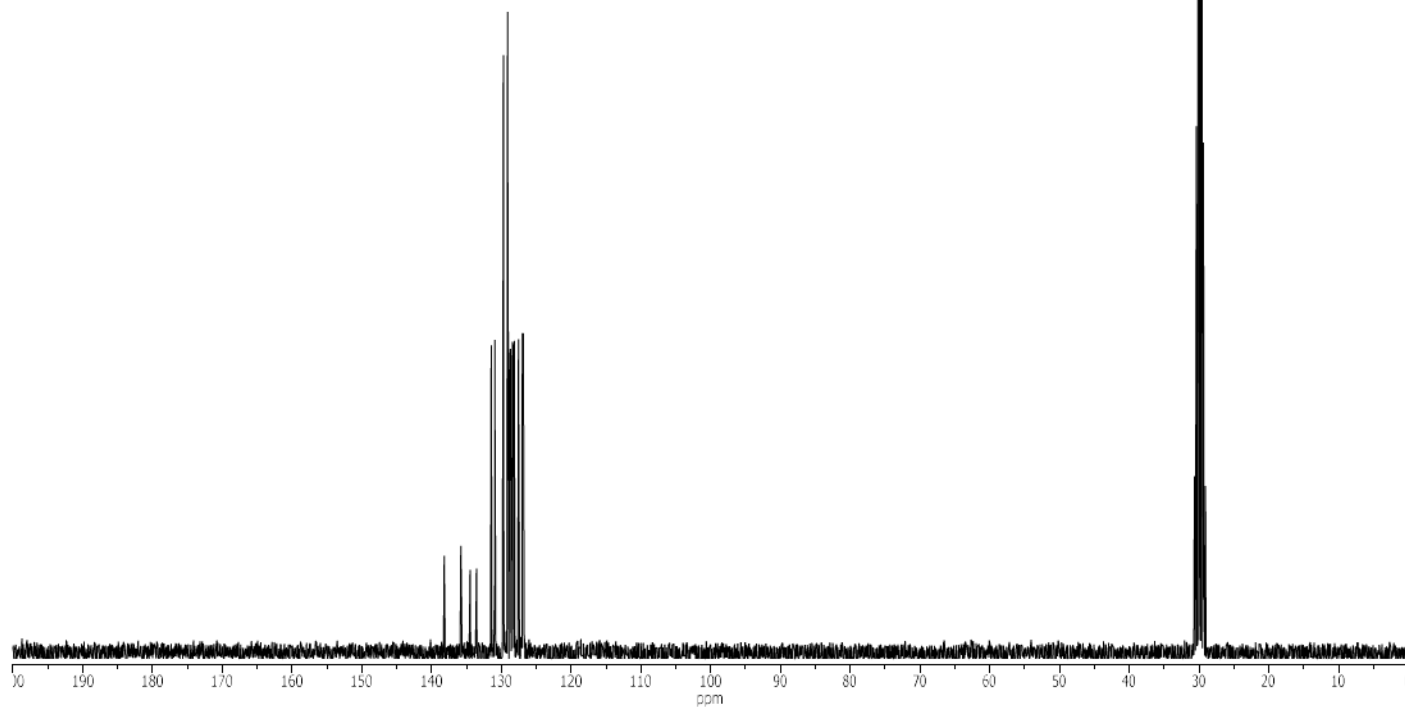
170920.1342.10.fid
1H Acetone



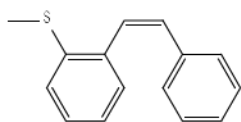
170920.1342.11.tid
13C Acetone



138.19
135.83
134.49
133.59
131.45
130.95
129.70
129.13
128.78
128.71
128.45
128.34
128.15
127.57
127.01
126.87

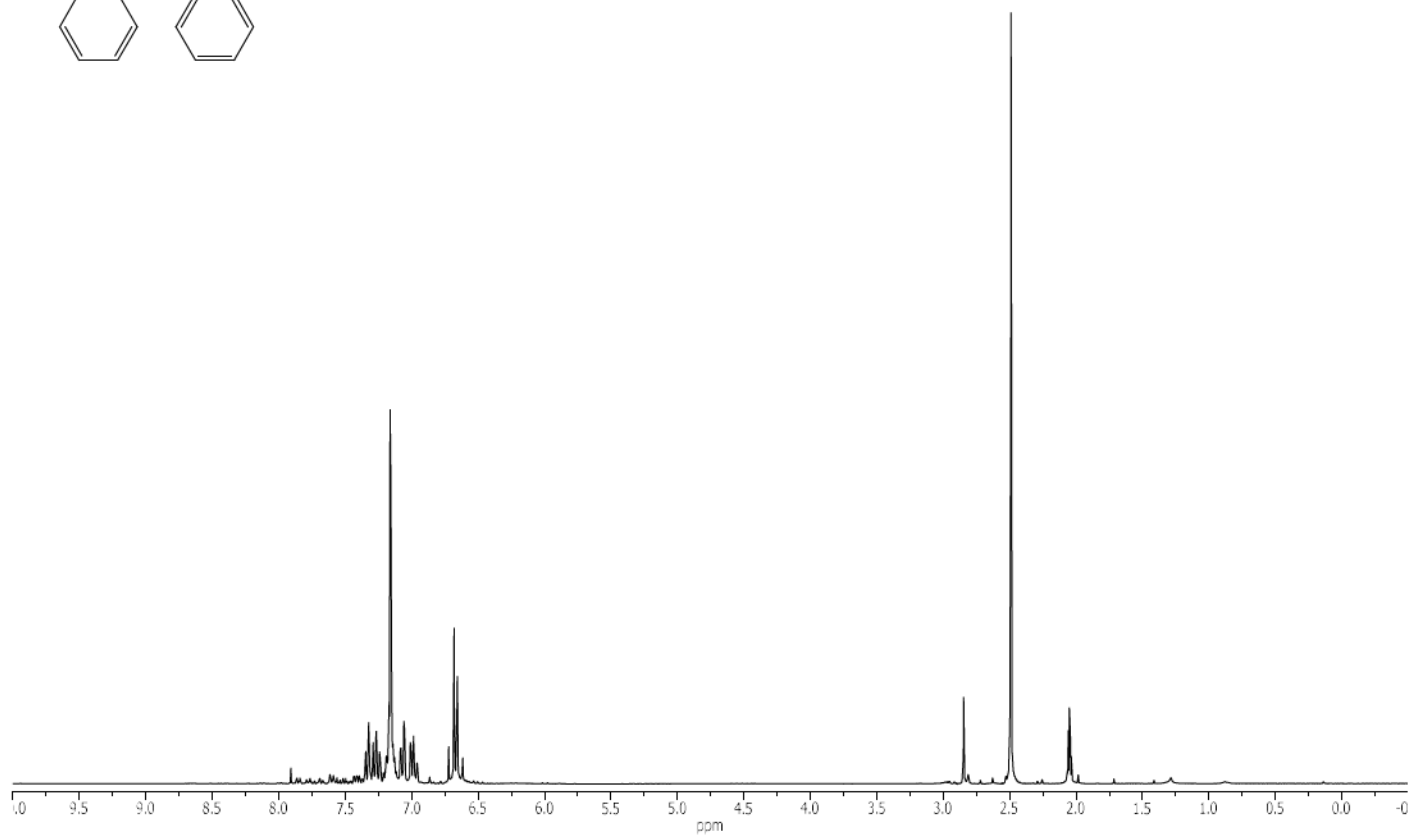


151204.330.10.tid
1H Acetone

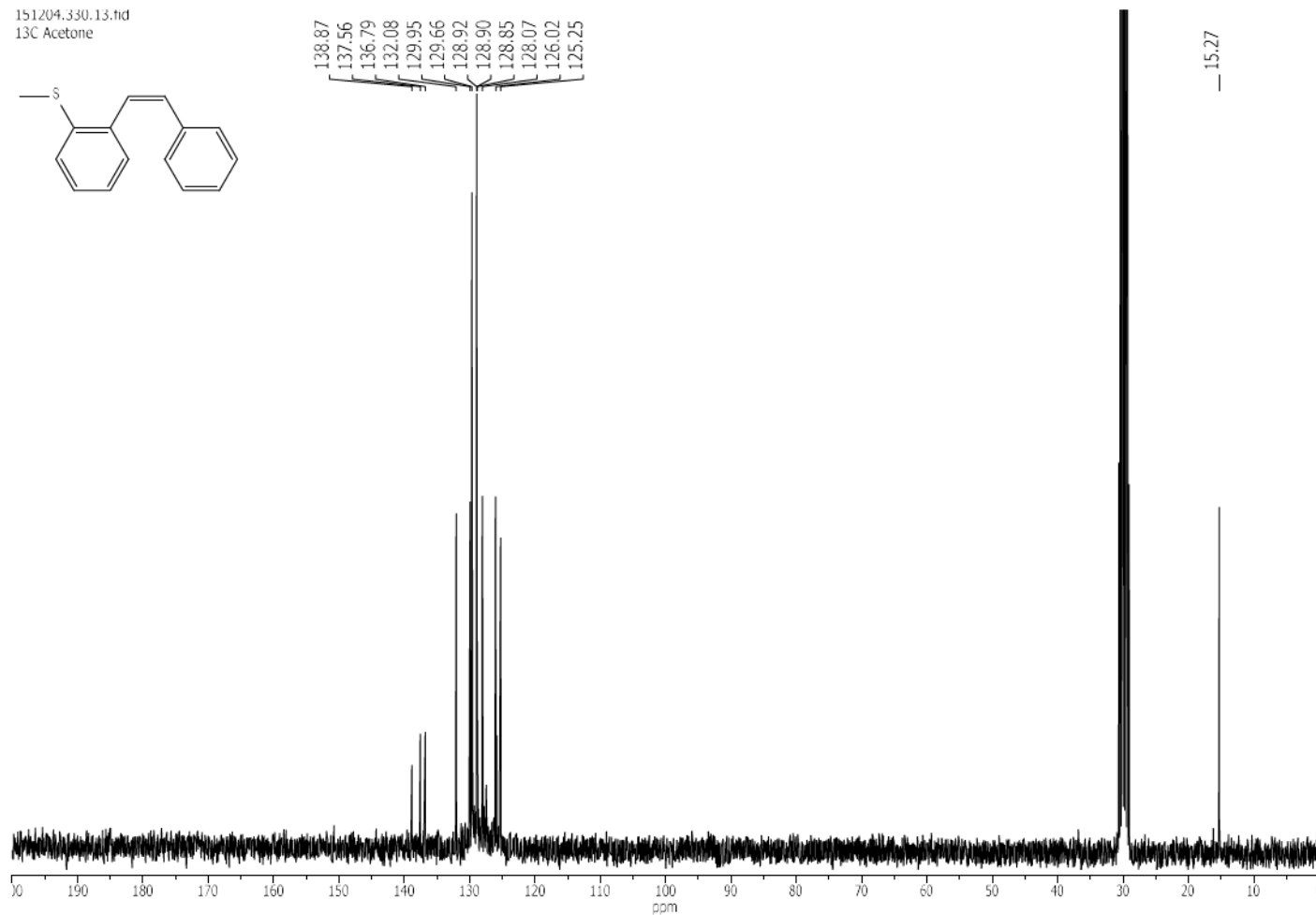
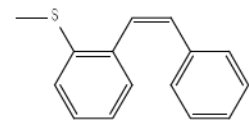


7.35
7.32
7.29
7.24
7.21
7.13
7.09
7.05
7.01
6.96
6.72
6.68
6.66
6.62

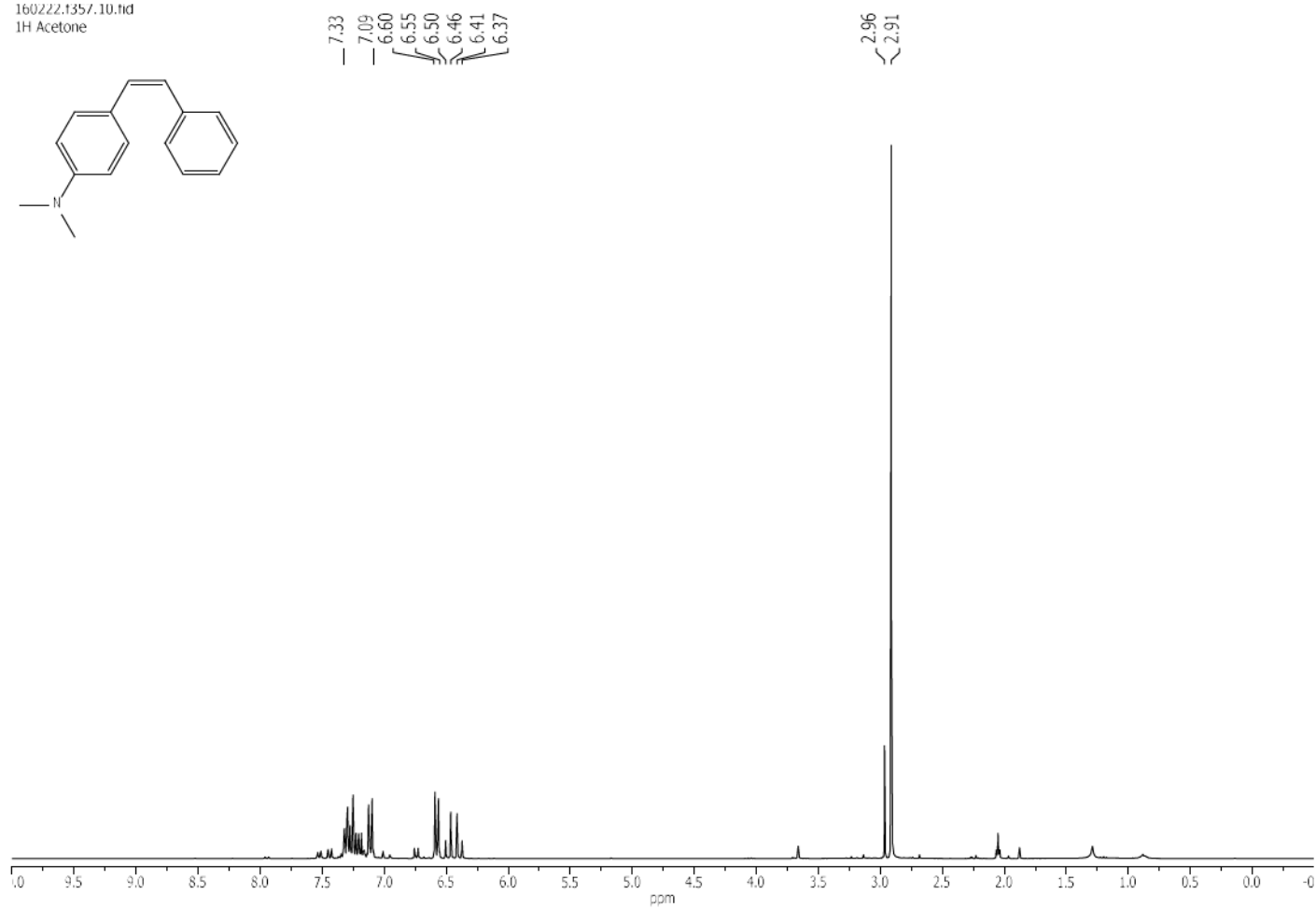
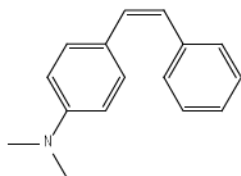
2.49



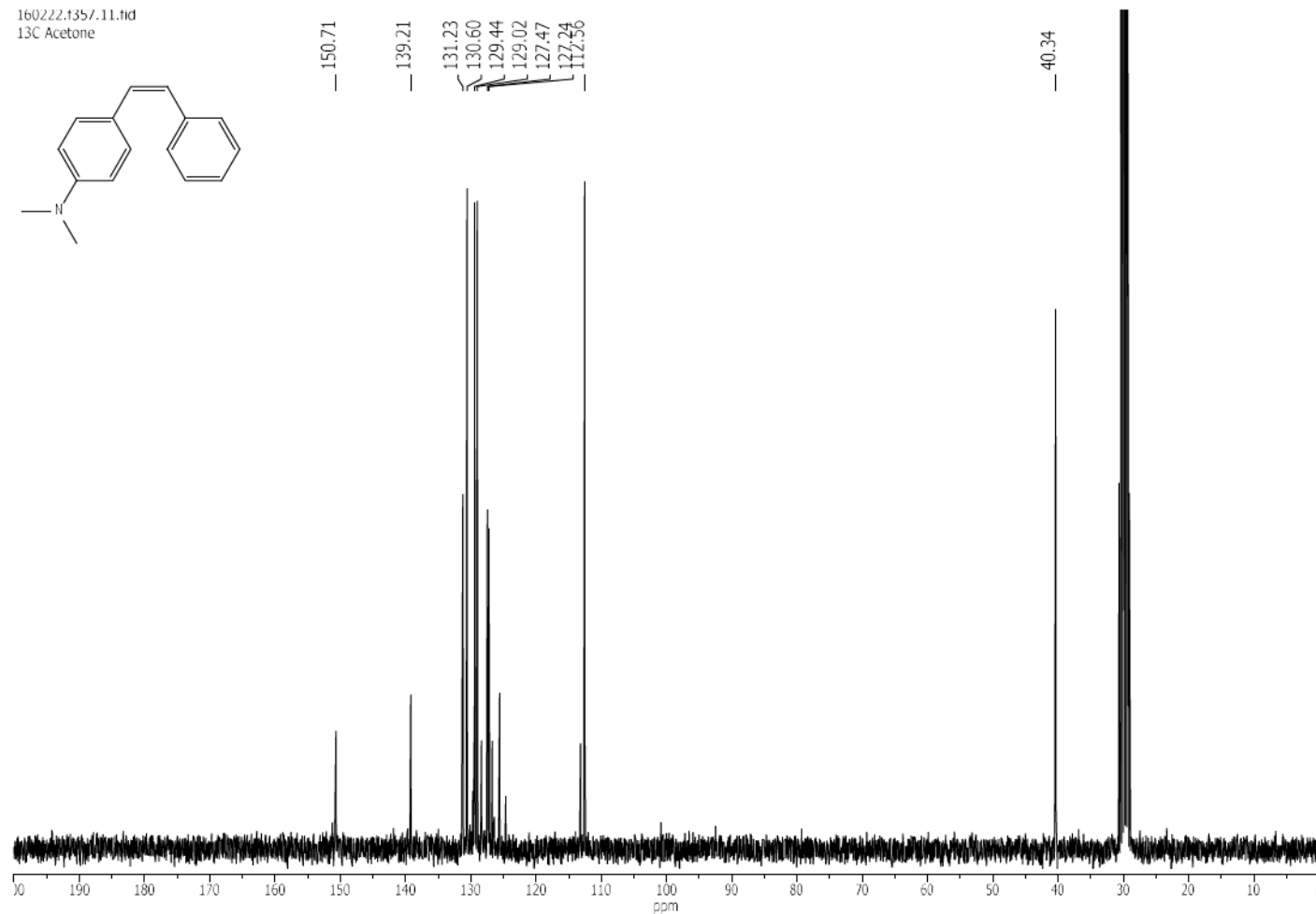
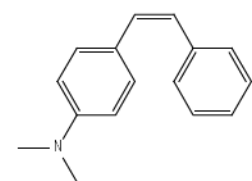
151204.330.13.fid
13C Acetone



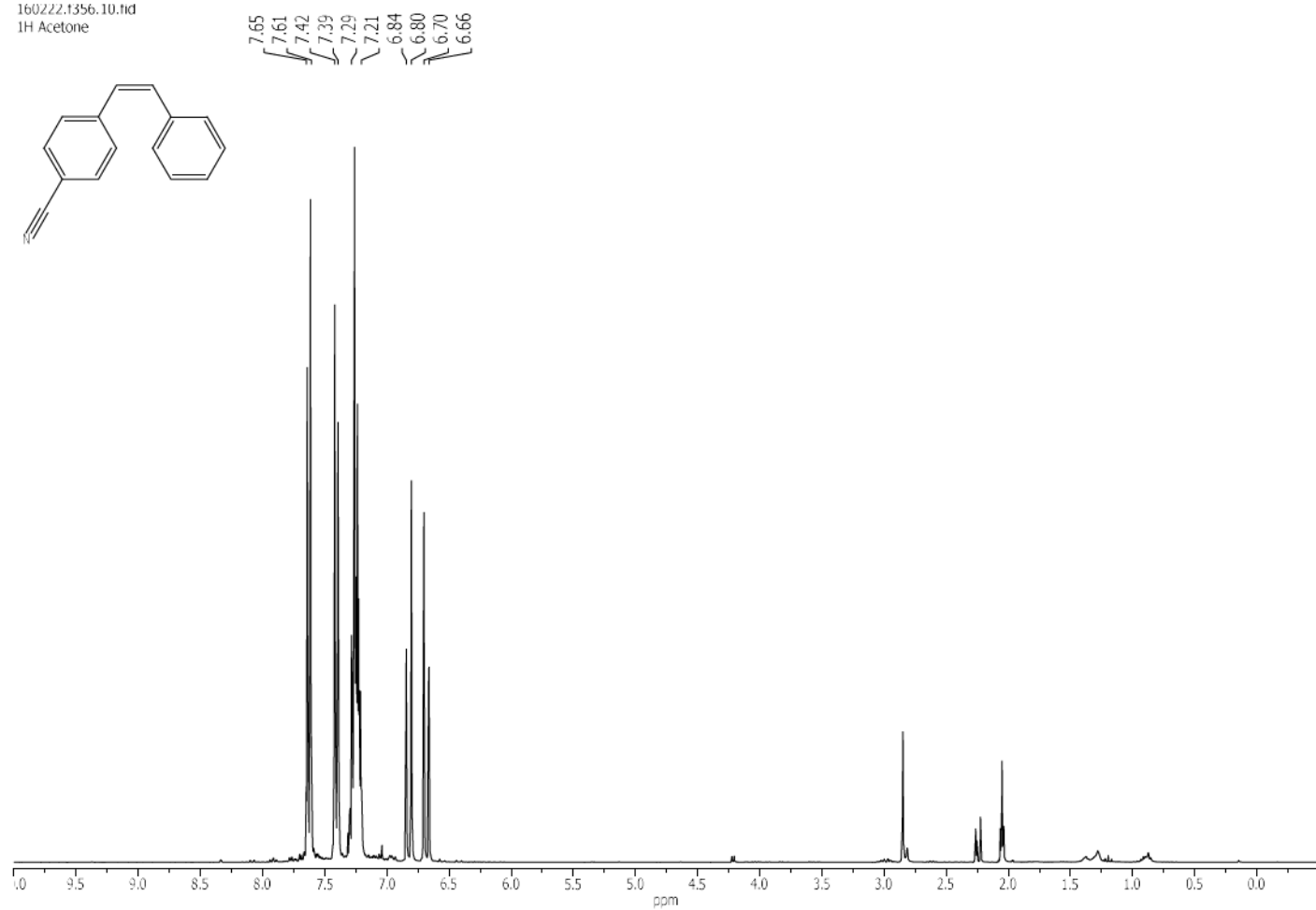
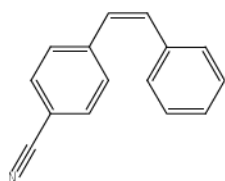
160222.1357.10.fid
1H Acetone



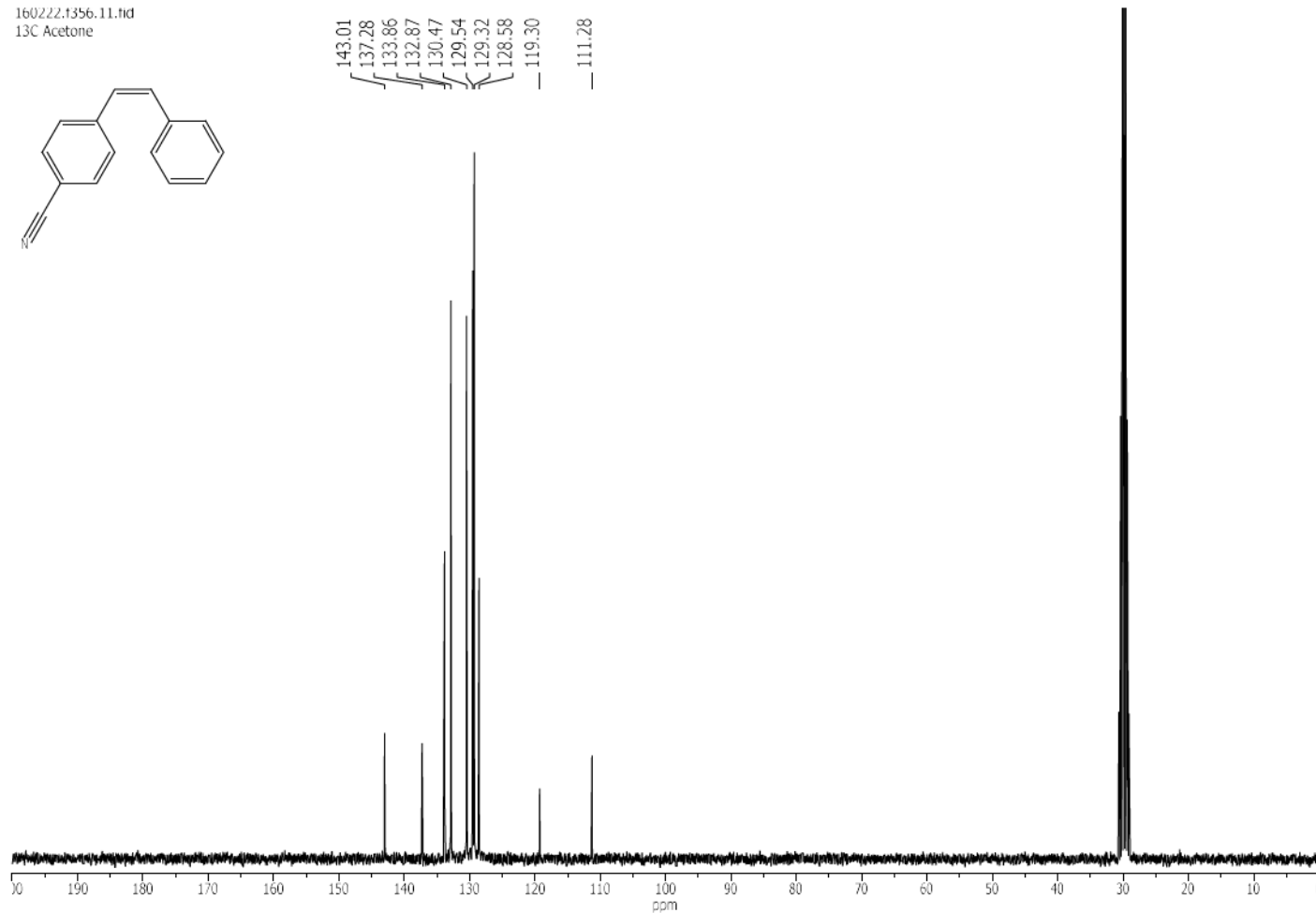
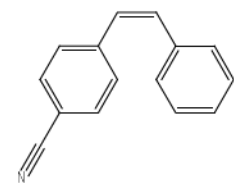
160222.1357.11.fid
13C Acetone



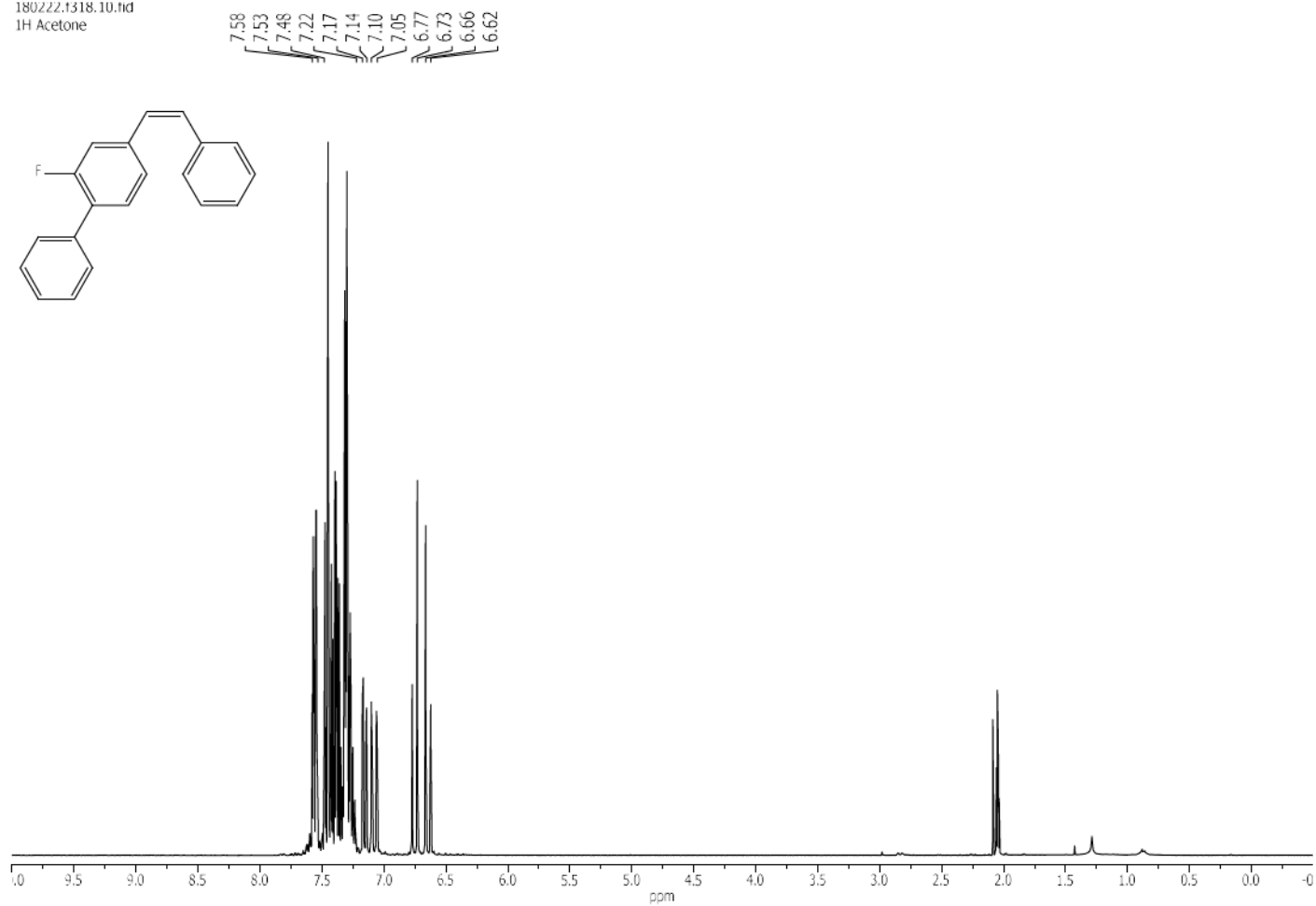
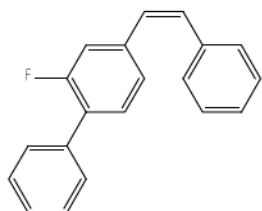
160222.1356.10.fid
1H Acetone



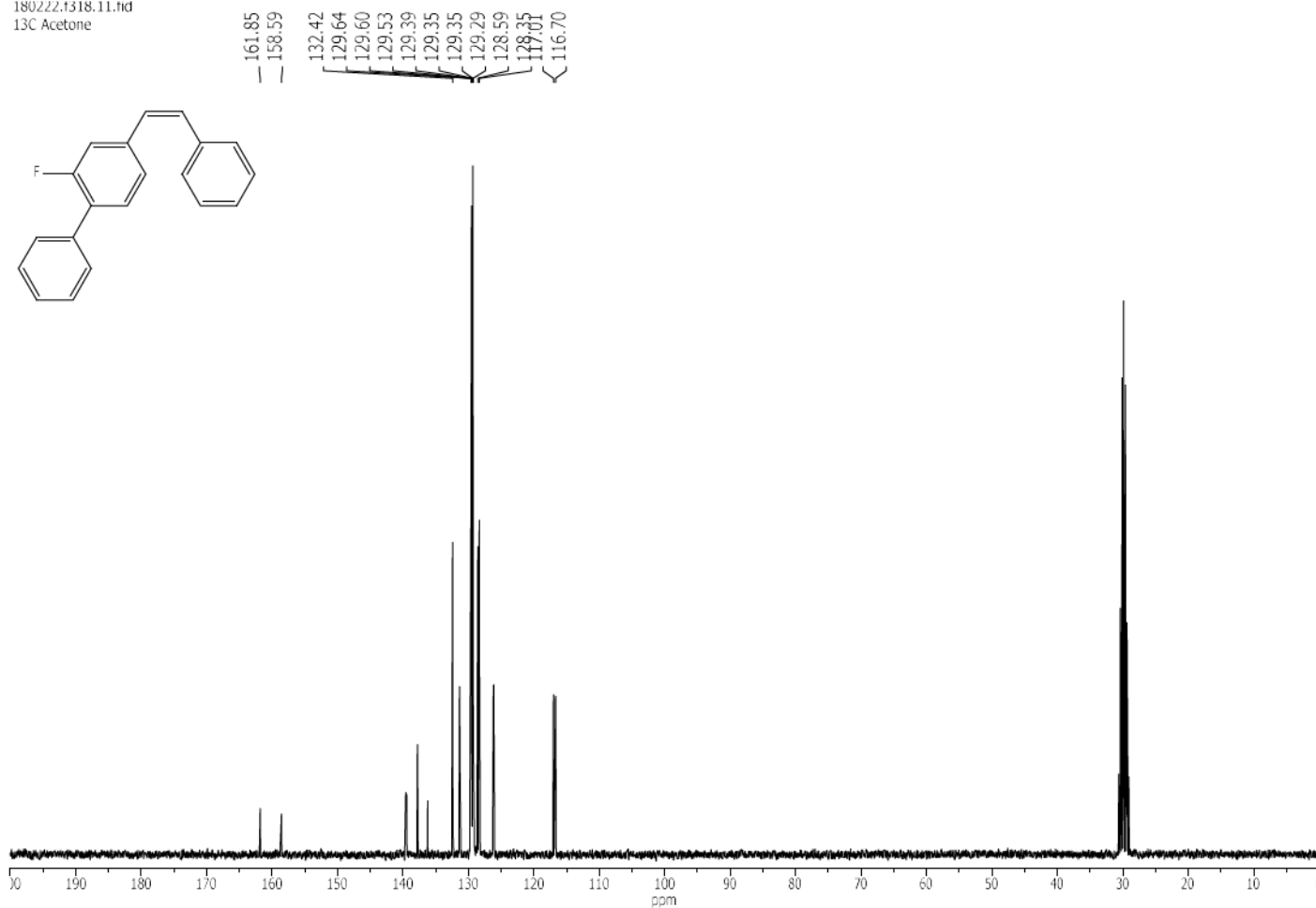
160222.1356.11.fid
13C Acetone



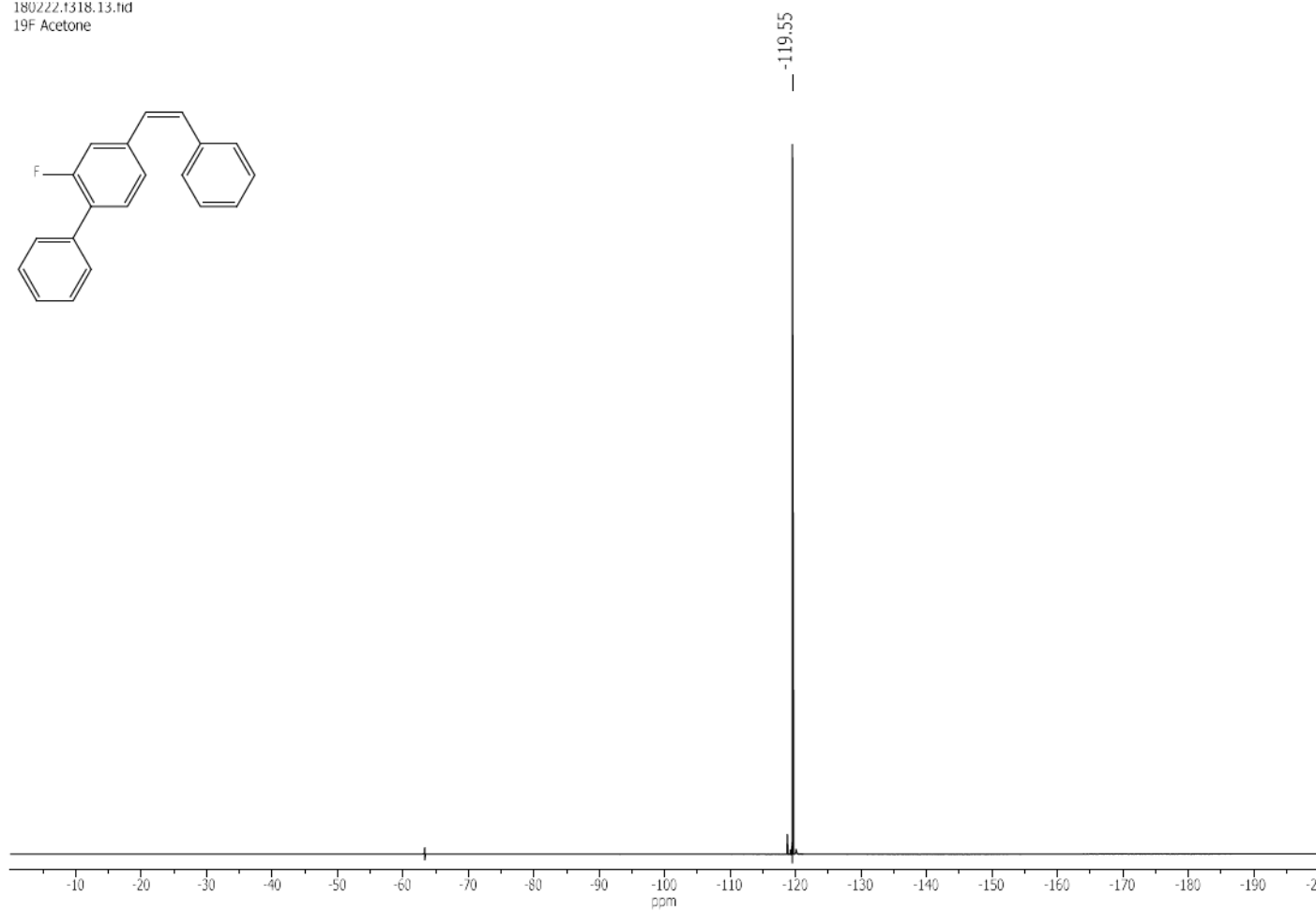
180222.1318.10.fid
1H Acetone



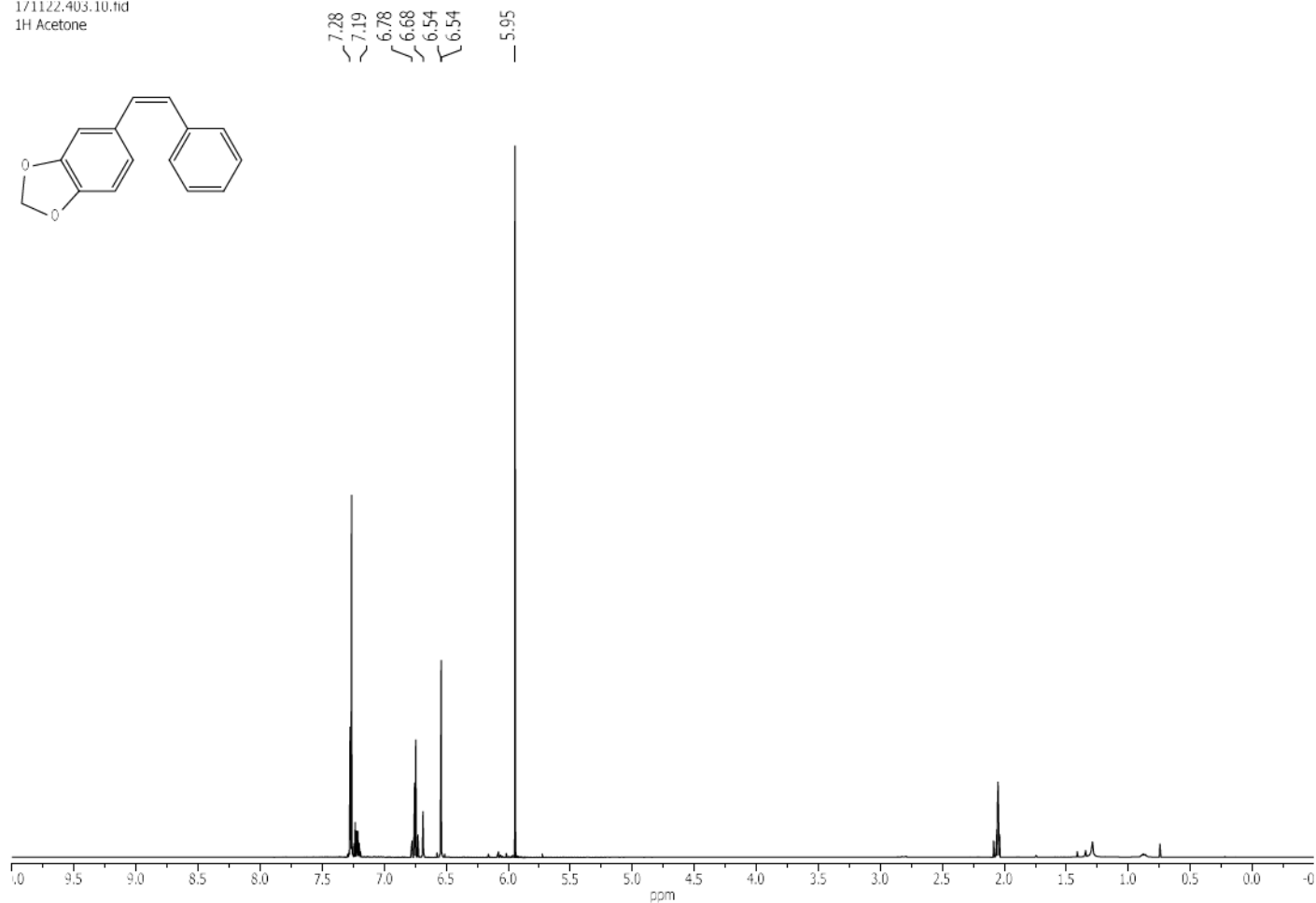
180222.1318.11.fid
13C Acetone



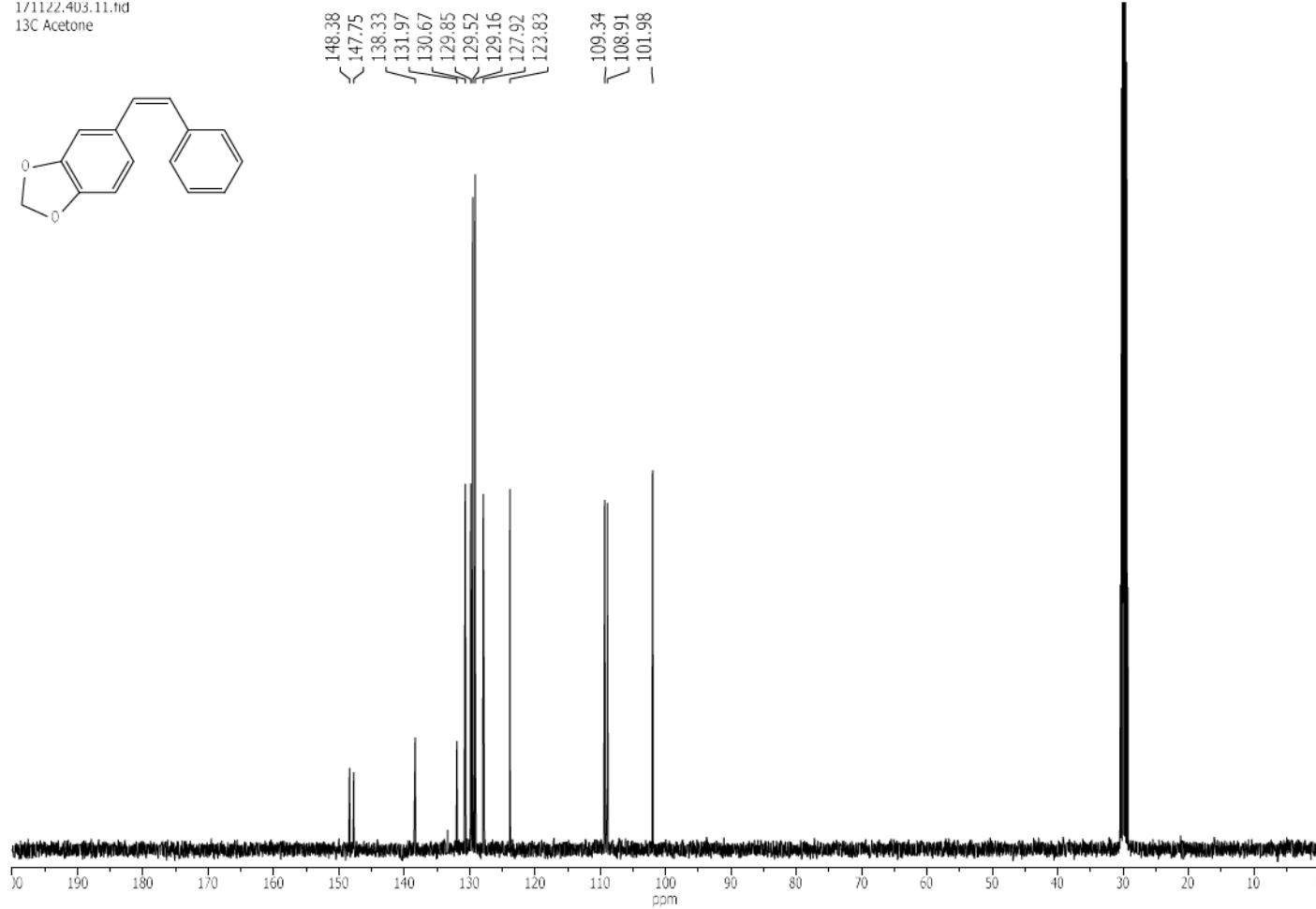
180222.1318.13.fid
19F Acetone



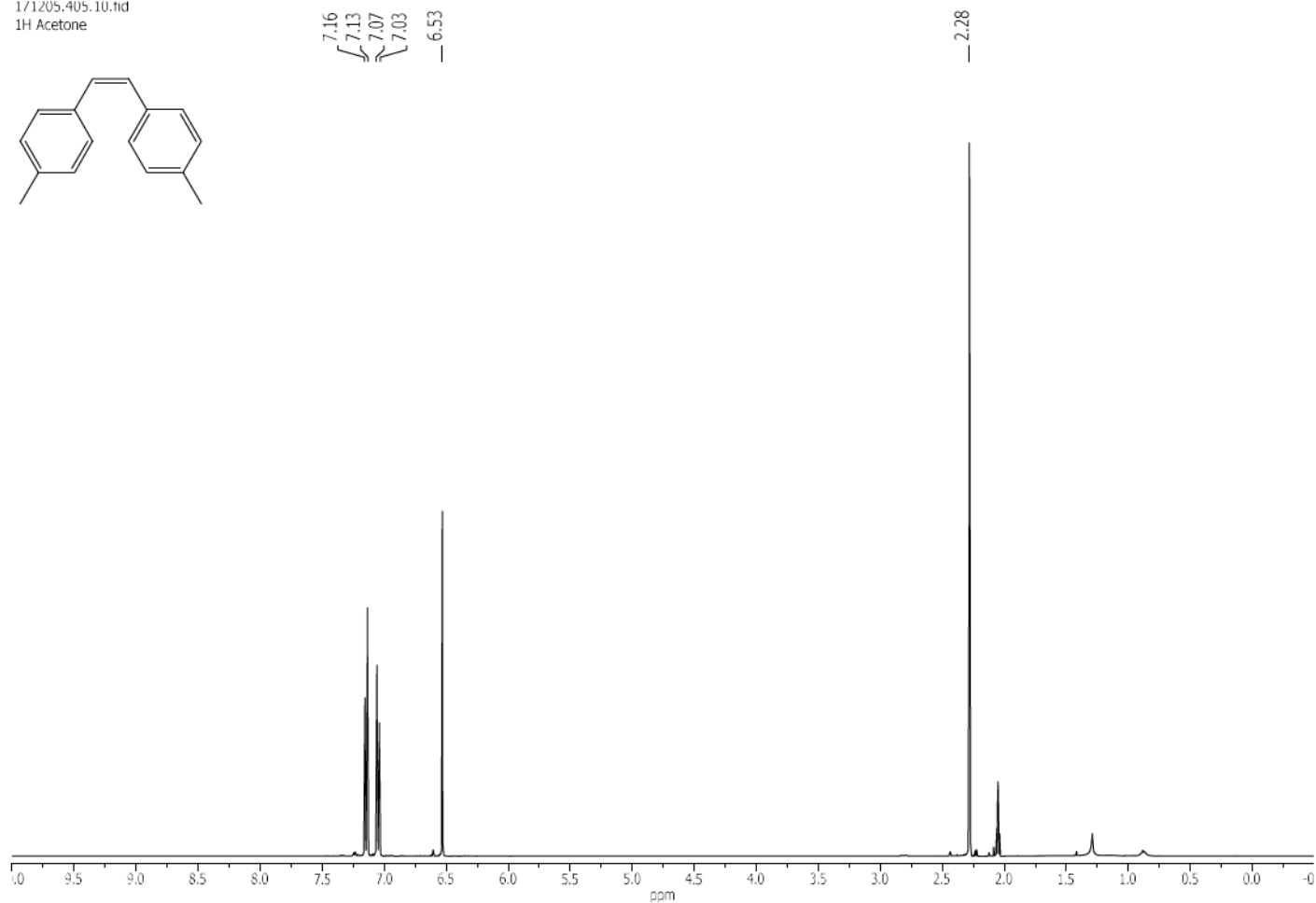
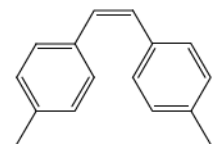
1/1122.403.10.tid
1H Acetone



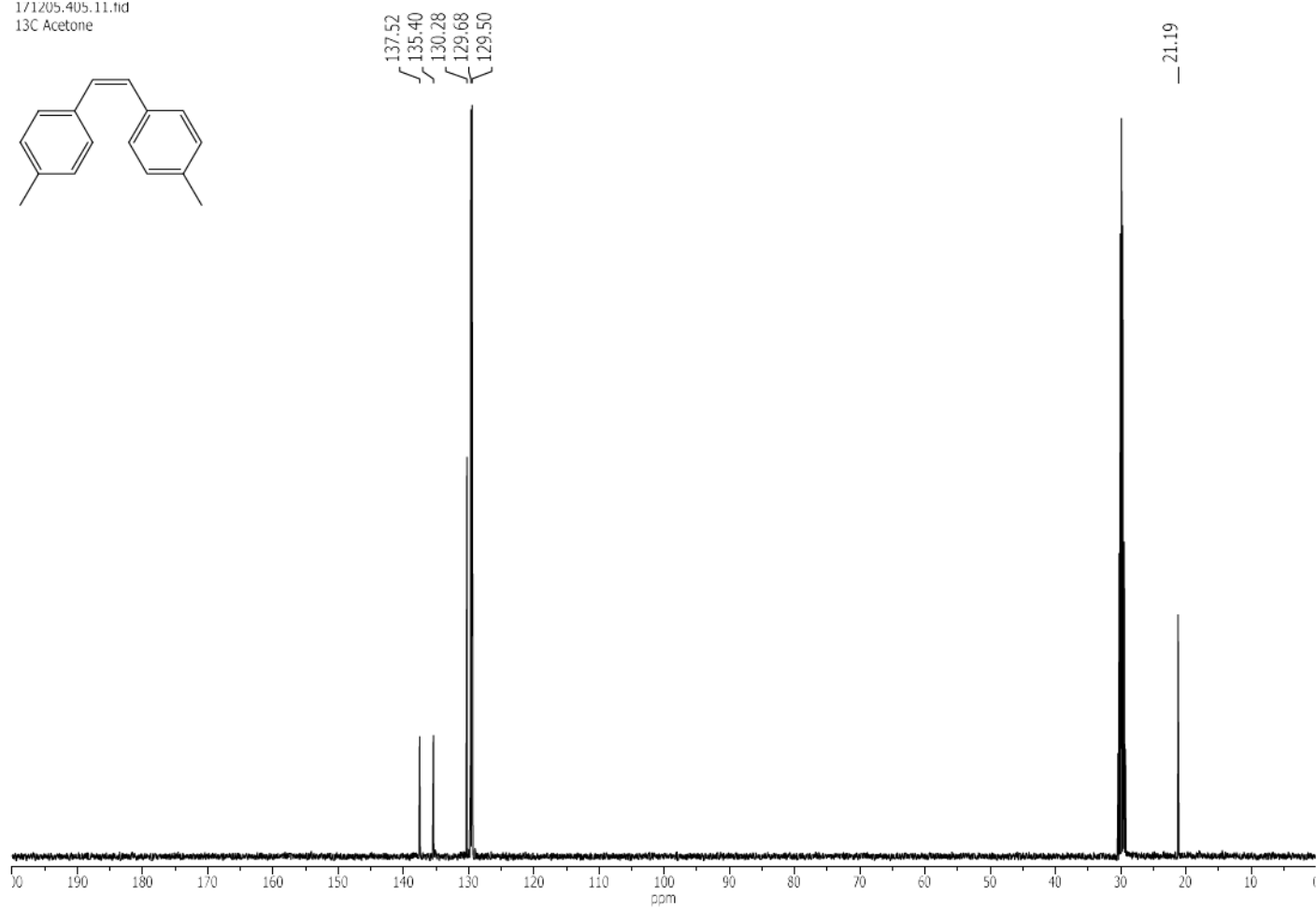
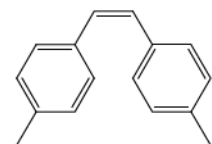
1/1122.403.11.tid
13C Acetone



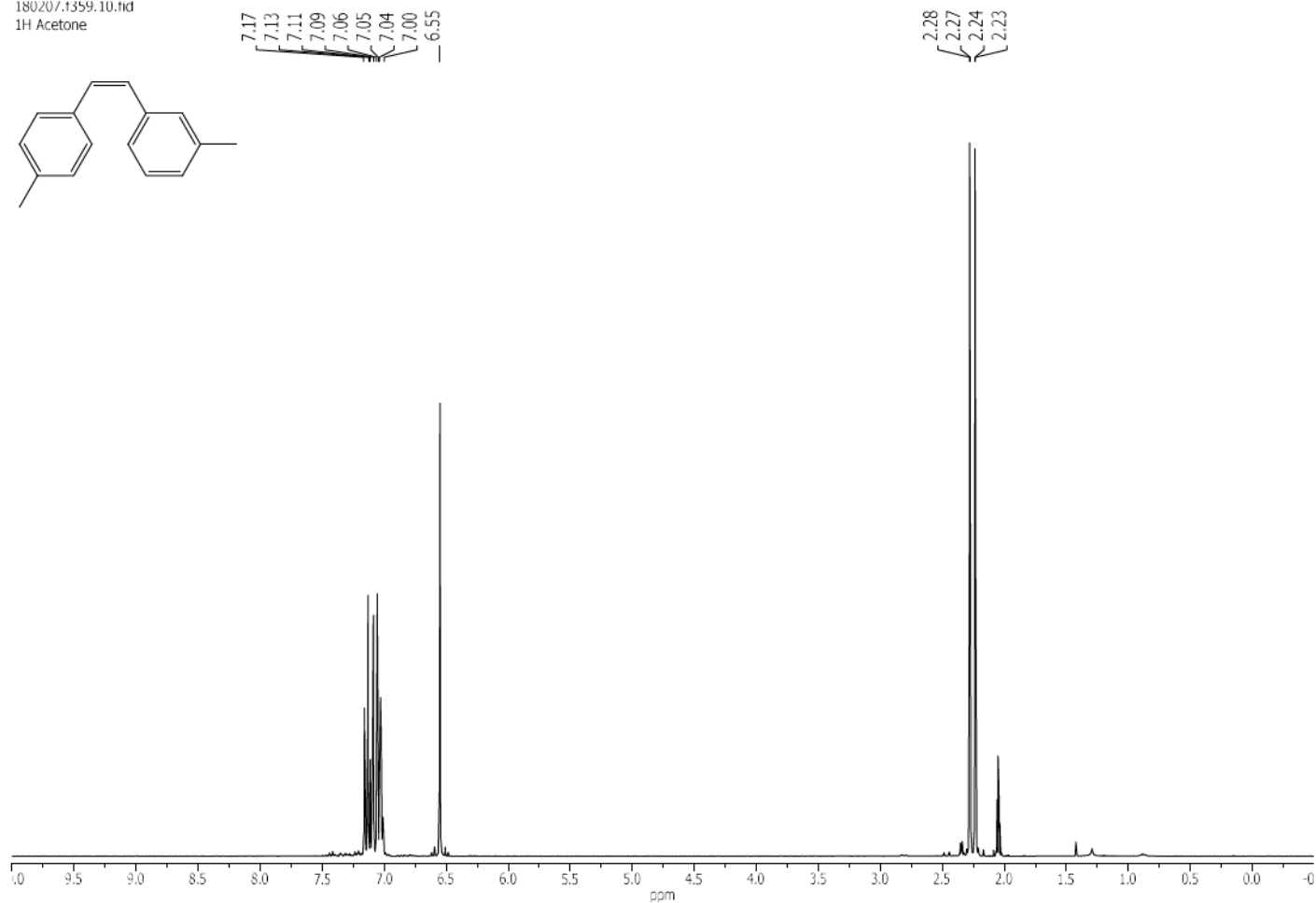
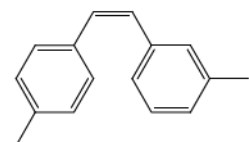
1/1205.405.10.tid
1H Acetone



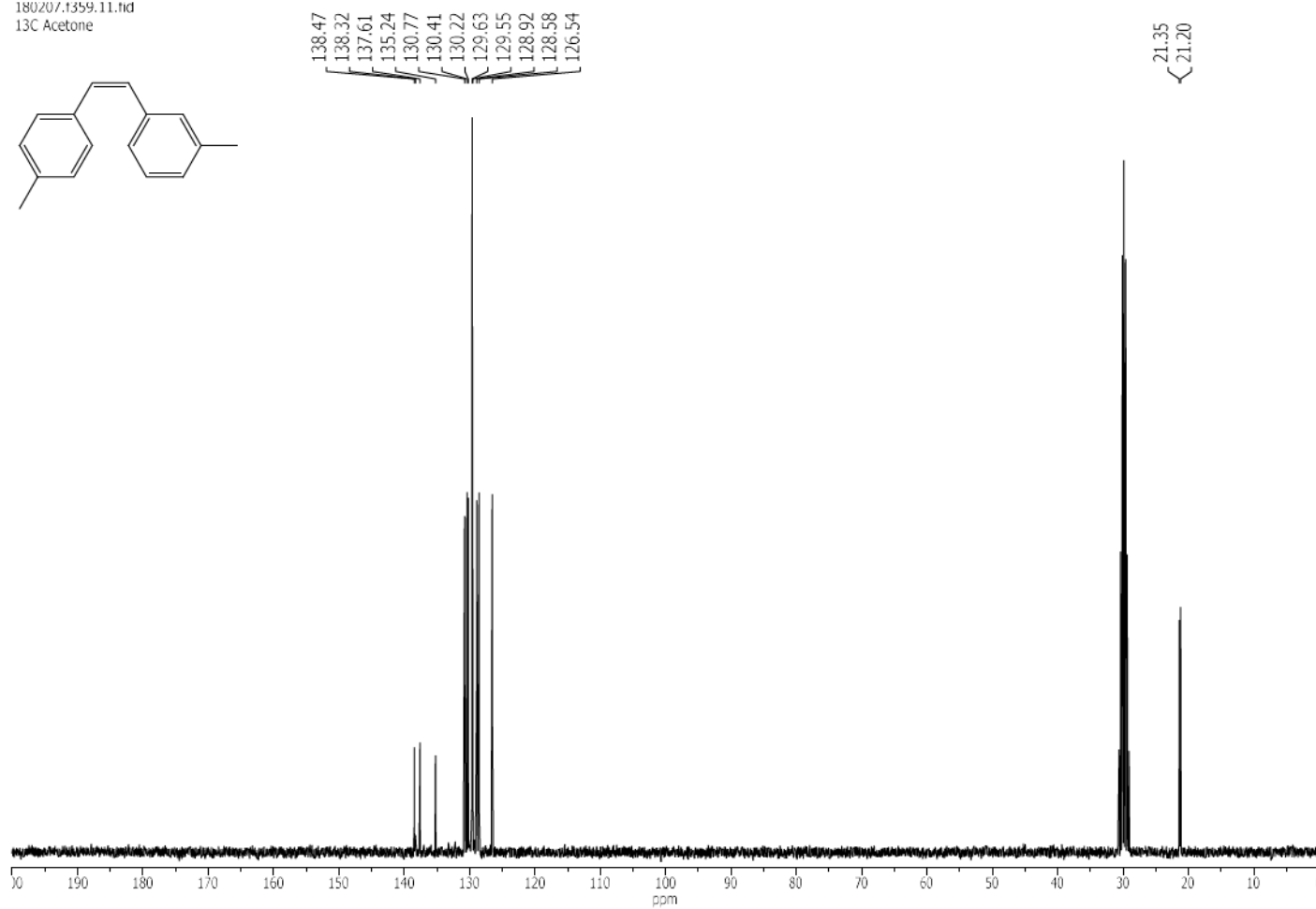
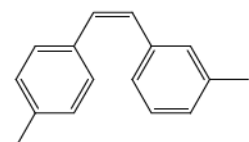
1/1205.405.11.tid
13C Acetone



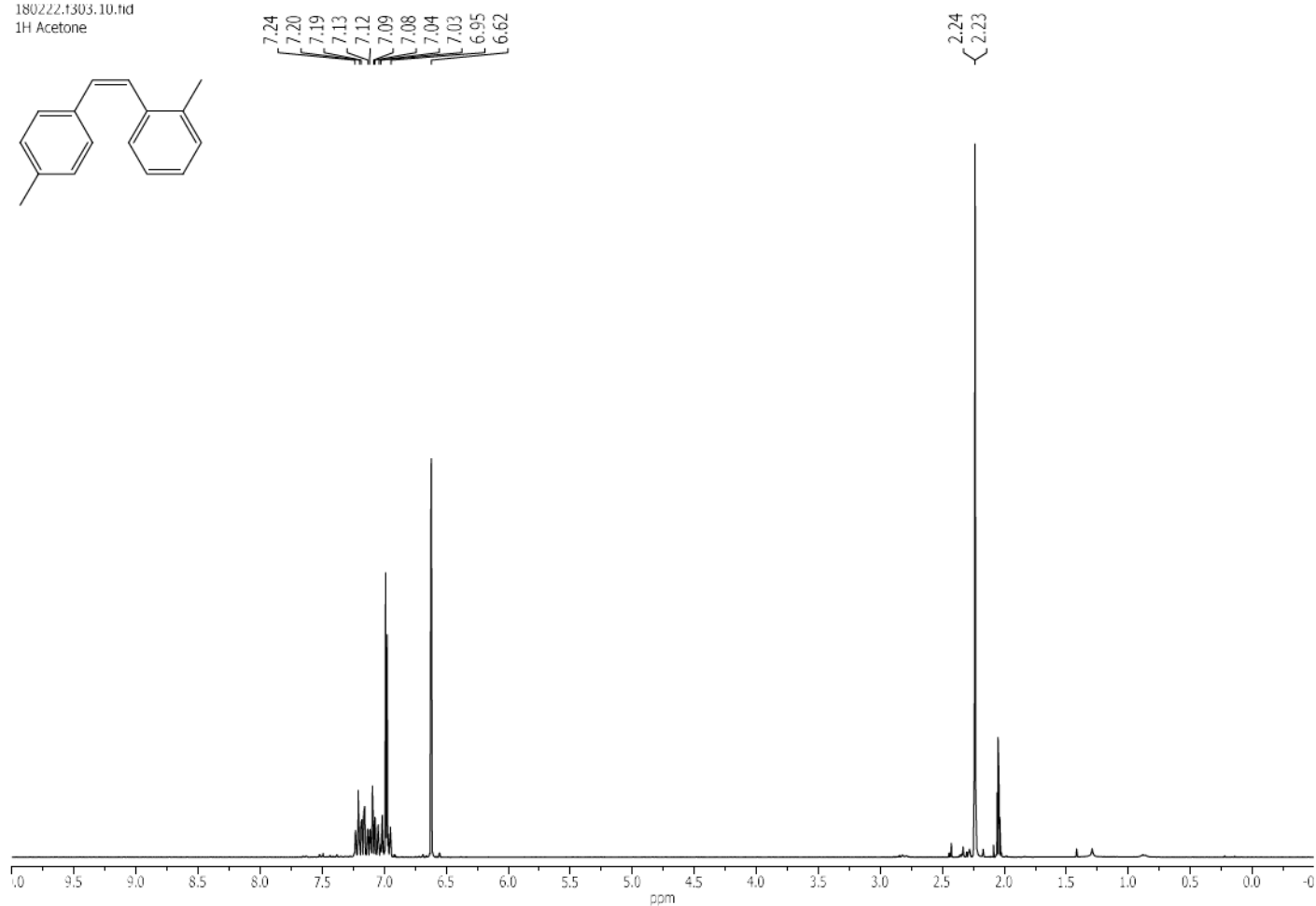
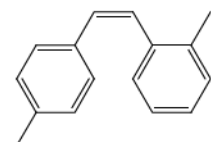
180207.1359.10.fid
1H Acetone



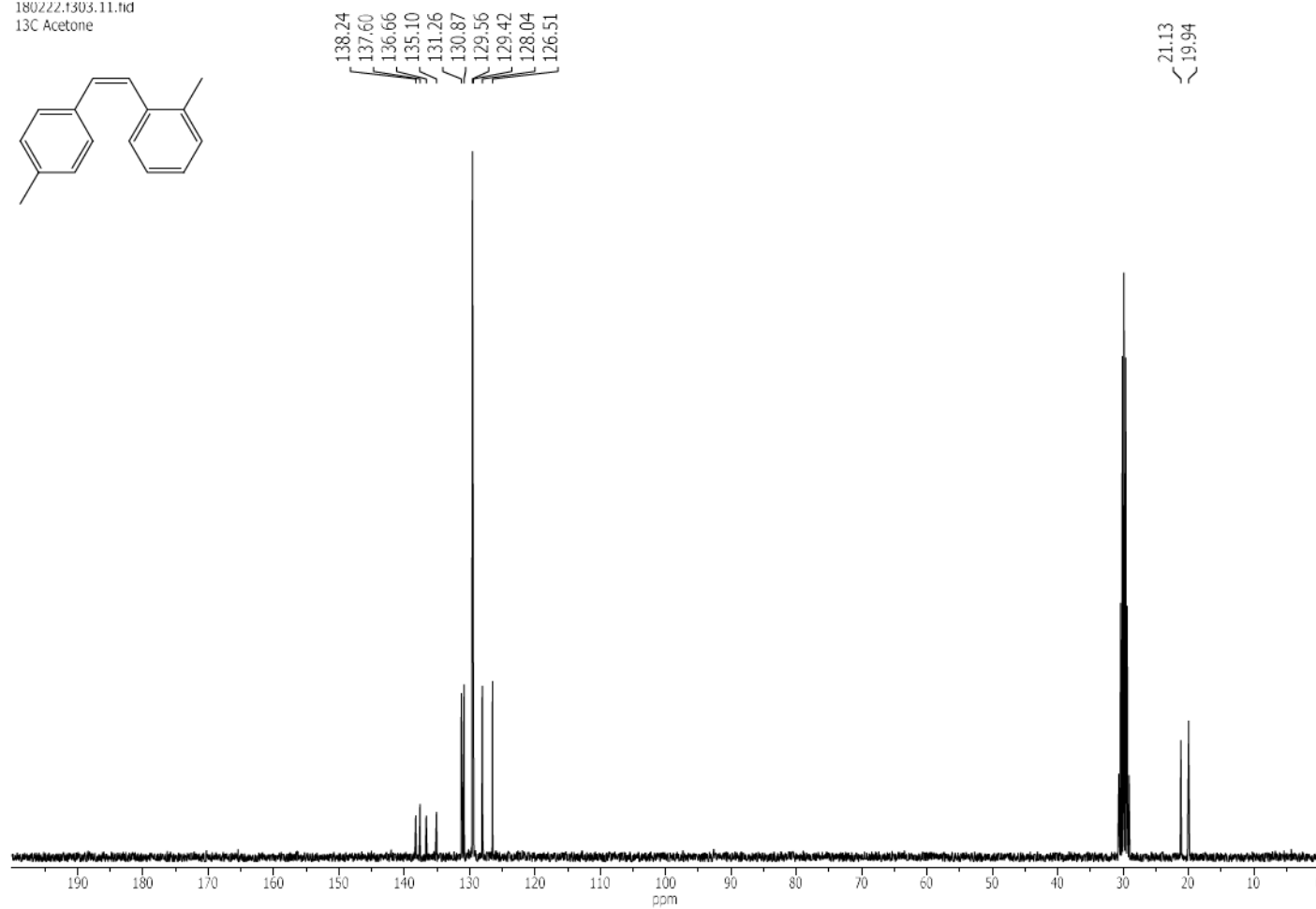
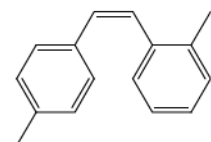
180207.1359.11.fid
13C Acetone



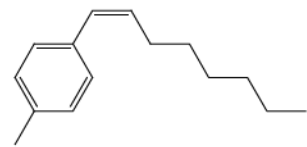
180222.1303.10.fid
1H Acetone



180222.1303.11.fid
13C Acetone



180320.1322.10.fid
1H Acetone



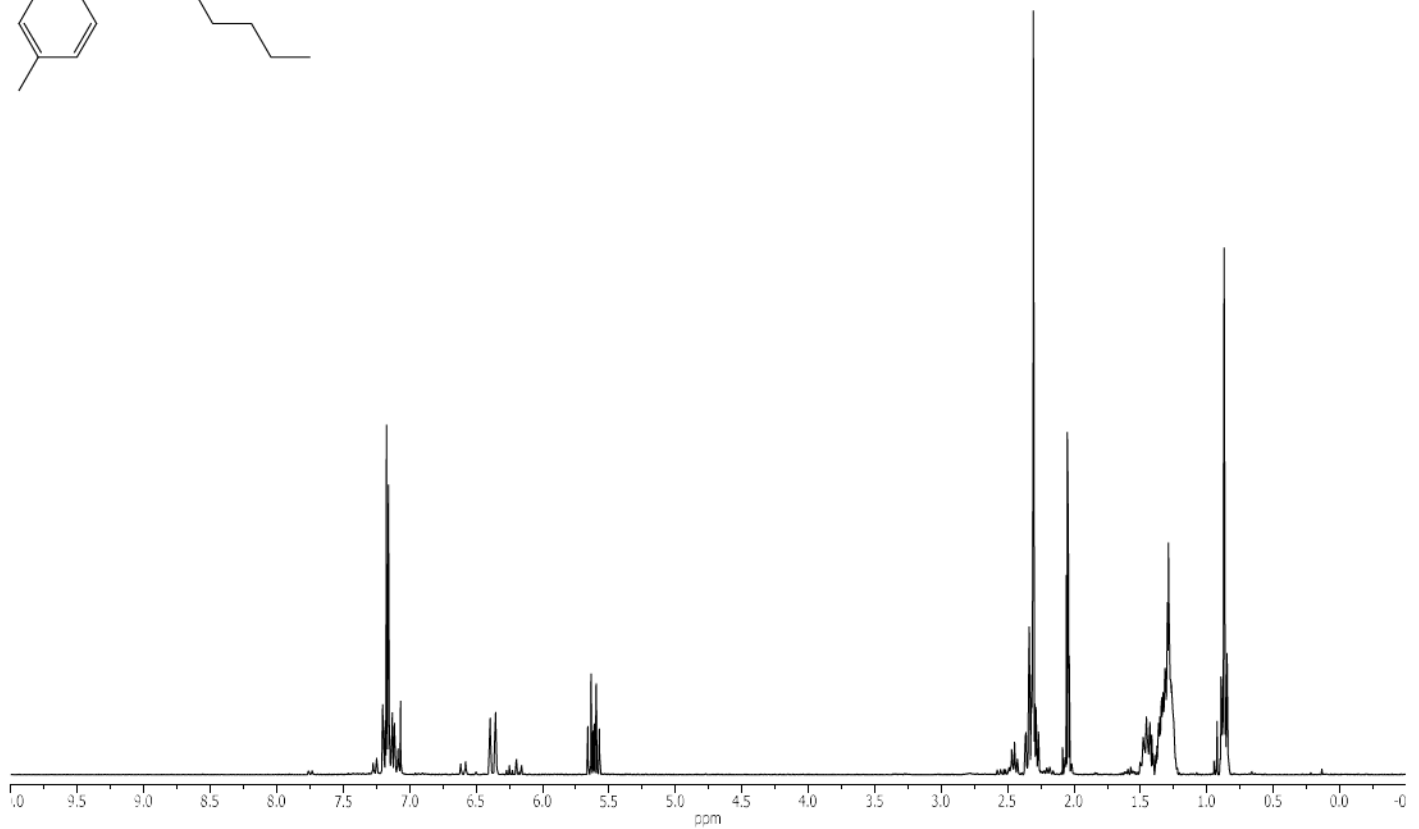
7.20
7.13

6.39
6.35

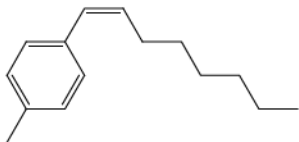
5.66
5.64
5.60
5.57

2.31

1.50
1.40
1.38
1.22
0.87

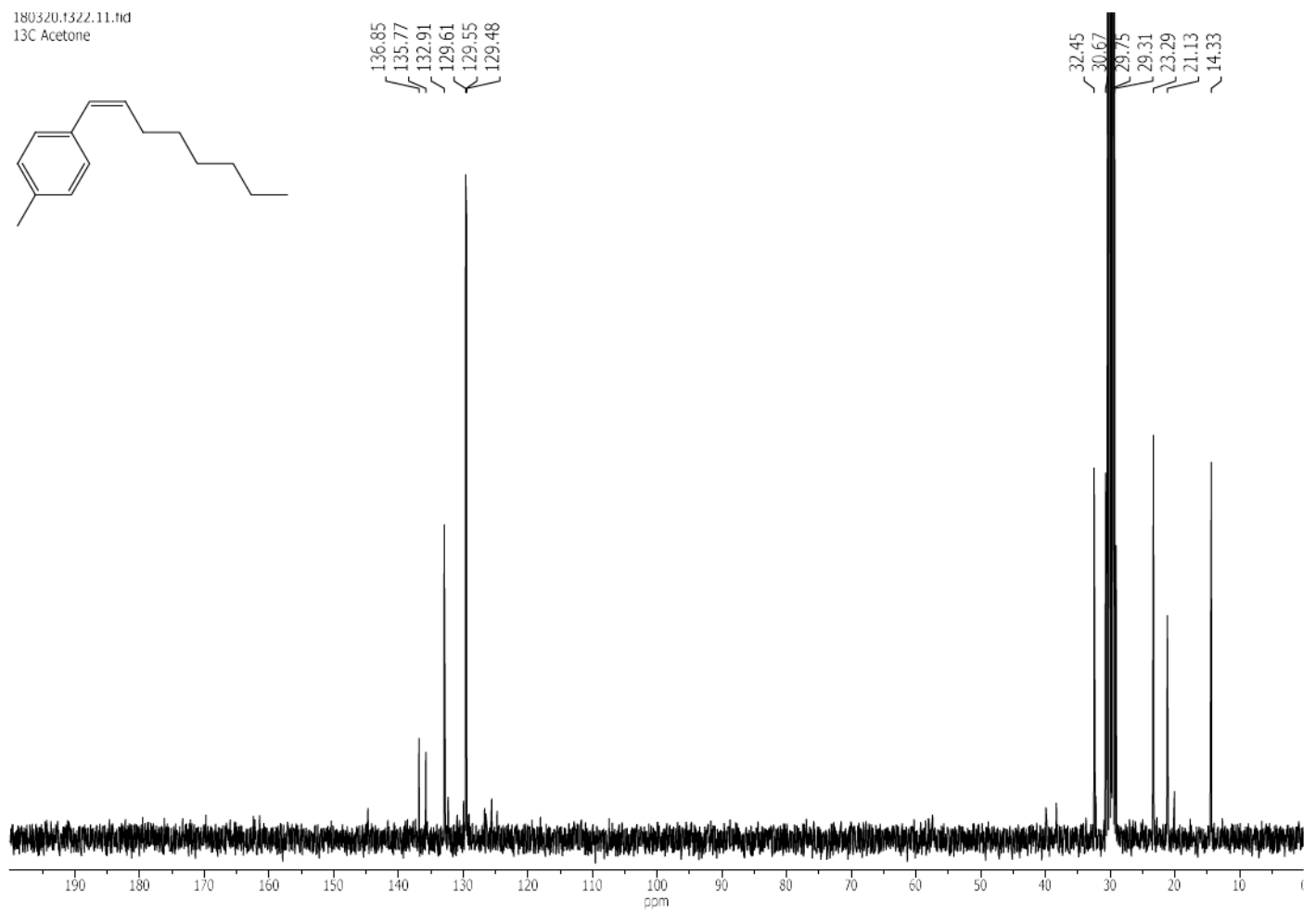


180320.1322.11.fid
13C Acetone

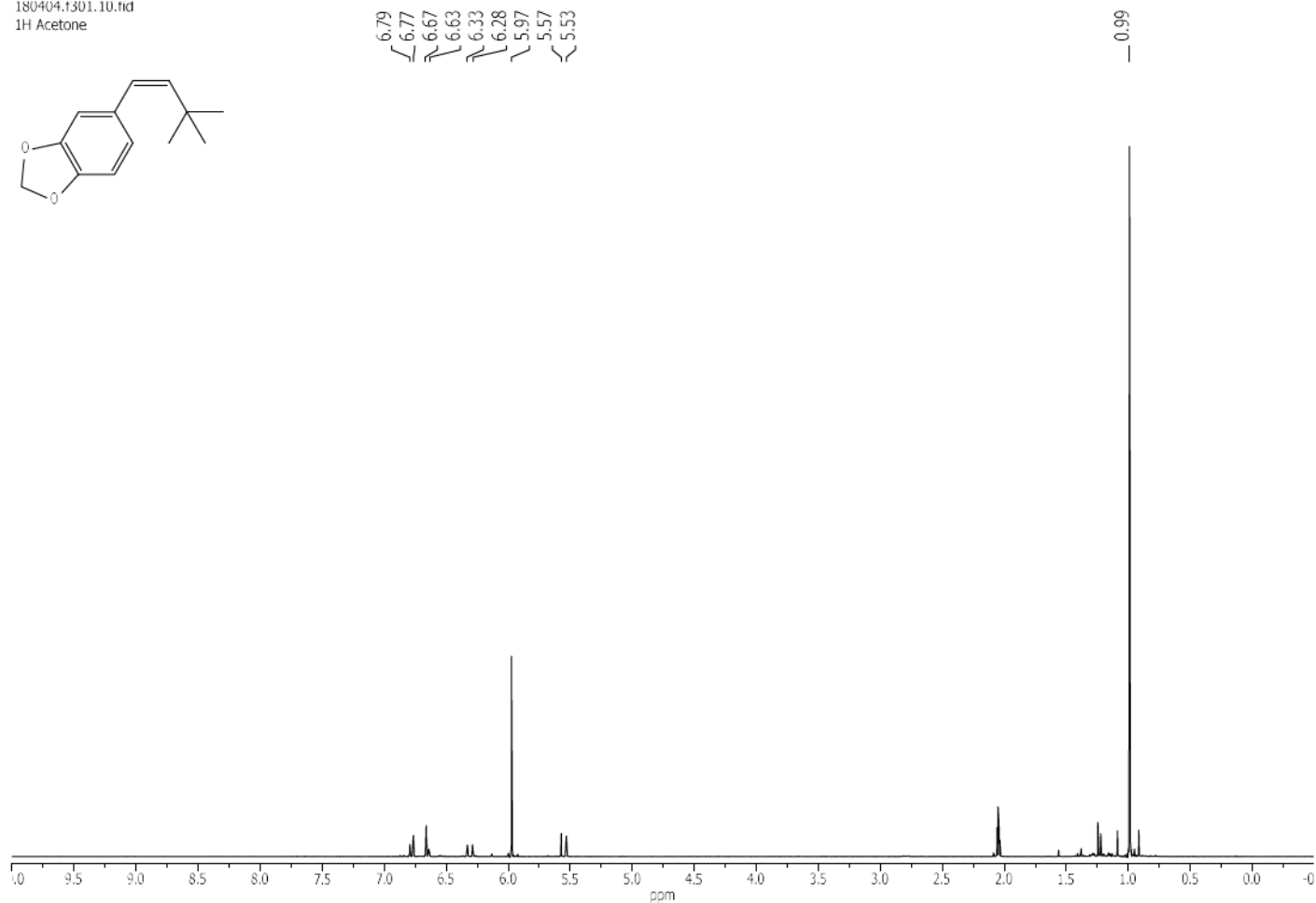
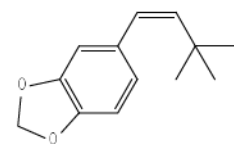


136.85
135.77
132.91
129.61
129.55
129.48

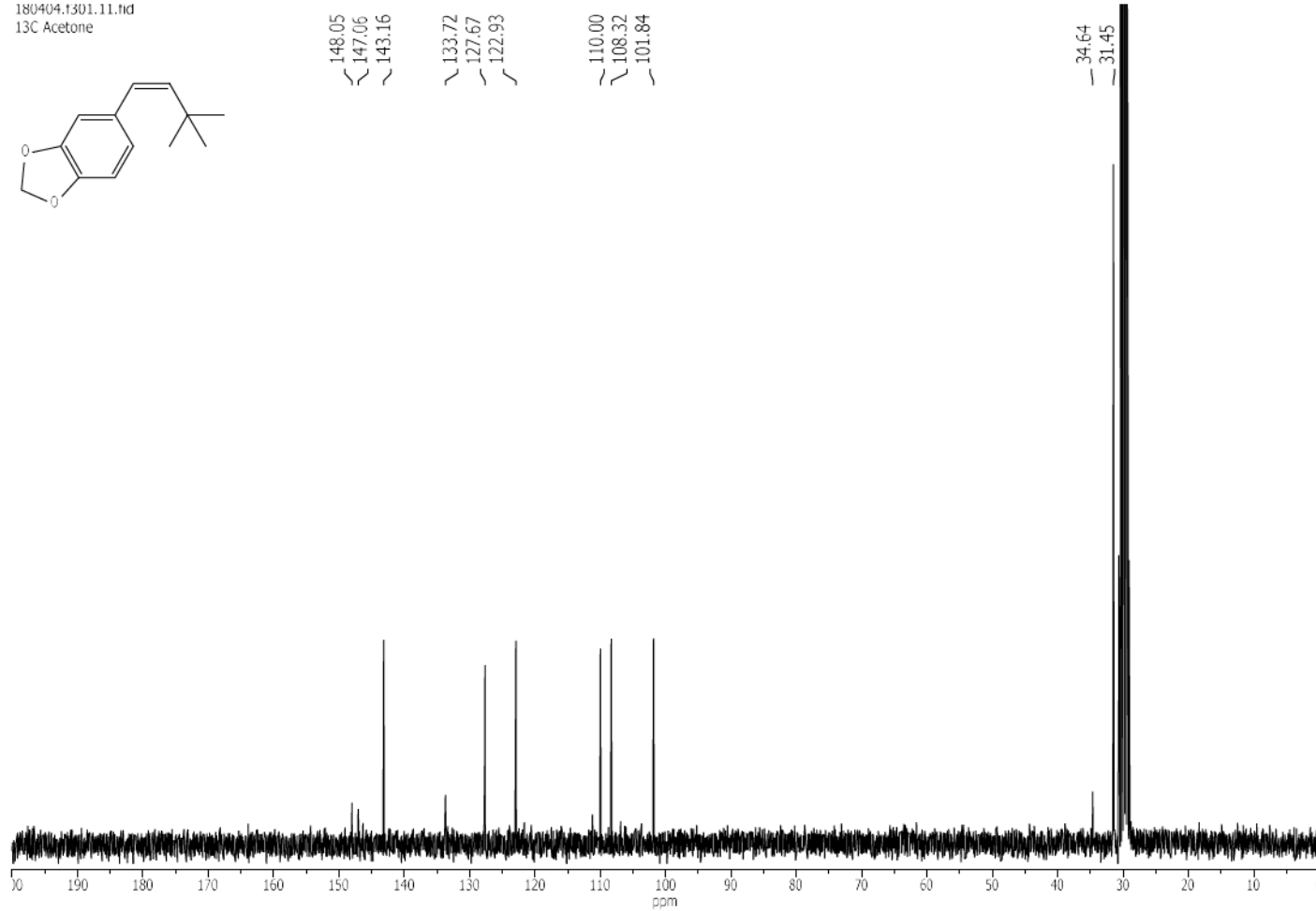
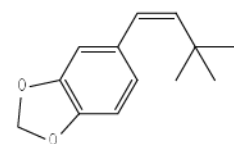
32.45
30.67
29.75
29.31
23.29
21.13
14.33



180404.1301.10.fid
1H Acetone



180404.1301.11.fid
13C Acetone



Analytical Instruments

NMR

- AV 400 (Bruker)
Build 2005, Magnetic field 9.4 Tesla, Proton-Resonance-Frequency 400 MHz.
- AV 300 (Bruker)
Build 2005, Magnetic field 7.0 Tesla, Proton-Resonance-Frequency 300 MHz.
- Fourier 300 (Bruker)
Build 2012, Magnetic field 7.0 Tesla, Proton-Resonance-Frequency 300 MHz.

HRMS

- Agilent 1200/6210 Time-of-Flight LC-MS

GC-MS

- Agilent HP-5890 with Agilent HP-5973 Mass Selective Detector (EI) and HP-5 capillary column

GC

- Agilent HP-5890 with FID detector and HP-5 capillary column

ICP-OES

- Varian/Agilent 715-ES

Flash chromatography

- Teledyne Isco CombiFlash R_f 200

Homogenous/Heterogeneous Catalysis

Development of a Palladium-Catalyzed Process for the Synthesis of Z-Alkenes by Sequential Sonogashira–Hydrogenation Reaction

Sören Hancker,^[a] Helfried Neumann,^[a] and Matthias Beller^{*[a]}

Abstract: A novel and selective sequential one-pot protocol for the synthesis of Z-alkenes via Sonogashira–semihydrogenation is reported. The efficiency of the methodology is increased by utilizing PdCl₂/BuPAD₂ as homogeneous catalyst for the Sono-

gashira coupling and subsequently transforming the transition metal complex into a heterogeneous Pd hydrogenation catalyst. This methodology represents one of the rare examples directly combining homogeneous and heterogeneous catalysis.

Introduction

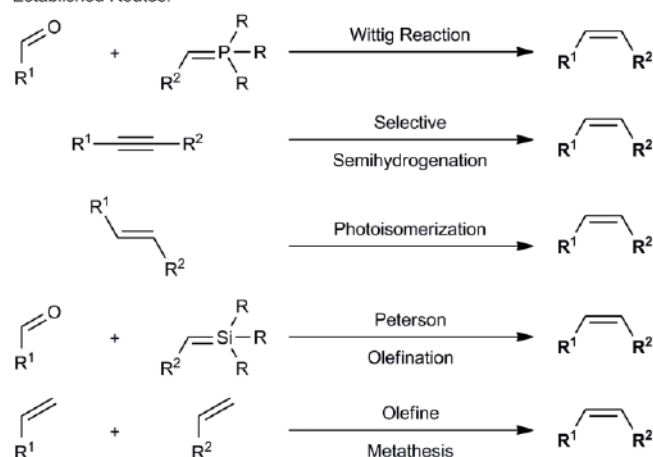
Catalysis represents a key technology for efficient and sustainable production in the chemical industry. In addition, academic laboratories and life science industries benefit from this well-established tool box for the synthesis of biologically active compounds and fine chemicals. Due to their respective advantages and disadvantages, both homogeneous and heterogeneous catalysts are applied in the manufacturing of numerous daily products.^[1] Traditionally, due to superior reusability and recyclability heterogeneous catalysts are favored for the synthesis of bulk chemicals. On the other hand, the demand for high selectivity and activity under mild conditions benefits the application of molecularly-defined homogeneous catalysts, specifically in the field of fine chemicals and specialties. However, in recent years there has been an increasing interest to develop more active and selective heterogeneous catalysts to overcome the conventional disadvantages of such materials while sustaining the benefits.^[2] Among other approaches, we and other groups demonstrated that the pyrolysis of distinct molecular complexes adsorbed on inorganic materials generates doped metal centers embedded into the support as catalytically active sites, which constitute highly efficient heterogeneous catalysts.^[3]

Interestingly, beside from this current approach, the methodology of utilizing a homogeneous complex for an initial chemical transformation prior to converting it into a heterogeneous material which is active in a sequential reaction step has been reported as early as 1994.^[4] Notably, this strategy turned the synthesis of the agrochemical Prosulfuron into an economically feasible process.^[5] Surprisingly, despite this success, this concept has rarely been applied in other areas.^[6]

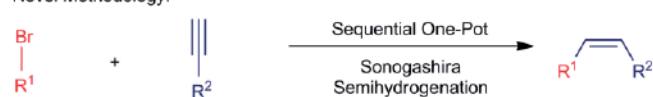
Inspired by all these reports, we present a new methodology for the selective synthesis of Z-alkenes including homogeneous and heterogeneous palladium catalyzed transformations. As an initial step, a Sonogashira reaction is performed followed by hydrogenation of the resulting alkyne catalyzed by a heterogeneous catalyst formed from the initially homogeneous metal complex. The resulting structural motif is found in various biologically active compounds and represents a valuable building block for organic syntheses.^[7]

In general, Z-alkenes are synthesized sequentially from the corresponding internal acetylene by hydrogenation (Scheme 1). For this second step, specific hydrogenation catalysts such as the Lindlar catalyst are typically used.^[8] In recent years other heterogeneous materials have been developed based on both

Established Routes:



Novel Methodology:



Scheme 1. Selected routes for the synthesis of Z-alkenes.

[a] Leibniz-Institut für Katalyse e.V. an der Universität Rostock,
Albert-Einstein-Straße 29a, 18059 Rostock, Germany
E-mail: Matthias.Beller@catalysis.de
www.catalysis.de

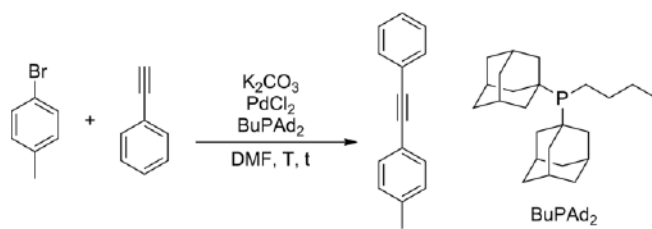
Supporting information and ORCID(s) from the author(s) for this article are available on the WWW under <https://doi.org/10.1002/ejoc.201800651>.

noble metals,^[9] and other transition metals.^[10] More traditionally, starting from aldehydes and phosphonium ylides, the Wittig reaction constitutes a stoichiometric approach leading to almost exclusively Z-alkenes under optimized conditions.^[11] The related Peterson olefination is another approach towards Z-alkenes.^[12] Herein, aldehydes are reacted with α -silyl carbanions followed by an acidic or basic work-up which determines the stereoselectivity. Furthermore, Z-alkenes can be synthesized by photoisomerization of E-alkenes.^[13] Finally, alkene metathesis provides access to Z-alkenes starting from easily available terminal olefins.^[14] However, the selectivity of this C–C bond forming transformation remains challenging especially for intermolecular reactions.

Results and Discussion

For our initial investigations, the reaction of 4-bromotoluene (**1**) and phenylacetylene (**2**) to give phenyl-*p*-tolyl-acetylene (**3**) was chosen as model system. Previously, it was shown that the combination of PdCl₂/BuPAd₂ with K₂CO₃ in DMF catalyzes Sonogashira reactions without the need of further additives (Cu salts, amines).^[15] Initially, the influence of the reaction temperature was evaluated applying this system. Even at room temperature, the reaction reached 68 % conversion and 65 % yield. However, 4 days were required and significant amounts of both starting materials remained unconverted (Table 1, entry 1).

Table 1. Optimization of the copper- and amine-free Sonogashira reaction.



Entry ^[a]	2 [mmol]	Pd/L [mol-%]	T [°C]	t [h]	Conversion ^[b,c] [%]	Yield ^[c] [%]
1	1	4:6	25	96	68	65
2	1	4:6	40	24	> 99	82
3	1	4:6	60	4	> 99	78
4	1.5	4:6	60	4	> 99	67
5 ^[d]	0.6	4:6	60	6	88 ^[e]	70
6	1	2:2	60	16	> 99	84
7	1	1:1	60	16	> 99	88
8 ^[d]	0.6	1:1	60	16	67 ^[e]	61
9	1	1:1	60	8	90	80
10	1	0.5:0.5	60	16	90	81
11	1	0.1:0.1	60	16	66	60
12	1	0:1	60	16	< 1	< 1
13	1	1:0	60	16	< 1	< 1

[a] Standard conditions (Entry 7): 0.5 mmol **1**, 1 mmol **2**, 1 mmol K₂CO₃, 1 mol-% PdCl₂, 1 mol-% BuPAd₂, 2 mL of DMF at 60 °C for 16 h. [b] Regarding **1**. [c] Determined by GC with hexadecane as internal standard. [d] **2** was dissolved in 1 mL of DMF and added continuously over the first 2 h of the experiment. [e] Conversion of **2**: > 99 %.

Simply increasing the temperature to 40 °C led to full conversion of the aryl bromide and 82 % of **3** were obtained after 24

hours (entry 2). At 60 °C, complete conversion was achieved after only 4 hours while the reaction provided 78 % of the desired compound (entry 3). Despite the decreased selectivity, the ongoing optimization was conducted at 60 °C due to the increased reaction rate and the desire to further lower the catalyst loading. Furthermore, the effect of the acetylene concentration was investigated since the complete consumption of **2** was observed in several experiments. Noteworthy, the yield further declined to 67 % when 3 equivalents of phenylacetylene were employed (entry 4).

The selectivity remained at 80 % compared to entries 2 and 3 when 1.2 equivalents were applied by adding the reagent continuously over a period of two hours (entry 5). However, significant amounts of the aryl bromide were detected while **2** was completely converted after the reaction. Upon reducing the catalyst and ligand loading to 2 mol-%, 84 % of the desired product was obtained (entry 6). Notably, the selectivity towards the internal acetylene was improved when lower catalyst loadings were applied (entries 6–13). Accordingly, the selectivity improved to 88 % at full conversion when 1 mol-% of the catalyst was utilized (entry 7). Attempts to decrease the necessary concentration of **2** resulted in lower product yields (entries 5 and 8). As expected lower catalyst loadings require longer reaction times since a conversion of 90 % was observed after 8 hours (entry 9). The necessity for longer reaction times under low catalyst loadings was emphasized by experiments applying 0.5 mol-% or 0.1 mol-% catalyst (entries 10 and 11). While the selectivity remained high, the conversion decreased to 90 % and 66 %, respectively. The control experiments proved that the palladium salt as well as the ligand is required for a successful reaction since the absence of either one of these compounds prevented the formation of the product (entries 12 and 13).

Next, different hydrogen sources were tested for the selective hydrogenation of **3**. Applying our catalytic system, hydrides, formic acid and alcohols failed to generate the product, whereas hydrogen gas afforded full conversion of the internal acetylene **3**. For the implementation of hydrogen, the reaction mixture was heated to 120 °C for 8 hours before the solution was cooled down to room temperature. Subsequently, hydrogen gas was bubbled through the reaction mixture for a specific time at 25 °C. The reaction provided full conversion, but no Z-alkene was detected after 150 min (Table 2, entry 1). Instead, quantitative amounts of the alkane (**6**) emerged as the reaction product. After a hydrogenation time of 80 min, 33 % of the desired product **4** was obtained, but the Z-selectivity and Z/E-ratio remained at low levels (entry 2). These parameters were further improved as the reaction time was decreased to 40 min (entry 3). Herein, the Z-selectivity was increased to 80 % at complete conversion and Z/E-ratio of 80:8. However, a hydrogenation period of 20 min gave the best result including 91 % overall yield at Z/E-ratio of 91:6 (entry 4). Experiments to further decrease the reaction time proved that the generation of the desired Z-alkene remained uncompleted as only 60 % of the desired Z-alkene was obtained (entry 5). Noteworthy, modifying the initial reaction step led to a decrease in the hydrogenation activity. In this case, the yields dropped to 38 % and 14 % after 20 min of hydrogenation when the first phase was reduced to

Table 2. Optimization of the selective-semihydrogenation.

Entry ^[a]	<i>t</i> ₁ [h]	<i>t</i> ₂ [min]	Conversion ^[b,c] [%]	Yield ^[c] 4 [%]	Z/E-Ratio ^[c] [%: %]	Z-Selectivity ^[d] [%]	Yield ^[c] 6 [%]
1	8	150	> 99	< 1	< 1:9	< 1	88
2	8	80	> 99	33	33:9	33	55
3	8	40	> 99	80	80:8	80	11
4	8	20	> 99	91	91:6	91	3
5	8	10	60	51	51:5	85	3
6	4	20	46	38	38:4	83	2
7	2	20	21	14	14:3	67	2

[a] Standard conditions (Entry 4): 0.5 mmol **3**, 1 mmol K₂CO₃, 1 mol-% PdCl₂, 1 mol-% BuPAD₂, 2 mL of DMF, 0.2 mL of H₂O at 120 °C for 8 h. Subsequently, hydrogen gas was bubbled through the solution at 25 °C for 20 min at 0.5 mL/s gas flow. [b] Regarding **3**. [c] Determined by GC with hexadecane as internal standard. [d] Referring to the ratio of yield to conversion.

4 and 2 hours, respectively (entries 6 and 7). It is important to note that without heterogenization of the initially applied homogeneous Pd complex, no hydrogenation occurred.

Finally, the separate reaction steps were combined to a sequential one-pot process. Therefore, the transformation was executed with the conditions developed in the optimization of the Sonogashira reaction (Table 1). Subsequently, water was added into the reaction mixture at room temperature before the solution was heated to 120 °C for 8 hours. In order to determine the optimal duration for the hydrogenation reaction, samples were prepared in specific intervals and analyzed for their composition. The results are depicted in Figure 1. The optimal duration was identified at 25 min of hydrogen flow and therefore slightly differing from the optimization results for the semihydrogenation step (Table 2).

Next, we examined the reactivity of different aryl bromides and terminal acetylenes to form preferentially Z-alkenes using this novel methodology (Table 3). Initially, we applied the previously optimized conditions to the reaction of methyl-substituted bromobenzenes such as *ortho*-, *meta*- and *para*-methyl-bromobenzene with phenylacetylene in order to study the effect of the substitution position. As shown in Table 3, entries 1–3, the corresponding intermediates **3a**, **3b** and **3c** were isolated with 85 %, 87 % and 84 % overall yield. Thus, no significant effect on the yield of the coupling reaction was observed. However, the semihydrogenation only provided the products in comparable yields 75 % (**4a**), 75 % (**4b**) and 72 % (**4c**) when the duration of the hydrogenation was adjusted. Herein, the *ortho*-substituted methyl-bromobenzene required longer reaction times presumably caused by steric hindrance of the methyl group. Due to the steric proximity of the *ortho*-substituent, the access of the catalysts surface to the internal acetylene is impeded. Therefore, the position of the substituent affects the semihydrogenation reaction, while the Sonogashira coupling displayed insignificant deviation based on the substituent position. Furthermore, the influence of the electron-withdrawing or

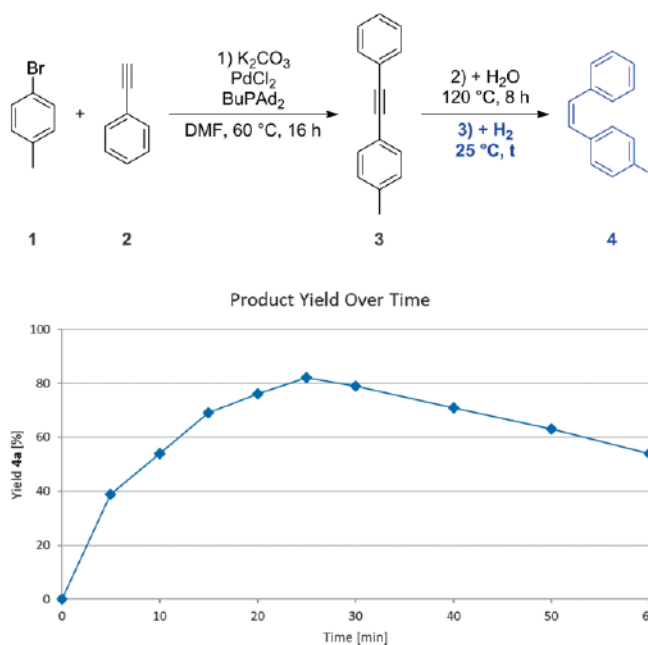


Figure 1. Product yield over time of the hydrogenation step in the sequential one-pot methodology. Conditions: 0.5 mmol **1**, 1 mmol **2**, 1 mmol K₂CO₃, 1 mol-% PdCl₂, 1 mol-% BuPAD₂, 2 mL of DMF at 60 °C for 16 h. Subsequently, 0.2 mL of H₂O was added at room temperature after which the solution was heated to 120 °C for 8 h. Finally, H₂ was bubbled through the reaction mixture at 25 °C for 25 min. Yield determined by GC with hexadecane as internal standard.

-donating nature of the substituent was investigated. Accordingly, 3-methoxy-bromobenzene (**1d**) as well as 3-trifluoromethyl-bromobenzene (**1e**) was evaluated for the productivity in the Sonogashira-semihydrogenation (entries 4 and 5). In agreement with literature findings, the electron-withdrawing group promotes the coupling reaction as 93 % of **3e** was formed. Conversely, only 72 % of intermediate **3d** was obtained suggesting that electron-donating groups decrease the reactiv-

ity of the aryl bromide. The complete reaction of **1d** and **1e** to the corresponding Z-alkenes revealed an additional influence of

the substituent on the hydrogenation result. The hydrogenation period had to be extended for substrate **1d** in order to achieve

Table 3. Substrate scope for the Sonogashira–semihydrogenation.^[a]

Entry ^[b]	Intermediate	Yield ^[c] [%]	Z-Alkene	Yield ^[c] [%]	Entry ^[b]	Intermediate	Yield ^[c] [%]	Z-Alkene	Yield ^[c] [%]
1		85		75	12 ^[ii]		68		64
2		87		75	13		87		0 ^[i]
3 ^[d]		84		72	14		83		0 ^[i]
4 ^[e]		72		68	15		86		0 ^[i]
5		93		83	16		82		76
6		88		79	17		84		76
7		82		72	18 ^[d]		80		71
8 ^[f]		69		35 ^[a]	19 ^[d]		90		85
9 ^[e]		70		41 ^[h]	20		80		0 ^[k]
10		98		84	21 ^[ii]		75		52
11		96		86	22 ^[m]		69		34

[a] General remark: For the isolated yields, the experiment was conducted twice. The first experiment was stopped after the Sonogashira step and the alkyne was isolated. The second experiment was conducted as described without purification of the intermediate and the Z-alkene was isolated. Therefore, the overall yield for the Z-alkene is obtained from **1** and **2** directly when the reaction is run without the isolation of **3**. [b] Standard conditions: 0.5 mmol **1**, 1 mmol **2**, 1 mmol K₂CO₃, 1 mol-% PdCl₂, 1 mol-% Bu₄Pd₂, 2 mL of DMF at 60 °C for 16 h. Subsequently, 0.2 mL of H₂O was added at room temperature followed by heating to 120 °C for 8 h. Finally, H₂ was bubbled through the reaction mixture at 25 °C for 25 min. [c] Isolated yield. [d] 30 min hydrogenation. [e] 35 min hydrogenation. [f] 180 min hydrogenation. [g] Significant amounts of the intermediate remained unconverted. [h] The isolated product contained significant amounts of the corresponding E-alkene which could not be removed by preparative methods. [i] 40 min hydrogenation. [j] The resulting complex mixture was not further isolated. [k] Despite prolonged hydrogenation, only insignificant amounts of the corresponding product were detected and not further isolated. [l] 80 min hydrogenation with 25 mol-% 3,6-dithia-1,8-octanediol (DTOD) at 0 °C. [m] 20 min hydrogenation at 0 °C.

full conversion (68 % yield) while the internal alkyne **3e** was completely hydrogenated after 25 min (83 % yield). The tendency of (strongly) coordinating functional groups to require prolonged hydrogenation periods was observed in several cases during the exploration of the substrate scope (entries 4, 8, 9, 12, 19). Based on the steric and electronic properties of the substrate, the optimal hydrogenation time varies for every reaction. Continuing our studies, we examined the reactivity of 4-trifluoromethyl-bromobenzene (**1f**) for both reaction steps (entry 6). Applying this starting material afforded 88 % of the intermediate **3f** and 79 % of the corresponding final product **4f**. When 2-bromonaphthalene was tested, the internal alkyne **3g** of the conversion with phenylacetylene was provided with 82 % overall yield while the hydrogenation gave 72 % of the *Z*-alkene **4g** (entry 7). 2-Methylthio-bromobenzene was successfully converted into the intermediate **3h** with an overall yield of 69 % despite the sulfur-containing functional group (entry 8). Albeit, the hydrogenation had to be extended to 3 hours, the process yielded 35 % of the *Z*-alkene **4h**. Nevertheless, a significant amount of the first-step product remained unconverted in the crude mixture despite the prolonged reaction time. Therefore, the methylthio-moiety displays a rather drastic example of the functional group effect on the hydrogenation. The transformation of 4-dimethylamino-bromobenzene (**1i**) offered 70 % of the intermediate product **3i** while the hydrogenation provided *Z*-alkene **4i** in 41 % overall yield (entry 9). However, the resulting product additionally contained 15 % *E*-alkene which could not be removed by preparative methods. Therefore, this substrate resulted in the most unfavorable *Z/E*-ratio (85:15). The aromatic nitrile **1j** was converted successfully to the corresponding intermediate **3j** in 98 % yield (entry 10). Subsequently, the hydrogenation afforded 84 % of the target *Z*-alkene **4j**. Furthermore, this result confirms the tendency of electron-withdrawing substituents to increase the reactivity of the aryl bromide in the coupling reaction. Next, we examined starting material **1k** in the transformation to the corresponding products and found both targets to be generated in 96 % (**3k**) and 86 % yield (**4k**), respectively (entry 11). Extending the list of different aryl bromides, intermediate **3l** was isolated in 68 % yield while the associated final product was obtained in 64 % (entry 12). Notably, also few functionalized substrates prevented the successful conversion to the desired products. In this respect, aldehyde- and nitro-containing substrates **1m** and **1n** smoothly converted into the corresponding intermediates in 87 % and 83 % yield; however, the hydrogenation led to a mixture of products including alkanes, alkenes and alkynes with either reduced or non-reduced aldehyde- or nitro-functional group (entries 13 and 14).

Using the ester-containing compound **1o**, provided the intermediate **3o** in 86 % yield (entry 15). Unfortunately, during heterogenization of the catalyst, the product was partially hydrolyzed in basic aqueous medium at 120 °C. Thus, a mixture of numerous compounds was obtained.

Moreover, we investigated the reactivity of different acetylenes in the one-pot Sonogashira–semihydrogenation process. To identify position effects, we compared the overall yields applying compounds **2p**, **2q** and **2r** (entries 16–18). The results

indicate a marginal effect for the coupling reaction as all three corresponding intermediates were isolated in 82 %, 84 % and 80 % overall yield. Regarding the final product, the tendency of *ortho*-substituents inhibiting the hydrogenation was observed as well. While the compounds **4p–4r** were obtained in similar quantities (76 %, 76 % and 71 %), the duration of the hydrogenation had to be extended in the case of *ortho*-methyl-phenyl-acetylene (**2r**) to 25 min in order to achieve complete conversion. Continuing our substrate scope, the conversion of aryl bromide **1a** and terminal acetylene **2s** provided the corresponding coupling product **3s** in 90 % and the semihydrogenation product **4s** in 85 % overall yield (entry 19). Unfortunately, the attempt to include 4-chloro-phenylacetylene in the list of convertible substrates failed although the intermediate **3t** was isolated in 80 % yield (entry 20). Here, various attempts to hydrogenate the C–C triple bond ended. To our delight, the transformation of **1a** with 1-octyne (**2u**) afforded the intermediate in 75 % yield (entry 21). Nevertheless, the initial hydrogenation results proved to be unsatisfactory/unsatisfying although promising. While the target was in fact formed and identified, the *Z*-selectivity accounted for only 58 %. The remaining starting material was already converted into the corresponding alkane. To increase the chemoselectivity, this reaction was performed in the presence of 3,6-dithia-1,8-octanediol (DTOD), also known as Lindlar Catalyst Poison.^[8a] Indeed, we discovered a positive effect of this additive for the hydrogenation of the intermediate **3u**. The results of the experiments with and without the additive are displayed in Figure 2.

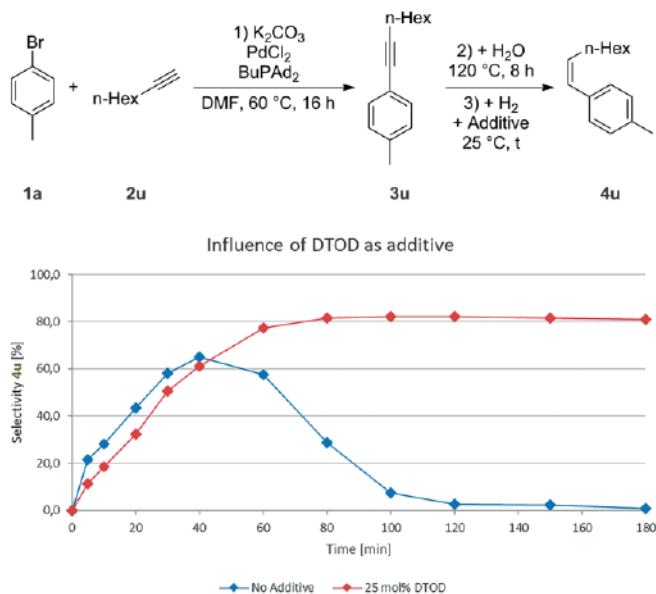
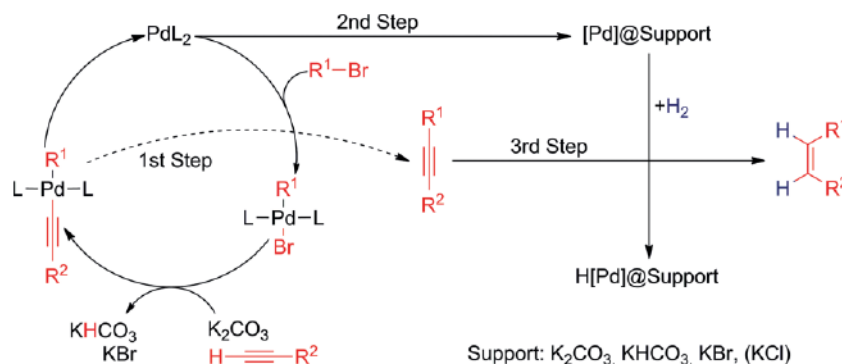


Figure 2. Influence of DTOD in the semihydrogenation step of internal acetylene **3u**. Conditions: 0.5 mmol **1a**, 1 mmol **2u**, 1 mmol K_2CO_3 , 1 mol-% PdCl_2 , 1 mol-% BuPA_{D_2} , 2 mL of DMF at 60 °C for 16 h. Subsequently, 0.2 mL of H_2O was added at room temperature after which the solution was heated to 120 °C for 8 h. Finally, the additive was added and H_2 was bubbled through the reaction mixture at 0 °C for 25 min. Yield determined by GC with hexadecane as internal standard.

Eventually, the final product **4u** was formed with 80 % *Z*-selectivity and an isolated yield of 52 % when the reaction was conducted with 25 mol-% DTOD at 0 °C for 80 min (Table 3,



Scheme 2. Postulated mechanism for the sequential Sonogashira-semihydrogenation.

entry 21). Consequently, alkyl-substituted acetylenes can be converted by aid of the additive with our methodology as well.

Nonetheless, when *tert*-butyl-acetylene (**2v**) was applied in combination with aryl bromide **1l**, the hydrogenation was prevented almost entirely in the presence of DTOD. Without the additive, the corresponding *Z*-alkene **4v** was obtained in 34 % yield when the reaction was conducted at 0 °C (entry 22).

To improve our understanding of the process, we analyzed the heterogeneous material and the reaction solution after each step for its palladium content by ICP-OES analysis. The results indicate that the palladium remains homogeneously dissolved after the Sonogashira reaction since no palladium was observed in the isolated particles. Overall 94 % of the originally applied palladium was detected in the homogeneous solution. In contrast, samples obtained after the heterogenization of the molecular catalyst as well as after the hydrogenation reaction contained detectable amounts of palladium. Herein, the homogeneous phase contained 69 % while the heterogeneous material incorporated 26 % of the employed transition metal. Obviously, the catalyst is not entirely heterogenized after the second reaction phase. To investigate the heterogeneous material XRD- and XPS-analysis were conducted. As expected, the material mainly consists of a K_2CO_3 - KHCO_3 mixture containing additional KBr and residual amounts of KCl . Unfortunately, the palladium content in the substance was too low (< 1 %) to get a defined understanding of the catalyst nature. XPS-analysis confirmed the composition of the material by O, C, K, Br and Cl. Herein, the chloride is presumably present as KCl stemming from PdCl_2 and K_2CO_3 .

Based on our findings, we postulate the mechanism depicted in Scheme 2 for the formation of *Z*-alkenes in the Sonogashira-semihydrogenation.

Initially, the synthesis of the internal acetylene is accomplished according to the generally accepted catalytic cycle for the Sonogashira reaction (first step).^[16] Herein, the active palladium complex undergoes oxidative addition with the aryl bromide. Next, the bromide ion is exchanged with the terminal acetylene through abstraction with K_2CO_3 . Aside from the formation of the aryl palladium acetylene complex, KBr and KHCO_3 are generated. Following the reductive elimination of the desired internal acetylene, the active palladium complex is regenerated and initiates a new catalytic cycle. During the partial heterogenization of the molecular Pd catalyst (second step), the

generated intermediate remains unconverted in the reaction mixture. Finally, the resulting heterogeneous palladium catalyst is activated by reduction with hydrogen. Hereupon, a palladium hydride surface is generated which serves as the active hydrogenation catalyst. Due to the specific surface, the selectivity of the catalyst allows for the hydrogenation of the internal acetylene towards the desired *Z*-alkene.

Conclusions

In summary, we developed a novel protocol for the synthesis of *Z*-alkenes making use of palladium twice, once as homogeneous complex and once as heterogenized hydrogenation catalyst. This methodology consists of three steps: 1. homogeneous Sonogashira reaction, 2. heterogenization of the homogeneous palladium complex and 3. selective semihydrogenation. It represents one of the rare examples in which a catalyst is transformed into a new form sequentially enabling an additional reaction. The synthesized *Z*-alkenes are an interesting substance class for fine chemical syntheses and life sciences. We further demonstrated the application on various substrates containing different functional groups and indicated the limitations regarding functional group tolerance.

Experimental Section

General Information: All manipulations were conducted under argon with exclusion of moisture and oxygen by using standard techniques for the manipulation of air sensitive compounds. Reaction temperatures refer to silicon oil in an additional pressure tube within the heated aluminium block. NMR spectroscopic data were recorded on Bruker ARX 300, Bruker ARX 400 and Bruker Fourier 300 spectrometers. ^{13}C and ^1H NMR spectra are given in ppm and referenced to signals of deuterated solvents and residual protonated solvents, respectively ($[\text{D}_6]\text{acetone}$: ^1H : 2.050 ppm, ^{13}C : 29.840 ppm. CD_2Cl_2 : ^1H : 5.320 ppm, ^{13}C : 54.000 ppm). The assignment of the carbon atoms was accomplished by aid of DEPT spectra. Gas chromatography analysis was performed on an Agilent HP-5890 instrument with a FID detector and HP-5 capillary column using argon as carrier gas. Gas chromatography-mass analysis was carried out on an Agilent HP-5890 instrument with an Agilent HP-5973 Mass Selective Detector (EI) and HP-5 capillary column using helium carrier gas. TOF HR-MS measurements were performed on an Agilent 1200/6210 Time-of-Flight LC-MS. Flash chromatography

was performed on a Teledyne Isco CombiFlash R_f 200 system. Chemicals were purchased from Sigma Aldrich, Alfa Aesar, TCI or Strem and were used as received. DMF was dried by a SPS from Innovative Technology while H_2O was flushed with argon for one hour. Solvents were stored in Aldrich Sure/store flasks under argon.

General Procedure for the Sonogashira–Semihydrogenation towards Z-Alkenes: In general, all steps are conducted subsequently without any intermediate work-up. Additives or solvents are only added after each step when indicated. In a glass pressure tube under argon, 4-bromotoluene (0.5 mmol, 63.5 μ L), phenylacetylene (1 mmol, 110 μ L) and DMF (2 mL) were added to the already present solids $PdCl_2$ (1 mol-%, 0.9 mg), $BuPAd_2$ (1 mol-%, 1.8 mg) and K_2CO_3 (1 mmol, 138 mg). The pressure tube was closed and the mixture was stirred in an aluminium block at 60 °C for 16 h. Afterwards, 0.2 mL of H_2O was added to reaction mixture under argon counter flow. The tube was closed again and heated to 120 °C for 8 h. Unless otherwise noted, hydrogen gas was passed through the reaction mixture at 0.5 mL/s gas flow at room temperature (25 °C) for a specific time without further additives. Afterwards, argon was passed through the solution for 10 min to remove dissolved hydrogen gas. For work-up, the product was purified by flash chromatography after initial extraction to give 73 mg (75 %) of **4a**. Detailed information can be obtained from the provided Supporting Information.

CCDC 1846870 (for TPAP 3) contains the supplementary crystallographic data for this paper. These data can be obtained free of charge from The Cambridge Crystallographic Data Centre.

Acknowledgments

We thank Patrick Piehl, Jacob Schneidewind, Max Hertrich, Sandra Leiminger, and the analytical department for fruitful discussions and technical support. The research was conducted as a part of the CHEM21 project funded by the EU and EFPIA. This work was supported by the state of Mecklenburg-Vorpommern, the BMBF, and the EU.

Keywords: Palladium · Z-Alkenes · Homogeneous catalysis · Heterogeneous catalysis · Sonogashira coupling · Hydrogenation

- [1] a) M. Beller, C. Bolm, *Transition Metals for Organic Synthesis*, Wiley-VCH, Weinheim, 2004; b) P. W. N. M. van Leeuwen, J. C. Chadwick, *Homogeneous Catalysis*, Wiley VCH, Weinheim, 2001.
- [2] a) M. J. Climent, A. Corma, S. Iborra, *Chem. Rev.* **2011**, *111*, 1072–1133; b) P. Munnik, P. E. de Jongh, K. P. de Jong, *Chem. Rev.* **2015**, *115*, 6687–6718; c) M. Sankar, N. Dimitratos, P. J. Miedziak, P. P. Wells, C. J. Kiely, G. J. Hutchings, *Chem. Soc. Rev.* **2012**, *41*, 8099–8139; d) H.-U. Blaser, A. Indolese, A. Schnyder, H. Steiner, M. Studer, *J. Mol. Catal. A* **2001**, *173*, 3–18; e) J. B. Ernst, C. Schwermann, G. I. Yokota, M. Tada, S. Muratsugu, N. L. Doltsinis, F. Glorius, *J. Am. Chem. Soc.* **2017**, *139*, 9144–9147; f) J. B. Ernst,

- S. Muratsugu, F. Wang, M. Tada, F. Glorius, *J. Am. Chem. Soc.* **2016**, *138*, 10718–10721.
- [3] a) R. V. Jagadeesh, K. Murugesan, A. S. Alshammari, H. Neumann, M. M. Pohl, J. Radnik, M. Beller, *Science* **2017**, *358*, 326–332; b) F. A. Westerhaus, R. V. Jagadeesh, G. Wienhofer, M. M. Pohl, J. Radnik, A. E. Surkus, J. Rabeah, K. Junge, H. Junge, M. Nielsen, A. Bruckner, M. Beller, *Nat. Chem.* **2013**, *5*, 537–543; c) R. V. Jagadeesh, A. E. Surkus, H. Junge, M. M. Pohl, J. Radnik, J. Rabeah, H. Huan, V. Schunemann, A. Bruckner, M. Beller, *Science* **2013**, *342*, 1073–1076; d) L. L. Zhang, A. Q. Wang, W. T. Wang, Y. Q. Huang, X. Y. Liu, S. Miao, J. Y. Liu, T. Zhang, *ACS Catal.* **2015**, *5*, 6563–6572; e) T. Cheng, H. Yu, F. Peng, H. Wang, B. Zhang, D. Su, *Catal. Sci. Technol.* **2016**, *6*, 1007–1015; f) J. Li, J. L. Liu, H. J. Zhou, Y. Fu, *ChemSusChem* **2016**, *9*, 1339–1347; g) Y. Li, Y. X. Zhou, X. Ma, H. L. Jiang, *Chem. Commun.* **2016**, *52*, 4199–4202; h) X. Ma, Y. X. Zhou, H. Liu, Y. Li, H. L. Jiang, *Chem. Commun.* **2016**, *52*, 7719–7722; i) Z. Z. Wei, Y. Q. Chen, J. Wang, D. F. Su, M. H. Tang, S. J. Mao, Y. Wang, *ACS Catal.* **2016**, *6*, 5816–5822.
- [4] P. Baumeister, G. Seifert, H. Steiner, EP0584043A1, **1994**.
- [5] P. Baumeister, W. Meyer, K. Oertle, G. Seifert, H. Steiner, *Chimia* **1997**, *51*, 144.
- [6] a) M. Picquet, *Platinum Met. Rev.* **2013**, *57*, 272–280; b) K. Geoghegan, S. Kelleher, P. Evans, *J. Org. Chem.* **2011**, *76*, 2187–2194.
- [7] C. Oger, L. Balas, T. Durand, J. M. Galano, *Chem. Rev.* **2013**, *113*, 1313–1350.
- [8] a) H. Lindlar, R. Dubuis, *Org. Synth.* **1966**, *46*, 89; b) H. Lindlar, *Helv. Chim. Acta* **1952**, *35*, 446–450.
- [9] a) S. Liang, G. B. Hammond, B. Xu, *Chem. Commun.* **2016**, *52*, 6013–6016; b) W. Niu, Y. Gao, W. Zhang, N. Yan, X. Lu, *Angew. Chem. Int. Ed.* **2015**, *54*, 8271–8274; *Angew. Chem.* **2015**, *127*, 8389; c) E. D. Slack, C. M. Gabriel, B. H. Lipshutz, *Angew. Chem. Int. Ed.* **2014**, *53*, 14051–14054; *Angew. Chem.* **2014**, *126*, 14275; d) R. Venkatesan, M. H. G. Precht, J. D. Scholten, R. P. Pezzi, G. Machado, J. Dupont, *J. Mater. Chem.* **2011**, *21*, 3030; e) O. Verho, H. Zheng, K. P. J. Gustafson, A. Nagendiran, X. Zou, J.-E. Bäckvall, *ChemCatChem* **2016**, *8*, 773–778; f) D. Köhler, M. Heise, A. I. Baranov, Y. Luo, D. Geiger, M. Ruck, M. Armbrüster, *Chem. Mater.* **2012**, *24*, 1639–1644.
- [10] a) F. Chen, C. Kreyenschulte, J. Radnik, H. Lund, A.-E. Surkus, K. Junge, M. Beller, *ACS Catal.* **2017**, *7*, 1526–1532; b) T. N. Gieshoff, A. Welther, M. T. Kessler, M. H. Precht, A. Jacobi von Wangelin, *Chem. Commun.* **2014**, *50*, 2261–2264; c) H. Konnerth, M. H. Precht, *Chem. Commun.* **2016**, *52*, 9129–9132; d) K. K. Tanabe, M. S. Ferrandon, N. A. Siladke, S. J. Kraft, G. Zhang, J. Niklas, O. G. Poluektov, S. J. Lopykinski, E. E. Bunel, T. R. Krause, J. T. Miller, A. S. Hock, S. T. Nguyen, *Angew. Chem. Int. Ed.* **2014**, *53*, 12055–12058; *Angew. Chem.* **2014**, *126*, 12251.
- [11] G. Wittig, U. Schöllkopf, *Chem. Ber.* **1954**, *87*, 1318–1330.
- [12] D. J. Peterson, *J. Org. Chem.* **1968**, *33*, 780–784.
- [13] a) H. Görner, H. J. Kuhn in *Adv. Photochem.* (Eds.: D. C. Neckers, D. H. Volman, G. v. Büna), John Wiley & Sons, New York, **2007**, pp. 1–117; b) J. Kagan in *Organic Photochemistry*, Academic Press, San Diego, **1993**, pp. 34–54.
- [14] G. C. Vougioukalakis, R. H. Grubbs, *Chem. Rev.* **2010**, *110*, 1746–1787.
- [15] a) X. F. Wu, H. Neumann, M. Beller, *Chem. Eur. J.* **2010**, *16*, 12104–12107; b) B. Agrahari, S. Layek, Anuradha, R. Ganguly, D. D. Pathak, *Inorg. Chim. Acta* **2018**, *471*, 345–354; c) S. Jadhav, A. Jagdale, S. Kamble, A. Kumbhar, R. Salunkhe, *RSC Adv.* **2016**, *6*, 3406–3420; d) S. J. Sabounchei, M. Ahmadi, Z. Nasri, E. Shams, M. Panahimehr, *Tetrahedron Lett.* **2013**, *54*, 4656–4660.
- [16] R. Chinchilla, C. Najera, *Chem. Rev.* **2007**, *107*, 874–922.

Received: April 26, 2018